

Water Science and Technology Library

Swatantra Kumar Dubey ·

Prakash Kumar Jha ·

Pankaj Kumar Gupta · Aliva Nanda ·

Vivek Gupta *Editors*

Soil-Water, Agriculture, and Climate Change

Exploring Linkages

 Springer

Water Science and Technology Library

Volume 113

Editor-in-Chief

V. P. Singh, Department of Biological and Agricultural Engineering & Zachry
Department of Civil and Environmental Engineering, Texas A&M University,
College Station, TX, USA

Editorial Board

R. Berndtsson, Lund University, Lund, Sweden

L. N. Rodrigues, Embrapa Cerrados, Brasília, Brazil

Arup Kumar Sarma, Department of Civil Engineering, Indian Institute of
Technology Guwahati, Guwahati, Assam, India

M. M. Sherif, Civil and Environmental Engineering Department, UAE University,
Al-Ain, United Arab Emirates

B. Sivakumar, School of Civil and Environmental Engineering, The University of
New South Wales, Sydney, NSW, Australia

Q. Zhang, Faculty of Geographical Science, Beijing Normal University, Beijing,
China

The aim of the *Water Science and Technology Library* is to provide a forum for dissemination of the state-of-the-art of topics of current interest in the area of water science and technology. This is accomplished through publication of reference books and monographs, authored or edited. Occasionally also proceedings volumes are accepted for publication in the series. *Water Science and Technology Library* encompasses a wide range of topics dealing with science as well as socio-economic aspects of water, environment, and ecology. Both the water quantity and quality issues are relevant and are embraced by *Water Science and Technology Library*. The emphasis may be on either the scientific content, or techniques of solution, or both. There is increasing emphasis these days on processes and *Water Science and Technology Library* is committed to promoting this emphasis by publishing books emphasizing scientific discussions of physical, chemical, and/or biological aspects of water resources. Likewise, current or emerging solution techniques receive high priority. Interdisciplinary coverage is encouraged. Case studies contributing to our knowledge of water science and technology are also embraced by the series. Innovative ideas and novel techniques are of particular interest.

Comments or suggestions for future volumes are welcomed.

Vijay P. Singh, Department of Biological and Agricultural Engineering & Zachry Department of Civil and Environment Engineering, Texas A&M University, USA
Email: vsingh@tamu.edu

All contributions to an edited volume should undergo standard peer review to ensure high scientific quality, while monographs should also be reviewed by at least two experts in the field.

Manuscripts that have undergone successful review should then be prepared according to the Publisher's guidelines manuscripts: <https://www.springer.com/gp/authors-editors/book-authors-editors/book-manuscript-guidelines>

Swatantra Kumar Dubey · Prakash Kumar Jha ·
Pankaj Kumar Gupta · Aliva Nanda · Vivek Gupta
Editors

Soil-Water, Agriculture, and Climate Change

Exploring Linkages

 Springer

Editors

Swatantra Kumar Dubey
Seoul National University of Science
and Environmental Engineering
Seoul, Korea (Republic of)

Pankaj Kumar Gupta
Faculty of Environment
University of Waterloo
Waterloo, ON, Canada

Vivek Gupta
Indian Institute of Technology Mandi
Himachal Pradesh, India

Prakash Kumar Jha
Kansas State University
Manhattan, KS, USA

Aliva Nanda
University of California
Merced, CA, USA

ISSN 0921-092X

ISSN 1872-4663 (electronic)

Water Science and Technology Library

ISBN 978-3-031-12058-9

ISBN 978-3-031-12059-6 (eBook)

<https://doi.org/10.1007/978-3-031-12059-6>

© The Editor(s) (if applicable) and The Author(s), under exclusive license to Springer Nature Switzerland AG 2022

This work is subject to copyright. All rights are solely and exclusively licensed by the Publisher, whether the whole or part of the material is concerned, specifically the rights of translation, reprinting, reuse of illustrations, recitation, broadcasting, reproduction on microfilms or in any other physical way, and transmission or information storage and retrieval, electronic adaptation, computer software, or by similar or dissimilar methodology now known or hereafter developed.

The use of general descriptive names, registered names, trademarks, service marks, etc. in this publication does not imply, even in the absence of a specific statement, that such names are exempt from the relevant protective laws and regulations and therefore free for general use.

The publisher, the authors, and the editors are safe to assume that the advice and information in this book are believed to be true and accurate at the date of publication. Neither the publisher nor the authors or the editors give a warranty, expressed or implied, with respect to the material contained herein or for any errors or omissions that may have been made. The publisher remains neutral with regard to jurisdictional claims in published maps and institutional affiliations.

This Springer imprint is published by the registered company Springer Nature Switzerland AG
The registered company address is: Gewerbestrasse 11, 6330 Cham, Switzerland

Contents

Part I Soil-Water Hydrological Consideration

- 1 Understanding Hydrology of Indian Himalayan Landscapes—A Review** 3
Manish Singh Rana, Manas Ranjan Panda,
Muhammad Shafqat Mehboob, Yeonjoo Kim,
and Chandan Mahanta
- 2 Development of a Semi-distributed Rainfall-Runoff Model for Water Budgeting in Macropore Dominated Hilly River Basins** 17
Suman Kumar Padhee, Chandan Pradhan, Ketan Kumar Nandi,
and Subashisa Dutta
- 3 Hydrological Simulation Using Coupled ANN-SCS Approach in Pagladiya Watershed: A Sub-catchment of Brahmaputra River Basin** 35
Sagar Debbarma, Swapnali Barman, Amulya Chandra Debnath,
Manoranjan Nath, and Sonu Kumar
- 4 Water Erosion Risks Mapping Using RUSLE Model in the Mohamed Ben Abdelkrim El Khattabi Dam Watershed (Central Coastal Rif, Morocco)** 53
Soukaina Ed-Dakiri, Issam Etebaai, Said El Moussaoui,
Mustapha Ikirri, Mohamed Ait Haddou, Salih Amarir,
Abdelhamid Tawfik, Hajar El Talibi, Hinde Cherkaoui Dekkaki,
Mohamed Abioui, Brahim Damnati, and Taoufik Mourabit

Part II Water-Agriculture-Climate Linkage

- 5 Estimating Soil Moisture Using Remote Sensing in Zimbabwe: A Review** 79
Never Mujere and Hardlife Muhoyi

6	Bivariate Copula Modelling of Precipitation and River Discharge Within the Niger Basin	93
	Samuel T. Ogunjo, Adeyemi O. Olusola, and Christiana F. Olusegun	
7	Remote Sensing and High-Throughput Techniques to Phenotype Crops for Drought Tolerance	107
	Sayantan Sarkar, Abhijit Rai, and Prakash Kumar Jha	
8	Sustainable Water Management Practices for Intensified Agriculture	131
	Manish Yadav, B. B. Vashisht, S. K. Jalota, Arun Kumar, and Dileep Kumar	
9	Deficit Irrigation: An Optimization Strategy for a Sustainable Agriculture	163
	Abhijit Rai, Sayantan Sarkar, and Prakash Kumar Jha	
 Part III Soil-Water Quality Consideration		
10	Recent Advances in the Occurrence, Transport, Fate, and Distribution Modeling of Emerging Contaminants—A Review	185
	Maliha Ashraf, Shaikh Ziauddin Ahammad, and Sumedha Chakma	
11	Management and Remediation of Polluted Soils Using Fertilizer, Sawdust and Horse Manure Under Changing Tropical Conditions	205
	Hassana Ibrahim Mustapha and Obumneme Sunday Okeke	
12	Impacts of Blend Diesel on Root Zone Microbial Communities: <i>Vigna Radiata</i> L. Growth Assessment Study	233
	Manvi Gandhi, Rakesh Kumar, Hassana Ibrahim Mustapha, Aprajita Jha, Pankaj Kumar Gupta, Nadeem Akhtar, and Prabhakar Sharma	
13	A Coherent Review on Approaches, Causes and Sources of River Water Pollution: An Indian Perspective	247
	Gaurav Singh, Tanu Jindal, Neelam Patel, and Swatantra Kumar Dubey	
 Part IV Techniques for Landscape Management Under Large Uncertainty		
14	Adapting to Climate Change: Towards Societal Water Security in Semi-arid Regions	275
	Manas Ranjan Panda and Yeonjoo Kim	

15 Challenges and Opportunities of Water Security in Latin America	291
Eduardo Saldanha Vogelmann, Juliana Prevedello, Kelen Rodrigues da Veiga, and Gabriel Oladele Awe	
16 Contribution of GIS to the Mapping of the Sensitivity of the Flood's Hybrid Multi-criteria Decision Approach: Example of the Wadi Tamlest Watershed (Agadir, Morocco)	309
Abderrahmane Wanaim, Mustapha Ikirri, Mohamed Abioui, and Farid Faik	
17 Flood Assessment Along Lower Niger River Using Google Earth Engine	329
Adeyemi O. Olusola, Oluwatola Adedeji, Lawrence Akpoterai, Samuel T. Ogunjo, Christiana F. Olusegun, and Samuel Adelabu	
18 Contribution of Geomatics to the Hydrological Study of an Ungauged Basin (Taguenit Wadi Watershed, Lakhssas, Morocco)	345
Mustapha Ikirri, Farid Faik, Said Boutaleb, Mohamed Abioui, Abderrahmane Wanaim, Amine Touab, Mouna Id-Belqas, and Fatima Zahra Echogdali	
Exploring Linkages Among Soil–Water, Agriculture, and Climate Change—A Summary	367
References	375

About the Editors

Swatantra Kumar Dubey is currently working as a researcher professor at Seoul National University of Science and Technology, Seoul, South Korea. His research focuses on water and food security indicators development using hydrological and crop modeling. He holds experience in the impacts of climate and land-use changes, water resources management, droughts, water quality, and climate extremes. He received M.Sc. (Tech) in environmental science and technology from the Banaras Hindu University, India, and graduated from the Central University of Rajasthan, India. He has worked with different institutes, i.e., CSIR-National Environmental Engineering Research Institute (CSIR-NEERI), Indian Agricultural Research Institute: ICAR (New Delhi), and Indian Institute of Science Education and Research (IISER) Bhopal, Madhya Pradesh. He has reviewed several research articles for reputed journals like River Research and Applications, International Journal of River Basin Management, Geology, Ecology, and Landscapes, Remote Sensing Letters, Sustainability, Water, Diversity, International Journal of Environmental Research and Public Health, ISH Journal of Hydraulic Engineering, and others. He is a lifetime member of the Indian Meteorological Society and a core member of the society of young agriculture and hydrology scholars of India (www.syahindia.org).

Dr. Prakash Kumar Jha is currently working as a postdoctoral researcher at the Feed the Future Sustainable Intensification Innovation Lab (SIIL), Kansas State University, USA. He is a crop modeler with an interest in sustainable agricultural systems. His specific research interests focus on investigating the influence of agronomic management on crop growth and development from field to ecological scale. He investigates complexities in agricultural systems, integrating crop simulation models, remote sensing, and climate forecast to formulate decision support systems for better management strategies at multiple scales of agroecosystems. He is passionate about teaching and the opportunity to mentor students interested in sustainable agricultural landscapes and fundamentals of digital agroecosystems. He has published more than 20 research papers and has reviewed several research articles for reputed journals like Agricultural Systems, Agronomy, Agronomy Journal, Computers and Electronics in

Agriculture, Crop and Pasture Science, Environmental Modeling & Software, Environmental Research Letters, Nature sustainability, Plant Methods, Plants, Scientific Reports, Sustainability, Water, and others.

Dr. Pankaj Kumar Gupta is a contaminant hydrogeologist; after having completed his Ph. D. from IIT Roorkee, he has been a Postdoctoral fellow at the University of Waterloo, Canada. Recently, he has been awarded the prestigious Ramanujan fellowship of the SERB (Govt. of India). The majority of his works focus on two areas: (1) understanding the soil moisture flow and pollutant mobility into soil–water systems and (2) developing water resource and pollution management strategies. He holds his in-depth experience in incorporating novel technologies (viz., geophysical investigations, groundwater modeling, aquifer mapping water quality assessment, etc.) to map aquifers of 30+ sites in India. He also teaches and guides Master's and Ph. D. students with diversified knowledge. He has received an AGU Travel Grant (2017), JPGU Travel Grant (2018), and EXCEED SWINDON and DAAD Germany Grant (2018). He serves as an editorial board member for SN Applied Sciences, Biochar, Carbon Research, and Frontiers in Water journals. He has published more than 20 research papers, approximately 30 book chapters, and edited 2 books and 2 popular science articles. He has reviewed several research articles for reputed journals including RSC Advances, Groundwater for Sustainable Development, ASCE JEE, ASCE Irrigation and Drainage, Env. Sc, Pollution Research, Eco-hydrology, Journal of Contaminant Hydrology, etc. Further, he has led many site restoration and remediation consultancy projects at polluted industrial sites in India. He is a core member of the society of young agriculture and hydrology scholars of India (www.yahindia.org), a network of early career researchers from the globe.

Dr. Aliva Nanda is currently working as a postdoctoral researcher at Sierra Nevada Research Institute, University of California, Merced, USA. Her research expertise includes understanding runoff generation mechanisms, pathways, and thresholds at micro- to macro-scale, modeling efficient irrigation systems, and optimizing irrigation efficiency. She is also exploring the ecohydrological processes of the forested catchment. She graduated from the Indian Institute of Technology Roorkee, India. During her Ph.D., she has done extensive field studies to understand the hydrological processes of the Himalayan landscapes. Her Master's and Bachelor's degree are in irrigation and drainage engineering and agricultural engineering, respectively. She also receives University Gold Medal and Governor's award for her outstanding academic performance. Besides these, she bagged many travel fellowships, i.e., Lloyd V. Berkner Travel Fellowship, American Geophysical Union (AGU) student travel grant, Japan Geophysics Union (JpGU) student travel grant, AGU early career travel grant, and academic awards till date. She has published her research in many reputed high-impact factor journals and presented at many international conferences. She is also a founding member of the Society of Young Agriculture and Hydrology scholars of India (www.yahindia.org), which aims to develop a collaborative network among graduate students, researchers, and professors.

Dr. Vivek Gupta is an assistant Professor at the School of Engineering at the Indian Institute of Technology Mandi, India. He completed his Ph.D. in Hydrology from IIT Roorkee and M. Tech. in Water Resources Engineering and Management from IIT Guwahati. After completing his Ph.D., he worked in industry for a short term and then joined as a Postdoctoral Scholar at the University of California at Merced in the USA. He has published more than 20 articles in several highly reputed international journals and conferences. His research interests are understanding the climate change impacts on water resources with a special focus on floods and droughts using physically based and data-based modeling, developing early warning and climate information systems, and utilizing remote sensing and GIS for studying hydrology at a large scale.

Part I
Soil-Water Hydrological Consideration

Chapter 1

Understanding Hydrology of Indian Himalayan Landscapes—A Review



Manish Singh Rana, Manas Ranjan Panda, Muhammad Shafqat Mehboob, Yeonjoo Kim, and Chandan Mahanta

Abstract Melt water from the glaciers and snow over the Himalayan mountainous range plays a vital role in the river hydrology where more than 200 million of people consume this water for domestic and agricultural purposes. The hydrology of this high-altitude glaciated range is quite complex and from a water resources management perspective a comprehensive hydrometeorological modeling system is mandatory to project the hydrological changes in response to climate change. Climate change has an impact on the basic components that control the formation and melting of glaciers and snow cover, consequently impacting the livelihood, hydropower generation, and agricultural practices. Several hydrological models from lumped to fully distributed, have been developed to understand the complex hydrological behavior of the Himalayan region, however, the impacts of climate change on the hydrology of the Himalayan region are still ambiguous. Some researchers agree with glaciers expansion while others showed a glacier retreat. Such contradictory views in the climate and glaciers threaten future water management and sustainability of water resources. The choice of hydrological models is purely dependent on the availability of the datasets and the goals to be achieved. Lack of in-situ meteorological datasets is one of the biggest challenges that researchers must face while estimating the hydrological variables. Satellite-based meteorological products, to some extent, provide a reasonable replacement of in-situ data but cascade the uncertainties in the final outputs. This chapter aims to demonstrate the complexity and understanding of the hydrology of Himalayan regions, and the challenges to developing the hydrological models in the Himalayan region.

Keywords The Himalayas · Climate change · Glaciers · Snow cover · Hydrological models

M. S. Rana (✉) · C. Mahanta
Department of Civil Engineering, IIT Guwahati, Assam, India
e-mail: manishsingh@iitg.ac.in

M. R. Panda · M. S. Mehboob · Y. Kim
Department of Civil and Environmental Engineering, Yonsei University, Seoul 03722, South Korea

1.1 Introduction

The Himalayas provide freshwater to over a quarter of the world's population (1.9 million people) (Bharti et al. 2020). In Asia, the Himalayan Mountain range divides the Indian subcontinent from the Tibetan Plateau, features one of the world's youngest, and most vulnerable systems due to ongoing geotectonic activities. The Hindu Kush Himalayan (HKH) area is a 3,500-km-long mountain range that runs from Afghanistan to Myanmar (Nepal et al. 2014a). The Himalayas are the source of many major rivers in Asia, and the water from these rivers is mostly used for hydropower generation in the hills and mountains. Many river basins that originate in this area range in elevation from near sea level to more than 8000 m above sea level (masl). As a result, the region's precipitation and temperature have complex spatial distribution features, adding to the already difficult issue of modeling mountainous hydrology. The Himalayas alone are the source of ten of Asia's largest rivers. However, the town in the Himalayan region experiencing severe drinking water shortages (Tamang et al. 2020). Natural rainfed springs are the primary source of household water, but most of the springs are drying up due to rapid climate change. Agriculture uses a large portion of the water in northern India and Nepal. At higher elevations, rain-fed agriculture predominates, with irrigation limited to the plains and lower to medium mountain region (approximately < 1500 m) (Tripathi and Sah 2001). In this region, rapid population growth rates of more than 2% per year have resulted in the rapid conversion of natural land into agriculture. The agricultural land area of Nepal's middle mountain region has increased by 10% to 25% in the previous 30 years. As a result of the increased demand for irrigation, water distribution linked with agricultural expansion has been put under growing strain. It is commonly acknowledged that global climate change is causing glaciers to decrease or retreat all across the planet. There is no exception in the Hindu Kush-Himalayan region. Subsequently, a vast number of glacial lakes have formed, many of which are prone to becoming unstable as their volume grows or as a result of surge waves resulting due to moraine dam overtopping triggered by ice and rock avalanche, earthquake, and other mass movements. Glacial lakes are extremely dynamic water reservoirs that expand in quantity, size, and volume in response to climate change (Bolch et al. 2019). In the Himalayas, more than 5000 glacier lakes are dammed due to climate change and rapid glacier recession, and similar patterns may be found in other mountain ranges. Various assessments on a global and regional scale across Asia demonstrate the expansion of glacier lakes and their harmful potential.

GLOFs are abrupt and large-scale discharges of dammed glacial lakes, which can cause catastrophic flooding and destruction in downstream areas (Linsbauer et al. 2016). Examples include the Breach of Chorabari lake in Mandakini river in Uttarakhand, India (Bhambri et al. 2016), the outburst of $1.1 \times 10^5 \text{ m}^3$ from Gongbatongshacuo in china (Allen et al. 2021), and outburst floods due to the rapid expansion of Cirenmaco in 1964 and 1981 (Wang et al. 2018). Because assessment information is frequently poor, glacial lake outburst flood (GLOF) spawning in transboundary basins can be extremely destructive. In the north of the subcontinent,

climate-induced glacial melt results in a large flow of sediment with heavy discharge of water. Himalayan eroded soil down to the riverine delta. Large areas of the country are flooded during the monsoon season, while dry season droughts caused by excessive heat evaporate the water and deposit silt in the river channel. This produces the storm which triggers the riverbank erosion, environmental degradation, and flooding of agriculture, urban settlements, and villages. It is vital to comprehend the present Glacial lakes and hydrological regimes of river systems in the Himalayan region. Understanding the features of a watershed and its responses to streamflow requires the use of hydrological models (Krause 2002). The data gathered from direct field observations are significantly used in hydrological models. However, our knowledge of the Himalayan hydrological cycle's timing and relative contributions is inadequate and many knowledge gaps exist about the Himalayan region's water resources and characteristics (Bajracharya and Shrestha 2011). As a result, the current chapter offers the findings of an extensive review of existing knowledge of the hydrology of the Himalayan region, gaps in our current understanding of the hydrology of catchment, and constraints in hydrological modeling. Many critical aspects in the management of water resources that are available in the Himalayan region have been recognized.

1.2 Hydrology of the Himalayan Region

The Western disturbances (WDs) and Indian summer monsoon (ISM) are two major weather systems responsible for precipitation in the Himalayas. The impact of these circulation systems is complex due to their occurrence and distribution (Bookhagen and Burbank 2010). Monsoon precipitation varies in intensity, timing, and magnitude from east to west, where the east experiences the longest monsoon and receives the higher rainfall. More than three-quarters of all precipitation falls in the eastern section of the region during the monsoon (Nepal 2012). Moreover, a third of total precipitation falls in the western region throughout the winter. On different mountain hydrological systems, the function of glaciers varies based on basin dynamics. The majority of the interpretations are based on the 'Alpine catchment', in which the majority of the yearly precipitation falls as snow throughout the winter season. The melting of the winter snow continues into the summer, resulting in seasonal high discharges when combined with glacier melt. Glaciers are crucial for river flow in such systems, particularly during the summer. A 'Himalayan catchment' differs dramatically from an 'Alpine catchment' because the monsoon coincides with the peak discharge of the annual hydrograph, temperature fluctuation, trends, ice, and snowmelt. As a result, the 'Himalayan catchment' is defined by peak runoff due to glacier melt responsible for annual streamflow during July and August (Thayyen and Gergan 2010).

When the snow melts in the summer, the water discharge increases by 20–50 times in Himalayan rivers. Furthermore, sediment load increases 500–1000 times due to the effect of high discharge in rivers, primarily from the western Tibetan plateau

and the Karakoram. The Himalayan Range's eastern portion is eroding quicker than the western side, contributing to the Brahmaputra's larger suspended load than the Ganges due to higher precipitation. In the Himalayas, there are several rain shadow zones, and the region's diverse geography creates both rainy and dry zones. Several studies of rainfall distribution with elevation in various Himalayan locations conveyed that precipitation has a direct relationship with altitude. According to Dhar and Rakhecha (1981), there is no linear relationship between precipitation and elevation. Other studies, on the other hand, have resulted that precipitation in the Himalayan region could increase continuously with elevation, but that precipitation begins to decline above a particular altitude. It indicates that the relationship between precipitation and elevation changes with time and location. Active tectonics is a major forcing factor impacting river channel dynamics, sediment load, and shape in any basin. The geology of the Indus drainage was mostly created by the 50 million-year-old collision between the Indian Plate and continental Asia (Inam et al. 2007). The surrounding ranges have been elevated to considerable heights due to continued tectonic activity. Himalayan rocks are separated from higher Himalayas in the north by major central thrust, and it is also separated from Siwalik in the south by main boundary thrust. Fracture zones, which form as a result of thrust, faults, and other lineaments, are ideal locations for springs because they encourage groundwater recharging while also controlling drainage.

Limitations in hydrological modeling

- Due to the lack of long-term data records and practical problems in data quality maintenance, there are certain ambiguities (Kattelmann 1987). Only a few climatological studies have been conducted in the entire Himalayan region. The local climate is influenced by the complex topography, which causes large variations in temperature and precipitation. Long-term climate data are frequently required for local-level development projects. However, only large-scale and regionalization of climate change data are available with overextended. Various models based on temporal and spatial data can be used to generate climate data. Cox and Isham (1994) identified three types of rainfall models: empirical statistical models that can be used to generate annual, monthly, and daily climate data, dynamic meteorology models that use physical processes in the catchment to represent real-world dynamics using nonlinear partial differential equations, and intermediate stochastic models that are primarily used for short-term data analysis. However, the uncertainty in future climate forecasts is mainly due to uncertainty in climate data modeling under climate change scenarios (Srikanthan and McMahon 2001).
- Due to a low rain gauge network density and a specific location where it is difficult to define dynamics of precipitation extremes of the Himalayan basin, representative data are scarce (Sharma et al. 2000). Rain gauges are the most effective tool for measuring precipitation, but due to topographic heterogeneity in the mountainous areas, it is impossible to install rain gauge stations uniformly for in situ rainfall measurement. The Indian meteorological department is continuously working to expand the rain gauge network in the Himalayan region, but the cost of expanding and maintaining these stations has proven very costlier.

Weather radars have grown more prevalent in recent years for detecting severe weather events (Bharti and Singh 2015). Although it has significant drawbacks, such as the need for a large and heavy antenna for long-range detection, the beam may not propagate properly, and it is susceptible to jamming. IMD installed multiple Doppler weather radar stations around India for a better understanding of the weather system; nevertheless, installing radar stations in the Himalayan region remains a difficult task.

- Incapacity of a model to reflect the various runoff components, such as the retreat of the glacier, snowmelt runoff, and baseflow, and to depict the dynamics of the riverine system in broad terms, such as increased water level during the monsoon season and low flows during the winter (Nepal et al. 2014b). Due to the uncertainty in the quality of existing data, hydrological modeling for the Himalayan region remains difficult. Furthermore, data scarcity makes accurate calibration in these models difficult (Pellicciotti et al. 2012). Several semi-distributed models (Shukla et al. 2021; Bhattarai et al. 2018), distributed models (Shrestha and Alfredsen 2011; Nepal et al. 2014a; Li et al. 2015), and glacier retreat models (Li et al. 2015) have been used for the Himalayan region, but a lack of clarity in understanding of hydrological processes creates uncertainty in modeling approaches under climate change scenarios.
- High cost of the monitoring operation in the study area. The utility of remote sensing and gridded models for many scientific types of research has increased in recent years, whereas studies relying on ground-based data have decreased worldwide due to their high operation cost and difficulty in handling (Yatagai et al. 2012). In situ observations are primarily utilized to confirm the model's reliability and play an important part in the calibration and validation process. According to literature, the Himalayan region's ground-based observation network is shrinking, resulting in a lack of understanding of physical processes and model inaccuracy.

1.3 Different Modeling Approaches

1.3.1 *Runoff Estimation Models*

Water availability assessment in gauged and ungauged regions in the Himalayan range is necessary to build management tools. Surface hydrology, particularly in ungauged watersheds, faces a significant challenge in estimating continuous streamflow in Himalayan regions. Ungauged basins are those with insufficient records of hydrological observations (Sivapalan et al. 2003). Because it is very essential to have a detailed knowledge of flow variability in data-scarce areas. Using proper hydrological models, reliable continuous streamflow forecasting is a key approach to watershed planning and management. The estimation of runoff is particularly essential in meteorology, especially in locations where there are no calibrated measuring stations. Previously, various hydrological models have been applied to estimate direct runoff in the ungauged region such as HEC-HMS (Akay et al. 2018), MOHYSE, HMETS,

GR4J (Arsenault et al. 2019), SWAT (Kanishka and Eldho 2020), VIC (Bao et al. 2012), and WASMOD (Yang et al. 2018) with the combination of regionalization methods.

In hydrology and water management engineering, machine learning widely applied in recent years. For monthly flow forecasting, Hussain and Khan (2020) found Random Forest (RF) outperformed multilayer perceptron (MLP) and support vector regression (SVR). The random forest model was able to simulate small and medium floods in a similar way to the HYDROMAD model (Schoppa et al. 2020). Wang and Wang (2020) showed that M5P model tree (M5P) and Multiple linear regression (MLR) performed better than k-nearest neighbor (KNN), Gaussian process (GP), multilayer perceptron (MLP), and random forest (RF) in the prediction of water level in Erie lake. However, there have been very few studies on using machine learning to predict hydrological model parameters.

It is a relatively new approach to use hydrological models to analyze the complex dynamics in the upper region of the Himalayas. As a result, certain modeling applications have been carried out without the use of glacier data (Sharma et al. 2000). However, the snowmelt-induced runoff has been highlighted in relation to climate change impact in recent years (Immerzeel et al. 2010). Snow and glacier melt have been approximated in the Himalayan region using empirical methodologies, such as snowmelt based on ablation gradients (Racoviteanu et al. 2013), threshold air temperature (Kour et al. 2016), and a degree-day factor (Immerzeel et al. 2010). Therefore, detailed knowledge for integrated hydrological system methodologies and investigation is limited due to the unavailability of data on catchment dynamics such as snow, discharge, infiltration properties, land cover change, and glacier ice melt.

1.3.2 Regionalization Approach

Streamflow forecasting in gauged and ungauged basins is predicted using various distributed models, semi-distributed models, physically-based models, data-driven and conceptual based models. The conceptual lumped model is commonly used to forecast streamflow due to its less complicated mechanism (Yadav et al. 2007). Model parameters obtained from physical catchment features for ungauged catchments using physically based models are fraught with risk and show ambiguity in prior distribution (Bulygina et al. 2011). It can lead to overparameterization and structural problems in the model. In comparison to conceptual or semi-distributed models, such models require a significant amount of data and human work. The model parameters in data-driven and conceptual/semi-distributed models must be determined by calibration process against observed discharge for adjustment in features and parameters until the catchment and model behavior become identical. Due to the low cost and well-known solution, regionalization is widely used for the estimation of streamflow time series in ungauged basins (Samuel et al. 2011). Regionalization can be used to transfer hydrological data across geographical objects and spatial dimensions. This approach can be used by employing predictive techniques such as extrapolating

hydrologic data from gauged to ungauged catchments (Goswami et al. 2007). Arora et al. (2005) evaluated three regionalization methods to construct a regional flow duration curve for the Chenab river basin, finding that flows in the upper region have larger variability than those in the lower region. Using a regionalization technique, Rees et al. (2004) estimated average water volume for the annual recession period for the Himalayan catchments. Liu et al. 2021 utilized a regionalization approach for Sino Himalaya to categorize floristic regions. In hydrological research, regionalization is often regarded as a difficult task. First, the chances of success of simulation are less due to the scarcity of discharge data, which is commonly used to calibrate model parameters (Sivapalan et al. 2003). Second, results from the literature review based on regionalization methods are inconsistent since they were conducted at diverse locations, and the available catchment parameters differ from one case to the next (Oudin et al. 2008).

The regionalization approach for estimating continuous streamflow can be accomplished using a hydrological model by transferring hydrological data through model parameters. The data-driven-based hydrologic model-independent method is an alternate method. Rainfall-runoff models for the ungauged region show some uncertainties due to flaws in model parameters estimation, the link between locally calibrated parameters and catchment feature, the distinctiveness of the basin (Wagener and Wheater 2006), and the complexity of the hydrological model. However, hydrologic model-independent methods prevent the complex mechanism of a hydrological model and estimation-based uncertainty in parameter and uncertainty due to calibration of the data-driven model. Data-driven methods typically require less data and knowledge, which could be advantageous in dealing with data-availability limits.

It is impossible to build a universal approach as the optimal way for all catchments because the regionalization process is integrally associated with employing catchment features. As a result, an investigation on any location of interest is required to determine the optimal technique among hydrologic model-dependent and independent methods.

1.3.3 Flow Duration Curve (FDC) and Low Flows Estimation

Headwater regions of the Himalayas have several low-flow rivers. These low flow rivers are tributaries of the Indus, Ganga, and the Brahmaputra, which are important in maintaining water flows in these rivers. As a result, accurate forecasts of low river flows in the Himalayan basins are extremely important for water resource management. When it comes to estimating reliable predictions of low flows, there are two major issues to consider. Firstly, most of the Himalayan basins are ungauged, therefore dependable and long-term hydrometeorological data is scarce. In these mountains, the stream gauging station network is poor. Second, the resource base is depleting at a higher rate than it was previously. According to a study, it is indicated that glaciers are retreating globally, including the Himalayan glaciers, retreating by hundreds of meters in the previous 20 years. Possible low-flow estimation approaches

in ungauged catchments in mountainous regions can be categorised into (i) those that use hydrological regionalization techniques to predict either specific low-flow indices or composite low-flow measures; and (ii) those that allow any low-flow characteristic to be estimated from synthetic flow time series. Furthermore, it can classify into (i) regional regression models; (ii) graphical methods; (iii) technique of spatial interpolation; and (iv) estimation of low flow using synthetic flow time series. In low-flow estimation for ungauged locations, the regional regression method is the most extensively employed. This method includes several steps such as a selection of low flow characteristics for regression model based on variable user requirements, streamflow database constraints, research aims, methodologies, etc., delineation of hydrologically homogeneous regions, and construction of regression. This establishes a link between dependent low-flow parameters and independent catchment and meteorological variables (Fouad et al. 2018).

Regional prediction curves, unlike regression models that estimate single low-flow attributes, allow for the estimation of various low-flow indices. FDC and low-flow frequency curves obtained from multiple homogeneous gauged catchments can be converted into identical scales, superimposed, and then averaged to generate a regional curve. All flows are standardized to make curves comparable with other catchments by area and mean or median flow. Another approach for low flow estimation is regional mapping and spatial interpolation. The interaction between flow field and natural elements which are zoned physiographically are the foundations for mapping flow features. Flow maps are built based on flow characteristics derived from gauged data, similar to regression relationships. The denser the gauging station network with adequate flow data is, the more accurate the maps-based estimates will be. The size of the catchments utilized for mapping should ideally represent the flow regime's zonal type. Moreover, very small rivers and very large rivers (running over multiple geographical zones) should not be chosen for flow mapping. For regional regressions and mapping, the upper and lower basin can be selected arbitrarily and may differ depending on physiographic conditions (Risley 1994).

Low flow in the ungauged area can be estimated using synthetic time series. The use of a time-series simulation method to produce sufficiently streamflow data of long length and low-flow indices from the simulated series is an alternate approach to low-flow estimate for ungauged sites. There are two types of simulation methods: stochastic and deterministic. The first generates a time series with 'realistic' statistical features, although it is not intended to imitate actual site flow sequences (Kelman 1980). The deterministic approach, on the other hand, usually incorporates a rainfall-runoff model that turns actual rainfall data in a simulated catchment into a continuous flow time series.

1.3.4 Climate Models for Himalayan Regions

Climate projections must be accurately estimated to assess the climate change impact and to be used in hydrological modeling. Under various scenarios, "Global Climate

Models” (GCMs) are the most widely acknowledged tools for producing reliable future projections (Iqbal et al. 2020). Even though GCMs give accurate representations of large-scale components of climate, the coarse resolution obtained from GCMs is not sufficient to resolve key features associated with regional scale (Wilby et al. 1999). The scale of a regional climate model (RCM) is substantially closer to real-world observations that affect the climate system, therefore it can resolve the heterogeneity of geographical regions, alleviating the uncertainty of GCMs (Lee et al. 2019). Despite the hard terrain and considerable variability in regional climate patterns, Dimri et al. (2013) proved that RCM may be used effectively to assess the impact of climate change in the Himalayan region. Jury et al. (2020) used an ensemble of 36 GCMs and 13 RCMs for two RCPs 4.5 and 8.5 for the lower river basins of the Himalayas and predicted that 2-m rise in air temperature and precipitation rate linked to the Indian summer monsoon.

Kulkarni et al. (2013) used Hadley Centre’s high-resolution regional of global warming to assess the global warming on the HKH and indicted that summer monsoon rainfall may be 20–40% higher in 2071–2098. Jasrotia et al. (2021) applied the Variable Infiltration Capacity (VIC) model to calculate the impact of climate change and found that precipitation projections had a significant impact on Jhelum watershed runoff. The freshwater-related risks of climate change can be analyzed using scenarios generated by GCMs as part of the Coupled Model Intercomparison Project phase 5 (CMIP5) (Taylor et al. 2012; Das et al. 2016). Multiple RCP experiments have used the Coordinated Regional Climate Downscaling Experiment (CORDEX) and CMIP5 model data to create various meteorological information at both regional and global scales.

1.4 Conclusions

The Himalayan region, which has abundant water resources, is experiencing a scarcity of water due to environmental and anthropogenic factors. Due to fast population growth and the related problem, governments in this region are confronting new and more difficult challenges in satisfying fundamental needs for water, food, and energy. Several studies have suggested that climate change has a negative impact on the hydrology of the western Himalayan river basins, which has a direct impact on the quantity and availability of water. The following are the highlights of this work:

- i. How variations in glacier melt will affect river discharge over the coming decades is one of the largest areas of uncertainty in Himalayan science. Therefore, there is a need to develop some methods or models on a regional scale to predict the impact of glacier melt on river flow.
- ii. A robust and dynamic hydrological model is required which can consider all disciplines such as the impact of climate change, glacier retreating, availability of water resources, and other water policy in a single frame.

- iii. Deforestation, habitat loss, and global warming are all known to be wreaking havoc on the Himalayan range, and its ability to serve as Asia's water tower, in the long run, is becoming increasingly doubtful. However, it can be managed sustainably using appropriate ecological models and policies.
- iv. There are several methodological challenges e.g. (a) lack of long-term data, (b) lack of accurate data, and (c) higher cost for field experiment and unavailability of field equipment which affects the research significantly. However, the regionalization approach can be used to estimate parameters for catchments without observed streamflow.
- v. In terms of water volume, low flows during roughly nine months of the year are more important than peak flows for three monsoonal months (July–September). Low flow measurements and accurate low flow estimating methods are crucial for proper water resource assessment, planning, and management, whether for hydropower, irrigation, or water delivery. Although there are several methods for estimating low flow, regional regression models are a widely accepted method for the same.
- vi. Climate change in the Himalayan range has a potential impact on snow melting, overland flow, streamflow, rainfall pattern, groundwater flow, infiltration rate, soil erosion, and water temperature. Henceforth, the influence of climate change on available water resources should be re-evaluated in the future.

References

- Akay H, Koçyiğit MB, Melih Yanmaz A (2018) Effect of using multiple stream gauging stations on the calibration of hydrologic parameters and estimation of hydrograph of ungauged neighboring basin. *Arabian J Geosci* 11(11):1–11
- Allen S et al (2021) Glacial lake outburst flood hazard under current and future conditions: first insights from a transboundary Himalayan basin. *Nat Hazards Earth Syst Sci Discuss*, 1–30
- Arora M et al (2005) Regional flow duration curve for a Himalayan river Chenab. *Hydrol Res* 36(2):193–206
- Arsenault R et al (2019) Streamflow prediction in ungauged basins: analysis of regionalization methods in a hydrologically heterogeneous region of Mexico. *Hydrol Sci J* 64(11):1297–1311
- Bajracharya SR, Shrestha BR (2011) The status of glaciers in the Hindu Kush-Himalayan region. International centre for integrated mountain development (ICIMOD)
- Bao Z et al (2012) Comparison of regionalization approaches based on regression and similarity for predictions in ungauged catchments under multiple hydro-climatic conditions. *J Hydrol* 466:37–46
- Bhambri R et al (2016) Devastation in the Kedarnath (Mandakini) Valley, Garhwal Himalaya, during 16–17 June 2013: a remote sensing and ground-based assessment. *Nat Hazards* 80(3):1801–1822
- Bharti V, Singh C (2015) Evaluation of error in TRMM 3B42V7 precipitation estimates over the Himalayan region. *J Geophys Res Atmosph* 120(24):12458–12473
- Bharti N et al (2020) Dynamics of urban water supply management of two Himalayan towns in India. *Water Policy* 22(S1):65–89
- Bhattarai S et al (2018) Hydrological modelling and climate change impact assessment using HBV light model: a case study of Narayani River Basin, Nepal. *Nat Environ Pollut Technol* 17(3):691–702

- Bolch T et al (2019) Status and change of the cryosphere in the extended Hindu Kush Himalaya region. *The Hindu Kush Himalaya Assessment*. Springer, Cham, pp 209–255
- Bookhagen B, Burbank DW (2010) Toward a complete Himalayan hydrological budget: Spatiotemporal distribution of snowmelt and rainfall and their impact on river discharge. *J Geophys Res Earth Surface* 115(F3)
- Bulygina N, McIntyre N, Wheeler H (2011) Bayesian conditioning of a rainfall-runoff model for predicting flows in ungauged catchments and under land use changes. *Water Resour Res* 47(2)
- Cox DR, Isham V (1994) Stochastic models of precipitation. *Statistics for the environment 2, Water issues* (1994): Barnett V, Turkman KF (Eds.), Wiley, New York, pp 3–18
- Das L, Meher JK, Dutta M (2016) Construction of rainfall change scenarios over the Chilka Lagoon in India. *Atmosph Res* 182:36–45
- Dhar ON, Rakhecha PR (1981) The effect of elevation on monsoon rainfall distribution in the central Himalayas. *Monsoon Dyn* 253:260
- Dimri AP et al (2013) Application of regional climate models to the Indian winter monsoon over the western Himalayas. *Sci Total Environ* 468:S36–S47
- Fouad G, Skupin A, Tague CL (2018) Regional regression models of percentile flows for the contiguous United States: Expert versus data-driven independent variable selection. *J Hydrol Regional Stud* 17:64–82
- Goswami M, O'connor KM, Bhattarai KP (2007) Development of regionalisation procedures using a multi-model approach for flow simulation in an ungauged catchment. *J Hydrol* 333(2–4):517–531
- Hussain D, Khan AA (2020) Machine learning techniques for monthly river flow forecasting of Hunza River, Pakistan. *Earth Sci Inform* 13(3)
- Immerzeel WW, Van Beek LPH, Bierkens MFP (2010) Climate change will affect the Asian water towers. *Science* 328(5984):1382–1385
- Inam A et al (2007) The geographic, geological and oceanographic setting of the Indus River. Large rivers: geomorphology and management, pp 333–345
- Iqbal Z et al (2020) Evaluation of global climate models for precipitation projection in sub-Himalaya region of Pakistan. *Atmosph Res* 245:105061
- Jasrotia AS et al (2021) Hydrological modeling to simulate stream flow under changing climate conditions in Jhelum catchment, western Himalaya. *J Hydrol* 593:125887
- Jury MW et al (2020) Climate projections for glacier change modelling over the Himalayas. *Int J Climatol* 40(3):1738–1754
- Kanishka G, Eldho TI (2020) Streamflow estimation in ungauged basins using watershed classification and regionalization techniques. *J Earth Syst Sci* 129(1):1–18
- Kattelmann R (1987) Uncertainty in assessing Himalayan water resources. *Mountain Res Dev*, 279–286
- Kelman J (1980) A stochastic model for daily streamflow. *J Hydrol* 47(3–4):235–249
- Kour R, Patel N, Krishna AP (2016) Assessment of temporal dynamics of snow cover and its validation with hydro-meteorological data in parts of Chenab Basin, western Himalayas. *Sci China Earth Sci* 59(5):1081–1094
- Krause P (2002) Quantifying the impact of land use changes on the water balance of large catchments using the J2000 model. *Phys Chem Earth Parts a/b/c* 27(9–10):663–673
- Kulkarni A et al (2013) Projected climate change in the Hindu Kush–Himalayan region by using the high-resolution regional climate model PRECIS. *Mountain Res Dev* 33(2):142–151
- Lee M-H, Im E-S, Bae D-H (2019) Impact of the spatial variability of daily precipitation on hydrological projections: a comparison of GCM-and RCM-driven cases in the Han River basin, Korea. *Hydrol Process* 33(16):2240–2257
- Li H et al (2015) Integrating a glacier retreat model into a hydrological model—Case studies of three glacierised catchments in Norway and Himalayan region. *J Hydrol* 527:656–667
- Linsbauer A et al (2016) Modelling glacier-bed overdeepenings and possible future lakes for the glaciers in the Himalaya—Karakoram region. *Ann Glaciol* 57(71):119–130
- Liu Y et al (2021) Influence of elevation on bioregionalisation: A case study of the Sino-Himalayan flora. *J Biogeogr* 48(10):2578–2587

- Nepal S (2012) Evaluating upstream downstream linkages of Hydrological Dyn Himalayan Region Nepal S, Flügel W-A, Shrestha AB (2014a) Upstream-downstream linkages of hydrological processes in the Himalayan region. *Ecol Process* 3(1):1–16
- Nepal S et al (2014b) Understanding the hydrological system dynamics of a glaciated alpine catchment in the Himalayan region using the J2000 hydrological model. *Hydrol Process* 28(3):1329–1344
- Oudin L et al (2008) Spatial proximity, physical similarity, regression and ungauged catchments: A comparison of regionalization approaches based on 913 French catchments. *Water Resour Res* 44(3)
- Pellicciotti F et al (2012) Challenges and uncertainties in hydrological modeling of remote Hindu Kush–Karakoram–Himalayan (HKH) basins: suggestions for calibration strategies. *Mountain Res Dev* 32(1):39–50
- Racoviteanu AE, Armstrong R, Williams MW (2013) Evaluation of an ice ablation model to estimate the contribution of melting glacier ice to annual discharge in the Nepal Himalaya. *Water Resour Res* 49(9):5117–5133
- Rees HG et al (2004) Recession-based hydrological models for estimating low flows in ungauged catchments in the Himalayas. *Hydrol Earth Syst Sci* 8(5):891–902
- Risley JC (1994) Estimating the magnitude and frequency of low flows of streams in Massachusetts. Vol. 94. No. 4100. US Department of the Interior, US Geological Survey
- Samuel J, Coulibaly P, Metcalfe RA (2011) Estimation of continuous streamflow in Ontario ungauged basins: comparison of regionalization methods. *J Hydrol Eng* 16(5):447–459
- Schoppa L, Disse M, Bachmair S (2020) Evaluating the performance of random forest for large-scale flood discharge simulation. *J Hydrol* 590:125531
- Sharma KP, Vorosmarty CJ, Moore B (2000) Sensitivity of the Himalayan hydrology to land-use and climatic changes. *Clim Change* 47(1):117–139
- Shrestha S, Alfredsen K (2011) Application of HBV model in hydrological studies of Nepali river basins: a case study. *Hydro Nepal J Water Energy Environ* 8:38–43
- Shukla S, Jain SK, Kansal ML (2021) Hydrological modelling of a snow/glacier-fed western Himalayan basin to simulate the current and future streamflows under changing climate scenarios. *Sci Total Environ* 795:148871
- Sivapalan M et al (2003) IAHS Decade on Predictions in Ungauged Basins (PUB), 2003–2012: Shaping an exciting future for the hydrological sciences. *Hydrol Sci J* 48(6):857–880
- Srikanthan R, McMahon TA (2001) Stochastic generation of annual, monthly and daily climate data: a review. *Hydrol Earth Syst Sci* 5(4):653–670
- Tamang L, Chhetri A, Chhetri A (2020) Sustaining local water sources: the need for sustainable water management in the hill towns of the eastern Himalayas. *Water Management in South Asia*. Springer, Cham, pp 123–131
- Taylor KE, Stouffer RJ, Meehl GA (2012) An overview of CMIP5 and the experiment design. *Bull Am Meteor Soc* 93(4):485–498
- Thayyen RJ, Gergan JT (2010) Role of glaciers in watershed hydrology: a preliminary study of a "Himalayan catchment". *Cryosphere* 4(1):115–128
- Tripathi RS, Sah VK (2001) Material and energy flows in high-hill, mid-hill and valley farming systems of Garhwal Himalaya. *Agr Ecosyst Environ* 86(1):75–91
- Wagener T, Wheater HS (2006) Parameter estimation and regionalization for continuous rainfall-runoff models including uncertainty. *J Hydrol* 320(1–2):132–154
- Wang W et al (2018) Integrated hazard assessment of Cirenmaco glacial lake in Zhangzangbo valley, Central Himalayas. *Geomorphology* 306:292–305
- Wang Q, Wang S (2020) Machine learning-based water level prediction in Lake Erie. *Water* 12(10):2654
- Wilby RL, Hay LE, Leavesley GH (1999) A comparison of downscaled and raw GCM output: implications for climate change scenarios in the San Juan River basin, Colorado. *J Hydrol* 225(1–2):67–91

- Yadav M, Wagener T, Gupta H (2007) Regionalization of constraints on expected watershed response behavior for improved predictions in ungauged basins. *Advance water Res* 30(8):1756–74
- Yang X, Magnusson J, Rizzi J, Xu CY (2018) Runoff prediction in ungauged catchments in Norway: comparison of regionalization approaches. *Hydrol Res* 49(2):487–505
- Yatagai A et al (2012) PHRODITE: constructing a long-term daily gridded precipitation dataset for Asia based on a dense network of rain gauges. *Bull Amer Meteorol Soc* 93(9):1401–1415

Chapter 2

Development of a Semi-distributed Rainfall-Runoff Model for Water Budgeting in Macropore Dominated Hilly River Basins



Suman Kumar Padhee, Chandan Pradhan, Ketan Kumar Nandi, and Subashisa Dutta

Abstract Hillslope-stream-groundwater interactions has been identified as one of the major unsolved scientific problems in hydrology. Research studies to understand hillslope response processes involves time, effort, and resources. Therefore, hydrological models prefer to eliminate the minor details from hillslope responses in aggregation approach to watershed scale. Such approaches are unsuitable for regions where hillslope processes are dominant. But there are not many hydrological models to address hillslope concepts. This paper presents a process-based semi-distributed rainfall-runoff model (Hilly Watershed Hydrologic Model, HWHM) for hilly watersheds to address the aggregation of hillslope response to watershed scale for a Himalayan River Basin. The prime objective of HWHM is to support the water management in this region by modelling the runoff response and water storage. HWHM operates by dividing the river basin into small grids ($\approx 1\text{km}^2$), each grid representing a micro-watershed and assumed to be made up of several hillslopes. The emphasis of HWHM is to mimic the runoff generation in hillslopes in space and time which includes runoff from both surface and subsurface. The surface runoff partition and water balance are conceptualized by the influence of three-layer soil matrix (A-, B-, and C- layer) and vertical macropore distribution in subsurface system. The A-layer depth (root zone) and macropore distribution is characterized by MODIS land use/land cover product, deduced from several sample dye-tracer experiments. Model parameterization includes the response controlling variables for surface (threshold for surface runoff generation (T_{sur}), and gradient of runoff generation rate (S)), and sub-surface (bedrock topography factor (a), saturated hydraulic conductivity (K_{sat}), and aquifer thickness (D_p)). The variability of T_{sur} in space is determined in the range of ($T_{sur} \pm 25\%$) defined by vegetation fraction, whereas variability in time depends upon the antecedent moisture condition in A-layer. S is standardized between a lower and higher limit as per the antecedent moisture condition in top soil layer.

S. K. Padhee (✉)

International Water Management Institute, New Delhi, India

e-mail: suman.iirs@gmail.com

S. K. Padhee · C. Pradhan · K. K. Nandi · S. Dutta

Department of Civil Engineering, Indian Institute of Technology Guwahati, Guwahati, India

The combined volumetric variability in A-layer depth and macropore distribution influence variable surface runoff generation. The subsurface is assumed to contain aquifer above bedrock with a maximum limit of aquifer thickness D_p and its ability to contribute as baseflow defined by K_{sat} . However, due to assumed dominance of preferential pathways, a high order factor of 10^a is multiplied with K_{sat} , where a is a standardized value between a range according to antecedent moisture condition of B-layer between its field capacity and wilting point. The standardization schemes for S and a helps to address the variation of runoff response in wet and dry seasons in surface and sub-surface respectively. With the help of satellite-based hydrometeorological inputs (CHIRPS precipitation, and FLDAS evapotranspiration) and modelled land surface variables (field capacity, wilting point, and K_{sat} from SOILGRIDS), HWHM is used to parameterize the spatio-temporal response of micro-watersheds, by calibration with the observed daily flow volume at the outlet. The controlling variables were simulated in combinations within stipulated ranges to find the best values ($T_{sur} = 1 \pm 0.25$ cm; $S = 0.7-0.1$; $K_{sat} \approx 10^5-10^{10}$ times original K_{sat} ; and $D_p \leq 1$ m) in calibration. Simulations from 2001–2007 produced a decent result of ($RMSE = 60$ MCM and $R^2 = 0.72$). The value of resulting K_{sat} was found to be of several times higher order than original K_{sat} (10^5-10^{10} times). This confirmed major domination of preferential pathways in runoff generation process at watershed scale. HWHM could be used for studies to further understand the influence of hillslope processes on water budget components at large scale watersheds with macropore dominated hilly regions.

Keywords Hillslope · Macropores · Semi-distributed model · Water balance

2.1 Introduction

It is presumed in distributed hydrological modelling that hydrological responses of small catchment units accumulate together to reflect the total surface runoff in water budget of large-scale basins. Therefore, integration of hydrological processes due to catchment responses is a common exercise in large-scale hydrological modelling. These catchment units involve several mechanisms for runoff generation including Hortonian flow (Horton 1932), saturation excess runoff (Hewlett and Hibbert 1967; Freeze 1972; Dunne et al. 1975), return flow (Dunne and Black 1970), and macropore flow (Beven and Germann 1982). Addressing these flow mechanisms through hydrological modelling is important for water resource management in various regions.

The hilly watersheds in humid tropical or sub-tropical regions are dominated by hillslope process where a threshold-based runoff generation is often seen (Williams et al. 2002; Das et al. 2014). Several research works have concluded the presence of macropores as the primary reason for occurrence of this threshold behaviour in surface runoff generation (Torres et al. 1998; Shougrakpam et al. 2010; Sharma et al. 2013; Sarkar et al. 2015). It is also evident from many research outcomes that

the bedrock topography linked through macropores in soil–bedrock interface, is an important factor in hillslopes (Dusek and Vogel 2016) and have controls on outflow variability in dry and wet seasons (Graham et al. 2010; Janzena and McDonnell 2015). Therefore, macropores are crucial representative in these two aspects of complexity in hillslope hydrology (runoff threshold and seasonal variability in outflow from a hilly watershed).

The Macropores are large pores in soil, usually greater than 0.08 mm in diameter which allow free movement of air and water by gravity (Chouksey et al. 2017). There are basically two types of macropores, main bypass (MB) (Hoogmoed and Bouma 1980) which is continuously interconnected with increase in depth and internal catchment (IC) (Bouma and Dekker 1978; Van Stiphout et al. 1987) which is not connected. Presence of macropore network triggers the preferential flow characteristics as the first draw from precipitation (Tromp-van Meerveld and McDonnell 2005; Graham et al. 2010; Penna et al. 2011) thereby delaying the surface runoff generation. It determines the fraction of precipitation that bypasses the root zone and directly contributes to subsurface flow (Menichino et al. 2014). Preferential flow drawn from rainfall due to presence of macropores is considered as the primary dominant control on runoff generation at hillslope scale. The variation of macropore distribution is often associated with different land covers due to which its impact on runoff generation is studied (Niehoff et al. 2002; Bachmair et al. 2009; Das et al. 2014; Mayerhofer et al. 2017). The presence of macropores changes the dynamics of runoff generation in contrast to the concepts of current hydrological models.

Majority of hydrological models for large-scale simulations have ignored the hydrological processes caused by macropore flow (Beven and Germann 2013) and it can eventually mislead the physical state of water storage. The process complexities due to macropores are generally not encountered in hydrological modelling by parameterization, but it is captured through the response functions with other numerically calibrated parameters. The exclusion of macropore flow could be due to the complexity in flow process itself (Weiler 2017) and considered as one of the major unsolved scientific problems in hydrological sciences (Blöschl et al. 2019). Further, there is no provision to integrate macropore flow within the schemes of popular hydrological models. Hence, a new semi-distributed rainfall-runoff model called Hilly Watershed Hydrologic Model (HWHM) has been developed for water balance in tropical hilly river basins which have soils dominated by macropores. This model is developed based on the evidences and data provided in several hillslope experiments which were conducted to address macropore flow. The grid responses were integrated to upscale the water budget at river basin scale. Since Himalayan watersheds are well-known for presence of soil macropores, the Subansiri River Basin from Eastern Himalayan region was selected as a pilot study area for testing and implementation of the HWHM.

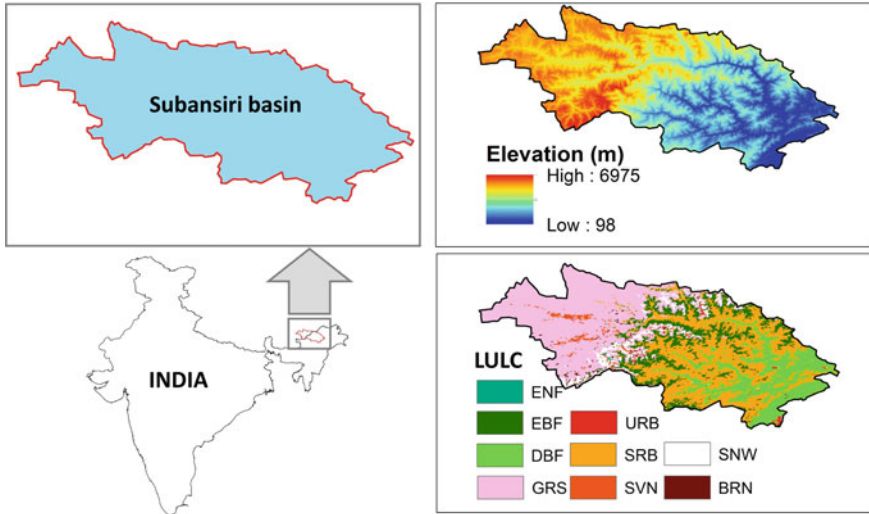


Fig. 2.1 Geographical Location of Subansiri river basin (*Note* Landuse in Subansiri basin: ENF-evergreen needleleaf forest, EBF-evergreen broadleaf forest, DBF-deciduous broadleaf forest, GRS-grassland, URB-urban area, SRB-shrubland, SVN-savanna, SNW-snow, BRN-barren land)

2.2 Materials and Methods

2.2.1 Study Area

The Subansiri River is a trans-Himalayan perennial river, which is situated in Eastern Himalayan Mountain ranges. It originates from the Tibetan Plateau in the western part of Mount Porom at an elevation of 5340 m. After traveling through the Himalayan range of Arunachal Pradesh, it enters the plain land and joins Brahmaputra River in Gerukamukh, Assam. The geographical extent of Subansiri river basin extends between latitude (26.90°N to 28.92°N) and longitude (91.55°E to 95.07°E). The total length of Subansiri River is about 442 km and its basin area is about 32,640 km², collectively in China and India. It is the largest tributary of Brahmaputra River (Shivam et al. 2017) and contributes around 12% of the annual flow of the Brahmaputra River. The geographical location, elevation and landuse maps of the study area are given in Fig. 2.1.

2.2.2 Methodology

a. Model concept

The HWHM is developed from process-based observations in a semi-distributed approach. A graphical abstract of the model is given in Fig. 2.2. It shows that the

model has three categorical inputs viz. daily initial conditions, daily forcing data and water balance parameters. The daily initial condition parameters are the various storage variables which define the antecedent condition of storages. Daily forcing files consists of daily incoming and outgoing water flux, i.e. precipitation (P) and evapotranspiration (ET), respectively, and leaf area index (LAI) for calculation of interception loss. The water balance parameters are storage restricting constants dependent upon soil texture (field capacity (θ_{FC}) and wilting point (θ_{WP})), and macropore volumes of IC and MB domains (V_{ic} and V_{mb}). Apart from these parameters, another set of parameters are user-defined which are calibrated from the observed data. These parameters are threshold (T_{sur}) and slope (S) values used in surface runoff generation and saturated hydraulic conductivity (K_{sat}) which control the daily base flow from sub-surface. The sources of various data used in HWHM are presented in Table 2.1.

The basic spatial and temporal resolutions for HWHM is user-defined. In the present study these two parameters are set as 1 km and daily scale, respectively. It is assumed that each 1 km grid at this scale represents a micro-watershed with inherent properties. These properties were defined as the volumetric capacity for storage according to the heterogeneity of LULC and soil texture in sub-surface characterization.

Fig. 2.2 Representation of a micro-watershed by a grid in HWHM

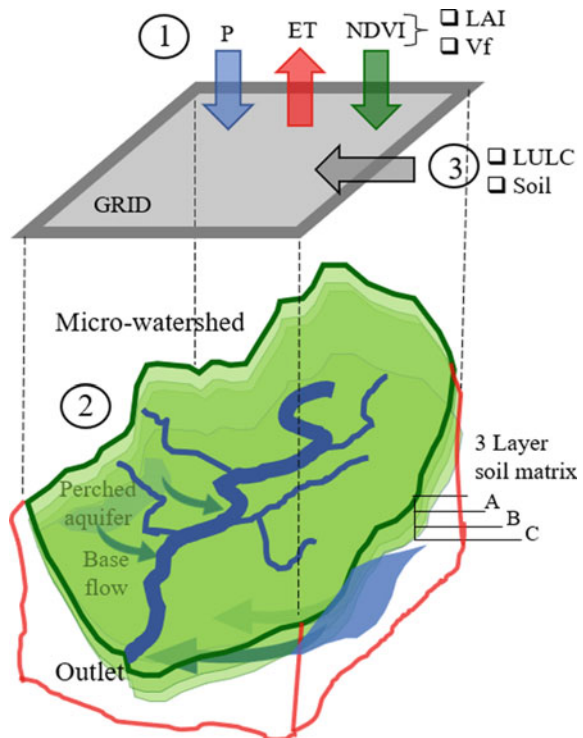


Table 2.1 Data used for HWHM setup and simulation

Variable name	Data used	Source
• Digital elevation model	• SRTM DEM	• https://dwtkns.com/srtm30m/
• Soil texture, field capacity, wilting point	• Soilgrids	• https://data.isric.org/geonet/work/srv/eng/catalog.search#/home/
• Land use & land cover	• MODIS	• https://lpdaac.usgs.gov/
• Precipitation	• CHIRPS (global daily)	• https://data.chc.ucsb.edu/products/CHIRPS-2.0/
• Evapotranspiration	• FLDAS Noah (global daily)	• https://disc.gsfc.nasa.gov/
• Leaf area index	• MODIS	• Interpolation of NDVI time-series by Padhee et al. (2019), and derivation of NDVI to LAI by Walthall et al. (2004)
• Saturated hydraulic conductivity	• Saturated hydraulic conductivity data for soilgrids (Dai et al. 2019)	• http://globalchange.bnu.edu.cn/research/soil5.jsp

b. *Sub-surface characterization*

The HWHM is based on the of concepts of SWAP model (Kroes and Dam, 2003; van Dam et al. 2008), which is used for solute transport modelling through macropores, and water balance with fill and spill approach (Graham and McDonnell 2010). Considering the importance of soil surface interaction with atmospheric processes, the HWHM focuses on the top horizon where a three-layer system is considered (A-, B- and C-horizon). The A-horizon is the root zone depth of various LULC, and it is taken from Das et al. (2014) (Table 2.2). The B- and C-horizons were considered to standard depth of 50 cm and 150 cm from the top of the ground surface.

The macropore volumetric proportions of the two domains, main bypass (V_{mb}) and internal catchments (V_{ic}) are calculated over each grid. The computation of macropore volumetric proportions is governed by three properties, viz. continuity, persistency, and horizontal distribution and its detailed description could be found in the ‘Alterra Report 1649—Swap32’ (Kroes and Dam 2003). Macropore geometry parameters changes with soil depth which is the basic indicator for macropore activeness. These parameters are determined by dye tracer experiments on vertical soil columns in field followed by analysis of the soil columns. The findings from a series of dye tracer field experiments conducted in several sites of Eastern Himalayan region (Das et al. 2014) are used in this study (Table 2.2).

Continuity: The continuity parameters of the model can be calculated from Eqs. 2.1 to 2.4 as given below:

$$P_{mb} = 1 - P_{ic} \quad (2.1)$$

Table 2.2 Macropore geometry parameters for various land use and land cover modified from Das et al. (2014). (Note LULC are coded as WTR-water, ENF-evergreen needleleaf forest, EBF-evergreen broadleaf forest, MXF-mixed forest, CRP-cropland, URB-urban area, VEG-natural vegetation, SNW-snow, SRB-shrubland, SVN-savanna, GRS-grassland, WTL-wetland; the modifications are in accordance with IGPB LULC classes in MODIS product)

Parameter	Description	LULC						
		ENF	EBF	MXF	SVN	SRB/VEG	CRP	GRS
• AH (cm)	• Bottom of A Horizon	-10	-4	-10	-4	-4	-2	-20
• Z_{ic} (cm)	• Bottom of IC domain	-30	-14	-30	-13	-13	-20	-30
• R_{ZAH}	• Cumulative frequency distribution at Bottom of A-Horizon	0.99	0.89	0.96	0.76	0.67	0.73	0.78
• M	• Shape factor	1.52	0.8	1.52	0.97	0.93	1.12	1.19
• V_{sr0} (cm ³ /cm ³)	• Static macropore volume fraction at the topsoil surface	0.06	0.06	0.09	0.04	0.06	0.03	0.06
• P_{ic} (cm ³ /cm ³)	• Volumetric proportion of IC domain	0.83	0.82	0.87	0.84	0.85	0.71	0.05
• d_{pmax}	• Maximum polygon diameter	32.07	32.32	35.95	33.2	34.04	17.59	32.39
• d_{pmin}	• Minimum polygon diameter	12.11	12.56	10.65	11.81	11.59	15.86	12.03

$$R = \begin{cases} R_{Zah} \left(\frac{Z}{Z_{Ah}} \right), & \text{for } 0 \geq Z \geq Z_{Ah} \\ R_{Zah} + (1 - R_{Zah}) \left[\left\{ \frac{Z_{Ah} - Z}{Z_{Ah} - Z_{ic}} \right\}^m \right], & \text{for } Z_{Ah} \geq Z \geq Z_{ic} \end{cases} \quad (2.2)$$

$$F = 1 - R \quad (2.3)$$

$$P_{ic} = \begin{cases} \left[\frac{F}{\left(\frac{1}{P_{ic0}} \right) + F - 1} \right], & \text{for } (0 \geq Z \geq Z_{ic}) \text{ and } (0 \leq P_{ic0} \leq 1) \\ 0, & \text{for } (Z \leq Z_{ic}) \text{ and/or for } (P_{ic0} = 0) \end{cases} \quad (2.4)$$

Here, the depths Z , Z_{Ah} and Z_{ic} are active depth, depth of A-horizon and depth of active IC domain, respectively. The value of m governs the distribution of IC

macropores with depth where ($m < 1$), ($m > 1$), and ($m = 1$) represents shallow, deep, and intermediate IC system. R_{Zah} is a parameter which describes increase of the volumetric distribution curve (R) over the layer thickness of the A-horizon. The curve (F) represents the fraction of IC macropores (Eq. 2.2) that is functional at a depth Z , and it is the complement of R curve. The volumetric proportion of IC macropore volume as a function of depth can be written in terms of the constant P_{ic0} and the function F as shown in Eq. 2.4. P_{ic0} represents volumetric proportion of IC at soil surface (cm^3/cm^3). The volumetric proportion of MB macropores as a function of depth is calculated from P_{ic} (Eq. 2.1).

Persistence: The total volume of macropores is defined by static and dynamic natures of macropores. Total macropores volume is ideally dynamic with time which is mainly reflected by dynamic macropores. However, due to large-scale hydrological modelling approach, the dynamic macropores are ignored in the development of HWHM. Therefore, the static macropore volume, which is also the permanent volumes of MB and IC macropores calculated in units (cm^3/cm^3), is equal to total macropore volume (V_{mp}). The parameter V_{mp} is a function of depth and it is constant with time. The parameter can be calculated from Eqs. 2.5 to 2.7

$$V_{mb} = \begin{cases} V_{stmb0}, & \text{for } 0 \geq Z \geq Z_{ic} \\ V_{stmb0} \left[\frac{Z - Z_{st}}{Z_{ic} - Z_{st}} \right], & \text{for } 0 \geq Z \geq Z_{st} \\ 0, & \text{for } Z \leq Z_{st} \end{cases} \quad (2.5)$$

$$V_{ic} = \begin{cases} V_{stic0}, & \text{for } 0 \geq Z \geq Z_{ic} \\ 0, & \text{for } Z \leq Z_{ic} \end{cases} \quad (2.6)$$

$$V_{mp} = V_{mb} + V_{ic} \quad (2.7)$$

Here, V_{mb} is volume fraction of MB flow domain, V_{ic} is volume fraction of IC domain, V_{stmb0} is static macropore volume fraction of MB flow domain at top, V_{stic0} is static macropore volume fraction of IC domain at top, V_{mp} is total macropore volume fraction. When these are accumulated from top of surface (depth = 0) to depth of static macropores (Z_{st}), the total volume fractions are obtained from Eq. 2.7.

Horizontal distribution: In the horizontal plane the distribution of macropore determines the functional horizontal shape of the macropores, which forms the basis of the calculation of several important parameters. It is determined by effective matrix polygon diameter (d_{pol}) as:

$$d_{pol} = \begin{cases} d_{pmax}, & \text{for } (V_{st} = 0), \text{ and } (P_{ic0} > 0) \\ d_{pmin} + \left(\frac{d_{pmax} - d_{pmin}}{1 - M} \right), & \text{otherwise} \end{cases} \quad (2.8)$$

$$M = \begin{cases} (V_{mp}/V_{st0}), & \text{for } V_{st0} > 0 \\ (P_{ic}/P_{ic0}), & \text{for } V_{st0} = 0, \text{ and } P_{ic0} > 0 \\ 1 - (Z/Z_{dpmax}), & \text{for } 1 - \left(\frac{Z}{Z_{dpmax}}\right) > 0 \\ 0, & \text{otherwise} \end{cases} \quad (2.9)$$

Here, M is relative macropore density, d_{pmin} is minimum polygon diameter, d_{pmax} is maximum polygon diameter, and Z_{dpmax} is depth of effective maximum polygon diameter.

The volume of soil matrix is limited between field capacity (θ_{FC}) and wilting point (θ_{WP}) multiplied by the depths of corresponding horizons as acquired. The water balance schemes (water gain and loss) in the soil matrix were carried out from top to bottom in order. The bedrock is considered beyond C-horizon where the storage is assumed to be held as a perched aquifer, which do not overlap with C-horizon. The thickness of this virtual aquifer could be variable, but it is assumed to reach a maximum value of 1 m thickness due to limitation of sub-surface specific data.

iii. *Water flow and storage*

The water flow and volumetric storage (gain and loss) in HWHM is formulated by fill and spill approach (also known as source and sink) from top to bottom order. Incoming water from precipitation (P) reaches to the soil surface after an interception loss due to vegetation canopy as shown in Eq. 2.10. The surface runoff response in a grid is developed based on the observations from several hillslope experiment studies. Plot scale hillslope experiments have shown that the presence of active macropores often makes infiltration to be the dominating hydrological process (Graham and McDonnell 2010; Sarkar and Dutta 2015). Hence, initial surface runoff response occurs after infiltration of water into different sub-surface domains (i.e. soil matrix, IC and MB macropores). The generation of surface runoff (R_{sur}) changes with seasonal variations (dry and wet seasons) (Das et al. 2014). To replicate the seasonal surface runoff response, slope (S), which is gradient in rainfall-runoff relationships, is assumed to vary from 0.1 (dry soil condition) to 0.7 (wet soil condition). The upper and lower limit values of S are selected from the study of Sarkar et al. (2015), where S is determined as a standardized value according to variation of antecedent moisture conditions of A-horizon ($\theta_{A,WP}$ to $\theta_{A,FC}$) as shown in Eq. 2.12. Remaining water is divided according to proportion of antecedent volumetric capacity of sub-surface domains. The proportion of water through MB macropores is directly added to storage in perched aquifer thickness with a maximum limit ($D_p \leq 1$ m), and any exceedance is considered as deep percolation. Brutsaert (2005) have presented a linearized form of Boussinesq equation especially for aquifers in hillslope. Later, D_p is used to calculate base flow (R_{bf}) from perched aquifer (Eq. 2.14) (Brutsaert 2005) and added with R_{sur} to get total runoff (R_{grid}) from a grid. The entire water balance process is summarized in Eqs. 2.10 to 2.14.

$$P_{sur} = P - (C \times LAI) \quad (2.10)$$

$$R_{grid} = R_{sur} + R_{bf} \quad (2.11)$$

$$R_{sur} = (S \times P_{sur}) - A(\theta_A - \theta_{A,FC}) + T_{sur} \quad (2.12)$$

$$S = \left[\frac{(\theta_A - \theta_{A,FC})}{(\theta_{A,FC} - \theta_{A,WP})} (S_{wet} - S_{dry}) \right] + S_{dry} \quad (2.13)$$

$$R_{bf} = \left[\frac{8(K_{sat} 10^a) p D_p^2 L^2}{Ar} \right] \times \exp \left[\frac{-\pi^2 (K_{sat} 10^a) p D_p L^2 t}{n_e Ar^2} \right] \quad (2.14)$$

Here, P and P_{sur} are the rainfall falling and reaching the ground surface, respectively; C is coefficient of interception (0.05–0.2 mm) linearly varying between lowest (Aston 1979) and highest (Toba and Ohta 2005) vegetation fraction; LAI is leaf area index computed from NDVI (Walthall et al. 2004); R_{grid} , R_{sur} and R_{bf} represents the total runoff in the grid, runoff originating from surface and base flow, respectively; T_{sur} is the surface runoff generation threshold (a calibrated parameter); S is the variable slope determined from antecedent moisture condition in A-horizon (θ_A) between the corresponding wilting point ($\theta_{A,WP}$) and field capacity ($\theta_{A,FC}$); K_{sat} is the saturated hydraulic conductivity of perched aquifer; a is a calibrated parameter called bedrock topography factor; p is constant adjustment parameter (0.3465) (Brutsaert 2005); D_p is the depth of perched aquifer; L is the length of all tributaries; Ar is the grid area (micro-watershed area); n_e is effective porosity (0.35–0.4) (Brutsaert 2005); and t is time. Additionally, snow covered grids are also considered where the runoff was calculated as snowmelt by using degree day algorithm (Martinec et al. 2008). The computation requires daily precipitation, maximum and minimum temperature data as inputs (Table 2.1), and the critical temperature is assumed at 1 °C for the study area (Singh et al. 2021).

iv. Calibration and validation scheme

The study area is a transboundary river basin, and the gauged observations of outflow discharge are labelled as classified records due to which direct calibration and validation is not possible. Rather, with modified data dissemination authorisation, monthly flow volume (May 2004–April 2005) is obtained from Central Water Commission, India (CWC). Additionally, daily flow volume from 2001 to 2007 was also obtained. These data were used to build the approach of calibration and validation used for HWHM.

The calibration is focused on the adjustment of overall runoff response with best possible Nash–Sutcliffe model efficiency coefficient (NSE) (Eq. 2.15) against monthly flow volume in 2004–2005. However, as the objective of HWHM is water balance, it is important to evaluate overall error in storage. Therefore, the root mean square error ($RMSE$) is taken as an appropriate indicator (Eq. 2.16).

$$NSE = \sum \frac{(Q_{obs} - Q_{mod})^2}{(Q_{obs} - Q_{mean})^2} \quad (2.15)$$

$$RMSE = \sqrt{\frac{\sum (Q_{obs} - Q_{mod})^2}{N}} \quad (2.16)$$

The HWHM provides the privilege to calibrate T_{sur} and a to describe seasonal changes (dry and wet soil) in surface runoff response and bedrock topography factor, respectively. The calibrated parameters are used to simulate HWHM for the river basin (year 2001–2007). The validation includes interpretation via comparison of monthly flow volume ranges (2001–2007) with observed flow volume during the specified period.

2.3 Results and Discussions

The initial infiltration concept used in HWHM are driven from the observations from experiments by Sarkar et al. (2015) at 20% surface slope hourly/sub-hourly scale of rainfall and runoff intensity. However, the aim of HWHM is to simulate water balance at/beyond daily scale. Conferring to data availability, the daily scale model needs a different generalization approach. Chen and Young (2006) concluded that the effect of surface slope on infiltration rate is applicable to a small time and this effect vanishes at prolonged time thereby making gravity as the dominant control mechanism. This concept is considered where effect of slope is negligible at large time scale. Also, there are evidences of variable infiltration capacities depending on vegetation density (Sarkar et al. 2015; Fatichi et al. 2016; Chouksey et al. 2017). However, no proper relationship has been developed ever by any study due to which this study generalized the spatial variation of rainfall-runoff partitioning scheme with $\pm 25\%$ variation of T_{sur} standardized between maximum and minimum values of vegetation fraction. This choice is completely under the control of user and dependent on the regional runoff response behaviour.

a. Calibration of HWHM

The calibration is carried out with combinations of the variables, T_{sur} (1 cm, 2.5 cm, 5 cm, 7.5 cm, and 10 cm), and a (0–10, with an interval of 2). These values are used together to observe the resulting NSE for monthly flow volumes during June 2004–May 2005. The simulated values for these combinations used for calibration are shown in Table 2.3. The optimum value for T_{sur} of 1 cm $\pm 25\%$ produces highest NSE value of 0.28. As the parameter T_{sur} is a linear influencer of surface runoff response (Eq. 2.12), it justifies the delay in surface runoff occurrence due to macropore dominance and antecedent soil conditions in initial partitioning of water (McGrath et al. 2007). Moreover, the high and low rates of surface runoff response in wet and dry seasons are justified by variable S (0.7–0.1), which uses top layer soil moisture content as an indicator of this rate (Sarkar and Dutta 2012).

Table 2.3 *NSE* values for various simulations used in calibration

T_{sur} (cm)	10^a factor multiplied to K_{sat}					
	10^0	10^2	10^4	10^6	10^8	10^{10}
1.00	0.19	0.19	0.19	0.28	0.21	-1.16
2.50	0.01	0.01	0.01	0.20	0.04	-0.91
5.00	0.00	0.00	0.01	0.19	0.04	-0.92
7.50	0.00	0.00	0.01	0.19	0.04	-0.92
10.00	0.00	0.00	0.01	0.20	0.04	-0.93

The results of HWHM simulations for the years 2001–2007 with the respective medians derived for comparison are shown in Fig. 2.3. Comparison through this approach (eg. medians, percentiles, flow duration curves, probability of exceedance, etc.) enables one to evaluate model performance under stationary assumptions, when observation time periods for discharge and model input data do not overlap (Westerberg et al. 2011). A fixed value of $a = 6$, as per the calibration, is used where generally dry seasons are seen to produce overestimated flow volume. In contrast, wet seasons produce underestimations when compared to the observed series (overall $RMSE = 161$ MCM). On the other hand, using variable a from (0–10) is seen to produce values nearer to the observed series with less error ($RMSE = 60$ MCM). Although, these values are found sensitive, the increase and decrease in flow volumes of variable a (0–10) series and observed series shows that variable K_{sat} is the key parameter for a right approach to address the flow complexity in hilly watersheds. However, it requires a separate study in tuning of water balance by analysis of parameter sensitivities, especially K_{sat} .

b. *Simulation and water balance in HWHM*

The scatter plot between observed and simulated daily flow volumes are shown in Fig. 2.4. Except certain extreme events, HWHM is able to simulate the daily flow volume with positive ($NSE = 0.23$) and good coefficient of determination ($R^2 = 0.72$). Interestingly, it is observed that even with one year of model calibration period, satisfactory results are produced from HWHM simulations. It demonstrates the strength of conceptualization from physically-based models in regions with dominant hillslope hydrological processes. Several earlier research experiments displayed that the events of surface runoff generation is rare in hillslopes (Graham and McDonnell 2010; Sarkar et al. 2015; Chouksey et al. 2017). The outcomes of water balance model were analysed for the number of surface runoff events. Figure 2.5 shows the percentage of surface runoff generation out of all rainfall events between 2001–2007 in Subansiri watershed. It is found that highest surface runoff generation ratio is at the snow-covered areas and near the outlet of the watershed where lowland starts. There is high distrust in these results as the scope of this work was very limited to snowmelt runoff estimation. Interestingly, forest and grassland regions show this proportion ranging between 0–5%. Most of the study area is covered with grassland in the upper regions and forest in the lower regions of the watershed. The forests are

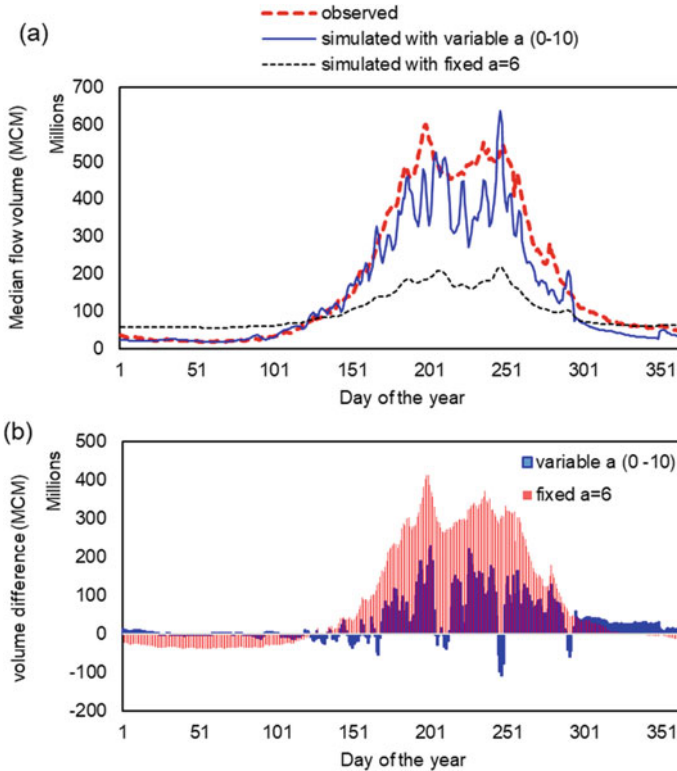


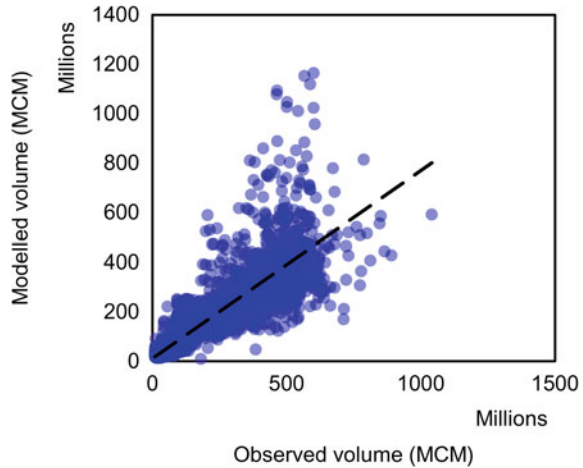
Fig. 2.3 **a** Daily median flow volume (2001–2007) derived from observed data, simulated from variable ($a = 0-10$) series, and fixed ($a = 6$) series. **b** Daily difference error in medians of observed and variable ($a = 0-10$) series, and observed and fixed ($a = 6$) series

known to have high density of soil macropore networks, due to which larger preferential contribution in outflow is possible. The results presented are in agreement with these findings as high average base flow runoff and low surface runoff generation ratio is observed.

2.4 Conclusion

The evidence of threshold-based runoff generation process in the hillslopes of humid tropical or sub-tropical regions is contrasting with most of the concepts used in hydrological models. Research studies have stated the reason for occurrence of this threshold is due to presence of macropores and bedrock storage which are mostly neglected in large scale hydrological modelling. It makes majority of the hydrological models unsuitable for hilly watersheds which have dominance of hillslope

Fig. 2.4 Scatter plot for observed and modelled daily flow volumes in Subansiri river basin (2001–2007)



processes. Therefore, considering Subansiri river basin as a pilot case, a process-based semi-distributed model called Hilly Watershed Hydrologic Model (HWHM) was developed by incorporating the findings from previous experiments and analyses. The model used daily ET and P as forcing data and it was calibrated with monthly flow volume observation records. During calibration process, it was revealed that HWHM simulates the flow with highest *NSE* value of 0.28 at $1 \text{ cm} \pm 25\%$ variation of threshold but at a much higher order of saturated hydraulic conductivity than expected. It might be due to the presence of a highly active preferential flow network. However, through model simulations with calibrated values for the years 2001–2007, it was evident that even a higher fixed hydraulic conductivity could not produce approximate water balance results. Therefore, an approach was taken to implement an active hydraulic conductivity according to antecedent subsurface saturation. This approach addressed the variability of flow contribution from bedrock storage with a variable bedrock topography factor (*a*). Though this perception might not be very accurate, but it was able to produce water balance results with good relevance. Hillslopes around the world with dominant soil macropores represent high complexity and a single case study is far from being conclusive. However, the present work demonstrated an approach to account for such complexities at large scale by developing a model (HWHM) to address the following issues: (a) rainfall-runoff partition by concentrating on delay in surface runoff and variation in seasonal runoff generation rate; (b) integration of subsurface macropore distribution in a model for water storage and flow partitioning; and (c) variation in subsurface flow due to variation in preferential paths in bedrock storage. It is important to integrate these hillslope concepts in large-scale hydrological modelling. The HWHM with $R^2 = 0.72$ against simulation from 2001–2007, can be considered as a reasonable model for water balance applications in humid tropical or sub-tropical hilly watersheds of India. The model can be checked for its applicability in other regions based on macropore geometry characterization through detailed experimental observations. The HWHM

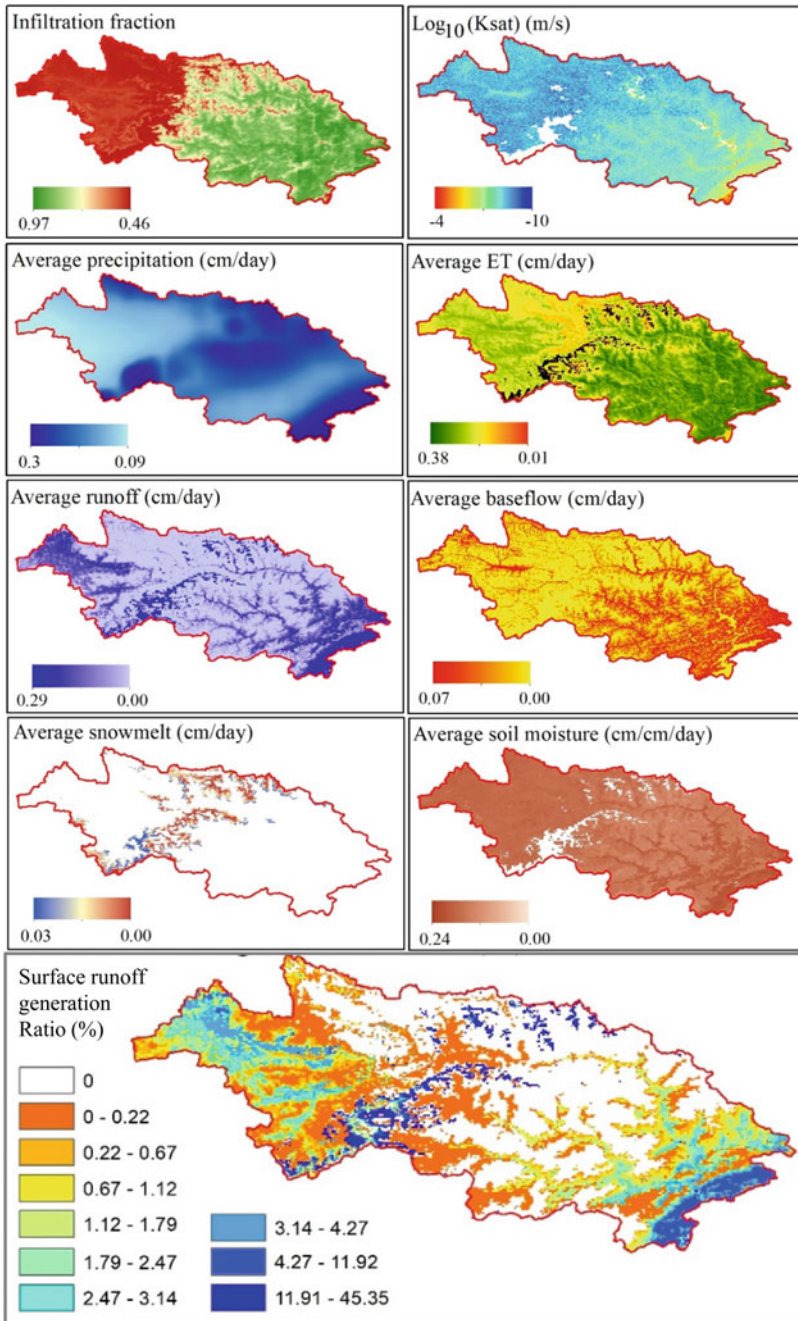


Fig. 2.5 Input and output of water balance simulation from 2001–2007 in Subansiri watershed

is seen to have highly sensitive runoff response due to which it is suggested for applications having large time interval (e.g. water budgeting) rather than small-time bound applications (e.g. flash floods, forecasting, etc.). Being a grid based hydrological model, HWHM is always open to integrate with experimental methods. The requirement for research to address hillslope water flow complexity is still at large and models like HWHM could provide a way forward in future research.

Acknowledgements Authors' sincere appreciation is extended to IIT Guwahati for providing computational facilities and SAC ISRO for funding. We are also obligated to data source authorities including USAID, NASA, NOAA, and SOILGRIDS for providing free access to geospatial data. Authors also acknowledge the editor and anonymous reviewers for their inputs.

Disclosure statement Authors declare no conflict of interest.

References

- Aston AR (1979) Rainfall interception by eight small trees. *J Hydrol* 42(3–4):383–396. [https://doi.org/10.1016/0022-1694\(79\)90057-X](https://doi.org/10.1016/0022-1694(79)90057-X)
- Bachmair S, Weiler M, Nützmann G (2009) Controls of land use and soil structure on water movement: Lessons for pollutant transfer through the unsaturated zone. *J Hydrol* 369:241–252. <https://doi.org/10.1016/J.JHYDROL.2009.02.031>
- Beven KJ, Germann PF (2013) Macropores and water flow in soils revisited. *Water Resour Res* 49:3071–3092. <https://doi.org/10.1002/wrcr.20156>
- Beven KJ, Germann PF (1982) Macropores and water flow in soils. *Water Resour Res* 18(5):1311–1325. <https://doi.org/10.1029/WR018i005p01311>
- Blöschl G, Bierkens MFP, Chambel A et al (2019) Twenty-three Unsolved Problems in Hydrology (UPH)—a community perspective. *Hydrol Sci J* 62(10):1141–1158. <https://doi.org/10.1080/02626667.2019.1620507>
- Bouma J, Dekker LW (1978) A case study on infiltration into dry clay soil I. Morphological observations. *Geoderma* 20:27–40. [https://doi.org/10.1016/0016-7061\(78\)90047-2](https://doi.org/10.1016/0016-7061(78)90047-2)
- Brutsaert W (2005) *Hydrology: an introduction*. Cambridge University Press, Cambridge, p 423
- Chen L, Young MH (2006) Green-Ampt infiltration model for sloping surfaces. *Water Resour Res* 42:1–9. <https://doi.org/10.1029/2005WR004468>
- Chouksey A, Lambey V, Nikam BR, Aggarwal SP, Dutta S (2017) Hydrological modelling using a rainfall simulator over an experimental hillslope plot. *Hydrology* 4(1):17. <https://doi.org/10.3390/hydrology4010017>
- Dai Y, Xin Q, Wei N, Zhang Y, Shangguan W, Yuan H, Zhang A, Liu S, Lu X (2019) A global high-resolution dataset of soil hydraulic and thermal properties for land surface modeling. *J Adv Model Earth Syst* 11(9):2996–3023. <https://doi.org/10.1029/2019MS001784>
- Das P, Islam A, Dutta S, Dubey AK, Sarkar R (2014) Estimation of runoff curve numbers using a physically-based approach of preferential flow modelling. *International association of hydrological sciences (IAHS) Publication*, vol 363, pp 443–448
- Dunne T, Black RD (1970) Partial area contributions to storm runoff in a small New England watershed. *Water Resour Res* 6(5):1296–1311
- Dunne T, Moore TR, Taylor CH (1975) Recognition and prediction of runoff-producing zones in humid regions. *Hydrol Sci Bull* 20:305–327
- Dusek J, Vogel T (2016) Hillslope-storage and rainfall-amount thresholds as controls of preferential stormflow. *J Hydrol* 534:590–605. <https://doi.org/10.1016/J.JHYDROL.2016.01.047>

- Fatichi S, Vivoni ER, Ogden FL, Ivanov VY, Mirus B, Gochis D, Downer CW, Camporese M, Davison JH, Ebel B, Jones N, Kim J, Mascaro G, Niswonger R, Restrepo P, Rigon R, Shen C, Sulis M, Tarboton D (2016) An overview of current applications, challenges, and future trends in distributed process-based models in hydrology. *J Hydrol* 537:45–60. <https://doi.org/10.1016/J.JHYDROL.2016.03.026>
- Freeze RA (1972) Role of subsurface flow in generating surface runoff: 2. Upstream source areas. *Water Resources Res* 8(5):1272–1283. <https://doi.org/10.1029/WR008I005P01272>
- Graham CB, McDonnell JJ (2010) Hillslope threshold response to rainfall: (2) Development and use of a macroscale model. *J Hydrol* 393:77–93. <https://doi.org/10.1016/j.jhydrol.2010.03.008>
- Graham CB, Woods RA, McDonnell JJ (2010) Hillslope threshold response to rainfall: (1) A field based forensic approach. *J Hydrol* 393:65–76. <https://doi.org/10.1016/J.JHYDROL.2009.12.015>
- Hewlett JD, Hibbert AR (1967) Factors affecting the response of small watersheds to precipitation in humid areas. *Forest Hydrology* 275–290:1967
- Hoogmoed WB, Bouma J (1980) A simulation model for predicting infiltration into cracked clay soil. *Soil Sci Soc Am J* 44:458–461. <https://doi.org/10.2136/sssaj1980.03615995004400030003x>
- Horton RE (1932) Drainage basin characteristics. *Trans Amer Geophys Union* 13:348–352
- Janzen D, McDonnell JJ (2015) A stochastic approach to modelling and understanding hillslope runoff connectivity dynamics. *Ecol Model* 298:64–74. <https://doi.org/10.1016/J.ECOLMODEL.2014.06.024>
- Kroes JG, van Dam JC (2003) Alterra-report 773 1 Reference Manual SWAP version 3.0.3. <https://edepot.wur.nl/35471>
- Martinez J, Rango A, Roberts R (2008) WinSRM 1.11—snowmelt runoffmodel user’s manual. ABD, Editörler: Gomez-Landesa E. ve Bleiweiss, PM, New Mexico State University, Las Cruces, New Mexico, USA
- Mayerhofer C, Meißl G, Klebinder K, Kohl B, Markart G (2017) Comparison of the results of a small-plot and a large-plot rainfall simulator—effects of land use and land cover on surface runoff in Alpine catchments. *CATENA* 156:184–196. <https://doi.org/10.1016/J.CATENA.2017.04.009>
- McGrath GS, Hinz C, Sivapalan M (2007) Temporal dynamics of hydrological threshold events. *Hydrol Earth Syst Sci* 11(2):923–938. <https://doi.org/10.5194/HESS-11-923-2007>
- Menichino GT, Ward AS, Hester ET (2014) Macropores as preferential flow paths in meander bends. *Hydrol Process* 28:482–495. <https://doi.org/10.1002/hyp.9573>
- Niehoff D, Fritsch U, Bronstert A (2002) Land-use impacts on storm-runoff generation: Scenarios of land-use change and simulation of hydrological response in a meso-scale catchment in SW-Germany. *J Hydrol* 267:80–93. [https://doi.org/10.1016/S0022-1694\(02\)00142-7](https://doi.org/10.1016/S0022-1694(02)00142-7)
- Padhee SK, Dutta S (2019) Spatio-temporal reconstruction of MODIS NDVI by regional land surface phenology and harmonic analysis of time-series. *GISci Remote Sens* 56(8). <https://doi.org/10.1080/15481603.2019.1646977>
- Penna D, Tromp-van Meerveld HJ, Gobbi A, Borga M, Dalla Fontana G (2011) The influence of soil moisture on threshold runoff generation processes in an alpine headwater catchment. *Hydrol Earth Syst Sci* 15:689–702. <https://doi.org/10.5194/hess-15-689-2011>
- Sarkar R, Dutta S (2012) Field investigation and modelling of rapid subsurface stormflow through preferential pathways in a vegetated hillslope of Northeast India. *J Hydrol Eng* 17(2):333–341. [https://doi.org/10.1061/\(ASCE\)HE.1943-5584.0000431](https://doi.org/10.1061/(ASCE)HE.1943-5584.0000431)
- Sarkar R, Dutta S (2015) Parametric study of a physically-based, plot- scale hillslope hydrological model through virtual experiments. *Hydrol Sci J* 60(3):448–467. <https://doi.org/10.1080/02626667.2014.897407>
- Sarkar R, Dutta S, Dubey AK (2015) An insight into the runoff generation processes in wet subtropics: field evidences from a vegetated hillslope plot. *CATENA* 128:31–43. <https://doi.org/10.1016/J.CATENA.2015.01.006>
- Singh V, Jain SK, Goyal MK (2021) An assessment of snow-glacier melt runoff under climate change scenarios in the Himalayan basin. *Stoch Env Res Risk Assess* 35:2067–2092. <https://doi.org/10.1007/s00477-021-01987-1>

- Sharma RD, Sarkar R, Dutta S (2013) Run-off generation from fields with different land use and land covers under extreme storm events. *Curr Sci* 104:1046–1053. <https://www.jstor.org/stable/24092192>
- Shivam, Goyal MK, Sarma AK (2017) Analysis of the change in temperature trends in Subansiri River basin for RCP scenarios using CMIP5 datasets. *Theoret Appl Climatol* 129:1175–1187. <https://doi.org/10.1007/s00704-016-1842-6>
- Shougrakpam S, Sarkar R, Dutta S (2010) An experimental investigation to characterise soil macro-porosity under different land use and land covers of northeast India. *J Earth Syst Sci* 119:655–674. <https://doi.org/10.1007/s12040-010-0042-5>
- Toba T, Ohta T (2005) An observational study of the factors that influence interception loss in boreal and temperate forests. *J Hydrol* 313(3–4):208–220. <https://doi.org/10.1016/J.JHYDROL.2005.03.003>
- Torres R, Dietrich WE, Montgomery DR, Anderson SP, Loague K (1998) Unsaturated zone processes and the hydrologic response of a steep, unchanneled catchment. *Water Resour Res* 34(8):1865–1879. <https://doi.org/10.1029/98WR01140>
- Tromp Van Meerveld I, McDonnell JJ (2005) Comment to "Spatial correlation of soil moisture in small catchments and its relationship to dominant spatial hydrological processes. *J Hydrol* 286: 113–134. *J Hydrol* 303:307–312. <https://doi.org/10.1016/j.jhydrol.2004.09.002>
- Van Dam JC, Groenendijk P, Hendriks RFA, Kroes JG (2008) Advances of modeling water flow in variably saturated soils with SWAP. *Vadose Zone J* 7:640–653. <https://doi.org/10.2136/vzj2007.0060>
- Van Stiphout TPJ, Van Lanen HAJ, Boersma OH, Bouma J (1987) The effect of bypass flow and internal catchment of rain on the water regime in a clay loam grassland soil. *J Hydrol* 95:1–11. [https://doi.org/10.1016/0022-1694\(87\)90111-9](https://doi.org/10.1016/0022-1694(87)90111-9)
- Walthall C, Dulaney W, Anderson M, Norman J, Fang H, Liang S (2004) A comparison of empirical and neural network approaches for estimating corn and soybean leaf area index from Landsat ETM+ imagery. *Remote Sens Environ* 92(4):465–474. <https://doi.org/10.1016/j.rse.2004.06.003>
- Weiler M (2017) Macropores and preferential flow—a love-hate relationship. *Hydrol Process* 31:15–19. <https://doi.org/10.1002/hyp.11074>
- Westerberg IK, Guerrero JL, Younger PM, Beven KJ, Seibert J, Halldin S, Freer JE, Xu CY (2011) Calibration of hydrological models using flow-duration curves. *Hydrol Earth Syst Sci* 15(7):2205–2227. <https://doi.org/10.5194/HESS-15-2205-2011>
- Williams JR, Arnold JG, Srinivasan R (2002) The APEX model, BRC Report No. 00–06. 121, Texas Agricultural Experiment Station, Blackland Research Centre, Texas A&M University, USA. https://www.nrcs.usda.gov/Internet/FSE_DOCUMENTS/nrcs143_013182.pdf

Chapter 3

Hydrological Simulation Using Coupled ANN-SCS Approach in Pagladiya Watershed: A Sub-catchment of Brahmaputra River Basin



Sagar Debbarma, Swapnali Barman, Amulya Chandra Debnath, Manoranjan Nath, and Sonu Kumar

Abstract A coupled Artificial Neural Network (ANN) and Soil Conservation Service (SCS) based method was developed for rainfall-runoff simulation in Pagladiya River Basin. Pagladiya River, a major northern sub-catchment of the Brahmaputra River Basin, significantly contributes to the mainstream Brahmaputra River. Because of this, the watershed is prone to both flood and erosion. In this study, runoff at different sub-catchments of the Pagladiya River Basin was simulated using the SCS-CN based approach. The Land Use Land Classification (LULC) was classified in ArcGIS using a supervised classification technique and a maximum likelihood classifier algorithm to estimate the curve number. Taking the runoffs at different sub-catchments as the inputs, an ANN model was developed in MATLAB for runoff simulation at the main outlet of Pagladiya. The ANN model's time series analysis employed the nonlinear autoregressive with exogenous inputs (NARX) method. The model efficiency was satisfactory with a coefficient of correlation (R), 0.91 for training, 0.88 validation, and 0.87 testings period. The overall value of R (0.90) indicates the utility of this ANN-SCS based coupled model for rainfall-runoff simulation.

Keywords ANN · SCS · Supervised classification · Runoff simulation · Pagladiya · Brahmaputra

S. Debbarma · A. C. Debnath · M. Nath
North Eastern Regional Institute of Water and Land Management, Tezpur 78420, India

S. Barman
North Eastern Regional Centre, National Institute of Hydrology, Guwahati 781006, India

S. Kumar (✉)
National Institute of Education, Earth Observatory of Singapore, Nanyang Technical University (NTU), Nanyang Ave, Singapore 639798
e-mail: nie22.sk2447@e.ntu.edu.sg

3.1 Introduction

River Brahmaputra originates from the Chema Yung-Dung in the Kailash range of southern Tibet at an altitude of 5300 m from MSL. After crossing through China, Bhutan, India, and Bangladesh, it empties into the Bay of Bengal. The average annual discharge and the suspended load of the Brahmaputra River are about 19,830 m³/s and 400 million metric tons at Pandu (Kotoky et al. 2015). The basin encounters heavy rainfall due to the southwest monsoon (Desai et al. 2012). Several tributaries join the Brahmaputra River from the north and south. Usually, the north bank tributaries flow in shallow braided channels with steep slopes and heavy silt charges. However, south bank tributaries have smoother slopes, deep meandering channels, and less sediment load. The selected tributaries of Brahmaputra River in this study, Pagladiya River, is one of the most critical north bank tributaries distinguished by its heavy discharge that causes heavy flooding downstream. Both rainfall and change in Land Use/Land Cover (LULC) that has taken place in the Pagladiya River Basin impact the difference in the river discharge. The rapid population growth has led to land use in terms of deforestation to improve agricultural production, leading to a decrease in infiltration rate and a rise in surface runoff (Ahmed 2004).

Runoff calculation of a river is essential because of its effect on flood and erosion downstream (Kumar et al. 2022). The complex and complicated physical processes that convert rainfall into runoff can be simulated with acceptable accuracy with the help of mathematical models and equations. In contrast to an empirical model representing data without any theoretical concept, a physically-based model has a theoretical concept that requires parameters and variables that are measured in the field (Gupta et al. 2020; Beven 1983). Artificial Neural Network (ANN) is a simple method that maps nonlinear relationships between precipitation and runoff (Lallahem, and Mania, 2003). However, This cannot characterize the physical processes of the basin. Therefore, an ANN-based hydrological model may not provide accurate results sometimes. Thus, non-consideration of a basin's physical processes is the main limitation of empirical models (Ahmad et al. 2015; Bhattacharjya 2020; Bhura et al. 2015). The physically-based models use numerous empirical interactions for estimating the parameter using the physically-based hydrological models (Wilcox et al. 1990). In hydrological studies, a common problem is an estimation of runoff from a watershed where only precipitation records are available. This, however, can be solved by comparing runoff characteristics with those of watershed characteristics, e.g., soil type and land use/land cover (Jabari et al. 2009).

Taking into consideration the pros and cons of various models and the severity of the impact of the discharge of Pagladiya River Basin in the flood and erosion problem downstream, this study represents a coupled model approach considering the SCS-CN and ANN-based model. The ANN-based model employs the NARX network to get the runoff. This coupled model approach used rainfall and LULC to estimate the Pagladiya river's runoff.

3.2 Materials and Methods

3.2.1 Study Area

Pagladiya river originating near Naningpho in the sub-Himalayan range of Bhutan at an altitude of 3000 m above MSL is one of the main north bank tributaries of the Brahmaputra. Most of the runoff of the watershed starts at the highland areas in Bhutan and travels downstream to the outlet of the watershed in River Brahmaputra (Talukdar 2019). Pagladiya River Basin lies between $91^{\circ}19'37.136''\text{E}$ to $91^{\circ}38'11.389''\text{E}$ longitude, $26^{\circ}17'24.664''\text{N}$ to $27^{\circ}1'50.936''\text{N}$ latitude. The location map of the basin is shown in Fig. 3.1. Its basin area is approximately 1015 km^2 . The Pagladiya River Basin elevation varies from 44 to 2536 m from MSL. Out of the total length of roughly 197 km, a significant part of the river falls in the Nalbari district of Assam and joins Brahmaputra at 2 km downstream from Chotemari village (Ahmed 2004). 55% of the Pagladiya River Basin lies within Assam, India and 45% of the upper reach lies in Bhutan (Fig. 3.1).

The study region has a mean maximum temperature of 29.1°C (2004–2017) with a maximum temperature recorded 34.52°C in April 2004 and a mean minimum temperature of 20.3°C (2004–2017) with a minimum temperature recorded 9.56°C

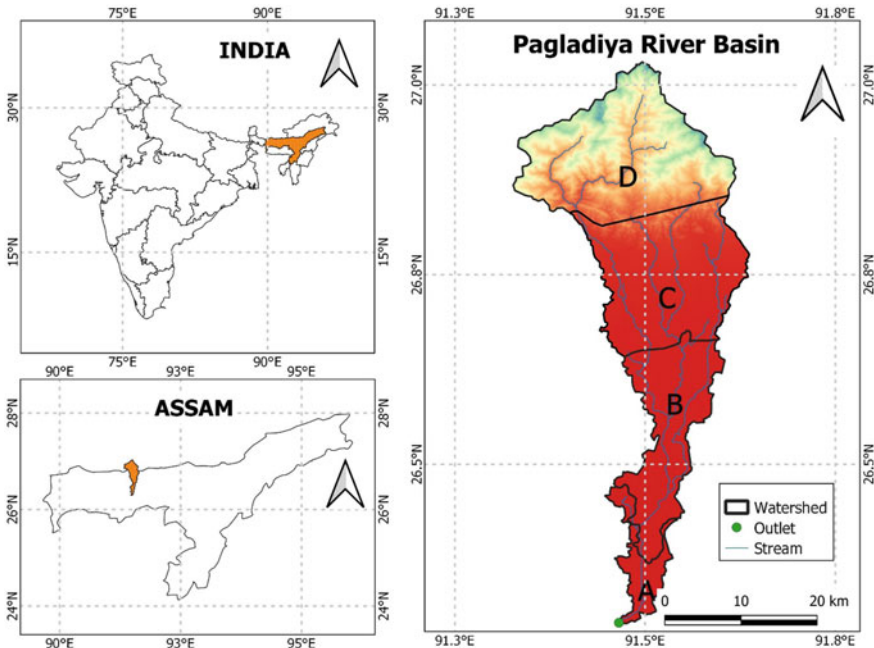


Fig. 3.1 Location map of the Pagladiya River Basin. Assam is one of India's northeastern states located in the central part of northeast India

in January 2011. The highest mean annual wind speed was observed at 5.78 m/s in April 2016, whereas the lowest yearly mean wind speed was observed at 0.38 m/s in January 2007. The mean relative humidity was changed from 50.77% to 87.43% in the region at 2 m. The watershed receives annual rainfall between 1586.07 mm to 2317.6 mm. All above data were collected from NASA's Prediction of Worldwide Energy Resources (POWER).

3.2.2 Materials

- (i) **Digital Elevation Model:** SRTM 90 m (Shuttle Rader Topographic Mission) Digital Elevation Model (DEM) were utilized for Pagladiya River Basin delineation in the research and analyzing the basin's topography.
- (ii) **Landsat:** Landsat-7 data of 30 m spatial resolution were employed to prepare the LULC maps for 2010.
- (iii) **Soil texture:** National Bureau of Soil Survey and Land Use Planning (NBSSLUP) and FAO-UNESCO soil maps were downloaded and employed to prepare the soil map of the selected study area.
- (iv) **Rainfall:** CHIRPS freely provides inclusive, consistent, reliable, up-to-date rainfall datasets for various applications, e.g., trend analysis of rainfall, flood, and drought analysis. CHIRPS datasets are developed using various Satellite, Reanalysis, and Gauge-based precipitation products, e.g., TRMM, CFS. Detailed information can be found in Funk et al. (2015) and Table 3.1.
- (v) **Discharge:** Daily observed discharge for 14 years from 2004 to 2017 was gathered from the Water Resources Department of Assam.

Table 3.1 A comprehensive summary of characteristics of various datasets used in this study, along with their sources

Data type	Data description	Spatial resolution	Temporal converge	Sources
Topography	SRTM, Digital Elevation Model (DEM)	90 m	2017	http://srtm.csi.cgiar.org/
Land Use and Land Cover	Landsat-7 & 8	30 m	2000 & 2010	https://earthexplorer.usgs.gov/
Soil Textura	NBSSLUP and FAO-UNESCO		2015	http://www.fao.org/geonetwork/srv/en/
Rainfall	CHIRPS	0.05°	2004–2017	https://climateserv.servirglobal.net/
Discharge	Nalbari Station	Point	2004–2017	Water Resources Department, Assam

3.2.3 Methodology

The step-wise explanations of the adopted methodology for the runoff-runoff simulation is described below in the following stages:

- I. Delineation of Pagladiya River Basin using SRTM DEM of 90 m spatial resolution in ArcGIS software,
- II. Preparation of LULC maps for the years 2000 and 2010 using supervised classification technique and maximum likelihood classifier algorithm in ArcGIS software,
- III. Preparation of soil map has using NBSSLUP and FAO soil maps,
- IV. Classification of suitable hydrological soil classes, namely, I, II, III & IV using soil texture information of the Pagladiya River Basin,
- V. Estimation of area-weighted for CN_{II} (AMC II), CN_I (AMC I), and CN_{III} (AMC III),
- VI. Extraction of CHIRPS gridded satellite rainfall data for various sub-basin using Python programming,
- VII. Estimation of runoff at every four sub-basins using the standard equation of SCS-CN technique,
- VIII. Finally, the overall runoff at the main outlet of Pagladiya River Basin was simulated using a coupled ANN-SCS model, where ANN was run utilizing time series analysis based on the NARX method. The model performance was analyzed based on the coefficient of correlation (R) values.

3.2.3.1 Preparation of LULC Maps

The LULC maps of Pagladiya River Basin were prepared using Landsat data of 30 m resolution for 2000 and 2010 using supervised classification technique and maximum likelihood classifier algorithm. Four LULC classes, viz., agricultural land, forest, rural built-up, and water bodies, were identified for the basin. A minimum number of 70–80 training samples were selected for each class to prepare the LULC maps.

3.2.3.2 Runoff Simulation of Pagladiya River Basin Using SCS-ANN Coupled Model

Theory Behind SCS Model

Estimating runoff is an essential aspect of hydrological modeling. A plethora of empirically-based methods for runoff calculation is available. However, the SCN method (SCS 1972) is the most popular (Ahmad et al. 2015; Bhattacharjya 2020; Bhura et al. 2015; Muthu and Santhi 2015; Vinithra and Yeshodha 2016), widely acceptable empirical-based model developed by the United States Department of Agriculture and Soil Conservation Service (USDA-SCS) to assess surface runoff. The Soil Conservation Service-Curve Number (SCS-CN) method is widely

used to determine direct runoff depth based on storm rainfall depth daily (Barman and Bhattacharjya 2020; Bhura et al. 2015). This method is prevalent due to its simplicity, flexibility, and reliance on only one Curve Number (CN) parameter for runoff computation. Hydrologic soil class, land use type, and antecedent moisture condition (AMC) are the essential basin properties applied for curve number computations (Ahmad et al. 2015; Subramanya 2008).

The central concept SCS-CN based method for estimating the runoff is based on the water balance equation and two essential assumptions.

The water balance equation is expressed as,

$$P = I_a + F + Q \quad (3.1)$$

where P , I_a , F , Q , and S are total rainfall depth (mm), initial abstraction rate (mm), cumulative infiltration excluding I_a , direct surface runoff rate (mm), and potential maximum retention rate (mm), respectively, which all in daily basis.

Two fundamental hypotheses are as follows:

- (i) The ratio of actual runoff (Q) to the maximum potential runoff ($P-I_a$) is equal to the ratio of actual retention (F) to the maximum potential retention (S),

$$\frac{Q}{P - I_a} = \frac{F}{S} \quad (3.2)$$

- (ii) Initial abstraction is equal to some fraction of maximum potential retention,

$$I_a = \lambda S \quad (3.3)$$

The potential maximum retention, S (mm), can vary between 0 to ∞ and is directly linked to CN (Curve Number).

$$S = \frac{25400}{CN} - 254 \quad (3.4)$$

From Eqs. (3.1), (3.2), and (3.3); the amount of direct runoff (mm) is found out as,

$$Q = \frac{(P - I_a)}{\{(P - I_a) + S\}} \quad (3.5)$$

The values of CN vary from 0 to 100 depending on soil type, hydrologic condition of the soil, land use, etc. For understating the hydrologic situation of the soil, AMC is used that expresses the wetness and availability of soil moisture storage before a rainfall event that can considerably affect runoff volume. Three stages of AMC, namely AMC-I, AMC-II, and AMC-III for dry, normal, and wet conditions, respectively, are employed in the CN method (Ahmad et al. 2015; Vinithra and Yeshodha 2016; Yuan et al. 2014). Apart from the AMC condition, much of the variability of

Table 3.2 Four classified hydrologic soil groups based on infiltration rate

Soil group	Infiltration (mm/hr)		Soil texture
	I	High	
II	Moderate	12.5 to 25	Loam and silt loam
III	Low	2.5 to 12.5	Sandy clay loam
IV	Very low	Less than 2.5	Silty clay, clay loam, sandy clay

CN was attributed to soils. Hydrologically soils are assigned into four groups based on water intake on the bare ground when thoroughly wetted (Table 3.2).

The CN value of AMCII(CNII) for various land use and soil type can be directly collected from the manual of SCN methods. However, the CN value for AMC I (CNI) and AMC III (CNIII) can be estimated using Eqs. (3.6 and 3.7) (USDA 1985):

$$CNI = \frac{4.2 \times CNII}{10 - (0.058 \times CNII)} \tag{3.6}$$

$$CNIII = \frac{23 \times CNII}{10 + (0.13 \times CNII)} \tag{3.7}$$

A general range of λ is lies between 0.1 to 0.4 based on the study conducted on the various geographical locations. Then it is found that $\lambda = 0.2$ on various experiments (SCS 1985), which is conducted in a small basin and is taken as a standard value. Using $\lambda = 0.2$ in Eq. (3.5) will become

$$Q = \frac{(P - 0.2S)}{P + 0.8S} \text{ for } P > 0.25S \tag{3.8}$$

This equation is known as the standard SCS-CN equation, where Q = daily runoff (mm), S = potential maximum retention (mm), and P = daily rainfall (mm).

The present study has divided the entire Pagladiya River Basin into four sub-catchments. The LULC maps of 2000 and 2010 have been used for runoff estimation for 2004–2009 and 2010–2017, respectively. The soil map of the Pagladiya River Basin was prepared for creating suitable hydrological soil classes. The weighted curve number was approximated based on the different LULC categories and hydrological soil classes. The standard SCS-CN technique was employed in ArcGIS and Microsoft Excel (Microsoft Excel is a suitable tool for developing the models) platforms to determine surface runoff for all selected four sub-basin from 2004 to 2017 on daily total rainfall.

ANN-Based Model

An ANN-based model was developed to simulate the surface runoff at the main outlet of Pagladiya River. The four sub-basin average runoffs were fed as input to the ANN-based model, and the ANN model was run using the time series analysis carried out in MATLAB using NARX approaches. The NARX is a dynamical neural

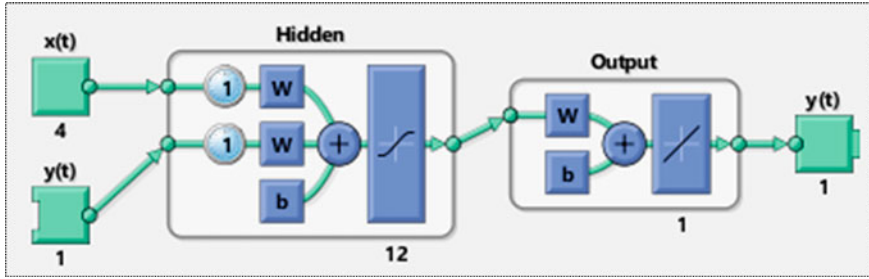


Fig. 3.2 Structure of NARX model for open-loop

architecture generally applied for input–output modeling of nonlinear dynamical systems can be scientifically denoted as

$$y(t) = f(x(t - 1), \dots, x(t - d), y(t - 1), \dots, y(t - d)) \quad (3.9)$$

where $y(t)$ and $x(t)$ represent the total surface runoff at the main outlet and each sub-basin of Pagladiya River Basin, and d denotes the tapped delay lines that store earlier estimates of the $x(t)$ and $y(t)$ sequences. The daily time series of observed available runoff from 2004 to 2017 was utilized for model development. The hydrological model was assembled employing a neural network toolbox in MATLAB 9.3 (R2017b). Out of the total observed available runoff data, 70% were carefully chosen for Training, 15% for validation, and the remaining 15% for testing. The network is created and trained in open-loop form, as shown in Fig. 3.2. The algorithm selected was the Levenberg–Marquardt algorithm. The number of hidden layers selected was 12, and the total number of delays was 1 for the optimum network.

3.3 Results and Discussions

3.3.1 Delineation of Watershed

Using SRTM DEM of 90 m spatial resolution, the Pagladiya River Basin was delineated. The basin was then divided into four small sub-basin. The topography of the study area ranges from the elevation of 44 to 2536 from MSL. As shown in Fig. 3.3, Approximately 60 percent of the entire Pagladiya River Basin falls in the floodplain area where the basin's elevations lie in the range of 44 to 278 m above MSL. The remaining northern region of the basin has elevation ranges from 278 to 2536 m above MSL. As obtained, the coordinates of the hypsometric curves of the four sub-basin of the Pagladiya River Basin were plotted in Fig. 3.4a-d. The hypsometric analysis provides information about the total horizontal cross-sectional area of the watershed at specific elevations (Sharma et al. 2013). The digital elevation map was

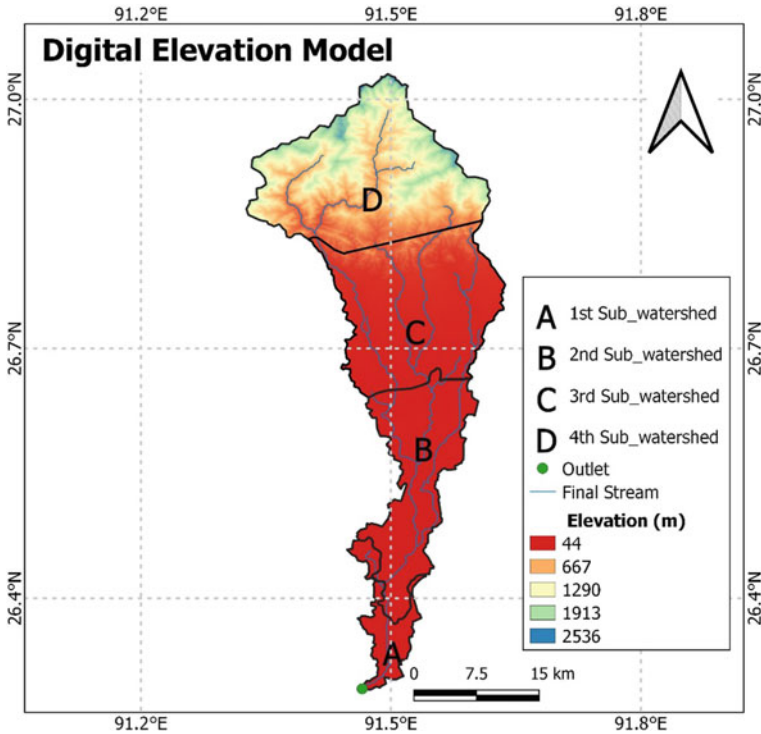


Fig. 3.3 Delineated Pagladiya River Basin, showing four different sub-catchments (solid black line), stream network (solid green line), main outlet (solid black point), and elevation (m) from MSL

employed to produce the relative area and elevation analysis data. It was noted from the hypsometric curves of four sub-basins that the seepage framework is achieving the monadnock stage from the experienced stage. The comparison between hypsometric curves of four sub-basins displayed in Fig. 3.4 revealed an insignificant difference in mass removal from the sub-basins of the Pagladiya River Basin.

3.3.2 Estimation of Rainfall Data

The daily accumulated rainfall for each sub-catchment was extracted using python scripts. The daily accumulated rainfall was determined by taking the arithmetic mean of all grids within each sub-basin of the Pagladiya River Basin. Figure 3.5 shows the spatial variation in seasonal monthly rainfall across the Pagladiya River Basin. The basin receives a high rainfall (approximately 15 mm/day) in the monsoon season (May-July) and less rainfall during the winter season from November to February. The upper part of the Pagladiya River Basin observed lower rainfall than the central part in May and July, but the lower and upper parts in July received a similar rainfall.

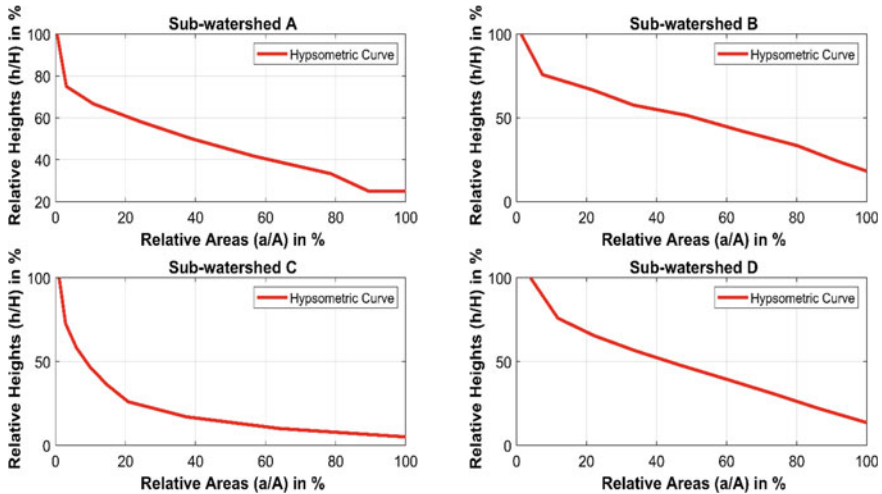


Fig. 3.4 Hypsometric curve for four sub-basins (a, b, c, and d) of Pagladiya River Basin

3.3.3 Land Use Change Estimation

When the remotely sensed records and study areas are recognized for land-use change study, selecting a suitable variation detection technique is significant in making a high-quality variation recognition concept (Anil et al. 2021). Change detection of land use is the effective use of Remote Sensing in the research because it helps users to detect changes in specific features within a particular interval. The investigation determined that satellite-based remote sensing concepts, including GIS, are often vital for planning and assessing LULC changes for its sustainability. The land cover features found in the study basin are agricultural land, forest, rural built-up, and water bodies. The four various classes for land use, namely agricultural land, forest, rural built-up, and water bodies, prepared in this study are shown in Fig. 3.6 for 2000 and 2010. The upper part of the basin is covered mainly by the forest, while the remaining three lower parts cover agricultural land in both selected years. The area covered by each LULC class and their changes from 2000 to 2010 is given in Table 3.3. It is seen from Table 3.3 that, compared to 2000, the area covered by rural built-up and agricultural land substantially got increased in 2010. However, the area covered by forest and water bodies got reduced during this decadal period. Generally, the land use land cover data during the study area's (2000–2010) indicated specific significant changes that can not show any significant environmental impact. However, these patterns should be firmly checked for the sustainability of the environment in the future.

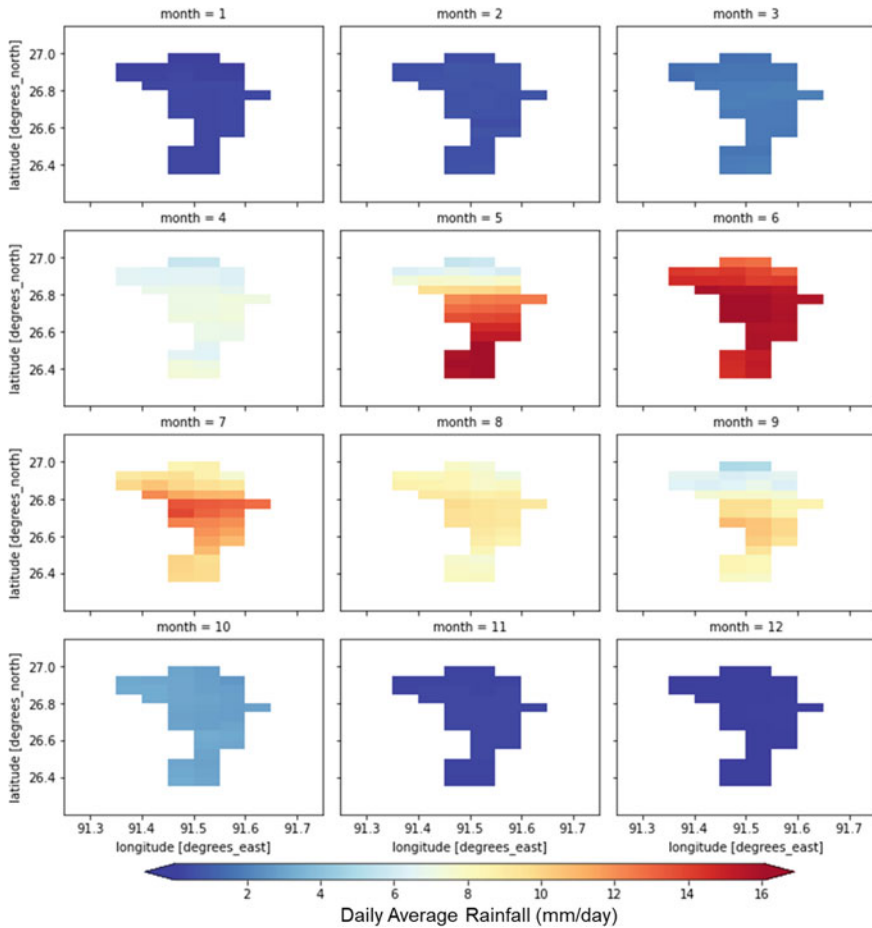


Fig. 3.5 Spatial variation in daily average rainfall across the Pagladiya River Basin from 2004 to 2018 for each seasonal month. Month 1, 2, 3, 4, 5, 6, 7, 8, 9, 10, 11, and 12 represents the name of month Jan, Feb, Mar, Apr, May, Jun, Jul, Aug, Sept, Oct, Nov, and Dec, respectively

3.3.4 Hydrological Soil Classes

The hydrological soil class type is based on soil texture. To determine the hydrological soil classes, the United States Department of Agriculture (USDA) soil texture should be recognized. Table 3.2 categorizes the hydrological soil classes by its USDA soil texture information, which was established corresponding to the sand, silt, and clay percentage. Based on the published data by the NBSSLUP and FAO-UNESCO soil map, soil texture was defined for the different soil types of the Pagladiya catchment, as illustrated in Table 3.4.

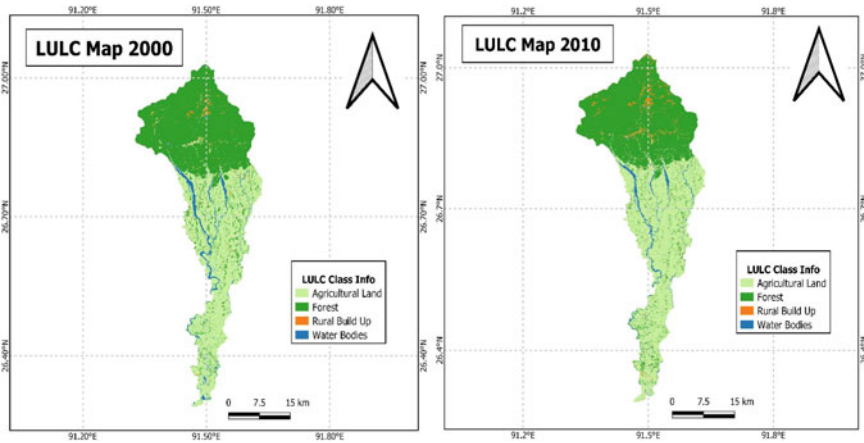


Fig. 3.6 Land use land cover maps of Pagladiya river basin for the years 2000 and 2010

Table 3.3 Area covered by different LULC classes in 2000 and 2010

Sl. No	LULC class	Area (km ²)		Change in area (km ²)	% Change
		2000	2010		
1	Agricultural land	450	465	15	3.33
2	Forest	512	495	-17	-3.32
3	Rural built-up	11	25	14	127.28
4	Water bodies	43	31	-12	-27.91

Table 3.4 Division of soil types according to hydrologic soil class

Soil type	Hydrological soil group
Acrisol	Group B
Nitrosol	Group B
Regosols	Group B
Typic Fluvaquents	Group C
Aeric Fluvaquents	Group C

The soil map for the basin was prepared in ArcGIS using NBSS-LUP soil and FAO-UNESCO soil map (Fig. 3.7). Five different soil types were classified for the basin; first, Acrisol is clay-rich subsoil related to humid, tropical climates, such as those found in forested areas. Second, Nitrosol is a deep, red, well-drained soil with more than 30% clay content and a blocky structure. The third is Regosols, which weakly developed mineral soil in unconsolidated materials. Fourth, fourth, Typic Fluvaquents (Coarse loamy), is a deep, well-drained, coarse loamy soil on a very gently sloping piedmont plain with a loamy surface with moderate erosion and slight

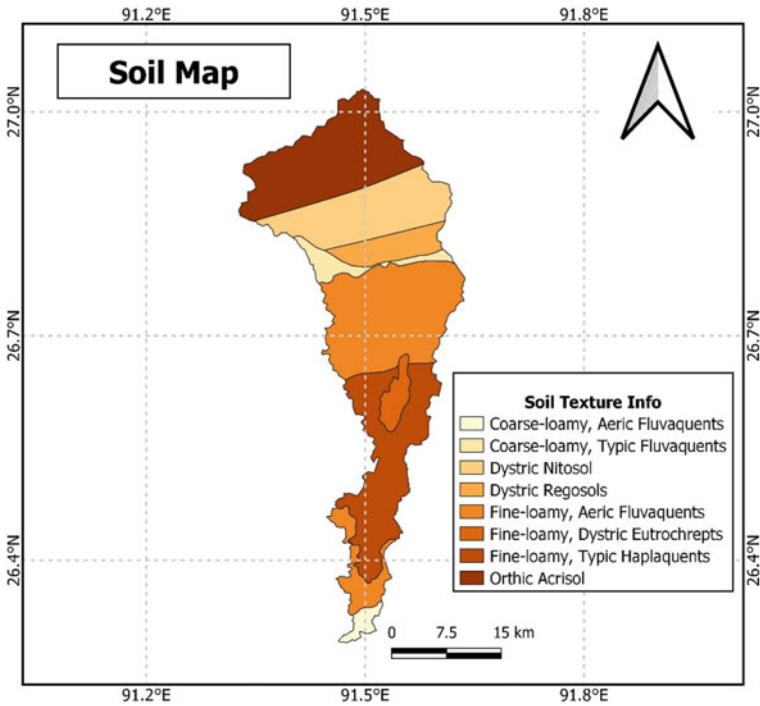


Fig. 3.7 Soil texture map of Pagladiya river basin

flooding. Lastly, Aeric Fluvaquents (Fine loamy) is a very deep, moderately well-drained, fine loamy soil on very gently sloping piedmont plains with a loamy surface with moderate erosion and slight flooding. These soil types into four Hydrologic soil classes, as given in Table 3.4.

3.3.5 Estimation of Weighted CN

In order to normalize CN, the weighted hydrologic CN of the Pagladiya River Basin was determined. The weighted CN acquired from the manual for AMC-II, corresponding to each sub-watershed, for AMC I and AMC III were determined using Eqs. 3.6 and 3.7, respectively. In terms of LULC and HSG combination, the lowest CN value was found to be 40 and 58 in forest areas, and the highest CN value was found to be 97 in water bodies for B and C groups, respectively. The curve number (CN) values for different LULC classes adopted in this study are shown in Table 3.5.

Table 3.5 CN values for different LULC classes adopted

LULC classes	Hydrological soil groups	
	Group B	Group C
Agricultural land	86	90
Forest	40	58
Rural built-up	69	79
Water bodies	97	97

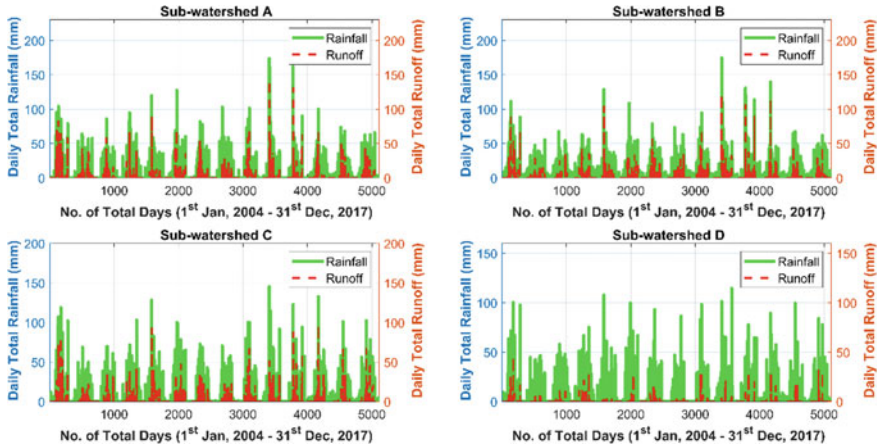


Fig. 3.8 Annual average rainfall and runoff for each sub-catchment. A clear picture of an increase in the runoff can be observed with respect to an increase in rainfall for different sub-catchments

3.3.6 Runoff Estimation

The runoff assessment is one of the most crucial aspects of hydrological modeling. This study collected the daily rainfall from the CHIRPS’ gridded satellite precipitation product for 14 years from 2004 to 2017. The potential maximum retention (S) is calculated for each sub-basin. If a rainfall event is more than the λS value, a runoff will be available for this rainfall event. Figure 3.8 shows the annual average rainfall and runoff for each sub-catchment. From Fig. 3.8,

3.3.7 Development of Coupled ANN-SCS Model and Runoff Simulation

The daily runoff at each sub-watershed of the Pagladiya River Basin was determined from 2004 to 2017 using the SCS-CN method. Runoff at the main outlet was simulated using an ANN model. The coefficient of correlation (R) values acquired for Training,

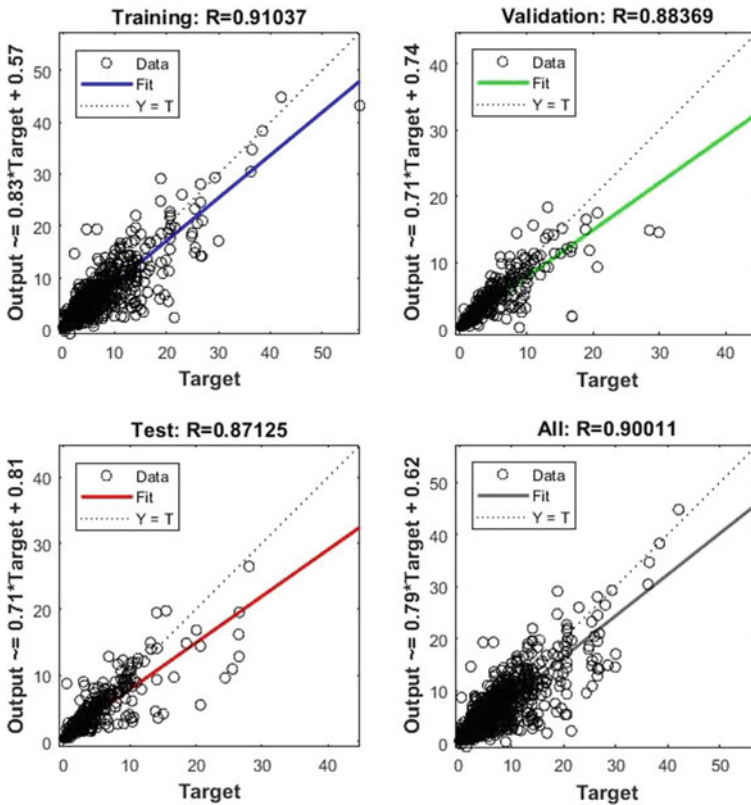


Fig. 3.9 Regression plots of ANN model

validation, and testing for the ANN model are 0.91, 0.88, and 0.87, respectively, with an overall R-value of 0.90. This indicates that the model is capable enough to be used for the simulation of runoff for the Pagladiya River Basin. The regression plots are shown in Fig. 3.9. The plots for observed and simulated runoffs are shown in Fig. 3.10.

3.4 Conclusions

This study simulated the runoff of the Pagladiya River Basin from 2004 to 2017 using a coupled ANN-SCS rainfall-runoff model. By dividing the entire basin into four different sub-watersheds, the runoff from each sub-watershed was first estimated using the SCS-CN approach. Then, the LULC maps were prepared for 2000 and 2010 using Landsat satellite-based data of 30 m resolution by supervised classification technique used for runoff simulation for the period 2004–09 and 2010–17, respectively. The basin's runoff at the main outlet was simulated using time series

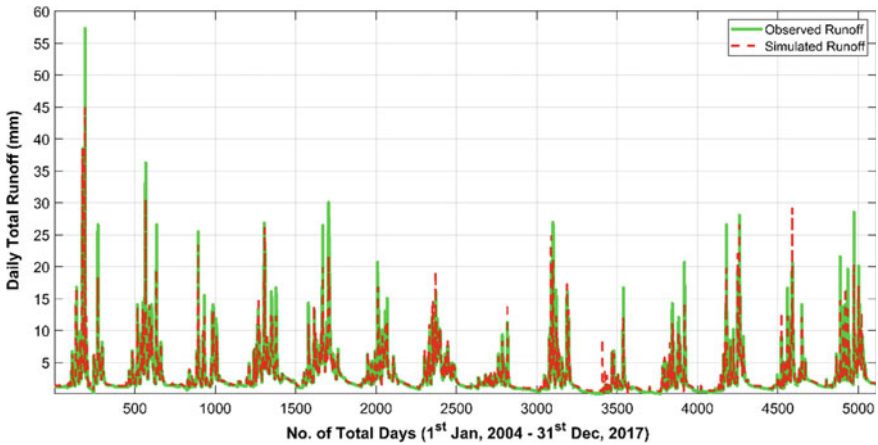


Fig. 3.10 Observed runoff versus simulated runoff graph as obtained from the ANN model

analysis in ANN, and the model's performance was analyzed based on the coefficient of correlation values. Satisfactory values for R as 0.91, 0.88, and 0.87 were obtained for Training, validation, and testing with an overall R-value of 0.90. This indicates the efficiency of the developed rainfall-runoff model in simulating runoff for the Pagladiya River Basin. The simulated surface runoff can be used further to plan for appropriate management of water and land in the study area. In this way, a hydrological model will help plan land use and carefully manage soil, water, and vegetation resources, employing suitable management practices and structural works.

Acknowledgements The authors are also thankful to the Water Resource Department, Government of Assam, for providing daily discharge data of the selected watershed site.

References

- Ahmad I, Verma V, Verma MK (2015) Application of curve number method for estimation of runoff potential in GIS environment. In: 2nd international conference on geological and civil engineering, vol 80, No 4, pp 16–20
- Ahmed JA (2004) Development of optimal operating policy for Pagladia multipurpose reservoir (Doctoral dissertation)
- Barman S, Bhattacharjya RK (2020) ANN-SCS-based hybrid model in conjunction with GCM to evaluate the impact of climate change on the flow scenario of the River Subansiri. *J Water Climate Change* 11(4):1150–1164
- Beven K (1983) Surface water hydrology-runoff generation and basin structure. *Rev Geophys* 21(3):721–730
- Bhura CS, Singh NP, Mori PR, Prakash I, Mehmood K (2015) Estimation of surface runoff for Ahmedabad urban area using SCS-CN method and GIS. *Int J Sci Technol Eng* 1(11):411–416
- Desai AJ, Naik SD, Shah RD (2012) Study on the channel migration pattern of Jia-Bhareli, Puthimari and Pagladiya tributaries of the Brahmaputra river using remote sensing technology; Hsu KL,

- Gupta HV, Sorooshian S (1995) Artificial neural network modeling of the rainfall–runoff process. *Water Resour Res.* 31:2517–2530
- Funk C, Peterson P, Landsfeld M, Pedreros D, Verdin J, Shukla S, Michaelsen J (2015) The climate hazards infrared precipitation with stations—a new environmental record for monitoring extremes. *Sci data* 2(1):1–21
- Gupta A, Himanshu SK, Gupta S, Singh R (2020) Evaluation of the SWAT model for analysing the water balance components for the upper Sabarmati Basin. In *Advances in water resources engineering and management* (pp 141–151). Springer, Singapore
- Jabari, S., Sharkh, M.A. and Mimi, Z. (2009). ‘Estimation of runoff for agricultural watershed using SCS curve number and GIS.’ Thirteenth International Water Technology Conference, IWTC 13, 2009, Hurghaba, Egypt.
- Kumar S, Yadav SR, Baghel T (2022) Estimating sediment rate through stage–discharge rating curve for two mountain streams in Sikkim, India. In *water resources management and sustainability* (pp 131–145). Springer, Singapore
- Kotoky P, Bezbaruah D, Sarma JN (2015) Spatio-temporal variations of erosion-deposition in the Brahmaputra River, Majuli—Kaziranga sector, Assam: implications on flood management and flow mitigation. In *environmental management of river basin ecosystems* (pp 227–251) Springer, Cham
- Lallahem S, Mania J (2003) A nonlinear rainfall-runoff model using neural network technique: example in fractured porous media. *Math Comput Model* 37(9–10):1047–1061
- Talukdar KK (2019) Watershed characteristics of Pagladiya river using GIS and digital elevation model. *Int J Res Appl Sci Eng Technol* 7(7):731–734
- Muthu AL, Santhi MH (2015) Estimation of surface runoff potential using SCS-CN method integrated with GIS. *Indian J Sci Technol* 8(28):1–5
- Sharma SK, Tignath S, Gajbhiye S, Patil R (2013) Use of geographical information system in hypsometric analysis of Kanhiya Nala watershed. *Int J Remote Sens Geosci* 2(3):30–35
- Subramanya K (2008) *Engineering Hydrology*. Tata McGraw-Hill Publishing, New Delhi
- USDA, SCS (1972) *National Engineering Handbook, Part 630 Hydrology, Section 4, Chapter 10*. Washington, DC: Natural Resources Conservation Service. U.S. Department of Agriculture
- Vinithra R, Yeshodha L (2016) Rainfall–runoff modelling using SCS–CN method: a case study of Krishnagiri District, Tamilnadu. *Int J Sci Res* 5(3):2319–7064
- Wilcox BP, Rawls WJ, Brakensiek DL, Wight JR (1990) Predicting runoff from rangeland catchments: A comparison of two models. *Water Resour Res* 26(10):2401–2410
- Yuan Y, Nie W, McCutcheon SC, Taguas EV (2014) Initial abstraction and curve numbers for semiarid watersheds in Southeastern Arizona. *Hydrol Proc* 28(3):774–783

Chapter 4

Water Erosion Risks Mapping Using RUSLE Model in the Mohamed Ben Abdelkrim El Khattabi Dam Watershed (Central Coastal Rif, Morocco)



Soukaina Ed-Dakiri, Issam Etebaai , Said El Moussaoui ,
Mustapha Ikirri, Mohamed Ait Haddou , Salih Amarir ,
Abdelhamid Tawfik, Hajar El Talibi , Hinde Cherkaoui Dekkaki ,
Mohamed Abioui , Brahim Damnati , and Taoufik Mourabit 

Abstract Water erosion poses serious problems by inducing the degradation and mobilization of soils and the silting up of dam reservoirs. The mapping of the vulnerability of land to erosion has been the subject of several studies in northern Morocco. This work is based on the RUSLE model (Revised Universal Soil Loss Equation) coupled with a Geographic Information System (GIS) to quantify soil loss rate. The

S. Ed-Dakiri (✉) · I. Etebaai · S. El Moussaoui · A. Tawfik · H. El Talibi ·
H. Cherkaoui Dekkaki · T. Mourabit

Laboratory of Research and Development in Engineering Sciences, Faculty of Science and
Technology of Al Hoceima, Abdelmalek Essaadi University, Tétouan, Morocco
e-mail: soukainaeddakiri@gmail.com

I. Etebaai
e-mail: i.etebaai@uae.ac.ma

S. El Moussaoui
e-mail: s.elmoussaoui@uae.ac.ma

A. Tawfik
e-mail: abdelhamid.tawfik@etu.uae.ac.ma

H. El Talibi
e-mail: hajar.el.talibi@gmail.com

H. Cherkaoui Dekkaki
e-mail: hcherkaouidekkaki@uae.ac.ma

T. Mourabit
e-mail: tmourabit@gmail.com

B. Damnati
Environment, Oceanology and Natural Resources Laboratory, Faculty of Science and Technology
of Tangier, Abdelmalek Essaadi University, Tétouan, Morocco
e-mail: b_damnati@yahoo.fr

M. Ikirri · M. Ait Haddou · S. Amarir · M. Abioui (✉)
Department of Earth Sciences, Faculty of Sciences, Ibn Zohr University, Agadir, Morocco
e-mail: m.abioui@uiz.ac.ma; abioui.gbs@gmail.com

study concerns the Mohamed Ben Abdelkrim El Khattabi (MBAK) watershed. It covers an area of 779 km² with land with sparse vegetation cover, friable substrates, and very rugged topography. The integration of the five factors of erosion in a GIS environment shows the susceptibility of this basin to the risk of water erosion. The average annual rate of soil loss is 6.44 t/ha/year. These results could assist decision-makers and planners in any decision to preserve and restore heavily eroded areas in the Mohamed Ben Abdelkrim El Khattabi Dam watershed.

Keywords Water erosion · RUSLE model · Mohamed Ben Abdelkrim El Khattabi Dam watershed · Rif Central · Morocco

4.1 Introduction

Soil erosion is a worrying environmental challenge in some regions such as Morocco. Combining climatic aggressiveness with inadequate human practices leads to significant or even irreversible soil degradation. It threatens large Mediterranean and semi-arid regions with a very aggressive climate with high rainfall intensities exceeding 45 mm.h⁻¹ (see Touaïbia et al. 2000). The precipitation in these mountainous areas generates torrential flows (Lu et al. 2004; Yahiaoui 2012; Tadrist and Debauche 2016). The flows resulting from this torrential regime pull particles from the soil transport them into the wadis and sediment behind the dams.

In the Rif's chain, the amount of soil lost reaches an average of 20 t/h/yr while it is only 5 to 10 t/ha/yr in the Middle and High Atlas. Clearing the protective vegetation cover has made the soils vulnerable to water erosion. The extent of erosion is more significant in the hills of the Perif, which cover only 6% of the national territory but produce 60% of the sediment. The excessive silting of most of the large dams in the northern part of Morocco has considerably limited their proper volume and thus their real storage capacity. Although solid transport by rainwater and runoff is a natural process, it is strongly accentuated by anthropogenic activities that weaken the soils that are sometimes degraded and leave the bedrock exposed (Dabral et al. 2008; Pandey et al. 2009; Bonilla et al. 2010; Bouimajjane et al. 2020).

Estimating the rate of sedimentation in dams and their lifespan requires knowledge of the solid inputs from the watershed. The spatial analysis of modeling based on rainfall erosivity, soil type, slopes, and vegetation cover will target the most sensitive watershed areas for development.

M. Ikirri

e-mail: mustapha.ikirri@edu.uiz.ac.ma; ikirimustapha@gmail.com

M. Ait Haddou

e-mail: mohamed.aithaddou@edu.uiz.ac.ma

S. Amarir

e-mail: salih.amarir@edu.uiz.ac.ma; amarir.salih.virgo@gmail.com

The solid transport problem and the extent of siltation in dams have been of interest to many researchers since 1950. Within the framework of this study, the MBAK dam watershed, affected by the siltation phenomenon, was chosen. In addition to its function as a drinking water supply reservoir, it is also used to recharge the water table located downstream.

To assess the risks of soil erosion and to establish conservation strategies and soil and water management plans, several models are currently being developed and used in several countries and different regions. Namely, empirical models such as the Universal Soil Loss Equation (USLE), which was developed by Wischmeier and Smith (1978) to estimate soil losses from a field on an annual basis (from parameters characterizing climate, soil, topography, vegetation cover, and erosion control) (Villeneuve et al. 1998). Physically, based distributed models such as the ANSWERS model (Areal Nonpoint Source Watershed Environmental Response Simulation) (Beasley 1977), CREAMS (Chemicals Runoff and Erosion from Agricultural Management Systems) (Knisel 1980), LISEM (Limburg Soil Erosion Model) (De Roo and Cremers 1996), and the SWRRB (Simulator for Water Resources in Rural Basins) model (Williams and Renard 1985).

The choice of model in the present study is made according to the availability of data, in particular the intensity of the precipitation. The chosen method is the most widely used on a national scale and more specifically in the Mediterranean region (Raissouni et al. 2016), it is the Revised Universal Soil Loss Equation (RUSLE) of Wischmeier and Smith (1978), based on the USLE model (Wischmeier and Smith 1978) which makes it possible to calculate and analyze the various factors which influence soil erosion.

The use of remote sensing and geographic information systems (GIS) is enabling estimation and spatialization of soil erosion at a reasonable cost (Wilson and Lorang 2000; Boggs et al. 2001; Jasrotia and Singh 2006). The principle consists in applying the RUSLE model (Revised Universal Soil Loss Equation) combined with a Geographic Information System (GIS) under Moroccan conditions at the watershed level of the MBAK dam to assess the extent of the erosion phenomenon and draw up the erosion hazard map.

This is achieved through two steps:

1. Mapping of the different factors related to the erosive process using GIS, which allows to store and structure of spatial information of different characteristics of the watershed.
2. Setting up an interactive database of erosion factors, integrating the model (RUSLE) in a GIS environment for localization of erosion-prone areas.

4.2 Study Area

The MBAK dam watershed is located in northeastern Morocco's eastern part of the inner Rif (Fig. 4.1). It is an elongated mountain basin with 779 km² and a perimeter of 173 km. It is drained by the Wadi Nekôr, which flows into the plain

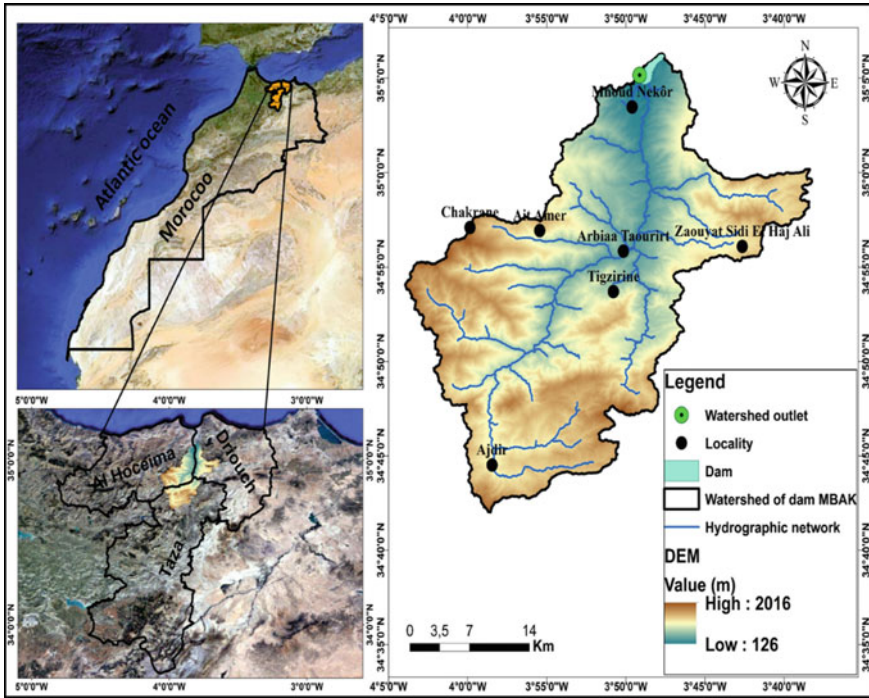


Fig. 4.1 Location of MBAK watershed, central coastal Rif, Morocco

of Al Hoceima. The average annual rainfall is about 344 mm from 1976 to 2006. Indeed, the altitudes range from 126 m at the dam to 2016 m on the highest peaks. The morphometric characteristics of the watershed show its elongated shape (Table 4.1). The overall slope index I_g equals 13.96 m/km, and according to the ORSTOM relief classification, its specific slope value characterizes an intense relief.

Geologically, this watershed is composed of Paleozoic shales of the Kétama unit, with alternating marl and limestone, as well as large blocks of sandstone (Albo-Aptian schistous and flysch) and also alluvium and silt of the recent Quaternary (Mourier 1982; Chafouq et al. 2018). The Quaternary formations show a thickness generally exceeding 100 m in depth (Salhi 2008). Lithological formations of more varied nature from the right bank; in the South, we have the sandstones of Jbel Kouine (Lower Miocene). In the South-West, the rigid limestone formations of Jbel Azrou Akechar (Lias) are surrounded by Jurassic shales. More in the North-East, towards the accident of Nekor, we meet essentially gypsiferous Triassic olistostromes, as well as the formations of shales, limestones, and marls/limestones of the Cretaceous period (Amil 1992; Arrebei et al. 2019) (Fig. 4.2).

Table 4.1 Topographic and morphometric characteristics of the MBAK dam watershed

Parameters	Value	Unit
Maximum elevation	2016	Meter
Minimum elevation	126	
Average elevation	1071	
Maximum slope	75	Degree
Minimum slope	0	
Average slope	37.5	
Perimeter	173	Km
Length of equivalent rectangle	93.08	
Width of equivalent rectangle	10.37	
Area	779	Km ²
Index of the global slope (Ig)	13.96	m/Km
Index of Gravelius (KG)	1.71	No unit

4.3 Materials and Methods

The Revised Universal Soil Loss Equation (RUSLE) (Renard et al. 1996) is a renovation of the USLE model of Wischmeier and Smith (1978) for estimating the average annual soil loss through water erosion. It is an empirical model that calculates soil erosion combining five factors (Fig. 4.3): (i) the erosivity of precipitation (the R-factor), it is the product of the kinetic energy of rainfall and the maximum intensity of rains for 30 min (Wischmeier and Smith 1978). It can also be considered as the average annual rain erosion index. However, due to the lack of datasets for our study area, we opted to use the available datasets for monthly and annual precipitation, (ii) the resistance of the soil, represented by the K-factor (soil erodibility) which quantitatively describes the inherent erodibility of each type of soil, the area studied is characterized by the association of the different types of soil: the association of little evolved soils and calcimagnesian soils, the association of little evolved soils and fersiallitic soils, the association of crude mineral soils, calcimagnesian soils and Brunified soils, and the association of little evolved soils, brunified soils and fersiallitic soils, (iii) the length of the slope and the inclination of the slope, represented by the LS-factor (topographic factor), which indicates the effects of topography on erosion, vegetation cover and soil particle size characterized by the area of study are the two parameters that influence the relationship between soil loss and slope inclination, (iv) the C-factor, which makes it possible to distinguish bare land from covered land in order to target the rate of alteration of the rock (Vegetation cover and agricultural techniques) and (v) the P-factor (prevention measures factor) which indicates the ratio of the soil loss observed on land mechanically tilled in one way and protected against erosion in another way compared to that which occurs on the reference plot where the land is plowed frequently in the direction of the greatest slope.

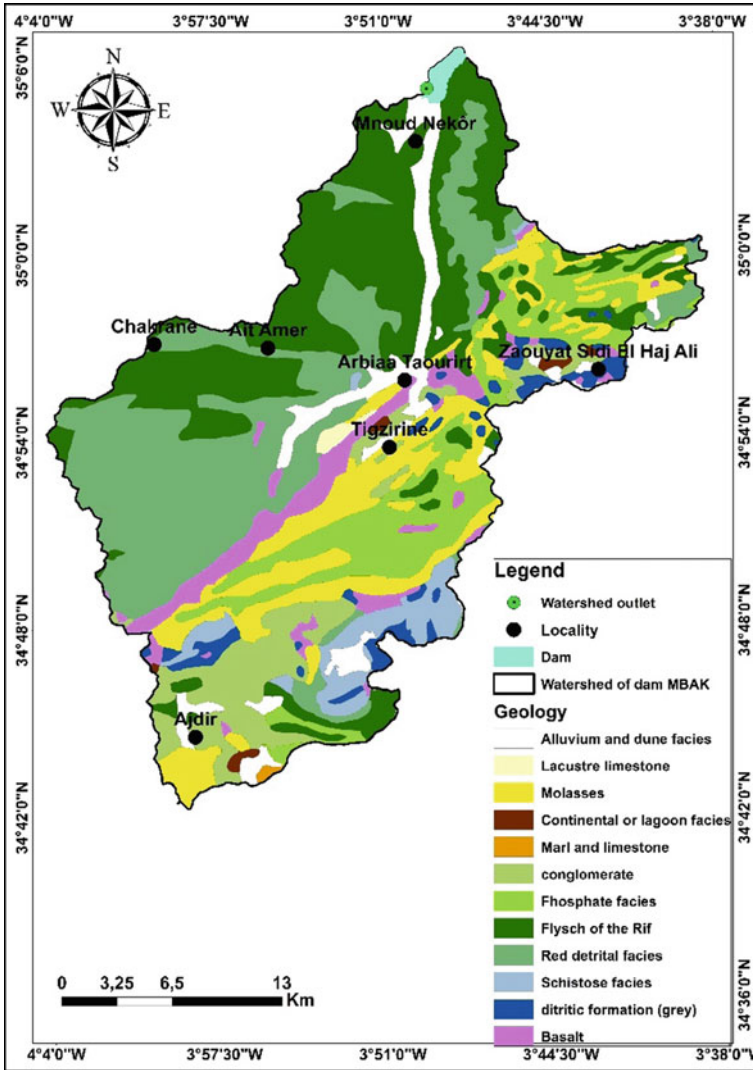


Fig. 4.2 Geological map of the study area (Compiled and modified from Mourier 1982)

This model has been recognized as the most used model for quantifying land loss and assisting in soil conservation to control water erosion (Millward and Mersey 1999). RUSLE is also applicable at a large scale (Xiong et al. 2018); it also provides insight into erosion at the watershed scale.

The soil loss equation is expressed in Eq. (4.1) (Renard et al.1996):

$$A = R.K.L.S.C.P \tag{4.1}$$

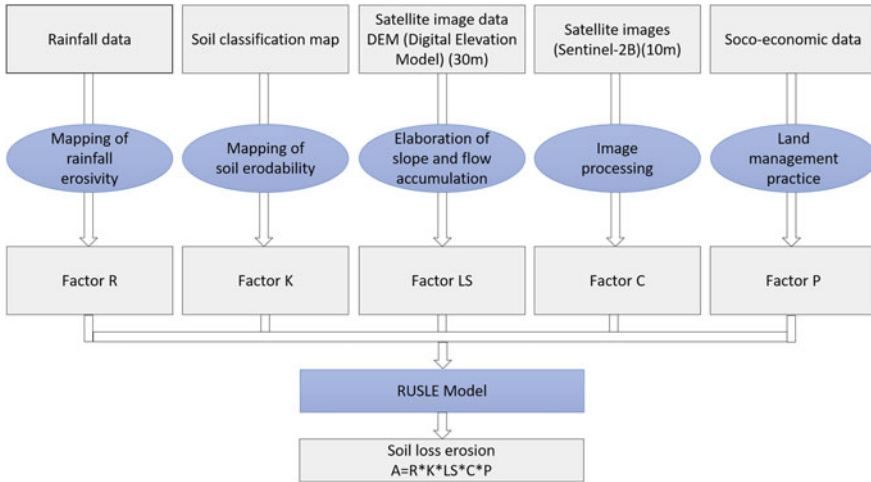


Fig. 4.3 Methodological framework of the RUSLE model

With:

A = Annual soil loss in tons/ha/year

R = Rainfall Erosivity Factor in MJ mm/ha/h/year

K = Soil Erodibility Factor in t. ha/MJ.mm

LS = Topographic factor representing the length (L in m) and slope (S in %)

C = Cover Management factor

P = Support Practice factor

Each RUSLE model factor contributes directly to the soil loss phenomenon and affects the severity of erosion. The methodology consists in multiplying all the obtained information layers related to the RUSLE factors gives a GIS to establish the erosion risk map giving the erosion value for each cell.

4.3.1 R-factor

Rainfall erosivity is the potential ability of rainfall to cause water erosion (Hudson 1981). It is one of the major factors in soil water erosion. When the soil is saturated, rainwater can no longer infiltrate and pull away from its particles. This factor depends on the height, intensity, kinetic energy, and rainfall distribution. According to Wischmeier and Smith (1978), the calculation of the R-factor requires kinetic energy (E_c) and average intensity over 30 min (I_{30}) of the raindrops of each shower. They are given by the empirical formula (Eq. 4.2) of Wischmeier and Smith (1978).

$$R = E_c I_{30} \tag{4.2}$$

Where

E_C = kinetic energy of the rain (MJ/ha)

I_{30} = maximum rainfall intensity in 30 min expressed in mm/h

However, in the absence of data on the average intensity of rainfall every 30 min, many equations allow the calculation of R as a function of monthly and annual rainfall or the Fournier index (Roose 1977; Renard et al. 1996). These equations have been applied in different works involving RUSLE modeling and have shown satisfactory results (Morschel and Fox 2004; El Garouani et al. 2008).

The empirical formula of Arnoldus (1980) seems the most appropriate for evaluating this climatic aggressiveness factor. The R factor is expressed as follows (Eq. 4.3):

$$\text{Log } R = 1.74 \cdot \text{Log} \sum \left(\frac{P_i^2}{P} \right) + 1.29 \quad (4.3)$$

Where

P_i = monthly precipitation in (mm)

P = annual rainfall in (mm)

The equation of Arnoldus (1977) since it is the most recent and the most adapted to Moroccan conditions (Issa et al. 2016; Elaloui et al. 2017). The application of this equation in the catchment area of the MBAK dam made it possible to calculate the R-factor at the various stations for which we have their climatic data located near the basin. This R factor was calculated separately for each station, and then we interpolated the results by the IDW interpolation method to have the map of the erosivity factor of the MBAK Dam watershed. The IDW interpolation method was chosen because it is based on the assumption that the estimated precipitation erosivity value of a point is more influenced by nearby known points than by those farther away (Weber and Englund 1992, 1994). In this study, the sampling points of the erosivity of the precipitations are measured during the interpolation so that the influence of the values of R are more important at the measured point, and they decrease when one moves away from the point.

4.3.2 *K-factor*

Soil erodibility depends essentially on the type of soil, climatic variability, and the types of agriculture applied (Roose and Sarrailh 1989). Soil erodibility K is expressed the vulnerability of soil particles to detachment and transport by rain and runoff. The K factor is determined based on some soil characteristics: texture, presence of organic matter, permeability, and depth (Safi et al. 2018; Bouimajane et al. 2020). The following equation (Eq. 4.4) was used to calculate the K factor:

$$K = [2.1 \times 10^{-4} \times (12 - MO)M^{1.14} + 2.5 \times (P - 3)] \quad (4.4)$$

where:

M = is calculated by the formula $M = (\% \text{ fine sand} + \text{Limon}) * (100 - \% \text{ clay})$

MO = percentage of organic matter

P = code of permeability ($1 < b < 4$)

S = structure code ($1 < c < 6$)

These data for the catchment area of Mohamed Ben Abdelkrim El Khattabi Dam are not being provided for all samples. This obliges us to make extrapolations based on the soil map obtained, and supplemented by the data of analyzes established on the same type of soil characterizing our basin (Billaux and Bryssine 1967; El Gharbaoui 1981; Inypsa 1987; Osrirhi et al. 2007; El Kamouné 2009) and using the Wischmeier monogram.

4.3.3 *LS-Factor*

The LS factor is a topographic index representing the terrain's morphology. It considers the length and slope gradient that affects sedimentary deposit production and transport (Roose 1994). The slope has an important influence on the process of water erosion. It exacerbates the effect of storm water runoff. Many formulas allow the calculation of this factor (Wischmeier and Smith 1978; Kalman 1967; Mitasova et al. 1996).

The LS factor was calculated from the Digital Elevation Model (DEM), which was downloaded from NASA (National Aeronautics and Space Administration) SRTM (Shuttle Radar Topography Mission) data in GeoTif format with 30 m resolution using the formula of Wischmeier and Smith (1978) (Eq. 4.5). It is expressed as follows:

$$LS = \left(\frac{L}{22.13} \right)^m (0.065 + 0.045S + 0.0065S^2) \quad (4.5)$$

Where

L = Length of the slope in (m)

S = Gradient of the slope in (%)

M = Factor which depends on the value of S (Wischmeier and Smith 1978):

- $m = 0.5$ for $S > 5.0\%$
- $m = 0.4$ for $3.5 < S < 4.5$
- $m = 0.3$ for $1.0 < S < 3.5$
- $m = 0.2$ for $S = 1.0$

The slope length was determined by the equation related to its average length (Eq. 4.6).

$$L = FA \times RS \quad (4.6)$$

Where

FA = Flow accumulation grid

RS = DEM model resolution (30 m)

4.3.4 C-Factor

The canopy factor C is used to determine the density of the vegetation cover; it is the factor that protects the soils and provides raindrop cushioning, slowing of surface water runoff, and infiltration (Roose 1996; Sabir and Roose 2004). C values range from 1 for bare fallow to 0.001 for fully covered soil (Wischmeier and Smith 1978).

This factor is determined for the BMAK Dam watershed using remote sensing data. A Normalized Difference Vegetation Index (NDVI) (Eq. 4.7) was calculated for the study area using a Sentinel-2B satellite image with a resolution of 10 m. The satellite image was acquired during February when the vegetation cover is at its maximum.

This index gives values between -1 and 1 , representing most of the patterns, where all negative values are mainly generated from clouds, water, and snow, values close to zero are mainly generated from rock and bare soil. Moderate values represent shrubs and grasslands. In contrast, high values indicate areas of dense vegetation cover (forests and matorrals) (Merchant 2000).

$$NDVI = \frac{IR - R}{IR + R} \quad (4.7)$$

Where

NIR = represents the near-infrared band

R = represents the red band

The latter allows estimating the values of the C-factor of the study area. Indeed, De Jong (1994) determined a function for calculating the C-factor from the NDVI (Eq. 4.8):

$$C = 0.431 - 0.805 \times NDVI \quad (4.8)$$

4.3.5 P-Factor

The anti-erosion practices factor P represents soil protection. Anti-erosion practices reduce runoff velocity and thus decrease the risk of water erosion. P values generally range from 0 in developed areas to 1, where soil and slope protection and development are almost absent, depending on the practice adopted and the slope (Wischmeier and Smith 1978). The most soil-conserving anti-erosion practices are contour, alternate

strip or terrace cropping, bench reforestation, ridging, and ridging. In the MBAK Dam watershed, the RUSLE model was run with a P-factor of 1, reflecting the desire for erosion potential under current conditions of no soil conservation practices (Renard et al. 1996; Hammad et al. 2004).

4.3.6 Evaluation of Soil Losses A

A is expressed as the average annual soil loss possible in the long term. Applying the equation of Wischmeier and Smith (1978) in the MBKA dam watershed allowed the estimation of soil losses and the mapping of potential erosion. This was done by superimposing the thematic maps obtained (five in number) and multiplying the corresponding indices by using the spatialization tools of the geographic information system (GIS) and remote sensing (Fig. 4.3).

The values of the corresponding indices are varied as follows:

- Climatic aggressiveness (R): from 27.48 to 32.76 MJ mm/ha/h/year
- Soil erodibility (K): from 0.15 to 1t. ha/MJ.mm
- Topography (LS): from 0 to 40.20
- Vegetation cover (C): from -0.54 to 0.46
- Anti-erosion practices (P): 1.

4.4 Results and Discussions

4.4.1 Rainfall Erosivity Factor (R)

The rainfall erosivity factor depends mainly on the rainfall data. The energy intensity of the precipitated water and the runoff water causes soil loss. The R-factor was calculated based on monthly and annual climate data from 7 meteorological stations surrounding the watershed (Table 4.2).

Table 4.2 Rainfall erosivity index (R) of weather stations

Meteorological station	Erosivity index R
Barrage MBAK	29.77
Al Hoceima	32.08
Aknoul	31.30
Boured	34.50
Tamassint	23.58
Ajdir	34.79
Tizi Oussli	29.90

The erosivity map made from climatic data represents the spatialization of the R factor in the watershed of the MBAK dam. Figure 4.4 shows that the value of R varies from 27.48 to 32.76 MJ/mm/ha/h/year. These results show that despite its semi-arid climate, the study area is subject to significant rainfall erosion. The distribution of the R factor on the map shows that the high values are recorded in the South and South-West of the basin (Upstream of the watershed); a large area is subject to moderate erosion, while the low values are recorded in the North-East of the watershed.

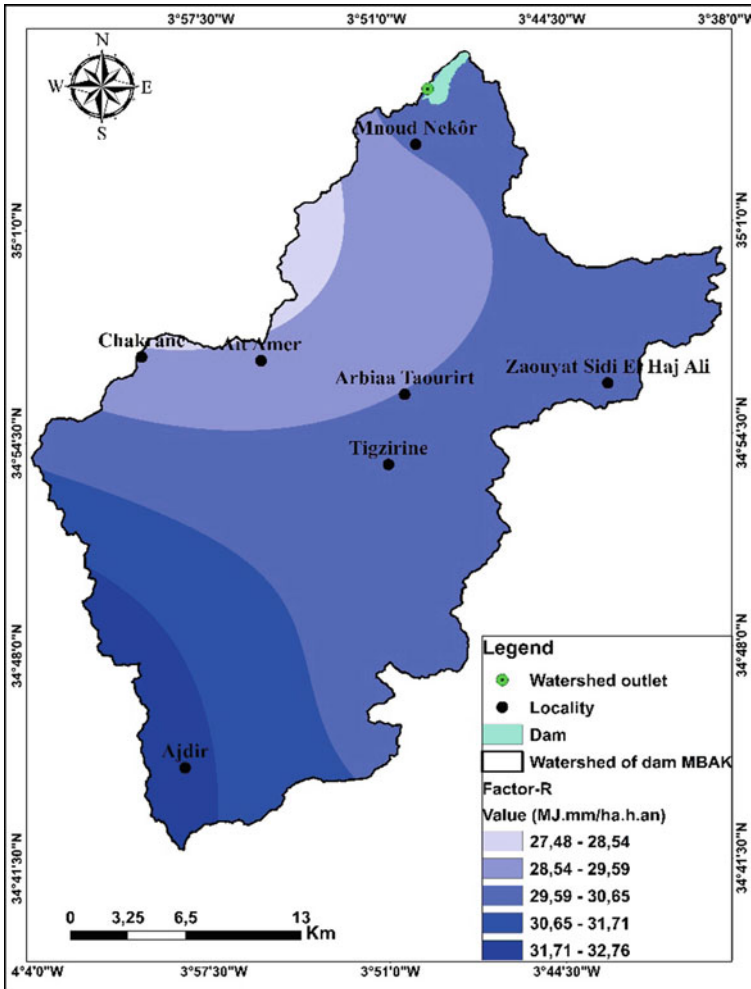


Fig. 4.4 Spatial distribution of rainfall erosivity factor (R) at MBAK

Table 4.3 Average K-factor values for each soil type

Type of soil	K-Factor
Association of raw mineral soils, calcimagnesian soils, and brunified soils	0.25
Association of crude mineral soils, little evolved soils, and fersiallitic soils	0.34
Association of poorly evolved soils and calcimagnesian Soils	0.41
Association of poorly evolved soils and fersiallitic soils	0.33
Association of poorly evolved soils, brunified soils, and fersiallitic soils	0.26
Brunified soils	0.15
Calcimagnesian soils	0.22
Fersiallitic soils	0.21
Crude mineral soils	0.38
Poorly evolved soils	0.44
Sodic soils	0.35

4.4.2 Soil Erodibility (K)

The evaluation of the k-index in the MBAK dam watershed was done based on the pedological map of the Rif oriental: At a scale of 1:500,000 (Ministry of Agriculture, Rural Development and Water and Forests, and National Institute of Agronomic Research) and completed by the data of the set of analyses of different types of soils characterized the watershed (Table 4.3).

The K values in the watershed are between 0.15 and 1 (Fig. 4.5), proving the soils' fragility (medium to high) and their susceptibility to erosion. Indeed, the synthetic map obtained shows that 13.97% of the watershed's surface has a high erodibility factor of 1, represented by the class of the association of soils not significantly evolved and calci-magnesian soils with K varying from 0.43 to 1. Almost 14.05% of the watershed's surface consists of elements that have an erodibility factor of 0.34, represented by the class of fersi-allitic soils with K varies between 0.34 and 0.43. In comparison, the association of crude mineral soils, calci-magnesian soils, and browned soils present a low erodibility of 0.25 with 27.74% of the watershed's surface. The rest of the studied surface presents relatively average values with a predominance of the not very evolved soils and fersi-allitic soils (28.11%), which shows a rather average erodibility with K varying from 0.15 to 0.34.

4.4.3 The Topographic Factor (LS)

The topographical factor depends on the slope and its length; the more significant the length of the plot, the greater the speed of runoff. The flowing water particles store a lot of energy, which causes the uprooting and digging of the soil. The topographic factor map was created by superimposing the slope map and the slope length map.

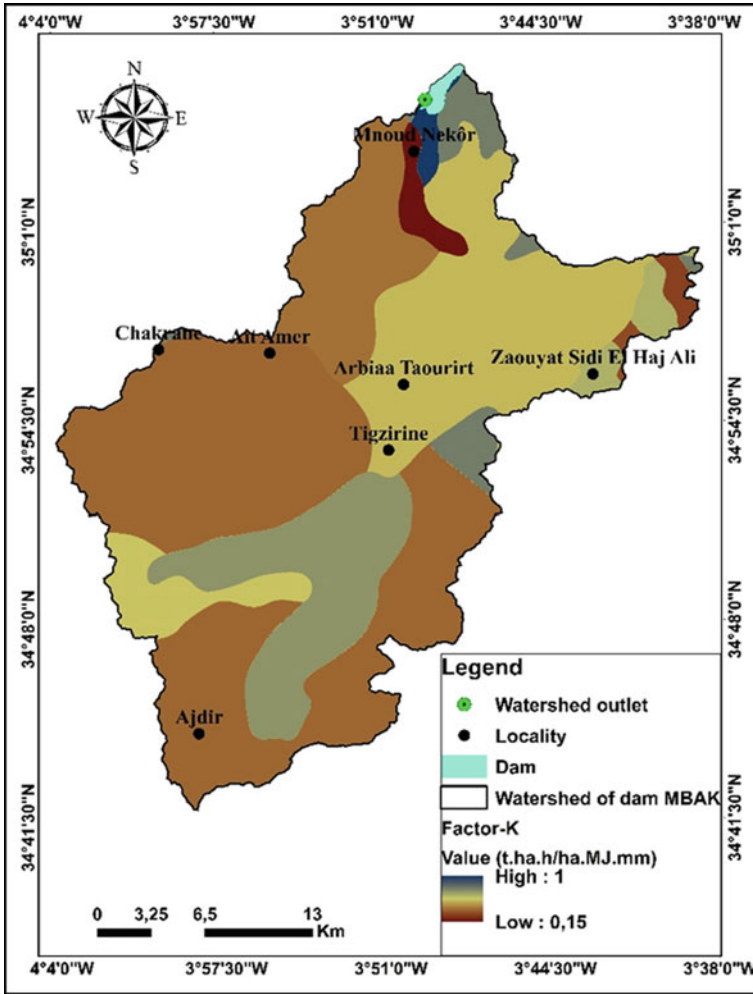


Fig. 4.5 Spatial distribution of soil erodibility factor K at MBAK basin

The values obtained for LS vary between 0 and 40.2. The topographic factor map (Fig. 4.6) shows that most basins have low LS values, while the average LS values are mostly placed towards the extremities and southwest of the basin.

4.4.4 The Vegetation Cover Factor (C)

The vegetation cover factor C map (Fig. 4.7) shows the distribution of vegetation cover over the entire watershed, while the large C values occupy small areas in the

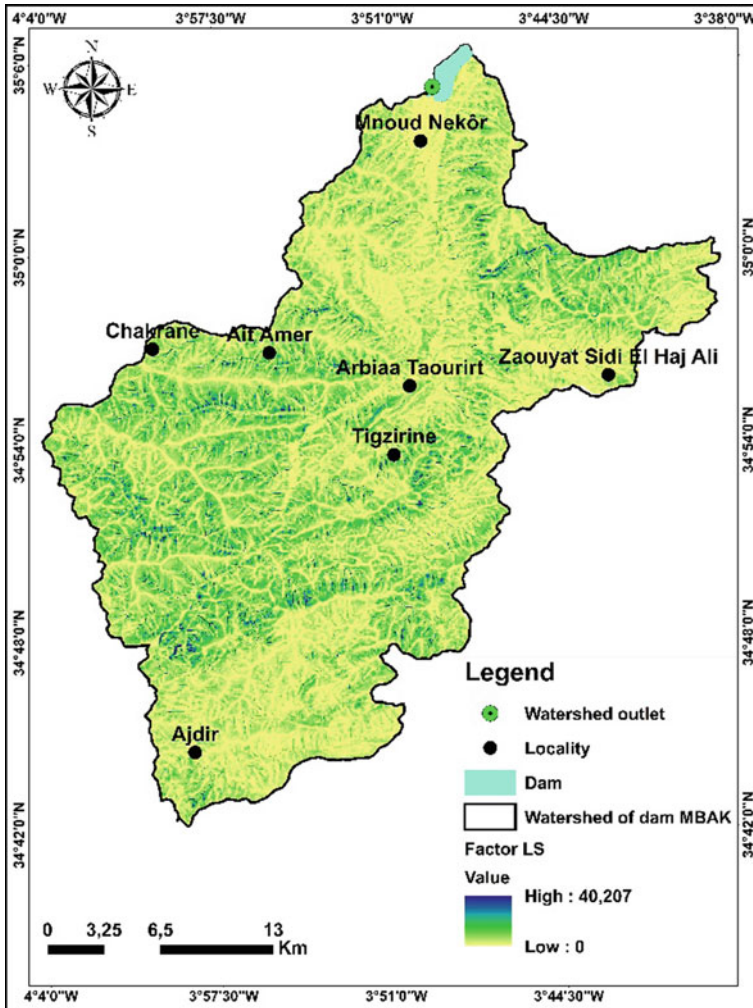


Fig. 4.6 Spatial distribution of topographic factor (LS) at MBAK basin

watershed. They are located at the ends and somewhat in the middle of the watershed, corresponding to dense medium vegetation and cultivated land. The minor C values present on a large surface correspond to water bodies and bare soils; they do not protect the soil against erosion, which leads us to say that erosion would probably be accentuated in this part of the watershed.

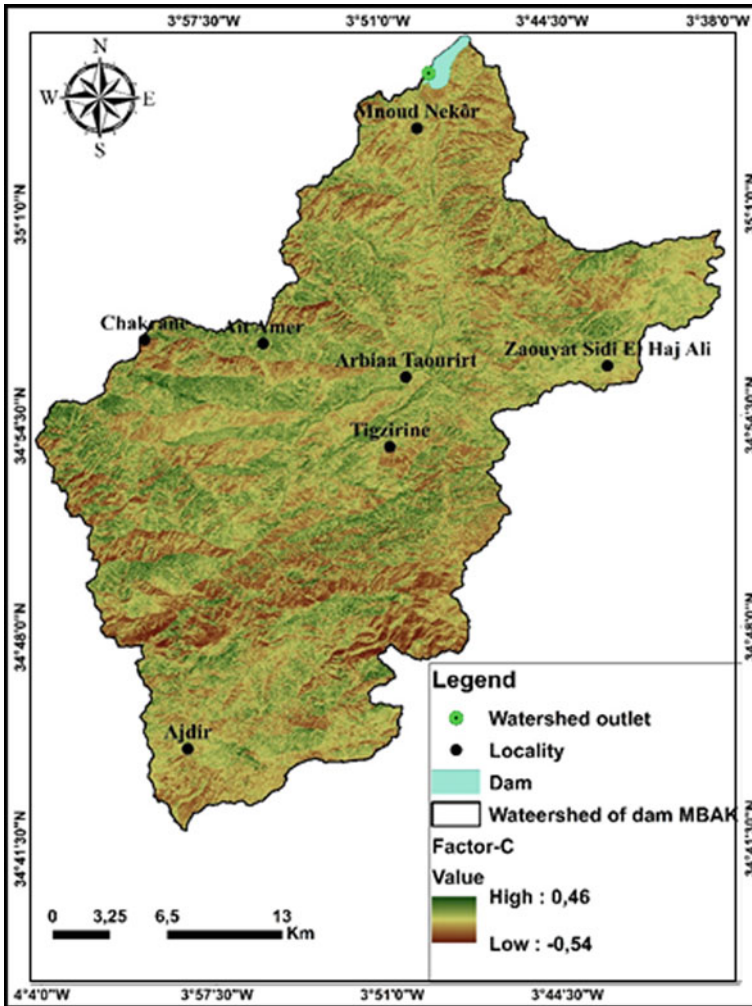


Fig. 4.7 Spatial distribution of vegetation coverage factor (C) at MBAK basin

4.4.5 Anti-erosion Practices Factor (P)

The values of the anti-erosion practices factor depend essentially on the practices adopted in each location. There are no erosion control measures in the entire MBak dam watershed, and farmers do not use erosion control practices. Crops are mostly cereal, and plowing is rarely parallel to the contour lines. A few attempts to rehabilitate forests by reforestation, but not by benching. In this context, the value $P = 1$ was assigned to the entire watershed.

4.4.6 Soil Losses A

The application of the Renard et al. (1996) equation in the MBAK watershed allowed for the estimation of soil losses and mapping of potential erosion, this was done by crossing the different factors of the RUSLE model, allowing us to elaborate a spatialized soil loss map in the entire watershed (Fig. 4.8).

The methodology used allowed us to establish the erosion risk map. It shows that the losses vary from 0 to 173.39 t/ha/year. The rate of erosion calculated by the model allows knowing the spatial distribution of erosive risks. It varies from one area

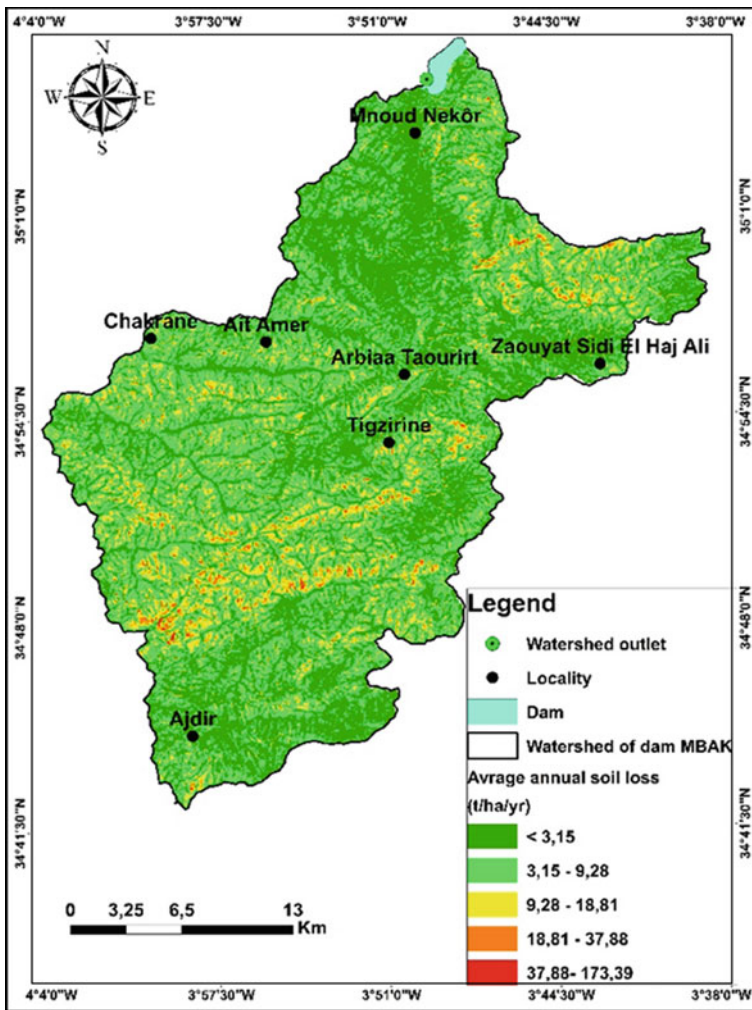


Fig. 4.8 Spatial distribution of potential erosion risk map of MBAK basin

to another of the watershed according to the influence of the different explanatory factors that control erosion: the slope, the climatic aggressiveness, the type and rate of vegetation cover, and the anthropic action.

Annual soil losses analysis shows that the very low values of soil loss (less than 3.15 t/ha/year) are located in large areas of the watershed (57%), represented by the alluvial terraces of wadis where there are flat losses at the very low slope (2° to 7°) and irrigated land or plantations (dense vegetation) that maintains the soil and therefore a solid resistance to erosion. However, 26.31% of the basin area represents a soil loss value between 9.28 and 18.81 t/ha/year. Almost 10.23% of the watershed area has an average A value between 18.81 and 37.88 t/ha/yr. The rest of the studied area has a relatively high to a very high value (3.75%), which shows a soil loss A of 37.88 to 173.39 t/ha/year at the level of steep and bare land. The values calculated by the empirical soil loss evaluation model (RUSLE) of Wischmeier and Smith (1978) are discussed. However, the method is among the decision support tools for planners, as it allows the simulation of soil protection and conservation scenarios to plan erosion control interventions, especially on slopes where water erosion is predominant (El Hafid et al. 2012).

This empirical model is the most widely used empirical method for estimating soil loss (Renard et al. 2011). However, it has several limitations and is subject to numerous criticisms. Indeed, Roose et al. (2012) observed that the topographic exposure of slopes is sometimes more important than the slope itself. Furthermore, many authors (e.g. Finlayson and Montgomery 2003; Nekhay et al. 2009; Rahmati et al. 2017; Pourghasemi et al. 2017; Ikirri et al. 2021; Aswathi et al. 2022; Ait Haddou et al. 2022; Ikirri et al. 2022; Benjmel et al. 2022; Echogdali et al. 2022a, b, c, d) have found that drainage density has a decisive impact on the vulnerability of soil subjected to floodwaters. Despite these imperfections, it remains a management and planning tool for decision-makers. These limitations must be considered and adapted by integrating GIS, which makes it possible, on the one hand, to quantify annual soil losses and, on the other hand, to map erosive risk areas that require intervention strategies for soil protection and to reduce the silting of certain hill dams. In any case, field verifications remain fundamental in this type of approach.

4.5 Conclusion

The catchment area of the MBAK dam is a favorable environment for the development of water erosion phenomena. The watershed has a length nine times greater than the width. The hypsometry shows that 52% of the basin corresponds to very high altitudes (1000–2000 m). The overall slope index is 13.96 m/km. The specific vertical drop is equal to 388.12 m which shows according to the ORSTOM classification that a substantial relief characterizes the basin. The study presents the results of a cartographic work based on the superposition of the maps of the factors of the Revised Universal Soil Loss Equation (RUSLE) of Wischmeier and Smith (1978)

using the Geographic Information System (GIS) to elaborate a water erosion map. The results of this study revealed that:

- 14% of the basin area is at high risk of water erosion with average annual losses between 18.81–173.39 t/ha/year.
- The low losses are located mainly on low slopes, low erodibility soils, and minimal precipitation values.
- The factors in the equation used (erodibility, topography, climatology, and vegetation cover) correlate well with soil losses. Soil degradation in the MBAK watershed has environmental effects (silting of the dam) and negative socio-economic consequences.
- The results obtained in this work can be used as a basis to assist in planning soil conservation activities and reducing dam siltation. The RUSLE model is a decision support tool for watershed management by erosion control administrations, although it is still under discussion for use.

In addition, many perspectives can be considered:

- Improve the accuracy of the RUSLE model, which could integrate new parameters or by “field” validation of the results.
- Use other models and techniques, such as the SWAT and radioactive labeling techniques (^{137}Cs and ^{210}Pb).
- Develop watershed land surface management and planning systems based on numerous studies on soil erosion and degradation in a given area.

Author Contributions The manuscript was written through the contributions of all authors. No seniority of authorship is implied by the order of names; this chapter is the product of a true and entirely equal collaboration. All authors have read and agreed to the published version of the manuscript.

Acknowledgements The authors are grateful to the co-editor Dr. Aliva Nanda (University of California, Merced, USA), and an anonymous reviewer for making time to review the manuscript and for their valuable comments and recommendations. The authors are much obliged to the Springer proofreading team for handling the work, sending reviews, and preparing the proof.

References

- Ait Haddou M, Wanaim A, Ikirri M, Aydda A, Bouchriti Y, Abioui M, Kabbachi B (2022) Digital elevation model-derived morphometric indices for physical characterization of the Issen basin (Western High Atlas of Morocco). *Ecol Eng Environ Tech* 23(5):285–298. <https://doi.org/10.12912/27197050/152161>
- Amil M (1992) Bassin versant du Nekor: Recherche des zones sources d’envasement de la retenue du barrage Mohamed Ben Abdelkrim Aïkhattabi (Maroc). Ph.D Dissertation, Université Cheikh Anta Diop

- Arrebei N, Sabir M, Naimi M, Chikhaoui M, Raclot D (2019) Reconstitution des données historiques et diagnostic de l'état actuel des aménagements antiérosifs dans le bassin versant Nekôr. Moroccan J Agron Vet Sci 7(2):287–306
- Arnoldus HMJ (1977) Methodology used to determine the maximum average soil loss due to sheet and rill erosion in Morocco. FAO Soil Bull 34:39–51
- Arnoldus HMJ (1980) An approximation of the rainfall factor in the universal soil loss equation. In: de Boodt M, Gabriels D (eds) Assessment of erosion. Wiley, Chichester, pp 127–132
- Aswathi J, Sajinkumar KS, Rajaneesh A, Oommen T, Bouali EH, Binojkumar RB, Rani VR, Thomas J, Thrivikramji KP, Ajin RS, Abioui M (2022) Furthering the precision of RUSLE soil erosion with PSInSAR data: an innovative model. Geocarto Int. <https://doi.org/10.1080/10106049.2022.2105407>
- Beasley DB (1977) A mathematical model for simulating the effects of land use and management on water quality. PhD Dissertation, Purdue University
- Benjmel K, Amraoui F, Aydda A, Tahiri A, Yousif M, Pradhan B, Abdelrahman K, Fnais MS, Abioui M (2022) A multidisciplinary approach for groundwater potential mapping in a fractured semi-arid terrain (Kerdous Inlier, Western Anti-Atlas, Morocco). Water 14(10):1553
- Billiaux P, Bryssine G (1967) Les sols du Maroc. Cah Rech Agron 1(24):59–101
- Boggs G, Devonport C, Evans K, Puig P (2001) GIS-based rapid assessment of erosion risk in a small catchment in the wet/dry tropics of Australia. Land Degrad Dev 12(5):417–434
- Bouimajjane L, Belfoul MA, Elkadiri R, Stokes M (2020) Soil erosion assessment in a semi-arid environment: a case study from the Argana Corridor, Morocco. Environ Earth Sci 79(18):409
- Bonilla CA, Reyes JL, Magri A (2010) Water erosion prediction using the revised universal soil loss equation (RUSLE) in a GIS framework, central Chile. Chile J Agric Res 70(1):159–169
- Chafouq D, El Mandour A, Elgettafi M, Himi M, Chouikri I, Casas A (2018) Hydrochemical and isotopic characterization of groundwater in the Ghis-Nekor plain (northern Morocco). J Afr Earth Sci 139:1–13
- Dabral PP, Baithuri N, Pandey A (2008) Soil erosion assessment in a hilly catchment of North Eastern India using USLE, GIS and remote sensing. Water Resour Manage 22(12):1783–1798
- De Jong SM (1994) Application of reflective remote sensing for land degradation studies in a Mediterranean environment. PhD Dissertation, University of Utrecht
- De Roo APJ, Wesseling CG, Ritsema CJ (1996) LISEM: a single-event physically based hydrological and soil erosion model for drainage basins. I: theory input and output. Hydrol Process 10(8):1107–1117
- Echogdali FZ, Kpan RB, Ouchchen M, Id-Belqas M, Dadi B, Ikirri M, Abioui M, Boutaleb S (2022a) Spatial Prediction of Flood Frequency Analysis in a Semi-Arid Zone: A Case Study from the Seyad basin (Guelmim Region, Morocco). In: Rai PK, Mishra VN, Singh P (eds) Geospatial Technology for Landscape and Environmental Management: Sustainable Assessment and Planning. Springer, Singapore, pp 49–71
- Echogdali FZ, Boutaleb S, Kpan RB, Ouchchen M, Bendarma A, El Ayady H, Abdelrahman K, Fnais MS, Sajinkumar KS, Abioui M (2022b) Application of fuzzy logic and fractal modeling approach for groundwater potential mapping in semi-arid Akka basin, Southeast Morocco. Sustainability 14(16):10205
- Echogdali FZ, Boutaleb S, Bendarma A, Saidi ME, Aadraoui M, Abioui M, Ouchchen M, Abdelrahman K, Fnais MS, Sajinkumar KS (2022c) Application of analytical hierarchy process and geophysical method for groundwater potential mapping in the Tata basin, Morocco. Water 14(15):2393
- Echogdali FZ, Boutaleb S, Taia S, Ouchchen M, Id-Belqas M, Kpan RB, Abioui M, Aswathi J, Sajinkumar KS (2022d) Assessment of soil erosion risk in a semi-arid climate watershed using SWAT model: case of Tata basin, South-East of Morocco. Appl Water Sci 12(6):137
- Elaloui A, Marrakchi C, Fekri A, Maimouni S, Aradi M (2017) USLE-based assessment of soil erosion by water in the watershed upstream Tessaoute (Central High Atlas, Morocco). Model Earth Syst Environ 3(3):873–885

- El Gharbaoui A (1981) La terre et l'Homme dans la péninsule tingitane : étude sur l'homme et le milieu naturel dans le Rif Occidental. *Trav Inst Sci* 15:1–439
- El Garouani A, Chen H, Lewis L, Triback A, Abahrour M (2008) Cartographie de l'utilisation du sol et de l'érosion nette à partir d'images satellitaires et du SIG IDRISI au Nord-Est du Maroc. *Téledétection* 8(3):193–201
- El Kamoune I (2009) Application du modèle STREAM pour la simulation de l'érosion dans le bassin versant Tleta (Rif occidental, Maroc). Mémoire de 3ème Cycle, Institut Agronomique et Vétérinaire Hassan II
- El Hafid D, Julia R, Akdim B (2012) Erosion, aménagement et risque hydrologique dans le bassin versant de l'oued Sidi Yahya (Oujda, Maroc). *Rev Géogr Maroc* 27:79–90
- Finlayson DP, Montgomery DR (2003) Modeling large-scale fluvial erosion in geographic information systems. *Geomorphology* 53(1–2):147–164
- Hammad AA, Lundekvam H, Børresen T (2004) Adaptation of RUSLE in the eastern part of the Mediterranean region. *Environ Manage* 34(6):829–841
- Hudson N (1981) Soil conservation, 2nd edn. Cornell University Press, Ithaca
- Ikirri M, Faik F, Boutaleb S, Echogdali FZ, Abioui M, Al-Ansari N (2021) Application of HEC-RAS/WMS and FHI models for the extreme hydrological events under climate change in the Ifni River arid watershed from Morocco. In: Nistor MM (ed) *Climate and Land Use Impacts on Natural and Artificial Systems: Mitigation and Adaptation*. Elsevier, Amsterdam, pp 251–270
- Ikirri M, Faik F, Echogdali FZ, Antunes IMHR, Abioui M, Abdelrahman K, Fnais MS, Wanaim A, Id-Belqas M, Boutaleb S, Sajinkumar KS, Quesada-Román A (2022) Flood hazard index application in arid catchments: case of the Taguenit Wadi watershed, Lakhssas, Morocco. *Land* 11(8):1178
- Inypsa (1987) Etude des sols au 1/100.000 (Edition au 1/50.000). *Projet Intégré de développement Agricole de Tanger-Tétouan, Secteur de Tétouan*. Inypsa—Maroc, S.A. & Direction Provinciale de l'Agriculture de Tétouan, Carte, 1p
- Issa LK, Lech-Hab KBH, Raissouni A, El Arrim A (2016) Cartographie quantitative du risque d'érosion des sols par approche SIG/USLE au niveau du bassin versant Kalaya (Maroc Nord Occidental). *J Mater Environ Sci* 7(8):2778–2795
- Jasrotia AS, Singh R (2006) Modeling runoff and soil erosion in a catchment area, using the GIS, in the Himalayan region, India. *Environ Geol* 51(1):29–37
- Kalman R (1967) Essai d'évaluation pour le pré-Rif du facteur couverture végétale de la formule de Wischmeier de calcul de l'érosion. In : *Rapport pour l'administration de la forêt et d'eau*, Rabat, pp 1–12
- Knisel WG (1980) Erosion and sediment yield models - an overview. In: *Proceedings of ASCE symposium on watershed management*, Boise, Idaho, vol 1, pp 141–150
- Lu D, Li G, Valladares GS, Batistella M (2004) Mapping soil erosion risk in Rondonia, Brazilian Amazonia: using RUSLE, remote sensing and GIS. *Land Degrad Dev* 15(5):499–512
- Merchant JW (2000) Remote sensing of the environment: an earth resource perspective. *Cartogr Geogr Inf Sci* 27(4):311–311
- Mitasova H, Hofierka J, Zlocha M, Iverson LR (1996) Modelling topographic potential for erosion and deposition using GIS. *Int J Geogr Inf Syst* 10(5):629–641
- Millward A, Mersey JE (1999) Adapting the RUSLE to model soil erosion potential in a mountainous tropical watershed. *Catena* 38(2):109–129
- Mourier T (1982) Etude géologique et structurale du Massif des Bokkoya (Rif oriental, Maroc) : étapes de structuration de la Dorsale et tectonique longitudinale. Ph.D Thesis, Paris-Sud University
- Morschel J, Fox D (2004) Une méthode de cartographie du risque érosif: application aux collines du Terrefort Lauragais. *Mappemonde* 76, 11p
- Nekhay O, Arriaza M, Boerboom L (2009) Evaluation of soil erosion risk using Analytic Network Process and GIS: a case study from Spanish mountain olive plantations. *J Environ Manage* 90(10):3091–3104

- Osirhi A, Eloumri M, Moussadek R (2007) Vocation agricole des terres de la province de Tanger- Rapport et cartes. Report, Institut National de la Recherche Agronomique, Rabat, 27p
- Pandey A, Mathur A, Mishra SK, Mal BC (2009) Soil erosion modeling of a Himalayan watershed using RS and GIS. *Environ Earth Sci* 59(2):399–410
- Pourghasemi HR, Yousefi S, Kornejady A, Cerdà A (2017) Performance assessment of individual and ensemble data-mining techniques for gully erosion modeling. *Sci Total Environ* 609:764–775
- Rahmati O, Tahmasebipour N, Haghizadeh A, Pourghasemi HR, Feizizadeh B (2017) Evaluation of different machine learning models for predicting and mapping the susceptibility of gully erosion. *Geomorphology* 298:118–137
- Raissouni A, Issa L, Lech-Hab K, Arrim AE (2016) Water erosion risk mapping and materials transfer in the Smir dam watershed (Northwestern Morocco). *J Geogr Environ Earth Sci Int* 5(1):1–17
- Renard KG, Foster GR, Weesies GA, McCool DK, Yoder DC (1996) Predicting soil erosion by water: a guide to conservation planning with the Revised Universal Soil Loss Equation (RUSLE). *Agriculture Handbook No. 703*, USDA-ARS, Washington
- Renard KG, Yoder DC, Lightle DT, Dabney SM (2011) Universal soil loss equation/revised universal soil loss equation. In: Morgan RPC, Nearing MA (eds) *Handbook of Erosion Modelling*. Blackwell Publishing Ltd., Hoboken, New Jersey, pp 135–167
- Roose E (1977) Use of the universal soil loss equation to predict erosion in West Africa. In: Foster GR (ed) *Soil erosion: prediction and control* (vol 21). Soil Conservation Society of America, Ankeny, pp 60–75
- Roose E (1994) Introduction à la gestion conservatoire de l'eau, de la biomasse et de la fertilité des sols (GCES). *Bull Pédol FAO* 70, 420p
- Roose E (1996) Méthodes de mesure des états de surface du sol, de la rugosité et des autres caractéristiques qui peuvent aider au diagnostic de terrain des risques de ruissellement et d'érosion, en particulier sur les versants cultivés des montagnes. *Bull Réseau Erosion* 16:87–97
- Roose E, Sarrailh JM (1989) Erodibilité de quelques sols tropicaux. Vingt années de mesure en parcelles d'érosion sous pluies naturelles. *Cah ORSTOM Pédol* 25(1–2):7–30
- Roose E, Sabir M, Arabi M, Morsl B, Mazour M (2012) Soixante années de recherches en coopération sur l'érosion hydrique et la lutte antiérosive au Maghreb. *Physio-Géo* 6:43–69
- Safi J, El-Nahhal Y, Safi M (2018) Particle size distribution and hydraulic conductivity in coastal non-agricultural land in Gaza coastal plain. *Int J Geosci* 9(10):619
- Sabir M, Roose E (2004) Influences du couvert végétal et des sols sur le stock de carbone du sol et les risques d'érosion et de ruissellement dans les montagnes méditerranéennes du Rif Occidental (Maroc). *Bull Réseau Erosion* 23:144–154
- Salhi A (2008) Géophysique, hydrogéologie et cartographie de la vulnérabilité et du risque de pollution de l'aquifère de Ghis-Nekor (Al Hoceima, Maroc). Ph.D Thesis, Abdelmalek Essaadi University
- Tadrist N, Debauche O (2016) Impact de l'érosion sur l'envasement des barrages, la recharge des nappes phréatiques côtières et les intrusions marines dans la zone semi-aride méditerranéenne : cas du barrage de Boukourdane (Algérie). *Biotechnol Agron Soc Envir* 20(4):453–467
- Touaibia B, Gomer D, Aidaoui A (2000) Estimation de l'index d'érosion de Wischmeier dans les micro-bassins expérimentaux de l'Oued Mina en Algérie du Nord. *Bull Réseau Erosion* 20:478–484
- Villeneuve J, Hubert P, Mailhot A, Rousseau A (1998) La modélisation hydrologique et la gestion de l'eau. *Rev Sci Eau* 11:19–39
- Weber DD, Englund EJ (1994) Evaluation and comparison of spatial interpolators II. *Math Geol* 26(5):589–603
- Weber DD, Englund EJ (1992) Evaluation and comparison of spatial interpolators I. *Math Geol* 24(4):381–391
- Wischmeier WH, Smith D (1978) *Predicting rainfall erosion losses—a guide to conservation planning*. US Department of Agriculture Press, Maryland

- Williams JR, Renard KG (1985) Assessments of soil erosion and crop productivity with process models (EPIC). In: Follett RF, Stewart BA (eds) *Soil Erosion and Crop Productivity*. American Society of Agronomy, Madison, WI, pp 68–102
- Wilson JP, Lorang MS (2000) Spatial models of soil erosion and GIS. In: Fotheringham AS, Wegener M (eds) *Spatial models and GIS: new potential and new models*. Taylor & Francis, Philadelphia, PA, pp 83–108
- Xiong M, Sun R, Chen L (2018) Effects of soil conservation techniques on water erosion control: A global analysis. *Sci Total Environ* 645:753–760
- Yahiaoui A (2012) Inondations torrentielles. Cartographie des zones vulnérables en Algérie du Nord (cas de l'oued Mekerra, Wilaya de Sidi Bel Abbès). Ph.D Dissertation, École Nationale Polytechnique

Part II
Water-Agriculture-Climate Linkage

Chapter 5

Estimating Soil Moisture Using Remote Sensing in Zimbabwe: A Review



Never Mujere and Hardlife Muhoyi

Abstract Soil moisture is an essential parameter for understanding the interactions and feedbacks between the atmosphere and the Earth's surface through energy and water cycles. Knowledge of the spatiotemporal distribution of land surface soil moisture for various environmental and socio-economic studies. Over recent past years, remote sensing using *electromagnetic spectra* from the optical/thermal to the microwave regions, have been intensively investigated for soil moisture retrieval, providing of several algorithms, models and products that are available for actual applications. However, the use of remote sensing technologies in estimating soil moisture is a challenge in low-income economies due to resource constraints. This present study gives a critical review of the remote sensing approaches applied in estimating soil moisture in Zimbabwe. The research findings show that remote sensing products have little been used in soil moisture monitoring in Zimbabwe.

Keywords GIS · Remote sensing techniques · Soil moisture · Zimbabwe

5.1 Introduction

At global scale, it is considered that at least 65% of precipitation returns to the atmosphere as green water while the remainder is either stored in the soil or become runoff (Bittelli 2011). Green water flow refers to water lost as actual evapotranspiration that is released back into the atmosphere via evaporation from both the soil, water bodies and transpiration from vegetation. Green water storage is also termed soil moisture or soil water. Soil moisture is the amount of water stored in the pore spaces between soil particles in the unsaturated soil zone or the vadose zone (Falkenmark and Rockström 2006). Soil moisture can also be grouped into surface soil moisture and root-zone

N. Mujere (✉)

Department of Geography Geospatial Sciences and Earth Observation, University of Zimbabwe, Harare, Zimbabwe
e-mail: nemuj@yahoo.co.uk

H. Muhoyi

Department of Geography and Geo-Information Sciences, Lupane State University, Bulawayo, Zimbabwe

soil moisture (Narasimhan and Srinivasan 2005). Surface soil moisture is the total amount of water found in the upper-most 10 cm of the soil profile. The water available in these first few centimetres of a soil layer is either stored or exchanged between the surface and atmosphere (Zhang et al. 2020). The amount of surface soil moisture determines how much rainfall is turned into runoff and, water movement and redistribution through infiltration, evaporation, percolation, and transpiration. Water available from the upper-most 200 cm of the soil profile is considered as root zone moisture. This is the water that is needed and available to be used by plants (Moran et al. 2004). Nevertheless, plants extract moisture from both the surface- and root-zone reservoirs through transpiration, but only the surface moisture zone is subject to evaporation. Vegetation growth development and their health are a function of the quantities of water as determined by the root zone moisture.

Soil moisture content is a soil property that is an essential parameter when it comes to appreciating the hydrological cycle and energy heat budget (Gumindoga et al. 2020; Zhang et al. 2020). It affects the critical hydrological, geomorphological, geological, ecological, and biogeochemical as well as the meteorological processes (Marumbwa et al. 2015). Knowledge of soil moisture variation in time and space is key in understanding both natural processes, water balance; and human activities e.g. irrigation scheduling. However, the concept of the term soil moisture varies depending on the area of application for example the farmer, water resource's manager and a meteorologist have got a different appreciation of the concept of soil moisture.

Therefore, depending on the field of specialisation and scale at which the measurements are taken, a calling for an accurate soil information forms part of the most important step for example in irrigation scheduling as in agricultural activities. When trying to maximise on food security, drought monitoring and yield forecasting as extrapolated from soil moisture modelling can promote economic and wise use of water, this is most relevant in the arid and semi-arid regions (Marumbwa et al. 2015). Moisture regimes affect the timing of irrigation, which must be applied at the right time, right place, and in the right amount for consistently high yields (Moran et al. 1994). Seed germination, plant growth, and plant nutrition require adequate amounts of soil moisture. Crop production in arid and semi-arid regions of the world, is determined by the available soil moisture either as derived from irrigation or precipitation (Marumbwa et al. 2015). Due to the high moisture content during the growing season which is mostly associated with rains or being supplemented by irrigation, crop yield has shown a linear relationship with soil moisture (Shafian and Maas 2015). It is from this understanding of the link between crop water requirement and crop productivity that accurate estimation of soil moisture is vital for activities such as irrigation scheduling.

Excessive water application lowers yield since excess water promotes leaching. This leads to nitrates being carried below reasonable depths of root penetration, displacing available soil air hence causing a lack of oxygen to the roots. Low soil moisture for sustained periods results in drought, reduced crop yields and plant water deficit and can potentially lead to wildfires. Conversely, high soil moisture leads to an increased risk of floods (Bittelli 2011).

Soil moisture is an essential variable for predicting global climate change because it affects the flow of energy, greenhouse gases, and water among the atmosphere, vegetation, and soils (Klemas et al. 2014). Soil moisture aids the processes of water loss from both the abiotic earth's surfaces (evaporation) and plants through transpiration making it key in the study of meteorology—weather development and formation of rainfall. Simulations with numerical weather prediction models have shown that improved characterisation of surface soil moisture, vegetation cover, and temperature can lead to significant forecast improvements. Moisture also drives infiltration and runoff during heavy rain events, affecting the amount of precipitation that runs off into nearby streams and rivers. Large-scale dry or wet surface regions have been observed to impart positive feedback on subsequent precipitation patterns (Arnold and Laymon 2012). In addition, the evaporation rate is strongly correlated to soil moisture that makes a strong connection between the land surface and atmosphere (Koster et al. 2004).

In water resources management and hydrologic studies, the soil moisture content is a hydrological parameter useful in water quality management, reservoir management and flood control (Gumindoga et al. 2020). In semi-arid ecosystems, dynamic information on soil moisture is critical to understanding groundwater recharge and drought conditions (Dumedah et al. 2014). The amount of soil moisture content serves as a solvent and carrier of nutrients, regulates soil temperature, and empowers microorganisms to conduct their metabolic activities. Soil moisture gradients together with nutrient fertility are used to classify forest types (Southee et al. 2012; Arnold and Laymon 2012).

Depending on the soil characteristics and surface water content, extreme events such as rainstorms and hurricanes can lead to flooding and landslides (Klemas 2009). Soil erosion and transport depend on soil moisture together with other soil properties including soil type, grain size and composition. Conversely, high soil moisture leads to an increased risk of flooding and erosion. Having accurate soil moisture data may lead to better predictions of such hazardous events and proper geotechnical engineering structures (Kerret et al. 2010; Zhang et al. 2020).

Near accurate estimation of soil moisture data usually achieved via traditional methods such as field and laboratory approaches (both direct and indirect). These approaches include use of gravimetric method and soil probes, and they point based where areal representation is achieved through kriging (Moran et al. 2004; Wang et al. 2020). However, with the invention and advancement in technology use of remote sensing approaches has recently gained competitive advantages over traditional approaches. The use of both passive and optical remote sensing especially in the microwave band of the electromagnetic spectrum; has been used in soil moisture estimation. This includes satellite images from sensors such as Landsat (Castelli et al. 2000), MODIS (Wang et al. 2020) and Sentinel (Vogels et al. 2019; Yang et al. 2019). Some of these sensors provide very coarse resolutions that might not be applied to patches of land of less than 10 m. for example MODIS has got a minimum spatial resolution of 250 m (Van doninck et al. 2011) while Landsat usable spatial resolution of 30 m (Chander et al. 2009) and Sentinel has a spatial resolution of 10 m (Vogels et al. 2019). However, out of these only MODIS has a higher temporal resolution of

a daily interval as opposed to Sentinel and Landsat (Van doninck et al. 2011). Therefore, it is not surprising that much research is restricted to handling soil moisture problems at a national, regional or global level to counter both spatial and temporal needs of the need for which soil moisture data is to be used (Bartsch et al. 2010a, b).

Even though many applications require soil moisture data, accurate assessment of this variable is difficult because typical field methods are complex and expensive. Also, local-scale variations in soil properties, terrain, and vegetation cover make the selection of representative field sites difficult if not impossible (Shafian and Maas 2015). Therefore, the purpose of this study is to review the remote sensing techniques applied in determining soil moisture with a particular focus on Zimbabwe, since the water for agriculture act as a key driver of its economic growth. Agriculture in the country is both rainfed and irrigated. Thus, there is a need for explicit soil moisture information in time and spatially, especially for irrigation scheduling.

5.2 Description of the Study Area

Zimbabwe is a landlocked country, located in southern Africa with a total area of 390,760 km² (Fig. 5.1). The country is bordered by five countries namely; Zambia (to the north), to the east of it is Mozambique, South Africa in the south while Botswana and Namibia border it in the west. It has a population of about 13 million people and its economy is highly dependent on agriculture, mining and tourism (FAO 2016).

Zimbabwe lies almost entirely over 300 m above sea level. Its principal physical feature is the broad ridge running from southwest to northeast across the entire country, the central watershed. The country has four major relief regions namely; the low veld (<600 m above mean sea level); middle veld (600–1,200 m); high veld (1,200–2,000 m); and eastern highlands (2,000–2,400 m). The highest point in the country lies at an altitude of 2,592 m along the eastern border with Mozambique.

Almost 70% of the country is covered by Precambrian Basement Complex and metavolcanic rocks. These rocks comprise gneisses and igneous rocks such as granite. Sedimentary rocks and metasediments occur in some parts of the country including the northwest (FAO 2016). Weathering of granite parent material resulted in residual soils including light sandy soils and -clays. Sands are highly leached and do not easily retain water because of their coarse texture. Except in areas where soils are of alluvial origin, soil depth is often less than 1 m (FAO 2016, 2020).

Zimbabwe has a tropical climate, with a dry season from April to October in which little rain falls and a rainy season that usually lasts from late November to March (FAO 2016). Mean annual ranges from less than 500 mm/year in the south and southwest; between 600 mm and 1,000 mm across much of the central part of the country to more than 1,000 mm in the eastern highlands. In Zimbabwe, rainfall amount increases from south to north as well as from west to east. The temperature gradient also tends to follow a west–east trend with temperatures getting lower as one moves from the south-eastern lowveld through the highveld to the east (FAO 2016).

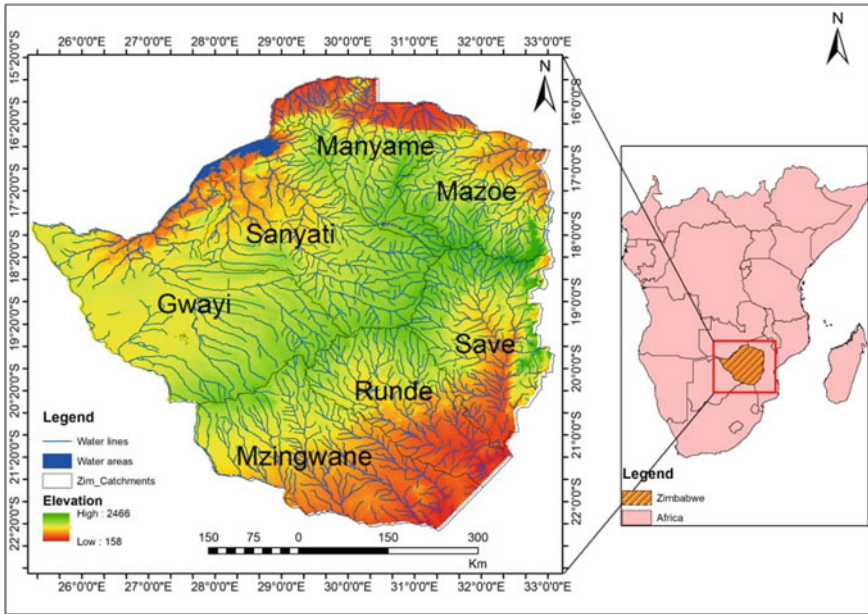


Fig. 5.1 Location of Zimbabwe in Africa and its river catchments

Vegetation of the country is predominantly tropical savanna comprising miombo and mopane trees with grasses. Tree growth is encouraged by the wet summers. Dry savanna with grass of up to 2 m height makes up a major part of Zimbabwe’s landscape (FAO 2016).

5.3 Estimation of Soil Moisture

5.3.1 Field and Laboratory Methods

In situ manual measurements using the gravimetric method and soil moisture probe are arguably the most accurate and reliable ways to obtain soil moisture data (Wang et al. 2020). Both of these manual methods are labour intensive and can take an extremely long time to properly analyse moisture content in large areas.

The soil moisture robe indirectly determines moisture content by the use of specialised probes that measure the electrical charge between two metallic hooks, thereby measuring the conduction of electricity in soil that can be translated to soil moisture. The gravimetric method directly estimates soil moisture content using a known volume of an undisturbed soil sample is collected from the field (using a ring, hovel, blade, plastic bag and a GPS) weighed, dried for 24 h at 105 °C, and then

reweighed. The gravimetric soil moisture content is calculated as the net difference between the mass of wet soil and dry soil, divided by the mass of dry soil. Gravimetric soil moisture content can be converted to a percentage by multiplying with 100.

Direct and indirect field and laboratory measurements of surface soil moisture are difficult, and the available techniques are limited by environmental and socio-economic factors. It is from this background that there is a key need for surface soil moisture assessment approaches that have got an explicit coverage both in time and space. This is critical especially for irrigated areas where there is a need for irrigation scheduling. Thus, it is without a doubt that remote sensing approaches are most appropriate compared to traditional field-based techniques. Poonia (2022) criticised the use of conventional and in-situ approaches at a regional scale because they failed to capture precisely the spatio-temporal dynamics of soil moisture.

5.3.2 *Satellite Remote Sensing of Soil Moisture*

The need for continuous measurements of surface soil moisture with regional and global coverage is critical for hydrological, ecological and climatological studies. In contrast with field measurements which represent single point locations, and cover relatively short periods of observation, satellite remote measurements have broad spatial coverage and temporal continuity at relatively low cost (Ahmad et al. 2010). Satellite remote sensing developments for soil moisture estimation began in 1975 when NASA launched Landsat to collect data using a passive sensor (Ahmad et al. 2010). Since then, various passive and active remote sensing techniques (ground-based, aerial, and space platforms) have been used in determining soil moisture content in different areas across the world.

Over last 60 years, *electromagnetic spectra*, from the optical/thermal to the microwave regions, have been intensively used to provide a number of algorithms, models and products that are available for soil moisture retrieval (Poonia 2022). Because the microwave wavelength can penetrate through the atmosphere and vegetation, it is suitable to detect soil moisture even during cloudy conditions (Poonia 2022). Studies using remote sensing observations to evaluate soil moisture conditions by employing measurements from solar reflectance, thermal infrared wavelengths, and microwaves have shown lots of potential in this area. It is without a doubt that remote sensing approaches are better as compared to traditional field-based soil moisture estimation techniques (Ahmad et al. 2011; Li et al. 2021).

Remotely sensed observations depend on reflected and emitted electromagnetic to produce spatially comprehensive measurements of surface environmental conditions. By relating variations in measured electromagnetic emittance to surface moisture conditions, regional variations and local spatial heterogeneity of soil moisture conditions are determined (Shafian and Maas 2015). The use of satellite imagery in determining the surface soil moisture is based on the principle that surface soil moisture interrupts with the surface characteristics that later emit an electromagnetic wavelength than can be observed through remote sensing. These include biophysical

factors such as vegetation cover, observed through vegetation indices (VI), and the surface energy balance, observed through surface temperature (T_s), is a good indicator of the energy balance on both regional and global scales. Surface temperature is one of the biophysical factors sensitive to soil moisture content. Stressed plants use a reflex through their stomata which close when maximising on water conservation while avoiding an accelerated transpiration hence results in a decreased latent heat flux. The energy flux balance is a function of an increase in sensible heat flux in association with warmer leaf temperatures and increased T_s . With decreasing soil moisture, VI decreases while T_s increases. Combining T_s and VI provides useful quantitative information for detecting the spatial and temporal distribution of soil moisture (Shafian and Maas 2015).

With remote sensing approaches, soil moisture data are retrieved from different from the electromagnetic spectrum (visible, infrared, thermal, and microwave) based on the sensitivity of the soil surface, the electromagnetic radiation as well as on the effectiveness of the reflected radiation from the soil surface that can be received by the sensor. Remotely sensed shortwave infrared transformed reflectance, the normalized difference vegetation index, and other such parameters are widely used to estimate soil moisture for drought detection or irrigation scheduling in low-income countries (Bartsch et al. 2010a, b; Marumbwa et al. 2015; Nhedzi 2008; Poonia 2022).

Measuring soil moisture using remote sensing at deep root zones below 5 cm from the surface is a challenge (Ahmad et al (2010)). Surface soil moisture depth is determined based on satellites' sensor frequency on that respective piece of land. Soil moisture depth reachable by electromagnetic radiation is referred to as skin or surface soil moisture (e.g. only a few mm for the optical and thermal band) or near-surface soil moisture (e.g. a few cm for microwave sensors). Depths exceeding 30 cm are rarely reachable by satellite cameras. In order to access deeper root zone soil moisture, combined statistical techniques based on energy balance or simplified water balance approaches are used (Ahmad et al. 2010; Lu et al. 2011).

Several remote sensing techniques are used for regular monitoring of soil moisture at various spatial and temporal scales. The remote sensing approach specifications and utilities can be found in well-documented literature but not limited to e.g. (Bartsch et al. 2010a, b; Marumbwa et al. 2015; Nhedzi 2008; Poonia 2022). The techniques for soil moisture SSM estimation vary from empirical and mechanistic models while the widely used methods are through satellite remote sensing of the active and passive for both optical and microwave. These approaches usually employ the linear relationship between land surface reflectance and soil moisture content either directly or through the development of empirical spectral indices. However, because the microwave wavelength is unlimited by weather and vegetation cover then this makes the microwave band the most suitable for estimating soil moisture as it can penetrate through the atmosphere and vegetation to detect soil moisture in the surface layer (Poonia 2022). It is thus well documented that different soil-moisture evaluation methods have been introduced in different regions (Bartsch et al. 2010a, b; Lu et al. 2011; Van doninck et al. 2011).

Although, remote sensing techniques are plausible for surface soil moisture retrieval, however, they do not properly provide a pattern for surface soil moisture column. Therefore, appropriate input data be incorporated in hydrologic models to provide an estimation of the spatial distribution of moisture for water balance estimates of any area (Moran et al. 2004; Samboko 2016). While the Normalized Difference Vegetation Index (NDVI) is an effective indicator of vegetation conditions, it is a rather conservative indicator of soil moisture status because there is a time lag between the time observed for a change in soil moisture and that time change as observed in NDVI. Thus, NDVI-based methods may not be effective in the rapid monitoring of soil moisture conditions.

Several shortcomings can be observed from the current remote sensing products used to estimated soil moisture. ASTER, MODIS or Landsat products are of coarser spatial resolutions (>10 km) when it comes to their applicability at the watershed or regional scale as soil moisture is highly variable with space and time. Therefore, there is a need to downscale these soil moisture products to finer spatial resolution, which can also be done by developing models with several covariates like vegetation, slope, soil texture, or to use the potential of Sentinel -2 which has got a better spatial resolution of at 10 m (Poonia 2022). Moreso, it is additionally acknowledged that different land cover reduces the classification accuracy of soil-moisture retrieval (Notarnicola 2004; Scipal et al. 2005; Zwieback et al. 2013).

5.4 Designing the Search Strategy

A well-designed search strategy (i.e., specific, unbiased, reproducible and including subject headings along with a range of keywords/phrases for the concepts) was designed to capture as many studies from various online databases as possible that meet the criteria for this systematic review. The search strategy involved the use of Boolean logic, phrase searching and truncations (Lackey 2013). Using Boolean logic, the following words or phrases were searched; “soil moisture” AND “remote sensing” AND “Zimbabwe”, (soil moisture* OR soil water) AND “remote sensing” AND “Zimbabwe”. During phrase searching, specific phrases were typed and enclosed in quotation marks. The database searched for the words typed; “soil moisture”, “moisture”, “soil water”, “remote sensing”, “Zimbabwe”. Some words were truncated in order to search for their different forms using the asterisk * as the truncation symbol.

5.5 Findings on the Use of Satellite Remote Sensing in Estimating Soil Moisture in Zimbabwe

Bartsch et al. (2010a, b) estimated soil moisture dynamics using radar satellite technology to develop the soil moisture information system for the Southern African

Development Community in which Zimbabwe is located. Medium resolution soil data (1 km) were obtained from ENVISAT's ASAR sensor operated in global mode (GM) with METOP scatterometer sensors and, coarse resolution soil moisture data (25–50 km) were derived from backscatter measurements acquired with METOP scatterometers on-board of the satellites ERS-1 and ERS-2 in near real-time via EUMETCast). The synergistic use of both systems allows frequent, medium resolution monitoring of regional soil moisture dynamics in the uppermost soil layer (<5 cm). However, the ENVISAT ASAR Global Mode soil moisture data had higher noise compared to the coarse resolution soil moisture products.

Shoko et al. (2015) showed that remotely sensed shortwave infrared (SWIR) transformed reflectance (TRSWIR), the normalized difference vegetation index (NDVI), and other such can be successfully used to estimate soil moisture at the surface level for large areas in low-income economies. The products can also be applied in drought detection or irrigation scheduling. Nevertheless, higher precision techniques for measuring soil moisture are required at depths that are physically hidden from current satellite cameras.

Gumindoga et al. (2020) applied the Surface Energy Balance System (SEBS) and the TOPographic driven MODEL (TOPMODEL) to estimate the spatio-temporal variation of soil moisture over a district in northern Zimbabwe from 2008 to 2013. Estimates of soil moisture were obtained by multiplying the relative evaporation from the SEBS algorithm by the average soil porosity and field capacity. After calibrating the TOPMODEL rainfall-runoff model with land surface inputs obtained from remote sensing, the spatial and temporal soil moisture estimates were compared with in situ measured soil moisture from the fifty-two sampling sites. Results show that the SEBS approach shows spatial and temporal soil moisture variability across the district simulated with a strong relationship ($R^2 = 0.796$) between in situ-based soil moisture measurements and SEBS based techniques for the period of March to July 2013. The study further revealed that there is a fair relationship ($R^2 = 0.60$) between ground soil moisture measurements and hydrologically modelled using TOPMODEL).

Samboko (2016) used the Topographic driven rainfall-runoff model (TOPMODEL) whose land surface inputs were obtained from remote sensing techniques to simulate soil moisture patterns from September 2008 to August 2010. Model results showed high levels of soil moisture along river channels, valleys and floodplains in northern Zimbabwe. However, a 12% difference was observed between the point and pixel-based soil moisture simulated by the model and retrieved by the data logger.

In Zimbabwe, the widely used approach for soil moisture estimation is the field-based gravimeter method. This is adopted by many commercial farmers as well as government departments such as the Agricultural Rural Extension Services, Meteorological Services and Zimbabwe National Water Authority. The use of remote approaches is still in its infancy as illustrated by our literature review. In most cases, this is applied at the academic or research level where sharing of knowledge will focus on marketing the new technology. Table 5.1 is an illustration for the comparison of field-based and remote sensing approaches in which they are applied in soil moisture estimation.

Table 5.1 A comparison of remote sensing and conventional methods in soil moisture estimation (Moran et al. 2004)

Approach	Merits	Limitations
Optical remote sensing (Visible, Near Infrared, Short-wave Infrared)	Fine spatial resolution; broad coverage; multiple sensors including hyperspectral sensors	Weak estimation of surface moisture, works only on clear weather; affected by vegetation cover, issue of temporal resolution
Thermal Infrared	Fine spatial resolution with broad coverage; multiple sensors available	Minimal surface penetration, affected by high humid weather, vegetation and atmospheric gas density
Microwave remote sensing	Broad coverage; satellite sensors available; strongly related to surface moisture estimation; surface penetration up to 5 cm and it is insensitive to weather patterns and atmospheric conditions	Affected by vegetation cover and surface roughness; ideally has got a coarse spatial resolution of approximately 30 km
Field-based methods (combined)	Near accurate estimates, addresses one's needs at a time; depth depends on the need; insensitive to earth's roughness and atmospheric condition	Point-based; time consuming and laborious;

5.6 Conclusion and Future Needs

This present review has shown that soil moisture is of great importance in closing hydrologic budgets, assessing soil–plant water interactions, studying climate change, controlling and regulating the interaction between the atmosphere and the land surface. It controls the ratio of runoff and infiltration, energy fluxes and nutrients, vegetation development and then carbon cycle. Moreso, soil moisture is an important factor in animal and plant productivity and can even sustain the interaction between the natural system and anthropogenic activity. Therefore, the distribution pattern of soil moisture, both spatially and temporally, is the key to climate modelling. Moreover, a long-term soil moisture data set on a regional scale, therefore, provide valuable information for research such as climate change and global warming and then improve weather forecasting and water resources management.

The review has shown that few studies using a combination of geostatistical approaches, remote sensing and hydrologic models has been conducted in Zimbabwe. However, the use of remote sensing in measuring soil moisture is promising in such data-scarce and water-limited regions. The issue of intense vegetation in Zimbabwe is a challenge in some areas, especially where there are significant topographical changes. This is so because the most accurate results from remote sensing data are achieved when there is no or low soil cover and most importantly applicable where the area is flat. Thus, the interaction of the emitted or reflected radiation from a

covered soil surface back to the remote sensor will no longer represent the actual soil surface-emission because part of the emitted/reflected radiation is either absorbed or enhanced by the soil cover.

Acknowledgements The great work done by anonymous reviewers of this paper is greatly appreciated.

Declaration of competing interest The authors declare no conflicts of interest.

References

- Ahmad S, Kalra A, Stephen H (2010) Estimating soil moisture using remote sensing data: a machine learning approach. *Adv Water Resour* 33:69–80
- Ahmad A, Zhang Y, Nichols S (2011) Review and evaluation of remote sensing methods for soil-moisture estimation. Society of photo-optical instrumentation engineers (SPIE). <https://doi.org/10.1117/1.3534910>. Downloaded From: <https://www.spiedigitallibrary.org/journals/SPIE-Reviews>. Accessed 4 Jan 2022
- Arnold JE, Laymon C (2012) NASA Soil moisture study. http://www.ghcc.msfc.nasa.gov/landprocess/lp_home.html.
- Bartsch A, Sabel D, Pathe C, Sinclair C, Vischel T, Doubkova M, Wagner W, Pegram G (2010a) Soil moisture dynamics from synthetic aperture radar for hydrometeorological applications in the southern African development community. International hydrological programme (IHP) and UNESCO, France
- Bartsch A, Doubkova M, Wagner W (2010b) ENVISAT ASAR GM soil moisture for applications in Africa and Australia. In: Earth observation and water cycle science. Presented at the ESA SP-674, ESA SP-674, Italy, p 6
- Bittelli M (2011) Measuring soil water content: a review. *Hort Techno* 21:293–300. <https://doi.org/10.21273/HORTTECH.21.3.293>.
- Castelli RM, Chambers JC, Tausch RJ (2000) Soil-plant relations along a soil-water gradient in Great Basin riparian meadows. *Wetlands* 20:251–266
- Chander G, Markham BL, Helder DL (2009) Summary of current radiometric calibration coefficients for Landsat MSS, TM, ETM+, and EO-1 ALI sensors. *Remote Sens Environ* 113:893–903. <https://doi.org/10.1016/j.rse.2009.01.007>
- Dumedah G, Walker JP, Chik L (2014) Assessing artificial neural networks and statistical methods for infilling missing soil moisture records. *J Hydrol* 515:330–344
- Gumindoga W, Murwira A, Rwasoka DT, Jahure FB, Chikwiramakomo L (2020) The spatio-temporal soil moisture variation along the major tributaries of Zambezi River in the Mbire District. Zimbabwe. *J Hydrol Reg Stud* 32:100753. <https://doi.org/10.1016/j.ejrh.2020.100753>
- Falkenmark M, Rockström J (2006) The new blue and green water paradigm: breaking new ground for water resources planning and management. *J water resour plann manage* 132(3):129–132
- FAO (2016) The state of world fisheries and aquaculture. Contributing to food security and nutrition for all. Rome (200 pp)
- FAO (2020) Crop and food security assessment mission to Zimbabwe. FAO Harare
- Kerr YH, Waldteufel P, Wigneron JP, Delwart S, Cabot F, Boutin J, Mecklenburg S (2010) The SMOS mission: new tool for monitoring key elements of the global water cycle. *Proc IEEE* 98(5):666–687
- Klemas VV (2009) The role of remote sensing in predicting and determining coastal storm impacts. *J Coast Res* 25(6):1264–1275
- Klemas V, Finkl CW, Kabbara N (2014) Remote sensing of soil moisture: an overview in relation to coastal soils. *J Coast Res* 30(4):685–696

- Koster RD, Dirmeyer PA, Guo Z, Bonan G, Chan E, Cox P, Gordon CT, Kanae S, Kowalczyk E, Lawrence D, Liu P, Lu CH, Malyshev S, McAvaney B, Mitchell K, Mocko D, Oki T, Oleson K, Pitman A, Sud YC, Taylor CM, Verseghy D, Vasic R, Xue Y, Yamada T (2004) Regions of strong coupling between soil moisture and precipitation, *Sci* 305:1138–1140. <https://doi.org/10.1126/science.1100217.6969-06981>
- Li X, Du Z, Huang Y, Tan Z (2021) A deep translation (GAN) based change detection network for optical and SAR remote sensing images. *ISPRS J Photogramm Remote Sens* 179:14–34
- Lu H, Koike T, Gong P (2011) Monitoring soil moisture change in Africa over past 20 years with using passive microwave remote sensing. In: 2011 19th international conference on geoinformatics. Presented at the 2011 19th international conference on geoinformatics, IEEE, Shanghai, China, pp 1–5. <https://doi.org/10.1109/GeoInformatics.2011.5980961>
- Marumbwa FM, Murwira A, Madamombe EK, Kusangaya S, Tererai F (2015) Remotely sensing of irrigation water use in Mazowe Catchment. *Zimbabwe* 5:11
- Moran MS, Clarke TR, Inoue Y, Vidal A (1994) Estimating crop water deficit using the relation between surface-air temperature and spectral vegetation index. *Remote sens environ* 49(3):246–263
- Moran MS, Peters-Lidard CD, Watts JM, McElroy S (2004) Estimating soil moisture at the watershed scale with satellite-based radar and land surface models 30:23
- Narasimhan B, Srinivasan R (2005) Development and evaluation of Soil Moisture Deficit Index (SMDI) and Evapotranspiration Deficit Index (ETDI) for agricultural drought monitoring. *Agric Meteorol* 133:69–88. <https://doi.org/10.1016/j.agrformet.2005.07.01>
- Nhedzi E (2008) Assessment of a catchment water balance using GIS and remote sensing techniques: Mazowe, Zimbabwe (MSc). ITC, Netherlands
- Notarnicola C (2004) Bayesian iterative inversion algorithm applied to soil moisture mapping using ground-based and airborne remote sensing data. In: Posa F (Ed), Presented at the remote sensing, Barcelona, Spain, p 116. <https://doi.org/10.1117/12.514413>
- Poonia RC (2022) Deep learning for sustainable agriculture. Deep learning for sustainable agriculture. Elsevier, India, pp 143–168
- Samboko H (2016) A remote sensing based approach to determine evapotranspiration in the Mbire District of Zimbabwe (MSc). University of Zimbabwe, Harare
- Scipal K, Scheffler C, Wagner W (2005) Soil moisture-runoff relation at the catchment scale as observed with coarse resolution microwave remote sensing. *Hydrol Earth Syst Sci* 5:11
- Shafian S, Maas SJ (2015) Index of soil moisture using raw Landsat image digital count data in Texas high plains. *Remote Sens* 7(3):2352–2372
- Shoko C, Dube T, Sibanda M, Adelabu S (2015) Applying the Surface Energy Balance System (SEBS) remote sensing model to estimate spatial variations in evapotranspiration in Southern Zimbabwe. *Trans Royal Soc South Africa* 70(1):47–55
- Southee FM, Treitz PM, Scott NA (2012) Application of lidar terrain surfaces for soil moisture modeling. *Photogram Eng Remote Sens* 78(12):1241–1251
- Van doninck J, Peters J, De Baets B, De Clercq EM, Ducheyne E, Verhoest NEC (2011) The potential of multitemporal Aqua and Terra MODIS apparent thermal inertia as a soil moisture indicator. *Int J Appl Earth Obs Geoinformation* 13:934–941. <https://doi.org/10.1016/j.jag.2011.07.003>
- Vogels M, de Jong S, Sterk G, Douma H, Addink E (2019) Spatio-temporal patterns of smallholder irrigated agriculture in the horn of Africa Using GEOBIA and sentinel-2 imagery. *Remote Sens* 11:143. <https://doi.org/10.3390/rs11020143>
- Wang C, Xie Q, Gu X, Yu T, Meng Q, Zhou X, Han L, Zhan Y (2020) Soil moisture estimation using Bayesian Maximum Entropy algorithm from FY3-B, MODIS and ASTER GDEM remote-sensing data in a maize region of HeBei province. China. *Int J Remote Sens* 41:7018–7041. <https://doi.org/10.1080/01431161.2020.1752953>
- Yang L, Feng X, Liu F, Liu J, Sun X (2019) Potential of soil moisture estimation using C-band polarimetric SAR data in arid regions. *Int J Remote Sens* 40:2138–2150. <https://doi.org/10.1080/01431161.2018.1516320>

Zhang D, Zhan J, Qiao Z, Župan R (2020) Evaluation of the performance of the integration of remote sensing and Noah hydrologic model for soil moisture estimation in Hetao irrigation region of inner Mongolia. *Can J Remote Sens* 46:552–566. <https://doi.org/10.1080/07038992.2020.1810003>

Zwieback S, Dorigo W, Wagner W (2013) Estimation of the temporal autocorrelation structure by the collocation technique with an emphasis on soil moisture studies. *Hydrol Sci J* 58:1729–1747. <https://doi.org/10.1080/02626667.2013.839876>

Chapter 6

Bivariate Copula Modelling of Precipitation and River Discharge Within the Niger Basin



Samuel T. Ogunjo, Adeyemi O. Olusola, and Christiana F. Olusegun

Abstract Rivers are important for domestic, industrial, agricultural, and geopolitical purposes. Within the tropics, rivers are fed by rainfall and underground recharge. Understanding the contribution of rainfall to the dynamics of river is necessary for several reasons. In this study, the best fit marginal probability distribution function for rainfall and river discharge from among Gamma, Beta, Gaussian, Student T, and Uniform were considered. Furthermore, the dependence between rainfall and river discharge was investigated using three copula functions: Gumbel, Clayton and Frank. Results obtained suggests that the Student T's distribution was best suited for rainfall and river discharge at Lokoja. It was also found that using the Akaike Information Criteria, that the Frank copula provides the best model for dependence between rainfall and river discharge. These results are important for an effective integrated water resources planning and management.

6.1 Introduction

The likelihood of climate change impact has increased the need for more knowledge about natural disasters such as flooding and drought. Understanding these disasters and their drivers involve the ability to model and simulate their occurrences. Scientists have used different approaches including Markov chain modelling (Ogunjo and Oluyamo 2021), stochastic models (Jimoh and Webster 1999), and other probability based models (Orimoloye et al. 2021). The ultimate aim is to be able to replicate hydrometeorological parameters considering minimal input with high accuracy. The

S. T. Ogunjo (✉)

Department of Physics, Federal University of Technology, Akure, Ondo, Nigeria
e-mail: stogunjo@futa.edu.ng

A. O. Olusola (✉)

Faculty of Environmental and Urban Change, York University, Toronto, Canada
e-mail: aolusola@yorku.ca

C. F. Olusegun

Faculty of Physics, Institute of Geophysics, University of Warsaw, Warsaw, Poland
e-mail: christiana.olusegun@fuw.edu.pl

use of probability based models is gaining attention due to its ability to generate synthetic data based on the underlying distribution of the data. The wide array of distribution functions allow for suitable choice of models given any spatio-temporal constraints. Furthermore, the use of probability in hydrometeorology is already established. The estimation of drought using indices such as standardized precipitation index requires the computation of suitable probability distribution (Ogunjo et al. 2019b). Given an appropriate probability distribution, samples can be drawn for further studies with high reliability.

Studies (Sharma and Singh 2010; Hanson and Vogel 2008; Al Mamoon and Rahman 2017; Ng et al. 2020) have shown that annual and seasonal rainfall were found to be best fit by lognormal and gamma distribution while different months of the years have different best fit distribution. According to Hanson and Vogel (2008), the Pearson type III distribution is the best probability distribution for daily rainfall over the United States of America. The annual precipitation in Qatar can best be described by the Generalized Extreme Value distribution (Al Mamoon and Rahman 2017). Similarly, the Generalized Extreme Value distribution was observed to be the best fit distribution for annual maximum rainfall in Malaysia (Ng et al. 2020). In Sudan, the annual rainfall are best fit with the normal and gamma probability distribution (Mohamed and Ibrahim 2016). ŞEN and Eljadid (1999) showed that the monthly precipitation in Libya can be predicted using the gamma probability distribution function. The log-Pearson type-III distribution was found to be the best fit probability distribution to the 24 h maximum precipitation in 5 out of 6 stations within Pakistan (Amin et al. 2016). In Bangladesh, the monthly precipitation in 3 out of four locations were found to be best described by the generalized extreme value precipitation while the remaining station was described by normal distribution (Ghosh et al. 2016). At different temporal and spatial resolution, the Pearson type-3 distribution was found to be the best distribution fit for precipitation in Singapore (Mandapaka and Qin 2013). The Gumbel distribution was reported to be the best fit for weekly and monthly maximum rainfall in India (Bhakar et al. 2008). Annual, monthly maximum, daily and consecutive days rainfall within Maharashtra state of India was found to be best described by the generalized extreme value distribution (Bajirao 2021). The annual precipitation in Upper Blue Nile basin area was found to follow a normal distribution (Ximenes et al. 2021). The annual and monthly precipitation in Japan have been reported to be best captured by the log-Pearson type 3 and Pearson type 3 distribution function respectively (Yue and Hashino 2007). Several studies have also been carried out to fit river discharge to probability density functions. Kroll and Vogel (2002) recommended the Pearson Type 3 and the 3-parameter lognormal distributions for fitting streamflows across different regions of the United States of America. The log-Pearson type 3 was recommended for the annual mean discharge on the Minab river in Iran (Khosravi et al. 2012). The annual one day maximum discharge at the Kulsi River Basin was found to be best predicted using the log-normal probability distribution function (Kalita et al. 2017). Gamma probability distribution was reported as the best fit for monthly river discharge at the Lower Murrumbidgee River, Australia (Wen and Ling 2011). The annual peak and maximum discharge at Karkheh River, Iran was found to fit the log-Pearson type 3 distribution (Machekposhti et al.

2016). The Generalized Pareto distribution was found suitable for annual maximum discharge at Kopili river (Bhuyan 2009). Chaibandit and Konyai (2012) reported that the extreme value distribution can capture the dynamics of the monthly river discharge of the Yom river. The best fit probability density function of river discharge has been found to change over time due to several mitigating factors (Githui et al. 2005). The annual mean flow on the Tana river was found to fit the lognormal and generalized extreme value probability distributions best (Langat et al. 2019). Both the four-parameter Kappa and three-parameter Generalized Pareto distributions were found to approximate daily streamflow dataset in Angola (Almeida et al. 2021). The Weibull probability distribution gave the best parameters when fitted to the monthly discharge in Strymon river, Greece (Antonopoulos et al. 2001). The Gumbel probability distribution function was found to be the best for predicting monthly river discharge at Kainji dam (Mohammed et al. 2017). Streamflow in 14 rivers with the northwest Iran were best fitted with the lognormal probability distribution function. These studies and some others (Ye et al. 2018) have shown that rainfall and streamflow (discharge) distribution can be explained based on various probability distribution functions. However, the dependence of interrelationships between these two hydrometeorology variables still begs for answers in the physical sciences. Despite the array of techniques that are available to unravel and show these interdependence, an emerging technique is the Copulas. Copulas are the mechanism which allows us to isolate the dependency structure in a multivariate distribution. The concept of copula was developed to measure the interdependence between two or more random variable joint probability distributions to their one-dimensional marginal distributions (Sklar 1959; Nelsen 2007). In the financial sector, copula has been used extensively for scenarios such as oil-stock diversification (Avdulaj and Barunik 2015), interdependence of oil prices and stock market indices (Sukcharoen et al. 2014), and gold and stock price returns (Boako et al. 2019). Copulas have also found application in the field of hydrometeorology. The idea has been employed to study the relationship between rainfall and temperature (Pandey et al. 2018), solar radiation and sky clearness index (Yet and Masseran 2021), drought frequency analysis (Mirabbasi and Dinpashoh 2012), and Covid-19 and maximum temperature (Novianti et al. 2021).

Tropical regions (latitude $\pm 23^\circ$) have been reported to have complex atmospheric dynamics and climate extremes (Fuwape et al. 2020; Ogunjo et al. 2019a). Water resources within the tropics is governed and determined by the amount of precipitation received. The network of rivers serve as sources of water for irrigation, industrial, and domestic use. It is particularly useful during the dry season and prolong periods of droughts. One of the most prominent rivers within tropical Africa is the River Niger. Studies at two ports along River Niger showed that the discharge exhibit chaotic behaviour influenced by dam construction (Ogunjo et al. 2022). Considering the role of rivers in the geopolitical balance of the West African region, it is pertinent to investigate the role of rainfall on its dynamics. In this study, the concept of copula was extended to study the relationship between river discharge and precipitation at a tropical location. The best marginal probability for each of river discharge and rainfall among five distributions was considered. Furthermore, three Archimedean copulas were investigated for their ability to model the dependence between river

discharge and rainfall within a tropical region. Results from this work will help in water resources management and planning within the region. It will also give insight into the role of rainfall in river dynamics within the tropics.

6.2 Methodology

In this section, the data sources used in the study were described. Furthermore, the location of study, as well as, the mathematical concept of copulas are introduced.

6.2.1 Study Area and Data

Two datasets were considered in this study—river discharge and precipitation data. The data were considered from January 1977 to December 1992. The monthly precipitation data were obtained from the archives of the Nigerian Meteorological Services. Daily river discharge were obtained from the Nigerian Hydrological Services Agency. The Nigerian Meteorological Services and Nigerian Hydrological Services Agency are located a few hundred metres from each other. The study location is Lokoja, a confluence town along both River Niger and River Benue.

6.2.2 Seasonal-Trend Decomposition Using LOESS (STL)

Both precipitation and river discharge data exhibit seasonal and annual cycles. Deseasonalization was carried out using the Seasonal Trend Decomposition using LOcally Estimated Scatterplot Smoothing (LOESS). A seasonal signal, X_t for months $t = 1, 2, 3, \dots, n$ can be decomposed into the seasonal component, S_t trend component, T_t and a residual component, R_t (Cleveland et al. 1990).

$$X_t = S_t + T_t + R_t \quad (6.1)$$

R_t from both precipitation and river discharge are further analyzed in this study. The use of STL has been reported for river discharge and precipitation (Apaydin and Falsafian 2021; Chao et al. 2018). STL has the advantage of being robust to outliers.

6.2.3 Probability Density Functions

There exists a probability distribution that can best describe a time series, x_i . In this study, five (6.5) probability density functions were considered for both precipitation and river discharge in Lokoja. The probability density functions considered are:

1. Gamma distribution

$$f(x, \alpha, \beta) = \frac{\beta^\alpha x^{\alpha-1} e^{-\beta x}}{\Gamma(\alpha)} \quad (6.2)$$

2. Beta distribution

This is defined as

$$f(x, a, b) = \frac{\Gamma(a+b)x^{a-1}(1-x)^{b-1}}{\Gamma(a)\Gamma(b)} \quad (6.3)$$

For $0 \leq x \leq 1, a > 0, b > 0$.

3. Gaussian distribution

$$f(x, \alpha) = \frac{1}{\sqrt{2\pi\sigma^2}} e^{-\frac{(x-\alpha)^2}{2\sigma^2}} \quad (6.4)$$

4. Student T distribution

$$f(x, v) = \frac{\Gamma\left(\frac{v+1}{2}\right)}{\sqrt{\pi v} \Gamma\left(\frac{v}{2}\right)} \left(1 + \frac{x^2}{v}\right)^{-(v+1)/2} \quad (6.5)$$

5. Uniform distribution This is defined as

$$f(x) = \begin{cases} \frac{1}{b-a}, & a \leq x \leq b; \\ 0, & x < a \text{ or } x > b \end{cases} \quad (6.6)$$

The *loc* and *scale* can be obtained by shifting and scaling of the distribution parameters.

6.2.4 Copula

Sklar (1959) introduced the concept of copulas to provide more comprehensive information about the relationships between two or more variables. The bivariate copula can be defined as

$$F(x, y) = C(f_x(x), f_y(y)) \quad (6.7)$$

where f_x, f_y are the marginal distribution functions and C is the copula function. In the Archimedean copula, a generator, \emptyset , exists such that

$$C(u, v) = \phi^{-1}\{\phi(u) + \phi(v)\} \tag{6.8}$$

In this study, three members of the Archimedean copula functions were considered.

1. Clayton

This is defined as

$$C(u, v) = (u^{-\theta} + v^{-\theta} - 1)^{1/\theta} \tag{6.9}$$

where the generator function is $((-\ln t)^\theta)$ with parameters in the range $[1, \infty)$.

2. Frank

The copula is defined as

$$C(u, v) = -\frac{1}{\theta} \left[1 + \frac{(e^{\theta u} - 1)(e^{\theta v} - 1)}{(e^\theta - 1)} \right] \tag{6.10}$$

where the generator function is given as $-\ln \frac{(e^{-\theta t} - 1)}{e^\theta - 1}$ with parameters in the range $(-\infty, \infty)$.

3. Gumbel

This is defined as

$$C(u, v) = \exp(-[\ln u^\theta + (-\ln v^\theta)])^{1/\theta} \tag{6.11}$$

where the generator function is given as $t^{-\theta} - 1$ with parameters in the range $[1, \infty)$.

A measure of dependence between the two variables under consideration can also be estimated from the generating function \emptyset . This is defined as (Karmakar and Simonovic 2009)

$$\tau = 1 + 4 \int_0^1 \frac{\phi(t)}{\phi'(t)} dt \tag{6.12}$$

where t is either of the variable.

6.2.5 Goodness of Fit

The performance of the different probability density functions and copula models were analyzed using the Akaike Information Criteria (AIC) (Akaike 1974). This is defined as

$$AIC = -2\ln L - 2Q$$

where L and Q are the maximum log-likelihood and number of parameters in the model respectively. The model with the lowest AIC values is considered as the most efficient model. where L and Q are the maximum log-likelihood and number of parameters in the model respectively. The model with the lowest AIC values is considered as the most efficient model.

6.3 Results and Discussion

6.3.1 Statistical Description

The temporal evolution of of river discharge at Lokoja station is shown in Fig. 6.1. The river discharge was observed to have seasonal variation over the period under consideration. Using STL, the trend and seasonal components were extracted from the time series to obtain the residue. There were two types of trend observed—a decreasing trend from 1978 till 1984 and an increasing trend from 1985 till 1990. The decrease between 1978 and 1984 could be tied to the prolonged drought period that occurred during that time (Badou et al. 2017). In their study on the evaluation of recent hydro-climatic changes in four tributaries of the Niger River Basin, Badou et al. (2017) provided information by laying claim to the fact that during the early 1970s, a break occurred in the hydro-climate of West Africa and this was followed by the great drought and famine of the 1980s. The STL decomposition of the precipitation data was also carried out (Fig. 6.2). The monthly precipitation were found to be as high as 400 mm per month, typical of a tropical station. The raining season at this location is characterized by two peaks in some years. This is influenced by the Tropical Maritime air mass from February to November while between December to January, the dry Tropical Continental air masses prevails. The meeting point of these two air masses is characterized by a relatively low pressure system known as the Inter-Tropical Discontinuity (ITD). Generally, during the raining season, the ITD migrates northward from over the ocean to further inland during the months of March/April (the beginning of the raining season along the Guinean coast) and reaches its northernmost position in July and August at about 21°N Sultan et al. (2007). The descriptive statistics of river discharge and rainfall over the location are shown in Table 6.1. Mean monthly river discharge was estimated to be 4765.73 m³ with a standard deviation of 4609.97 m³. Monthly river discharge is positively

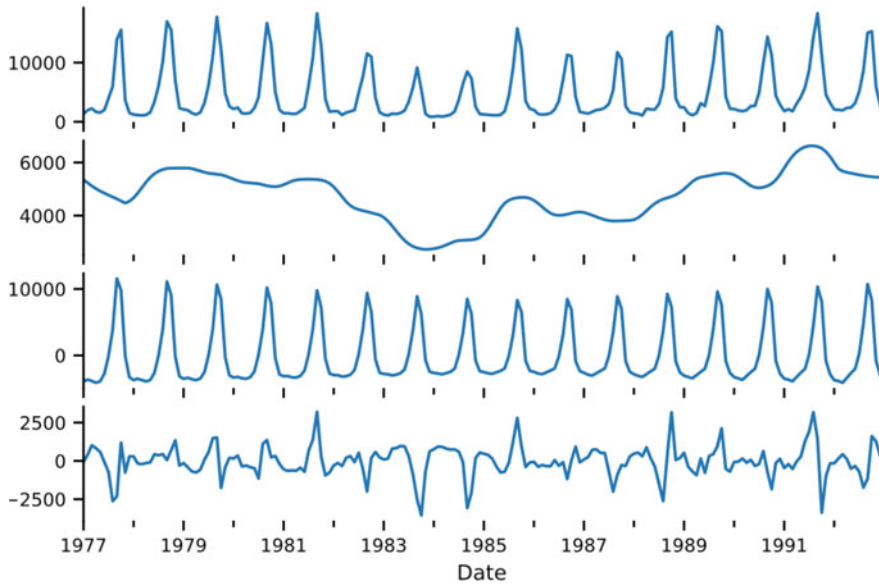


Fig. 6.1 Temporal evolution of river discharge at Lokoja including the trend, seasonal and residue components after STL analysis

skewed with a Kurtosis of 0.8652. The minimum and maximum values of monthly river discharge were 859.72 m^3 and $18,379.55 \text{ m}^3$ respectively. Similarly, the mean and standard deviation of monthly rainfall were 97.57 mm and 96.17 mm respectively. Rainfall was also positively skewed with a small kurtosis of 0.000495. The maximum monthly rainfall was obtained as 423.5 mm .

6.3.2 Marginal Probability Distribution

Five probability distribution functions were fitted to both river discharge and rainfall at Lokoja. The results, as well as, goodness of fit parameter are shown in Table 6.2. Negative values were obtained for the location parameter (*loc*) in all the distributions considered, except for river discharge (Student T distribution) and Rainfall (Gaussian distribution). However, all the distributions were found to have positive values of scale parameter. The Student T distribution was observed to be the best fit with the lowest AIC values for both river discharge and rainfall. This is a departure other best probability density function for rainfall such as Pearson Type III (Hanson and Vogel 2008), generalized extreme value distribution (Ghosh et al. 2016; Bajirao 2021), gamma distribution (ŞEN and Eljadid 1999), three parameter lognormal distribution (Ozonur et al. 2020), Pearson type 3 (Yue and Hashino 2007), and normal distribution (Ismawati and Rosmaini 2018). Similarly, our result differs from reports on best fit

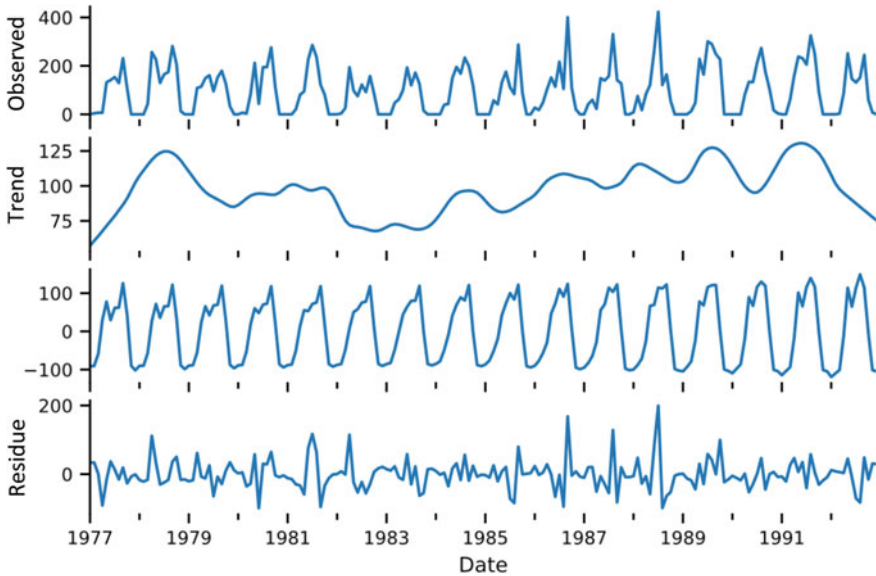


Fig. 6.2 Temporal evolution of precipitation at Lokoja including the trend, seasonal and residue components after STL analysis

Table 6.1 Descriptive statistics for monthly rainfall and river discharge at Lokoja

Statistics	Discharge	Rainfall
Mean	4765.73	97.57
Standard deviation	4609.97	96.17
Skewness	1.43	0.8
Kurtosis	0.8652	0.000495
Min	859.72	0
Max	18,379.55	423.5

probability density function for river discharge such as gamma probability function (Wen and Ling 2011), Extreme value distribution (Chaibandit and Konyai 2012), Weibull (Antonopoulos et al. 2001), Gumbel propability distribution (Mohammed et al. 2017), lognormal (Tabari et al. 2013), lognormal and generalized extreme value distribution (Langat et al. 2019).

6.3.3 Bivariate Copula Estimation

Three Archimedean based copula were used to model the relationship between river discharge and precipitation at Lokoja. The parameter (θ) of the copulas: Clayton,

Table 6.2 Estimated parameters and goodness of fit values for probability distribution models of precipitation and river discharge at Lokoja

PDF	Parameter	a	b	loc	Scale	AIC
Gamma	Discharge	367.88		-19,677.2	53.46	3207.02
	Rainfall	0.78		-99.3	2.47	16,158.27
Beta	Discharge	165.09	1098.63	-3564.16	6762.42	206,741.2
	Rainfall	26.61	983.67	-99.3	298.73	127,816.7
Gaussian	Discharge			-4.81	1012.4	3204.18
	Rainfall			0.19	44	2000.03
Student T	Discharge			27.79	634.55	3170.93
	Rainfall			-2.63	27.96	1970.71
Uniform	Discharge			-3564.16	6762.42	3388.55
	Rainfall			-99.3	298.73	2190.62

Frank, and Gumbel were found to be 0.98, 3.27, and 1.49 respectively. These are similar to reported values such as (0.62–0.96) Clayton, (2.64–4.40) Frank, and (1.39–1.86) Gumbel (Zhang and Singh 2012); 0.75 (Clayton), 2.65 (Frank), and 1.36 (Gumbel) (Abdollahi et al. 2019). However, the values obtained in this study are less than 2.15 (Clayton), 11.44 (Frank), and 2.61 (Gumbel) (Golian et al. 2012). Based on the AIC, the best joint distribution between river discharge and precipitation in Lokoja was found to be the Frank copula while the worst performing copula was the Clayton copula. This contrast best copulas reported in other regions including Galambos copula (Zhang and Singh 2012), Joe copula family (Golian et al. 2012),

Ali-Mikhail-Haq copula (Abdollahi et al. 2019), Gumbel (Huang et al. 2015), Student t copula and Frank copula (Dodangeh et al. 2020), Clayton copula (Sabaghi et al. 2021).

The correlation value for the three copulas were found to be identical at 0.33 (Table 6.3). This is within the range of correlation reported by 0.276–0.475 (Zhang and Singh 2012), 0.30 (Abdollahi et al. 2019), but lower than 0.45–0.82 (Huang et al. 2015). This shows an r^2 value of 0.1, implying that precipitation account for 10% of the river discharge volume at Lokoja. These can be attributed to a number of reasons. Firstly, the influence of the dam upstream moderates the impact of the flow irrespective of the amount of rainfall received, secondly, land use activities along river Niger affect the discharge volume at Lokoja. thirdly, the river discharge volume is largely driven by the black and white flood, not precipitation. The black flood originates from high rainfall area in the headwaters. The flood arrives at Kainji in November and lasts until March at Jebba after attaining a peak in February (Oyebande 1995; Jimoh 2007). The white flood becomes prominent only downstream of Sabon-gari soon after the river enters Nigeria. Usually heavy-laden with silt and other suspended particles. The flood derives its flow from the local tributaries and reaches Kainji in August in the pre-dam period, and attains peak between September and October in Jebba (Jimoh 2007), lastly, the role of river Benue on the discharge volume at Lokoja cannot be ruled out.

Table 6.3 Parameter estimates and goodness of fit to the bivariate copula models for river discharge and precipitation at Lokoja

Copula	Theta	Tau	AIC
Clayton	0.98	0.33	-32.00
Frank	3.27	0.33	-161.66
Gumbel	1.49	0.33	-56.32

6.4 Conclusion

This work has shown the distribution of river discharge and rainfall at-a-station (Lokoja, Nigeria) between 1977 and 1992. The distribution provides an insight into the pattern of these two hydrometeorological variables and their behaviour over time. The imprint of antecedent events, prolonged drought, was clearly visible on the trend of the river discharge. However, despite the alteration in rainfall pattern, due to the drought event, the double maxima seasonality is now restored in recent times as evidenced from the study.

Despite the existing knowledge on rainfall-runoff regarding their dependence, the observed association using the copula as presented in this study provides new insights. As against existing interpretations and expectations, the hydrology of the Lower Niger River is influenced largely as a result of the Kainji Dam, black and white floods. The contribution of rainfall to river discharge at Lokoja station as presented in this study is 10 percent, this suggests that other factors account for 90 percent of the river discharge distribution. Therefore, to carefully plan for conjunctive use of water within the Lower Niger Basin calls for a thorough understanding of the entire flow distribution of the Lower Niger River in relation to rainfall to aid an effective integrated river basin planning and management.

References

- Abdollahi S, Akhoond-Ali AM, Mirabbasi R, Adamowski JF (2019) Probabilistic event based rainfall-runoff modeling using copula functions. *Water Resour Manage* 33(11):3799–3814
- Akaike H (1974) A new look at the statistical model identification. *IEEE Trans Autom Control* 19(6):716–723
- Al Mamoon A, Rahman A (2017) Selection of the best fit probability distribution in rainfall frequency analysis for Qatar. *Nat Hazards* 86(1):281–296
- Almeida M, Pombo S, Rebelo R, Coelho P (2021) The probability distribution of daily streamflow in perennial rivers of Angola. *J Hydrol* 603:126869
- Amin M, Rizwan M, Alazba A (2016) A best-fit probability distribution for the estimation of rainfall in northern regions of Pakistan. *Open Life Sciences* 11(1):432–440
- Antonopoulos VZ, Papamichail DM, Mitsiou KA (2001) Statistical and trend analysis of water quality and quantity data for the strymon river in Greece. *Hydrol Earth Syst Sci* 5(4):679–692
- ApaydinH SattariMT, FalsafianK PrasadR (2021) Artificialintelligencemodelling integrated with singular spectral analysis and seasonal-trend decomposition using loess approaches for stream-flow predictions. *J Hydrol* 600:126506

- Avdulaj K, Barunik J (2015) Are benefits from oil–stocks diversification gone? new evidence from a dynamic copula and high frequency data. *Energy Econ* 51:31–44
- Badou DF, Kapangaziwiri E, Diekkrüger B, Hounkpè J, Afouda A (2017) Evaluation of recent hydro-climatic changes in four tributaries of the Niger River Basin (West Africa). *Hydrol Sci J* 62(5):715–728
- Bajirao TS (2021) Comparative performance of different probability distribution functions for maximum rainfall estimation at different time scales. *Arabian J Geosci* 14(20):1–15
- Bhakar S, Iqbal M, Devanda M, Chhajed N, Bansal AK (2008) Probablity analysis of rainfall at Kota. *Indian J Agric Res* 42(3):201–206
- BhuyanA BorahM (2009) Bestfittingprobabilitydistributionsforannualmaximum discharge data of the river Kopili, Assam. *J Appl Nat Sci* 1(1):50–52
- Boako G, Tiwari AK, Ibrahim M, Ji Q (2019) Analysing dynamic dependence between gold and stock returns: evidence using stochastic and full-range tail dependence copula models. *Finan Res Lett* 31
- Chaibandit K, Konyai S (2012) Using statistics in hydrology for analyzing the discharge of Yom River. *APCBEE Proc* 1:356–362
- Chao Z, Pu F, Yin Y, Han B, Chen X (2018) Research on real-time local rainfall prediction based on mems sensors. *J Sens*
- Cleveland RB, Cleveland WS, McRae JE, Terpenning I (1990) Stl: a seasonal-trend decomposition. *J Off Stat* 6(1):3–73
- Dodangeh E, Shahedi K, Pham BT, Solaimani K (2020) Joint frequency analysis and uncertainty estimation of coupled rainfall–runoff series relying on historical and simulated data. *Hydrol Sci J* 65(3):455–469
- Fuwape I, Oluyamo S, Rabiou B, Ogunjo S (2020) Chaotic signature of climate extremes. *Theoret Appl Climatol* 139(1):565–576
- Ghosh S, Roy MK, Biswas SC (2016) Determination of the best fit probability distribution for monthly rainfall data in Bangladesh. *Am J Math Stat* 6:170–174
- Githui F, Opere A, Bauwens W (2005) Statistical and trend analysis of rainfall and river discharge: Yala river basin, kenya. In: *Proceedings of the international conference of UNESCO Friend/Nile project: towards a better cooperation*, pp 171–181
- Golian S, Saghafian B, Farokhnia A (2012) Copula-based interpretation of continuous rainfall–runoff simulations of a watershed in Northern Iran. *Can J Earth Sci* 49(5):681–691
- Hanson LS, Vogel R (2008) The probability distribution of daily rainfall in the united states. In: *World environmental and water resources congress 2008: Ahupua`A*, pp 1–10
- Huang S, Chang J, Huang Q, Chen Y (2015) Identification of abrupt changes of the relationship between rainfall and runoff in the Wei River Basin, China. *Theoret Appl Climatol* 120(1):299–310
- Ismawati P, Rosmaini E (2018) Monthly rainfall distributions in pematangsiantar. In: *Journal of physics: conference series*, IOP Publishing, vol 1116, p 022018
- Jimoh O (2007) Impact of dams on hydrology of river Niger at Lokoja, Nigeria. *Arid Zone J Eng Technol Environ* 5:1–12
- Jimoh O, Webster P (1999) Stochastic modelling of daily rainfall in Nigeria: intraannual variation of model parameters. *J Hydrol* 222(1–4):1–17
- Kalita A, Bormudoi A, Saikia MD (2017) Probability distribution of rainfall and discharge of Kulsi River Basin. *Int J Eng Adv Technol (IJEAT)* 6(4):31–37
- Karmakar S, Simonovic S (2009) Bivariate flood frequency analysis. Part 2: a copula-based approach with mixed marginal distributions. *J Flood Risk Manag* 2(1):32–44
- Khosravi G, Majidi A, Nohegar A (2012) Determination of suitable probability distribution for annual mean and peak discharges estimation (case study: Minab River-Barantin Gage, Iran). *Int J Probab Stat* 1:160–163
- Kroll CN, Vogel RM (2002) Probability distribution of low streamflow series in the United States. *J Hydrol Eng* 7(2):137–146
- Langat PK, Kumar L, Koech R (2019) Identification of the most suitable probability distribution models for maximum, minimum, and mean streamflow. *Water* 11(4):734

- Machekposhti KH, Sedghi H, Telvari A, Babazadeh H (2016) Determination of suitable probability distribution for annual discharges estimation (case study: Karkheh River at Iran). *Int J Probab Stat* 5:73–81
- Mandapaka PV, Qin X (2013) Analysis and characterization of probability distribution and small-scale spatial variability of rainfall in singapore using a dense gauge network. *J Appl Meteorol Climatol* 52(12):2781–2796
- Mirabbasi R, Fakheri-Fard A, Dinpashoh Y (2012) Bivariate drought frequency analysis using the copula method. *Theoret Appl Climatol* 108(1):191–206
- Mohamed TM, Ibrahim AAA (2016) Fitting probability distributions of annual rainfall in Sudan. *J Eng Comput Sci* 17(2)
- Mohammed JM, Otache YM, Jibril I, Mohammed I (2017) Evaluation of best-fit probability distribution models for the prediction of inflows of Kainji Reservoir, Niger State, Nigeria. *Air Soil Water Res* 10
- Nelsen RB (2007) *An introduction to copulas*. Springer Science & Business Media
- Ng J, Yap S, Huang Y, Noh NM, Al-Mansob R, Razman R (2020) Investigation of the best fit probability distribution for annual maximum rainfall in kelantan river basin. In: *IOP conference series: earth and environmental science*, IOP Publishing, vol 476, p 012118
- Novianti P, Kartiko S, Rosadi D (2021) Application of clayton copula to identify dependency structure of covid-19 outbreak and average temperature in jakarta Indonesia. In: *Journal of physics: conference series*, IOP Publishing, vol 1943, p 012154
- Ogunjo S, Fuwape I, Oluyamo S, Rabiun B (2019a) Spatial dynamical complexity of precipitation and temperature extremes over Africa and South America. *Asia-Pacific J Atmosph Sci*, 1–14
- Ogunjo S, Ife-Adediran O, Owoola E, Fuwape I (2019b) Quantification of historical drought conditions over different climatic zones of Nigeria. *Acta Geophys* 67(3):879–889
- Ogunjo S, Fuwape I, Oluyamo S, Rabiun A (2021) Second-order markov chain models of rainfall in Ibadan, southwest nigeria. In: *IOP conference series: earth and environmental science*, IOP Publishing, vol 655, p 012001
- Ogunjo ST, Olusola AO, Fuwape IA, Durowoju OS (2022) Temporal variation in deterministic chaos: the influence of kainji dam on downstream stations along the lower niger river. *Arabian J Geosci* Accepted, 1–14
- Orimoloye IR, Olusola AO, Ololade O, Adelabu S (2021) A persistent fact: Reflections on drought severity evaluation over Nigerian Sahel using mod13q1. *Arab J Geosci* 14(19):1–18
- Oyebande L (1995) Effects of reservoir operation on the hydrological regime and water availability in Northern Nigeria. *IAHS Publ Ser Proc Reports-Intern Assoc Hydrol Sci* 230(1995):25–34
- Ozonur D, Pobocikova I, de Souza A (2020) Statistical analysis of monthly rainfall in central west brazil using probability distributions. *Model Earth Syst Environ*, 1–11
- Pandey P, Das L, Jhajharia D, Pandey V (2018) Modelling of interdependence between rainfall and temperature using copula. *Modeling Earth Syst Environ* 4(2):867–879
- Sabaghi B, Bajestan MS, Aminnejad B (2021) Uncertainty analysis of rainfall–runoff relationships using fuzzy set theory and copula functions. *Iranian Journal of science and technology, transactions of civil engineering*, pp 1–10
- Şen Z, Eljadid AG (1999) Rainfall distribution function for libya and rainfall prediction. *Hydrol Sci J* 44(5):665–680
- Sharma MA, Singh JB (2010) Use of probability distribution in rainfall analysis. *New York Sci J* 3(9):40–49
- Sklar M (1959) Fonctions de repartition an dimensions et leurs marges. *Publ Inst Statist Univ Paris* 8:229–231
- Sukcharoen K, Zohrabayan T, Leatham D, Wu X (2014) Interdependence of oil prices and stock market indices: a copula approach. *Energy Econ* 44:331–339
- Sultan B, Janicot S, Drobinski P (2007) Characterization of the diurnal cycle of the west african monsoon around the monsoon onset. *J Clim* 20(15):4014–4032
- Tabari H, Nikbakht J, Talaei PH (2013) Hydrological drought assessment in northwestern iran based on streamflow drought index (sdi). *Water Resour Manage* 27(1):137–151

- Wen L, Rogers K, Ling J, Saintilan N (2011) The impacts of river regulation and water diversion on the hydrological drought characteristics in the lower Murrumbidgee River, Australia. *J Hydrol* 405(3–4):382–391
- Ximenes PDSMP, Silva ASAD, Ashkar F, Stosic T (2021) Best-fit probability distribution models for monthly rainfall of northeastern Brazil. *Water Sci Technol* 84(6):1541–1556
- Ye L, Hanson LS, Ding P, Wang D, Vogel RM (2018) The probability distribution of daily precipitation at the point and catchment scales in the United States. *Hydrol Earth Syst Sci* 22(12):6519–6531
- Yet ZR, Masseran N (2021) Modeling dependence of solar radiation and sky clearness index using a bivariate copula. *Meteorol Atmos Phys* 133(5):1495–1504
- Yue S, Hashino M (2007) Probability distribution of annual, seasonal and monthly precipitation in Japan. *Hydrol Sci J* 52(5):863–877
- Zhang L, Singh VP (2012) Bivariate rainfall and runoff analysis using entropy and copula theories. *Entropy* 14(9):1784–1812

Chapter 7

Remote Sensing and High-Throughput Techniques to Phenotype Crops for Drought Tolerance



Sayantana Sarkar , Abhijit Rai, and Prakash Kumar Jha

Abstract Drought is an inevitable consequence of climate change. Therefore, newer crop varieties are required which are resilient to drought stress. Though there are extensive breeding programs for numerous crops, traditional breeding process is slow. Phenotyping crops for physiological and morphological traits could be used as proxies for drought tolerance traits. However, extensive in-situ field data collection is constrained by time and resources. Remote data collection and machine learning techniques for analysis offer a high-throughput phenotyping (HTP) alternative to manual measurements that could help breeding for stress tolerance. In this chapter we would discuss recent advances and future of HTP techniques that could help in faster selection of desired genotypes. These techniques could be further extended to aid in variable rate input application such as irrigation and be a step towards precision agriculture. In this chapter we advocate for the use of newer technologies such as remote sensing, machine learning, and computer vision in plant breeding and agronomic decision making.

Keywords Remote sensing · High-throughput phenotyping (HTP) · Aerial imagery · Drought tolerance · Low-moisture stress

S. Sarkar (✉)

Blackland Research and Extension Center, Texas A&M Agrilife Research, Temple, TX 76502, USA

e-mail: sarkarsayantana@hotmail.com

A. Rai

Department of Plant Sciences, College of Agriculture and Bioresources, University of Saskatchewan, Saskatoon, SK S7N 5A8, Canada

P. K. Jha

Feed the Future Innovation Lab for Collaborative Research on Sustainable Intensification, Kansas State University, Manhattan, KS 66506, USA

e-mail: pjha@ksu.edu

7.1 Introduction

Crop production ensures food and nutritional security of burgeoning population globally (El Bilali et al. 2019). However, crop production system faces acute pressure with changing diet, variability in climate and are sensitive to biotic and abiotic stresses (Bharadwaj 2012; Richards et al. 2015). Variability in climatic conditions persist for longer period and can be attributed directly to human activity. Crop production is generally sensitive to environmental extremes like temperature and precipitation (Huang 2004; Ahmed et al. 2011; Ayyogari et al. 2014; Araya et al. 2022). Higher temperatures, lowers crop yield by reducing carbon assimilation directly (Boonekamp 2012; Yadav et al. 2022) and impact indirectly by causing erratic precipitation leading to droughts, floods, and storms. Global water scarcity limits the crop productivity via water stress leading to poor germination, stunted shoots, smaller leaves, less flowering, aborted pollens and ovules, poor seed set, and increased diseases incidences (Nuruddin 2001; Rakshit et al. 2009; Minaxi et al. 2011; Sarkar 2020; Bennett et al. 2021). Water deficit stress to plants has significant effects on crop morphology and physiology which significantly reduces crop yield at the end of the crop growth season (Jha et al. 2018, 2021, 2022; Jha 2019; Balota et al. 2021a) (Fig. 7.1a).

Drought stress affects assimilate partitioning by allocating more dry matter to the roots instead of the reproductive sinks such as tubers, pods, and seeds (Blum 2011; Balota and Sarkar 2020). On a cellular level, reduced water availability causes loss of cell turgor pressure, leading to poor cell elongation (Burow et al. 2021). Drought stress in plant cells leads to activation of abscisic acid (ABA) signaling genes which causes over expression of ABA producing genes. This triggers a cascade of physiological changes starting in guard cells to roots (Osakabe et al. 2014). Moreover, drought environments result in high evapotranspiration of soil causing higher concentration of residual solutes in it, thereby increasing soil salinity (Prasad and Chakravorty 2015).

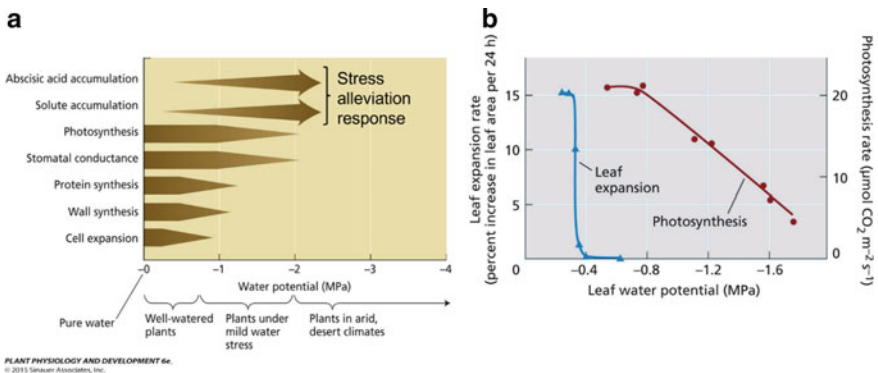


Fig. 7.1 Effect of drought stress on plant at **a** cellular level and **b** physiological level (Adapted from Taiz et al. 2015)

Salinity stress have shown to adversely affect economically important parts of crops by causing cellular and anatomical modifications (Maksimovic and Ilin 2012).

Field and simulated water management studies have shown that crop production system remain resilient if proper practices were adopted at critical crop growth stages (Singh and Lal al. 2010; Jha 2019; Eeswaran et al. 2021). However, the development of stress tolerant cultivars remains a priority of breeders and alteration of crop calendar have been suggested by agronomists to manage drought stress (Parajuli et al. 2019). The phenomics technologies characterizes crop responses to drought stress using imageries which include, leaf color and biomass conditions. In this chapter, we will discuss plant responses to drought stress and different techniques of phenotyping crop for drought tolerance.

7.2 Plant Response to Drought Stress

Plants respond to environmental stress through various morphological, physiological, and metabolic adaptations. These adaptations have direct effect on growth and development, biomass accumulation, yield, and quality of the crop (Mishra and Singh 2010). Adaptations for drought tolerance can be classified as escape, avoidance, and tolerance adaptations (Stebbins 1952; Chapin et al. 1993; Kooyers 2015; Basu et al. 2016). Drought escape mechanisms are referred as “earliness.” The plants grow quickly and end their reproductive cycle before the dry weather arrives. The plants can modulate their vegetative and reproductive phases based on water availability. These mechanisms apply mostly to the annual plants with low vegetative growth (Blum 2009). These plants are adapted to have fast phenological growth and produce fewer seeds before depletion of the available soil water. Drought avoidance involves mechanisms that allow plants to keep high turgidity under low cellular water potential; in this way, they can “avoid” severe stress. In this instance, plants use water more efficiently by modifying physiological activities (i.e., lowering transpiration and minimizing stomatal conductance,) and morphological characteristics (i.e., more succulent leaves, limiting vegetative growth from reduced plant height and leaf area, and increasing root growth) (Blum 2011). Drought tolerance involves adaptations to allow plants endure low tissue water content. The underlying mechanisms are cellular protection mechanisms under low cellular turgidity (Sung et al. 2021). For example, plants can withstand dry weather by osmotic adjustment, sugar and other metabolites accumulation, and production of osmoprotectants which help stabilize proteins (Basu et al. 2016; Kooyers 2015).

Drought resistance involves physiological alterations. These alterations are further controlled by phytohormones and other molecular mechanisms which are regulated by gene expressions (Osakabe et al. 2014). All these events are integrated into molecular networks and mechanisms for the plant to adapt and survive. Comparative studies on drought resistant *vs.* drought susceptible wheat and cotton genotypes showed that overexpression of certain genes resulted in accumulation of glucose, fructose, proline, and glycine in plant cells (Patil et al. 2016). These solutes accumulation helped with

osmotic adjustment and turgor pressure maintenance for cell growth and mitosis even under low water potential conditions. These solutes also detoxified membranes from the reactive oxygen species (ROS) and maintained membrane integrity and enzyme stability (Chaves and Oleiveira 2004; Serraj and Sinclair 2002). A study on rice suggested that *HARDY* (*HRD*) gene in HRT lines of rice were responsible for drought tolerance. This gene was responsible for higher shoot biomass accumulation under well-watered conditions whereas, under drought and salt stress, the over expression of the *HRD* gene was responsible for increased root biomass development and production of thicker leaves with more chloroplast bearing mesophylls. This resulted in better water use efficiency (WUE) and enhanced photosynthesis during drought conditions (Karaba et al. 2007; Jha et al. 2018; Rai et al. 2020; Shekoofa et al. 2022). Therefore, drought resistant genotypes can be developed through selection for traits that favor drought tolerance, including maintained cell turgor pressure under low moisture conditions, compact canopy to reduce transpiration, and higher chlorophyll stability, better WUE, and photosynthesis during low moisture stress.

The current breeding approach has been successful in selection of high yielding and stress resistant cultivars, but traditional methods of manually selecting lines for trait of interest are slow and uneconomical for large breeding populations (Jones and Vaughan 2010; Branch et al. 2014; Tester and Langridge 2010). Several morphological and physiological traits are associated with tolerance to water deficit stress and breeding for these traits is superior to breeding for yield alone (Nigam et al. 2005). Measuring these phenotypic traits, breeders can select genotypes with tolerance to water deficit stress including early biomass accumulation, leaf area index (LAI), leaf wilting, plant height, and rooting depth (Kiniry et al. 2005; Nigam and Aruna 2007; Arunyanark et al. 2008). Early to mid-season LAI variations were indicators of drought, therefore LAI was recommended as a useful physiological characteristic in breeding for drought tolerance (Ma et al. 1992; Nutter and Littrell 1996). Shortening of the main axis and cotyledonary branches of crops under soil moisture stress has been reported by Chung et al. (1997) and thoroughly discussed by Reddy et al. (2003). Reduction in plant height under soil water deficit was attributed to reduction of internodal length, and it was suggested to change dry matter partitioning, plant density, spatial arrangements of the plants, and light interception under drought (Bell et al. 1993; Collino et al. 2001; and Pandey et al. 1984). In maize, plant height was related with yield and proposed as a selection tool for this crop (Freeman et al. 2007; Yin et al. 2011).

Low soil moisture has been associated with deep rooting pattern of the plants. Deep roots uptake water from lower soil horizon during drought stress (Comas et al. 2013; Fukai and Cooper 1995; Henry et al. 2011). Leaf wilting has been related to WUE and leaf water potential of crops (Sarkar et al. 2021b). A plant trait to avoid heat stress is transpiration cooling to decrease canopy temperature but is not favorable under drought stress as water conservation is a priority for the plant to survive (Julia and Dingkuhn 2013; Lin et al. 2017). Slow transpiring or limited transpiring plants with higher canopy temperature than susceptible cultivars would have better WUE and chance of survival in drought stress. Therefore, canopy temperature could be a phenotypic selection tool (Sarkar et al. 2022a). However, measurements of

these traits over large breeding populations or acreages are difficult and impractical because substantial number of data points are needed to generate representative trait information. Therefore, phenotyping for drought stress remotely could be a better option (Tattaris et al. 2016; Sarkar 2020).

7.3 High-Throughput Techniques and Remote Sensing for Phenotyping

High-throughput (HT) techniques involve using advanced technologies for faster and accurate collection, extraction, and analysis of data (Sarkar and Jha 2020). The data collection is automated, non-destructive, and takes lesser time (Sarkar et al. 2020). It allows for measurement of a large area over a period of time (temporal variability) and include small variations within the same field (spatial variability). Phenotyping over a time period at frequent time intervals is crucial for determining stress response over the mapped area. Determining spatiotemporal variations within the field can help to select desirable genotypes within a large pool. Spectral wavelength quantifying sensors such as aerial multispectral and hyperspectral cameras mounted on an automated unmanned aerial vehicle (UAV) can be used for aerial imagery (Fig. 7.2) (Sarkar et al. 2019; Balota et al. 2021b). This process of remote collection of data is called remote sensing and is the most crucial part of HT technology (Sadeghpour et al. 2017a; Oakes et al. 2019).

Aerial and proximal imagery in different visible and in-visible wavelengths from the electromagnetic spectrum are collected to determine the extent to which different wavelengths are reflected by the plants (Table 7.1) (Sadeghpour et al. 2017b; Sarkar et al. 2018; Oakes et al. 2020). This reflected part of the electromagnetic spectrum is known as the reflectance (Ladoni et al. 2010). Based on this reflectance, various methods have been developed for data acquisition, band selection, model estimation and verification of remote sensing data (Sarkar 2021). Aerial imagery is used to capture this reflectance to be analyzed in a lab (Sarkar et al. 2020, 2021a). Apart from that, the infrared reflectance or thermal imagery can also be calibrated and used to estimate canopy temperature of plants (Fig. 7.3). Thermal imagery or thermography represents use of thermal long wave infrared (TIR) sensors (or simply thermal camera) to record thermal radiation and provide raster with temperature value pixel (Pineda et al. 2020). Aerial thermography can be used to measure leaf or canopy temperature of field crops as a stress phenotyping trait for virtually any crop. Measuring canopy temperature is an important physiological trait owing to its occurrence before any visual symptom (Chaerle and Straeten 2001).

Apart from reflectance, aerial imagery can be used to determine colors of vegetation using red–green–blue (RGB) color space models. A color space model is a geometric representation of colors in space, usually in three dimensions. It is the way

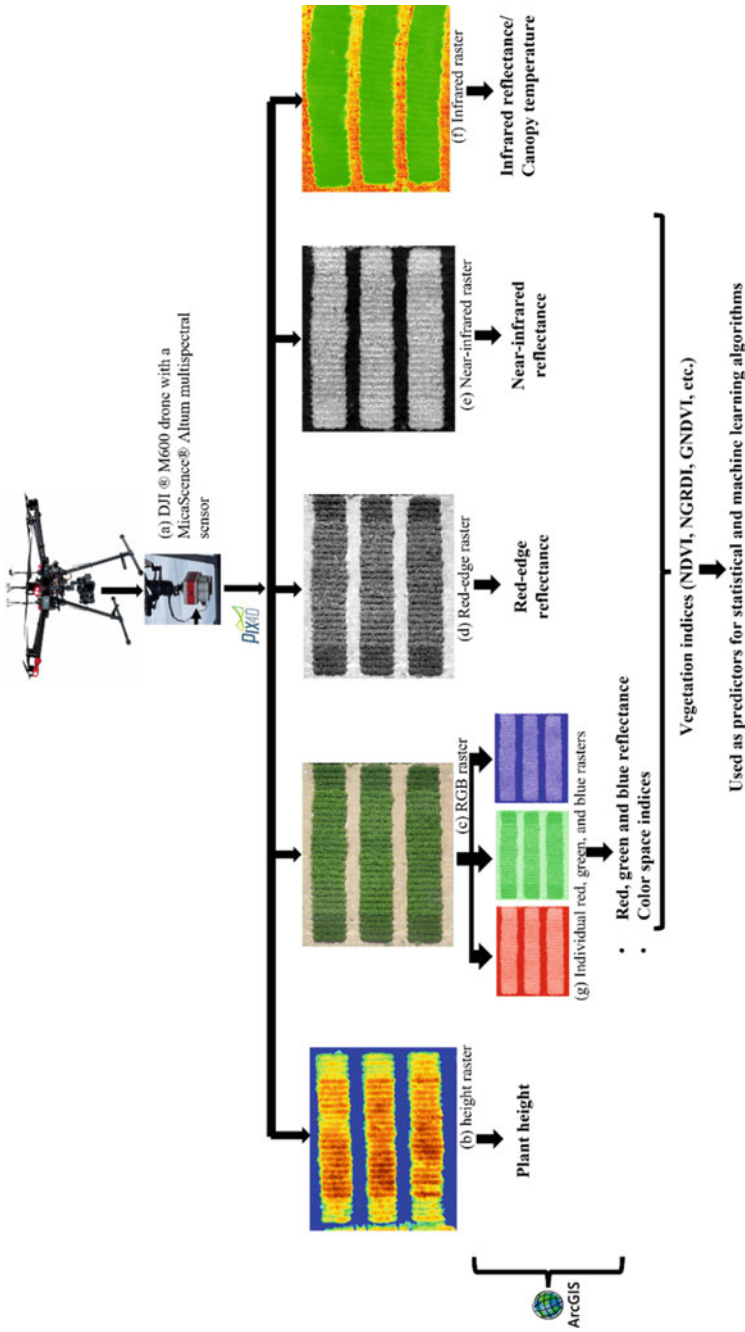


Fig. 7.2 Schematic diagram of using aerial imagery and reflectance to phenotype crops

Table 7.1 Sensors for high-throughput imagery and their use on corresponding traits (Adapted from Kim et al. 2020. <https://doi.org/10.1590/1678-992X-2019-0300> under creative commons Attribution 4.0 International (CC BY 4.0) license)

Sensors	Wavelength	Features	Traits
RGB (Red, green, blue) sensor	400–700 nm	Sensing visible wavelengths. Most easily accessible sensor	Vegetation indices, plant height, plant structure, growth rates, and morphological traits
NIR (Near infrared) sensor	700–1400 nm	Sensing highest reflectance of plant green area in 700–1300 nm, while beyond 1300 nm shows more absorbance by water than the visible spectrum	Chlorophyll conductance, water status, and vegetation indices
Hyperspectral sensor	–	Sensing thousands of bands per pixel. More detailed images can be obtained than the multispectral imaging if the requirements are set	Vegetation and water indices, soil cover status, photosynthesis rates, and levels of phytochemicals
Thermal sensor	700–106 nm	Sensing emitted radiation of object that increases with the object temperature above absolute zero. Suitable to image temperature changes	Canopy temperature, transpiration rates, and water stress responses
Fluorescence sensor	180–800 nm	Sensing fluorescence emitted by short wave light absorption of susceptible molecule	Chlorophyll conductance, photosynthetic rates, and pigment composition
LiDAR (Light Detection and Ranging)	250–2000 nm	Surface scan of target objects and distance measurement by analyzing the reflected light	Canopy and leaves, vegetation cover, plant height, and nitrogen status
Others -MRI	–	Feasible to screen underground structures of plant by 3D imaging and transport processes in natural porous media	Water contents, stem structures, root structures, transport processes
Others -Gravimetric sensor	–	Capable of measuring plant physiological changes by non-imaging process. Requires other sensors for screening	Weight, water use efficiency, water status, transpiration rates, biomass

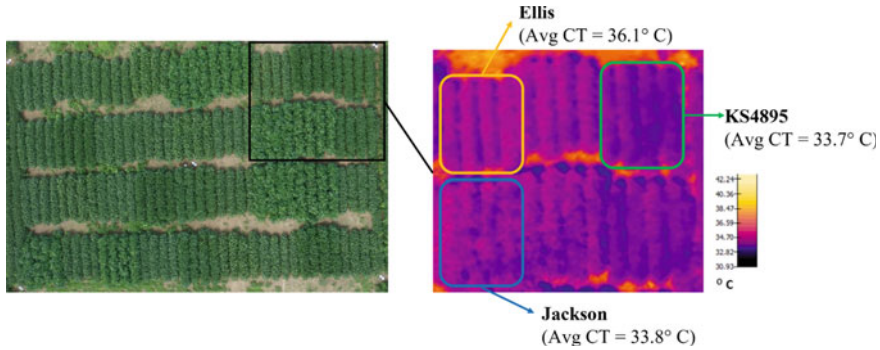


Fig. 7.3 Canopy temperature (CT) estimation using thermal imagery. Ellis, Jackson, and KS4895 are soybean varieties

human eyes can visualize color through its attributes such as hue angle and brightness. Distinct color space models are available for different applications (Schanda 2007; Lee et al. 2020). The color space models used for crop phenotyping are CIE-Luv and CIE-Lab. L in Luv and Lab represents luminance whereas u and v in Luv, and a and b in Lab represents chrominance. Chrominance ranges from red (+a) to green (−a); and from yellow (+b) to blue (−b). Other indices such as green area (GA) and greener area (GGA) have been developed based on the position of the color within chrominance and hue angle. GA includes pixels ranging from 60° to 120° Hue angle, and GGA includes pixels from 80° to 120° on CIE-Lab (Schanda 2007). RGB color space indices have been previously used in estimating leaf wilting (Sarkar et al. 2021b) (Table 7.2).

Aerial images can also be used to create a three-dimensional model built by Structure from Motion (SfM) photogrammetry. SfM photogrammetry is a three-dimensional reconstruction of structures from a moving sensor (Fig. 7.4). It is a low supervision and expertise required technique of using consumer grade digital cameras to derive high resolution structural images with accurate spatial information (Westoby et al. 2012; James and Robson 2012; Fonstad et al. 2013; Micheletti et al. 2015a, b). SfM photogrammetry uses multiple overlapping images acquired from multiple viewpoints. A software algorithm then identifies common feature points across the overlapped image sets. The common points identified are used to determine spatial data of the elevation of the point in an arbitrary 3-D coordinate system. The algorithm then transforms these elevation points on coordinate system covering the system also known as point cloud. The last step is intensifying the point clouds to generate high resolution 3-D models by isolating gross errors (Snavely et al. 2008; Furukawa and Ponce 2010; Rothermel et al. 2012; Remondino et al. 2014). UAV and SfM photogrammetry have been successfully used to estimate plant height, canopy width, crop architecture, crop growth rate, and above ground biomass in plants (Freeman et al. 2007; Bendig et al. 2013; Holman et al. 2016; Watanabe et al. 2017; Demir et al. 2018; Lottes et al. 2017; Han et al. 2018; Wang et al. 2018, Yuan et al. 2018).

Table 7.2 Red–green–blue (RGB) color space indices and their basis of derivation (Adapted from Sarkar et al. 2021b. <https://doi.org/10.3389/fpls.2021.658621> under creative commons Attribution 4.0 International (CC BY 4.0) license)

RGB color indices*	Basis of derivation*
Intensity	Measures intensity or greyness in 0 (black) to 1 (white) scale in Hue Saturation Intensity (HSI) color space ^a
Hue	Color judgement based on position in HSI color space [0° to 360° (0°-red; 60°-yellow; 120°-green; 240°-blue)] ^a
Saturation	Measures dilution of pure color (hue) with white light in HSI color space (ranges from 0 to 1) ^a
Lightness	Light reflected by a non-luminous body [0 (black) to 100 (white) scale] ^b
a	Measures color shift from green (–a) to red (+a) in CIE-Lab ^c color space ^b
b	Measures color shift from blue (–b) to yellow (+b) in CIE-Lab color space ^b
u	Measures color shift from green (–a) to red (+a) in CIE-Luv ^c color space ^b
v	Measures color shift from blue (–b) to yellow (+b) in CIE-Luv color space ^b
Green Area (GA)	Percentage of pixels in 60°–120° hue angle in CIE-Lab ^c
Greener Area (GGA)	Percentage of pixels in 80°–120° hue angle in CIE-Lab ^c

^aWelch et al. (1991)

^bSchanda (2007)

^cCasadesús et al. (2007)

^dKefauver et al. (2017)

^eL represents Lightness in both CIE-Lab and CIE-Luv, and a and u represent the red–green spectrum of chromaticity and b and v represent yellow–blue color spectrum (Schanda 2007)

The images and 3-D models are further processed using image processing software and analyzed using GIS software to extract reflectance values of each pixel (Sadeghpour et al. 2018; Balota et al. 2021b). These state-of-art software programs run using high-processing power computer gives an edge to the HT system by making data extraction faster (Sarkar et al. 2021b). The analysis of the data involves statistical and machine learning tools for stepwise multiple linear regression (SMLR), partial least square regression (PLSR), multivariate adaptive regression splines (MARS), principal component regression, and artificial neural networks (ANN) to derive phenotypic estimation models (Araya et al. 2021; Saravi et al. 2021). Therefore, phenotyping using HT techniques is called high-throughput phenotyping (HTP).

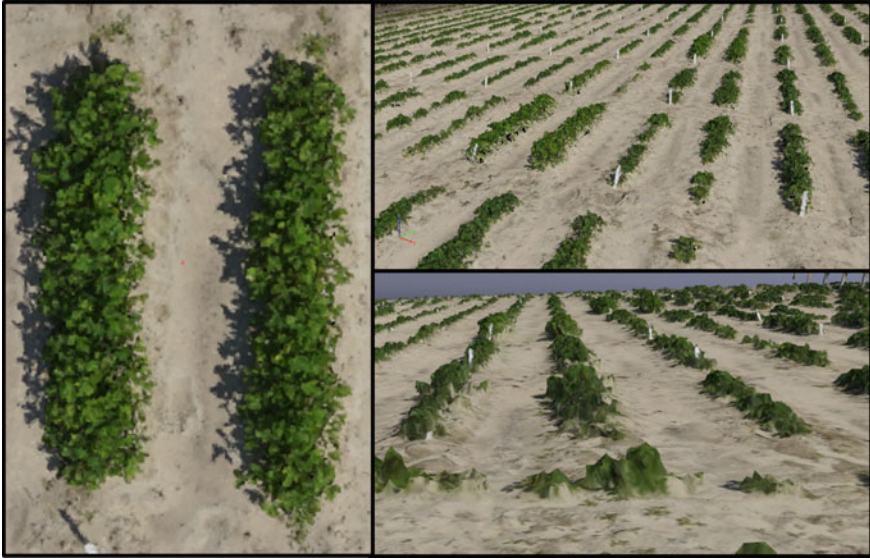


Fig. 7.4 Three dimensionally reconstructed peanut canopies using surface to motion (SfM) photogrammetry

7.4 High-Throughput Phenotyping for Drought Tolerance in Plants

7.4.1 Use of Reflectance and Vegetation Indices

Aerially derived RGB, NIR, and infra-red imagery derived vegetation indices (NDVI, GNDVI, RGRI, SAVI, NGRDI, and NSSI) were used to estimate leaf area, leaf wilting, biomass, and yield of several agronomic and horticultural crops including wheat, maize, barley, soybean, dry beans, peanuts, grapes, tomato, and spinach (Zakaluk and Ranjan 2008; Behmann et al. 2014; Raza et al. 2014; Wenting et al. 2014; Luis et al. 2016; Sankaran et al. 2019; Zhang et al. 2019; Banerjee and Krishnan 2020; Zhou et al. 2020; Sarkar et al. 2021b). Aerially estimated NDVI can be used as a drought phenotyping tool similar to any other physiological trait or grain yield (Rutkoski et al. 2016; Khan et al. 2018). NDVI has shown to preserve the variability within wheat varieties required for breeding selection. Other indices such as green NDVI and red NDVI have shown to improve genomic and pedigree selection for grain yield in wheat (Rutkoski et al. 2016). These indices showed high broad sense heritability ($H^2 > 0.8$) for what grain yield at early growth stages even during high to low drought stages. This is very helpful for selection of drought tolerant genotypes earlier in the season. Indices normalized difference water index (NDWI)

and normalized multi-band drought index (NMDI) have been used to detect relative water content in soybean leaves, even when the water low water deficit (Braga et al. 2021). These indices were derived using short wave infra-red (SWIR) bands. Vegetation indices being successfully used to detect vegetation water content at low water deficit can be used to detect early drought symptoms in crops. Biomass yield of 50 perennial ryegrass cultivars were correlated ($r = 0.6\text{--}0.8$) to aerially derived NDVI (Wang et al. 2019a). The study hypothesized that this method would be more rapid and cost effective for forage breeders as compared to traditional visual scoring. It was also observed that NDVI was a proxy for yield and could be used to delineate and select genotypes. Several vegetation indices such as NGRDI, NDVI, and NDRE were used to estimate plant height, leaf number, and biomass in fench and faba beans (r -values ± 0.7 to ± 0.9) (Travlos et al. 2017). This study on legumes also concluded that visible RGB vegetation indices are better suited for legumes than invisible NIR or red-edge ones.

Further studies also showed that aerially measured RGB vegetation indices could be used to phenotype peanuts and soybean for leaf area, above ground biomass, yield, and harvest quality (Vollmann et al. 2011; Sarkar et al. 2021a). A recent study showed that drought and salinity stress on basil (*Ocimum basilicum* L.) caused variation in greenness index (GI), NDVI, plant senescence reflectance index (PSRI), and Anthocyanin Reflectance Index (ARI) (Lazarević et al. 2021). The study concluded that GI is related to leaf morphology, thickness, water content, and light scattering; PSRI represents chlorophyll to carotenoid ratio and is related to leaf senescence; and ARI is related to anthocyanin accumulation in stressed leaves causing plants' darker green color. Quantitative trait loci (QTL) analysis of durum wheat showed that 46 significant QTLs affected NDVI across platforms; several of which effects leaf chlorophyll content, leaf greenness, leaf rolling and biomass under terminal drought stress (Condorelli et al. 2018). Therefore, it can be concluded that vegetation indices can be measured aerially and used for HTP of crops for drought tolerance. However, fewer studies are available on heritability and effect of QTLs of different crops on vegetation indices and more investigation is required before indices could be used as traits themselves instead of using them to estimate crop traits.

7.4.2 Use of Thermal Imagery/thermography

Thermal imaging of crops is increasingly used by crop physiologist, pathologists, and geneticists for high-throughput field and greenhouse phenotyping (Prashar and Jones 2014). Since canopy temperature of crops vary on several different factors such as relative humidity, wind speed, light intensity and canopy structure, thermal imagery requires several corrections and calibrations to accurately represent canopy temperature. These corrections and calibrations on thermal imagery result in values known as thermal long wave infrared (TIR) stress indices (Pineda et al. 2020). Among stress indices, crop water stress index (CWSI), has been used to study leaf transpiration and senescence due to water stress on wheat foliage (Jackson et al. 1981).

This study found that maximum transpiration coincided with minimum CWSI and discussed using CWSI for irrigation scheduling of crops. Further, this study used the difference of canopy and air temperature, canopy temperature depression (CTD), correlated to vapor pressure deficit of wheat, which was affected by evapotranspiration rate. Another stress index, index of stomatal conductance (I_G), is based on leaf temperature of wet and dry leaves and is linearly correlated to leaf stomatal conductance (Jones 1999). This study used I_G for irrigation scheduling of runner beans (*Phaseolus coccineus* L.) under different moisture regimes. Normalized relative canopy temperature (NRCT) is a valid estimation of crop water status in barley (*Hordeum vulgare* L.) (Elsayed et al. 2015). NRCT could also estimate barley grain yield ($R^2 = 0.5 - 0.7$) under well-watered and drought stressed conditions. Simple use of IRT has been successful in disease phenotyping of tobacco (*Nicotiana tabacum* L.) (Simko et al. 2017).

It was found that leaves infected by tobacco mosaic virus (TMV) showed a pre-symptomatic rise in temperature 8 h before cell death (Chaerle et al. 2001). This study concluded that thermography was a better than visual detection of TMV necrosis in tobacco leaves for amelioration measures. Thermography using IRT has been used to phenotype corn landraces for drought tolerance (Costa et al. 2015). In this study leaf temperature of several corn landraces was measured every 48 h, which is very difficult manually. Another study phenotyped 92 corn genotypes for drought stress using thermography and CWSI by observing the time interval between anthesis and blister stage (Romano et al. 2011). Therefore, thermography can accelerate drought phenotyping process and when done aerially could be a HTP tool. However, canopy temperature might be caused by several biotic and abiotic stresses simultaneously. Therefore, it is suggested that thermography cannot be used independently and should be used in combination with other spectral indices (Pineda et al. 2020). Moreover, there is a need for universal calibration and correction protocol for conversion of thermal reflectance to canopy temperature.

7.4.3 Use of Color Space Indices

Vegetation indices can be derived from RGB color space indices (also known as color indices), which represent international standards for color perception by the human eye and were adopted by the Commission Internationale de l'Eclairage (CIE) in 1976 (Yam and Papadakis 2004; Trussell et al. 2005; Kefauver et al. 2015; Chapu et al. 2022). Color indices (a^* , u^* , NDLab, NDLuv) were used to estimate persistence and biomass of drought stressed forage crop *Festuca arundinacea* Schreb. with high accuracy (r -values above ± 0.9) (Swaef et al. 2021). Color indices have also been used to phenotype grain yield and leaf N content in corn (Vergara-diaz et al. 2016); and grain yield and disease severity in durum wheat (Vergara-diaz et al. 2015). In both studies color indices outperformed spectral indices such as NDVI in phenotype assessment. The studies hypothesized that quantifying visual colors is a better representation and more direct measurement of traits than spectral reflectance of foliage.

Similar results were observed using color indices such as Hue, a^* , b^* , GA, and GGA to estimate LAI and biomass for breeding selection of tritordeum, wheat and triticale genotypes (Casadesús et al. 2007; Casadesús and Villegas 2014). These studies concluded that NDVI is related to red and NIR reflectance due to photosynthesis, cereals reach maximum photosynthesis very early during their life cycle.

Therefore, color indices outperform NDVI because the later saturates and loses sensitivity at the end of vegetative phase of cereals. Color indices, saturation, a^* , and b^* were used to differentiate effects of different rates of plant growth regulators (PGR) on cotton (Sarkar et al. 2022b). This study concluded that cotton with higher rates of PGR had darker green foliage compared to lower rates. This difference in greenness can be used to optimize efficiency of PGR application using aerial imagery. Color index b^* has been used to predict green leaf area and onset of senescence for phenotyping grain yield and protein concentration of winter wheat during drought stress (Kipp et al. 2013). A similar study used color indices to predict leaf wilting in peanuts and soybean which corresponded to leaf water potential and specific leaf area (Zhou et al. 2020; Sarkar et al. 2021b). The peanut study used images from aerial as well as handheld cameras with accuracies above 90%. This shows that color indices have the potential to be used in algorithm of a cell phone app to estimate leaf wilting and leaf water content for irrigation scheduling. A recent study has also argued that vegetation and color indices can be used as proxy traits for drought phenotyping owing to their high heritability (H^2 value higher than 0.7) (Balota et al. 2021b; Swaef et al. 2021).

7.4.4 Use of SfM Photogrammetry

SfM photogrammetry using aerial stereo images were successfully used to determine plant height in sorghum, wheat, barley, peanuts, cotton, and corn using digital surface models (Freeman et al. 2007; Han et al. 2018; Wang et al. 2018; Yuan et al. 2018; Sarkar et al. 2020, 2022b). Plants affected by drought stress are usually stunted, making plant height an important drought phenotyping trait. SfM photogrammetry and LiDAR were used to create 3-D models of wheat plant to assess plant height and growth rates (Holman et al. 2016). These aerially assessed growth rates correlated with wheat growth stages and fertilizer applications. This study concluded that SfM photogrammetry using RGB images is as good as LiDAR in terms of accuracy while bettering in cost and efficiency. Surface models derived using SfM photogrammetry were used to phenotype corn plants for plant height, lodging area, and canopy LAI at different growth stages with reasonable accuracy ($R^2 > 0.7$) (Su et al. 2019). These phenotypic traits could be used for faster selection of drought tolerant genotypes of corn. SfM photogrammetry was used to phenotype tomato for leaf area and main stem height (Rose et al. 2015). The study hypothesized that tomato genotypes with higher leaf surface area (hence more stomata) is more prone to wilting because of higher transpiration rates. Therefore, HTP of leaf area in crops is important for drought phenotyping. Digital 3-D plant models using SfM photogrammetry were

used to measure leaf area and biomass in basil affected by drought and salinity stress (Lazarević et al. 2021). Digitally measured morphological traits showed a profound reduction in leaf area and biomass of basil subjected to stress. Though SfM photogrammetry is an advanced and high-throughput technique for phenotyping, creation of surface models requires technical expertise in use of hardware and software. Therefore, developing technology with user friendly interface is required for SfM photogrammetry.

7.4.5 Use of Machine Learning

Machine learning algorithms have been used to train models for estimation of drought phenotyping traits (Hien et al. 2021). One such study estimated yield by identifying rice, wheat, and sorghum panicles using convoluted neural network (CNN) from RGB images (Xiong et al. 2017; Hasan et al. 2018; Ghosal et al. 2019). Another study in wheat identified flowering stage of wheat from digital images using CNN architecture (Wang et al. 2019b). The CNN architecture used training-validation-testing approach to predict awn phenotype among several wheat lines. Another study used spatial pyramid matching (SPM) and support vector machines (SVM) as learning models to identify and differentiate between flowering and heading stage of wheat (Sadeghi-Tehran et al. 2017). These studies on wheat demonstrated that deep learning using breeder trained models from aerial or proximal images can accurately classify plant morphology, which are important traits for drought phenotyping. Leaf area index of peanuts was estimated using multiple linear regression (MLR) and artificial neural network (ANN) using vegetation indices as predictors with very high accuracy ($R^2 = 0.085 - 0.97$) (Sarkar et al. 2021a). LAI is an important drought phenotyping trait in peanuts. Machine learning and computer vision approach using *k*-means and CNN were used to create root system architecture using RGB images in soybean (Falk et al. 2020).

Root architecture is a very important phenotypic trait for drought tolerance in virtually all plants. Evapotranspiration rates in 48 chickpea (*Cicer arietinum* L.) genotypes were forecasted using machine learning tools such as SVM, ANN, and Random Forests (RF) by 3-D scanning around 5000 plants every 2 h (Kar et al. 2021). Machine learning approaches for such huge amounts of data, also known as big data, requires cutting edge technologies such as larger storage devices, faster computing processors, and rapid internet connection. Ordinal and binary logistic regression were used to train models for peanut leaf wilting prediction on 0–5 scale as well as wilted/not wilted binary scale using several color indices as predictors (Sarkar et al. 2021b). The study was further extended to predict leaf wilting from aerial images using computer vision and SVM with better accuracy (*unpublished*). Comparing both the approaches to estimate peanut leaf wilting concludes that different statistical and machine learning approaches to analyze the same data can yield different results. Therefore, advanced analysis of aerial and spectral data is important, making machine learning algorithms for big data analysis the backbone of HTP technology.

7.5 Conclusion

Using HTP for drought tolerant cultivar selection is feasible. Drought tolerant cultivars are required to make agriculture sustainable in the future. Using HTP methods such as remote sensing, statistics, and machine learning can be faster options to phenotype plants for better water use efficiency and drought tolerance. Along with direct measurements, using aerially derived vegetation indices can be used as predictors for phenotype estimation. Vegetation indices are directly linked to plant physiology, leaf pigments, photosynthesis, photosystem II, and leaf water content. Whereas color indices show direct linkage with physical appearance; lighter green color of crop foliage due to drought or disease stress on leaves; or darker green foliage due to PGR or fertilizer application. Therefore, variations in aerially measured indices can be used not only as proxies for physiological traits but as individual traits itself. Similarly, thermography and TIR stress indices are often more reliable than actual temperature values. Digital crop models and machine learning approaches can help in faster and more accurate phenotyping of crops. Machine learning can also be used to convert the derived indices and crop models into a field map. HTP using machine learning and aerial imagery can facilitate creation of high-resolution spatiotemporal field maps for individual phenotypes or vegetation indices which is easier to visualize. This field map can not only be used for breeding but for agronomic purposes to pinpoint requirements of amelioration and corrective measures instead of blanket application of farm inputs. The application rate of farm inputs such as irrigation, fertilizers, and pesticide could be varied over a single field with the help of a field map showing variable stress. This variable rate application is a step towards precision agriculture and can prevent over application and wastage of resources. Therefore, we see that HTP can not only help select drought tolerant cultivars but prevent excessive use of irrigation water and other resources in a drought situation.

References

- Ahmad J, Alam D, Haseen MS (2011) Impact of climate change on agriculture and food security in India. *Int J Agricult Environ Biotechnol* 4(2):129–137
- Araya A, Prasad P, Ciampitti I, Jha P (2021) Using crop simulation model to evaluate influence of water management practices and multiple cropping systems on crop yields: a case study for Ethiopian highlands. *Field Crop Res* 260:108004
- Araya A, Jha PK, Zambreski Z, Faye A, Ciampitti IA, Min D, ... Prasad PVV (2022) Evaluating crop management options for sorghum, pearl millet and peanut to minimize risk under the projected midcentury climate scenario for different locations in Senegal. *Clim Risk Manag* 100436
- Arunyanark A, Jogloy S, Akkasaeng C, Vorasoot N, Kesmala T, Nageswara Rao R, Wright G, Patanothai A (2008) Chlorophyll stability is an indicator of drought tolerance in peanut. *J Agron Crop Sci* 194(2):113–125
- Ayyogari K, Sidhya P, Pandit MK (2014) Impact of climate change on vegetable cultivation-a review. *Int J Agricult Environ Biotechnol* 7(1):145
- Balota M, Sarkar S (2020) Transpiration of Peanut in the field under Rainfed production. Paper presented at the American Peanut research and education society annual meeting 2020, Virtual

- Balota M, Sarkar S, Cazenave A, Kumar N (2021a) Plant characteristics with significant contribution to Peanut yield under extreme weather conditions in Virginia, USA. Paper presented at the ASA, CSSA, SSSA international annual meeting, Salt Lake City, UT
- Balota M, Sarkar S, Cazenave A, Burow M, Bennett R, Chamberlin K, Wang N, White M, Payton P, Mahan J (2021b) Vegetation indices enable indirect phenotyping of Peanut physiologic and agronomic characteristics. Paper presented at the American Peanut research and education society annual meeting, Virtual
- Banerjee K, Krishnan P (2020) Normalized Sunlit Shaded Index (NSSI) for characterizing the moisture stress in wheat crop using classified thermal and visible images. *Ecol Ind* 110:105947
- Basu S, Ramegowda V, Kumar A, Pereira A (2016) Plant adaptation to drought stress. *F1000Research*, 5
- Behmann J, Schmitter P, Steinrücken J, Plümer L (2014) Ordinal classification for efficient plant stress prediction in hyperspectral data. In: International archives of the photogrammetry, remote sensing & spatial information sciences
- Bell M, Wright G, Harch G (1993) Environmental and agronomic effects on the growth of four peanut cultivars in a sub-tropical environment II. Dry matter partitioning. *Exp Agricult* 29(4):491–501
- Bendig J, Bolten A, Bareth G (2013) UAV-based imaging for multi-temporal, very high resolution crop surface models to monitor crop growth variability monitoring des Pflanzenwachstums mit Hilfe multitemporaler und hoch auflösender Oberflächenmodelle von Getreidebeständen auf Basis von Bildern aus UAV-Befliegungen. *Photogrammetrie-Fernerkundung-Geoinformation* 2013(6):551–562
- Bennett RS, Chamberlin K, Morningweg D, Wang N, Sarkar S, Balota M, Burow M, Chagoya J, Pham H (2021) Response to drought stress in a subset of the U.S. Peanut mini-core evaluated in three states. *Peanut Sci* 49(1). <https://doi.org/10.3146/>
- Bhardwaj ML (2012) Effect of climate change on vegetable production in India. In: Vegetable production under changing climate scenario, pp 1–12
- Blum A (2009) Effective use of water (EUW) and not water-use efficiency (WUE) is the target of crop yield improvement under drought stress. *Field Crop Res* 112(2–3):119–123
- Blum A (2011) Plant breeding for water-limited environments. Springer
- Boonekamp PM (2012) Are plant diseases too much ignored in the climate change debate? *Eur J Plant Pathol* 133(1):291–294
- Braga P, Crusiol LGT, Nanni MR, Caranhato ALH, Fuhrmann MB, Nepomuceno AL, ... Mertz-Henning LM (2021) Vegetation indices and NIR-SWIR spectral bands as a phenotyping tool for water status determination in soybean. *Precis Agricult* 22(1):249–266
- Branch W, Breneman T, Hookstra G (2014) Field test results versus marker assisted selection for root-knot nematode resistance in peanut. *Peanut Sci* 41(2):85–89
- Burow M, Balota M, Sarkar S, Bennett R, Chamberlin K, Wang N, White M, Payton P, Mahan J, Dobrev I (2021) Field measurements, yield, and grade of the U.S. Minicore under water deficit stress. Paper presented at the American Peanut Research and Education Society Annual Meeting 2021, Virtual
- Casadesús J, Villegas D (2014) Conventional digital cameras as a tool for assessing leaf area index and biomass for cereal breeding. *J Integr Plant Biol* 56(1):7–14
- Casadesús J, Kaya Y, Bort J, Nachit MM, Araus JL, Amor S, ... Villegas D (2007) Using vegetation indices derived from conventional digital cameras as selection criteria for wheat breeding in water-limited environments. *Ann Appl Biol* 150(2):227–236
- Chaerle L, Van Der Straeten D (2001) Seeing is believing: imaging techniques to monitor plant health. *Biochimica et Biophysica Acta (BBA)-Gene Struct Exp* 1519(3):153–166
- Chaerle L, De Boever F, Montagu MV, Straeten DVD (2001) Thermographic visualization of cell death in tobacco and Arabidopsis. *Plant Cell Environ* 24(1):15–25
- Chapin FS III, Autumn K, Pugnaire F (1993) Evolution of suites of traits in response to environmental stress. *Am Nat* 142:S78–S92

- Chapu I, Kalule DO, Okello RC, Odong TL, Sarkar S, Balota M (2022) Re-designing late leaf spot and groundnut rosette disease phenotyping in groundnut breeding in Uganda. *Front Plant Sci* 13. <https://doi.org/10.3389/fpls.2022.912332>
- Chaves MM, Oliveira MM (2004) Mechanisms underlying plant resilience to water deficits: prospects for water-saving agriculture. *J Exp Bot* 55(407):2365–2384
- Chung S-Y, Vercellotti JR, Sanders TH (1997) Increase of glycolytic enzymes in peanuts during peanut maturation and curing: evidence of anaerobic metabolism. *J Agric Food Chem* 45(12):4516–4521
- Collino D, Dardanelli J, Sereno R, Racca R (2001) Physiological responses of argentine peanut varieties to water stress.: Light interception, radiation use efficiency and partitioning of assimilates. *Field Crops Res* 70(3):177–184
- Comas L, Becker S, Cruz VMV, Byrne PF, Dierig DA (2013) Root traits contributing to plant productivity under drought. *Front Plant Sci* 4:442
- Condorelli GE, Maccaferri M, Newcomb M, Andrade-Sanchez P, White JW, French AN, Sciara G, Ward R, Tuberosa R (2018) Comparative aerial and ground based high throughput phenotyping for the genetic dissection of NDVI as a proxy for drought adaptive traits in durum wheat. *Front Plant Sci* 9(893). <https://doi.org/10.3389/fpls.2018.00893>
- Costa JM, Tejero IFG, Zuazo VHD, da Lima RSN, Chaves MM, Patto MCV (2015) Thermal imaging to phenotype traditional maize landraces for drought tolerance. *Comunicata Scientiae* 6(3):334–343
- Demir N, Sönmez NK, Akar T, Ünal S (2018) Automated measurement of plant height of wheat genotypes using a DSM derived from UAV imagery. Paper presented at the multidisciplinary digital publishing institute proceedings
- De Swaef T, Maes WH, Aper J, Baert J, Cougnon M, Reheul D, Steppe K, Roldán-Ruiz I, Lootens P (2021) Applying RGB- and thermal-based vegetation indices from UAVs for high-throughput field phenotyping of drought tolerance in forage grasses. *Remote Sens* 13(1):147. <https://www.mdpi.com/2072-4292/13/1/147>
- Devries JD, Bennett J, Boote K, Albrecht S, Maliro C (1989a) Nitrogen accumulation and partitioning by three grain legumes in response to soil water deficits. *Field Crop Res* 22(1):33–44
- Devries J, Bennett J, Albrecht S, Boote K (1989b) Water relations, nitrogenase activity and root development of three grain legumes in response to soil water deficits. *Field Crop Res* 21(3–4):215–226
- Eeswaran R, Nejadhashemi AP, Kpodo J, Curtis ZK, Adhikari U, Liao H, Li S-G, Hernandez-Suarez JS, Alves FC, Raschke A (2021) Quantification of resilience metrics as affected by conservation agriculture at a watershed scale. *Agr Ecosyst Environ* 320:107612
- El Bilali H, Callenius C, Strassner C, Probst L (2019) Food and nutrition security and sustainability transitions in food systems. *Food Energy Secur* 8(2):e00154
- Elsayed S, Rischbeck P, Schmidhalter U (2015) Comparing the performance of active and passive reflectance sensors to assess the normalized relative canopy temperature and grain yield of drought-stressed barley cultivars. *Field Crop Res* 177:148–160
- Falk KG, Jubery TZ, Mirnezami SV, Parmley KA, Sarkar S, Singh A, ... Singh AK (2020) Computer vision and machine learning enabled soybean root phenotyping pipeline. *Plant Methods* 16(1):1–19
- Fonstad MA, Dietrich JT, Courville BC, Jensen JL, Carbonneau PE (2013) Topographic structure from motion: a new development in photogrammetric measurement. *Earth Surf Proc Land* 38(4):421–430
- Freeman KW, Girma K, Arnall DB, Mullen RW, Martin KL, Teal RK, Raun WR (2007) By-plant prediction of corn forage biomass and nitrogen uptake at various growth stages using remote sensing and plant height. *Agron J* 99(2):530–536
- Fukai S, Cooper M (1995) Development of drought-resistant cultivars using physiomorphological traits in rice. *Field Crop Res* 40(2):67–86
- Furukawa Y, Ponce J (2010) Dense 3d motion capture from synchronized video streams. In: *Image and geometry processing for 3-D cinematography*. Springer, pp 193–211

- Ghosal S, Zheng B, Chapman SC, Potgieter AB, Jordan DR, Wang X, Singh AK, Singh A, Hirafuji M, Ninomiya S (2019) A weakly supervised deep learning framework for sorghum head detection and counting. *Plant Phenomics*
- Gitelson AA, Viña A, Arkebauer TJ, Rundquist DC, Keydan G, Leavitt B (2003) Remote estimation of leaf area index and green leaf biomass in maize canopies. *Geophys Res Lett* 30(5)
- Han X, Thomasson JA, Bagnall C, Pugh NA, Horne DW, Rooney WL, Malambo L, Chang A, Jung J, Cope DA (2018) Calibrated plant height estimates with structure from motion from fixed-wing UAV images. Paper presented at the autonomous air and ground sensing systems for agricultural optimization and phenotyping III
- Hasan MM, Chopin JP, Laga H, Miklavcic SJ (2018) Detection and analysis of wheat spikes using convolutional neural networks. *Plant Methods* 14(1):1–13
- Hein NT, Ciampitti IA, Jagadish SVK (2021) Bottlenecks and opportunities in field-based high-throughput phenotyping for heat and drought stress. *J Exp Bot* 72(14):5102–5116. <https://doi.org/10.1093/jxb/erab021>
- Henry A, Gowda VR, Torres RO, McNally KL, Serraj R (2011) Variation in root system architecture and drought response in rice (*Oryza sativa*): phenotyping of the OryzaSNP panel in rainfed lowland fields. *Field Crop Res* 120(2):205–214
- Holman FH, Riche AB, Michalski A, Castle M, Wooster MJ, Hawkesford MJ (2016) High throughput field phenotyping of wheat plant height and growth rate in field plot trials using UAV based remote sensing. *Remote Sens* 8(12):1031
- Huang S (2004) Global trade patterns in fruits and vegetables. USDA-ERS Agriculture and Trade Report No. WRS-04–06
- Jackson RD, Idso SB, Reginato RJ, Pinter PJ Jr (1981) Canopy temperature as a crop water stress indicator. *Water Resour Res* 17(4):1133–1138
- James MR, Robson S (2012) Straightforward reconstruction of 3D surfaces and topography with a camera: Accuracy and geoscience application. *J Geophys Res: Earth Surf* 117(F3):n/a–n/a. <https://doi.org/10.1029/2011jf002289>
- Jha PK (2019) Agronomic management of corn using seasonal climate predictions, remote sensing, and crop simulation models. Michigan State University
- Jha PK, Kumar SN, Ines AV (2018) Responses of soybean to water stress and supplemental irrigation in upper Indo-Gangetic plain: field experiment and modelling approach. *Field Crop Res* 219:76–86
- Jha PK, Ines AV, Singh MP (2021) A multiple and ensembling approach for calibration and evaluation of genetic coefficients of CERES-maize to simulate maize phenology and yield in Michigan. *Environ Model Softw* 135:104901
- Jha PK, Ines AV, Han E, Cruz R, Prasad PV (2022) A comparison of multiple calibration and ensembling methods for estimating genetic coefficients of CERES-Rice to simulate phenology and yields. *Field Crop Res* 284:108560
- Jones HG (1999) Use of infrared thermometry for estimation of stomatal conductance as a possible aid to irrigation scheduling. *Agric for Meteorol* 95(3):139–149
- Jones HG, Vaughan RA (2010) Remote sensing of vegetation: principles, techniques, and applications. Oxford University Press
- Julia C, Dingkuhn M (2013) Predicting temperature induced sterility of rice spikelets requires simulation of crop-generated microclimate. *Eur J Agron* 49:50–60
- Kanning M, Kühling I, Trautz D, Jarmer T (2018) High-resolution UAV-based hyperspectral imagery for LAI and chlorophyll estimations from wheat for yield prediction. *Remote Sens* 10(12):2000
- Kar S, Purbey VK, Suradhaniwar S, Korbu LB, Kholová J, Durbha SS, ... Vadez V (2021) An ensemble machine learning approach for determination of the optimum sampling time for evapotranspiration assessment from high-throughput phenotyping data. *Comput Electron Agricult* 182:105992
- Karaba A, Dixit S, Greco R, Aharoni A, Trijatmiko KR, Marsch-Martinez N, Krishnan A, Nataraja KN, Udayakumar M, Pereira A (2007) Improvement of water use efficiency in rice by expression

- of HARDY, an Arabidopsis drought and salt tolerance gene. *Proc Natl Acad Sci* 104(39):15270–15275
- Kefauver SC, El-Haddad G, Vergara-Díaz O, Araus JL (2015) RGB picture vegetation indexes for high-throughput phenotyping platforms (HTPPs). In: *Remote sensing for agriculture, ecosystems, and hydrology XVII*, vol 9637. International Society for Optics and Photonics, p 96370J
- Kefauver SC, Vicente R, Vergara-Díaz O, Fernandez-Gallego JA, Kerfal S, Lopez A, ... Araus JL (2017) Comparative UAV and field phenotyping to assess yield and nitrogen use efficiency in hybrid and conventional barley. *Front Plant Sci* 8:1733
- Khan Z, Rahimi-Eichi V, Haefele S, Garnett T, Miklavcic SJ (2018) Estimation of vegetation indices for high-throughput phenotyping of wheat using aerial imaging. *Plant Methods* 14(1):1–11
- Kim J, Kim K-S, Kim Y, Chung YS (2020) A short review: comparisons of high-throughput phenotyping methods for detecting drought tolerance. *Scientia Agricola* 78
- Kiniry J, Simpson C, Schubert A, Reed J (2005) Peanut leaf area index, light interception, radiation use efficiency, and harvest index at three sites in Texas. *Field Crop Res* 91(2–3):297–306
- Kipp S, Mistele B, Schmidhalter U (2013) Identification of stay-green and early senescence phenotypes in high-yielding winter wheat, and their relationship to grain yield and grain protein concentration using high-throughput phenotyping techniques. *Funct Plant Biol* 41(3):227–235
- Kooyers NJ (2015) The evolution of drought escape and avoidance in natural herbaceous populations. *Plant Sci* 234:155–162
- Ladoni M, Bahrami HA, Alavipanah SK, Norouzi AA (2010) Estimating soil organic carbon from soil reflectance: a review. *Precision Agric* 11(1):82–99
- Lazarević B, Šatović Z, Nimac A, Vidak M, Gunjača J, Politeo O, Carović-Stanko K (2021) Application of phenotyping methods in detection of drought and salinity stress in basil (*Ocimum basilicum* L.). *Front Plant Sci* 12:174
- Lee K, Seong J, Han Y, Lee WH (2020) Evaluation of applicability of various color space techniques of UAV images for evaluating cool roof performance. *Energies* 13(16):4213
- Lin H, Chen Y, Zhang H, Fu P, Fan Z (2017) Stronger cooling effects of transpiration and leaf physical traits of plants from a hot dry habitat than from a hot wet habitat. *Funct Ecol* 31(12):2202–2211
- Lottes P, Khanna R, Pfeifer J, Siegwart R, Stachniss C (2017) UAV-based crop and weed classification for smart farming. Paper presented at the 2017 IEEE international conference on robotics and automation (ICRA)
- Luis JM, Ozias-Akins P, Holbrook CC, Kemerait RC Jr, Snider JL, Liakos V (2016) Phenotyping peanut genotypes for drought tolerance. *Peanut Sci* 43(1):36–48
- Ma L, Gardner F, Selamat A (1992) Estimation of leaf area from leaf and total mass measurements in peanut. *Crop Sci* 32(2):467–471
- Maksimovic I, Ilin Z (2012) Effects of salinity on vegetable growth and nutrients uptake. *Irrigat Syst Pract Challenge Environ* 9
- Mathews AJ, Jensen JL (2013) Visualizing and quantifying vineyard canopy LAI using an unmanned aerial vehicle (UAV) collected high density structure from motion point cloud. *Remote Sens* 5(5):2164–2183
- Micheletti N, Chandler JH, Lane SN (2015a) Investigating the geomorphological potential of freely available and accessible structure-from-motion photogrammetry using a smartphone. *Earth Surf Proc Land* 40(4):473–486
- Micheletti N, Lane SN, Chandler JH (2015b) Application of archival aerial photogrammetry to quantify climate forcing of alpine landscapes. *Photogram Rec* 30(150):143–165
- Minaxi RP, Acharya KO, Nawale S (2011) Impact of climate change on food security. *Int J Agricult Environ Biotechnol* 4(2):125–127
- Mishra AK, Singh VP (2010) A review of drought concepts. *J Hydrol* 391(1–2):202–216
- Nigam S, Aruna R (2007) Improving breeding efficiency for early maturity in peanut. *Plant Breeding Rev* 30:295–322
- Nigam S, Chandra S, Sridevi KR, Bhukta M, Reddy A, Rachaputi NR, Wright G, Reddy P, Deshmukh M, Mathur R (2005) Efficiency of physiological trait-based and empirical selection approaches for drought tolerance in groundnut. *Ann Appl Biol* 146(4):433–439

- Nuruddin MM (2001) Effects of water stress on tomato at different growth stages
- Nutter FW Jr, Littrell RH (1996) Relationships between defoliation, canopy reflectance and pod yield in the peanut-late leafspot pathosystem. *Crop Prot* 15(2):135–142
- Oakes J, Balota M, Thomason WE, Cazenave AB, Sarkar S, Sadeghpour A (2019) Using unmanned aerial vehicles to improve n management in winter wheat. Paper presented at the ASA, CSSA, SSSA international annual meeting 2019, San Antonio, TX
- Oakes J, Balota M, Thomason W, Cazenave A, Sarkar S (2020) Using UAVs to improve nitrogen management of winter wheat. In: Annual wheat newsletter, vol 66. Wheat Genetic and Genomic Resources Center at Kansas State University, p 103
- Osakabe Y, Osakabe K, Shinozaki K, Tran LS (2014) Response of plants to water stress. *Front Plant Sci* 5:86. <https://doi.org/10.3389/fpls.2014.00086>
- Pandey R, Herrera W, Villegas A, Pendleton J (1984) Drought response of grain legumes under irrigation gradient: III. Plant growth I. *Agron J* 76(4):557–560
- Parajuli R, Thoma G, Matlock MD (2019) Environmental sustainability of fruit and vegetable production supply chains in the face of climate change: a review. *Sci Total Environ* 650:2863–2879
- Patil S, Kumar K, Jakhar DS, Rai A, Borle U, Singh P (2016) Studies on variability, heritability, genetic advance and correlation in maize (*Zea mays* L.). *Int J Agricult Environ Biotechnol* 9(6):1103–1108
- Pineda M, Baron M, Perez-Bueno ML (2020) Thermal imaging for plant stress detection and phenotyping. *Remote Sens* 13(1):68
- Prasad BVG, Chakravorty S (2015) Effects of climate change on vegetable cultivation—a review. *Nat Environ Pollut Technol* 14(4):923
- Prashar A, Jones HG (2014) Infra-red thermography as a high-throughput tool for field phenotyping. *Agronomy* 4(3):397–417
- Rai A, Sharma V, Heitholt J (2020) Dry bean [*Phaseolus vulgaris* L.] growth and yield response to variable irrigation in the arid to semi-arid climate. *Sustainability* 12(9):3851
- Rakshit A, Sarkar NC, Pathak H, Maiti RK, Makar AK, Singh PL (2009) Agriculture: a potential source of greenhouse gases and their mitigation strategies. In: IOP conference series. earth and environmental science, vol 6, no 24. IOP Publishing
- Raza S-E-A, Smith HK, Clarkson GJ, Taylor G, Thompson AJ, Clarkson J, Rajpoot NM (2014) Automatic detection of regions in spinach canopies responding to soil moisture deficit using combined visible and thermal imagery. *PLoS One* 9(6):e97612
- Reddy T, Reddy V, Anbumozhi V (2003) Physiological responses of groundnut (*Arachis hypogea* L.) to drought stress and its amelioration: a critical review. *Plant Growth Regulat* 41(1):75–88
- Remondino F, Spera MG, Nocerino E, Menna F, Nex F (2014) State of the art in high density image matching. *Photogram Rec* 29(146):144–166
- Richards G, Lénia M, Mein K, Marques L, Mein K (2015) Summary for policymakers. In Stocker TF, Qin D, Plattner G-K, Tignor M, Allen SK, Boschung J, Nauels A, Xia Y, Bex V, Midgley PM (eds) Climate change 2013—the physical science basis: contribution of working group I to the fifth assessment report of the intergovernmental panel on climate change (Climate Change 2013—the physical science basis). Cambridge University Press/UNEP. <https://doi.org/10.1017/CBO9781107415324.004>
- Romano G, Zia S, Spreer W, Sanchez C, Cairns J, Araus JL, Müller J (2011) Use of thermography for high throughput phenotyping of tropical maize adaptation in water stress. *Comput Electron Agric* 79(1):67–74
- Rose JC, Paulus S, Kuhlmann H (2015) Accuracy analysis of a multi-view stereo approach for phenotyping of tomato plants at the organ level. *Sensors* 15(5):9651–9665
- Rothermel M, Wenzel K, Fritsch D, Haala N (2012) SURE: photogrammetric surface reconstruction from imagery. Paper presented at the proceedings LC3D workshop, Berlin
- Rutkoski J, Poland J, Mondal S, Autrique E, Pérez LG, Crossa J, ... Singh R (2016) Canopy temperature and vegetation indices from high-throughput phenotyping improve accuracy of pedigree and genomic selection for grain yield in wheat. *G3: Genes Genomes Genet* 6(9):2799–2808

- Sadeghi-Tehran P, Sabermanesh K, Virlet N, Hawkesford MJ (2017) Automated method to determine two critical growth stages of wheat: heading and flowering. *Front Plant Sci* 8:252
- Sadeghpour A, Oakes J, Sarkar S, Balota M (2017a) Precise Nitrogen management of biomass Sorghum using vegetation indices. Paper presented at the ASA, CSSA and SSSA international annual meetings 2017, Tampa, FL
- Sadeghpour A, Oakes J, Sarkar S, Pitman R, Balota M (2017b) High throughput phenotyping of biomass sorghum using ground and aerial imaging. Paper presented at the ASA, CSSA and SSSA international annual meetings 2017, Tampa, FL
- Sadeghpour A, Oakes J, Sarkar S, Balota M (2018) Seeding rate and harvesting time effect on biomass Sorghum production in Virginia. Paper presented at the ASA, CSSA and CSA international annual meetings 2018, Baltimore, MD
- Sankaran S, Quirós JJ, Miklas PN (2019) Unmanned aerial system and satellite-based high resolution imagery for high-throughput phenotyping in dry bean. *Comput Electron Agric* 165:104965
- Saravi B, Nejadhashemi AP, Jha P, Tang B (2021) Reducing deep learning network structure through variable reduction methods in crop modeling. *Artif Intell Agricult* 5:196–207
- Sarkar S (2020) Development of high-throughput phenotyping methods and evaluation of morphological and physiological characteristics of peanut in a sub-humid environment. Virginia Polytechnic Institute and State University
- Sarkar S (2021) High-throughput estimation of soil nutrient and residue cover: a step towards precision agriculture. In: *Soil science: fundamentals to recent advances*. Springer, Singapore, pp 581–596
- Sarkar S, Jha PK (2020) Is precision agriculture worth it? Yes, may be. *J Biotechnol Crop Sci* 9(14):4–9
- Sarkar S, Cazenave AB, Oakes J, McCall D, Thomason W, Abbot L, Balota M (2020) High-throughput measurement of peanut canopy height using digital surface models. *Plant Phenome J* 3(1):e20003
- Sarkar S, Oakes J, Balota M (2018) High-throughput phenotyping of Peanut and biomass Sorghum using proximal sensing and aerial imaging for the mid-atlantic U.S. Paper presented at the 2018 GIS and remote sensing research symposium
- Sarkar S, Oakes J, Balota M (2019) Use of proximal and remote sensing technologies for high-throughput phenotyping in peanuts. Paper presented at the advanced environmental, chemical, and biological sensing technologies XV
- Sarkar S, Cazenave AB, Oakes J, McCall D, Thomason W, Abbot L, Balota M (2021a) Aerial high-throughput phenotyping of peanut leaf area index and lateral growth. *Sci Rep* 11(1):1–17.
- Sarkar S, Ramsey AF, Cazenave A-B, Balota M (2021b) Peanut leaf wilting estimation from RGB color indices and logistic models. *Front Plant Sci* 12:713
- Sarkar S, Shekoofa A, McClure A, Gillman JD (2022a) Phenotyping and Quantitative Trait Locus analysis for the limited transpiration trait in an upper-mid south soybean recombinant inbred line population ('Jackson' × 'KS4895'): high throughput aquaporin inhibitor screening. *Front Plant Sci* 3175
- Sarkar S, Wedegaertner K, Shekoofa A (2022b) Using aerial imagery to optimize the efficiency of PGR application in cotton. Paper presented at the Beltwide cotton conference 2022b, San Antonio, TX
- Schanda J (2007) *Colorimetry: understanding the CIE system*. Wiley
- Serraj R, Sinclair T (2002) Osmolyte accumulation: can it really help increase crop yield under drought conditions? *Plant Cell Environ* 25(2):333–341
- Shekoofa A, Sheldon K, Sarkar S, Raper TB (2022) Variety selection: a valuable tool in the management of water relations in cotton production. Paper presented at the Beltwide cotton conference 2022, San Antonio, TX
- Simko I, Jimenez-Berni JA, Sirault XR (2017) Phenomic approaches and tools for phytopathologists. *Phytopathology* 107(1):6–17
- Singh JP, Lal SS (2010) Climate change and potato production in India. *ISPRS Archives XXXVIII-8*. In: W3 workshop proceedings: impact of climate change on agriculture, pp 115–117

- Snavely N, Seitz SM, Szeliski R (2008) Skeletal graphs for efficient structure from motion. Paper presented at the 2008 IEEE conference on computer vision and pattern recognition
- Stebbins GL Jr (1952) Aridity as a stimulus to plant evolution. *Am Nat* 86(826):33–44
- Su W, Zhang M, Bian D, Liu Z, Huang J, Wang W, ... Guo H (2019) Phenotyping of corn plants using unmanned aerial vehicle (UAV) images. *Remote Sens* 11(17):2021
- Sung C, Balota M, Sarkar S, Bennett R, Chamberlin K, Wang N, Payton P, Mahan J, Chagoya J, Burow M (2021) Genome-wide association study on Peanut water deficit stress tolerance using the U.S. minicore to develop improvement for breeding. Paper presented at the American Peanut research and education society annual meeting 2021, Virtual
- Taiz L, Zeiger E, Møller IM, Murphy A (2015) *Plant physiology and development*. Sinauer Associates Incorporated
- Tattaris M, Reynolds MP, Chapman SC (2016) A direct comparison of remote sensing approaches for high-throughput phenotyping in plant breeding. *Front Plant Sci* 7:1131
- Tester M, Langridge P (2010) Breeding technologies to increase crop production in a changing world. *Science* 327(5967):818–822
- Tian M, Ban S, Chang Q, You M, Luo D, Wang L, Wang S (2016) Use of hyperspectral images from UAV-based imaging spectroradiometer to estimate cotton leaf area index. *Trans Chin Soc Agricult Eng* 32(21):102–108
- Travlos I, Mikroulis A, Anastasiou E, Fountas S, Bilalis D, Tsiropoulos Z, Balafoutis A (2017) The use of RGB cameras in defining crop development in legumes. *Adv Anim Biosci* 8(2):224–228
- Trussell HJ, Saber E, Vrhel M (2005) Color image processing: Basics and special issue overview. *IEEE Signal Process Mag* 22(1)
- Venkateswarlu B, Maheswari M, Saharan N (1989) Effects of water deficit on N₂ (C₂H₂) fixation in cowpea and groundnut. *Plant Soil* 114(1):69–74
- Vergara-Díaz O, Kefauver SC, Elazab A, Nieto-Taladriz MT, Araus JL (2015) Grain yield losses in yellow-rusted durum wheat estimated using digital and conventional parameters under field conditions. *Crop J* 3(3):200–210
- Vergara-Díaz O, Zaman-Allah MA, Masuka B, Hornero A, Zarco-Tejada P, Prasanna BM, ... Araus JL (2016) A novel remote sensing approach for prediction of maize yield under different conditions of nitrogen fertilization. *Front Plant Sci* 7:666
- Vollmann J, Walter H, Sato T, Schweiger P (2011) Digital image analysis and chlorophyll metering for phenotyping the effects of nodulation in soybean. *Comput Electron Agric* 75(1):190–195
- Wang X, Singh D, Marla S, Morris G, Poland J (2018) Field-based high-throughput phenotyping of plant height in sorghum using different sensing technologies. *Plant Methods* 14(1):53
- Wang J, Badenhorst P, Phelan A, Pembleton L, Shi F, Cogan N, ... Smith K (2019a) Using sensors and unmanned aircraft systems for high-throughput phenotyping of biomass in perennial ryegrass breeding trials. *Front Plant Sci* 1381
- Wang X, Xuan H, Evers B, Shrestha S, Pless R, Poland J (2019b) High-throughput phenotyping with deep learning gives insight into the genetic architecture of flowering time in wheat. *GigaScience* 8(11):giz120
- Watanabe K, Guo W, Arai K, Takanashi H, Kajiya-Kanegae H, Kobayashi M, Yano K, Tokunaga T, Fujiwara T, Tsutsumi N, Iwata H (2017) High-throughput phenotyping of sorghum plant height using an unmanned aerial vehicle and its application to genomic prediction modeling. *Front Plant Sci* 8(421). <https://doi.org/10.3389/fpls.2017.00421>
- Welch E, Moorhead R, Owens JK (1991, April) Image processing using the HSI color space. In: *IEEE proceedings of the SOUTHEASTCON'91*. IEEE, pp 722–725
- Wenting H, Yu S, Tengfei X, Xiangwei C, Ooi SK (2014) Detecting maize leaf water status by using digital RGB images. *Int J Agricult Biol Eng* 7(1):45–53
- Westoby MJ, Brasington J, Glasser NF, Hambrey MJ, Reynolds JM (2012) 'Structure-from-Motion' photogrammetry: a low-cost, effective tool for geoscience applications. *Geomorphology* 179:300–314. <https://doi.org/10.1016/j.geomorph.2012.08.021>

- Williams JH, Phillips TD, Jolly PE, Stiles JK, Jolly CM, Aggarwal D (2004) Human aflatoxicosis in developing countries: a review of toxicology, exposure, potential health consequences, and interventions. *Am J Clin Nutr* 80(5):1106–1122
- Xiong X, Duan L, Liu L, Tu H, Yang P, Wu D, Chen G, Xiong L, Yang W, Liu Q (2017) Panicle-SEG: a robust image segmentation method for rice panicles in the field based on deep learning and superpixel optimization. *Plant Methods* 13(1):1–15
- Yadav MR, Choudhary M, Singh J, Lal MK, Jha PK, Udawat P, ... Prasad PV (2022) Impacts, tolerance, adaptation, and mitigation of heat stress on wheat under changing climates. *Int J Mol Sci* 23(5):2838
- Yam KL, Papadakis SE (2004) A simple digital imaging method for measuring and analyzing color of food surfaces. *J Food Eng* 61(1):137–142
- Yin X, McClure MA, Jaja N, Tyler DD, Hayes RM (2011) In-season prediction of corn yield using plant height under major production systems. *Agron J* 103(3):923–929
- Yuan H, Yang G, Li C, Wang Y, Liu J, Yu H, Feng H, Xu B, Zhao X, Yang X (2017) Retrieving soybean leaf area index from unmanned aerial vehicle hyperspectral remote sensing: analysis of RF, ANN, and SVM regression models. *Remote Sens* 9(4):309
- Yuan W, Li J, Bhatta M, Shi Y, Baenziger PS, Ge Y (2018) Wheat height estimation using LiDAR in comparison to ultrasonic sensor and UAS. *Sensors* 18(11):3731
- Zakaluk R, Ranjan R (2008) Predicting the leaf water potential of potato plants using RGB reflectance. *Canadian Biosyst Eng* 50
- Zhang L, Niu Y, Zhang H, Han W, Li G, Tang J, Peng X (2019) Maize canopy temperature extracted from UAV thermal and RGB imagery and its application in water stress monitoring. *Front Plant Sci* 10:1270
- Zhou J, Zhou J, Ye H, Ali ML, Nguyen HT, Chen P (2020) Classification of soybean leaf wilting due to drought stress using UAV-based imagery. *Comput Electron Agric* 175:105576

Chapter 8

Sustainable Water Management Practices for Intensified Agriculture



Manish Yadav, B. B. Vashisht, S. K. Jalota, Arun Kumar, and Dileep Kumar

Abstract Water is considered the most critical resource for sustainable agricultural development worldwide. Irrigated areas will increase in forthcoming years, while fresh water supplies will be diverted from agriculture to meet the increasing demand for domestic use and industry. Furthermore, the efficiency of irrigation is very low, since less than two third of the applied water is actually used by the crops. The sustainable use of irrigation water is a priority for agriculture in arid areas. So, under scarcity conditions and climate change, considerable effort has been devoted over time to introducing policies aiming to increase water efficiency based on the assertion that more can be achieved with less water through better management. Better management usually refers to the improvement of water allocation and/or irrigation water efficiency. Looking at current and future trends of agricultural production worldwide, it is clear that irrigation is essential to meet current food demand and that irrigation will have to increase in the future. The use of large amounts of water by crops is dictated by the evaporative demand of the environment and is tightly associated with biomass production and yield. Increases in potential biomass production per unit of water transpired during the next 10–20 years will be small despite promises from biotechnology. Breeding for yield potential will also provide a small contribution in the near future, so the real opportunity to increase the productivity of water resides in closing the current large gap between actual and potential yields. To increase the effectiveness of irrigation in a sustained fashion, without detrimental impacts on the environment, a number of measures need to be considered, particularly: improving water management at farm and district levels and reforming institutions to allow for user participation.

M. Yadav (✉) · B. B. Vashisht · S. K. Jalota
Department of Soil Science, Punjab Agricultural University, Ludhiana, Punjab 141004, India
e-mail: manish.soil017@gmail.com; manish-2016001@pau.edu

A. Kumar
Department of Agronomy, Punjab Agricultural University, Ludhiana, Punjab 141004, India

D. Kumar
Micronutrient Research Scheme (ICAR), Anand Agricultural University, Anand, Gujarat 388110, India

Keywords Biotechnology · Breeding · Efficiency · Irrigation · Sustainable and Water

8.1 Introduction: Sustainable Water Use

Water is the crucial input for agriculture and food security. Irrigated agriculture covers 20% of agricultural land and 40% of global food production. The productivity of irrigated agriculture is at least twice more than rainfed agriculture that ensures crop intensification as well as diversification. Access to water resources is necessary for the economic productivity of numerous human activities (D’Odorico et al. 2018). With about 24% of the world’s geographical area comes under severe water scarcity (Alcamo et al. 2003) and 35% of the world’s human population living under water-scarce areas (Rockstrom et al. 2014), overexploitation of water resources commonly occurs as a result of economic development (Savenije and van der Zaag 2002), resulting in ecological damage (Sullivan 2002).

Agriculture is the major consumer of water resources (Green et al. 2015). Irrigation accounts for over 70% of worldwide freshwater withdrawals, ensuring global food production (Rockstrom et al. 2017). Irrigated regions make for 18% of world farmland yet account for over 40% of world food production (Chartzoulakis and Bertaki 2015; FAO 2019). Simultaneously, 40% of worldwide irrigation techniques are non-sustainable due to the depletion of ecological and groundwater reserves (Wada and Bierkens 2014; Rosa et al. 2018). The strong link between economic and environmental demands for water reserves raises critical questions at the heart of the water sustainability debate: how can human appropriation of water reserves support economic deeds, such as agriculture, without depleting water reserves, habitats of aquatic ecosystems and other relevant ecosystem services? (Rosa et al. 2018; D’Odorico et al. 2018).

Sustainable irrigation strategies in agriculture must allow for increased crop production to satisfy growing food demands while also ensuring that natural resources (groundwater reserves, freshwater and water quality) are not irreparably depleted (Rosa et al. 2018; Borsato et al. 2020). The term “sustainability” is frequently used to refer to the management, use, and protection of natural assets in such a way that forthcoming generations will have access to them (FAO 2013; Borsato et al. 2020). In more anthropocentric words, “sustainability” refers to a state that permits the current generation’s requirements to be met “without jeopardizing future generations’ capacity to fulfill their own needs”. The emphasis is on human needs rather than preserving the natural resource. A “weak” definition of sustainability has resulted from a failure to recognize the fundamental role of natural resources and environmental benefits, sometimes called as “natural capital,” and it comes under the definition of sustainability (Solow 1974).

“Weak sustainability” refers to circumstances in which natural capital may be substituted by man-made capital as long as its total value does not decline over time (Hartwick 1978). As a result, forthcoming generations will have access to the

same total amount of endowments or assets as their forefathers (Groenfeldt 2019). Natural and human capital is interchangeable in a weakly sustainable system and natural capital can be destroyed in the course of creating man-made wealth. Crop production and their earnings, for example, might come at the expense of marine environment loss and depletion of groundwater (Wada et al. 2010; Jagermeyr et al. 2017). “Strong sustainability,” on the other hand, guarantees that natural capital is not substituted by human capital and it is not damaged in the process of human capital generation. Thus, weak and strong sustainability conceptions may be used to examine both the ecological and economic elements of sustainability, highlighting the contradiction of balancing the cost of environmental degradation with human capital (Rennings and Wiggering 1997) (Fig. 8.1).

The reduction in the cost of manufactured and natural capital, as well as the influence of humans on natural resources, may be used to assess weak and strong sustainability (Dietz and Neumayer 2007). Since water is a renewable resource, it is possible to aspire for great sustainability when it comes to irrigation. Of course, water resources may be non-renewable on a local level, like in arid regions with low rainfall and large non-renewable groundwater reserves. The exploitation of groundwater (commonly referred to as “groundwater mining”) is a classic example of

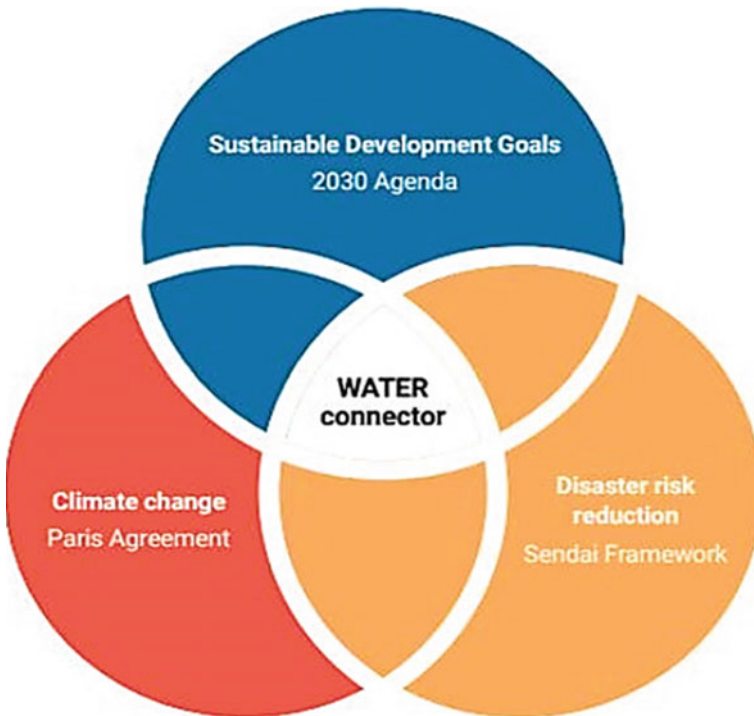


Fig. 8.1 Water as a connector among global commitments adopted in 2015. *Source* The United Nation World Water Development Report (2020)

Table 8.1 Utilization of irrigation water and effective agricultural water withdrawal in some selected countries (Kumar 2021)

Country	Effective renewable water resource per capita (m ³)	Effective agricultural water withdrawal (m ³ per capita)	Actual irrigation water use (m ³ per capita)
Australia	42,823	18,966	951
Brazil	47,150	1772	218
China	2530	670	341
Egypt	835	873	858
France	3783	447	67
Germany	2028	269	113
India	1340	741	560
Israel	315	256	210
Philippines	6080	445	285
Russia	32,790	836	93
United States	11,485	1826	712

unsustainable water usage in such areas (Konikov and Likhodedova 2011) (Table 8.1).

Sustainable irrigation must ensure that water reserves viz. aquifers, rivers, or lakes are not depleted by keeping withdrawal rates below those of natural replenishment. In sustainable irrigation practices, the withdrawals from water bodies do not result in the loss of aquatic habitat and irreversible ecosystem degradation. These practices should not result in other types of environmental damage for example, soil salinization with associated losses of ecosystem services and functions, here collectively referred to as “natural capital” (de Perthuis and Jouvet 2015). Indices that specify the efficiency of an irrigation system in terms of its ability to supply the water needed by agriculture without losses of natural capital and from the aspect of economic viability are frequently used to define sustainability, when irrigation does not deplete either natural or human capital, strong sustainability can be attained (Aeschbach-Hertig and Gleeson 2012).

In order to be economically sustainable, the cost of irrigation must not surpass the value of irrigation’s marginal productivity when compared to rainfed crops. Appropriate sustainability indicators might be a useful tool in evaluating irrigation sustainability and implementing appropriate policy responses (Juwana et al. 2012). Furthermore, a separate study for surface water bodies and aquifers may be required to guarantee that environmental flows and groundwater reserves do not get exhausted (Vanham et al. 2018).

8.2 Perspectives for Agricultural Land and Water Use Towards 2050

Population growth, urbanization, and climate change, all of which influence agriculture, are expected to increase competition for water supplies. The world's population is expected to exceed 10 billion people by 2050, and this population, whether urban or rural, will require food and fibre to meet their basic requirements. Agricultural production would need to expand by roughly 70% by 2050 when paired with the higher intake of calories and more sophisticated meals that come with rising wealth in emerging countries (Alexandratos and Bruinsma 2012). Rising demand will be met by both irrigated and rainfed agriculture. From existing established land and water resources, a doubling of present output may be achieved. Other land and water resources could be used for agricultural production, but in most cases, they already provide vital environmental and economic services. Conversion to crop production would necessitate a previous assessment of the trade-off between gains and the loss of current ecological and socio-economic services.

Intensification will likely account for the majority of future crop production increase in developing nations, with irrigation playing an increasingly important role due to enhanced water supplies, water use efficiency (WUE) improvements, yield growth, and greater cropping intensities. The irrigated area and agricultural water use are predicted to grow slowly: land under irrigation is expected to rise by 6% from 301 Mha in 2009 to 318 Mha in 2050 (Dubois 2011). Any increase, however, would need compromises, notably in terms of inter-sectoral water distribution and environmental implications. On private farms, supplemented and pressured irrigation is projected to develop significantly. Agricultural withdrawals will need to climb to more than 2900 km³yr⁻¹ by 2030 and about 3000 km³ yr⁻¹ by 2050, based on current agricultural water-use efficiency and productivity improvements. Between now and 2050, this represents a net rise of 10% (Table 8.2).

As land and water limitations become more obvious, the rivalry between municipal and industrial needs will grow more intense, and intra-sectoral competition within agriculture between non-food crops, livestock and staples, including liquid biofuels will become more prevalent. Municipal and industrial water needs will expand significantly faster than agricultural water demands, crowding out agricultural allocations. Meanwhile, soil management and water application efficiency will need to improve to keep up with rising agricultural production. Intra-sectoral competition for scarce land and water will increase, and the ultimate supply of naturally accessible freshwater and groundwater will be severely impacted. Temperature, precipitation, and river flow are important to agricultural systems; all these are projected to vary as a result of climate change. While certain agricultural systems at higher latitudes may gain from increased temperatures as more land becomes viable for crop development, lower latitudes are projected to bear the brunt of the negative consequences. Droughts and flooding in subtropical areas are anticipated to become more frequent and intense as a result of global warming, and Sea-level rise is expected to have a negative impact on deltas and coastal areas. Long-term changes in base flows are also projected in

Table 8.2 Factors driving agricultural water productivity in different regions of the world

Region	Arable land suitable for cultivation (mha ⁻¹)	Arable land in use (mha ⁻¹)	Projected growth in arable land use (%)	Projected growth in irrigation (%)	Pressure on water resources (%)
World	4495	1592	0.10	0.10	7.20 ^a
Sub-Saharan Africa	1073	240	0.44	0.50	3.80
Latin America and the Caribbean's	1095	202	0.49	0.30	1.60
Near East/North Africa	95	84	0.00	0.20	54.10
South Asia	195	206	0.08	0.10	40.0–42.0 ^a
East Asia	410	236	0.00	0.20	10.0–11.0 ^a
Developed countries	1592	624	-0.14	0.00	4.00

Source Alexandratos and Bruinsma (2012)

^aKumar (2021)

mountain or highland and irrigated systems that rely on summer snowmelt. Droughts, excessive rainfall, and other severe events are all present and foreseeable concerns; thus adaptation and mitigation efforts should focus on enhancing the resilience of farming systems to lower existing and future risks.

8.3 Water-Saving Practices for Intensified Agriculture

The amount of water stored in the earth is comparable to the amount of money in a bank account. If you withdraw money quicker than you deposit fresh money, you'll soon run out of money in your account. Pumping water out of the earth faster than it can be replenished generates similar issues in the long run. Pumping causes the volume of groundwater in storage to decrease in many parts of the United States and South Asia especially India (Fig. 8.2).

i. Optimum groundwater withdrawn

Continuous groundwater pumping is the primary cause of groundwater depletion. Some of the negative consequences of groundwater depletion include:

- i. Wells drying up
- ii. Water reduction in streams and lakes
- iii. Water quality deterioration
- iv. Higher pumping expenses

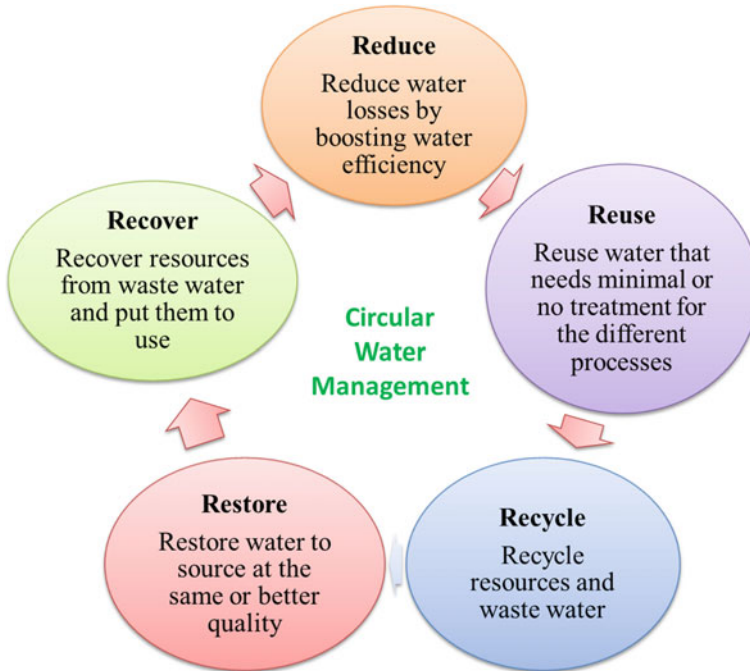


Fig. 8.2 Circular water management for sustainable use. *Source* World Business Council for Sustainable Development (2017)

v. Subsidence of the land

Groundwater abstraction has proven to be a vital supply of accessible irrigation water, although it is difficult to control. As a result, locally intense groundwater withdrawals in important cereal-producing areas in high, middle, and low income nations surpass natural replenishment rates. Because many critical food production regions rely on groundwater, diminishing aquifer levels and continuous non-renewable groundwater abstraction pose an increasing threat to local and global food supply (Dubois 2011). Groundwater usage in irrigation is rapidly growing, with about 40% of irrigated land currently relying on groundwater as a major source or in combination with surface irrigation. By boosting allocation efficiency among sectors and adopting technology and a governance structure that promote efficient water use, multilevel stakeholder engagement across land and water systems may greatly improve water productivity and reduce stress. Participatory community irrigation and groundwater management are two examples (Fig. 8.3).

ii. Rain water-harvesting

Rainwater harvesting is a basic approach for collecting and storing rainwater for later use. Rainwater from natural or man-made catchment areas, such as rooftops,

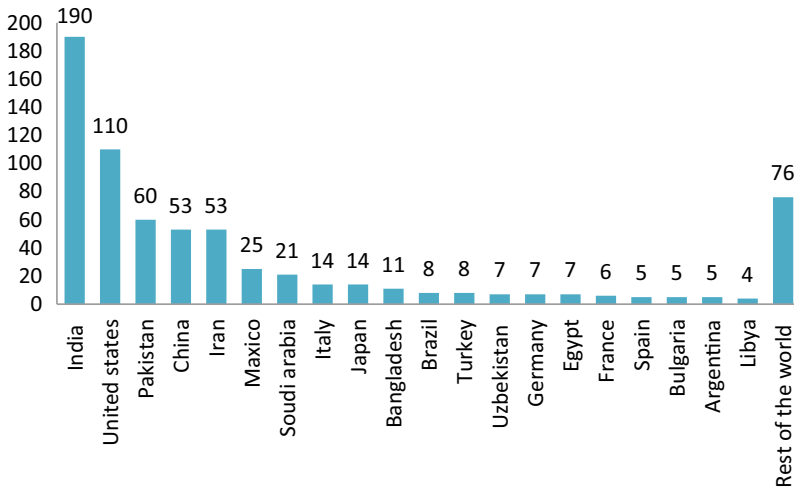


Fig. 8.3 Groundwater use km³ per year (Jakeman et al. 2016)

complexes, rocky surfaces, hill slopes, or intentionally repaired impervious or semi-pervious land surfaces, is collected and stored using artificially built systems. Rainwater harvested from surfaces where rain falls can be filtered, conserved, and used in a variety of ways, or it can be used immediately for recharge. Rainwater harvesting is limited by impurities, has a lower storage cost, and ease of maintenance other than occasional cleaning. With diminishing groundwater levels and changing climate conditions, this approach can go a long way towards reducing the negative consequences of growing water shortages. Reserving rainwater can aid in the replenishment of rivers and aquifers, the reduction of urban floods, and, most importantly, the availability of water in water-scarce areas.

Advantages of rain water harvesting

1. Supply water for supplemental irrigation
2. Reduces withdrawn on groundwater
3. Save energy and cost for pumping groundwater
4. Ecological benefit
5. Reduces flooding and soil erosion

Techniques of rainwater harvesting

1. Surface runoff harvesting

Rainwater is collected as surface runoff and stored for later use in this approach. The flow of minor creeks and streams can be diverted into surface or subsurface reservoirs to collect surface water. It can offer water for agriculture, animals, and ordinary household usage. In metropolitan cities, surface runoff collection is the best option. In metropolitan cities, rooftop rainwater and storm runoff can be collected

via recharge pits, recharge trenches, tubewells, and recharge wells, among other methods.

2. Ground water recharge

Groundwater recharge is a hydrologic process in which water travels downhill from surface to groundwater. Recharge is the most common way for water to enter an aquifer. The aquifer also functions as a mechanism of distribution. Using artificial recharge techniques, the excess precipitation may subsequently be used to recharge the groundwater aquifer. In rural locations, rainwater can be collected using gully plugs, contour bunds, dugwell recharge, percolation tanks, check dams, and recharge shafts, among other methods.

iii. Watershed management

In recent decades, significant progress has been made in understanding the interplay between on-farm irrigation and basin hydrology. As a result, more people are realizing that irrigation losses on the farm aren't always losses in the basin. The reason for this is that losses from one farm's runoff and deep percolation enter the basin's general drainage network and may be recovered as part of the water supply of another farm downstream. As a result, irrigation losses are at least somewhat recoverable within a basin and if water conservation is the goal, measures for enhancing irrigation water usage efficiency must first consider the nature of the possible water savings. Measures that reduce irrecoverable water losses result in a net decrease in the basin's consumptive consumption. The techniques used to reduce recoverable losses will not lessen basin water needs and may potentially affect downstream customers' water supplies. To demonstrate the significance of these disparities, consider the findings of a research on irrigation water consumption in the Western United States (Interagency Task Force Report 1979). The study looked at a variety of on-farm and off-farm water conservation and irrigation efficiency strategies to see if they may help reduce irrigation water needs. While the anticipated reduction in irrigation diversions was greater than 30 million acre-feet, the majority of that water was reused, and the irrecoverable losses, which constitute the expected net water savings, were just two to five million acre-feet.

Even though the concept and practice of water reuse are obvious, they are not typically considered in water supply estimates for irrigation at the watershed or regional levels. It is commonly considered that once water is taken, it is no longer usable. In many circumstances, evaluating water use in diverse industries purely on diversions without considering water reuse might be inaccurate. For example, because most water diverted for irrigation is reused for various purposes within a basin, the estimate that 72% of water consumption goes to irrigation (Seckler 1993) probably overestimates irrigation water use. Most worldwide data sets on countries' water supplies overlook water-recycling impacts (Seckler et al. 1998), for example, in Spain's national hydrologic studies; a single statistic of 20% of diversions is used as the average reuse in irrigation for the whole country. The fact is that locating and measuring recoverable water within and across basins is a complex undertaking, and the amount and quality of hydrologic data available for this purpose is typically

insufficient. As a result, additional efforts are needed to gather credible data for assessing irrigation reuse at the basin and regional levels.

iv. Reduce water losses from field

Water balance equation can be written as follows

$$(\Delta S + \Delta V) = (P + I + U) - (R + D + E + T)$$

where ΔS = Water stored in the root zone

ΔV = Increment of water stored in the vegetation

P = Precipitation

I = Irrigation

U = Upward capillary flow of water into root zone

R = Runoff

D = Drainage out of the root zone

E = Evaporation from soil surface

T = Transpiration by plants

All the quantities of water in the field water balance are estimated in volume of water per unit area.

a. Reducing evaporation from the soil

Evaporation rates are generally high when soils are wet, and they are related to the solar radiation incident on the surface. Evaporation rates drop dramatically as soon as the soil surface dries out in one or two days due to limitations in soil water transfer to the surface. The quantity of radiant energy impinge on the soil surface is the most important determinant of evaporation loss. Thus, evaporation rates may be high when crop cover is low, such as during the early phases of crop development when soil is often wetted by rain or irrigation. Evaporation is low when the crop canopy completely shaded the ground, possibly 10% of evapotranspiration (ET) or less. Evaporation may be a significant component of ET when averaged over a season, especially in rainfed crops when minimal growth and the soil surface is exposed for much of the season. On the other hand, rapid growth rates under irrigation lower seasonal evaporation values for field crops to a mainly inevitable fraction of 20–35% of ET.

Drip irrigation reduces soil evaporation compared to other irrigation systems that moisten the whole ground surface. Although drip irrigation can save crucial water in young orchards by reducing evaporation, the approach is not suitable for watering of major field crops. Even if drip irrigation were cost-effective, evaporation savings in row crops would be minor or non-existent, as demonstrated in a research comparing drip and furrow irrigation in processing tomatoes (Pruitt et al. 1984). According to Bonachela et al. (1999), the potential evaporation savings from switching from surface to subsurface drip irrigation in an olive grove is less than 7% of the seasonal irrigation depth. In water-scarce areas, such savings might be significant, but in most circumstances, they are insufficient to warrant changing irrigation methods.

b. Reducing irrigation system losses

Science and technology have developed a variety of irrigation technologies and procedures that can enhance irrigation efficiency while reducing losses due to runoff and deep percolation. Recent advances in surface irrigation optimization have provided guidance for the design of surface systems with minimal losses. If soil heterogeneity and terrain make surface systems impractical, a range of sprinkler and drip systems with high potential efficiency and uniformity are available. As a result, a variety of technical solutions are available to handle most irrigation concerns on a field-by-field basis. Changing water delivery techniques and flows, land consolidation, and modifications in the design and operation of distribution networks may be required to optimize the design and operation of current surface irrigation systems. Such improvements need both financial investments and agreements among numerous users. Other physical infrastructure upgrades are required to implement pressured systems in community irrigation networks (reservoirs). As a result, there must at the very least be economic incentives and money available to implement the modifications required to raise the system's potential efficiency and uniformity.

Before implementing solutions to decrease irrigation system losses, it is necessary to understand the possible net water savings. Quantifying water sources and sinks at the district and basin levels has been difficult due to major scientific and technological restrictions. The assessment of irrigation return flows and the consequences of various on-farm conservation strategies on net water savings and environmental implications at the basin level are now possible because of new technological breakthroughs based on modelling, remote sensing, and GIS.

8.4 Enhancing Water Productivity Under Intensified Agriculture

Until recently, water was not considered a limited resource. With increasing water shortages and concerns about water quality, there is a growing interest in increasing water productivity, a subclass of partial factor productivity. Crop output per cubic meter of water is the most common way to measure water productivity. Productivity and partial water productivity are two terms that are often used interchangeably. Water productivity is a word that is defined and applied in various ways, and there isn't a single definition that applies to all circumstances. One of the key goals of the International Water Management Institute (IWMI) is to **“increasing the crop per drop”**.

The following is a physical or economic expression of partial water productivity.

1. The quantity of output divided by the quantity of input is known as pure physical productivity. For example, crop yield per hectare or each cubic meter of water applied or consumed by the crop.

2. Productivity is defined as the gross or net present value of a product (economic product) divided by the amount of water diverted or consumed by the crop, incorporating both physical and economic aspects.
3. Economic productivity is calculated by dividing the product's gross or net present value by the value of the water diverted or used by the crop, which may be expressed in terms of the value or opportunity cost of the highest alternative usage.

Choosing water-efficient crops or variety, avoiding wasteful water losses, and maintaining optimum agronomic conditions for agricultural production are the key ways to improve crop water productivity (Rockstrom and Barron 2007). Agronomic strategies for healthy, fast-growing crops favour more transpiration and productive water losses. Avoiding water stress can increase water productivity in other stressors (nutrient deficits, diseases, and weeds) are also alleviated (Bouman 2007), implying that water management should be done in conjunction with fertilizer and soil management. The various interventions for enhancing crop water productivity improvement have included precision and supplemental irrigations, drainage, reduced tillage practices, recommended fertilizer applications, conservation of soil moisture, and the use of disease and drought-resistant crop cultivars (Gowda et al. 2009; Molden and de Fraiture 2010; Balwinder-Singh et al. 2011). Under irrigated and rainfed environments, water productivity varies greatly between agricultural systems. It's been predicted that raising the productivity of low-yield agricultural systems to 80% of the productivity of high-yield farming systems on equivalent land may provide three-quarters of the additional food we need for our rising population. There is much room for improvement, especially if yield discrepancies are large (Cai et al. 2011). In this regard, low-yielding rainfed regions in impoverished pockets spanning most of Sub-Saharan Africa and South Asia have the most considerable potential of increases in crop water productivity (Rockstrom et al. 2010). Because many of the world's poorest people reside in low-yielding rainfed areas, increasing water and land productivity in these places would have several advantages. Thus, by maximizing the value of currently unused rainfall, agricultural land growth would be controlled and disadvantaged men and women's livelihoods would be enhanced without jeopardizing other ecosystem services. According to a new global review on decreasing yield gaps, proper nutrient and water management is critical and must be done in tandem (Mueller et al. 2012) (Table 8.3).

Access to water and other inputs like seeds and fertilizers are frequently connected to gaps in agricultural water productivity, highlighting the relevance of markets and infrastructure (Ahmad and Giordano 2010). However, in areas with high productivity, caution is advised regarding the potential for increased water productivity of crops (Molden and de Fraiture 2010). The biomass output per unit of transpiration has a crop-dependent biophysical limit (Gowda et al. 2009), and while plant breeders have been able to improve the harvest index of crops, increases in harvest index appear to have peaked. The canopy expansion associated with rising yields restricts the potential for minimizing water losses because doubling the yield needs nearly double the amount of transpiration (Descheemaeke et al. 2011). Because irrigated

Table 8.3 Crop water productivity of major crops in different countries (Kumar 2021)

Crop	Countries ^a	Location for highest CWP ^b : CWP (kg m ⁻³)	Water productivity range (kg m ⁻³)
Rice	8	China (2.2)	0.6–1.6
Wheat	13	China (2.67)	0.6–1.7
Cotton	9	China and Israel (0.35)	0.14–0.33
Maize	10	China (3.99)	1.1–2.7

^aNumber of countries considered

^bCWP—Crop Water Productivity

agriculture is the greatest consumer of water resources, it is critical to consider the possibilities for lowering irrigation water demand globally when planning for the future. The primary purpose of irrigation is to increase agricultural output per unit of irrigation water. To boost irrigation water productivity, you'll need to do the following:

1. Increase biomass output per unit of water transpired.
2. Increase harvestable output per unit of water transpired

These are the following strategies to improve the water productivity under intensive cropping systems.

- i. Agronomic measures
- ii. Advanced irrigation technologies
- iii. Use of remote sensing and modelling.

i. Agronomic measures

Scientific Irrigation Scheduling

Optimizing the amount of water for irrigation and spatial zone for its application scientifically requires irrigation scheduling. Scientific irrigation scheduling (SIS) is an efficient tool that calculates projected water needed over short periods to meet crop demands and avoid excess or under the application. These scheduling approaches involve past short-term climate data to predict water use for the next 2–3 weeks to forecast the date for the upcoming irrigation.

- Irrigation scheduling was created to satisfy full irrigation needs, but the ideas may also be used to deficit irrigation. Schedules can also be computed based on the energy balances concept, i.e., known crop response functions, or based on crop responses to stress such as plant water potentials, change in stem diameters, canopy temperature, inter-node lengths, measured soil water content, or combinations of these methods with climate-based irrigation scheduling.
- Scientific irrigation scheduling often improves water productivity, mainly because of the synchronization of crop water demand with water applications. However, it is usually impossible to separate scheduling effects from other improved management practices that are typically followed in the on-farm irrigation scheduling

program. Shifting to improved irrigation practices from surface irrigation to pressurized drip or sprinkler irrigation systems can facilitate irrigation scheduling, especially when the system is automated and controlled based on pre-installed in-situ soil moisture sensors.

Managed Deficit Irrigations

There are three main irrigation scenarios for lowering agricultural water supply; each has its own set of management issues, and all need some type of scientific irrigation scheduling. In the first scenario, a fixed amount is available for allocate for a fixed land area over the growing season as the grower sees fit under full season drought control. In the second, partial season drought management may only make a limited amount of water accessible over a fixed land area for a short period over a fixed land area. The third section discusses spatial optimization techniques such as relocating agricultural production to places with the highest yield potential due to water availability and soil conditions. Each of the mentioned water supply scenarios may include complete or partial land retirement. Both annual and perennial crops face different challenges under such conditions.

- These three situations include integrated techniques that stress crops at various phases of development, distribute limited water throughout the growing season, or manage restricted water that is accessible just part of the year. Annual and biennial crops may be more tolerant of partial-season drought management tactics than perennials, although long-season annuals like potatoes may not tolerate full-season deficit watering schemes.

Full Season Drought Management

- Weather changes, soil spatial variability, irrigation system failures, and other external factors can cause crop yields to plummet fast in deficit conditions. Furthermore, water transport and regulatory restrictions may limit managing deficit irrigations. As a result, deficit irrigation strategies will demand a system-wide rethink, encompassing everything from delivery infrastructure to crop insurance and other agricultural safety net measures.
- There are three primary forms of controlled root zone irrigation solutions when a restricted quantity of water is available for the whole crop growing season (1) regulated deficit irrigation (2) controlled late-season deficit irrigation and (3) fallowing land. The first approach has grown in popularity among tree and vine crops, but it's also been utilized on various annual crops (Fereris and Soriano 2007).

Regulated Deficit Irrigation

When utilizing typical irrigation systems, regulated deficit irrigation (RDI) is a common option for high-value perennial crops in dry areas with insufficient summer

rainfall. Partially drying the root zone is a method of managed deficit irrigation in which water is applied from one side of the plant to the other, necessitating two irrigation systems. This method purposely uses daily sprinkler or micro-irrigation techniques to impose various plant water stresses during specific developmental periods but only replaces 10–30% of the plant's daily water needs- the volume of wetted soil contracts from the sides and bottom of the root zone.

- Regulated deficit irrigation usually needs sufficient late-season water allocations to preserve quality and size at harvest, as well as a system intended to apply at least peak crop water usage daily throughout the growing season. For maximal regulated deficit irrigation control, automated micro-irrigation is frequently employed. RDI has primarily been studied on perennial crops to date, although certain annual crops could also benefit. Many tree crops and grapes have been tried using regulated deficit irrigation, with generally positive results, particularly product quality. These management tactics use particular crop's physiological reactions to drought stress, which cause a decrease in vegetative output in favour of fruit yield. In Australia, beneficial responses have been observed in peaches (Chalmers 1981) and pears (Mitchell et al. 1984); in Washington, beneficial responses have been observed in apples (Drake and Evans 1997), citrus (Goldhamer and Salinas 2000), grapes and other crops (McCarthy et al. 2000). These findings suggest that, depending on rootstocks and cultivars, carefully regulating the intensity and duration of a uniform, consistent degree of water stress on vital perennial crops can benefit crop quality. RDI has been shown to reduce vegetative growth, advance fruit maturity and accelerate fruiting and increase soluble solids and fruit precocity.
- The key to RDI performance is good water management to decrease soil water levels, limiting vegetative development, but water must be accessible throughout the growing season. It can be challenging to execute in many regions because water savings are often made early in the season when water is most plentiful.
- Fereres and Soriano (2007) predict that using regulated deficit irrigation methodologies, yearly water diversions can be decreased by up to 40% from full evapotranspiration (ET), depending on the particular crop and crop quality needs. However, compared to annual and perennial field crops, the overall area planted to high-value permanent crops appropriate for RDI is relatively tiny. For example, a 40% reduction in the irrigated area on only 1% of the total irrigated area will have little influence on water conservation in a watershed.

Controlled Deficit Irrigation

- Late-season deficit irrigation or controlled irrigation refers to irrigation systems in which water resources are plentiful early in the growing season but become scarce later. This is an ordinary circumstance in many regions where late-season water applications are in short supply. Due to late-season drought stressors, irrigation reduces detrimental physiological reactions on annual or perennial crops during

crucial growth phases. Control deficit irrigation is commonly employed as a water conservation practice with perennial crops in dry places, such as plums, peaches, or cherries that are harvested in the early to midsummer. However, postharvest stressors must be carefully managed to minimize detrimental yield consequences on the following year's crop. Water savings will range from 10 to 25% per year or higher.

Fallowing Irrigated Lands

- As part of multiyear rotations, one field or part of land may occasionally be “fallowed” (not watered) for 1 or 2 years, with the water savings used to irrigate the limited area. The semi “fallowed” area might be planted in dryland crops, converted to dryland grazing, or managed to save as much water as possible for later irrigated crops.

Partial Season Drought Management

- Making a set amount of water accessible just during the early growing season is one of the most typical decreased water scenarios. In the long run, this will very certainly result in a shift in crops and lower fertilizer, water, and chemical inputs. Drought-related output decreases are minimized by implementing irrigation systems to deliver water at significant periods and growth stages. Vegetables and other high-value short-season crops can be replaced on a smaller scale for longer-season crops.

Supplemental Irrigation

- Irrigation is, by definition, a complement to natural precipitation. Supplemental irrigation is a tactical tool in temperate and humid places, such as the Mississippi River region and the SE-United States, to augment relatively ample rainfall and sustain output despite short-term droughts. However, this topic is mainly focused on dry and semi-arid regions, where only 1 or 2 irrigations each season may be feasible. This is a type of controlled deficit irrigation in which the timing and use of restricted water supply may have a significant beneficial impact compared to rain-fed agriculture (Solomon and Labuschagne 2003). These methods are used to administer water during vital periods of development. When rainfall is insufficient at planting time, for example, even a small amount of irrigation shortly before or after planting will aid in optimal germination, resulting in a strong stand and greater yield potential. Similarly, a second watering at pollination might help assure a greater harvest for many crops.

Crop Selection

- There is expected to be a shift to crops that develop quickly viz. tiny grains, cold season oil seeds or different pulse crops such as peas and lentils, in arid and semi-arid locations where irrigation water delivery cuts result in repeated partial season droughts. To make the most of the water stored in the soil, farmers may switch to drought resistant and deep-rooted, crops like safflower and sunflower.

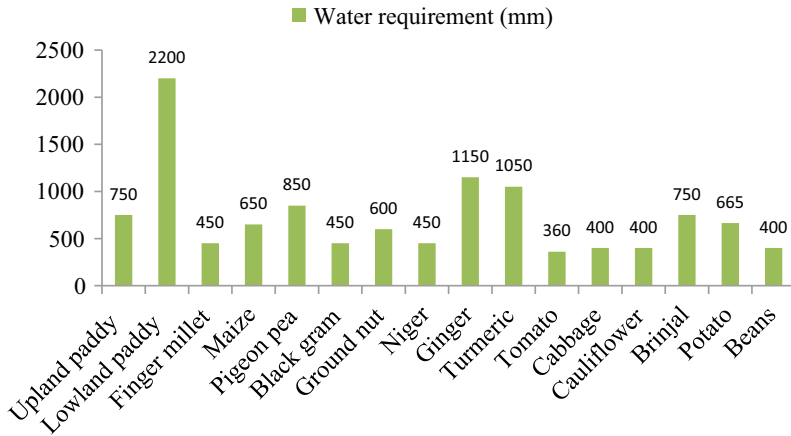


Fig. 8.4 Water requirements of the crops in lachhaputraghati watershed of South-West Asia (Adhikary et al. 2015)

Long season crops viz., maize has lower yields and quality depending on climatic circumstances during the season (Fig. 8.4).

Spatially Optimizing Production

- This method for increasing water delivery productivity is to optimize its geographical distribution. Geographically shifting particular crops to their most favourable locations and soil conditions, lowering irrigation volumes, increasing overall efficiency, and stop giving irrigation in other places are all examples of spatially optimum land use.

Geographic Optimization of Crop Production

- The economic efficient use of natural resources would be to relocate certain crops to climatic locations and type of soil that is best suited for maximum yield. Relocation involves what is produced, produced, and produced for each field, irrigation district, farm, area or watershed. Individual fields to entire regions can be affected by such land use alternatives, with significant economic and environmental consequences. Lands abandoned by geographic relocations would be transformed to non-irrigated dry land pastures/crops, relocated to more “appropriate” irrigated crops, or completely retired from production.

Total or Partial Retirement of Lands

The entire season and partial season drought management is the whole or partial permanent retirement of fields from irrigation. Most typically, a section of the irrigated land is “retired” from irrigation so that the remaining area can be fully irrigated. Retired areas are usually turned to dryland agricultural or animal grazing. To ensure

maximum productivity, available water resources are then utilized in smaller regions. Retirements of land may also be transitory as a result of a brief drought.

- Purchases by metropolitan areas for water or other command initiatives might result in land being permanently retired. Locally, leaving salty or shallow soil parts, as well as degraded and extremely erodible places, can work effectively. The Westland Irrigation District in California, for example, acquired 40,000 acres of very salty, low-yielding fields and shifted the water to more productive regions. Several communities along Colorado's Front Range have acquired tens of thousands of hectares of property to secure water rights for urban usage. Another city, Arizona, and Tucson has had a similar land acquisition scheme that only around 25% of traditionally cultivated areas are now in agricultural production. In reaction to changes in climatic or economic conditions, land may be involuntarily retired.

ii. **Advanced irrigation technologies**

Irrigation has been performed for over the 6000 years ago (Postel 1999), but in the last 100 years, more innovation has happened in this field than in the previous centuries combined. Pumping, diversion works, filtration, distribution, conveyance, application methods, power sources, drainage, scheduling, chemigation, fertigation, erosion control, soil water measurement, land grading, and water conservation are just a few of the areas where irrigation has seen significant innovation.

- Irrigation technology has progressed from early ditches dug by hand to encompass large reservoirs and canal networks to fulfill surface gravity irrigation systems, mechanically and manually operated sprinkler, and a range of low-flow rate systems known as micro-irrigation. Irrigation used to be done using gravity-based technologies to distribute and apply water.
- The invention of low cost aluminium (Al) and then Polyvinyl Chloride (PVC) pipe improved sprinkler technology, and sprinklers now irrigate more area in the many parts of the world than gravity systems.
- Irrigation management and technologies that make better use of soil water have been found to save money and energy while also improving water quality. Reduced water and nutrient stresses have been demonstrated to boost the productivity and quality of fruit and vegetable crops using high-frequency drip irrigation and other micro-irrigation systems. Micro-irrigation can have an application efficiency of 95% or better without drought stress when tied to effective soil water monitoring program, good design, and appropriate management practices. Combining highly effective micro irrigation systems with biodegradable plastic mulches to prevent soil evaporation and further boost potential water savings is another efficient approach.

Improved Irrigation Systems

Surface irrigation systems can be such as effective under certain situations particularly level basins. These techniques need accurate topographic grading, high instant flow rates, and high degrees of management and automation.

- **Micro-irrigation**, which comprises trickle or surface drip, subsurface drip, micro sprinklers, and bubblers, is a slow water delivery rate at discrete sites at low pressures. In the last three decades, it has gone a long way and is now the current standard for effective irrigation procedures that conserve water and allow plants to respond optimally. Small diameter tubing, either on the surface or underground, is installed in the field with small water application devices that supply water directly to a plant at low pressures.
- Self-propelled irrigation systems include centre pivots, which move in a circle around a central point using long, single-pipe laterals, and linear motion sprinkler irrigation systems, which move in straight lines. These systems use miniature sprinklers, sprayers, or bubblers to distribute water slightly above or in the plant canopy as they travel over a field. Water is applied consistently throughout the field, independent of topography, soil type, or plant variances. Low-growing crops including, alfalfa, rice, small grains, soybeans, sugar beet, vegetables and taller crops like sugarcane and corn are most suited for these systems. Low-energy precision applications, or LEPA, are a very efficient water application version using self-propelled irrigation devices. Water is sprayed between plant rows at ground level. Some people call this technique “traveling drip,” since water bursts out of the application device into the furrow. The phrase precision is a little deceptive because it does not provide water more precisely in space than a sprinkler, but it does not fulfill plant demands accurately.
- One of the most compelling reasons for producers to enhance these irrigation systems is to minimize labour expenses through automation while also conserving water. Another advantage is that it allows them to increase their irrigated area while maintaining irrigation capacity, known as “water spreading” in certain jurisdictions.
- Water loss may be reduced using a variety of management strategies. Furrow diking or digging tiny pits or basins (little reservoirs) in sprinkler-irrigated fields to store water that falls from both irrigation and precipitation can be advantageous (this may be required under LEPA systems). Reduced acreage of irrigated and fertilized crops left unharvested for any reason will diminish non-beneficial usage. Evaporation losses can be reduced by irrigating at night. Weeds are extensive non-beneficial use of water that must be controlled, but chemical management is expensive and can have unintended environmental repercussions. Mulches may minimize non-beneficial ET and soil evaporation when used for weed control. Soil evaporation losses can be reduced using reduced tillage practices. Drip irrigation reduces soil evaporation and increases crop water yield, which helps to save water. Alternative cropping systems (ACS), such as deep-rooted cultivars and winter crops might be incorporated into these techniques to optimize the utilization of stored nutrients and soil moisture.

- Nonetheless, without modern irrigation methods, the deficit irrigation tactics outlined above would not be achievable, and the ability to conserve water is dependent on the irrigation system's and operator's ability to execute water saving practices and technology. Linear or self-propelled centre pivot motion sprinklers, as well as different micro-irrigation systems, are viable options for increasing efficiency by applying site-specific and precise watering at various places over a field. Other precision agricultural methods, such as site-specific fertilizer inputs, will also benefit these technologies.

Site-Specific Irrigation

Agricultural producers' incapacity to regulate inputs in ways that accommodate varying growth conditions throughout a field is one of the most significant barriers to managing increased production and water quality. Infiltration rates vary between irrigation episodes and places within the field, as has long been recognized. Tillage methods and crop rotations may also have an influence. Thus, instead of managing the entire field as a single unit, it may be more desirable to vary water applications across a field to accommodate possible productivity disparities and environmental repercussions from the diversity of these multiple elements. Alternatively, the goal is to administer water in a non-uniform manner over non-uniform soils and field conditions to give ideal growth circumstances. Irrigation equipment, designers makers, managers, researchers, and growers will face significant obstacles and possibilities, but they may prove to be highly profitable at the end (Sadler et al. 2007).

- Because of their present degree of automation and extensive area coverage with a single lateral pipe, self-propelled centre pivot and linear move irrigation systems are remarkably adaptable to site-specific techniques. Potential water savings employing site-specific technology under non-stress conditions (maximum yield) are likely in the range of 15–30% but might be average of 5% or less. (Sadler et al. 2005).
- The development of control and management technologies that allow “precision” self-propelled irrigation systems to spatially and temporally direct the amount and frequency of water (and appropriate agrochemical) applications would be a powerful tool for increasing productivity while minimizing negative water quality impacts. More effective ways of administering crop supplements (fertilizers, insecticides, and growth regulators) are also needed to minimize use, enhance profit margins, and lessen environmental consequences.

Micro-irrigation

With its precise, high-level administration, micro-irrigation can save much water and is a very versatile watering system. In general, their high cost and intense management requirements limit their application to limited field areas. Micro-irrigation is adaptable to nearly every farming condition and climate zone. It may be placed as a surface water application system (Schwank and Hanson 2007) or a subsurface water application system (Lamm and Camp 2007). Micro-irrigation, as previously said,

is employed on <1% of the world's fields, owing to its new creation and expensive initial capital cost.

- Micro-irrigation may be used on most crops, but due to its relatively high cost and care needs, it is most commonly utilized on high-value specialty crops such as vegetables, ornamentals, vines, berries, olives, avocados, nuts, fruit crops, and greenhouse plants. In many circumstances, it may also be used for field crops, golf greens, fairways, cotton, and sugarcane. However, the criteria for optimal designs and management in humid environments vary significantly from those in dry places; therefore, good technology and practices in one area may not be appropriate in another.
- Micro-irrigation is becoming more popular worldwide, and it is projected to remain a viable irrigation strategy for agricultural output in the near future. With rising demands on limited water supplies and a desire to reduce irrigation's environmental impact, this technology will surely become even more significant in the future. Micro-irrigation has a variety of agronomic, water, and energy-saving benefits that solve many of the issues that irrigated agriculture faces.
- Farmers and other micro-irrigation users are always looking for new uses, such as wastewater reuse, which will keep designers and irrigation managers on their toes. Despite its various variations, significant gains are potential if micro-irrigation can be made less expensive, allowing producers to accept and use these technologies, particularly in impoverished nations.

iii. Use of remote sensing and modelling

Developing accurate, timely information on plant and field to make decision will be required to ensure the success of irrigated agricultural companies. Current plant models capable of forecasting a crop's physiological demands across time and place are sophisticated and only function with a single set of precisely defined input parameters based on a single location in a field, making them unrealistic for real time on farm management. On the other hand, simple models may be precise plenty, but they need to be refined. Such models would very indeed rely on automated regular updates, sensor systems in field to alter the model variables, ensuring suitable field monitoring as well as spatial forecasts for model improvements.

The information on soil and plant nutrition and water content may be obtained by remote sensing and utilizing aerial satellite, integrated satellite and field level soil and plant based sensor systems (Table 8.4).

However, this technique requires additional research to enhance temporal-spatial modelling and apply for district irrigation operations and on-farm management. Improved techniques and procedures for assessing particular plant characteristics (water and nutrient status, disease infections, competitive weeds) on a time step are becoming accessible, and they are likely to offer the data needed to improve crop modelling and hence within-season management.

Table 8.4 Sensors or satellites that provide images suitable for agricultural water management (Bastiaanssen et al. 2000)

Purpose	SPOT	IRS	MSS	ERS-SAR	ERS-ALT	Meteosat	TM	ERS-ATSR	GMS
Precipitation						✓			✓
Irrigated area							✓	✓	
Land use	✓	✓	✓				✓	✓	
LAI	✓	✓	✓				✓	✓	
Transpiration coefficient	✓	✓	✓				✓	✓	
Surface roughness				✓	✓				
Potential ET						✓	✓	✓	✓
Actual ET							✓	✓	
Root-zone moisture							✓	✓	
Soil salinity				✓			✓		
River discharge				✓	✓				
Cartographic information	✓	✓					✓		
Cropping pattern				✓			✓		
Crop yield	✓	✓	✓				✓	✓	
Surface moisture				✓					
Water logging	✓	✓	✓	✓			✓		
Crop coefficient	✓	✓	✓				✓		

SPOT: Satellite pour Observation de la Terre; *IRS*: Indian Remote Sensing Satellite; *TM*: Thematic Mapper; *MSS*: Multi spectral Scanner; *ERS*: European Remote Sensing Satellite; *SAR*: Synthetic Aperture Radar; *ALT*: Altimeter; *ATSR*: Along-Track Scanning Radiometer; *GMS*: Geostationary Meteorological Satellite

- When based on distributed networks of farm-level microclimate and soil water sensor stations that feed into a microprocessor control system to manage irrigations according to rules pre-established by the producer real time irrigation application could be effective in improving water use efficiency. Expanded agricultural weather networks with increased geographical density and grower-friendly information delivery systems that schedule irrigations in terms of pest control and marketing information are required to assist this effort.
- While improved irrigation methods usually need less field labour, they sometimes necessitate more extensive management. As a result, support aids that increase

the producer's capacity to execute choices quickly and readily must be developed; nevertheless, this also necessitates the development of control and monitoring systems. To make timely judgments based on complicated inputs, decision support systems are required. Climate change and insect outbreaks necessitate daily and seasonal water and chemical treatments that are carefully timed and put. The decision support process must also give accurate projections of crop water demand, application efficiency, and uniformities to increase management flexibility.

8.5 Real-Time Crop and Water Management Options for Intensified Agriculture

An innovative paradigm for enhancing crop and water management is included in FAO research on climate change adaptation (Turrall et al. 2011). The framework is made up of the following components:

On-Farm Management

1. Farm and crop management
2. Crop selection and calendar
3. Fertilizer management
4. Farm water management
5. Farm irrigation technology
6. Accounting for depletion
7. Flood prevention and erosion
8. Commercial agriculture

Irrigation System Level

1. Allocation of water
2. The efficiency of the system
3. Calendars and cropping patterns
4. Irrigation policy actions
5. Conjunctive usage of ground and surface water

River Basin and National Level

1. Irrigation policy
2. Managing to droughts
3. Dealing with floods
4. Interventions, both structural and non-structural
5. Aquifer recharge management
6. Evaluation of adaption alternatives to assure the security of irrigation supply

Policies, Institutions, and the Subsector's Structure

1. Allocation mechanism

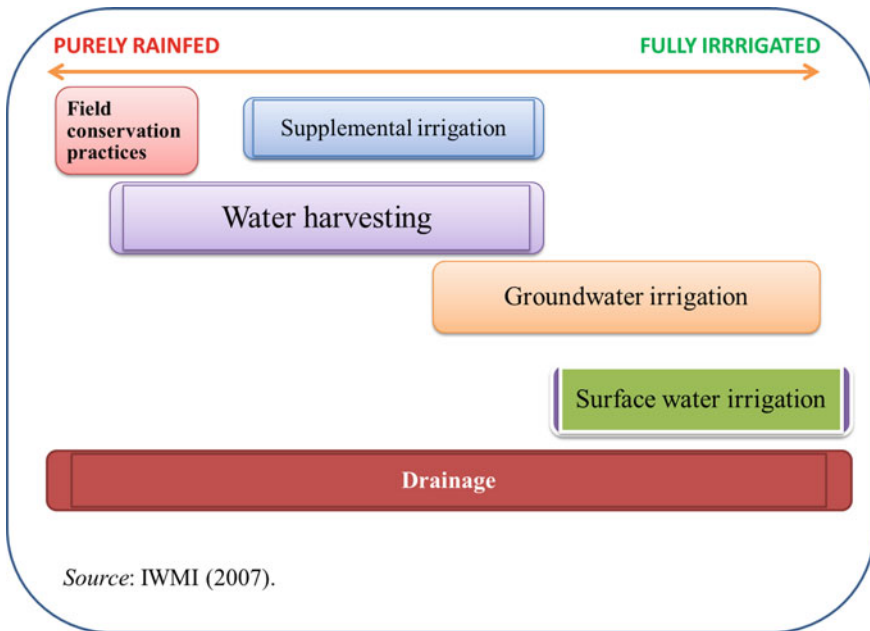


Fig. 8.5 Diverse options for agricultural water management

2. Problems of national food policy (NFP)

Institutions

1. Implications of long-term investment for agricultural water management (Fig. 8.5 and Tables 8.5, 8.6).

8.6 Breeding for Enhancing Water Productivity

Plant breeding has boosted water productivity indirectly (in conjunction with other production parameters) during the last century since yields have grown with no additional water usage. Improved varieties have resulted from traditional breeding programs that prioritized production per unit of land. The majority of the increases have been attributable to advances in the harvest index (the ratio of marketable product to total biomass, often known as the grain-to-straw ratio), which in many of our key crops may now be reaching its theoretical limit (Richards et al. 1993). The most significant improvements in yield stability are usually due to the development of appropriate phenology through genetic modification. The duration of the vegetative and reproductive periods is as close as possible to the regular water supply or the absence of crop hazards. Planting, blooming, and maturity dates all have a role in coordinating optimal crop development with minimal saturation vapour-pressure

Table 8.5 Categorization of different management interventions for sustainable water management

Theme	Category	Intervention
Water	On-field irrigation methods	Border or furrow irrigation
		Sub-surface irrigation
		Drip irrigation
		Sprinkler irrigation
	On-field irrigation management	Regulated deficit irrigation
		Supplemental irrigation
		Alternate wetting and drying
		Surge irrigation
	Irrigation infrastructure	Pipes
		Canal lining
	Moisture recycling	Hydroponics
		Greenhouse
	Soil and land	Land grading
Block-end or soil bunds		
Terracing		
Agronomic interventions	Supplements	Growth enhancers
		Fertilizers
	Crop selection	Crop rotation
		Variety: high yield
		Variety: rooting depth
		Variety: short duration
		Timing of sowing
	Coverage	Planting density
		Weed control
		Shading
		Mulching
	Salinity management	Cover crops
		Leaching
Salt-tolerant crop types		

Table 8.6 Inventory summary of different management interventions with average recorded changes (%) in irrigation (I), evapotranspiration (ET), crop yield (Y), water productivity based on ET (ET-WP), and irrigation water productivity (I-WP)

	Count	Irrigation (%)	ET (%)	Yield (%)	ET-WP (%)	I-WP (%)
Agronomy	54	-4	-6	19	27	12
Coverage	24					
Mulching	24	0	-3	14	14	0
Selection of crop	18					
Variety: high yields	3		0	10	15	
Variety: short duration	3	-23	-18	-2	29	22
Crop rotation	4	8	-19	-14	1	15
Date of sowing	6	-4	-20	36	7	-2
Supplement inputs	12					
Fertilizers/nutrients	12			84	62	24
Water management	131	-38	-5	14	41	50
On-farm irrigation	124					
Furrow/border irrigation	3	15		0		5
Alternate wetting-drying	3	-37	0	1	-7	31
Deficit irrigation (DI)	27	38	-27	-23	-13	57
Sprinkler irrigation	12	-27		14		-2
Drip irrigation	67	-46	9	29	11	87
Surge irrigation	6	-22	0	0	-3	6
Sub-surface irrigation	6	-15	-10	62		33
Irrigation infrastructure	6					
Soil and land	40	-18	3	10	2	18
Pipes	4	-28	4	20		
Tillage practices	26					
Zero tillage	25	-14	6	8	2	14
Land leveling	14					
Field levelling	14	-23	-2	15	3	52
Grand total	240	-32	-4	13	20	37

deficits, and these traits may be genetically manipulated. Modifying canopy growth to prevent evaporation from the soil surface is one technique to increase water productivity genetically. As a result, great effort has gone into selecting big leaf areas throughout the vegetative phase to boost early vigour.

Biotechnology is thought to offer much potential for developing drought- or salt-tolerant crops, although it hasn't been completely realized yet. The genetic complexity of the trait and its interaction with the environment is often blamed for the poor development in drought tolerance breeding. Improved environmental simulations used for germ plasm screening and analysis, defining how the impact of water deficit on growth and yield components changes during the growth stages, and discovering the regulatory genes underlying the plant's responses to water deficit are all complementary approaches being taken to address this issue. Quantitative trait loci (QTL) research is one potential way to finding the genes responsible for drought effects on yield components. The suppression of panicle growth by hormonal signals from stressed leaves and roots and the reduction of carbon transfer from leaves to the growing grain are examples of indirect effects. The genetic modulation of cytokinin production, for example, may be able to avoid early drought-induced leaf loss. However, it may be argued that traditional breeding would be more effective in altering these processes. For years, traditional plant breeding has introduced several good qualities for dealing with drought stress. Changes to the timing of sensitive stages and the length of the growing season are among them, as are selections for tiny leaves and early stomatal closure to minimize transpiration, deep-rooted systems, intense root activity and resistance to salt. In a nutshell, traditional breeding practices and current biotechnology-based breeding procedures should be viewed as complementary.

The four genetic enhancement options for improving legume and grain crop tolerance to drought-prone areas are:

1. The development of short-duration genotypes capable of surviving drought.
2. For drought-prone locations, conventional breeding of genotypes with improved yield potential.
3. Breeding for drought-resistant genotypes.
4. Identification of quantitative trait loci for drought tolerance and their application in marker-assisted breeding.

Despite biotechnology's promises, substantial gains in enhancing key crops' potential yield or harvest index are unlikely to be achieved in the next 10–20 years. This is due to the fact that crop output is determined by a number of genes and their interactions with the environment. Plants have also been subjected to billions (in the case of photosynthesis) to thousands of years of selection (in the case of harvestable yields). Currently, biotechnology has effectively addressed crop development goals by dealing with characteristics dependent on one or a few genes, selecting for certain defect changes and pest, herbicide, and disease resistance. In the next one to two decades, breeding for drought resistance utilizing existing and future technologies as they become available would only result in modest, incremental gains in crop productivity under constrained water supplies.

8.7 Role of Institutions and Policymakers

There are technologies available that might improve irrigation efficiency across the planet. Improved water management, as well as institutional reforms, are necessary to actualize this promise. Irrigation scheduling strategies, which decide the timing and amount of irrigation, can help optimize on-farm water management. Most irrigation scheduling approaches have already been created, while feasible further enhancements. Due to a lack of economic incentives and adequate legislation, farmers in industrialized nations have not extensively implemented such approaches. Some signs irrigation scheduling technologies are being used more widely in the more sophisticated irrigated regions. The idea to use irrigation scheduling techniques in underdeveloped nations, where irrigation networks are frequently constructed to supply only a portion of crop demand is not viable. In those circumstances, the first step would be to gather basic soil and meteorological data that might be used to determine seasonal requirements for district or watershed planning reasons.

Institutional reforms, such as introducing market forces to deal with water as an economic good, are advised for more effective management of water resources in agriculture. There are two requirements to considering water as an economic good so that market forces may determine how much water is allocated to agriculture in many parts of the world. The first is water supply to farmers, and the second is water rights that are guaranteed and specified. Both are frequently inadequate in poorer nations, where irrigation rights are sometimes ambiguous. However, in industrialized nations, the use of market forces to control water in irrigated agriculture is desired for increasing irrigation effectiveness, especially in water-scarce conditions. Many experts have studied the global irrigation demand for 2025. Although the study may only be a poor approximation to the actual world due to uncertain data quality, it is refreshing to get a worldwide perspective on this crucial issue. According to one of the study's findings, greater irrigation effectiveness through conservation may provide roughly half of the expected rise in demand from 1990 to 2025.

References

- Adhikary PP, Madhu M, Dash CJ, Sahoo DC, Jakhar P, Naik BS, Dash B (2015) Prioritization of traditional tribal field crops based on RWUE in Koraput district of Odisha. *Indian J Tradition Knowl* 14(1):88–95
- Aeschbach-Hertig W, Gleeson T (2012) Regional strategies for the accelerating global problem of groundwater depletion. *Nat Geosci* 5(12):853–861
- Ahmad MUD, Giordano M (2010) The Karkheh River basin: the food basket of Iran under pressure. *Water Int* 35(5):522–544
- Alcamo J, Doll P, Henrichs T, Kaspar F, Lehner B, Rosch T, Siebert S (2003) Global estimates of water withdrawals and availability under current and future “business-as-usual” conditions. *Hydrol Sci J* 48(3):339–348
- Alexandratos N, Bruinsma J (2012) *World agriculture towards 2030/2050: the 2012 revision*

- Balwinder-Singh, Humphreys E, Eberbach PL, Katupitiya A, Yadvinder-Singh, Kukal SS (2011) Growth, yield and water productivity of zero till wheat as affected by rice straw mulch and irrigation schedule. *Field Crops Res* 121:209–225
- Bastiaanssen WG, Molden DJ, Makin IW (2000) Remote sensing for irrigated agriculture: examples from research and possible applications. *Agric Water Manag* 46(2):137–155
- Bonachela S, Orgaz F, Villalobos FJ, Fereres E (1999) Measurement and simulation of evaporation from soil in olive orchards. *Irrig Sci* 18(4):205–211
- Borsato E, Rosa L, Marinello F, Tarolli P, D’Odorico P (2020) Weak and strong sustainability of irrigation: a framework for irrigation practices under limited water availability. *Front Sustain Food Syst* 4:17
- Bouman BAM (2007) A conceptual framework for the improvement of crop water productivity at different spatial scales. *Agric Syst* 93(1–3):43–60
- Cai X, Molden D, Mainuddin M, Sharma B, Ahmad MUD, Karimi P (2011) Producing more food with less water in a changing world: assessment of water productivity in 10 major river basins. *Water Int* 36(1):42–62
- Chalmers DJ (1981) Control of peach tree growth and productivity by regulated water supply, tree density, and summer pruning. *J Amer Soc Hort Sci* 106:307–312
- Chartzoulakis K, Bertaki M (2015) Sustainable water management in agriculture under climate change. *Agricult Agric Sci Procedia* 4:88–98
- D’Odorico P, Davis KF, Rosa L, Carr Joel A, Chiarelli D, Dell’Angelo J et al (2018) The global food-energy-water nexus. *Rev Geophys* 56(3):456–531
- De Perthuis C, Jouvet PA (2015) Green capital. A new perspective on growth. Columbia University Press, New York, NY. <https://doi.org/10.7312/columbia/9780231171403.001.0001>
- Descheemaeker K, Amede T, Haileslassie A, Bossio D (2011) Analysis of gaps and possible interventions for improving water productivity in crop livestock systems of Ethiopia. *Exp Agric* 47(S1):21–38
- Dietz S, Neumayer E (2007) Weak and strong sustainability in the SEEA: concepts and measurement. *Ecol Econ* 61(4):617–626
- Drake SR, Evans RG (1997) Irrigation management influence on fruit quality and storage life of ‘Redspur’ and ‘Golden Delicious’ apples. *Fruit Varieties J (USA)* 51(1):7–12
- Dubois O (2011) The state of the world’s land and water resources for food and agriculture: managing systems at risk. Earthscan
- Fereres E, Soriano MA (2007) Deficit irrigation for reducing agricultural water use. *J Exp Bot* 58(2):147–159
- Food and Agriculture Organization (2013) Sustainability assessment of food and agriculture systems. Guidelines Version 3.0. FAO, Rome
- Food and Agriculture Organization (2019) FAOSTAT. Food and Agriculture data [WWW Document]
- Goldhamer DA, Salinas M (2000) Evaluation of regulated deficit irrigation on mature orange trees grown under high evaporative demand. In: *Proceedings of internat soc citriculture IX congress*, pp 227–231
- Gowda CLL, Serraj R, Srinivasan G, Chauhan YS, Reddy BVS, Rai KN, Nalini M (2009) Opportunities for improving crop water productivity through genetic enhancement of dryland crops. In: *Rainfed agriculture: unlocking the potential*, vol 7, pp 133–163
- Green PA, Vörösmarty CJ, Harrison I, Farrell T, Sáenz L, Fekete BM (2015) Freshwater ecosystem services supporting humans: pivoting from water crisis to water solutions. *Glob Environ Chang* 34:108–118
- Groenfeldt D (2019) *Water ethics: a values approach to solving the water crisis*, 2nd edn. Routledge
- Hartwick JM (1978) Intergenerational equity and the investing of rents from exhaustible resources. *Am Econ Rev* 67(5):972–974
- Interagency Task Force Report (1979) *Irrigation water use and management*. USDI, USDA and EPA, Washington, DC, 133 pp

- International Water Management Institute [IWMI] (2007) *Water for food water for life: a comprehensive assessment of water management in agriculture*, IWMI, Columbo, Sri Lanka
- Jagermeyr J, Pastor A, Biemans H, Gerten D (2017) Reconciling irrigated food production with environmental flows for sustainable development goals implementation. *Nat Commun* 8:15900
- Jakeman AJ, Barreteau O, Hunt RJ, Rinaudo JD, Ross A (2016) *Integrated groundwater management*. Springer Nature, p 762
- Juwana I, Muttil N, Perera BJC (2012) Indicator-based water sustainability assessment—a review. *Sci Total Environ* 438:357–371
- Konikov E, Likhodedova O (2011) Global climate change and sea-level fluctuations in the Black and Caspian Seas over the past 200 years. In: *Geology and geoarchaeology of the black sea region: beyond the flood hypothesis*, vol 473, p 59
- Kumar MD (2021) *Water productivity and food security: global trends and regional patterns*, vol 3. Elsevier
- Lamm FR, Camp CR (2007) Subsurface drip irrigation. In: Lamm FR, Ayars JE, Nakayama FS (eds) *Microirrigation for crop production*, Chap. 13. Elsevier, New York, pp 473–551
- McCarthy MG, Loveys BR, Dry PR (2000) Regulated deficit irrigation and partial Rootzone drying as irrigation practices-water reports 22. FAO, Rome
- Mitchell PD, Jerie PH, Chalmers DJ (1984) The effects of regulated water deficits on pear tree growth, flowering, fruit growth, and yield. *J Am Soc Hortic Sci* 109(5):604–606
- Molden D, de Fraiture C (2010) *Comprehensive assessment of water management in agriculture*. *Agricult Water Manag* (Print) 97(4)
- Mueller ND, Gerber JS, Johnston M, Ray DK, Ramankutty N, Foley JA (2012) Closing yield gaps through nutrient and water management. *Nature* 490(7419):254–257
- Postel S (1999) *Pillar of sand: can the irrigation miracle last?* WW Norton & Company
- Pruitt WO, Fereres E, Martin PE, Singh H, Henderson DW, Hagan RM, Chandio B (1984) Microclimate, evapotranspiration, and water-use efficiency for drip and furrow-irrigated tomatoes. In: *International commission on irrigation and drainage (ICID)*. 12th congress, Fort Collins, pp 367–393
- Rennings K, Wiggering H (1997) Steps towards indicators of sustainable development: linking economic and ecological concepts. *Ecol Econ* 20(1):25–36
- Richards RA, López-Castañeda C, Gomez-Macpherson H, Condon AG (1993) Improving the efficiency of water use by plant breeding and molecular biology. *Irrig Sci* 14(2):93–104
- Rockstrom J, Barron J (2007) Water productivity in rainfed systems: overview of challenges and analysis of opportunities in water scarcity prone savannahs. *Irrig Sci* 25(3):299–311
- Rockstrom J, Falkenmark M, Allan T, Folke C, Gordon L, Jägerskog A, Varis O (2014) The unfolding water drama in the Anthropocene: towards a resilience-based perspective on water for global sustainability. *Ecohydrology* 7(5):1249–1261
- Rockstrom J, Karlberg L, Wani SP, Barron J, Hatibu N, Oweis T, Qiang Z (2010) Managing water in rainfed agriculture—the need for a paradigm shift. *Agric Water Manag* 97(4):543–550
- Rockstrom J, Williams J, Daily G, Noble A, Matthews N, Gordon L, Smith J (2017) Sustainable intensification of agriculture for human prosperity and global sustainability. *Ambio* 46(1):4–17
- Rosa L, Rulli MC, Davis KF, Chiarelli DD, Passera C, D’Odorico P (2018) Closing the yield gap while ensuring water sustainability. *Environ Res Lett* 13(10):104002
- Sadler EJ, Camp CR, Evans RG (2007) New and future technology. *Irrigat Agricult Crops* 30:607–626
- Sadler EJ, Evans R, Stone KC, Camp CR (2005) Opportunities for conservation with precision irrigation. *J Soil Water Conserv* 60(6):371–378
- Savenije HH, Van Der Zaag P (2002) Water as an economic good and demand management paradigms with pitfalls. *Water Int* 27(1):98–104
- Schwankl LJ, Hanson LR (2007) Surface drip irrigation. In: *Developments in agricultural engineering*, vol 13. Elsevier, pp 431–472
- Seckler D (1993) *Designing water resources strategies for the twenty-first century*. Water Resources and Irrigation Division. Discussion Paper 16. Winrock International, Arlington, Virginia, USA

- Seckler DW (1998) World water demand and supply, 1990 to 2025: scenarios and issues, vol 19. Iwmi
- Solomon KF, Labuschagne MT (2003) Variation in water use and transpiration efficiency among durum wheat genotypes grown under moisture stress and non-stress conditions. *J Agric Sci* 141(1):31–41
- Solow RM (1974) Intergenerational equity and exhaustible resources. *Rev Econ Stud* 41:29–45
- Sullivan C (2002) Calculating a water poverty index. *World Dev* 30(7):1195–1210
- Turrall H, Burke J, Faurès JM (2011) Climate change, water and food security, no 36. Food and Agriculture Organization of the United Nations (FAO)
- Vanham D, Hoekstra AY, Wada Y, Bouraoui F, De Roo A, Mekonnen MM, Bidoglio G (2018) Physical water scarcity metrics for monitoring progress towards SDG target 6.4: an evaluation of indicator 6.4. 2 “Level of water stress.” *Sci Total Environ* 613:218–232
- Wada Y, Berkers MF (2014) Sustainability of global water use: past reconstruction and future projections. *Environ Res Lett* 9(10):104003
- Wada Y, Van Beek LP, Van Kempen CM, Reckman JW, Vasak S, Bierkens MF (2010) Global depletion of groundwater resources. *Geophys Res Lett* 37(20)
- World Business Council for Sustainable Development (WBCSD) (2017) Reporting matters. Striking a balance between disclosure and engagement. <https://www.wbcd.org/Projects/Reporting/Reporting-matters/Resources/Reporting-Matters-2017>. Accessed 1 Feb 2018

Chapter 9

Deficit Irrigation: An Optimization Strategy for a Sustainable Agriculture



Abhijit Rai, Sayantan Sarkar , and Prakash Kumar Jha

Abstract Nearly 70% of the global renewable water resources are annually used for irrigation. It is projected that the demand for irrigation will continuously increase over time due to increasing climatic variability, reduction in water quantity and quality, increasing competition for freshwater resources from other sectors of the economy, and changes in water policy. Water use in agriculture is interconnected with soil, weather, land use pattern and allocation of available water resources. For sustainable agriculture, efficient water use and productivity with implication on socioeconomic aspects needs to be discussed thoroughly. This chapter discusses the concepts and rationale of deficit irrigation (DI), different popular DI approaches in the world, and discusses the challenges and limitations of each one. Furthermore, the chapter will discuss different practical tools and resources required for the successful implementation of DI and discuss the physiological and biochemical basis of DI.

Keywords Deficit irrigation (DI) · Crop evapotranspiration (ET) · Yield response factor (Ky) · Sustained deficit irrigation (SDI) · Partial root-zone drying (PRD) · Stage-based deficit irrigation (SBDI) · Supplemental irrigation (SI)

A. Rai

Department of Plant Sciences, College of Agriculture and Bioresources, University of Saskatchewan, Saskatoon, SK S7N 5A8, Canada
e-mail: abr922@usask.ca

S. Sarkar (✉)

West Tennessee AgResearch and Education Center, University of Tennessee, Jackson, TN 38301, USA
e-mail: sarkarsayantan@hotmail.com

P. K. Jha

Feed the Future Innovation Lab for Collaborative Research on Sustainable Intensification, Kansas State University, Manhattan, KS 66506, USA
e-mail: pjha@ksu.edu

9.1 Introduction

World agricultural production has increased in the past because of intensified irrigated agriculture to meet the food demand of growing population, however pressing challenges of limited water availability due to climate variability constrained the growth in food production. At present, agriculture accounts for 70% of the world's water withdrawal, the majority of which is employed for irrigation. A study under Water Futures and Solutions Initiative (WFaS) project analyzed three future scenarios: *Sustainability*, *middle of the road*, and *regional rivalry* (Burek et al. 2016). The study concluded that there would be a 20–30% increase in water demand by agricultural, industrial, and domestic sectors in all the scenarios by 2050. Though the agricultural sector will have the highest water demand, the other two sectors will show a significant increase too. However, agriculture not only faces challenges from other sectors for water allocation but also complications arising from climate change from field to watershed scale (Eswaran et al. 2021).

Agriculture is vulnerable to the changes that occur in climate, mostly due to the dependence of agriculture systems on the climate (Balota and Sarkar 2020, Sarkar 2021; Balota et al. 2021a). Some of the adverse effects of climate change on agriculture are; increased variability in precipitation on an interannual basis, increased frequency and magnitude of extreme events like droughts, floods (Hirabayashi et al. 2008; Wilhite et al. 2007; Baule et al. 2018; Araya et al. 2021), and heat stress which impact yield (Mazdiyasi and AghaKouchak 2015; Yadav et al. 2022). In addition, the increased temperature may result in increased water demand, and higher spring runoff of rivers in the colder semi-arid regions (Barnett, et al. 2005), which can complicate the already vulnerable supply–demand balance by decreasing the available water supply. Therefore, maximizing agriculture productivity in a water-scarce era should be of prime focus with an efficient use of the precision agriculture (Sarkar and Jha 2020).

Deficit irrigation (DI) is an optimizing strategy that can reduce the demand for irrigation and improve water productivity. DI is used as a water-saving irrigation strategy around the world where water supply is limited under erratic climate conditions with minimal yield loss (Feres and Soriano 2007). An efficient application of DI requires careful assessment of crop water requirements, knowledge of water-sensitive growth stages and proper irrigation scheduling based on the DI approach adopted (Jha et al. 2018; Pereira et al. 2002). Moreover, an understanding of the role of factors such as crop (and cultivar), soil, climate and different management practices under limited water scenarios is required for implementing DI at the field. The present chapter seeks to provide an overview of the deficit irrigation concepts and strategies for its efficient implementation.

9.2 Deficit Irrigation Concepts and Rationale

The concept of DI was first introduced by James and Lee (1971), and the earliest research into DI can be traced to the early 1980s (English and Nuss 1982; Hargreaves and Samani 1984). English (1990) defined DI as the “deliberate and systematic under-irrigation of crops”. Under DI crops are exposed to certain levels of water stress either during a growth stage or throughout the growing season in a manner that does not result in a significant reduction of yield. The marginal yield reduction is justified by the economic benefits derived from increased irrigation efficiency, reduced costs of irrigation, and the opportunity cost of water (English 1990). Several researchers have assessed the economic viability of DI and have concluded that net farm income can be increased using the DI technique (Dudley et al. 1971; Rodrigues and Pereira 2009).

On the water-saving front, studies have reported on the positive effects of DI on water productivity. Yonts et al. (2018) reported that by reducing irrigation by 25% for dry beans, irrigation water use efficiency (IWUE) can be increased by 26% with a yield loss of 6% in comparison to full irrigation. Early deficit application in potatoes has shown to save 32–54% of water over full irrigation without yield penalty (Yactayo et al. 2013). Greaves and Wang (2017) assessed maize yield response to four DI levels of 0.3, 0.5, 0.6 and 0.8 fraction of full irrigation. They reported <12% decrease in the yield of maize for irrigation levels of 0.8 and 0.6 of full irrigation with higher water productivity. Comparable results have been observed for maize by Irmak et al. (2016) with irrigation levels of 0.25, 0.5, 0.75 of full irrigation. Mugabe and Nyakatawa (2000) applied 75 and 50% of irrigation requirements in wheat and observed yield decreases of 12 and 20% in two years, respectively. Sezen et al. (2011) reported water-saving of 36 and 33% increase in IWUE with DI, with a 15% reduction in seed yield for sunflower.

However, some studies have reported a yield increase in response to DI. Du et al. (2008) have reported an increase of 5–20% in seed cotton yield with DI over full irrigation because of improved harvest index, and Zhang et al. (2006) has reported an increase in wheat yield, and approximately 40% in water use efficiency under DI in comparison to full irrigation treatment (Kirda et al. 1995). As evident, the positive benefits of DI are established but the crop response can vary with the crop and cultivar types (Lanna et al. 2016; Emam et al. 2012; Singh et al. 2009; Sung et al. 2021; Shekoofa et al. 2022), soil types-land use patterns (Daryanto et al. 2015; Bennett et al. 2021; Burow et al. 2021; Hota et al. 2022), climate conditions, and DI levels adopted. Thus, any decisions on the DI level or approach for any crop or region require careful assessment of crop response to DI based on local experiments.

Table 9.1 Review of selected deficit irrigation studies in the literature

Year	Crop	Country	Climate	Soil	DI method	Main effects	References
2014-2016	Tomato	Saudi Arabia	Semi-Arid	Clayey sand	SDI	20% reduction in Irrigation resulted in decrease of 18% of yield	Al-Chobari and Dewidar (2018)
2016-2017	Potato	Morocco	Greenhouse	Sandy soil	PRD and DI	No difference in Yield between PRD and DI	Elhami et al. (2019)
2012-2013	Maize	China	Semi-arid	Brown loess loam	SBDI and SDI	80% irrigation between V8 and R6 growth stage had overall higher yield than 100% irrigation	Zou et al. (2021)
2012-2013	Maize	USA	Semi-arid	Sandy loam	SBDI	DI at late vegetative stage resulted in 15-17% of ET saving with no yield loss	Comas et al. (2019)
2018-2019	Wheat	Pakistan	Semi-arid	Sandy loam	SBDI	50% water deficit at the grain maturity stage improved WUE without significant yield reduction	Memon et al. (2021)
2010-2015	Dry bean	USA	Semi-arid	Sandy loam	SDI	75% FT increased IWUE by 26% and only 6% yield reduction	Yonts et al. (2018)
2003-2004	Wheat	China	Semi-arid	Loam	SBDI	Yield and WUE improved for medium stress at jointing and grain filling stage	Zhang et al. (2006)
2010	Potato	Peru	Semi-arid	Sandy loam	PRD and SDI	Early PRDs with mild water restriction allow drought hardness	Yacutayo et al. (2013)
2010-2012	Sorghum	USA	Subtropical	Clay loam	SBDI and SDI	Yield was stabilized by increasing seeds per panicle under Managed Deficit Irrigation	Bell et al. (2018)
2006-2007	Cotton	India	Semi-arid	Loam	SDI	Reducing irrigation by 20% decreased yield by 9.3%	Singh et al. (2010)
2006-2007	Sunflower	Turkey	Mediterranean	Clay loam	PRD and SDI	Reducing irrigation by 36% under PRD reduced yield by 15%	Sezen et al. (2011)
2017-2019	Dry bean	USA	Semi-arid	Sandy loam	SDI	Reducing irrigation by 25% below FT resulted in an average reduction of 30% in yield	Rai et al. (2020)
2008	Chickpea	Iran	Continental	Sandy loam	SBDI	Drought stress at anthesis phase reduced seed yield more severe than that on vegetative stage	Mafāheri et al. (2010)

(continued)

Table 9.1 (continued)

Year	Crop	Country	Climate	Soil	DI method	Main effects	References
1988	Pigeon pea	India	Tropical	Clay	SBDI	The harvest index was significantly reduced (22%) by stress at pod development but not by stress at late vegetative stage	Lopez et al. (1996)
2006–2007	Common bean, Mung bean	Uzbekistan	Continental	Silt loam	SDI	Moderate stress reduced seed yield significantly for both Common and mung bean	Bourgault et al. (2010)
2017–2019	Alfalfa	China	Arid	Loam sandy	SBDI and SDI	Deficit irrigation at single stage maintained a higher forage yield than slightly stressed irrigation during whole growth	Liu et al. (2021)
2016–2018	Sugar beet	USA	Semi-arid	Clay loam	SDI	Deficit irrigation at 66ETc did not affect the sugar beet root yield, sucrose concentration, and sugar yield	Nilahyane et al. (2020)
2012–2014	Peanut	India	Arid	Loamy sand	SDI	Reducing irrigation by 20% increased WUE by 17.1% with only marginal reduction in economic benefit and yield	Rathore et al. (2021)

SDI is sustained deficit irrigation

SBDI is Stage based deficit irrigation

PRD is partial root drying

FTT is full irrigation treatment

ET is evapotranspiration

WUE is irrigation water use efficiency

9.3 Deficit Irrigation Approaches

The selection of an efficient irrigation strategy, specific to local needs, requires appropriate knowledge of the evapotranspiration needs of the crop (crop water demand). A distinction needs to be made between supplemental and deficit irrigation. Deficit irrigation is the deliberate application of irrigation below the full evapotranspiration requirement for a crop (Chai et al. 2016). Full evapotranspiration can be considered the level of water supply beyond which no additional positive effects in yield are realized provided the crop does not suffer from any stress. Whereas, supplemental irrigation involves the application of limited amounts of irrigation water to rainfed crops during inadequate rainfall for healthy growth, yield improvement and stabilization (Oweis and Hachum 2012; Jha et al. 2018). There are multiple direct and indirect ways to determine crop evapotranspiration or crop water use with methods varying in the parameters required for determination. The two most used inexpensive methods are the Penman–Monteith equation (Eq. 9.1) and the soil water balance approach (Eq. 9.3) (Allen et al. 1998).

The Penman–Monteith equation utilizes weather data to compute reference evapotranspiration from the reference crop surface under no water limitation. The two standardized reference surfaces used are grass (height of 0.12 m), and alfalfa (0.50 m).

$$ET_{ref} = \frac{0.408\Delta(R_n - G) + \gamma\left(\frac{C_n}{T+273}\right)u_2(e_s - e_a)}{\Delta + \gamma(1 + C_d u_2)} \quad (9.1)$$

where ET_{ref} is short (ET_o) or tall (ET_r) standardized reference crop evapotranspiration (mm day^{-1} for daily time steps or mm h^{-1} for hourly time steps); R_n is net radiation at the crop surface ($\text{MJ m}^{-2} \text{day}^{-1}$ for daily time steps); G is soil heat flux density at the soil surface ($\text{MJ m}^{-2} \text{day}^{-1}$); T is mean daily or hourly air temperature at 1.5–2.5 m height ($^{\circ}\text{C}$); u_2 is mean daily, or hourly wind speed at 2 m height (ms^{-1}); e_s is mean saturation vapor pressure at 1.5 to 2.5 m height (kPa); e_a is mean actual vapor pressure at 1.5–2.5 m height (kPa); Δ is the slope of the vapor pressure–temperature curve ($\text{kPa } ^{\circ}\text{C}^{-1}$); γ is psychrometric constant ($\text{kPa } ^{\circ}\text{C}^{-1}$); C_n is numerator constant for reference type, and C_d is denominator constant for a reference type.

The ET_{ref} can be further adjusted for different crops and cultivars by multiplying ET_{ref} with crop coefficients (K_c), which are experimentally determined. In addition, further adjustments can be made to represent the actual water deficit in the soil by multiplying the K_c with a stress coefficient (K_s), assumed 1 for no water stress based on the dual crop coefficient approach (Allen et al. 1998), and is expressed as

$$ET_{cadj} = (K_s K_c) ET_{ref} \quad (9.2)$$

whereas the soil water balance approach (9.3) is based on the principle of conservation of mass which considers irrigation, precipitation, and groundwater contribution as inputs. While ET_c , deep percolation, and runoff are considered as outputs. This is

a simple and inexpensive way to determine ET_c but the complexity may increase depending on the estimation of the individual parameters in the equation.

$$ET_c = P + I + U - RO - DP \pm \Delta S \quad (9.3)$$

where ‘ P ’ is precipitation (mm), ‘ I ’ is irrigation (mm), U is upward water flux, RO is a runoff (mm), DP is deep percolation below the crop root zone (mm), and ΔS is the change in soil water content.

The two above-listed methods are not the most accurate methods to calculate the crop ET but provide good estimations for practical applications. The other methods which are more accurate utilize energy balance (Eddy covariance and Bowen ratio method), and lysimeter (direct method), in addition, stomatal conduction has been used to quantify transpiration rate directly, but the cost of specialized instruments can be extremely high apart from the skill required to handle and interpret data. There are many other methods available for ET estimation, some are based on temperature (Thorntwaite 1948; Hargreaves and Samani 1984), and some on radiation (Makkink 1957; Priestley and Taylor 1972). However, the general accuracy of the different methods may vary (Lang et al. 2017; Ghiat et al. 2021). The evaluation of all methods can be achieved by large-scale weighing lysimeter because it is the most accurate instrument for field ET measurement (Allen et al. 1998; Chávez et al. 2009; Howell et al. 1995; Young et al. 1997). However, lysimeters require an extremely high degree of meticulousness and skill, in addition, installation difficulties and cost.

Furthermore, Dorenboos and Kassam (1979) concluded that the pattern of crop stress is affected by its response to water deficits. Several researchers have used different DI strategies which have resulted in different water-stress patterns which resulted in different yield responses but the three most common and mostly applied are sustained deficit irrigation (SDI), stage-based deficit irrigation (SBDI), and partial root-zone drying (PRD) (Feres and Soriano 2007; Capra et al. 2008; Chai et al. 2016).

9.3.1 Sustained Deficit Irrigation (SDI)

Under SDI, the available water supply under water-limited conditions is distributed uniformly over the entire growing season. In the SDI approach crops are expected to adapt to water deficit conditions by allowing the stress to develop slowly and over time. This results from the uniform application of reduced irrigation amount over the growing season and depletion of soil water reserve resulting in a progressive increase in water deficit in the season. The principle behind SDI is that if soil moisture deficits are maintained above a certain threshold (management allowed depletion, MAD), the impact on crop growth and yield is negligible. Several past studies have focused on assessing the best SDI level for different crops under different management practices (Rai et al. 2020; Greaves and Wang 2017; Sharma 2021; Irmak et al. 2016). However, crop response to SDI and levels can be affected by many factors, including climatic



Fig. 9.1 Sustained deficit irrigation (SDI)

conditions, crop species and cultivars, and agronomic management practices, among others. Overall, the SDI should be designed at elevated levels of irrigation supply to avoid significant yield losses (Musick et al. 1994; Oweis et al. 2004, 2005), and crops or crop varieties with a short growing season and some degree of tolerance to drought are more suited for deficit irrigation (Stewart et al. 1983) (Fig. 9.1).

9.3.2 Stage Based Deficit Irrigation (SBDI)

Stage-based deficit irrigation is the application of irrigation at critical growth stages to meet full evapotranspiration need and withholding it at non-critical stages based on the DI approach. SBDI is based on the principle that water stress induced due to DI at non-critical crop stages may not negatively impact growth and yield. Therefore, identification of the most sensitive crop growth stages to water deficit is critical, and like SDI the response can be influenced by many factors. For example, the most water sensitive growth stage for wheat (*Triticum aestivum*) are stem elongation and booting stage under Mediterranean climate (García Del Moral et al. 2003). Whereas

Kang et al. (2002) observed wheat crops to be more sensitive to water deficit at post-tillering than in the early stages in the North China Plains. Moreover, agronomic management also influences crop sensitivity to water stress. Different agronomic management studies on winter wheat and sorghum showed changes in water deficit sensitivity in North America (Oakes et al. 2019; Sadeghpour et al. 2017a, 2018). Overall, it is accepted that high-yielding varieties are more sensitive to water stress than low-yielding varieties (Dorrenbos and Kassam 1979), and sensitivity at the reproductive stage is higher than the vegetative stage (Chai et al. 2016).

9.3.3 *Partial Root-Zone Drying (PRD)*

Partial root-zone drying is one of the most popular approaches to DI. The concept of PRD was derived during the 1980s by alternate drying and wetting of root zone study as the process acclimatized the plant for drought stress (Caradus and Snaydon 1986; Kirkham 1983; Kang and Zhang 2004). Alternate rows of crops are subjected to PRD by applying a percentage of crop evapotranspiration. Part of the root system is in contact with wet soil all the time resulting in half of the root system being irrigated with a full amount and the other half exposed to dry soil. Studies have argued that this causes stomatal closure resulting from a root-source signal to shoot to limit transpirational water loss during partial root drying under PRD (Liu et al. 2006; Sobeih et al. 2004). This limited transpiration during reduced water application helps reduce water loss with little or no impact on crop photosynthesis (De Souza et al. 2005; Liu et al. 2004; Sarkar et al. 2022a). The other possible mechanism includes a reduction in the surface areas for soil water evaporation, and growth of secondary roots and higher root activity which improves uptake of soil nutrients that enhance nutrient recovery in plants (Chai et al. 2016). Several studies on PRD have shown positive effects of partial root-zone irrigation on increase in water use efficiency without significant reduction in crop vegetative growth and yield (Dry et al. 1996; Loveys et al. 1997; Liu et al. 2006). Meanwhile, Kirda et al. (2004) reported 10–27% additional marketable tomato yield with PRD over a DI treatment receiving the same amount.

Therefore, mild to moderate water deficits in all DI approaches have shown strong positive experimental evidence on major crops. However, the yield response of different crops to water stress during defined growth stages or throughout the life cycle needs to be studied before implementing a DI in relation to prevalent climate and soil conditions (Kirda and Kanber 1999). In addition, the selection of an appropriate DI approach should be based on the production goals and available resources. For example, PRD is more suited to drip and furrow irrigation (Capra et al. 2008) while sprinkler irrigation systems are more suited for SDI, whereas stage-based DI can be practiced under all kinds of irrigation systems (Fig. 9.2).



Fig. 9.2 Partial root drying

9.4 Yield Response Factor (K_y)

Yield response factor (K_y) is defined as the relative decrease in yield to the relative deficit in ET_c . It was introduced by Doorenbos and Kassam (1979) in the FAO Irrigation and drainage paper no. 33, and has been extensively used in irrigation research (Doorenbos and Kassam 1979; Kirda and Kanbar 1999; Singh et al. 2010; Shrestha et al. 2010; Kuscü et al. 2013; Jha 2019). The crop yield response factor (>1) implies that relative yield decreases for a given evapotranspiration deficit is proportionately greater than the relative decrease in evapotranspiration. The reference is only made on above-ground biomass production and yield, given the difficulties in quantifying root biomass under field conditions. K_y relationship can be effectively

used to differentiate crop response to water deficit under a range of conditions and criteria to determine the best applicable DI strategy and approach and is expressed as:

$$K_y = \frac{\left[1 - \frac{Y_c}{Y_m}\right]}{\left[1 - \frac{ET_c}{ET_m}\right]} \tag{9.4}$$

where Y_c is the actual seed yield (kg ha^{-1}), Y_m is the maximum seed yield (kg ha^{-1}) corresponding to full irrigation, ET_c is actual crop evapotranspiration (mm), and ET_m is maximum crop evapotranspiration (mm) corresponding to full irrigation, $1 - (Y_c/Y_m)$ is the reduction in relative yield, and $1 - (ET_c/ET_m)$ is the reduction in relative crop ETc (Fig. 9.3).

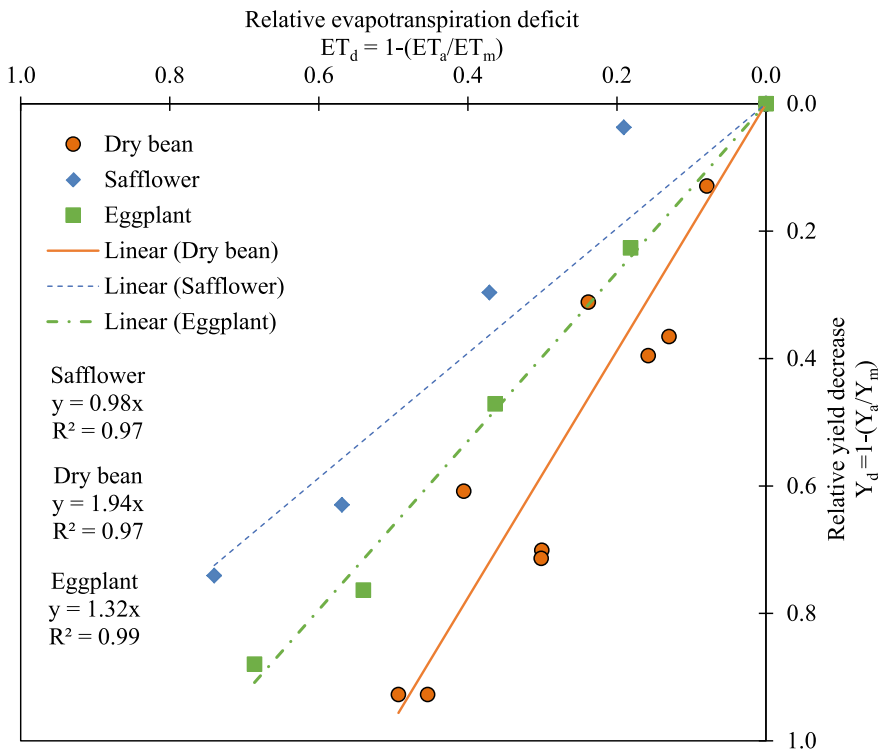


Fig. 9.3 Yield response factor (K_y) for Dry bean, Safflower, and Eggplant (Redrawn from Sharma and Rai 2022; Lovelli et al. 2007)

9.5 Physiological and Biochemical Basis of Deficit Irrigation

DI involves the application of irrigation below crop to meet full evapotranspiration demands of crops. The basic rationale behind DI is that under milder to moderate stress, the crop can turn on its drought resistance mechanism from organ to cellular level and escape a significant decline in biomass and yield. Thus, a relative decrease in ET deficit compared to full ET does not result in a similar reduction in yield and therefore, water productivity under DI is improved.

The primary response to water stress is inhibition of above-ground growth by inducing stomatal closure. This allows plants to reduce the surface area available for transpiration which in turn causes reduced photosynthesis and root uptake and the essential solutes are diverted from growth requirement to osmotic adjustments that enhance cell water retention and leaf turgor (Neumann 2008; Jha et al. 2021). If prolonged, the water stress may result in a substantial reduction in leaf area and photosynthetic ability of the plant thereby reducing crop yield significantly. Several studies have reported reduced growth and yield in response to the water deficits caused by the decrease in plant height, leaf area, biomass, and yield components i.e., pods plant⁻¹, seeds pod⁻¹, seed weight (Emam et al. 2012; Asemanrafat and Honar 2017; Mathobo et al. 2017; Jha et al. 2018; Sarkar et al. 2020, 2021a). These reductions have been attributed to a decrease in the photosynthetic and transpiring ability of the plants (Balota et al. 2021b; Chaves et al. 2002; Mafakheri et al. 2010; Sarkar et al. 2021b; Talukdar 2013). The reductions in photosynthesis and transpiration in response to water stress are regulated by complex drought coping pathways, about which still not everything is well understood (Chai et al. 2016). However, several researchers work have shed some light on the physiological and biochemical control of this complex mechanism.

The plant under water stress results in lowering of the leaf water content (Perez-Pastor et al. 2014) which generates hydraulic signals along with chemical signals that lead to a reduction in leaf area expansion and partial or complete closure of stomata (Shahnazari et al. 2007), depending on the stress level. The principal component of the signaling process is a plant hormone called abscisic acid (ABA), which is produced in roots, shoot, and transferred to leaves through xylem where it triggers stomatal closure (Schroeder et al. 2001), thus decreasing photosynthesis and transpiration rates.

Interestingly, root growth in corn at low water potentials is a result of stress-induced abscisic acid (ABA) accumulation (Saab et al. 1990). In addition, Glinka (1980) reported an increase in hydraulic conductivity in response to an increase in exogenous ABA in soybean. Moreover, root water deficit responds by increased sap levels of ABA, and this increase results in increased water-use efficiency and partially reduces stomatal opening by inhibiting water transport to a slightly greater degree than carbon dioxide transport (Kang et al. 1998). Apart from the discussed ABA signaling theory, plants also increase the production of antioxidative enzymes to reduce plant cell damage from water stress (Hu et al. 2010). In such plants reduced

chlorophyll concentration and chlorophyll fluorescence is offset by these enzymes in stressed tissues. Furthermore, water stress may induce the production of low molecular weight non-enzymatic substances like sugars, proline, carotenoids, anthocyanin etc. (Mansouri-Far et al. 2010; Mishra et al. 2013; Sarkar et al. 2018; Tahkokorpi et al. 2007). These substances regulate osmotic potential in plants to reduce osmotic stress and enhance plant water holding capacity under limited water conditions.

However, these drought coping responses can vary with crop species and genotypes. Under the same level of water deficit, Bourgault et al. (2010) reported a higher photosynthesis rate than common bean (*Phaseolus vulgaris*) compared to mung bean (*Vigna radiata*) with the same levels of transpiration. Within species, plant genotypes express varying degrees of water stress response due to their photosynthetic rate, stomatal conductance, and transpiration rate (Hongbo et al. 2005; Sadeghpour et al. 2017b; Sarkar 2020; Sarkar et al. 2022b). Moreover, Chaitanya et al. (2009) showed variation among water-stressed plant species and cultivars related to antioxidant enzyme activity. However, DI aims to take advantage of these drought coping mechanisms of crops and improve water productivity by managing water stress at levels where no significant reduction in aboveground growth takes place thereby only a minor decrease in yield may occur.

9.6 Conclusion

Irrigation is by far the largest component of agricultural water use in the world. Competition for water allocation from other sectors of the economy is forcing farmers, researchers, and policymakers alike to rethink current irrigation management practices. Deficit irrigation (DI) is a viable strategy to optimize water productivity across the globe especially for the future scenarios of water scarcity. However, DI is not usually adopted as a practical alternative to full irrigation by either practitioners or researchers, despite studies across the globe validating the utility of the strategy for a range of crops, climate, and soils. The major hurdles to its adoption have been a lack of proper understanding of the concepts and methodology. In addition, DI involves the use of advanced precision irrigation and knowledge of a wide range of disciplines from plant physiology to engineering. Furthermore, there is no one-fit-all approach in the DI due to the lack of standard and uniform responses to the DI method that can be implemented effectively and efficiently across different conditions with certainty. Thus, the present paper seeks to fill gaps in knowledge by providing a simple overview of the DI concepts and tools required to successfully implement DI.

References

- Al-Ghobari HM, Dewidar AZ (2018) Integrating deficit irrigation into surface and subsurface drip irrigation as a strategy to save water in arid regions. *Agric Water Manag* 209:55–61
- Allen RG, Pereira LS, Raes D, Smith M (1998) Crop evapotranspiration—Guidelines for computing crop water requirements—FAO Irrigation and Drainage Paper 56, vol 300, no 9. Fao, Rome, p D05109
- Araya A, Prasad P, Ciampitti I, Jha P (2021) Using crop simulation model to evaluate influence of water management practices and multiple cropping systems on crop yields: a case study for Ethiopian highlands. *Field Crop Res* 260:108004
- Asemanrafat M, Honar T (2017) Effect of water stress and plant density on canopy temperature, yield components and protein concentration of red bean (*Phaseolus vulgaris* L. cv. akhtar). *Int J Plant Prod* 11(2):241–258
- Balota M, Sarkar S (2020) Transpiration of Peanut in the field under Rainfed production. Paper presented at the American Peanut research and education society annual meeting 2020, Virtual
- Balota M, Sarkar S, Cazenave A, Kumar N (2021a) Plant characteristics with significant contribution to Peanut yield under extreme weather conditions in Virginia, USA. Paper presented at the ASA, CSSA, SSSA international annual meeting 2021, Salt Lake City, UT
- Balota M, Sarkar S, Cazenave A, Burow M, Bennett R, Chamberlin K, Wang N, White M, Payton P, Mahan J (2021b) Vegetation Indices enable indirect phenotyping of Peanut physiologic and agronomic characteristics. Paper presented at the American Peanut research and education society annual meeting 2021, Virtual
- Barnett TP, Adam JC, Lettenmaier DP (2005) Potential impacts of a warming climate on water availability in snow-dominated regions. *Nature* 438:303
- Baule WJ, Jha PK, Ines AV (2018) Quantifying the impacts of early and late growing season precipitation on midwestern US corn production: a downscaling and modeling approach. In: AGU fall meeting 2018. AGU
- Bell JM, Schwartz R, McInnes KJ, Howell T, Morgan CL (2018) Deficit irrigation effects on yield and yield components of grain sorghum. *Agric Water Manag* 203:289–296
- Bennett RS, Chamberlin K, Morningweg D, Wang N, Sarkar S, Balota M, Burow M, Chagoya J, Pham H (2021) Response to drought stress in a subset of the U.S. Peanut mini core evaluated in three states. Paper presented at the American Peanut research and education society annual meeting 2021, Virtual
- Bourgault M, Madramootoo CA, Webber HA, Stulina G, Horst MG, Smith DL (2010) Effects of deficit irrigation and salinity stress on common bean (*Phaseolus vulgaris* L.) and mungbean (*Vigna radiata* (L.) Wilczek) grown in a controlled environment. *J Agron Crop Sci* 196(4):262–272
- Burek P, Sato Y, Fischer G, Kahil MT, Scherzer A, Tramberend S, ... Hanasaki N (2016) Water futures and solution-fast track initiative
- Burow M, Balota M, Sarkar S, Bennett R, Chamberlin K, Wang N, White M, Payton P, Mahan J, Dobrev I (2021) Field measurements, yield, and grade of the U.S. minicore under water deficit stress. Paper presented at the American Peanut research and education society annual meeting 2021, Virtual
- Capra A, Consoli S, Scicolone B (2008) Deficit irrigation: theory and practice. *Agricultural irrigation research progress*. Nova Science Publishers, USA, pp 53–82
- Caradus JR, Snaydon RW (1986) Plant factors influencing phosphorus uptake by white clover from solution culture. *Plant Soil* 93(2):165–174
- Chai Q, Gan Y, Zhao C, Xu HL, Waskom RM, Niu Y, Siddique KH (2016) Regulated deficit irrigation for crop production under drought stress: a review. *Agron Sustain Dev* 36(1):3
- Chaitanya KV, Rasineni GK, Reddy AR (2009) Biochemical responses to drought stress in mulberry (*Morus alba* L.): evaluation of proline, glycine betaine and abscisic acid accumulation in five cultivars. *Acta Physiologiae Plantarum* 31(3):437–443

- Chaves MM, Pereira JS, Maroco J, Rodrigues ML, Ricardo CPP, Osório ML, ... Pinheiro C (2002) How plants cope with water stress in the field? Photosynthesis and growth. *Ann Botany* 89(7):907–916
- Chávez JL, Howell TA, Copeland KS (2009) Evaluating eddy covariance cotton ET measurements in an advective environment with large weighing lysimeters. *Irrig Sci* 28(1):35–50
- Comas LH, Trout TJ, DeJonge KC, Zhang H, Gleason SM (2019) Water productivity under strategic growth stage-based deficit irrigation in maize. *Agric Water Manag* 212:433–440
- Daryanto S, Wang L, Jacinthe P-A (2015) Global synthesis of drought effects on food legume production. *Rev Sci Instr* 71(2 II):902–905. <https://doi.org/10.1371/journal.pone.0127401>
- Del Moral LG, Rharrabti Y, Villegas D, Royo C (2003) Evaluation of grain yield and its components in durum wheat under mediterranean conditions: an ontogenic approach. *Agron J* 95(2):266–274
- de Souza CR, Maroco JP, dos Santos TP, Rodrigues ML, Lopes C, Pereira JS, Chaves MM (2005) Control of stomatal aperture and carbon uptake by deficit irrigation in two grapevine cultivars. *Agric Ecosyst Environ* 106(2–3):261–274
- Doorenbos J, Kassam AH (1979) Yield response to water. *Irrigat Drain Pap* 33:257
- Dry PR, Loveys BR, Düring H, Botting DG (1996) Effects of partial rootzone drying on grapevine vigour, yield composition of fruit and use of water. In: Stokley CS, Sas AN, Johnstone RS, Lee TH (eds) *Proceedings of 9th Australian wine industry technical conference*. Winetitles, Adelaide, Adelaide, Australia, pp 128–131
- Du T, Kang S, Zhang J, Li F (2008) Water use and yield responses of cotton to alternate partial root-zone drip irrigation in the arid area of north-west China. *Irrig Sci* 26(2):147–159
- Dudley NJ, Howell DT, Musgrave WF (1971) Optimal intraseasonal irrigation water allocation. *Water Resour Res* 7(4):770–788. <https://doi.org/10.1029/WR007i004p00770>
- Elhani S, Haddadi M, Csákvári E, Zantar S, Hamim A, Villányi V, ... Bánfalvi Z (2019) Effects of partial root-zone drying and deficit irrigation on yield, irrigation water-use efficiency and some potato (*Solanum tuberosum* L.) quality traits under glasshouse conditions. *Agricult Water Manag* 224:105745
- Emam Y, Shekoofa A, Salehi F, Jalali AH, Pessaraki M (2012) Drought stress effects on two common bean cultivars with contrasting growth habits. *Arch Agron Soil Sci* 58(5):527–534. <https://doi.org/10.1080/03650340.2010.530256>
- English M (1990) Deficit irrigation. I: Analytical framework. *J Irrigat Drain Eng* 116(3):399–412
- English MJ, Nuss GS (1982) Designing for deficit irrigation. *J Irrigat Drain Eng, ASCE* 108(2):91–106
- Eeswaran R, Nejadhashemi AP, Kpodo J, Curtis ZK, Adhikari U, Liao H, ... Jha PK (2021) Quantification of resilience metrics as affected by conservation agriculture at a watershed scale. *Agricult Ecosyst Environ* 320:107612
- Fereris E, Soriano MA (2007) Deficit irrigation for reducing agricultural water use. *J Exp Bot* 58(2):147–159
- Ghiat I, Mackey HR, Al-Ansari T (2021) A review of evapotranspiration measurement models, techniques and methods for open and closed agricultural field applications. *Water* 13(18):2523
- Glinka Z (1980) Abscisic acid promotes both volume flow and ion release to the xylem in sunflower roots. *Plant Physiol* 65(3):537–540
- Greaves GE, Wang YM (2017) Yield response, water productivity, and seasonal water production functions for maize under deficit irrigation water management in southern Taiwan. *Plant Prod Sci* 20(4):353–365
- Hargreaves GH, Samani ZA (1984) Economic considerations of deficit irrigation. *J Irrigat Drain Div, ASCE* 110(4):343–358
- Hirabayashi Y, Kanae S, Emori S, Oki T, Kimoto M (2008) Global projections of changing risks of floods and droughts in a changing climate. *Hydrol Sci J* 53(4):754–772. <https://doi.org/10.1623/hysj.53.4.754>
- HongBo S, ZongSuo L, MingAn S, ShiMeng S, ZanMin H (2005) Investigation on dynamic changes of photosynthetic characteristics of 10 wheat (*Triticum aestivum* L.) genotypes during two vegetative-growth stages at water deficits. *Colloids Surf B: Biointerf* 43(3–4):221–227

- Hota S, Mishra V, Mourya KK, Giri K, Kumar D, Jha PK, ... Ray SK (2022) Land use, landform, and soil management as determinants of soil physicochemical properties and microbial abundance of Lower Brahmaputra Valley, India. *Sustainability* 14(4):2241
- Howell TA, Schneider AD, Dusek DA, Marek TH, Steiner JL (1995) Calibration and scale performance of Bushland weighting lysimeters
- Hu T, Yuan L, Wang J, Kang S, Li F (2010) Antioxidation responses of maize roots and leaves to partial root-zone irrigation. *Agric Water Manag* 98(1):164–171
- Irmak S, Djaman K, Rudnick DR (2016) Effect of full and limited irrigation amount and frequency on subsurface drip-irrigated maize evapotranspiration, yield, water use efficiency and yield response factors. *Irrig Sci* 34(4):271–286
- James LD, Lee RR (1971) *Economics of water resources planning*. McGraw-Hill, New York, USA, p 325
- Jha PK, Kumar SN, Ines AV (2018) Responses of soybean to water stress and supplemental irrigation in upper Indo-Gangetic plain: field experiment and modeling approach. *Field Crop Res* 219:76–86
- Jha PK (2019) Agronomic management of corn using seasonal climate predictions, remote sensing, and crop simulation models. Michigan State University
- Jha PK, Ines AV, Singh MP (2021) A multiple and ensembling approach for calibration and evaluation of genetic coefficients of CERES-maize to simulate maize phenology and yield in Michigan. *Environ Model Softw* 135:104901
- Kang S, Liang Z, Hu W, Zhang J (1998) Water use efficiency of controlled alternate irrigation on root-divided maize plants. *Agric Water Manag* 38(1):69–76
- Kang S, Zhang L, Liang Y, Hu X, Cai H, Gu B (2002) Effects of limited irrigation on yield and water use efficiency of winter wheat in the Loess Plateau of China. *Agric Water Manag* 55(3):203–216
- Kang S, Zhang J (2004) Controlled alternate partial root-zone irrigation: its physiological consequences and impact on water use efficiency. *J Exp Bot* 55(407):2437–2446
- Kirda C, Kanber R, Tulucu K (1995) Yield response of cotton, maize, soybean, sugar beet, sunflower, and wheat to deficit irrigation (No. INIS-MA-007). Joint FAO/IAEA Division of Nuclear Techniques in Food and Agriculture
- Kirda C, Kanber R (1999) Water, no longer a plentiful resource, should be used sparingly in irrigated agriculture. In: *Crop yield response to deficit irrigation*, pp 1–20
- Kirda C, Çetin M, Dasgan Y, Topçu S, Kaman H, Ekici B, ... Ozguven AI (2004) Yield response of greenhouse grown tomato to partial root drying and conventional deficit irrigation. *Agric Water Manag* 69(3):191–201
- Kirkham MB (1983) Physical model of water in a split-root system. *Plant Soil* 75(2):153–168
- Kuscu H, Karasu A, Mehmet OZ, Demir AO, Turgut I (2013) Effect of irrigation amounts applied with drip irrigation on maize evapotranspiration, yield, water use efficiency, and net return in a Suba Humid Cli. *Turk J Field Crops* 18(1):13–19
- Lang D, Zheng J, Shi J, Liao F, Ma X, Wang W, ... Zhang M (2017) A comparative study of potential evapotranspiration estimation by eight methods with FAO Penman–Monteith method in southwestern China. *Water* 9(10):734
- Lanna AC, Mitsuzono ST, Terra TGR, Pereira Vianello R, Carvalho MADF (2016) Physiological characterization of common bean (*Phaseolus vulgaris* L.) genotypes, water-stress induced with contrasting response towards drought. *Austr J Crop Sci* 10(1):1–6
- Liu F, Shahnazari A, Andersen MN, Jacobsen SE, Jensen CR (2006) Effects of deficit irrigation (DI) and partial root drying (PRD) on gas exchange, biomass partitioning, and water use efficiency in potato. *Sci Hortic* 109(2):113–117
- Liu LX, Xu SM, Woo KC (2004) Deficit irrigation effects on photosynthesis and the xanthophyll cycle in the tropical tree species *Acacia auriculiformis* in North Australia. *NZ J Bot* 42(5):949–957
- Liu M, Wang Z, Mu L, Xu R, Yang H (2021) Effect of regulated deficit irrigation on alfalfa performance under two irrigation systems in the inland arid area of midwestern China. *Agric Water Manag* 248:106764
- Lopez FB, Johansen C, Chauhan YS (1996) Effects of timing of drought stress on phenology, yield, and yield components of short duration pigeonpea. *J Agron Crop Sci* 177(5):311–320

- Lovelli S, Perniola M, Ferrara A, Di Tommaso T (2007) Yield response factor to water (Ky) and water use efficiency of *Carthamus tinctorius* L. and *Solanum melongena* L. *Agricult Water Manag* 92(1–2):73–80
- Loveys B, Grant J, Dry P, McCarthy M (1997) Progress in the development of partial rootzone drying
- Mafakheri A, Siosemardeh AF, Bahramnejad B, Struik PC, Sohrabi Y (2010) Effect of drought stress on yield, proline, and chlorophyll contents in three chickpea cultivars. *Aust J Crop Sci* 4(8):580–585
- Makkink GF (1957) Testing the Penman formula by means of lysimeters. *J Inst Water Eng* 11:277–288
- Mansouri-Far C, Sanavy SAMM, Saberali SF (2010) Maize yield response to deficit irrigation during low-sensitive growth stages and nitrogen rate under semi-arid climatic conditions. *Agric Water Manag* 97(1):12–22
- Mathobo R, Marais D, Steyn JM (2017) The effect of drought stress on yield, leaf gaseous exchange and chlorophyll fluorescence of dry beans (*Phaseolus vulgaris* L.). *Agric Water Manag* 180:118–125
- Mazdiyasn O, AghaKouchak A (2015) Substantial increase in concurrent droughts and heatwaves in the United States. *Proc Nat Acad Sci* 112(37):11484–11489
- Memon SA, Sheikh IA, Talpur MA, Mangrio MA (2021) Impact of deficit irrigation strategies on winter wheat in semi-arid climate of sindh. *Agric Water Manag* 243:106389
- Mishra M, Kumar U, Prakash V (2013) Influence of salicylic acid pre-treatment on water stress and its relationship with antioxidant status in *Glycine max*. *Int J Pharma Bio Sci* 4:B81–B97. <https://doi.org/10.1.1.405.7109>
- Mugabe FT, Nyakatawa EZ (2000) Effect of deficit irrigation on wheat and opportunities of growing wheat on residual soil moisture in southeast Zimbabwe. *Agric Water Manag* 46(2):111–119
- Musick JT, Jones OR, Stewart BA, Dusek DA (1994) Water-yield relationships for irrigated and dryland wheat in the US southern plains. *Agron J* 86(6):980–986
- Neumann PM (2008) Coping mechanisms for crop plants in drought-prone environments. *Ann Bot* 101(7):901–907
- Nilahyane A, Chen C, Afshar RK, Sutradhar A, Stevens WB, Iversen W (2020) Deficit irrigation for sugarbeet under conventional and no-till production. *Agrosyst Geosc Environ* 3(1):e20114
- Oakes J, Balota M, Thomason WE, Cazenave AB, Sarkar S, Sadeghpour A (2019) Using unmanned aerial vehicles to improve N management in winter wheat. Paper presented at the ASA, CSSA, SSSA international annual meeting 2019, San Antonio, TX
- Oweis T, Hachum A (2012) Supplemental irrigation, a highly efficient water-use practice. ICARDA, Aleppo, Syria
- Oweis T, Hachum A, Pala M (2004) Lentil production under supplemental irrigation in a Mediterranean environment. *Agric Water Manag* 68(3):251–265
- Oweis T, Hachum A, Pala M (2005) Faba bean productivity under rainfed and supplemental irrigation in northern Syria. *Agric Water Manag* 73(1):57–72
- Pereira LS, Oweis T, Zairi A, Santos L (2002) Irrigation management under water scarcity. *Agric Water Manag* 57(3):175–206
- Pérez-Pastor A, Ruiz-Sánchez MC, Domingo R (2014) Effects of timing and intensity of deficit irrigation on vegetative and fruit growth of apricot trees. *Agric Water Manag* 134:110–118
- Priestley CHB, Taylor RJ (1972) On the assessment of surface heat flux and evaporation using large-scale parameters. *Mon Weather Rev* 100(2):81–92
- Rai A, Sharma V, Heitholt J (2020) Dry bean [*Phaseolus vulgaris* L.] growth and yield response to variable irrigation in the arid to semi-arid climate. *Sustainability* 12(9):3851
- Rathore VS, Nathawat NS, Bhardwaj S, Yadav BM, Kumar M, Santra P, ... Yadav OP (2021) Optimization of deficit irrigation and nitrogen fertilizer management for peanut production in an arid region. *Sci Rep* 11(1):1–14
- Rodrigues GC, Pereira LS (2009) Assessing economic impacts of deficit irrigation as related to water productivity and water costs. *Biosys Eng* 103(4):536–551

- Saab IN, Sharp RE, Pritchard J, Voetberg GS (1990) Increased endogenous abscisic acid maintains primary root growth and inhibits shoot growth of maize seedlings at low water potentials. *Plant Physiol* 93(4):1329–1336
- Sadeghpour A, Oakes J, Sarkar S, Balota M (2018) Seeding rate and harvesting time effect on biomass sorghum production in Virginia. Paper presented at the ASA, CSSA and CSA international annual meetings 2018, Baltimore, MD
- Sadeghpour A, Oakes J, Sarkar S, Balota M (2017a) Precise Nitrogen management of biomass sorghum using vegetation indices. Paper presented at the ASA, CSSA and SSSA international annual meetings 2017, Tampa, FL
- Sadeghpour A, Oakes J, Sarkar S, Pitman R, Balota M (2017b) High throughput phenotyping of biomass sorghum using ground and aerial imaging. Paper presented at the ASA, CSSA and SSSA international annual meetings 2017, Tampa, FL
- Sarkar S (2020) Development of high-throughput phenotyping methods and evaluation of morphological and physiological characteristics of peanut in a sub-humid environment. Virginia Polytechnic Institute and State University
- Sarkar S (2021) High-throughput estimation of soil nutrient and residue cover: a step towards precision agriculture. In: *Soil science: fundamentals to recent advances*. Springer, Singapore, pp 581–596
- Sarkar S, Jha PK (2020) Is precision agriculture worth it? Yes, may be. *J Biotechnol Crop Sci* 9(14):4–9
- Sarkar S, Oakes J, Balota M (2018) High-throughput phenotyping of Peanut and biomass Sorghum using proximal sensing and aerial imaging for the Mid-Atlantic U.S. Paper presented at the 2018 GIS and remote sensing research symposium, Blacksburg, VA
- Sarkar S, Cazenave AB, Oakes J, McCall D, Thomason W, Abbot L, Balota M (2020) High-throughput measurement of peanut canopy height using digital surface models. *Plant Phenome J* 3(1):e20003
- Sarkar S, Cazenave AB, Oakes J, McCall D, Thomason W, Abbot L, Balota M (2021a) Aerial high-throughput phenotyping of peanut leaf area index and lateral growth. *Sci Rep* 11(1):1–17
- Sarkar S, Ramsey AF, Cazenave A-B, Balota M (2021b) Peanut leaf wilting estimation from RGB color indices and logistic models. *Front Plant Sci* 12:713
- Sarkar S, Shekoofa A, McClure A, Gillman JD (2022a) Phenotyping and quantitative trait locus analysis for the limited transpiration trait in an Upper-mid south soybean recombinant inbred line population ('Jackson' × 'KS4895'): high throughput aquaporin inhibitor screening. *Front Plant Sci* 3175
- Sarkar S, Wedegaertner K, Shekoofa A (2022b) Using aerial imagery to optimize the efficiency of PGR application in cotton. Paper presented at the Beltwide cotton conference 2022, San Antonio, TX
- Schroeder JI, Kwak JM, Allen GJ (2001) Guard cell abscisic acid signalling and engineering drought hardiness in plants. *Nature* 410(6826):327–330
- Sezen SM, Yazar A, Tekin S (2011) Effects of partial root zone drying and deficit irrigation on yield and oil quality of sunflower in a Mediterranean environment. *Irrig Drain* 60(4):499–508
- Shahnazari A, Liu F, Andersen MN, Jacobsen SE, Jensen CR (2007) Effects of partial root-zone drying on yield, tuber size and water use efficiency in potato under field conditions. *Field Crop Res* 100(1):117–124
- Sharma V (2021) Impact of irrigation and nitrogen management strategies on Sugarbeet (*Beta vulgaris* L.) yield, evapotranspiration, and crop water productivity. In: 6th decennial national irrigation symposium, 6–8 December 2021, San Diego, California. American Society of Agricultural and Biological Engineers, p 1
- Sharma V, Rai A (2022) Dry Bean (*Phaseolus vulgaris* L.) crop water production functions and yield response factors in an arid to semi-arid climate. *J ASABE* 65(1):51–65
- Shekoofa A, Sheldon K, Sarkar S, Raper TB (2022) Variety selection: a valuable tool in the management of water relations in cotton production. Paper presented at the Beltwide cotton conference 2022, San Antonio, TX

- Shrestha N, Geerts S, Raes D, Horemans S, Soentjens S, Maupas F, Clouet P (2010) Yield response of sugar beets to water stress under Western European conditions. *Agric Water Manag* 97(2):346–350
- Singh SP, Terán H, Muñoz-Perea CG, Lema M, Dennis M, Hayes R, ... Smith J (2009) Dry bean landrace and cultivar performance in stressed and nonstressed organic and conventional production systems. *Crop Sci* 49(5):1859–1866
- Singh Y, Rao SS, Regar PL (2010) Deficit irrigation and nitrogen effects on seed cotton yield, water productivity and yield response factor in shallow soils of semi-arid environment. *Agric Water Manag* 97(7):965–970
- Sobeih WY, Dodd IC, Bacon MA, Grierson D, Davies WJ (2004) Long-distance signals regulating stomatal conductance and leaf growth in tomato (*Lycopersicon esculentum*) plants subjected to partial root-zone drying. *J Exp Bot* 55(407):2353–2363
- Stewart BA, Musick JT, Dusek DA (1983) Yield and water use efficiency of grain sorghum in a limited irrigation-dryland farming system
- Sung C, Balota M, Sarkar S, Bennett R, Chamberlin K, Wang N, Payton P, Mahan J, Chagoya J, Burow M (2021) Genome-wide association study on Peanut water deficit stress tolerance using the U.S. minicore to develop improvement for breeding. Paper presented at the American Peanut research and education society annual meeting 2021, Virtual
- Tahkokorpi M, Taulavuori K, Laine K, Taulavuori E (2007) After-effects of drought-related winter stress in previous and current year stems of *Vaccinium myrtillus* L. *Environ Exp Botany* 61(1): 85–93
- Talukdar D (2013) Comparative morpho-physiological and biochemical responses of lentil and grass pea genotypes under water stress. *J Nat Sci Biol Med* 4(2):396
- Thornthwaite CW (1948) An approach toward a rational classification of climate. *Geogr Rev* 38(1):55–94
- Wilhite DA, Svoboda MD, Hayes MJ (2007) Understanding the complex impacts of drought: a key to enhancing drought mitigation and preparedness. *Water Resour Manage* 21(5):763–774
- Yadav MR, Choudhary M, Singh J, Lal MK, Jha PK, Udawat P, Gupta NK, Rajput VD, Garg NK, Maheshwari C, Hasan M, Gupta S, Jatwa TK, Kumar R, Yadav AK, Prasad PV (2022) Impacts, tolerance, adaptation, and mitigation of heat stress on wheat under changing climates. *Int J Mol Sci* 23(5):2838
- Yactayo W, Ramírez DA, Gutiérrez R, Mares V, Posadas A, Quiroz R (2013) Effect of partial root-zone drying irrigation timing on potato tuber yield and water use efficiency. *Agric Water Manag* 123:65–70
- Yonts CD, Haghverdi A, Reichert DL, Irmak S (2018) Deficit irrigation and surface residue cover effects on dry bean yield, in-season soil water content and irrigation water use efficiency in western Nebraska high plains. *Agric Water Manag* 199:138–147
- Young MH, Wierenga PJ, Mancino CF (1997) Monitoring near-surface soil water storage in turfgrass using time domain reflectometry and weighing lysimetry. *Soil Sci Soc Am J* 61(4):1138–1146
- Zhang B, Li FM, Huang G, Cheng ZY, Zhang Y (2006) Yield performance of spring wheat improved by regulated deficit irrigation in an arid area. *Agric Water Manag* 79(1):28–42
- Zou Y, Saddique Q, Ali A, Xu J, Khan MI, Qing M, ... Siddique KH (2021) Deficit irrigation improves maize yield and water use efficiency in a semi-arid environment. *Agricult Water Manag* 243:106483

Part III
Soil-Water Quality Consideration

Chapter 10

Recent Advances in the Occurrence, Transport, Fate, and Distribution Modeling of Emerging Contaminants—A Review



Maliha Ashraf, Shaikh Ziauddin Ahammad, and Sumedha Chakma

Abstract The increasing technological and scientific development to cater the anthropogenic needs has caused a substantial increase of Emerging Contaminants (ECs) in the environment, posing threats to the ecosystem due to their hazardous nature. A successful treatment system for the removal is still not developed because of diversity in the physico-chemical nature of ECs and cost constraints. The mathematical model serves as a good alternative in predicting the transport and fate of the contaminants in the environment. The output of the models may serve as a risk assessment tool and shall be utilized for policy making and control of emerging contaminants in the environment. The paper discusses the processes of transport, fate, and distribution of the ECs in the environment. Also, several models currently in practice have been discussed highlighting their limitations to give clarity of the model to be used for a specific category of contaminant. The paper aims to ease the selection of models for a specific category of EC, scenario, and requirement of the user. The identified limitations will serve a medium for future researchers to easily select a suitable model by applying suitable modifications and performing risk assessment studies.

Keywords Emerging contaminants · Fate and transport · GIS-based models

M. Ashraf (✉)

School of Interdisciplinary Research, Indian Institute of Technology, Delhi, India

e-mail: Maliha.Ashraf@sire.iitd.ac.in

S. Z. Ahammad

Department of Biochemical Engineering and Biotechnology, Indian Institute of Technology, Delhi, India

e-mail: zia@dbeb.iitd.ac.in

S. Chakma

Department of Civil Engineering, Indian Institute of Technology, Delhi, India

e-mail: chakma@civil.iitd.ac.in

10.1 Introduction

The everyday practice of releasing effluents from industries, domestic use, agricultural use, and hospitals directly to nearby drains or after partial treatment has led to an increase in the pollution of the environment globally (Tijani et al. 2016). The released wastewater pollutants load both the conventional pollutants as well as emerging contaminants/pollutants (ECs) (Žur et al. 2018). Conventional pollutants are those pollutants that have rules and regulations defined for them before release into the environment and the ECs are those compounds that pose potential threats to the ecosystem as well as to human health but have not been studied before and are not included by the existing regulations for water-quality (Lamastra et al. 2016). The ECs possess the following features, i.e., potential risks to ecology, present recorded in low concentration (ng/l to $\mu\text{g/l}$), and the regulation is missing due to lack of information and knowledge. (Gavrilescu et al. 2015; Žur et al. 2018).

Keeping in view the harm posed due to these ECs, an effective treatment system needs to be developed for their removal before being discharged from the treatment plants but unfortunately, the wastewater treatment system designed to treat the polluted water is effective only in treating the conventional pollutants thereby releasing the ECs without being treated (Grassi et al 2012). The treatment strategies employed depend on the physical and chemical characteristics of the ECs, which makes it almost impossible to design a treatment system for every EC, thus calling for an alternative solution to keep a check on the increasing concentration in the environment. With the increase in the variety of contaminants every day, and due to limited knowledge of the pathways of the release of the ECs, it is spatially and temporally cumbersome as well as expensive for routine monitoring of each contaminant whose behavior being dynamic in all the environmental compartments/media (Trinh et al. 2016). Mathematical modelling technique is a good tool to predict the contaminants concentration in various media with good accuracy (Lindim et al. 2017). Multimedia models serves as useful tools complimenting field monitoring and assisting in forecasting human health issues (Cohen and Cooter 2002b).

The study here, deals with an insight of transport and fate of the ECs in multimedia environment. Various mathematical models available for fate and transport study have been discussed. The output of the model may serve as a tool for risk assessment and further policy making to control the use of ECs posing detrimental health effects.

10.2 Modeling Fate and Transport of Contaminants in the Environment

In order to accurately design a model governing transport and fate of the ECs, the possible sources of emissions of the ECs concerned, their physical, chemical and biological characteristics, transport pathways (inter-compartmental/inter-media transfer, the physical process of transport accompanying such as diffusion, advection

and dispersion, various physical) and bio-geochemical processes leading to loss of contaminant's concentration and the distributions (fate) of the contaminants in the environment needs to be thoroughly studied (Cohen and Cooter 2002b). The distribution of contaminant in the environment is a result of chemical, biological and physical processes (Cohen et al. 1990; Cohen and Cooter 2002b). The media/compartments of the natural environment, i.e., the atmosphere, surface waters, and the subsurface, can each contain multiple phases (i.e., gas, aqueous, solid, and NAPL phases) (Dunnivant and Anders 2005). The steps in the study of fate and transport has been depicted in Fig. 10.1. and explained further. The first step in fate and transport study is the identification of the type of pollutant, which can be classified based on chemical state, physical state or by the risk posed by them (the limit in which they exist is more hazardous) (Dunnivant and Anders 2005). The next step includes the assessment of sources of the pollutants of interest, i.e., whether the source of pollutant is point or non-point source. Point sources are well defined sources such as smoke stack, end of the pipe, drains etc. and non-point sources include sources that are not well defined (such as application of pesticides, insecticides to agriculture) but contain all such sources where the point sources can be pin-point. (Dunnivant and Anders 2005), The ECs can be released from its source either just instantaneously or it may be continuous. The third step is the development of appropriate model for the fate and transport study which includes identification of suitable model and the parameters of the model, i.e., various physical, chemical and biological process that occurs during transport of the pollutant from its sources till its destination (Dunnivant and Anders 2005).

The various parameters required for modeling of pollutants fate and transport includes pH of the solvent in which the contaminant is present, contaminants activity that is the effective concentration of any ion, solubility of the contaminants, contaminant's vapor pressure, Henry's Law Constant for that contaminant, acid–base as well as oxidation–reduction reactions, equilibrium sorption, complexation reactions, equilibrium sorption phenomenon that includes ionic exchange reactions of the contaminants and partitioning co-efficient between different media (a measure of the pollutant's distribution across the solid (or particulate) phase and the water

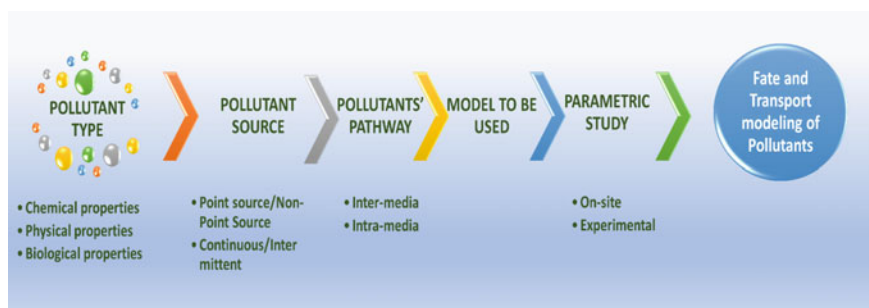


Fig. 10.1 Steps in fate and transport study of any contaminant

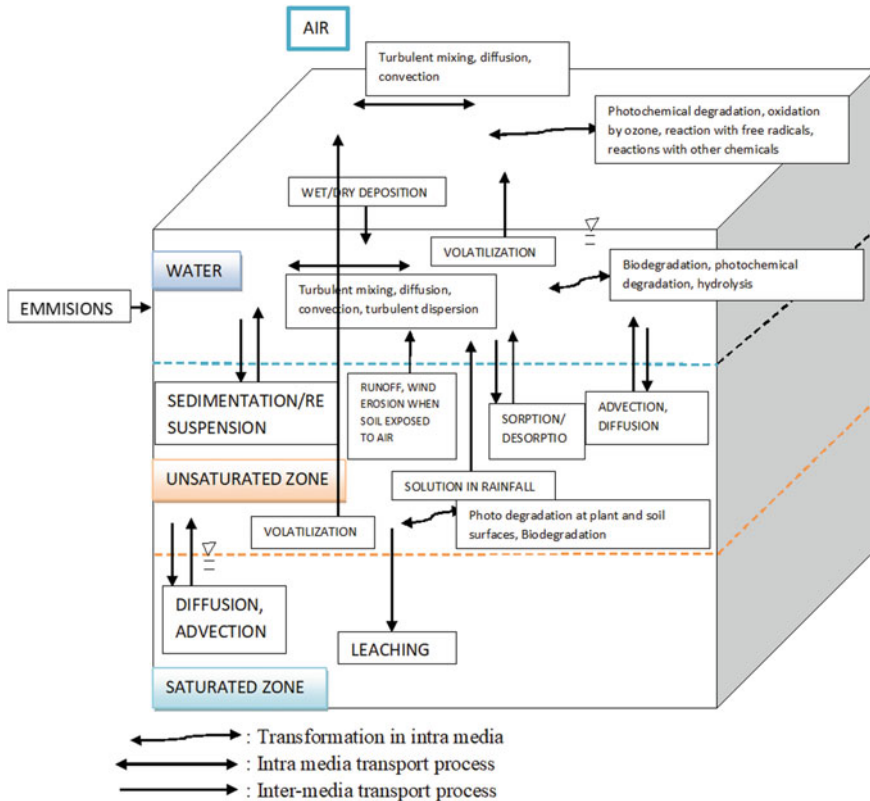


Fig. 10.2 A physical multimedia model depicting with the fate and transport processes

phase, transformation/degradation reactions that includes Abiotic Chemical transformations/ degradations, photochemical transformation/degradation reactions, nuclear and biological reactions (Dunnivant and Anders 2005) as can be seen in Fig. 10.2. The outcome of the fate and transport study can be utilized in risk assessment due to the EC of concern as well as policy making and framing of environment laws.

10.3 Models Available for Fate and Transport Study in the Environment

Modeling of contaminants in general has been in practice since late 1970s and early 1980s, by Mackay as well as Peterson where initially single or coupled compartments were in consideration. Later, many other compartments were incorporated in the model and all these compartments were treated to be well mixed and homogeneous. The models were earlier used for screening level and risk management for

regulatory purposes evaluation of fate of toxic contaminants in the environment. Also, these models served the purpose of rough estimation of the concentration of contaminants present in the environment for they were less complex (Hollander 2008). Later, concern was raised for those contaminants which are persistent, long-ranged and easily removed from the compartments, as these contaminants though emitted locally, their effect was observed locally as well as globally (Ciuffo and Sala 2013) which further led to the division of the regions into various sub-region, in which initially the sub-regions were treated as multi-box units having coarser resolution and these models can be successfully used for ranking of chemicals and establishing partitioning tendencies of the contaminants in the environmental compartment. Since this type of models didn't portray a realistic scenario, spatially explicit multimedia models with finer resolution was introduced, and the emissions as well as different environmental characteristics varying with the location was modelled, and these models were successful at local scale and when emissions occur in soil and also when dynamic simulations are involved. Further realism was introduced when the GIS came into practice which led to the possibility of defining geo-referenced parameters in the model varying at regular intervals leading to precise modelling and simulation of concentration, fluxes and loads of contaminants in the environment (Semplice et al. 2012).

For successful application of an environment fate model in a screening level assessment of risk and to be used as a decision making tool, the model must incorporate all sources of contamination, as well all compartments and all the important mechanisms of transport and fate process (Zhang et al. 2003). The decision of which type of model to be adopted for measuring contaminant concentration depends on situation, availability of data and requirement of user (Armitage et al. 2007; Klepper and Den Hollander 1999). Environmental multimedia models have advanced over ages from just evaluation models to mass-balance models on a regional scale, further to 'multi-region models, then global models and finally coupling of these models with GIS (Caudeville et al. 2012). The mathematical equation describing the environment is written in the form of mass, energy or momentum conservation equations. Generally, in the mass-balance models, the input and output of a contaminant in each spatial compartment and environmental medium is balanced. This mass balance equation may be written either in terms of concentration or fugacity.

Fugacity based Approach

Fugacity is actually a surrogate for concentration and the fugacity expressions are algebraically similar to concentration expression (Mackay and Paterson 1986). Fugacity based models are very well developed and documented models and extensively used to predict the fate of contaminants at several scales, i.e., single compartmental scale, global scale and regional (Zhang et al. 2015). The concept of fugacity came into existence as an equilibrium criterion by G.N. Lewis in 1901. This concept is based on the belief that chemicals which are present in a system has equal potential in all the compartments, i.e., the system will achieve minimal Gibbs free energy. The potential of a chemical varies logarithmically with concentration, whereas fugacity varies logarithmically with chemical potential, therefore fugacity is linearly related

to chemical potential of a contaminant shown in Eq. (10.1), therefore more practical for modelling behavior of contaminant.

$$f_j = \frac{C_j}{Z_j} \quad (10.1)$$

f_j is the contaminant's fugacity in any phase j , C_j is the concentration in the phase j and Z_j is the constant of proportionality which is known as fugacity capacity of that phase j , which is contaminant specific, medium specific and dependent on temperature (Diamond 1989). Fugacity is generally referred as the escaping tendency of any contaminant in a given phase, whereas fugacity capacity represents the capacity of partitioning of that phase. The net diffusive flux of the contaminant between any two n phases will be from higher fugacity phase to lower one until state of equifugacity is attained. And the phase having higher fugacity will attain a higher concentration than a phase with low fugacity capacity as fugacity capacity is inversely proportional to the concentration in any phase. In this approach, instead of using concentration as the controlling variable, fugacity is used and finally concentration is calculated as $C = Fz$ (Diamond 1989).

Limitation of this approach is its application to ionizing compounds as ionizing compounds are assumed to have negligible vapor pressure as it has no Henry's Law constant therefore fugacity capacity of any phase cannot be calculated. Also, uncertainties associated with key chemical and physical properties of the data make this model cumbersome. The solution to this is to assign very negligible of air–water partitioning co-efficient value to anion, the error will be insignificant in broader context (Rong-Rong et al. 2012). Another solution to this is the use of equilibrium criterion of activity as activity is calculated from a water phase base (Diamond 1989). Fugacity based models therefore, considers various transport process as well the chemical reactions, assuming that the environmental media to be well mixed (Rong-Rong et al. 2012).

The mass balance differential equation for fugacity-based approach for a particular compartment can be written as shown in Eq. (10.2) (Warren et al. 2005).

$$\frac{df_i}{dt} Z_i \times V = E \pm \sum_{i=1}^{i=n} [f_i \times \sum_{t=1}^{t=n} (D_i)_t] \quad (10.2)$$

where, df/dt being the rate of fugacity change of any phase/compartment i (Pa/h), Z being the fugacity capacity (mol/m³/Pa), V being the volume of the compartment considered, E being the emissions to that particular compartment. $(D_i)_t$ being the transport co-efficients for various t types of transport and transformation processes in that compartment I (mol/h/Pa), $+$ indicates that there is input of contaminant to the system and $-$ indicates the contaminant is going out from the system through that particular transport or degradation process.

A fugacity based model has been classified into four classes as tabulated in Table 10.1 (Mackay and Arnot 2011; Mackay and Paterson 1986; Rong-Rong et al. 2012;

Trinh et al. 2016). By formulation of fugacity models compared to concentration models, the equilibrium as well as kinetic parameters will be in such a form that it will promote interpretation of model output as well as assist in the identification of dominant processes in the fate and transport of these emerging contaminants (Goyena 2019; Mackay and Paterson 1986). While using concentration expression, there is a high possibility to encounter equations that contains various mass transfer co-efficient, partitioning co-efficient, path lengths, diffusivities, uptake times and rate constants, hence the algebraic complexity will tend to murk the nature of the fundamental phenomenon that is being simulated (Mackay and Paterson 1986).

The Mathematical models for transport and fate study of ECs is broadly classified based on three approaches (Chen and Yuan, 2009; Cohen and Cooter, 2002b; Su et al. 2019; Yan et al. 2010); Compartments in consideration, i.e., single media model/multimedia compartmental model; Homogeneity, i.e., Spatial versus non-spatial compartments and GIS based models. Single Media models consider just single media/compartment into consideration while simulating the fate and transport of contaminants (Kim et al. 2010). Single media model generally employs the use of advection–dispersion analytical solution for modelling (Chen and Yuan 2009).

Table 10.1 Classification of fugacity-based models

Fugacity model	Key findings	Temporal resolution
Level I	<ul style="list-style-type: none"> • Equilibrium or equi-fugacity among all compartments in the closed system • The mass of the contaminant is constant in the compartment • Simple multimedia partitioning occurs with no losses or reaction 	Steady state
Level II	<ul style="list-style-type: none"> • Introduction of the rate of chemical reaction, advection, degradation • Assumption of equilibrium between compartments • Equilibrium partitioning occurs with losses due to reaction and flow/advection 	Steady state
Level III	<ul style="list-style-type: none"> • Equilibrium constraint removed • Contaminant allowed to enter and move out of the compartments • Contaminants mode of entry to each compartment is specified • Valuable insights obtained such as residence time, overall chemical persistence, potential of long-range transport in water or air 	Steady state
Level IV	<ul style="list-style-type: none"> • Mass flux constraint removed • The contaminant simultaneously goes into the system as well as comes outside therefore the concentration of contaminant inside any compartment varies with time • Useful when the system is recovering by a contamination from a persistent contaminant • Involves solution of differential equations of mass balance 	Unsteady state

Multimedia compartmental models are those models which consider more than one compartment for simulation of concentration in various compartments of the model (Yuan et al. 2011a). General multimedia models consist of multimedia compartmental models without considering spatial variability and are referred to as non-spatial multimedia models whereas recently developed multimedia models include space and time variations of the parameters involved in the models and are referred to as spatially explicit models (Yuan et al. 2011a) as described further. A multimedia compartment model not only considers simple advection–dispersion equation but additionally includes sources of emission of pollutants as well as the reactions taking place in the compartments (Rong-Rong et al. 2012). Based on homogeneity, two different approaches of modelling fate of contaminants in the multimedia environment have been developed; firstly, treating the whole region where the contaminant is being modelled to be homogeneous in each compartment and which are referred to as non-spatial models and the other is spatial models in which splitting the regions (all compartments) being modelled is done on the basis of geographic as well as climate variability or spatial and temporal variability (Rong-Rong et al. 2012).

10.3.1 Non-Spatial Models

Non-Spatial models includes multimedia compartmental models where the compartments are treated to be homogeneous. The contaminant's concentration obtained is an averaged value for each compartment and is based on transport (advection, diffusion, inter-media transport/exchange processes), inter-media partitioning, and various degradation process. The multimedia compartmental models are solved using mass balance equations that are based on either fugacity or concentration. These type of models have relatively less complexity, therefore often used in risk assessment/screening assessment of large number of contaminants (Hollander et al. 2008). The advantage of non-spatial models are that they are low data demanding, application of model being straightforward, output relatively easy to process and interpret; also minimal error prone (Hollander et al. 2012). Non-spatial models are likely to be accurate while assessment of dispersed emission sources, except in the case of presence of large-stagnant water bodies in the modelled area (Between et al. 2005; Hollander 2008). For, persistent and long range contaminants; and for those that are removed swiftly from the environmental media, use of non-spatial models will introduce substantial errors in the concentrations predicted (Hollander et al. 2012). The models of this type includes Spatially Uniform Spherical model (Scheringer 1996), Global Model (Scheringer et al. 2000), ClimoChem model (Schenker et al. 2007, 2008), simple Box model, CalTox, GloBox (Sleeswijk 2003; Sleeswijk 2011; Sleeswijk and Heijungs 2010), OECD tool (Wegmann et al. 2009).

10.3.2 *Spatially Explicit Models*

The use of non-spatial models for contaminants that are persistent in nature and exhibit long range transport will introduce substantial errors in the concentrations predicted (Hollander et al. 2012). Therefore, the compartments need to be treated as spatially as well as temporally varying. The spatial models are based on formulation similar to multimedia compartmental models but spatial models use maps of varying environment properties and emission patterns instead of simply averaging the values (Klepper and Den Hollander 1999). There are basically three type of approaches adopted in spatially explicit modelling: numerical simulation of advective-dispersion equation simultaneously applied; treating the whole considered region as a collection of various box models; development of meta models (Hansen et al. 2006; Pistocchi et al. 2010a, b). The spatially varying model may be studied at large scale/finer resolution or small scale/coarse resolution depending upon the requirement. Earlier during 1990s and early 2000s, coarser spatial models were developed where the targeted region was split into multiple linear box models and each model represented a region (Environmental and Centre 2001; Pistocchi et al. 2010a, b; Wania and Mackay 1995). The advancement of computer-aided technology has led to the division of the targeted region into finer resolution of few hundred kilometers, and each region/cell has for itself well defined explicit emissions (local), transport and removal of the contaminants entering and exiting the surrounding cells. The mass balance equation is written separately for each cell/region and solved for steady or transient state (Pistocchi et al. 2010a, b). Parameters assigned in these models are based upon the actual existing landscape and climate conditions. The spatial models too adopt average value of climate and landscape properties over a large stretch of region where the values remain constant with time; also the intra-media transport currents is very difficult to estimate; therefore, usually the result obtained from spatial and non-spatial models are similar with little difference (Armitage et al. 2007). Various contaminants travel long distances of more than 1000 s of kilometer before degrading or permanently being isolated in sediments or soil (Woodfine et al. 2001), therefore it is very important in such cases to adapt spatially explicit models to account for region wise emissions as well as environmental characteristics. Spatial models also predict the chemical fluxes and the direction of water and air flows simultaneously. The spatial models prove to be very useful when chemical emissions are not known and need to be calculated, in this case contaminants concentration is monitored at various sites and inverse modelling of emissions from concentration can be done (Pistocchi et al. 2010a, b). Spatial models can be further classified into multimedia box models, integrated spatial compartmental models, linked spatial single media models and extended environment multimedia compartmental models.

10.3.2.1 Multimedia Box Models

This modelling is done by splitting the considered region into various sections/boxes and then the boxes are connected. The formulation of the models is done using 2-D or 3-D advection–dispersion equation (ADE) including various compartments. This ADE is applied to each region separately and the regions are interconnected by various fluxes from one region to another which is based on empirical relationships rather than fundamental physical relationships. Also, the numerical solution of ADE carries some unavoidable artifacts, also these models are computation extensive, overwhelmingly data demanding and run time is longer in comparison to simple models which turns out to be expensive (Pistocchi 2008; Pistocchi et al. 2010a, b). Some of the multimedia box models include ChemGL, Evn-BETR, IMPACT-2002 and SESAMe. models.

10.3.2.2 Linked Spatial Single Media Models

These models comprise of single-media transport models being linked together. The model formulation initiates with calculating concentration of contaminant in a media/compartments, followed by calculation of rates of inter-media transfer for that particular media which serves as an input for the contaminant concentration in the adjoining media (Rong-Rong et al. 2012). The model does not provide numerical solution model but gives a high degree of spatial resolution (Chen and Yuan 2009). The model is employed for risk assessment due to exposure of human to hazardous contaminants (Rong-Rong et al. 2012). Some of this type of models include MEPAS, MMSOILS, RESRAD and 3MRA.

LSSMM have suffered various limitation such as: (Yuan 2009).

- i. Empirical algorithm used to estimate gaseous emissions
- ii. Gaseous advection not considered in the polluted soil
- iii. Leachate release was considered at steady state.

10.3.2.3 Integrated Spatial Compartmental Models

ISCMs are hybrid models which combines single media models and compartmental models to avoid simplification of the model and to provide a good spatial resolution and unified via inter-media physical boundary conditions (Rong-Rong et al. 2012). All media, biological and non-biological are considered in one single system. Generally, soil and sediments are considered non-uniform while other compartments are considered uniform. Fugacity model is applied to uniform compartments and mass balance to non-uniform media (Rong-Rong et al. 2012). One of the limitation of ISMC is that it does not incorporate variability/uncertainty into the model and constitutes both well mixed and spatially explicit compartments (Yuan et al. 2011b). Mend-Tox I & II are currently practiced ISCM (Cohen and Cooter 2002b; Cooter and Cohen 2001).

10.3.2.4 Extended Environmental Multimedia Compartmental Models

EEMCM is the first model to address multimedia pollution problem in multi-dimension. The model is an improved version of LSSMMs, incorporating flux transportation through various compartments in order to characterize the space and time dynamics in the general non-uniform multimedia problems (Yuan et al. 2011b). It is solved numerically using.

both finite element as well as finite difference methods (Huang et al. 2014; Chen and Yuan 2009) for temporal and spatial considerations (Chen and Yuan 2009). Flux being the basic quantitative concept, best captures the usefulness of continuity equation on the issue of mobility of the contaminant (Valsaraj and Thibodeaux 2010). Flux is of prime importance as it is continuous across any two phases while, concentration is discontinuous (Valsaraj and Thibodeaux 2010). The flux equates the equilibrium and transport process to a single linear equation obtained by the product of fugacity and a kinetic parameter for quantification of mobility (Valsaraj and Thibodeaux 2010). The EEMCM is a distinguished risk assessment tool useful for assessing impacts on quality of water resource, fate of emerging pollutants, biodiversity, climate change etc. (Yuan et al. 2020). An EEMCM have been used for modeling landfill sites (Chen and Yuan 2009; Yuan and Elektorowicz 2020a, b). Few of the practiced variants of EEMCM have been depicted in Table 10.2.

10.4 GIS Based Models

GIS based modelling is sought to be a simple as well as cost effective technique which also allows the time variable parameters to be included in modelling such as emissions, climate variability etc. and therefore allows simple yet spatially explicit description of fate of chemical (Pistocchi et al. 2010a, b). The GIS plays a vital role in gathering and further processing of environmental data, i.e., the geo-referenced parameters used in modelling for accuracy and efficiency and in displaying and interpreting results obtained from model assessment (Woodfine et al. 2001; Tsihrintzis et al. 1996). For evaluating the risk due to these emerging contaminants, it is very crucial for obtaining pollutants information, including its spatial distribution in different sub-regions and its transportation routes, and this can be incorporated easily into the model using GIS (Song and Xu 2011). The main challenge of using GIS with any model is the difficulty of the model integration with GIS. Some of the GIS based models are GREAT-ER, PhATE, BETR North America, BETR-Global, BETR-World, G-CIEMS, QMX-R, QMX-F and Hydro-ROUT.

There are various catchment scale water quality models including REACH model (Bowman and Calster 2007; Foss et al. 2007; Franco et al. 2013; Öberg and Iqbal 2012; Wielen 2007), SWAT model (Documentation 2009; Luo and Zhang 2009) GWAVA model (Dumont et al. 2012; Johnson et al. 2013), SIMCAT model (Fryer et al. 2006), TOMCAT (Keller 2006), RQP model (Berry and Wells 2004) etc. and

Table 10.2 The variants of Extended Environmental Multimedia Model

Variant of the models	Compartments	Key findings	Limitations	Spatial scale	Temporal scale	Key authors
IEMMS (Improved environmental multimedia modelling systems)	Air, soil- saturated and unsaturated	<ul style="list-style-type: none"> Assessment of impact of landfill on the surroundings i.e., air, soil and groundwater 	<ul style="list-style-type: none"> Rainwater and related phenomenon not considered Various air compartment phenomenon such as dry and wet deposition not considered Only one emission source of benzene considered, i.e., diffused sources not considered Uniform as well as non-uniformity of media considered 	Site-specific, local	Unsteady state	(Yuan et al. 2011b)
FEEMMS (Fuzzy-set enhanced environmental modelling system)	polluting source module, air dispersion module, vadose zone and groundwater module	<ul style="list-style-type: none"> The developed model may serve estimation of spatial and time varying contaminant concentration in soil, air, groundwater Can be used for risk assessment and uncertainty analysis Fuzzy set methodology incorporated in the FEEMMS 	<ul style="list-style-type: none"> Diffusion co-efficients obtained empirically, hence may contribute to imprecision for different field conditions, seepage velocities obtained using Darcy's law, which may deviate from assumptions as well as with time Uncertainty analysis not combined with sensitivity analysis 	Regional, continental, global	Steady state	(Chen et al. 2018; Zhan et al., 2015)

(continued)

Table 10.2 (continued)

Variant of the models	Compartments	Key findings	Limitations	Spatial scale	Temporal scale	Key authors
A novel EEMMS	Air, Landfill, vadose zone, groundwater	<ul style="list-style-type: none"> • Used for fate and transport modeling of benzene • Uncertainty analysis through Monte-Carlo method • Numerical solutions based on FEM and FDM 	<ul style="list-style-type: none"> • Sediments, groundwater and many other compartments not considered 	Regional scale	Unsteady state	(Yuan and Elektorowicz, 2020b)

some geo-referenced single media models for predicting “down the drain” contaminants include PhATE, LF2000-WQX (Johnson et al. 2007; Keller et al. 2015; Price et al. 2010a; Price et al. 2010a, b), iSTREEM model, ePiE model (Oldenkamp et al. 2018), MAPPE model.

Many software have been developed for multimedia modeling of fate and transport of contaminants such as GREAT-ER software (GREAT-ER 2.0 and GREAT-ER 4.0) (Koormann et al. 2006; Kehrein et al. 2015); BETR-Global (Macleod et al. 2011); BETR-Research (Macleod et al. 2011); Mend-Tox (Cohen and Cooter 2002a); PhATE software Version 4.0 which is available on Mgarvin@phrma.org (Caldwell et al. 2019).

10.5 Summary and Conclusions

Environmental pollution has been attracting great attention since two decades due to their hazardous consequences. Urgent actions are required on formulation of policies to control the emerging contaminants being emitted. To achieve the goal, in depth understanding of occurrence, emissions, fate, transport and distribution of contaminants is necessary. The Emerging contaminants once emitted in any medium can travel via various transport processes and reach other media/compartments. Therefore, the purpose of the review is (1) to get a complete insight of fate, transport and distribution processes of ECs once released in the environment, (2) to understand the modeling techniques and (3) to study the available models to predict the occurrence, fate, transport and distribution of various ECs and their effect on human health. The results from the model can further be utilized in risk assessment and formulation of policies to control the ECs in the environment.

The study indicates that the selection of appropriate model depends on the type of contaminant which is posing risk, emissions source, scenario/conditions existing and requirement of user. Various challenges are associated with modeling such as (a) analytical challenges due to the presence of ECs in low concentration, typically ng/l to $\mu\text{g/l}$ (Wilkinson et al. 2017; Žur et al. 2018), (b) due to complicated structure of the ECs, only limited studies have been done for the evaluation of fate and transport including PPCPs in water resources (Trinh et al., 2016), (c) The inclusion of all the multimedia diverse compartments, along with all the parameters affecting fate and transport of ECs with realistic depiction of the conditions existing in the environment; that varies spatially as well as temporally in a single multimedia model is still a challenge. With GIS, there has been advancement in inclusion of geo-referenced parameters in the model and the resolution of the region is successfully incorporated till 1 km. like in the case of PhATE model, which is still not realistic.

Based on review conducted in this study, EEMCM is found to be successful in predicting transport behaviour of ECs in all the compartments and the compartments linked via well established boundary conditions. However, there are few limitations as described below.

- a. Large number of parameters and data is required, which limited the applicability of model in case of data-scarcity.
- b. The model does not consider other compartments such as surface water, sediments, rock fractures as well as various other phases in each compartment.
- c. Point type emission source such as landfill was considered only.

Therefore, for risk assessment study, requirement of appropriate model is of utmost importance. The results of which can be utilized in policy making and hence controlling emerging contaminants in nature.

References

- Armitage JM, Cousins IT, Hauck M, Harbers V, Huijbregts MAJ (2007) Empirical evaluation of spatial and non-spatial European-scale multimedia fate models : results and implications for chemical risk assessment. *J Environ Monitor* 572–581. <https://doi.org/10.1039/b700680b>
- Berry JA, Wells PG (2004) Integrated fate modeling for exposure assessment of produced water on the Sable Island Bank (Scotian Shelf, Canada). *Environ Toxicol Chem* 23(10):2483–2493. <https://doi.org/10.1897/03-458>
- Between AC, Multimedia THE, Models E, Assessment FORL, On B, Population THE, Fraction I, Pollutants OFT (2005) Comparaison entre devenir et exposition Huijbregts 2005.pdf. 24(2):486–493
- Bowman DM, Van Calster G (2007) Does REACH go too far ? 2:1–2
- Caldwell DJ, Aco VD, Davidson T, Kappler K, Murray-smith RJ, Owen SF, Robinson PF, Simonhettich B, Oliver J, Tell J (2019) Chemosphere environmental risk assessment of metformin and its transformation product guanylurea: II. Occurrence in surface waters of europe and the united states and derivation of predicted no-effect concentrations. *Chemosphere* 216:855–865. <https://doi.org/10.1016/j.chemosphere.2018.10.038>
- Caudeville J, Bonnard R, Boudet C, Denys S, Govaert G, Cicolella A (2012) Development of a spatial stochastic multimedia exposure model to assess population exposure at a regional scale. *Sci Total Environ* 432:297–308. <https://doi.org/10.1016/j.scitotenv.2012.06.001>
- Chen Z, Yuan J (2009) An extended environmental multimedia modeling system (EEMMS) for landfill case studies. *Environ Forensics* 10(4):336–346. <https://doi.org/10.1080/15275920903347396>
- Chen Z, Zhang RR, Wang ZP (2018) An enhanced environmental multimedia modelling system (FEMMS): Part II—user interface and field validation. *Environ Eng Manag J* 17(4):1009–1020
- Ciuffo B, Sala S (2013) Climate-based archetypes for the environmental fate assessment of chemicals. *J Environ Manage* 129:435–443. <https://doi.org/10.1016/j.jenvman.2013.08.016>
- Cohen Y, Tsai W, Chetty SL, Mayer GJ (1990) Dynamic partitioning of organic chemicals in regional environments: a multimedia screening-level modeling approach. *Environ Sci Technol* 24(10):1549–1558. <https://doi.org/10.1021/es00080a015>
- Cohen Y, Cooter EJ (2002a) Multimedia environmental distribution of toxics Mend-Tox II : software implementation and case studies. 6:87–101. [https://doi.org/10.1061/\(ASCE\)1090-025X\(2002\)6](https://doi.org/10.1061/(ASCE)1090-025X(2002)6)
- Cohen Y, Cooter EJ (2002b) Multimedia environmental distribution of toxics (Mend-Tox). I: hybrid compartmental-spatial modeling framework. *Pract Period Hazard, Toxic, Radioact Waste Manag* 6(2):70–86. [https://doi.org/10.1061/\(ASCE\)1090-025X\(2002\)6:2\(70\)](https://doi.org/10.1061/(ASCE)1090-025X(2002)6:2(70))
- Cooter EJ, Cohen Y (2001) Model evaluation of dry deposition to vegetation for volatile and semi-volatile organic compounds in a multimedia environment. *Air-Surf Exch Gases Part* 2000:285–294. https://doi.org/10.1007/978-94-010-9026-1_28
- Diamond, 1989 Diamond M (1989) No Title. 18(1980):1343–1365

- Documentation T (2009) SWAT 2009 theoretical documentation
- Dumont E, Williams R, Keller V, Voß A, Tattari S (2012) Modélisation d'indicateurs de sécurité de l'eau, de pollution de l'eau, et de biodiversité aquatique en Europe. *Hydrol Sci J* 57(7):1378–1403. <https://doi.org/10.1080/02626667.2012.715747>
- Dunnivant and Anders, 2005 Dunnivant FM, Anders E (2005) A basic introduction to pollutant fate and transport. <https://doi.org/10.1002/0471758132>
- Environmental C, Centre M (2001) BETR North America: a regionally segmented multimedia contaminant fate model for North America 8(3):156–163
- Foss S, Carlsen L, Tickner JA (2007) Chemicals regulation and precaution: does REACH really incorporate the precautionary principle. 10:395–404. <https://doi.org/10.1016/j.envsci.2007.01.001>
- Franco A, Ferranti A, Davidsen C (2013) An unexpected challenge: Ionizable compounds in the REACH chemical space. 321–325. <https://doi.org/10.1007/s11367-010-0165-6>
- Fryer M, Collins CD, Ferrier H, Colville RN, Nieuwenhuijsen MJ (2006) Human exposure modelling for chemical risk assessment: a review of current approaches and research and policy implications. *Environ Sci Policy* 9(3):261–274. <https://doi.org/10.1016/j.envsci.2005.11.011>
- Gavrilescu M, Demnerová K, Aamand J, Agathos S, Fava F (2015) Emerging pollutants in the environment: Present and future challenges in biomonitoring, ecological risks and bioremediation. *New Biotechnol* 32(1):147–156. <https://doi.org/10.1016/j.nbt.2014.01.001>
- Goyena R (2019) A Quantitative water, air, sediment interaction (QWASI) fugacity model for describing the fate of chemicals in lakes. *J Chem Inf Model* 53(9):1689–1699. <https://doi.org/10.1017/CBO9781107415324.004>
- Grassi M, Kaykioglu G, Belgiorno V, Lofrano G (2012) Removal of emerging contaminants from water and wastewater by adsorption process, pp 15–37. https://doi.org/10.1007/978-94-007-3916-1_2
- Hansen KM, Prevedouros K, Sweetman AJ, Jones KC, Christensen JH (2006) A process-oriented inter-comparison of a box model and an atmospheric chemistry transport model: insights into model structure using α -HCH as the modelled substance. *Atmos Environ* 40(12):2089–2104. <https://doi.org/10.1016/j.atmosenv.2005.11.050>
- Hollander A, Scheringer M, Shatalov V, Mantseva E, Sweetman A, Roemer M, Baart A, Suzuki N, Wegmann F, Van De Meent D (2008) Estimating overall persistence and long-range transport potential of persistent organic pollutants: a comparison of seven multimedia mass balance models and atmospheric transport models. *J Environ Monit* 10(10):1139–1147. <https://doi.org/10.1039/b803760d>
- Hollander A, Hauck M, Cousins IT (2012) Assessing the relative importance of spatial variability in emissions versus landscape properties in fate models for environmental exposure assessment of chemicals. pp 577–587 <https://doi.org/10.1007/s10666-012-9315-5>
- Hollander A (2008) Spatial variation in multimedia mass balance models. <http://hdl.handle.net/2066/53744%0APlease>
- Huang Y, Dai Z, Zhang W (2014) Geo-disaster modeling and analysis: an SPH-based approach 2008. 1–189. <https://doi.org/10.1007/978-3-662-44211-1>
- Johnson AC, Keller V, Williams RJ, Young A (2007) A practical demonstration in modelling diclofenac and propranolol river water concentrations using a GIS hydrology model in a rural UK catchment. *Environ Pollut* 146(1):155–165. <https://doi.org/10.1016/j.envpol.2006.05.037>
- Johnson AC, Dumont E, Williams RJ, Oldenkamp R, Cisowska I, Sumpter JP (2013) Do concentrations of ethinylestradiol, estradiol, and diclofenac in European rivers exceed proposed EU environmental quality standards? *Environ Sci Technol* 47(21):12297–12304. <https://doi.org/10.1021/es4030035>
- Kehrein N, Berlekamp J, Klasmeier J (2015) Modeling the fate of down-the-drain chemicals in whole watersheds: new version of the GREAT-ER software. *Environ Model Softw* 64:1–8. <https://doi.org/10.1016/j.envsoft.2014.10.018>
- Keller V (2006) Risk assessment of “down-the-drain” chemicals: search for a suitable model. *Sci Total Environ* 360(1–3):305–318. <https://doi.org/10.1016/j.scitotenv.2005.08.042>

- Keller VDJ, Lloyd P, Terry JA, Williams RJ (2015) Impact of climate change and population growth on a risk assessment for endocrine disruption in fish due to steroid estrogens in England and Wales. *Environ Pollut* 197:262–268. <https://doi.org/10.1016/j.envpol.2014.11.017>
- Kim GN, Moon JK, Lee KW (2010) An analysis of the effect of hydraulic parameters on radionuclide migration in an unsaturated zone. *Nucl Eng Technol* 42(5):562–567. <https://doi.org/10.5516/NET.2010.42.5.562>
- Klepper O, Den Hollander HA (1999) A comparison of spatially explicit and box models for the fate of chemicals in water, air and soil in Europe. *Ecol Model* 116(2–3):183–202. [https://doi.org/10.1016/S0304-3800\(98\)00161-6](https://doi.org/10.1016/S0304-3800(98)00161-6)
- Koormann F, Rominger J, Schowanek D, Wagner JO, Schröder R, Wind T, Silvani M, Whelan MJ (2006) Modeling the fate of down-the-drain chemicals in rivers: an improved software for GREAT-ER. *Environ Model Softw* 21(7):925–936. <https://doi.org/10.1016/j.envsoft.2005.04.009>
- Lamastra L, Balderacchi M, Trevisan M (2016) Inclusion of emerging organic contaminants in groundwater monitoring plans. *MethodsX* 3(May):459–476. <https://doi.org/10.1016/j.mex.2016.05.008>
- Lindim C, Gils JV, Cousins IT, Kühne R, Georgieva D, Kutsarova S, Mekenyan O (2017) Model-predicted occurrence of multiple pharmaceuticals in Swedish surface waters and their flushing to the Baltic Sea*. *Environ Pollut* 223:595–604. <https://doi.org/10.1016/j.envpol.2017.01.062>
- Luo Y, Zhang M (2009) Management-oriented sensitivity analysis for pesticide transport in watershed-scale water quality modeling using SWAT. *Environ Pollut* 157(12):3370–3378. <https://doi.org/10.1016/j.envpol.2009.06.024>
- Mackay D, Arnot JA (2011) The application of fugacity and activity to simulating the environmental fate of organic contaminants. 1348–1355. <https://doi.org/10.1021/je101158y>
- Mackay D, Paterson S (1986) The fugacity approach to multimedia environmental modeling. In: *Pollutants in a multimedia environment 1978*, pp 117–131. https://doi.org/10.1007/978-1-4613-2243-6_6
- Macleod M, Waldow HV, Tay P, Armitage JM, Wöhrnschimmel H, Riley WJ, Mckone TE, Hungerbühler K (2011) Short communication BETR global e a geographically-explicit global-scale multimedia contaminant fate model. *Environ Pollut* 159(5):1442–1445. <https://doi.org/10.1016/j.envpol.2011.01.038>
- Öberg T, Iqbal MS (2012) Chemosphere the chemical and environmental property space of REACH chemicals. 87:975–981. <https://doi.org/10.1016/j.chemosphere.2012.02.034>
- Oldenkamp R, Hoeks S, Čengić M, Barbarossa V, Burns EE, Boxall ABA, Ragas AMJ (2018) A high-resolution spatial model to predict exposure to pharmaceuticals in European surface waters: EPIE. *Environ Sci Technol* 52(21):12494–12503. <https://doi.org/10.1021/acs.est.8b03862>
- Pistocchi A (2008) A GIS-based approach for modeling the fate and transport of pollutants in Europe. *Environ Sci Technol* 42(10):3640–3647. <https://doi.org/10.1021/es071548+>
- Pistocchi A, Sarigiannis DA, Vizcaino P (2010a) Spatially explicit multimedia fate models for pollutants in Europe: state of the art and perspectives. *Sci Total Environ* 408(18):3817–3830. <https://doi.org/10.1016/j.scitotenv.2009.10.046>
- Pistocchi A, Zulian G, Vizcaino P, Marinov D (2010b) Multimedia assessment of pollutant pathways in the environment, European scale model (MAPPE-EUROPE). JRC Scientific and Technical Reports EUR 24256 EN–2010b. In *Mappe-Europe 24256*, <https://doi.org/10.2788/63765>
- Price OR, Williams RJ, van Egmond R, Wilkinson MJ, Whelan MJ (2010a) Predicting accurate and ecologically relevant regional scale concentrations of triclosan in rivers for use in higher-tier aquatic risk assessments. *Environ Int* 36(6):521–526. <https://doi.org/10.1016/j.envint.2010.04.003>
- Price OR, Williams RJ, Zhang Z, van Egmond R (2010b) Modelling concentrations of decamethyl-cyclopentasiloxane in two UK rivers using LF2000-WQX. *Environ Pollut* 158(2):356–360. <https://doi.org/10.1016/j.envpol.2009.09.013>
- Rong-Rong Z, Che-Sheng Z, Zhong-Peng H, Xiao-Meng S (2012) Review of environmental multimedia models. *Environ Forensics* 13(3):216–224. <https://doi.org/10.1080/15275922.2012.702328>

- Schenker U, Scheringer M, Hungerbühler K (2007) Including degradation products of persistent organic pollutants in a global multi-media box model. *Environ Sci Pollut Res* 14(3):145–152. <https://doi.org/10.1065/espr2007.03.398>
- Schenker U, Scheringer M, Hungerbühler K (2008) Investigating the global fate of DDT: model evaluation and estimation of future trends. *Environ Sci Technol* 42(4):1178–1184. <https://doi.org/10.1021/es070870h>
- Scheringer M (1996) Persistence and spatial range as endpoints of an exposure-based assessment of organic chemicals. 30(5):1652–1659. <https://doi.org/10.1021/es9506418>
- M Scheringer F Wegmann K Hungerbu 2000 Investigation of the cold condensation of persistent organic pollutants with a global multimedia fate model. *Environ Sci Technol* 34(9):1842–1850. <https://doi.org/10.1021/es991085a>
- Semplice M, Ghirardello D, Morselli M, Di Guardo A (2012) Guidance on the selection of efficient computational methods for multimedia fate models. <https://doi.org/10.1021/es201928d>
- Sleeswijk AW, Heijungs R (2010) Science of the total environment GLOBOX: a spatially differentiated global fate, intake and effect model for toxicity assessment in LCA. *Sci Total Environ* 408(14):2817–2832. <https://doi.org/10.1016/j.scitotenv.2010.02.044>
- Sleeswijk AW (2003) General prevention and risk minimization in LCAA combined approach. 10(1):69–77
- Sleeswijk AW (2011) Regional LCA in a global perspective. A basis for spatially differentiated environmental life cycle assessment. 106–112. <https://doi.org/10.1007/s11367-010-0247-5>
- Song HM, Xu LY (2011) A method of urban ecological risk assessment: combining the multimedia fugacity model and GIS. *Stoch Env Res Risk Assess* 25(5):713–719. <https://doi.org/10.1007/s00477-011-0476-6>
- Su C, Zhang H, Cridge C, Liang R (2019) Science of the total environment a review of multimedia transport and fate models for chemicals: principles, features and applicability. *Sci Total Environ* 668:881–892. <https://doi.org/10.1016/j.scitotenv.2019.02.456>
- Tijani JO, Fatoba OO, Babajide OO, Petrik LF (2016) Pharmaceuticals, endocrine disruptors, personal care products, nanomaterials and perfluorinated pollutants: a review. *Environ Chem Lett* 14(1):27–49. <https://doi.org/10.1007/s10311-015-0537-z>
- Trinh HT, Adriaens P, Lastoskie CM (2016) Fate factors and emission flux estimates for emerging contaminants in surface waters. 3:21–44. <https://doi.org/10.3934/environsci.2016.1.21>
- Tsihrintzis VA, Hamid R, Fuentes HR (1996) Use of geographic information systems (GIS) in water resources: a review. *Water Resour Manage* 10(4):251–277. <https://doi.org/10.1007/BF00508896>
- Valsaraj KT, Thibodeaux LJ (2010) On the physicochemical aspects of the global fate and long-range atmospheric transport of persistent organic pollutants. *J Phys Chem Lett* 1(11):1694–1700. <https://doi.org/10.1021/jz100450f>
- Wania F, Mackay D (1995) A global distribution model for persistent organic chemicals. *Sci Total Environ* 160–161(C):211–232. [https://doi.org/10.1016/0048-9697\(95\)04358-8](https://doi.org/10.1016/0048-9697(95)04358-8)
- Warren C, Mackay D, Whelan M, Fox K (2005) Mass balance modelling of contaminants in river basins: a flexible matrix approach. 61:1458–1467. <https://doi.org/10.1016/j.chemosphere.2005.04.118>
- Wegmann F, Cavin L, MacLeod M, Scheringer M, Hungerbühler K (2009) The OECD software tool for screening chemicals for persistence and long-range transport potential. *Environ Model Softw* 24(2):228–237. <https://doi.org/10.1016/j.envsoft.2008.06.014>
- Wielen A (2007) REACH: next Step to a Sound Chemicals Management. <https://doi.org/10.1038/sj.jes.7500598>
- Wilkinson J, Hooda PS, Barker J, Barton S, Swinden J (2017) Occurrence, fate and transformation of emerging contaminants in water: an overarching review of the field. *Environ Pollut* 231:954–970. <https://doi.org/10.1016/j.envpol.2017.08.032>
- Woodfine DG, MacLeod M, Mackay D, Brimacombe JR (2001) Development of continental scale multimedia contaminant fate models: integrating GIS. *Environ Sci Pollut Res* 8(3):164–172. <https://doi.org/10.1007/BF02987380>

- Yan S, Subramanian SB, Tyagi RD, Surampalli RY, Zhang TC (2010) Emerging contaminants of environmental concern: Source, transport, fate, and treatment. *Pract Periodic Hazard Toxic Radioactive Waste Manag* 14(1):2–20. [https://doi.org/10.1061/\(ASCE\)HZ.1944-8376.0000015](https://doi.org/10.1061/(ASCE)HZ.1944-8376.0000015)
- You K (n.d.) Development of fate and transport department of urban and environmental engineering graduate school of UNIST
- Yuan J, Elektorowicz M, Chen Z (2011a) Improved environmental multimedia modeling and its sensitivity analysis. *Water Sci Technol* 63(10):2155–2163. <https://doi.org/10.2166/wst.2011.343>
- Yuan J, Elektorowicz M, Chen Z (2011b) Improved environmental multimedia modeling and its sensitivity analysis. 10:2155–2164. <https://doi.org/10.2166/wst.2011.343>
- Yuan J, Elektorowicz M (2020) Extended environmental multimedia modeling system assessing the risk carried by pollutants in interacted air-unsaturated-groundwater zones. *J Hazard Mater* 381:120852
- Yuan J, Elektorowicz M (2020b) Extended environmental multimedia modeling system assessing the risk carried by pollutants in interacted air-unsaturated-groundwater zones. *J Hazard Mater*, 381:120852. <https://doi.org/10.1016/j.jhazmat.2019.120852>
- Yuan J (2009) Development of an extended environmental multimedia modeling system (EEMMS). In: *Aspectos Generales De La Planificación Tributaria En Venezuela*, (Issue December)
- Zhan C, Zhang R, Song X, Liu B (2015) An enhanced environmental multimedia modeling system based on fuzzy-set approach: I. theoretical framework and model development. *Front Environ Sci Eng* 9(3):494–505. <https://doi.org/10.1007/s11783-013-0609-x>
- Zhang Q, Crittenden JC, Shonnard D, Mihelcic JR (2003) Development and evaluation of an environmental multimedia fate model CHEMGL for the Great Lakes region. *Chemosphere* 50(10):1377–1397. [https://doi.org/10.1016/S0045-6535\(02\)00760-9](https://doi.org/10.1016/S0045-6535(02)00760-9)
- Zhang Q-Q, Ying G, Chen Z (2015) Basin-scale emission and multimedia fate of triclosan in whole China. 10130–10143. <https://doi.org/10.1007/s11356-015-4218-z>
- Žur J, Piński A, Marchlewicz A, Hupert-Kocurek K, Wojcieszynska D, Guzik U (2018) Organic micropollutants paracetamol and ibuprofen—toxicity, biodegradation, and genetic background of their utilization by bacteria. *Environ Sci Pollut Res* 25(22):21498–21524. <https://doi.org/10.1007/s11356-018-2517-x>

Chapter 11

Management and Remediation of Polluted Soils Using Fertilizer, Sawdust and Horse Manure Under Changing Tropical Conditions



Hassana Ibrahim Mustapha and Obumneme Sunday Okeke

Abstract Auto-mechanic workshops in developing countries such as Nigeria are a major source of potentially toxic substances which can leach into the water table and contaminate groundwater. Several physical and chemical methods have been employed to remediate pollutants in oil-contaminated soils, some of these methods are simply a transfer of contaminants from one place to another, which may also require additional treatments. A combination of treatments consisting of the application of NPK (nitrogen, phosphorous, and potassium) fertilizer, sawdust, horse manure and exposure to oxygen was evaluated in situ during 70 days for the remediation of cadmium, chromium, lead and total petroleum hydrocarbon in used engine oil-contaminated soils. The soils received 447.6 kg of horse manure, 48 kg of sawdust and 4.2 kg of NPK fertilizer per 2 m² of surface area. The total heterotrophic bacteria count at the start-up of the experiment was 0.018×10^6 CFU/g in the contaminated soil and thus increased to 80.5×10^6 CFU/g during the 70 days treatment. In addition, the combined treatment showed 87% total petroleum hydrocarbon degradation, 71% Cd and 62% Pb reduction. Hence, the results of this study showed that nutrient enhanced bioremediation can achieve the degradation of petroleum hydrocarbon and heavy metals in oil-contaminated soils under the prevailing tropical conditions of Nigeria.

11.1 Introduction

Soil is one of the most vital resources of the world alongside air and water. It is a key component for a sustainable ecosystem (Obasi et al. 2013). The major source of pollution in soil, water and groundwater is due to the release of contaminants into the environment naturally, anthropogenically, or accidentally (Achile and Yillian 2010; Abioye 2011). The rate at which soil is being degraded has overwhelmed the self-cleaning capacity of the soil (Garbisu and Alkorta 2003). Thus, affecting

H. I. Mustapha · O. S. Okeke (✉)

Department of Agricultural and Bioresources Engineering, Federal University of Technology, Minna, Nigeria

e-mail: okekeosunday@gmail.com

the physical, chemical and biological properties of the soil, subsequently, adversely affecting public health, crop production and productivity, quality and utility of the soil (Agamuthu et al. 2013; Idzi et al. 2013; Ojuederie and Babalola 2017). Incidentally, contaminated soils are common environmental problem all over the world (Garbisu and Alkorta 2003). However, the extent of contamination and the priority given to the problem differs from country to country. For instance, Nigeria is a developing and oil-producing country that has diverse environmental problems with no effective regulatory policies on the environment (Onuoha 2013). In this context, therefore, this chapter presents an alternative measure to reduce soil contamination input by an ecologically and economically feasible technique by assessing the efficacy of the combined effects of horse manure, sawdust, NPK fertilizer and aeration in treating total petroleum hydrocarbon and some selected heavy metals in engine oil-polluted soils. Also, the rate of biodegradation of hydrocarbon in soils, biostimulation efficiency as well as net loss was discussed in the chapter.

11.1.1 Soil Contamination: Types, Causes and Its Effects

A contaminated soil contains toxic chemicals above its threshold limits thus posing risks to human health as well as the ecosystem. Contamination of soil may be a result of many causes (van Straalen 2002). In Nigeria for instance, the most important sources of soil pollution (Table 11.1) are auto-mechanic workshops (Onianwa et al. 2003; Adeniyi and Afolabi, 2002), solid waste dumps (Osakwe et al. 2012; Musa et al. 2018); petrol stations (Adeniyi and Afolabi, 2002; Onianwa et al. 2003), motor parks (Onianwa et al. 2003), bush burning, agricultural activities (Adamu and Nganje, 2010; Mustapha and Adeboye 2014), exploration and exploitation of crude oil (Uzoekwe and Oghosanine 2011) and refineries (Mustapha et al. 2018a, b, c, d).

Soil contamination types include soil pollution by industrial discharges, solid wastes, agricultural soil pollution, and pollution due to urban activities. The major causes of soil pollution are industrial discharges (Mustapha and Lens 2018), agricultural pesticides (Zhang and Qiao 2002), fertilizers and insecticides (Zhang and Qiao 2002), fuel leakage from automobiles and seepage of toxic from dumpsites (Musa et al. 2018). In addition, soil fertility is negatively affected by contamination with industrial effluent (Hamza et al. 2012), exploitation and exploration of crude oil (Uzoekwe and Oghosanine 2011; Mustapha et al. 2018a, b, c, d) and automobile discharges (Abioye 2011; Chindo 2016).

Petroleum industries are a major contributor of contaminants into the environment by their various activities ranging from exploration, exploitation, transportation, distribution and usage of refined products (Tyagi et al. 2011; Benson et al. 2016). The companies generate solid waste and sludge composed of heavy metals, organic and inorganic compounds (Uzoekwe and Oghosanine 2011), its improper disposal can lead to soil contamination which can pose serious threats to groundwater (Pal et al. 2010). Furthermore, used and unused engine oil are discriminately disposed of on the ground surface at auto-mechanic workshops, in water drains and open channels

Table 11.1 Major sources of soil pollution in Nigeria

Activity	Location	Types	Concentrations ($\mu\text{g/g}$)	Sources	Reference
Oil exploration	Niger Delta, Imo river and Oginni canal	Polyaromatic hydrocarbons compounds: phenanthrene, anthracene, fluoranthene, pyrene	65–331 and 24–120	Sediments and soil in rivers and canals	Samuel Sojину et al. (2010)
Urban soils (industrial and agricultural areas)	Ibadan	Cd, Cu, Mn, Mo, Ni, Pb, Zn, As, Cr,	8.4, 46.8, 1097.9, 2.2, 20.2, 95.1, 228.6, 3.9, 64.4	Soil	Odebande and Abimbola (2008)
Dump slag	Ibadan	Pb, Zn and Ni	34.8–41,500, 16.3–849 and ND–48.2; 9.2–9700, 16.0–271 and 2.83–36.9; 4.55670, 8.00–174 and ND–322	Soil, plant root and plant shoot	Ogundiran and Osibanjo (2008)
Auto-repair workshops, gas-stations and motor-parks	Ibadan	Pb, Zn, Cd, Cu, Cr, Co and Ni	Pb–95.8, Cu–117; gas stations: Pb–46.6, Cu–33.5; motor-parks: Pb–31.6, Cu–16.8	Soil	Onianwa et al. (2003)
Auto-mechanic workshop	Four geo-political zones of Nigeria	Cu, Cd, Pb and Zn	NI		Nkwoada et al. (2018)
Petroleum stations and mechanic workshop,	Lagos	TPH and heavy metals	399.83 \pm 106.19 and 450.83 \pm 90.58 $\mu\text{g/g}$; 362.60 \pm 185.84 and 428.55 \pm 119.00 $\mu\text{g/g}$	Soil	Adeniyi and Afolabi (2002)
Tanker loading point	Niger Delta	Total PAH	47.2 \pm 31.2 mg PAH _{tot} /kg OC	Soil	Abbas and Brack (2006)
Land use pattern	Benue	Pb, Zn, Cd, As		Mineralized soils, urban soils, forest soils and agricultural soils	Adamu and Nganje (2010)
Municipal waste dumpsites	Asaba	Cu, Pb, Mn, Zn	47.91, 60.32, 82.24, 63.21%	Soil	Osakwe et al. (2012)
Wastewater irrigation	Minna	Mn, Mg, Cu, Zn, Pb, Fe, Cd	3.20, 6.85, 31.0, 25.46, 10.0, 60.96, and 0.05	Soil	Mustapha and Adeboye (2014)

(continued)

Table 11.1 (continued)

Activity	Location	Types	Concentrations ($\mu\text{g/g}$)	Sources	Reference
Municipal waste dumpsites	Kafanchan	Cd, Cr, Cu, Ni and Pb	11.38–30.67 mg/kg, 106.52–158.42 mg/kg, 52.09–119.69 mg/kg 94.19–308.35 mg/kg and 98.43–332.83 mg/kg	Soil	Chindo (2016)
Municipal waste dumpsites	Owerri	Cu, Pb, Zn and Cd	0.08–0.10 mg/kg, 0.84–1.48 mg/kg, 0.13–0.79 mg/kg, 1.40–34.89 mg/kg	Soil	Onwudike et al. (2017)
Oil exploration	Niger Delta	Cd, Zn, Pb, As, Fe,	36.71 mg/kg, 22.24 mg/kg, 72.26 mg/kg, 13.41 mg/kg and 27,930 mg/kg	Soil	Idzi et al. (2013)

Note NI—Not Indicated

in Nigeria (Abdulyekeen et al. 2016) and many other developing countries (Abioye et al. 2008; Aleer et al. 2011). The effects of the discharge of pollutants into the environment are numerous. Firstly, this practice is unsafe, and it will continuously release persistent, bioaccumulative and toxic chemicals into the environment as long as the world's demand for oil for transport and continuous dependence on automobiles is on the rise (Aler et al. 2011). Secondly, the contaminants can find their way into plant tissues, animals and human beings through migration and ingestion (Abdulyekeen et al. 2016), which could increase the risks of liver and kidney damage as well as cause cancer in people living in the affected environment (Aler et al. 2011). Oil spills can cause displacement of air pore spaces in soil particles, this effect can cause wide deforestation and pollution of aquatic and terrestrial ecosystems (Mustapha and Lens 2018). In addition, effects of spent and fresh motor oil spills on soils are; increase in acidity of the soils, halt cellular respiration and roots of plants are starved of vital oxygen (Idzi et al. 2013; Abdulyekeen et al. 2016). Accordingly, Ebuehi et al. (2005) reported the impact of oil spillage on microorganisms and man through the introduction of non-organic, carcinogenic and toxic substances into the soil and Uzoekwe and Oghosanine (2011) reported a positive correlation between contamination of water and sediments with aromatic hydrocarbons from refinery effluents with an adverse threat on the health of aquatic organisms.

Heavy metals are essential for normal healthy growth by plants and animals at low but critical concentrations and toxic at high concentrations (Osakwe et al. 2012; Ojuederie and Babalola 2017). They are major pollutants in soil (Chen et al. 2015) because they are not biodegradable and have long-lasting effects in soil due to their relatively strong adsorption on humid and clay colloids (Osakwe et al. 2012). Tables 11.1 and 11.2 present various heavy metal and their sources of contamination in the environment. The main sources of heavy metals in the environment are industrial waste, electronic waste, auto-mechanic workshops, dumpsites, mining,

soil parent material, energy and fuel production, electroplating, plumbing, wastewater sludge and agriculture (Abioye, 2011; WHO 2011; Ali et al. 2013; Su et al. 2014; Nkwoada et al. 2018). The heavy metals of significant biological toxicity commonly found in soils are mercury (Hg), cadmium (Cd), lead (Pb), chromium (Cr), nickel (Ni), zinc (Zn) and copper (Cu) (Table 11.2; Abioye 2011; Ali et al. 2013; Su et al. 2014). These heavy metals can bioaccumulate in plants as well as surface waters and tend to be toxic to aquatic organisms (Nkwoada et al. 2018).

The contamination of soils has resulted in severe environmental deterioration (Su et al. 2014). For instance, waste-derived fuels are especially prone to contain heavy metals (Abioye 2011) and waste oil from lubricants, gasoline, diesel, and by-products of used and spent engine oil contain heavy metals such as Va, Pb, Zn, Cd, Cr, Cu, Al and Ni (Abioye 2011; Nkwoada et al. 2018). However, whatever may be the source of releasing heavy metals, the ultimate destination of the heavy metals is in the soil and water environment (Uddin et al. 2016). Therefore, these persistent problems that release toxic materials into the environment such as oil spills from spent and fresh motor oil, oil and gas production, industrial and municipal discharges, stormwater discharges, runoff from roads, vandalism, war, forest and grass fires (Ogunfowokan et al. 2003), needs to be given priority attention due to the increased health risks associated with it as well as the increased rate of depletion of soil and water resources (Belmount et al. 2004; Tabari et al. 2011).

11.2 Treatment Methods for Petroleum Contaminated Soils

11.2.1 Conventional Treatment Methods

Conventional treatment methods are mainly physical and chemical processes (Marrot et al. 2006). They have been employed for the remediation of pollutants in oil-contaminated soils, some of these methods are simply a transfer of contaminants from one place to another (Mazzeo et al. 2010), which may also require additional treatments. Moreover, the methods are energy-intensive, expensive, and generate by-products that are often toxic to both humans and the environment (Mustapha et al. 2018a). Conventional treatment methods are also known to destroy the biological component of the soil or change the chemical or physical characteristics of the soil (Lin and Mendelsohn 2009). Examples include incineration, thermal vaporization, solvent washing, and soil washing techniques (Table 11.2; Mustapha 2018). Zhang and Qiao (2002) highlighted some benefits as well as disadvantages of using some conventional treatment methods such as chemical treatment and volatilization, they said that although the method is feasible, is problematic in that large volume of acids and alkalis are produced and subsequently must be disposed of. In addition, they stated that incineration is the most reliable method for the destruction of toxic compounds, since the public is opposing potentially toxic emission, and it is also economically restrictive.

Table 11.2 Heavy metals and hydrocarbons in soils

Contaminants	Sources	Effects on soil	Techniques	Limitations	References
Heavy metal					
Essential: Fe, Mn, Cu, Zn, Ni Non-essential: Cd, Pb, As, Hg, Cr	Natural: weathering of minerals, erosion and volcanic activity Anthropogenic: mining, smelting, electroplating, use of pesticides and phosphate fertilizers, biosolids in agriculture, sludge dumping, industrial discharge, atmospheric deposition	Toxicological effects on soil microbes may lead to a decrease in their number and activities Oxidative stress by the formation of free radical Severe soil erosion and off-site pollution	Physical, chemical and biological approaches Conventional remediation methods: In situ vitrification, soil incineration, excavation and landfill, soil washing, soil flushing, solidification, and stabilization of electro-kinetic systems	the physical and chemical methods suffer from limitations like high cost, intensive labour, irreversible changes in soil properties and disturbance of native soil microflora Chemical methods can also create secondary pollution problems	Ali et al. (2013)
Heavy metals: Hg, Cd, Pb, Cr, Zn, As, Cu	Anthropogenic: Industrial waste, electronic waste, mining, energy & fuel production, electroplating, wastewater sludge and agriculture		Physical, chemical degradation, photodegradation	Methods leave behind daughter compounds which are toxic to the environment than the parent compounds	Abioye (2011)
Hydrocarbons: Volatile and semi-volatile organic compounds; PAH, PCBs, dioxins	Oil spills, oil waste discharge from refineries, factories or shipping		Soil vapour extraction	The method cannot be used for removal of heavy oils, metals, PCBs, or dioxins	Abioye (2011)
			In situ steam injection vapour extraction, Air sparging, Excavation	High unit cost for transportation and final off-site disposal	

(continued)

Table 11.2 (continued)

Contaminants	Sources	Effects on soil	Techniques	Limitations	References
Heavy metals: Hg, Cd, Cr, As, Pb, Cr, V, Ni Cu and Zn,	Atmospheric deposition, sewage irrigation, improper stacking of the industrial solid waste, mining activities, the use of pesticides and fertilizers	Inhibit microbial biomass and activity of the soil, reduces activities of enzymes in the soil, can interfere with crop photosynthesis and protein synthesis and may cause membrane damage	Replacement of contaminated soil, soil removal and soil isolation	Cost a large amount of manpower and material resources, so they can only be applied to a small area of soils	Su et al. (2014)

11.2.2 Natural Treatment Methods

Natural systems can be exploited in soil management for treating a wide variety of contaminants simultaneously by the combined action of the microorganisms growing on the medium and plant species (Mustapha et al. 2018b). They are known to be low-cost (Stottmeister et al. 2003; Al-Baldawi et al. 2014), have low maintenance (Chen et al. 2006), requires less energy (Hazra et al. 2011; Aslam et al. 2007), as well as being an ecologically friendly alternative to conventional treatment methods (Mustapha 2018). However, the method is slow, with the addition of organic and inorganic materials, supplying oxygen and by maintaining suitable conditions of temperature, pH and moisture the process of remediation can be accelerated (Ebuehi et al. 2005; Hamoudi-Belarbi et al. 2018). Natural treatment systems include phytoremediation and bioremediation.

Phytoremediation is a plant-assisted bioremediation technique (Wenzel 2009). It uses plants and or associated microorganisms to remove organic and/or inorganic contaminants from soil, uptake and conversion into non-toxic forms, or stabilization of inorganic into a less soluble form (Abou-Shanab et al. 2007; Isitekhale et al. 2013). Phytoremediation of contaminated sites is a cost and environmentally effective approach (Isitekhale et al. 2013). This natural approach supports the goal of sustainable development by helping to conserve soil as a resource, bring the soil back into beneficial use, preventing the spread of pollution to air and water, and reducing the pressure for development on green or agricultural field sites (Oh et al. 2014). The fundamental processes involved in phytoremediation are phytostabilization (and immobilization), phytovolatilization, rhizovolatilization, phytoextraction, and phytodegradation, rhizodegradation (Wenzel 2009; Pal et al. 2010). Garbisu and Alkorta (2003) described plants as solar-driven pumps because of their abilities to

uptake essential and non-essential metals in the course of remediation of polluted sites.

Bioremediation is the use of natural microbial capacity to reduce or eliminate hazardous substances from the environment (Zhang and Qiao 2002; Aleer et al. 2011). In addition, Agamuthu et al. (2013) referred to bioremediation as the removal, destruction, or transformation of pollutants to less harmful constituents. Bioremediation of contaminated soils is a widely accepted technology in which native introduced microorganisms and/or biological wastes, such as compost, animal manure and plant residues are used to detoxify or transform toxic contaminants into less toxic forms (Ashokkumar et al. 2014). Also, the process can range from simply allowing indigenous organisms to degrade toxic substances under natural conditions, to supplying oxygen to the contaminated soils and active augmentation by artificial means to accelerate the process of biodegradation (Zhang and Qiao 2002; Aleer et al. 2011).

Bioremediation may be classified into three main types; biostimulation and bioaugmentation (Tyagi et al. 2011) and intrinsic bioremediation (natural attenuation) (Aleer et al. 2011). Bioremediation technology can be classified into ex situ and in situ as well as the techniques involved in bioremediation are also classified into in situ and ex situ (Agamuthu et al. 2013). *Ex-situ* technologies involve the physical movement of contaminant materials to another area for treatment while treatment in place is called in situ. Examples of ex situ technology include biopiles, landfarming and composting and in situ are bioventing, bioaugmentation, biosparging and biostimulation (Pal et al. 2010; Aleer et al. 2011). However, many factors such as nutrients, pH, temperature, moisture, oxygen, soil properties, strain selection, microbial ecology, type of contaminants and concentration of contaminants can limit bioremediation techniques (Tyagi et al. 2011; Ofoegbu et al. 2015). Bioremediation is a cost-effective means of remediation of soil contaminated with petroleum (Gupta et al. 2020). The process involves the stimulation of the catabolic activity of indigenous microorganisms by the addition of organic and inorganic biostimulants (Hamoudi-Belarbi et al. 2018). For instance, Agamuthu et al. (2013) biostimulated indigenous microorganisms by the use of organic and inorganic wastes, they achieved a 94 and 82% degradation of used lubricant oil-contaminated soils after 98 days of exposure from cow dung and sewage sludge, respectively. Also, Ebuehi et al. (2005) treated a crude oil-contaminated sandy soil during a 10 weeks study using remediation by enhanced natural attenuation (RENA) technique. Their study revealed a reduction in TPH content in the contaminated soils from 1.1004×10^4 mg/kg to 282 mg/kg. RENA is a full-scale bioremediation technology in which contaminated soils, sediments and sludge are periodically tilled to aerate the waste (Ebuehi et al. 2005).

Biostimulation agents are cheap, readily available and environmentally friendly and they are capable of improving the nutrient or aeration status of the soil. Organic manures are used to improve soil fertility (Benson et al. 2016; Obasi et al. 2013), aeration, pH, water-holding capacity, ion-exchange capacity and conservation of soil texture (Hamoudi-Belarbi et al. 2018). They could come from both animals and plant sources including domestic birds and livestock such as chicken, ram, sheep, cow, goat, horse, sawdust, rice husk, yam peel, banana skin, carrot peel, and palm kernel husk (Ofoegbu et al. 2015; Hamoudi-Belarbi et al. 2018). Hamoudi-Belarbi et al.

(2018) reported that these biostimulants provide nutrients that enhance the growth of hydrocarbon-degrading bacteria and also release biosurfactants that increase the bioavailability of poorly soluble hydrocarbons compounds. Thus, making them effective amendments for the bioremediation of used lubricant contaminated soils (Agamuthu et al. 2013).

Inorganic fertilizers (NPK) are a good supplement for the growth of petroleum utilizing bacteria in oil-contaminated soils. They have been reported to increase the carbon to nutrient ratios to stimulate and sustain microbial activity (Isitekhale et al. 2013). The application of organic and inorganic manures to oil-contaminated soils has been reported by various researchers. For instance, Isitekhale et al. (2013) achieved net remediation of 86.97 and 76.42% from poultry manure and NPK fertilizer mixture. They concluded that both organic and inorganic fertilizer mixtures are effective in the remediation of crude oil-contaminated soils (Gupta, 2020a, b; Basu et al. 2020; Yadav and Gupta, 2021, Ali et al. 2021, Mahajan et al. 2021, Kumar et al. 2021a, b). Thus, for an efficient bioremediation process to occur a competent microbe, water, oxygen and nutrients are vital parameters to be considered (Tyagi et al. 2011).

11.3 Description of the Study Site

The investigation was undertaken at a mechanic workshop located at western by-pass, Mechanic village in Bosso Local Government Area of Minna, Nigeria (Fig. 11.1). Minna lies between latitude 9° 40' N and longitude 6° 33' E of the Equator at an elevation of about 400 m above sea level, it falls within the southern Guinea Savanna vegetation zone with a sub-humid climate (Egharevba and Ibrahim 2006). Its climate is influenced mainly by the rain-bearing South West winds from the oceans and the dry dusty or harmattan North East winds (air masses) from the Sahara Desert (Musa et al. 2016). There are two main seasons; the rainy and the dry (harmattan). The rainy season starts in April and ends in October while the dry season commences in October /November and ends March. It has a mean annual rainfall of between 1038.3 and 1423.4 mm and a mean annual temperature of between 32° and 29° during the dry season (Mustapha 2010). The texture of the soil profile is an Alfisol and varied from sandy loam in the upper horizons to sandy clay in the deeper horizons with very low cation exchange capacity (Egharevba and Ibrahim 2006).

Horse manure and sawdust were collected from a stable and a carpentry workshop. Samples were collected in sacks and transported to the experimental site while NPK fertilizer was bought from a commercial dealer, all samples were collected in Minna, Nigeria.

Minna is the capital of Niger State, it is situated in the North Central Nigeria with a population of about 447, 959 (Minna's 2020 population; latest revision of UN World Urbanization Prospects) and Niger state with a land mass of 76, 363 km². It is severely faced with different types of environmental pollution problems that requires urgent attention.

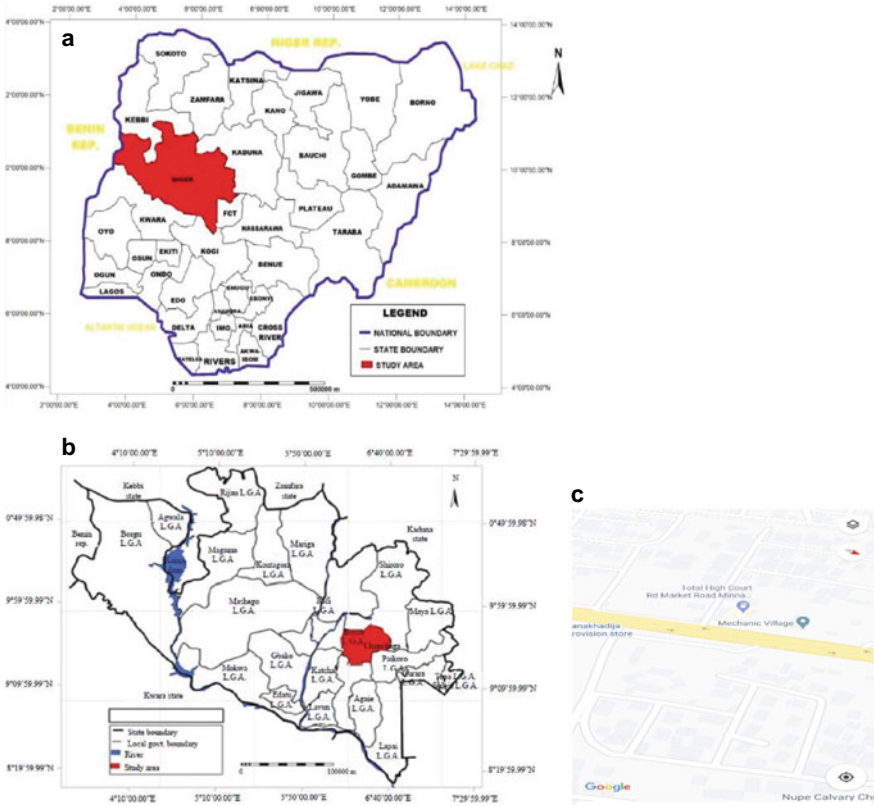


Fig. 11.1 Map of Nigeria showing Niger State **a** and Bosso Local Government Area **b** in red and **c** Goggle map of Mechanic village (the study area) in Minna, Bosso L.G.A, Niger State, Nigeria. *Source* (Oguh et al. (2019) for **a** and **b**

11.3.1 Experimental Design

A plot cell measuring 100 cm by 200 cm was used for this study, it was ploughed to a depth of 30 cm such that the depth and exposed surface area of the soil, its temperature, nutrient concentration, moisture content and oxygen availability, could be controlled. The plot cell was demarcated with the aid of pegs and ropes to avoid intrusion and interruption (Fig. 11.2). The experiment was conducted during the rainy season (June to September 2009) as such the plot cells received excess runoffs. This was unavoidable since the remediation study took place in the open air and therefore exposed to the rains.

The study consisted of three treatment cells: treatment cell A (engine oil contaminated + application of NPK fertilizer + horse manure + sawdust + tilling): received combined treatment of 4.2 kg of NPK fertilizer, 48 kg of sawdust and 448 kg of horse



Fig. 11.2 a. Engine oil contaminated soil at an auto mechanic workshop in Minna, Nigeria. Bio-stimulants used for the experiment are: b. Horse dung; c. NPK fertilizer and d. Sawdust. They are reported to add nutrients to the soil and improve the quality of the soil. Thus, application of the stimulants revived the engine oil contaminated soil back to useful value

manure during the remediation period; treatment cell B (engine oil contaminated soil + tilling): received tilling (aeration) and no amendment and treatment cell C (uncontaminated soil) which served as the control cell (i.e., did not receive any treatment and was also not affected by the activities of automobile repairs and maintenance).

11.3.2 Soil Characterization

The composite samples were air-dried, ground to fine particles, homogenized then passed through a 2 mm mesh sieve. The physiochemical parameters of the soils were measured according to standard methods, particle size analysis was determined by hydrometer method, total hydrocarbon content was determined by a photometric method using DR/4000 Spectrophotometer at a wavelength of 420 nm, pH and electrical conductivity were recorded using the conductivity meter. Organic carbon and organic matter content were determined by wet oxidation method and Walkley–Black acid digestion method respectively, chromium, cadmium and lead using the bulk atomic absorption spectrometer (AAS). Determination of available phosphorus

was calorimetric, potassium was by flame photometer, nitrogen content was determined by Kjeldahl digestion method and dilution plate method was used to determine soil microbial content.

11.3.2.1 Physiochemical Characterization of Contaminated and Uncontaminated Soils

The physiochemical qualities of treatment A, treatment B (engine oil contaminated soil + tilling) and treatment C (uncontaminated soil) are presented in Tables 11.3, 11.4 and 11.5. Treatment A soil was characterized with low moisture content, has a C: N of 13 which decreased to 2 during the degradation process. The soil pH was slightly acidic, it decreased at the end of the experiment, has low available nutrients thus inability to suit plant and animal lives (Table 11.3).

Over 70 days of treatment, treatment A soil showed an increment in its moisture content, organic matter and a decrease in organic carbon content (Table 11.3). The organic matter content ranged from 0.53 to 5.27%. The total organic matter increased when treatment began (1.78%) compared with the content before treatment and subsequently throughout the experiment. The total organic carbon content decreased from 5.85 to 1.03%. The nutrient (nitrogen, phosphorus and potassium) contents of the soil increased after the treatment and a decrease in the content was observed afterward toward the termination of the experiment.

Table 11.4 present the physicochemical qualities of the soil samples taken as untreated contaminated soil at the start-up (day 0) and termination (day 70) of the experiment. The pH of the untreated soil was slightly acidic at the start-up and alkaline at the termination of the experiment as well. The organic carbon content ranged from 5.85 to 3.20%, this decreased the C: N from 13.0 to 8.42%. This is an indication of natural attenuation of total petroleum hydrocarbon in the engine oil-polluted soils, implying slow degradation of the contaminants in the contaminated

Table 11.3 Soil physiochemical characteristics of treatment cell A (engine oil contaminated soil + NPK fertilizer + horse manure + sawdust + tilling) during 70 days of remediation

Parameters	Sampling period (days)					
	0	14	28	42	56	70
Moisture content (%)	6.50	8.70	11.20	12.40	14.10	16.30
pH	6.90	6.78	6.70	6.50	6.13	6.06
Organic carbon (%)	5.85	4.82	3.16	2.70	1.96	1.03
Organic matter (%)	0.53	1.78	2.32	3.04	4.53	5.27
Total Nitrogen (%)	0.45	0.66	0.60	0.55	0.53	0.51
Available Phosphorus (mg/kg)	0.17	2.18	2.06	1.73	1.70	1.55
Sodium (mg/kg)	0.32	0.67	0.60	0.74	0.42	0.36
Potassium (mg/kg)	0.12	0.91	0.30	0.44	0.20	0.17

Table 11.4 Physiochemical characteristic of untreated contaminated (control) site at start-up and endpoint

Parameters	Sampling period (days)	
	0	70
Moisture content (%)	6.50	8.20
pH	6.20	6.03
Organic carbon (%)	5.85	3.20
Organic matter (%)	0.53	3.74
Nitrogen (%)	0.45	0.38
Available phosphorus (mg/kg)	0.17	0.09
Sodium (mg/kg)	0.32	0.41
Potassium (mg/kg)	0.12	0.06
Total petroleum hydrocarbon (mg/kg)	3.23×10^3	2.42×10^3
Cadmium (mg/kg)	0.0464	0.0364
Chromium (mg/kg)	0.4215	0.4113
Lead (mg/kg)	0.6154	0.6030
Sand (%)	96.36	–
Silt (%)	3.9	–
Clay (%)	–0.156	–
Texture	Sandy clay	–

Table 11.5 Soil physiochemical characteristic of uncontaminated soil (control site)

Parameters	Soil	Horse dung	Sawdust
Moisture content (%)	30.0	45	10.80
Organic carbon (%)	7.50	40.47	60.00
Organic matter (%)	1.26	48.5	3.64
Nitrogen (%)	0.06	0.90	1.10
pH	5.90	6.68	5.95
Available phosphorus (mgkg ⁻¹)	2.10	18.70	10.22
Potassium (mgkg ⁻¹)	0.37	0.64	0.78
Lead (mgkg ⁻¹)	0.30	–	–
Chromium (mgkg ⁻¹)	0.0	–	–
Cadmium (mgkg ⁻¹)	0.0	–	–
Sand (%)	94.2	–	–
Silt (%)	5.28	–	–
Clay (%)	0.52	–	–
Texture	Sandy silt	–	–

soils by utilizing microorganisms. The untreated contaminated soils contained low nutrient concentrations (nitrogen, phosphorus and potassium).

The physicochemical characteristic of the uncontaminated soils is presented in Table 11.5 and it is classified as sandy silt with acidic pH, low nutrient (0.06–2.10 mg/kg) content, organic carbon and organic matter (1.26–7.50%) (Table 11.5). Soil pH can control the availability, mobility and toxicity of heavy metals in the soils. In this present study, the uncontaminated soil contained 0.30 mg/kg of lead while cadmium and chromium were not detected in the soil samples.

Horses are generally known to produce a large amount of manure. They have a high carbon to nitrogen ratio (Keskinen et al. 2017). For instance, the horse manure used for this study had a C: N of 40:1, their bedding may have mixed with their manure to contribute to a large amount of carbon. The horse dung had a 55% moisture content, this is ideal for microbial metabolism, 0.90% N, 0.64 and 18.70 mg/kg of K and P, respectively (Table 11.5).

Sawdust ash has been proven to be an effective organic fertilizer (Awodun 2007). The sawdust properties for this study are shown in Table 11.5 as 1.10% N, 10.22 mg/kg P, and 0.78 mg/kg K. It is also known to contain high content of oxygen (>33%) (Phonphuak and Chindapasirt 2015) and hydrogen (5.32%). Sawdust has a liming effect with a pH value of 5.95. The C: N ratio for the sawdust was 55.

11.3.2.2 Influence of Soil Physicochemical Parameters on Biostimulation Process

The physicochemical characteristics of soil indicate the health of soil (Benson et al. 2016). The engine oil-contaminated soil was slightly acidic at the inception of the experiment, this may be related to petroleum oil contaminants in polluted soil (Benson et al. 2016). Consequently, at the termination of the experiment, the pH of treated contaminated soils showed a decrease in acidity. This may be due to the effect of the addition of horse dung, sawdust, NPK fertilizer and aeration of the soil, indicative of a high rate of fertilization of the added nutrients (Singwane and Malinga 2012). In addition, organic manures have a buffering effect on petroleum-contaminated soils (Benson et al. 2016). The pH of a soil can also affect the physicochemical properties of the soil, thus, an increase in pH and a corresponding decrease in TPH was observed, which may have favored the microbial degradation of oil as well as aided organic matter breakdown and mineralization of carbon in the contaminated soil (Obasi et al. 2013). However, this was different for the controlled soil, with higher pH, lower organic matter content and lower degradation of TPH in the soil.

The contaminated soil showed low moisture content (Table 11.3), which is in agreement with the findings of Benson et al. (2016), they reported that oil-contaminated soils have water repellent property thereby making the soils to be water deficient. However, with the addition of the biostimulation agents, the moisture content improved. Also, the moisture content was within the range (12–25%) favorable for microbial growth, proliferation and metabolism (Tyagi et al. 2011; Abdulyekeen et al. 2016). Thus, these agents are capable of improving the soil's

physical and chemical conditions as well as aeration of the soils (Benson et al. 2016).

Soil organic carbon content was observed to have decreased with an increase in microbial growth and a corresponding decrease in the TPH concentrations. The degradation of TPH is due to the stimulated microbial growth which led to the synthesis of enzymes necessary for the degradation of the contaminants (Hamoudi-Belarbi et al. 2018). This decrease may also be attributed to the utilization of carbon as an energy source, mineralization of hydrocarbons and organic matter breakdown by the microorganisms present in the contaminated soils (Nduka et al. 2012). This was brought about by the conducive environmental conditions provided by biostimulation of the engine oil-contaminated soil; a pH close to neutrality with the availability of nutrients (Ebuehi et al. 2005; Obasi et al. 2013; Benson et al. 2016), adequate supply of oxygen and increased moisture content (Hamoudi-Belarbi et al. 2018).

Soils contaminated with oil are limited in soil nitrogen, phosphorus and oxygen (due to the hydrophobic properties of oil) as well as an increase in carbon content (Obasi et al. 2013; Abdulyekeen et al. 2016). This is in line with this present study, lower nutrient was observed in the contaminated soil and consequently, the nutrient content increased with lower TPH towards the end of the experiment (Fig. 11.3) with horse dung, sawdust and NPK fertilizer amendment. The soil organic matter content of the treated contaminated soil was improved, nutrient and moisture content of the soil increased as well as the microbial activities, showing an improvement in physical, chemical and biological properties of the treated contaminated soil (Table 11.1; Figs. 11.1 and 11.2; Singwane and Malinga 2012).

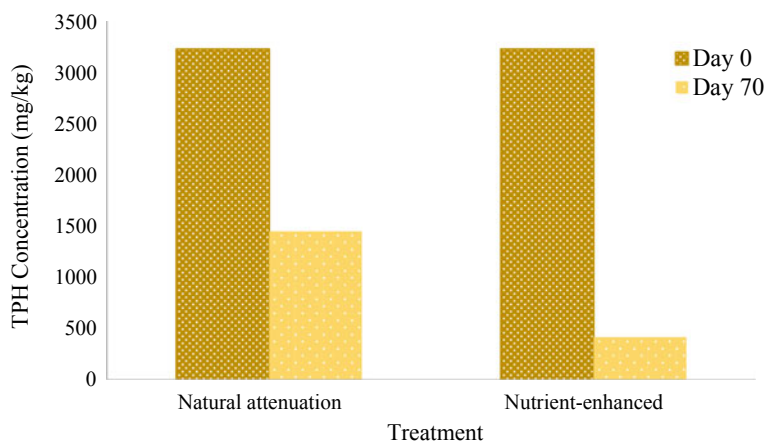


Fig. 11.3 Bioremediation of Total petroleum hydrocarbon (TPH) in engine oil-contaminated soil. Nutrient-enhancement (biostimulation) of the contaminated soil was more effective compared to the naturally attenuated technique during the 70 days of remediation. Biostimulation is aimed at enhancing the activities of the indigenous microorganisms that are capable of degrading hydrocarbons in oil-contaminated soils

11.3.3 Bioremediation Procedure

The engine oil contaminated soil was tilled to a depth of 15 cm and the lumps were broken to fine particles to increase the surface area with the aid of digger, shovel and rake (on day 0) and allowed for three days in an open-air for proper aeration and to activate the soil microorganisms (composite samples were taken for analysis). The composite samples consisted of 5 sub-samples taken at equally spaced intervals within the collection treatment cells. On day 4, 1 kg of NPK fertilizer was applied to the treatment cells at the rate of 1 kg of NPK fertilizer per 2 m² of soil surface. NPK: 20.20.10 fertilizer was selected for its relatively high nitrogen content and availability in the market. Plots were tilled again to incorporate these materials to the depth of 15 cm. On day 14, approximately 48 and 448 kg of a mixture of dry sawdust and horse manure were applied once to the plot cells, covering the plot cell to a depth of 10 cm or deeper and then tilled into the soil (composite samples were taken for analysis). On day 28 (4th week of remediation), soils were tilled before the collection of composite samples. 5 g of these composite soil samples were collected as described by Abioye et al. (2009). Following sample collection, NPK fertilizer was applied at the rate of 1 kg/m² to the plot cells and then tilled to mix nutrients and aerate. The soil plot was tilled every two days for proper aeration and to avoid compaction to generate an aerobic condition that can enhance the activities of aerobic micro-organisms. The third composite samples were taken on day 42, after tilling to a depth of 30 cm to identify any possible deep leaching of hydrocarbons. NPK fertilizer was applied at the rate of 0.6 kg/m² and tilled into the soil. Subsequently, other composite samples were taken on day 56 and finally on day 70 for isolation and enumeration of heterotrophic bacteria and determination of total petroleum hydrocarbon. The samples for the total hydrocarbon content (THC) measurements were placed in one-litre glass bottle and sealed with aluminum foil. This procedure was undertaken three times. The bags and glasses were immediately transferred to the laboratory for analysis.

11.3.3.1 Determination of Total Hydrocarbon Content

The total petroleum hydrocarbon content in engine oil contaminated soil was determined as described in Abioye et al. (2009). 10 g of soil samples were weighed into a volumetric flask and 20 mL of toluene was added. The mixture was then placed on an orbital shaker for 30 min, and the liquid phase measured at 420 nm using DR/4000 Spectrophotometer. The total petroleum hydrocarbon (TPH) in soil was estimated with reference to a standard curve derived from fresh used lubricating oil diluted with toluene.

The degree of degradation (D) was calculated using the equation from Ofoegbu et al. (2015):

$$\% D = \frac{\text{Initial TPH content, mg/kg} - \text{Residual TPH content, mg/kg}}{\text{Initial TPH concentrations, mg/kg}} \times 100 \quad (11.1)$$

The biostimulation efficiency (BE) of treatment A and treatment B was calculated using the equation from Ofoegbu et al. (2015):

$$\%BE = \frac{\%TPH_{(T)} - TPH_{(U)}}{TPH_{(T)}} \quad (11.2)$$

Where % TPH $_{(T)}$ is the percentage removal of TPH in biostimulated soil and % TPH $_{(U)}$ is the percentage removal of TPH in unbiostimulated soil.

The equation for net % loss in TPH was adopted from Agamuthu et al. (2013).

$$\text{Net \% loss} = \% \text{ loss in TPH of engine oil contaminated soil with combined treatment} \\ - \% \text{ loss in TPH of untreated soil} \quad (11.3)$$

11.3.3.2 Biodegradation of Engine-Oil Contaminated Soils

The degradation of total petroleum hydrocarbon (TPH) in engine oil contaminated soil was investigated over 70 days. This is illustrated in Fig. 11.3. The figure showed high degradation of TPH in the nutrient-enhanced treatment (contaminated soils + horse manure + NPK fertilizer + sawdust + tilling) compared to the natural attenuated (contaminated soil + tilling) treatment. Furthermore, the nutrient-enhanced treatment showed an 87% degradation while the natural-attenuated treatment showed a 55% reduction and a net percentage oil loss of 31.95% at the termination of the experiment.

11.3.4 Efficacy of Biostimulation Process

Bioremediation of engine oil contaminated soil with indigenous microorganisms stimulated with a combination of NPK fertilizer, horse manure, sawdust application and tillage was more effective compared to the natural attenuation (Table 11.2 and Figs. 11.1, 11.2, 11.3 and 11.4). Thus, the addition of NPK fertilizer, horse manure, sawdust increased the nutrient contents of the engine oil contaminated soil, hence the increase in microbial growth and activities and therefore restoring the engine oil-contaminated soil. The contaminated soil had a TPH concentration of 3230 mg/kg at inception, after 28 days of treatment with organic and inorganic stimulants, there was a 52% TPH in the contaminated soil. Subsequently, at days 56 and 70, there were 82 and 87% TPH removal while the natural attenuation treatment system had total removal of 55% TPH. The biostimulation efficiency (BE) and the net loss of the

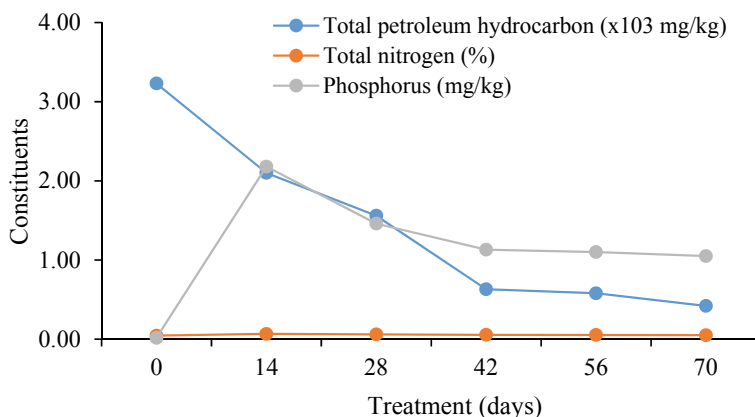


Fig. 11.4 Effects of nutrients on the treatability of TPH in engine oil-contaminated soil

nutrient-enhanced and natural attenuation treatment systems were 36.78 and 31.95%, respectively.

11.3.4.1 Total Petroleum Hydrocarbon

The level and toxicity of petroleum oil-contaminated soils can be determined by the content of TPH in the soil (Benson et al. 2016). Biostimulation of the contaminated engine oil soils was restored by the addition of organic (horse manure and sawdust), inorganic (NPK fertilizer) and tilling of the contaminated soil. This observation is illustrated in Fig. 11.4. The nutrient-enhanced treated soils (treatment A) had higher degradation of TPH than the naturally attenuated treated soil (treatment B). This is particularly due to the nutrient contents of the manure and fertilizer. This observation is in agreement with the findings of Agamuthu et al. (2013), Benson et al. (2016); Ebuehi et al. (2005) and Obasi et al. (2013). Agamuthu et al. (2013) reported accelerated biodegradation of petroleum in soil with the addition of N and P to an oil-polluted soil. Abdulyekeen et al. (2016) achieved 84 and 79% degradation of oil and grease in soil contaminated with used motor oil after 6 weeks of biostimulating with elephant and horse dung. Similarly, Onuoha (2013) reported a 79.2, 81.6, 92.6 and 97.8% for unamended control soil, cow dung amended soil, poultry amended soil and goat dung amended soil respectively after six months for soil contaminated with 5000 mg/kg (0.5%) spent oil.

Furthermore, the degradation of TPH in both the nutrient-enhanced treatment and the natural-attenuated treatment may be related to the fact that tropical soils have a high rate of decomposition (Singwane and Malinga 2012). Also, as reported by Tyagi et al. (2011) temperature can influence the growth and degradation potentials of microorganisms as well as the physical and chemical composition of the oil.

There was a decrease in TPH content and a corresponding increase then a decrease in the nutrient content. The decrease in the nutrient content may be due to the utilization of the nutrient by the microorganisms in the contaminated soil. In addition, Isitekhale et al. (2013) also reported a 75% hydrocarbon degradation in crude oil contaminated soil 2 weeks after the application of chicken manure.

Petroleum-contaminated soils are characterized by low nutrients. The contaminated soils were stimulated by organic and inorganic stimulants, the figure showed an increase in nutrients then a decline in the available nutrients, this is likely to happen when a microbial community begins to degrade contaminants.

11.3.4.2 Total Heterotrophic Bacteria in Engine-Oil Contaminated Soil

Figure 11.5 present the effects of reduction of contaminants in contaminated soil on the growth of total heterotrophic bacteria. At the start-up of the experiment, total heterotrophic bacteria (THB) was 0.018×10^6 CFU /g in the engine-oil contaminated soil and the uncontaminated soil sample had a bacteria count of 1.22×10^6 CFU/g. On day 28 of the experimentation period, THB had increased to 2.26×10^6 CFU /g with a corresponding decrease in TPH (1.56×10^3 mg/kg). Similarly, on day 42, lower TPH and lower THB were observed, and at the termination of the experiment, lower TPH corresponded to increased THB.

The engine oil-contaminated soils showed a low presence of microorganisms (Fig. 11.5). There was an increase in the microbial population of the treated engine oil-contaminated soils over time. There was more THB count in the nutrient-enhanced treatment compared to the natural-attenuated treatment, owing to the presence of

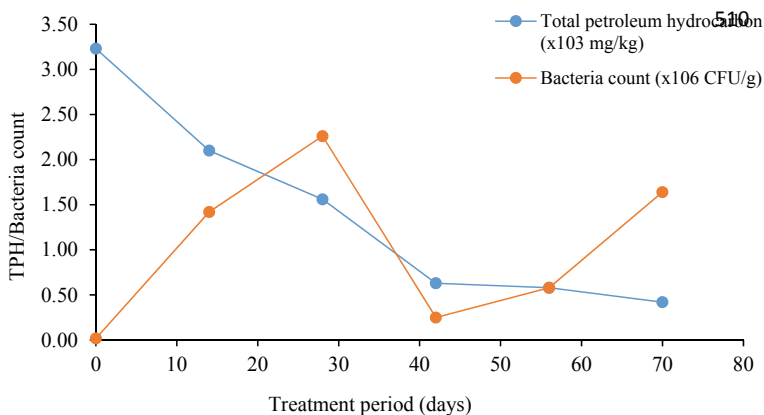


Fig. 11.5 Effects of biodegradation on reduction of total petroleum hydrocarbon and growth of total heterotrophic bacteria in treatment cell. The bioremediation of total petroleum hydrocarbon is shown to be effective with continuous reduction of the TPH compounds during the period of remediation. Meanwhile, there was a growth of the indigenous microorganisms then a decline and then a gradual increment in the microbial biomass. However, this did not affect the remediation process

macro and microelements (N, P, K, Cu and Zn) in the combined manure (Agamuthu et al. 2013) which could have stimulated microbial growth in the contaminated soil. Also, an increase in THU is indicative of increased biodegradation as observed by Ebuehi et al. (2005). They achieved a decrease in TPH, nitrogen and phosphorus from crude oil-contaminated soil amended with fertilizer and aeration from 1.10×10^4 mg/kg, 24,6 mg/kg and 22.8 mg/kg to 300, 0,12 and 1.7 mg/kg, respectively for TPH, nitrogen and phosphorus after 10 weeks of remediation by natural attenuation of crude oil contaminated sandy soil. Similarly, Benson et al. (2016) recorded a higher presence of total heterotrophic bacteria (THB) and hydrocarbon utilizing bacteria after amendment with cow dung in crude oil-contaminated soil. In addition, increasing the amount of nitrogen and phosphorus in soil under aerobic conditions increased the activities of the indigenous microorganisms consequently increasing the degradation of TPH to carbon and water (Abioye 2011; Ebuehi et al. 2005). Thus, N and P are very important nutrients needed by hydrocarbon utilizing bacteria to carry out effective and efficient biodegradation of petroleum contaminants (Agamuthu et al. 2013).

11.3.4.3 Fate of Heavy Metals in Treatment Cells

Figure 11.6 presents the reduction in heavy metal concentrations in used engine oil contaminated soils amended with horse dung, NPK fertilizer, sawdust and tilling. On day 0, Cr, Cd and Pb were relatively low in the engine-oil contaminated soil (Fig. 11.6). Gradually, there was a decrease in the concentration of Pb and Cd and an increase in Cr concentration in the treated soil towards the termination of the experiment. The treatment cell A showed 71 and 64% Cd and Pb removal, respectively while Cr showed adsorption onto the soil particles of the treatment.

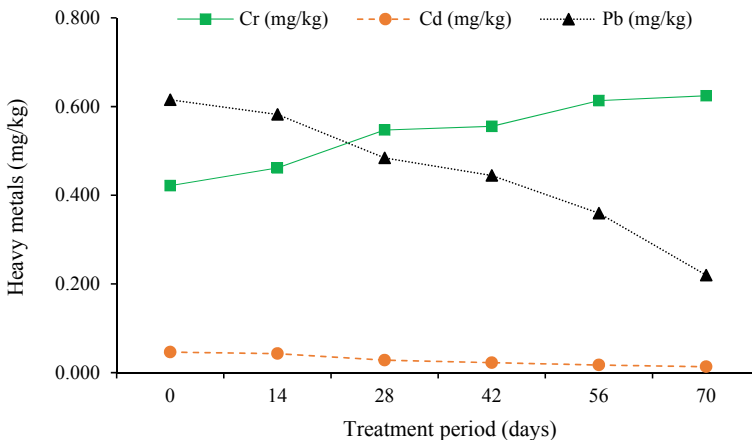


Fig. 11.6 Change in heavy metal concentration during biostimulation process

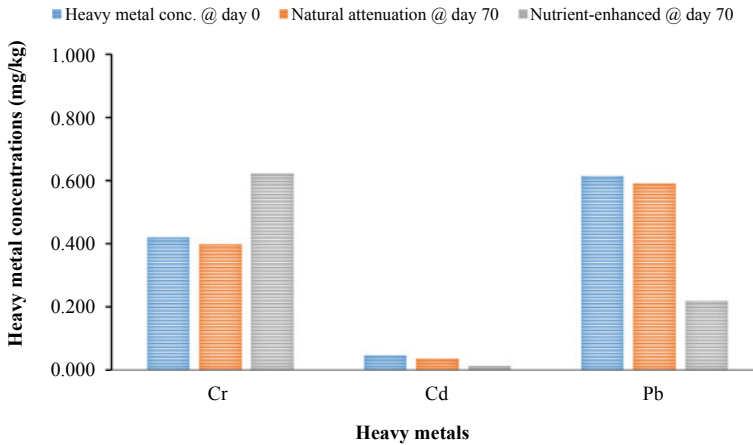


Fig. 11.7 Fate of heavy metals in treatment cells. Cd and Pb were reduced in the natural attenuated and nutrient enhanced systems. Cr showed an increased concentration, this may be as a result of both anthropogenic and natural processes

Figure 11.7 presents the heavy metal concentrations in the treatment cell soils at the start-up and termination of the experiment. The heavy metal concentrations in the soils of the treatment cells at the start-up of the treatment were in the order of $Pb > Cr > Cd$ and at the termination of the experiment the order was $Cr > Pb > Cd$. The concentrations were relatively low and Pb had the highest concentration (0.615 mg/kg).

Cd and Pb were removed/treated in the engine-oil contaminated soil while Cr was shown increasing in concentration.

The fate of heavy metals and their transport in soils depends on their chemical form and speciation (Evanko and Dzombak 1997). Evanko and Dzombak (1997) stated that primary processes influencing the fate of Pb in soil include adsorption, ion exchange, precipitation and complexation with sorbed organic matter, these processes limit the amount of Pb that can be transported into surface water or groundwater and Cr mobility depends on sorption characteristics of the soil, including clay content, iron oxide content and the amount of organic matter present while Cd removal is by sorption which is influenced by cation exchange capacity of clays, carbonate minerals, and organic present in soils and sediment. Heavy metal removal mechanisms include sedimentation, flocculation, absorption and cations and anion exchange, complexation, precipitation, oxidation/reduction, microbiological activity and uptake (Shafik 2008; Ojuederie and Babalola 2017). Metals are more soluble in acidic pH, hence toxicity problems are more severe in acidic soil than alkaline soil (Damodaran et al. 2011). The study site was slightly acidic, with low concentrations of Cd, Pb and Cr. These were found to be within the threshold limits of 50 mg Cr/kg, 100 mg Pb/kg and 2 mg Cd/kg (Fabiatti et al. 2010).

There was a decrease in Cd and Pb concentrations corresponding to a 71 and 64% removal respectively during the course of bioremediation of the engine-oil contaminated soil, while the natural attenuation had a removal efficiency of 22 and 4% respectively for Cd and Pb this may have been influenced by amendment with organic and inorganic biostimulants. In contrast to no Cr removal in the nutrient-enhanced bioremediation, natural attenuation had a 5% Cr removal efficiency.

Meanwhile, the release of Cr in the process of bioremediation of the engine oil-contaminated soils was observed. This release may be attributed to the application of organic and inorganic stimulants. These findings are supported by Wuana and Okieimen (2011), who reported that application of numerous biosolids (e.g., livestock manures, composts, and municipal sewage sludge) to land can unintentionally lead to the accumulation of heavy metals such as Cd, Cr, Cu, Pb, Hg, Ni and Zn in the soil. Also, the release of Cr in the treated soil may be related to microbial degradation of Cr(IV) to nontoxic immobile Cr(III) in either aerobic or anaerobic conditions in the soil (Das and Mishra 2010).

Phytoremediator plant species have a unique ability to extract and transport metals from substrates to plant parts (Kumar et al. 2013). Therefore, the presence of macrophytes can play an important role in effectively removing Cr from polluted water and soil. Effective treatment of Cr in plant-assisted bioremediation (phytoremediation) of secondary treated refinery wastewater was reported by Mustapha et al (2018c). Thus, phytoremediation and biostimulation can be used as complementary techniques for the remediation of used engine oil-contaminated soils.

11.4 Conclusions

- Biostimulating agents (horse dung and sawdust) are cheap, environmentally friendly, are widely available, and are capable of stimulating indigenous microorganisms in enhancing mineralization of hydrocarbons and bioaccumulation of heavy metals in engine oil-contaminated soils, therefore, restoring the contaminated soil.
- Horse dung and sawdust were able to improve the engine oil-contaminated soil and also added nutrients to the soil. The results showed positive effects of combining horse manure, sawdust, NPK fertilizer and tilling in enhancing remediation of engine oil contaminated soil compared to the contaminated un-amended soil with only tilling (natural attenuation), with the nutrient-enhanced treatment showing a higher degradation of TPH (87%) than the natural attenuated treatment (40%).
- Biostimulation of used engine oil contaminated soil improved the physicochemical properties of the soils, hence stimulated the growth and metabolism of indigenous soil microbes, thus enhancing the degradability potentials of the microbes.
- More researches should be dedicated to environmental management issues such as the extent of soil contamination and effects on crop production and productivity, particularly in affected communities.

- The problem of petroleum contamination will continue to linger on as we continue to depend on fossil fuel, therefore, more researches in the area of bioenergy/biofuel should be sponsored. This is expected to reduce environmental threats and health implications.

References

- Abbas OO, Brack W (2006) Polycyclic aromatic hydrocarbons in Niger Delta soil: contamination sources and profiles. *Int J Environ Sci Technol* 2(4):343–352. <https://doi.org/10.1007/BF03325895>
- Abduleykeen KA, Muhammad IM, Giwa SO, Abdulsalam S (2016) Bioremediation of used motor oil contaminated soil using elephant and horse dung as stimulants. *IOSR J Environ Sci Toxicol Food Technol* 10(12):73–78. Retrieved from www.iosrjournals.org
- Abioye OP, Agamuthu P, Abdul Aziz AR (2008) Phytotreatment of soil contaminated with used lubricating oil using *Hibiscus cannabinus*. *Biodegradation* 19(4):1–12. <https://doi.org/10.1007/s10532-011-9506-9>
- Abioye PO (2011) Biological remediation of hydrocarbon and heavy metals contaminated soil. In: Pascucci S, Pascucci S (eds) *Soil contamination*. InTech, London. <https://doi.org/10.5772/927>
- Abioye PO, AbdulAziz A, Agamuthu P (2009) Enhanced biodegradation of used engine oil in soil amended with organic wastes. *Water Air Soil Pollut* 1–7. <https://doi.org/10.1007/s11270-009-0189-3>
- Abou-Shanab R, Ghanem N, Ghanem K, Al-Kolaibe A (2007) Phytoremediation potential of crop and wild plants for multi-metal contaminated soils. *Res J Agric Biol Sci* 3(5):370–376
- Achile GN, Yillian L (2010) Mineralization of organic compounds in wastewater contaminated with petroleum hydrocarbon using Fenton's reagent: a kinetic study. *Am J Sci* 6(4):58–66. Retrieved from <http://www.americanscience.org>
- Adamu CI, Nganje TN (2010) Heavy metal contamination of surface soil in relationship to land use patterns: a case study of Benue State, Nigeria. *Mater Sci Appl* 1:127–134. <https://doi.org/10.4236/msa.2010.13021>
- Adeniyi AA, Afolabi JA (2002) Determination of total petroleum hydrocarbons and heavy metals in soils within the vicinity of facilities handling refined petroleum products in Lagos metropolis. *Environ Int* 28(1–2):79–82. [https://doi.org/10.1016/S0160-4120\(02\)00007-7](https://doi.org/10.1016/S0160-4120(02)00007-7)
- Agamuthu A, Tan YS, Fauziah SH (2013) Bioremediation of hydrocarbon contaminated soil using selected organic wastes. *Procedia Environ Sci* 18:694–702. <https://doi.org/10.1016/j.proenv.2013.04.094>
- Al-Baldawi IA, Abdullah SR, Abu Hasan H, Suja F, Anuar N, Mushrifah I (2014) Optimized conditions for phytoremediation of diesel by *Scirpus grossus* in horizontal subsurface flow constructed wetlands (HSFCWs) using response surface methodology. *J Environ Manage* 140:152–159. <https://doi.org/10.1016/j.jenvman.2014.03.007>
- Aleer S, Adetutu EM, Makadia TH, Patil S, Ball AS (2011) Harnessing the hydrocarbon-degrading potential of contaminated soils for the bioremediation of waste engine oil. *Water Air Soil Pollut* 218:121–130. <https://doi.org/10.1007/s11270-010-0628-1>
- Ali H, Khan E, Sajad MA (2013) Phytoremediation of heavy metals—concepts and applications. *Chemosphere* 91:869–881. <https://doi.org/10.1016/j.chemosphere.2013.01.075>
- Ali Y, Zarka Z, Baba Z, Gupta PK, Hamid B (2021) World trend of pesticide consumption and assessment of pesticide toxicity on earthworms using different biomarkers. *Environ Chem Lett* 1–24

- Ashokkumar B, Jothiramalingam S, Thiyagarajan SK, Hildhayathullakhan T, Nalini R (2014) Removal of heavy metals from contaminated soil using phytoremediation. *Int J Chem Phys Sci* 3(5):88–94
- Aslam MM, Malik M, Baig M, Qazi I, Iqbal J (2007) Treatment performances of compost-based and gravel-based vertical flow wetlands operated identically for refinery wastewater treatment in Pakistan. *Ecol Eng* 3:34–42. <https://doi.org/10.1016/j.ecoleng.2007.01.002>
- Awodun MA (2007) Influence of sawdust ash on soil chemical properties and cowpea performance in southwest Nigeria. *Int J Soil Sci* 2(1):78–91
- Basu S, Yadav BK, Mathur S, Gupta PK (2020) In situ bioremediation of LNAPL polluted vadose zone: integrated column and wetland study. *CLEAN—Soil Air Water* 2000118
- Belmont MA, Cantellano E, Thompson S, Williamson M, S´anchez A, Metcalfe CD (2004) Treatment of domestic wastewater in a pilot-scale natural treatment system in central Mexico. *Ecol Eng* 23:299–311. <https://doi.org/10.1016/j.ecoleng.2004.11.003>
- Benson DM, Ochekwu EB, Tanee F (2016) Enhancement of crude oil polluted soil by applying single and combined cow-dung and hydrogen peroxide as remediating agents. *J Appl Sci Environ Manag* 20(4):1137–1145
- Chen M, Xu P, Zeng GZ, Yang C, Huang D, Zhang J (2015) Bioremediation of soils contaminated with polycyclic aromatic hydrocarbons, petroleum, pesticides, chlorophenols and heavymetals by composting: applications, microbes and future research needs. *Biotechnol Adv* 33:745–755. <https://doi.org/10.1016/j.biotechadv.2015.05.003>
- Chen TY, Kao CM, Yeh TY, Chien HY, Chao AC (2006) Application of a constructed wetland for industrial wastewater treatment: a pilot scale study. *Chemosphere* 64:497–502. <https://doi.org/10.1016/j.chemosphere.2005.11.069>
- Chindo SY (2016) Determination of some heavy metals in dumpsite soil and abelmoschus esculentus fruit grown near dumpsites in Kafanchan metropolis, Kaduna state, Nigeria. Ahmadu Bello University, Zaria, Department of Chemistry. Zaria: Ahmadu Bello University, Zaria
- Damodaran D, Suresh G, Raj MB (2011) Bioremediation of soil by removing heavy metals using *Saccharomyces cerevisiae*. In: 2011 2nd International conference on environmental science and technology, vol. 6. Singapore: IPCBEE, pp. V2–22–27
- Das AP, Mishra S (2010) Biodegradation of the metallic carcinogen hexavalent chromium Cr(IV) by an indigenous isolated bacterial strain. *J Carcinogen* 9:6. <https://doi.org/10.4103/1477-3163.63584>
- Ebuehi OA, Abibo IB, Shekwolo P, Sigismund K, Adoki A, Okoro IC (2005) Remediation of crude oil contaminated soil by enhanced natural attenuation technique. *J Appl Sci Environ Manag* 9(1):103–106
- Egharevba NA, Ibrahim H (2006) Prediction of sediment yield in runoff from agricultural land in the Southern Guinea Savannah Zone of Nigeria. *West African J Appl Ecol* 10:131–138
- Evanko CR, Dzombak DA (1997) Remediation of metals-contaminated soils and groundwater. Ground-Water Remediation Technologies Analysis Center (GWRTAC), Pittsburgh, PA. Retrieved from <http://www.gwrtac.org>
- Fabiatti G, Biasioli M, Barberis R, Ajmone-Marsan F (2010) Soil contamination by organic and inorganic pollutants at the regional scale: the case of Piedmont, Italy. *J Soils Sediments* 10:290–300. <https://doi.org/10.1007/s11368-009-0114-9>
- Garbisu C, Alkorta I (2003) Basic concepts on heavy metal soil bioremediation. *Europ J Mineral Proc Environ Protect* 3(1):58–66
- Gupta PK (2020a) Fate, transport and bioremediation of biodiesel and blended biodiesel in subsurface environment: a review. *ASCE J Environ Eng* 146(1):03119001
- Gupta PK (2020b) Pollution load on Indian soil-water systems and associated health hazards: a review. *ASCE J Environ Eng* 146(5):03120004
- Gupta PK, Sharma D (2018) Assessments of hydrological and hydro-chemical vulnerability of groundwater in semi-arid regions of Rajasthan, India. *Sustain Water Resour Manag* 1(15):847–861

- Gupta PK, Gharedaghloo B, Lynch M, Cheng J, Strack M, Charles TC, Price JS (2020) Dynamics of microbial populations and diversity in NAPL contaminated peat soil under varying water table conditions. *Environ Res* 191:110167
- Hamoudi-Belarbi L, Hamoudi S, Belkacemi K, Nouri L, Bendifallah L, Khodja M (2018) Bioremediation of polluted soil sites with crude oil hydrocarbons using carrot peel waste. *Environments* 5(124):1–12. <https://doi.org/10.3390/environments5110124>
- Hamza UD, Mohammed IA, Sale A (2012) Potentials of bacterial isolates in bioremediation of petroleum refinery wastewater. *J Appl Phytotechnol Environ Sanitat* 1(3):131–138. Retrieved from <http://www.trisanita.org/japes>
- Hazra M, Avishek K, Pathak G (2011) Developig an artificial wetland system for wastewater treatment: a designing perspective. *Int J Environ Protect* 1(1):8–18. Retrieved July 24, 2016, from www.ijep.org
- Idzi AA, Abdullahi S, Paul I, Shekwonyadu I (2013) Chemical composition analysis of soil from selected oil producing communities in the Niger Delta region of Nigeria. *Int J Basic Appl Chem Sci* 3(1):84–92. Retrieved from <http://www.cibtech.org/jcs.htm>
- Isitekhale HH, Aboh SI, Edion RI, Abhanziyoa MI (2013) Remediation of crude oil contaminated soil with inorganic and organic fertilizer using sweet potato as a test crop. *J Environ Earth Sci* 3(7):116–121
- Keskinen R, Saastamoinen M, Nikama J, Sarkijarvi S, Myllymaki M, Salo T, Uusi-Kamppa J (2017) Recycling nutrients from horse manure: effects of bedding type and its compostability. *Agric Food Sci* 26:68–79
- Kumar N, Bauddh K, Kumar S, Dwivedi N, Singh D, Barman S (2013) Accumulation of metals in weed species grown on the soil contaminated with industrial waste and their phytoremediation potential. *Ecol Eng* 491–495. <https://doi.org/10.1016/j.ecoleng.2013.10.004>
- Kumar R, Gupta PK, Jha PK, Sharma P, Singh RP, Prasad V (2021a) Bioaccumulation of fluoride in plants and its microbially-associated re-mediation: a review of physical processes and technology performance. *Processes* 9(12):2154
- Kumar R, Sharma P, Verma A, Jha PK, Singh P, Gupta PK, Chandra R, Prasad PVV (2021b) Effect of physical characteristics and hydrodynamic conditions on transport and deposition of microplastics in riverine ecosystem. *Water* 13:2710
- Lin Q, Mendelsohn IA (2009) Potential of restoration and phytoremediation with *Juncus roemerianus* for diesel-contaminated coastal wetlands. *Ecol Eng* 35(1):85–91. <https://doi.org/10.1016/j.ecoleng.2008.09.010>
- Mahajan M, Singh A, Gupta PK, Vaish B, Singh RP, Kothari R (2021) A comprehensive study on aquatic chemistry, health risk and remediation techniques of cadmium in groundwater. *Sci Total Environ*. <https://doi.org/10.1016/j.scitotenv.2021.151784>
- Marrot B, Barrios-Martinez A, Moulin P, Roche N (2006) Biodegradation of high phenol concentration by activated sludge in an immersed membrane bioreactor. *Biochem Eng J* 30:174–183. <https://doi.org/10.1016/j.bej.2006.03.006>
- Mazzeo DE, Levy CE, de Angelis DD, Marin-Morales MA (2010) BTEX biodegradation by bacteria from effluents of petroleum refinery. *Sci Total Environ* 4334–4340. <https://doi.org/10.1016/j.scitotenv.2010.07.004>
- Musa JJ, Bala JD, Mustapha HI, Musa ET, Yerima I, Daniel SE, Akos M (2018) Longitudinal and transverse mobility of Some heavy metals on receiving soils of dumpsites in Niger State, Nigeria. *ABUAD J Eng Res Dev* 393–398. Retrieved from www.ajerd.abuad.edu.ng/
- Musa JJ, Mustapha HI, Yerima YI, Kuti IA, Abogunrin ME (2016) Evaluation of irrigation efficiency: case study of Chanchaga irrigation scheme. *Arid Zone J Eng Technol Environ* 12:58–64. www.azojete.com.ng
- Mustapha HI (2010) Water quality assessment of river Chanchaga, Minna, Nigeria for irrigation purposes. In: 10th International conference of Nigeria Institution of Agricultural Engineers, vol 30. Enugu: NIAE, pp 304–309
- Mustapha HI (2018) Treatment of petroleum refinery wastewater with constructed wetlands. Wageningen University and IHE Delft, Institute for Water Education, Delft, the Netherlands,

- Environmental Engineering and Water Technology. Leiden: CRC Press/Balkema. <https://doi.org/10.18174/444370>
- Mustapha HI, Adeboye BO (2014) Heavy metals accumulation in edible part of vegetables irrigated with untreated municipal wastewater in tropical savannah zone, Nigeria. *Afr J Environ Sci Technol* 8(8):460–463. <https://doi.org/10.5897/AJEST2013.1531>
- Mustapha HI, Lens P (2018) Constructed wetlands to treat petroleum wastewater. In: Prasad R, Aranda E, Aranda RP (eds), *Approaches in bioremediation, the new Era of environmental microbiology and nanobiotechnology*, 1st edn. Springer Nature, Switzerland AG, pp 1–403. https://doi.org/10.1007/978-3-030-02369-0_10
- Mustapha HI, Gupta PK, Yadav BK, van Bruggen J, Lens P (2018a) Performance evaluation of duplex constructed wetlands for the treatment of diesel contaminated wastewater. *Chemosphere* 205:166–177. <https://doi.org/10.1016/j.chemosphere.2018.04.036>
- Mustapha HI, van Bruggen HJ, Lens PN (2018b) Vertical subsurface flow constructed wetlands for the removal of petroleum contaminants from secondary refinery effluent at the Kaduna refining plant (Kaduna, Nigeria). *Environ Sci Pollut Res* 25(30):30451–30462. <https://doi.org/10.1007/s11356-018-2996-9>
- Mustapha HI, van Bruggen JJ, Lens PN (2018c) Fate of heavy metals in vertical subsurface flow constructed wetlands treating secondary treated petroleum refinery wastewater in Kaduna Nigeria. *Int J Phytoremed* 20(1):44–56. <https://doi.org/10.1080/15226514.2017.1337062>
- Mustapha HI, van Bruggen JJ, Lens PN (2018d) Optimization of petroleum refinery wastewater treatment by vertical flow constructed wetlands under tropical conditions: plant species selection and polishing by a horizontal flow constructed wetland. *Water Air Soil Pollut* 229:137–154. <https://doi.org/10.1007/s11270-018-3776-3>
- Nduka JK, Umeh LN, Okerulu IO, Umedum LN, Okoye HN (2012) Utilization of different microbes in bioremediation of hydrocarbon contaminated soils stimulated with inorganic and organic fertilizers. *Petrol Environ Biotechnol* 3(116):1–9. <https://doi.org/10.4172/2157-7463.1000116>
- Nkwoada AU, Alisa CO, Amakom CM (2018) Pollution in Nigerian auto-mechanic villages: a review. *IOSR J Environ Sci Toxicol Food Technol* 12(7 Ver I):43–54
- Obasi NA, Eze E, Anyanwu DI, Okorie U (2013) Effects of organic manures on the physicochemical properties of crude oil polluted soils. *Afr J Biochem Res* 7(6):67–75. <https://doi.org/10.5897/AJB R11.113>
- Odewande AA, Abimbola AF (2008) Contamination indices and heavy metal concentrations in urban soil of Ibadan metropolis, southwestern Nigeria. *Environ Geochem Health* 30(3):243–254. <https://doi.org/10.1007/s10653-007-9112-2>
- Ofoegbu RU, Momoh YO, Nwaogazie IL (2015) Bioremediation of crude oil contaminated soil using organic and inorganic fertilizers. *J Pet Environ Biotechnol* 6(1):1–6. <https://doi.org/10.4172/2157-7463.1000198>
- Oguh CE, Chima UC, Wisdom OO, Ugwu CV, Tochi AP, Blessing OC, Kelechi E (2019) Risk assessment on bioaccumulation of potentially toxic elements on soil and edible vegetables *Corchorus olitorius* and *Amaranthus cruentus* grown with water treatment sludge in Chanchaga Minna, Niger state, Nigeria. *J Res Environ Sci Toxicol* 8(2):92–103. <https://doi.org/10.14303/jrest.2019.033>
- Ogundiran MB, Osibanjo O (2008) Heavy metal concentrations in soils and accumulation in plants growing in a deserted slag dumpsite in Nigeria. *Afr J Biotechnol* 7(17):3053–3060. Retrieved from <http://www.academicjournals.org/AJB>
- Ogunfowokan AO, Asubiojo OI, Fatoki O (2003) Isolation and determination of polycyclic aromatic hydrocarbons in surface runoff and sediments. *Water, Air, Soil Pollution* 147(1):245–261. <https://doi.org/10.1023/A:1024573211382>
- Oh K, Cao T, Li T, Cheng H (2014) Study on application of phytoremediation technology in management and remediation of contaminated soils. *J Clean Energy Technol* 2(3):216–220. <https://doi.org/10.7763/JOCET.2014.V2.126>
- Ojuederie OB, Babalola OO (2017) Microbial and plant-assisted bioremediation of heavy metal polluted environments: a review. *Int J Environ Res Public Health* 14:1504–1530. <https://doi.org/10.3390/ijerph14121504>

- Onianwa PC, Jaiyeola OM, Egekenze RN (2003) Heavy metals contamination of topsoil in the vicinities of auto-repair workshops, gas stations and motor-parks in a Nigerian City. *Toxicol Environ Chem* 84(1–4):33–39. <https://doi.org/10.1080/02772240309820>
- Onuoha SC (2013) Stimulated biodegradation of spent lubricating motor oil in amended with animal droppings. *J Nat Sci Res* 3(12):106–116
- Onwudike SU, Igbozurike CI, Ithem EE, Osisi F, Ukah CI (2017) Quantification of heavy metals using contamination and pollution index in selected refuse dumpsites in Owerri, Imo State South-east Nigeria. *Int J Environ Agric Biotechnol* 2(3):1202–1208. <https://doi.org/10.22161/ijeab/2.3.25>
- Osakwe SA, Akpoveta OV, Okoh BE, Ize-Iyamu OK (2012) Chemical forms of heavy metals in soils around municipal waste dumpsites in Asaba Metropolis, Delta State Nigeria. *Chem Speciat Bioavailabil* 24(1):23–30. <https://doi.org/10.3184/095422912X13255245250543>
- Pal S, Patra AK, Reza SK, Wildi W, Poté J (2010) Use of bio-resources for remediation of soil pollution. *Nat Resour* 110–125. <https://doi.org/10.4236/nr.2010.12012>
- Phonphuak N, Chindapasirt P (2015) Typs of waste, properties, and durability of pore-forming waste-based fired masonry bricks. In *Eco-efficient masonry bricks and blocks, design, properties and durability*. Science Direct, pp 103–127. <https://doi.org/10.1016/B978-1-78242-305-8.00006-1>
- Samuel Sojину OS, Wang J.-Z, Sonibare OO, Zheng EY (2010) Polycyclic aromatic hydrocarbons in sediments and soils from oil exploration areas of the Niger Delta, Nigeria. *J Hazard Mater* 174(1–3):641–647. <https://doi.org/10.1016/j.jhazmat.2009.09.099>
- Shafik MA (2008) Phytoremediation of some heavy metals by *Dunaliella salina*. *Glob J Environ Res* 2(1):1–11
- Singwane SS, Malinga P (2012) Impacts of pine and Eucalyptus forest plantations on soil organic matter content in Swaziland—Case of Shisel Weni Forests. *J Sustain Dev Africa* 14(1):137–151
- Stottmeister U, Wiefner A, Kusch P, Kappelmeyer M, Kästner M (2003) Effects of plants and microorganisms in constructed wetlands for wastewater treatment. *Biotechnol Adv* 22:93–117. <https://doi.org/10.1016/j.biotechadv.2003.08.010>
- Su C, Jiang L, Zhang W (2014) A review on heavy metal contamination in the soil worldwide: Situation, impact and remediation techniques. *Environ Skeptics Crit* 3(2):24–38. Retrieved from <http://www.Iaees.org/publications/journals/environsc/online-version.asp>
- Tabari M, Salehi A, Mohammadi J, Aliarab A (2011) Heavy Metal Contamination of Zn, Cu, Ni and Pb in Soil and Leaf of *Robina pseudoacacia* Irrigated with Municipal Wastewater in Iran. In: Einschlag PF (ed.) *Waste water—evaluation and management*. In Tech, pp 341–350. Retrieved July 19, 2016, from <http://www.intechopen.com/books/waste-water-evaluation-and-management/heavy-metal-contamination-of-zn-cu-ni-and-pb-in-soil-and-leaf-of-robiniapseud-acacia-irrigated-with>
- Tyagi M, da Fonseca MM, de Carvalho C (2011) Bioaugmentation and biostimulation strategies to improve. *Biodegradation* 22:231–241. <https://doi.org/10.1007/s10532-010-9394-4>
- Uddin MN, Wahid-Uz-Zaman M, Rahman MM, Islam MS, Islam MS (2016) Phytoremediation potentiality of lead from contaminated soils by fibrous crop varieties. *Am J Appl Sci Res* 2(5):22–28. <https://doi.org/10.11648/j.ajars.20160205.11>
- Uzoekwe SA, Oghosanine FA (2011) The effect of refinery and petrochemical effluent on water quality of Ubeji Creek Waar, Southern Nigeria. *Ethop J Environ Stud Manag* 4(2):107–116. <https://doi.org/10.4314/ejesm.v4i2.12>
- van Straalen NM (2002) Assessment of soil—a functional perspective. *Biodegradation* 13:41–52
- Wenzel WW (2009) Rhizosphere processes and management in plant-assisted bioremediation (phytoremediation) of soils. *Plant Soil* 385–408. <https://doi.org/10.1007/s11104-008-9686-1>

- Wuana RA, Okieimen FE (2011) Heavy Metals in contaminated soils: a review of sources, chemistry, risks and best available strategies for remediation. *Int Scholar Res Netw* 2011:1–21. <https://doi.org/10.5402/2011/402647>
- Yadav BK, Gupta PK (2021) Thermally enhanced bioremediation of hydrocarbon polluted soils. *Pollutants*. <https://doi.org/10.3390/pollutants2010005>
- Zhang JL, Qiao CL (2002) Novel approaches for remediation of pesticide pollutants. *Int J Environ Pollut* 18(5):423–433. <https://doi.org/10.1504/IJEP.2002.002337>

Chapter 12

Impacts of Blend Diesel on Root Zone Microbial Communities: *Vigna Radiata* L. Growth Assessment Study



Manvi Gandhi, Rakesh Kumar, Hassana Ibrahim Mustapha, Aprajita Jha, Pankaj Kumar Gupta, Nadeem Akhtar, and Prabhakar Sharma

Abstract Petroleum hydrocarbons are a severe environmental problem globally due to their persistence and toxicity to soil and human health. This research aims to analyze the impact of diesel and its blends on root zone microbial communities using a small-scale *Vigna radiata* L. growth assessment experiment. Five plate setups were prepared with organic soils and spilled with diesel, neat biodiesel, two blends of diesel (B5 and B20), and a control. Straight-chain saturated hydrocarbons, *n*-alkanes persisting in the blended diesel contaminated soil samples were analyzed using gas chromatography-mass spectrometry (GC-MS). A 16S rRNA gene amplicon sequencing was performed to identify the microbial communities and their abundance. Results showed that concentrations of C₈, C₁₀, C₃₀, and C₃₂ hydrocarbons were higher in diesel contaminated tray than biodiesel and its blend spilled trays. Proteobacteria benefited bacteria due to the addition of carbon sources and thus dominated in contaminated soils. Acidobacteria was prevalent in soil samples prior to contamination, decreasing significantly after contamination. No significant change was observed for Chlamydiae, Planctomycetes, Verrucomicrobia, and Dependuntiae in all soil samples, in the relative abundance, before and after contamination. Plant growth index was 1.22% in case of neat biofuel containing tray, with a more significant

M. Gandhi

Faculty of Sciences, University of Adelaide College, Adelaide, SA 5000, Australia

R. Kumar (✉) · P. Sharma

School of Ecology and Environment Studies, Nalanda University, Rajgir 803116, Bihar, India

e-mail: rakesh.kumar.PhD@nalandauniv.edu.in

H. I. Mustapha

Department of Agricultural and Bioresources Engineering, Federal University of Technology, Minna, Nigeria

A. Jha

School of Biotechnology, Kalinga Institute of Industrial Technology, Bhubaneswar 751024, Odisha, India

P. K. Gupta

Faculty of Environment, University of Waterloo, Waterloo, ON N2L 3G1, Canada

N. Akhtar

Department of Animal Biosciences, University of Guelph, Guelph, ON N1G 2W1, Canada

growth percentage than control tray, i.e., 1%. This indicates the positive impact of neat biofuel as a substrate or plant stimulator. We conclude that neat biofuel application in soil improves proteobacterial communities to take care of hydrocarbon-polluted soils.

Keywords Diesel · Seed germination · Microbial communities · Bioremediation · Plant growth

12.1 Introduction

Diesel is a petroleum-based conventional and non-renewable fuel that fulfills energy demand. Diesel and biodiesel are two distinct compounds with similar functionality (Junior et al. 2009). However, emerging concerns, such as energy protection, political instability, financial and environmental benefits, including reduced greenhouse gas emissions compared to traditional fuels, have catalyzed the development of biofuels (Hawrot-Paw et al. 2020). Biofuel possesses readily degradable hydrocarbon contents (Gupta 2020), and thus low particulate matter emissions can be expected for multiple uses (Bamgbose and Anderson 2020). Biodiesel consists of methyl, ethyl, or propyl esters of fatty acids derived from animal and plant oils (Junior et al. 2009). Nevertheless, biodiesel contains methanol, produced as a by-product of reverse transesterification reactions (Hawrot-Paw et al. 2019). For example, pure biodiesel (B100) or in combination with traditional petrol-diesel oils (B2–B20) can be called a blend, depending upon various concentrations of biodiesel (Gupta 2020; Hawrot-Paw and Izwikow 2015). Badzinski et al. (2021) reported that biodiesel has lesser environmental impacts than traditional mineral diesel oils. However, one can not ignore the potential ecotoxicity of biodiesel that may be associated with its blends with mineral diesel oils, as highlighted by Gupta (2020). Gupta (2020) also highlighted that biodiesel is radially biodegradable, but it may cause profound soil–water quality due to its dissolution if spilled high volume, which is yet to receive proper attention.

Microbes preferentially degrade biodiesel first if it is co-existed with mineral diesel oils and thus may hinder hydrocarbon compounds like BTEX (Benzene, toluene, ethylbenzene, and xylene) degradation, especially in anaerobic conditions (Gupta 2020; Corseuil et al. 2011; Ramadass et al. 2018; Ramos et al. 2013; Thomas et al. 2017). Different soil microorganisms play an integral role in re/cycling essential soil nutrients and influence organic matter dynamics that diesel–biodiesel spills can impact (Badzinski et al. 2021; Woźniak-Karczewska et al. 2019; Silva et al. 2012). Consequently, the toxicity of blended fuels can impact microbial populations and their diversity in the soil. Hawrot-Paw et al. (2020) evaluated the ecotoxicity of blend diesel contaminated soil and observed an inversely proportional relationship between the blend diesel contaminants and the population of lipolytic and amylolytic organisms in clayey soils obtained from 0–15 cm topsoil in Szczecin. This study also observed that blend diesel favors the survival of tolerable species; therefore,

Pseudomonas was displaced by intolerant microbial *Azotobacter species* in blend fuels contaminated soils. Thus, the performance of microbial communities in soils spilled with varying levels of diesel–biodiesel may help to understand hydrocarbon biodegradability in the root zone.

Different remediation approaches, for example, chemical treatments (Nwaogu et al. 2008), natural attenuation (Penet et al. 2006), bioremediation, and phytoremediation (Afzal et al. 2012), have been applied to remediate the menace caused by blend diesel contamination in soils (Gupta 2020). Pardo et al. (2014) reported the use of the Fenton process, which involved the utilization of hydrogen peroxide as an oxidizing agent, trisodium citrate as a chelator, and ferric ions as a catalyst to treat soils contaminated with B20 blend biodiesel. Bioremediation approaches involve utilizing naturally occurring biochemical processes to remediate target pollutants persisting in the contaminated soils (Sarkar et al. 2005). This approach is highly dependent on the microbial population naturally residing in the contaminated sites (Penet et al. 2006). Phyto-rhizoremediation applies indigenous or selected green plants and their associated microorganisms in the rhizosphere to degrade, extract, and immobilize pollutants in the contaminated sites (Hussain et al. 2018; Mustapha and Lens n.d.; Mustapha et al. 2018). This is due to the symbiotic relationship between plant roots and soil microorganisms. Plant roots provide carbon and energy for microbial growth, and root growth increases the tolerance stress (Afzal et al. 2012; Hussain et al. 2018; Akpan and Usuah 2014). Consequently, microorganisms uptake, metabolize and remediate the contaminants persisting in the soil (Vergani et al. 2017). Likewise, Nwaogu et al. (2008) reported a significant reduction in plant growth and germination in blend diesel spilled contaminated soils on different species *Bacillus cereus*, *Bacillus subtilis*, *Trichoderma harzanium*, and *Trichothercium roseum*. Interestingly, it was observed that amount of diesel oil reduced with respect to time as *Bacillus subtilis* used diesel oil for potential carbon sources in plants. Similarly, Hawrot-Paw et al. (2015) also reported inhibition of photosynthetic and respiratory processes, deformation of cells, vascular obstruction, accumulation of oil in plant tissues, and eventually dehydration of plants. It was observed that 4 plant species, *Glycine max (L.) Merrill*, *Helianthus annuus L.*, *Lupinus luteus L.*, and *Pisum sativum L.* showed resistance to diesel oil in the soil, regardless of fuel types and dose, out of 19 plants species.

Previous studies focused on the impact of blend diesel contaminated soil's microbes; however, limited to single blend levels; thus, implications of varying blend levels on soil microbes especially present in the root zoon are yet to be systematically investigated. The present research aims to determine the influence of varying biodiesel blend spills on (a) plant growth and (b) colonization of microbial communities in the rhizosphere. Alternatively, in this research, we tested the performance of neat biodiesel as a plant and microbes biostimulator to improve hydrocarbon degradations. This study provides future approaches to identify favorable microbes and neat biodiesel to cut the remediation cost in the field.

12.2 Materials and Methods

12.2.1 Experimental Setup

High-organic content (wetland) soil was collected (10–15 cm depth) from a local wetland located in Southern Ontario, Canada, and analyzed for hydro-physical properties like porosity, bulk density, etc. Porosity and bulk density were estimated using the standardized oven-dry method. 500 g of loose soils were taken in a tray (7 cm × 7 cm) where 20 seeds of *Vigna radiata* were added to each tray at $t = 0$ days. *Vigna radiata*, commonly known as Green gram, was selected as a plant to be studied because it has a wide range of adaptability and early maturity. According to nitrogen fixation machinery, *Vigna radiata* is a leguminous crop with high protein (approximately 25–28% digestible protein). Because of its wide range of adaptability, it is extensively distributed throughout tropical and subtropical regions. 0.5 mL of pure biodiesel/biofuel (B100), 20% blend diesel (B20), neat diesel, and 5% blend diesel (B5) were spilled to tray B, tray C, tray D, and tray E, respectively at day 5, i.e., after initial germination (Fig. 12.1). One tray was kept as a control, refers as sample A. 1 mL of hydrocarbons were spilled uniformly on the surface on 5th day carefully to avoid direct toxicity to below surface germinating cells of *Vigna radiata*. All the soil samples were kept under similar conditions, i.e., room temperature, which varies from 15–25 °C, ~32% relative humidity, and the outdoor light intensity with 80% watering throughout the experiment. Water saturation in soils was maintained at about 80% of porosity (i.e., 45%) and volume of soils in the tray, as estimated by Gupta et al. (2020). The rate of above surface growth of *Vigna radiata* was monitored on the 10th day and 20th day (i.e., the final phase of the experiment). In addition, soil samples were collected on the initial and final days of the investigation. Samples collected on day 5th before hydrocarbon spills from tray A-E were referred to as A0-E0, respectively. Likewise, samples collected on 20th day of the experiment from tray A-E were referred to as A1-E1, respectively. A0-E0 and A1-E1 samples were used for microbial analysis, while only A1-E1 samples were used for hydrocarbon analysis.

12.2.2 Hydrocarbon Gas Sampling and Analysis

Hydrocarbons were extracted using Dichloromethane (DCM) and sub-samples in 2 mL vials for gas chromatography (GC) (GC; Shimadzu GC2014) to facilitate sampling through PTFE septa (Canadian Life Science). As soon as the samples were taken, they have instantly inserted into the GC auto-injection vials of 2 mL, which were impenetrable due to PTFE/silicone septa caps. A capillary column (Rxi-5Sil, Column, 30 m × 0.25 mm × 0.25 μm) was used in the experiment. A carrier gas (Helium) was employed, and its flow rate was sustained at 5 mL/min. The infusion port temperature of the GC chromatograph was kept at 250 °C while that of MS was 230 °C. However,

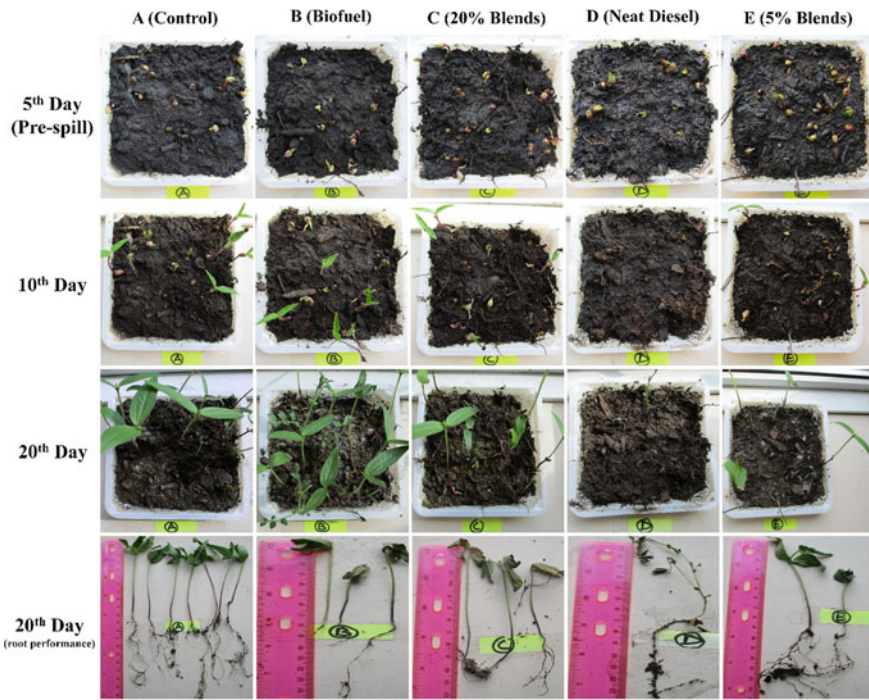


Fig. 12.1 Performance for seed germination in contaminated soils, control (A), biofuel (B), 20% blend (C), neat diesel (D), and 5% blend (E)

after the initiation of the procedure, the temperature was increased from 60 °C to 280 °C at the rate of 20 °C/min. Nevertheless, the temperature of the diffusion line between GC and MS was kept at 250 °C. Twelve grams of soil were taken underneath each soil pot and transferred in a conical tube (M0). All collected soil samples were preserved at 4 °C, followed by disposition in their corresponding try.

12.2.3 Seed Germination and Plant Growth Indices

Seed germination index (SGI) and plant growth index (PGI) were calculated as:

$$\text{Seed Germination Index, SGI(\%)} = \frac{\text{Number of normally germinated seeding}}{\text{number of seeds sown}} \times 100 \tag{12.1}$$

$$\text{Plant Growth Index, PGI(\%)} = \frac{G_w R L_w S L_w}{G_C R L_C S L_C} \tag{12.2}$$

where G_w , RL_w , SL_w represent the seed germination (%), root elongation (cm), and shoot elongation (cm), respectively, and G_c , RL_c , and SL_c are their corresponding control values.

12.2.4 Statistical Analysis

16S rRNA Amplicon sequencing was performed as per the details given in Gupta et al. (2020). QIIME 2 was used to analyze ASV (Amplified Sequence Variant) data presented in detail with respect to species to phylum level. n-alkanes analysis in blend biodiesel contaminated soils is analyzed in triplicate and presented with their mean values. ASV structure was prepared for downstream analysis, as the details provided in Gupta et al. (2020).

12.3 Results

12.3.1 *N-alkanes Analysis in Blend Biodiesel Contaminated Soils*

On the 20th day, *n*-alkanes, i.e., straight-chain saturated hydrocarbons, for example, *n*-C₈, *n*-C₁₂, *n*-C₃₀, and *n*-C₃₂ pollutants persisting in the blended diesel contaminated soil samples, were analyzed using GC–MS, collected from different tray setups. Minimum, maximum, and average values for different alkane degradation have been highlighted in Fig. 12.2. *n*-C₁₂ values were found in the range of 1–3.12 mg/l, 2.5–4.8 mg/l, 4.3–6.0 mg/l, 3.5–5.1 mg/l for soil samples biofuel (B), 20% blend (C), neat diesel (D), and 5% blend (E), respectively. However, *n*-C₁₂ concentrations in neat diesel and 5% blend soil samples exceeded the *n*-C₈ concentrations with a range of 4.3–6 mg/l and 3.5–5.1 mg/l, respectively. High-chain alkanes, *n*-C₃₂ and *n*-C₃₀, were observed with similar average concentrations in all samples.

12.3.2 *Plant Growth Assessment*

Data of SGI and PGI of plant *Vigna radiata* at different levels of diesel blends and in neat diesel are presented in Table 12.1. Maximum SGI (92%) with an improved PGI (1.2%) was observed when the seedlings were grown in biofuel (B), whereas the lowest SGI (20%) and PGI (0.13%) were seen in neat diesel treatment. With an increase (from 5 to 20%) in percent blends, a 42.86% increase was observed in the SGI, with an 87.50% increase in PGI.

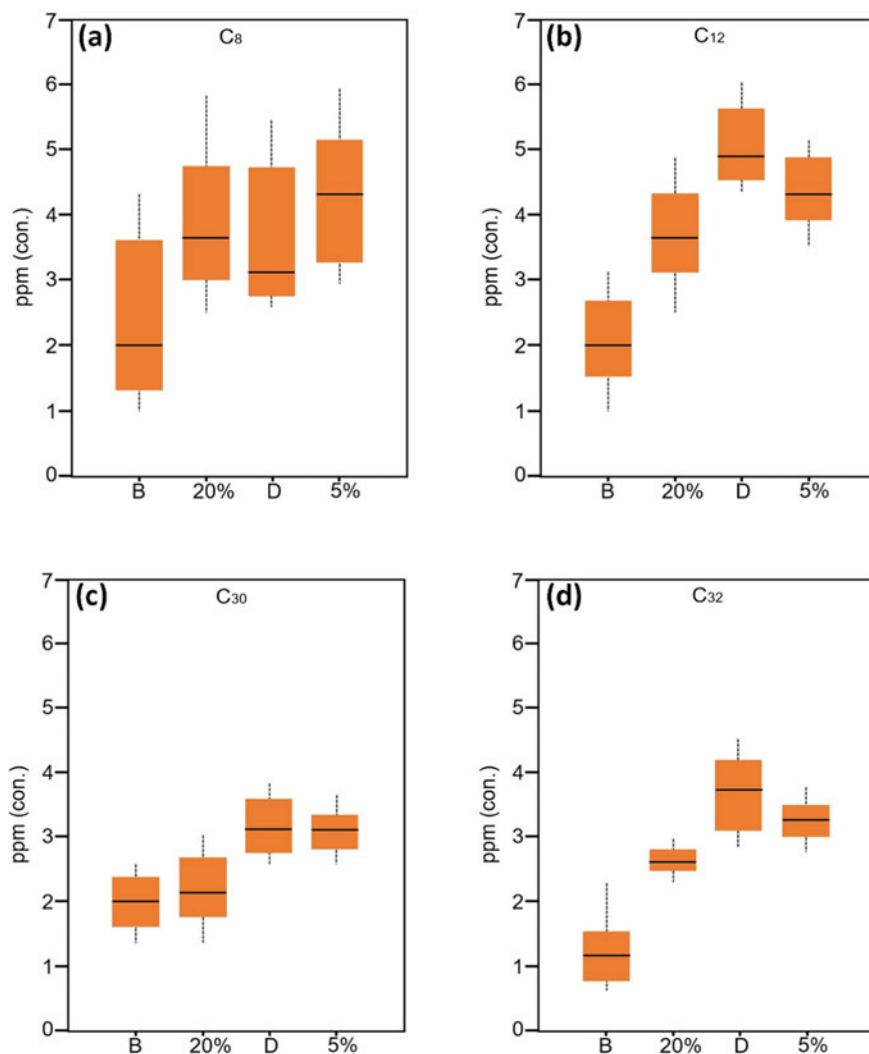


Fig. 12.2 Concentrations of *n*-alkanes hydrocarbons in biofuel (b), 20% blend, neat diesel (d), and 5% blend contaminated soils for a C₈, b C₁₂, c C₃₀, and d C₃₂ hydrocarbons. [Box plot explains the range of respective hydrocarbons, black line denotes mean value, and dot lines are their minimum and maximum values; unit: 1 mg/l = 1 ppm]

Table 12.1 Plant growth assessment at the different levels of diesel blends

Particulars	A (Control)	B (Biofuel)	C (20% Blends)	D (Diesel)	E (5% Blends)
SGI (%)	90	92	50	20	35
PGI (%)	1	1.22	0.45	0.13	0.24

12.3.3 Microbial Communities

Considerable fluctuations in abundance were observed for the majority of the bacterial phylum. Proteobacteria persisted in low abundance in most samples before contamination, with relative abundances of 30.19%, 28.65%, and 47.51% in samples from tray A, B, and C pre-spilled days, refer as A0, B0, and C0, respectively (Fig. 12.3). However, the relative abundances surged to 47%, 87%, and 71.23% after contamination in samples A1, B1, and C1 (Fig. 12.4). In D0 and E0 samples, the relative abundance of Proteobacteria before the contamination was 62.73% and 63.12%, respectively, which reduced to 20% in sample D1 and remained unchanged in sample E1 after contamination. Acidobacteria is prevalent in soil samples before contamination with relative abundances of 43.96%, 61.03%, 40.36%, and 21.94% in A0, B0, C0, and D0 samples, respectively, which significantly reduced to 20%, 2%, 5%, and 2% respectively in A1, B1, C1 and D1 samples after contamination. Besides this, the relative abundance of Acidobacteria remained the same in samples E0 and E1 before and after the contamination.

The relative abundance of *Geobacter* in samples A1, B1, and C1 were found to be 2.91%, 1.02%, and 2.89% after contamination, which was the same as that of the abundances in samples A0, B0, and C0 before contamination. However, relative abundance of *Geobacter* increased rapidly to 80% and 60% after contamination in D1 and E1 samples, with an initial relative abundance of 0.96% and 0.83% in D0 and E0 samples, respectively. In addition to this, no significant change in relative abundance was observed for Chlamydiae, Planctomycetes, Verrucomicrobia, and Dependientiae in all soil samples, before and after contamination. A similar trend was exhibited for Actinobacteria, Bacteroidetes, and Cyanobacteria, *except* for a few soil samples.

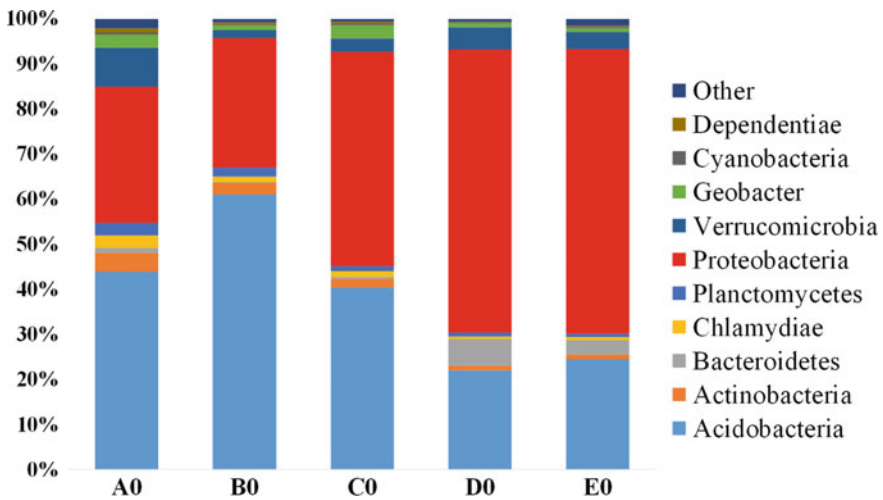


Fig. 12.3 Relative abundance of microbial communities on the first day of germination and before the addition of pollutants

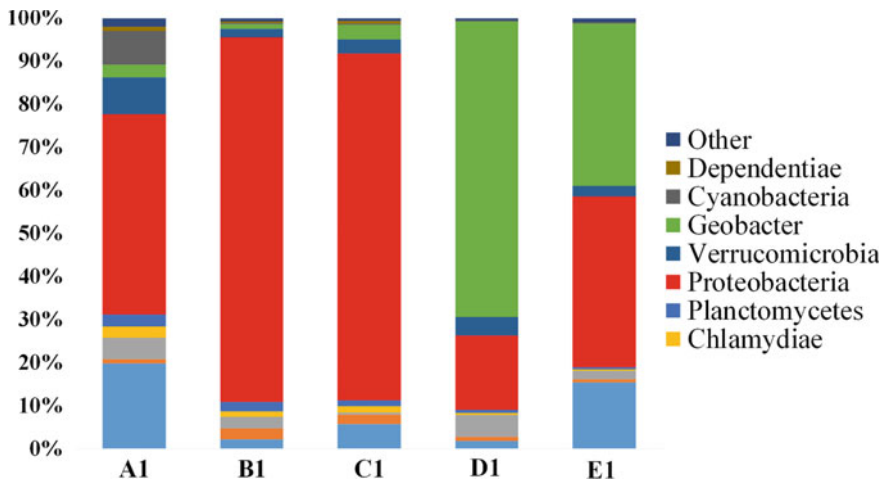


Fig. 12.4 Relative abundance of microbial communities on the 20th day of germinations and the end of the experiment

The relative abundance of Actinobacteria was 4.16% for soil sample A0 before contamination which was reduced to 1% for soil sample A1 after contamination.

Nevertheless, the relative abundances of Actinobacteria in all soil samples remained the same. On the contrary, the relative abundance of Cyanobacteria was 0.46% for soil sample A0 before contamination, which increased to 8% after the contamination, with no change observed in the remaining soil samples. Also, the relative abundance of Bacteroidetes was 1.10% and 0.21% in soil samples A0 and B0 before contamination which surged to 5% and 2.63% after contamination, respectively, while the abundance remained the same in other soil samples.

12.4 Discussion

Petroleum and its products will continue to affect plant growth negatively. Soil and groundwater contaminated with petroleum products contain varying levels of organic and inorganic pollutants, including total petroleum hydrocarbons, metals, and their derivatives. The soil pollutants may affect the health of living organisms in diverse ways, including uptake of soil pollutants by plants and seepage of these pollutants through the soil into groundwater and surface water for potable purposes. These pollutants also exhibit long-term toxicity in the environment.

Since the ultimate objective of remediation approaches is to prevent contamination from contaminated sites through cost and time-saving approaches, several methodologies of soil remediation were applied to petroleum-contaminated soil, including chemical and physical methods, viz. thermal treatment, soil washing, solidification, and stabilization. These methods are expensive, energy-intensive, and disruptive to

the environment. The relative costs of these methods range from US\$80–340 (Khalid et al. 2017; Mahajan et al. 2021). These treatment methods can also lead to incomplete pollutant decomposition that may generate by-products that require further treatment because they are often toxic to plants and other environmental components. However, the relative costs of biological approaches range from US\$ 10–35 for phytoremediation and US\$ 50–150 for bioremediation (Khalid et al. 2017; Mahajan et al. 2021). The performance evaluation of bioremediation methods is well documented with efficient results, extensive application, minimal maintenance, and operating costs (Mahajan et al. 2021). These methods rely on microorganisms' intrinsic activities, which vary with initial substrate concentrations of hydrocarbons to remove total hydrocarbon and decontaminate the soil, land surface, and groundwater (Gupta and Yadav 2020).

This manuscript is focused on the effects of different biodiesel blends and deterioration capacity on the soil microbes. Alphaproteobacteria, Gammaproteobacteria, Actinobacteria, Betaproteobacteria, Cyanobacteria, Geobacter, and Planctomycetes, were pronounced, benefiting biodiesel-based bioremediation (Gupta 2020). Our results are in-line with the findings of Owsianiak et al. (2009), who observed that blends with higher than 30% biodiesel contributed to the stimulation of biodegradation efficiency. Likewise, Chen et al. (2019) demonstrated high biodegradation performance with high biodiesel blends and neat biodiesel with the dominating bacterial community, viz. *Comamonas testosterone*, *Gordonia alkanivorans*, *P. aeruginosa*, *Alcaligenes sp.*, *Gordonia terrae*, *Gordonia desulfuricans*, and *Rhodococcus erythropolis*. Woźniak-Karczewska et al. (2019) suggested that higher quantities of biodiesel favored the new growth of specialized species during the experimental durations. Likewise, Lisiecki et al. (2014) reported that an increase in the quantity of biodiesel in which fuel corresponds to an increase in the abundance of *Citrobacter*, indicating that they were responsible for the metabolism of oxidation products of alkane biotransformation since fatty acid methyl esters, which have enhanced their growth. High abundant sequence types affiliated with the *Geobacter* were present in neat diesel spilled try. Notably, the Alphaproteobacteria, Gammaproteobacteria, and Betaproteobacteria were high in neat biodiesel compared to its blends.

12.5 Conclusions

The present study illustrates the impacts of diesel and its blends on root zone microbial populations in high organic content wetland soils. Significant increase in PGI was witnessed when seedlings of *Vigna radiata* were grown in blend diesel (5% to 20%) polluted soils. In addition to this, maximum SGI (92%) with an improved PGI (1.2%) was observed with the use of biofuels. The relative abundances of different microbial populations were enhanced upon contamination of blended diesel in wetland soils. This is encouraging findings for simultaneous biodegradation of high blends and biodiesel in contaminated soil–water systems. Our results provide small-scale laboratory evidence that managed application of neat biodiesel may be suitable

for the remediation and management of hydrocarbon-polluted soils. We advise that increased microbial abundance along with the ratio of Proteobacteria and Acidobacteria can be utilized as key indicators to estimate neat diesel contamination, which can further aid in assessing the progress of site remediation after diesel spills in different soils. Consequently, in order to better understand ecological mechanisms that favor microbial populations, it is strongly recommended to perform large-scale experiments to determine the distribution of microbiota and its role in the effective biodegradation of hydrocarbon contaminants persisting in soils.

Acknowledgements All authors thank their respective organization for supporting their research activities. Authors would also thank SYAHI for providing a communication platform.

References

- Afzal M, Yousaf S, Reichenauer TG, Sessitsch A (2012) The inoculation method affects colonization and performance of bacterial inoculant strains in the phytoremediation of soil contaminated with diesel oil. *Int J Phytorem* 14(1):35–47. <https://doi.org/10.1080/15226514.2011.552928>
- Akpan GU, Usuah PE (2014) Phytoremediation of diesel oil polluted soil by fluted pumpkin (*Telfairia occidentalis* Hook F.) in Uyo, Niger Delta Region, Nigeria. *J Environ Earth Sci* 4(1):6–15
- Badzinski C, Ramos RF, Godoi B, Daroit DJ (2021) Soil acidification and impacts over microbial indicators during attenuation of soybean biodiesel (B100) as compared to a diesel-biodiesel blend (B8). *Fuel* 289:119989. <https://doi.org/10.1016/j.fuel.2020.119989>
- Bamgbose IA, Anderson TA (2020) Ecotoxicity of three plant-based biodiesels and diesel using, *Eisenia fetida*. *Environ Pollut* 260:113965. <https://doi.org/10.1016/j.envpol.2020.113965>
- Chen Y-A, Liu P-WG, Whang L-M, Wu Y-J, Cheng S-S (2019) Biodegradability and microbial community investigation for soil contaminated with diesel blending with biodiesel. *Process Saf Environ Prot* 130:115–125. <https://doi.org/10.1016/j.psep.2019.07.001>
- Corseuil HX, Monier AL, Gomes AP, Chiaranda HS, do Rosario M, Alvarez PJ (2011) Biodegradation of soybean and castor oil biodiesel: implications on the natural attenuation of monoaromatic hydrocarbons in groundwater. *Groundwater Monit Remed* 31(3):111–118. <https://doi.org/10.1111/j.1745-6592.2011.01333.x>
- Gupta PK (2020) Fate, transport, and bioremediation of biodiesel and blended biodiesel in subsurface environment: a review. *J Environ Eng* 146(1):03119001. [https://doi.org/10.1061/\(ASCE\)EE.1943-7870.0001619](https://doi.org/10.1061/(ASCE)EE.1943-7870.0001619)
- Gupta PK, Yadav BK (2020) Three-dimensional laboratory experiments on fate and transport of LNAPL under varying groundwater flow conditions. *J Environ Eng* 146(4):04020010. [https://doi.org/10.1061/\(ASCE\)EE.1943-7870.0001672](https://doi.org/10.1061/(ASCE)EE.1943-7870.0001672)
- Gupta PK, Gharedaghloo B, Lynch M, Cheng J, Strack M, Charles TC, Price JS (2020) Dynamics of microbial populations and diversity in NAPL contaminated peat soil under varying water table conditions. *Environ Res* 191:110167. <https://doi.org/10.1016/j.envres.2020.110167>
- Hawrot-Paw M, Ratomski P, Mikiciuk M, Staniewski J, Koniuszy A, Ptak P, Golimowski W (2019) Pea cultivar Blauwschokker for the phytostimulation of biodiesel degradation in agricultural soil. *Environ Sci Pollut Res* 26(33):34594–34602. <https://doi.org/10.1007/s11356-019-06347-9>
- Hawrot-Paw M, Koniuszy A, Zajac G, Szyzslak-Barglowicz J (2020) Ecotoxicity of soil contaminated with diesel fuel and biodiesel. *Sci Rep* 10(1):1–9. <https://doi.org/10.1038/s41598-020-73469-3>
- Hawrot-Paw M, Izwikow M (2015) Ecotoxicological effects of biodiesel in the soil. *J Ecol Eng* 16(5)

- Hawrot-Paw M, Wijatkowski A, Mikiciuk M (2015) Influence of diesel and biodiesel fuel-contaminated soil on microorganisms, growth and development of plants. *Plant Soil Environ* 61(5):189–194. <https://doi.org/10.17221/974/2014-PSE>
- Hussain I, Puschenreiter M, Gerhard S, Schöftner P, Yousaf S, Wang A, Syed JH, Reichenauer TG (2018) Rhizoremediation of petroleum hydrocarbon-contaminated soils: improvement opportunities and field applications. *Environ Exp Bot* 147:202–219. <https://doi.org/10.1016/j.envexpbot.2017.12.016>
- Junior JS, Mariano AP, de Angelis D (2009) Biodegradation of biodiesel/diesel blends by *Candida viswanathii*. *African J Biotechnol* 8(12)
- Khalid S, Shahid M, Niazi NK, Murtaza B, Bibi I, Dumat C (2017) A comparison of technologies for remediation of heavy metal contaminated soils. *J Geochem Explor* 182:247–268. <https://doi.org/10.1016/j.gexplo.2016.11.021>
- Lisiecki P, Chrzanowski Ł, Szulc A, Ławniczak Ł, Białas W, Dziadas M, Owsianiak M, Staniewski J, Cyplik P, Marecik R (2014) Biodegradation of diesel/biodiesel blends in saturated sand microcosms. *Fuel* 116:321–327. <https://doi.org/10.1016/j.fuel.2013.08.009>
- Mahajan M, Gupta PK, Singh A, Vaish B, Singh P, Kothari R, Singh RP (2021) A comprehensive study on aquatic chemistry, health risk and remediation techniques of cadmium in groundwater. *Sci. Total Environ*, 151784. <https://doi.org/10.1016/j.scitotenv.2021.151784>
- Mustapha HI, Gupta PK, Yadav BK, van Bruggen J, Lens P (2018) Performance evaluation of duplex constructed wetlands for the treatment of diesel contaminated wastewater. *Chemosphere* 205:166–177. <https://doi.org/10.1016/j.chemosphere.2018.04.036>
- Mustapha HI, Lens PN (2018) Constructed wetlands to treat petroleum wastewater. In: Prasad R, Aranda E (Eds), *Approaches in Bioremediation*, Springer 2018, pp 199–237. https://doi.org/10.1007/978-3-030-02369-0_10
- Nwaogu L, Onyeze G, Nwabueze R (2008) Degradation of diesel oil in a polluted soil using *Bacillus subtilis*. *Afr J Biotech* 7(12):1939–1943. <https://doi.org/10.5897/AJB07.889>
- Owsianiak M, Chrzanowski Ł, Szulc A, Staniewski J, Olszanowski A, Olejnik-Schmidt AK, Heipieper HJ (2009) Biodegradation of diesel/biodiesel blends by a consortium of hydrocarbon degraders: effect of the type of blend and the addition of biosurfactants. *Biores Technol* 100(3):1497–1500. <https://doi.org/10.1016/j.biortech.2008.08.028>
- Pardo F, Rosas JM, Santos A, Romero A (2014) Remediation of a biodiesel blend-contaminated soil by using a modified Fenton process. *Environ Sci Pollut Res* 21(21):12198–12207. <https://doi.org/10.1007/s11356-014-2997-2>
- Penet S, Vendeuvre C, Bertoncini F, Marchal R, Monot F (2006) Characterisation of biodegradation capacities of environmental microflorae for diesel oil by comprehensive two-dimensional gas chromatography. *Biodegradation* 17(6):577–585. <https://doi.org/10.1007/s10532-005-9028-4>
- Ramadass K, Megharaj M, Venkateswarlu K, Naidu R (2018) Bioavailability of weathered hydrocarbons in engine oil-contaminated soil: Impact of bioaugmentation mediated by *Pseudomonas* spp. on bioremediation. *Sci. Total Environ*. 636:968–974. <https://doi.org/10.1016/j.scitotenv.2018.04.379>
- Ramos DT, da Silva MLB, Chiaranda HS, Alvarez PJ, Corseuil HX (2013) Biostimulation of anaerobic BTEX biodegradation under fermentative methanogenic conditions at source-zone groundwater contaminated with a biodiesel blend (B20). *Biodegradation* 24(3):333–341. <https://doi.org/10.1007/s10532-012-9589-y>
- Sarkar D, Ferguson M, Datta R, Birnbaum S (2005) Bioremediation of petroleum hydrocarbons in contaminated soils: comparison of biosolids addition, carbon supplementation, and monitored natural attenuation. *Environ Pollut* 136(1):187–195. <https://doi.org/10.1016/j.envpol.2004.09.025>
- Silva GS, Marques EL, Dias JC, Lobo IP, Gross E, Brendel M, da Cruz RS, Rezende RP (2012) Biodegradability of soy biodiesel in microcosm experiments using soil from the Atlantic Rain Forest. *Appl Soil Ecol* 55:27–35. <https://doi.org/10.1016/j.apsoil.2012.01.001>

- Thomas AO, Leahy MC, Smith JW, Spence MJ (2017) Natural attenuation of fatty acid methyl esters (FAME) in soil and groundwater. *Q J Eng GeolHydrogeol* 50(3):301–317. <https://doi.org/10.1144/qjegh2016-130>
- Vergani L, Mapelli F, Zanardini E, Terzaghi E, Di Guardo A, Morosini C, Raspa G, Borin S (2017) Phyto-rhizoremediation of polychlorinated biphenyl contaminated soils: an outlook on plant-microbe beneficial interactions. *Sci Total Environ* 575:1395–1406. <https://doi.org/10.1016/j.scitotenv.2016.09.218>
- Woźniak-Karczewska M, Lisiecki P, Białas W, Owsianiak M, Piotrowska-Cyplik A, Wolko Ł, Ławniczak Ł, Heipieper HJ, Gutierrez T, Chrzanowski Ł (2019) Effect of bioaugmentation on long-term biodegradation of diesel/biodiesel blends in soil microcosms. *Sci Total Environ* 671:948–958. <https://doi.org/10.1016/j.scitotenv.2019.03.431>

Chapter 13

A Coherent Review on Approaches, Causes and Sources of River Water Pollution: An Indian Perspective



Gaurav Singh, Tanu Jindal, Neelam Patel, and Swatantra Kumar Dubey

Abstract Non-contaminated water or sustaining each sector of fresh water is essential for the survival of all living beings in current and upcoming generations. However, the degradation of freshwater qualities is a significant concern in developing countries (India). The need for clean water is increasing sharply to meet rising human demands constantly. River water is rich in ecological community and plays a vital role in surviving all living beings. Still, presently it is the most threatened ecosystem due to various human-made activities. Hence, meticulous monitoring of river water qualities (RWQs), assessment of numerous variables (physicochemical, bacteriological, pathogenic), and heavy metals content are imperative indicators for finding out the actual health of river water ecosystems. Upsetting the concentration of multiple RWQ variables and metals content leads to deteriorating the RWQ and ultimately affects human well-being. Simultaneously, applying a multivariate statistical approach and computing water quality index (WQI) and comprehensive pollution index (CPI) is also a vital role in understanding the actual status of RWQ. This comprehensive study is focused on various processes, causes, and sources of river water pollution in India. It provides extensive information and better understanding to enable policymakers, preservationists, and environmentalists to develop strategies to mitigate river pollution and strengthen aquatic ecosystems rejuvenation.

Keywords Water · River water pollution · Heavy metals · Multivariate statistics · Water quality index · Comprehensive pollution index

G. Singh (✉) · T. Jindal

Amity Institute of Environmental Sciences, Amity University Uttar Pradesh, Noida, UP, India

e-mail: singhaurav.env@gmail.com

N. Patel

National Institution for Transforming India (NITI Aayog), New Delhi, India

S. K. Dubey

Department of Environmental Engineering, Seoul National University of Science and Technology, Seoul, South Korea

13.1 Highlights

- This review covers various aspects of river water, and possible causes and sources of river pollution in developing nation like India.
- Point sources like industrials and municipal wastewaters, and non-point source like agricultural runoff are the primary source of river pollution in India.
- Multivariate statistical approaches and water quality indexes are promising tools for river water quality assessment.
- Periodic monitoring of river water quality status by analyses inorganic and organic contaminants and efficient and continuous treatments of wastewater by adopting ETPs and STPs are suggested.

13.2 Introduction

Water is a principal constituent and key resource requisite to sustain life on the earth. It is recognized as a fundamental individual right worldwide, thus a necessity to be handled effectively and efficiently to secure worldwide requirements. Water distribution across the globe is uneven, and water scarcity is now a primary global concern. The significant water utilizes in agricultural, industrial (comprises industrial actions, energy, and mining, etc.), and recreational, domestic/municipal, as well as ecological water application which has a significant effect on the availability of water via physical water abstraction and deterioration of water (Plessis et al. 2017). Human activities are mainly responsible for threatened freshwater ecosystems and stand to be further influenced by climate change. Presently, water scarcity is affecting one-fifth of the global populace, and a quarter of the global public faces a lack of technology to restore freshwater from ponds and rivers (Xiao-jun et al. 2014). Therefore, a framework to investigate the significant threats to water safety at a range of geographical scales from local to worldwide is urgently required (Vörösmarty et al. 2010).

The entire freshwater resources on the planet are evaluated to be 43,750 km³ year⁻¹. The demand for agricultural freshwater is increasing at an alarming rate due to the continuous increase in the human population and urbanization. The global assessment shows that freshwater's requirement is affected by industrial development, agricultural production, and population expansion in addition to climate change. Globally, freshwater extraction is predicted at 3800 km³, out of which 70% is for agricultural irrigation with significant fluctuation among and the nations. As the equilibrium between water requirement and availability has arrived at a critical level in various parts of the planet and increasing need for water and agricultural production is probable in the forthcoming, a sustainable way of water resource management is become important (Ayyam et al. 2019).

India is the second-most populated and the seventh-biggest country on the planet, with an entire geographical area of 32,87,590 km² (Garg 2012). It is located in the northern part of the Indo-Australian plate as well as north of the equator at 8°4'

and 37°6' N and 68°7' and 97°25' E. India is home to nearly 18% of the world's populace and has approximately 4% of the world's freshwater resources. The rapid population growth has drive pressure on water resources in the country. Rivers and groundwater are significant sources of freshwater provide to the nation. India received approximately 75% of the annual precipitation, 48% mean surface water during monsoons. Overall, the country received <4,000,000 MCM (million cubic meters) of precipitation every year, which also comprises snowfall (Poddar et al. 2014). Besides rapid population growth, climate change also generates extra pressure on the hydrological cycle and changes the aquatic resources structures. According to Central Water Commission (CWC 2013–2014), the potential of water resources in India is predicted to be 1,869,000 MCM given both grounds and surface water (Manju and Sagar 2017).

About 329 million hectares of land in India consists of numerous small and big rivers, some of which are among the world's largest rivers (CWC 2005). Because of limitations in water resources, per capita, water availability (PCWA) also decreases (5177 to 1140 m³/year) with an increasing populace (361 to 1640 million) from 1951 to 2050 (Fig. 13.1). The country's situation may be classified as water-stressed, when water availability is <700 m³/capita/year, and water-scarce when water availability is <1000 m³/capita/year (MoWR 2008; Manju and Sagar 2017). Among the world's 17 'extremely water-stressed nations, India has 13th ranked and is under extremely high levels of baseline water stress (WRI 2019).

Rivers are amongst the essential natural resources of water for humans and other living beings. Rivers aid human development as they meet water demands for irrigation, household use, industrial use, and aquaculture and sustain roles for different fauna and flora. They have founded reservoirs of ecological diversity,

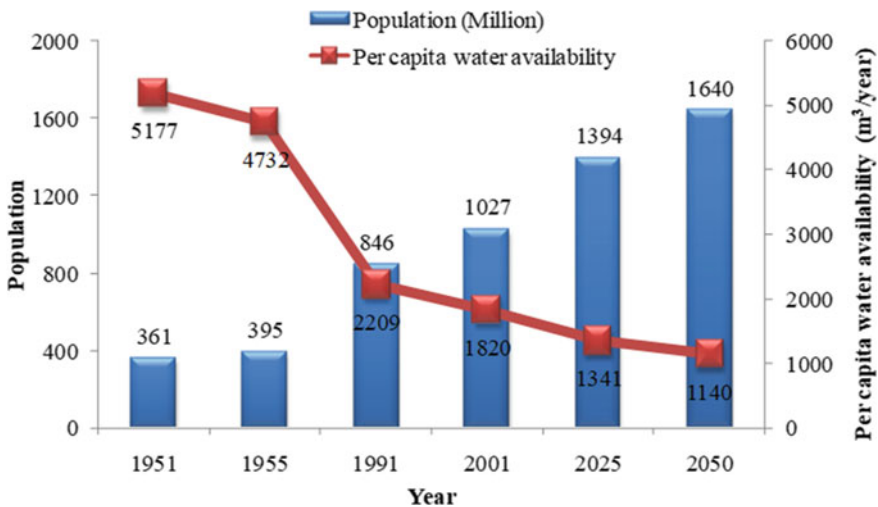


Fig. 13.1 Per capita water availability in India

provide adequate services to the public, and economic benefits. These rivers played a vital role in the development of Indian culture, religious and spiritual life. Most ancient civilizations grew along the river's banks. Even today, millions of people live in the cities developed along the bank of rivers and depend on them for their survival. India is bestowed with an extensive river network and blessed with high rainfall due to the southwestern monsoon, accounting for 75% of the yearly precipitation (Ghosh and Mistri 2015).

India is affluent with 13 major river basins that cover 20,000 km² (82.4% of the total river basin of the country) and contributing 85% of the total surface flow and nearly 80% of the country's populace is dwelling in these basins (Dadhwal et al. 2014). Main river basins of the country include the Brahmaputra, Indus (including Satluj and Beas Sub Basin), Ganga (including Yamuna Sub Basin), Krishna, Godavari, Mahanadi, Cauvery, Narmada, Brahmini (including Baitarni Sub Basin), Mahi, Sabarmati, Pennar and Tapi, (CWC 2015).

Government of India (GoI) is focused to clean Ganga River comprise its tributaries for conservation and rejuvenation, which catchment basin covered almost northern India, by launching Namami Gange scheme under National Mission for Clean Ganga (NMCG), Ministry of Jal Shakti. Along with various government bodies like State Project Management Group (SPMG) in Uttarakhand, Uttar Pradesh, Bihar, Jharkhand and West Bengal, CPCB, CWC and affiliated agencies also working on rejuvenation of river water quality in holistic approaches i.e. cleaning of surface river, ghats, biodiversity conservation, afforestation and upgrading or establishment of STPs and ETPs. Hence, the objective of this review summarizes the literature of various sources and causes of river water pollution in India with respective of monitoring of various parameter and pollution status of Indian rivers. This review helps to intensive sympathetic for upcoming researchers, preservationists, and environmentalists in developing strategies to mitigate river water pollution and rejuvenation.

13.3 River Water Pollution

Degradation of surface water quality due to various human activities such as random urbanization and moderately treated or non-treated industrial effluent released, poor hygiene, inappropriately managed landfills, and other sources of pollution viz pesticides and fertilizers runoff from the farming sector is an area of serious concern (CGWB 2017). In India, just 62% of effluents from industries and 37% sewage from municipal sources are treated (MoEFCC 2019). Several districts have contaminated water sources, thus influencing human wellbeing on a broad scale (CGWB 2017).

Rivers are among the most diversified and vulnerable ecosphere on the globe. The ever-increasing anthropogenic pressure has severely altered these ecosystems. However, various protection and management approaches for rivers have been prepared and executed worldwide to counters this problem. Assessment of rivers' actual status or "health" has become imperative to all such strategies (Srivastava et al. 2017). Diminished river water quality (RWQ) upsets the balance of the aquatic

ecosystem and leads to fatal consequences both for humans and animals. It is an environmental concern and a socio-economic issue that needs to be immediately resolved (Pathak and Mishra 2020). It is recognized that elevated spatial–temporal fluctuations describe streams and rivers, and traditional investigative water quality evaluation techniques involving physicochemical parameters have been considered insufficient (Srivastava et al. 2017). Contamination level in any aquatic body is monitored by comprehensive observation of various physical and chemical variables, bacteriological/coliform, heavy metals, and computing water quality indexes. These parameters act as an indicator to find out the level of contamination. Excessive levels of contaminants through various anthropogenic reasons, which ultimately affect the biological system of aquatic flora and fauna and human beings, should be addressed first.

13.3.1 Major Causes and Sources of River Water Pollution

Numerous sources cause river water pollution on national and international levels. The contaminants include a broad spectrum of organic, inorganic, chemicals, and pathogens. Mainly, river water pollution is caused by point and non-point sources. When pollutants have come into the water body is from a detectable source like industrial effluents/effluent treatment plants (ETPs), major drains, as well as municipal waste/sewage treatment plants (STPs), is called point source (PS) pollution. However, the source of water pollution is not well-known, or pollutants that are not entered from a single disconnected source are called non-point source (NPS) pollution. NPS pollutions are the leading cause of water pollution on national and international scales (Jain et al. 1998; Schwarzenbach et al. 2010; Chaudhry and Malik 2017). As per the Centre for Science and Environment (CSE), about 75–80% of the river water pollution is caused by industrial runoff, municipal sewage, and other wastes are discharged into surface water bodies, including rivers, and it totals over 3000 million liters of wastes per day (Misra 2010; Gaur 2018). The remaining is disposed directly into water bodies, polluting three-fourths of our surface water resources. For example, in northern India, rivers such as the Yamuna are polluted due to numerous sources like agricultural, industrial, urban stormwater runoff, organic contaminants, nutrients, and pathogens (Fig. 13.2).

13.3.1.1 Agricultural Pollutants

Surface runoff from adjacent agricultural fields is a major NPS of pollution and is largely recognized as being more difficult to decrease than point sources. In past decades, organic nutrients have been mainly applied in the agriculture field that might cause eutrophication. But due to the high yield and modernization of agriculture practices after the green revolution (associated with agricultural production through

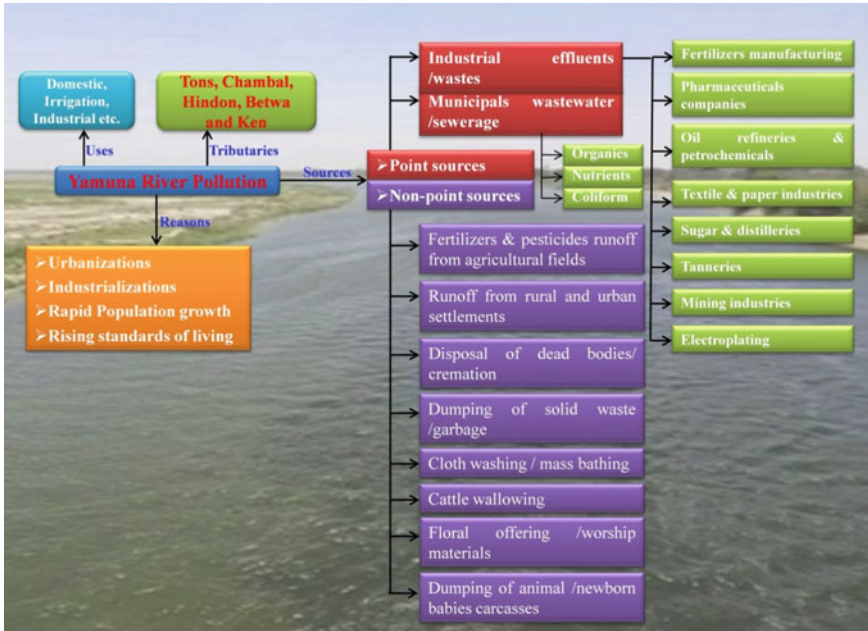


Fig. 13.2 Various sources and causes of Yamuna River pollution

the use of chemical fertilizers, pesticides, i.e., insecticides, fungicides and herbicides, and machinery), surface/river water pollution increase many times since last few decades (Lal et al. 2016; Chaudhry and Malik 2017; Wato et al. 2020). Chemical fertilizers, pesticides, and herbicides contain metals and metalloids, complex compounds that reach natural water bodies through runoff and may be hazardous to flora and fauna. Some of them are persistent, which takes time to degrade, are more harmful. Therefore, it contaminates water, soil, and irrigated plants and causes various health problems to aquatic flora and fauna, which ultimately affect human wellbeing through the food web (Anju, et al. 2010; Schwarzenbach et al. 2010; Chaudhry and Malik 2017).

13.3.1.2 Industrial Pollutants

Industrial units situated along or close by rivers frequently discharge their effluents and wastes indirectly or directly into the streams/rivers. Most of these manufacturing effluents are toxic to living beings that use contaminated river water. Effluents from electroplating, textile, diamond, chemical, and fertilizer industries, etc., are very chronic. India has numerous types of industrial sectors viz mining, thermal power plant, electroplating, distilleries, sugar, paper, and pulp mills, automobile manufacturing, oil refineries, chemical and pesticide production units, hydropower unit, and so

Table 13.1 Pollution index and category of the different industrial units

PI Score	Category	Approximate industries
60 and above	Red	60
41–59	Orange	83
21–40	Green	63
Upto 20	White*	36

**Newly introduced White group have industrial segments which are non-contaminating*

on adjacent to surface water body (Gaur 2018). Development/establishment of small and large industrial units are increasing day by day due to increasing population, demand, and upgrading living standards.

In compliance with GoI acts and rules related to environment protection, Central Pollution Control Board (CPCB) has fixed and categorized the industrial sectors in 2016, based on having pollution index (PI) (Table 13.1). PI of the industrial segment is a number between 0–100, and the rising value of PI indicates the increasing amount of pollutants load generated from the industries. The CPCB also formulated and applied the effluent discharge limit for different categories of industries. But following the rules and monitoring of these compliances is very tough at ground levels.

13.3.1.3 Urban Storm Water Runoff

Among various anthropogenic activities, urban regions are accounted to impose the most consistent and ever-present effects on the RWQ, habitat modification, and decline in biodiversity attributed to both the considerable pollutants load from point and non-point sources. In peri-urban and urban regions, buildings cover and pavement lots of the land surface; hence, when there is precipitation or melting of snow, the water does not absorb/soak into the land. This runoff water brings contaminants such as lawn fertilizers, dirt, chemicals, and oil straight to streams and rivers, ultimately a source of water pollution (Letchinger 2000). In ordinary land, these contaminants are captured into soil's pores, and water is filtered. However, as water cannot absorb/penetrate the ground in metropolitan cities, it washes away all of these contaminants into surface water bodies (Chaudhry and Malik 2017). Walsh et al. (2005) formulated “urban stream syndrome” after studying the degradation of streams draining urban runoff. This term addresses problems like negative changes in flow regime, amplification of pollutant loads, riverbed morphology.

13.3.1.4 Sediment Pollution

Sedimentation because of runoff affects RWQ. It decreases the capacity of navigation channels, streams, ditches, and rivers and also reduces sunlight penetration into the water due to disturbed underwater flora. Therefore, the fishes and other

aquatic fauna nourishing on that vegetation were also disrupted, and the entire food web was disrupted. Contaminants such as phosphorus and pesticides are carried and collected because of sedimentation. Sediment particles also affix to fish gills and cause respiratory problems; ultimately, the death of fish may also occur. In addition, sediments bring hazardous chemicals, viz petroleum products, and pesticides, to surface reservoirs, consequently polluting them (Letchinger 2000; Chaudhry and Malik 2017).

13.3.1.5 Heavy Metals Pollution

“Heavy metals (HMs)” is a cluster of metals with an atomic weight $>4 \text{ g/cm}^3$, or 5 times or more, higher than water (Hawkes 1997). HMs are of serious concern among the contaminants because of their accumulation characteristics through the food web and generate ecological troubles (Paul and Sinha 2015). Commonly, the majority of the HMs come in the river from different sources, which can be either natural by weathering and erosion or human activities (Kashyap et al. 2016; Paul 2017). HMs concentrations at high levels may form toxic complex compounds, which significantly affect the various biotic systems. The occurrence of HMs in industrial effluents is a possible threat to the ecological community. The occurrence of toxic metals in sediments is because of the precipitation of their hydroxides, sulfides and carbonates, which set down and form the fraction of sediments. The industries which characteristic toxic metals in surface water are commonly metal industries, varnishes, pigment, paints, rayon, paper and pulp, distillery, rubber, tannery, steel plant, thermal power plant, mining industries, cotton textiles as well as random application of toxic metal-containing fertilizer and pesticides in farming fields (Suthar et al. 2009; Paul 2017). A concise summary of metal sources and possible harmful effects on human wellbeing has been presented in Table 13.2.

The most vital HMs concerning water contamination is arsenic (As), Cu, Cd, Ni, mercury (Hg), Cr, Pb, and Zn. Some metals (e.g. Zn, Mn, Fe and Cu) are essential as nutrients in trace quantities for plants and microbes’ biological processes but become noxious at elevated concentrations. The Bureau of Indian Standards (BIS) and CPCB have fixed permissible limits of essential metals concentration in drinking water and discharge for a natural water body. Others like chromium, lead, and cadmium has no role in biotic activities but are toxic metal (Ghannam et al. 2015). These HMs are not easily degradable and bio-accumulates in the human and animal bodies to an excessive noxious quantity leading to abominable effects beyond an acceptable limit (Pandey and Madhuri 2014; Paul 2017). Lethal diseases like nephritis, nasal mucous membranes, eyelid edema, renal tumor, anuria, and pharynx congestion, headache, increment cardiovascular diseases, and blood pressure, cancer, osteoporosis, and impairment of various biological systems caused by toxic metals (Jaishankar et al. 2014; Vaishaly et al. 2015). They are also well-known to inhibit the hormone’s metabolism and synthesis (Paul 2017).

India is a nation of intensive gala/ritual where a significant number of festivals are celebrated. Many persons take bathe in the river and discard behind worship

Table 13.2 Heavy metals sources and probable toxic effects on human wellbeing

Metals	Source of heavy metals	Toxic effects
Cadmium (Cd)	Batteries, fertilizer, electroplating, pesticides, nuclear fission plant, welding	Nausea, vomiting, diarrhea, and death
Iron (Fe)	Mining	Congestion of blood vessels, quick increase in respiration, pulse rate, hypertension and drowsiness, noxious for marine life
Chromium (Cr)	Cotton Textiles, electroplating, mining, tannery industries	Sensitization/ulceration of the skin, lung cancer,
Copper (Cu)	Electroplating, pesticides, mining	Sporadic fever, coma, hypertension, noxious for marine life, death
Lead (Pb)	Automobile emission, burning of coal, mining, paint, batteries, pesticides	Lead poisoning, death, anemia
Manganese (Mn)	Welding, fuel addition, Ferromanganese production	Fever, sexual impotence, central nervous system disorder, growth retardation, blindness and muscular fatigue
Nickel (Ni)	Electroplating, batteries industry, zinc base casting,	Lung and nasal cancer
Zinc (Zn)	Metal plating, brass manufacture, refineries, immersion of painted idols	Liver and kidney damage, headache, noxious for marine life

Sources Sundaray et al. (2012), Paul (2017)

goods, clay idols, plastic bags, account books, human excreta, and flower gifts in the river that raise the floating matters and contaminants in the river water. Additionally, several small towns and villages are situated all alongside the river, the most of them don't have satisfactory hygiene amenities. Thus, several persons utilize the river drainage field for excretion, a source of pathogenic and organic pollution in river water. Also, the public has the tradition of discarding the un-burnt dead bodies of humans and cattle into the river. As per superstition, the dead body has certain diseases (tuberculosis, asthma, snake bite, leprosy, poisoning, etc.), and infants, holy men, and unmarried persons are discarded into the river. People having meager incomes also abandon dead bodies into the river water to save the expensive wood incineration (Gaur 2018). Dumping garbage and solid waste is one more contaminating cause and contaminating activities by Indian people, whose appropriate supervision is inescapable in rivers.

13.4 Reviews on River Water Pollution in India

About 70% of rivers in India are polluted due to rapid industrialization and urbanization (Jindal and Sharma 2011). In developing nations, the majority of the rivers

nearby urban cities are the primary sinks for wastes released from industries (Suthar et al. 2009). The release of urban wastewater into river drainage basins is a significant problem in sustaining RWQ. These effluents and urban sewage negatively influence public well-being through various processes/routes of the food chain (Gomez-Baggethun et al. 2013). Regarding progress plans in India, cleaning up of rivers is often not optimally prioritized; hence, continuous evaluation of the status of pollution of the rivers by human activities is needed.

CPCB monitored 445 rivers throughout the country, of which 302 river stretches were identified polluted. These polluted river stretches were further classified under different priority classes (CPCB 2015). Accordingly, CPCB has assessed present sewage generation based on India's urban population and projecting the population for 2020, considering the growth rate for the year 2001 to 2011. The rate of sewage generation is taken as 80% of the water supply. Total sewage generation and treatment capacity in India is presented in Fig. 13.3. Out of this, Uttar Pradesh (UP) generates 8263 MLD (million liters per day), with 3374 MLD (41%) installed capacity. Out of total sewage generation, 2510 MLD (30%) is treated (CPCB 2021).

Girija et al. (2007) have evaluated the water quality of Bharalu tributary's (Brahmaputra River, Assam) in different seasons. They reported 'poor' water quality, with significant spatial and seasonal fluctuation. Urban runoff was found to have the leading role in hardness, alkalinity, and BOD, and the catchment region has a noticeable influence on chloride concentration and conductivity. Sulfate (SO_4^{2-}) content showed noticeable seasonal fluctuation, influenced by dilution and occurrence of

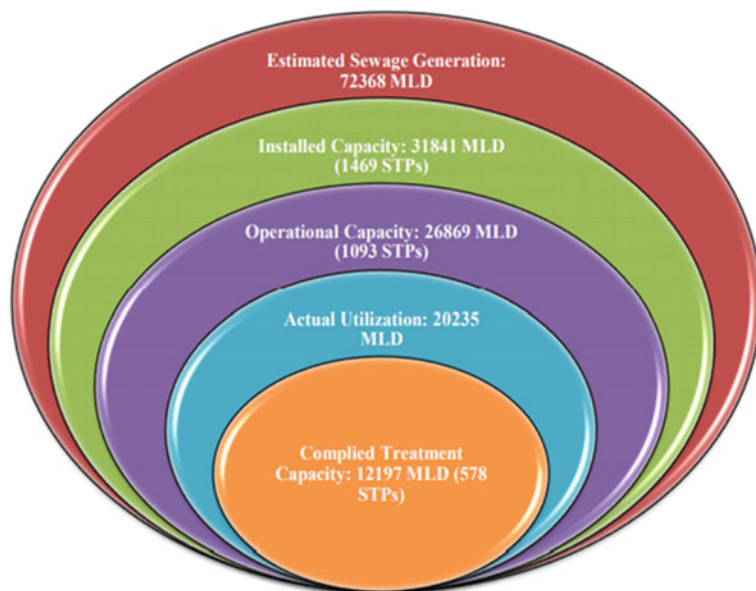


Fig. 13.3 Venn diagram depicting sewage generation, installed treatment capacity, operational capacity, actual utilization, and complied treatment capacity (Sources CPCB 2021)

bacteria, iron, and phosphorus was high in all the sites promoting extreme growth of weeds and inducing more stress on dissolved oxygen (DO) of the water channel. Chatterjee et al. (2010) evaluated environmental and bacteriological variables of Damodar River (West Bengal) at a point source location following chemometric methods from 2004 to 2007. The results show that contamination of metals, coliform counts, and organic pollutants at beyond the acceptable limits for domestic uses. Besides different industrial's effluents near the sampling location, the random inclusion of domestic sewage may be contributed to the increment of the pollutants.

Mandal et al. (2010) investigated the spatial and seasonal fluctuation of Yamuna RWQ in Delhi during 2000–2005. The result reveals that the release of partially treated and non-treated wastewater is the leading cause of Yamuna River pollution. The seasonal fluctuation and interrelationship of the chosen variables may be helpful to in the regular examination of RWQ. Banerjee and Gupta (2013) characterized the industrial effluents discharged from different industries and heavy metals distribution in effluent releases channel and their impact on Damodar River. The results of enrichment factors (EF) and the pollution load index (PLI) (1.305) confirm that effluent channels have deteriorated from important heavy metal pollution following urbanization and industrialization. Compared to baseline data, the surface sediment layers explain high enrichment across the channel and at its release point. Factor analysis (FA) also explains three factors i.e., surface runoff inputs, industrial sources, and background lithogenic factors, which clarify the observed variance of the environmental parameters.

Further, Haldar et al. (2014) assessed the water quality of the Sabarmati River (Gujarat) using physicochemical variables, microbiological (total and chosen bacterial count), and biological (phytoplankton). The results showed that the river stretch from Ahmedabad -Vasana barrage to Vataman was extremely contaminated due to continuous waste releases primarily from industries and municipal drainage. The study also showed moderate to poor Sabarmati RWQ concerning physicochemical and biological contaminants. The river has significantly lost self-purification capacity among Ahmedabad to Vataman due to a lack of minimum flow. Numerous small and medium-scale industries situated along the river water body are causing river water pollution.

Sharma et al. (2014) assessed the Hindon RWQ of various point sources contributing to a river in pre-and post-monsoon seasons in 2012. The high amount of BOD and COD content noticed in the drains showed a high level of organic contamination represented the water inappropriately even for bathing purposes. Almost sampling locations of the u/s and m/s of Hindon River, DO content was found to be 0 mg/L due to huge organic load. BOD content varied between 3.3–65 mg/L, and COD content is varied between 28–338 mg/L in pre-monsoon. However, during post-monsoon BOD varied between 0–139 mg/L, and COD varied between 24–388 mg/L. Further, RWQ has been evaluated using WQI and water quality was found to be 'bad' at each sampling location. Results showed that point sources have a huge organic pollution load that degrades overall Hindon RWQ. Moreover, pollution risk estimation based on QUAL2E-UNCAS simulations of Hindon and its tributary Kali flowing through Uttar Pradesh shows the imperceptible concentration of DO with

higher levels of BOD equal to 56.7 mg/L in Kali and 86.5 mg/L in Hindon elucidated the effect of slightly treated to non-treated waste releases into both rivers. The simulations of water quality were conducted and the study indicated that both rivers are in pollution stress and, particularly Hindon River is not able to recover even in winter seasons when it is generally expected that the high absorptive capability of rivers (Babbar 2014).

Gurjar and Tare (2019) evaluated the RWQ and natural absorptive capacity of Ramganga River, which confluence with Ganga River. Despite the huge organic load in midstream (m/s) of Ramganga, the recorded values of DO were >4 mg/L at approximately every location on the main stem, even in a lean flow time of a year. Assessment of Ramganga before and after the confluence with Ganga, RWQ for lean flow period declared that Ramganga is not considerably contributed to the deterioration in Ganga RWQ concerning variables like heavy metals and DO. RWQ at 12 sites were classified as good, 9 sites as satisfactory and 2 sites as poor according to irrigation criteria described by CPCB (2011). Pathak and Mishra (2020) also investigated Ganga RWQ at 6 urban centers (Anupshahar, Kannauj, Kanpur, Prayagraj, Mirzapur, and Varanasi) of UP. Four RWQ [DO, BOD, Fecal Coliform (FC), and Total Coliform (TC)] monitoring data of the UP-Pollution Control Board were used for the analysis. Anupshahar and Kannauj were less polluted centers with downstream values slightly higher than the upstream values that signified a slight accumulation of pollutants. The maximum differences in the BOD level and pathogenic concentration between the u/s and d/s sides were observed at Kanpur and Varanasi, signifying massive interference of human activities in the river ecosystem in Kanpur and Varanasi. Prayagraj showed a continuous decline in pollution, signifying improving water quality. The decreasing trend of pollution levels in the Ganga River water stream showed that the efforts from the government sector and participation from the general community are in the right direction.

The current situation of HMs (Cu, Fe, Co, Cd, Cr, Hg, Mn, Zn, Ni, and Pb) pollution in the Ganga River was reviewed by Paul (2017). Numerous researches of HMs contamination confirm that the concentration of different toxic metals in Ganga River water and sediment is beyond the permissible limits. HMs at elevated levels in the river ecosystem shows a chronic risk to human wellbeing. HMs exposure is associated with various cancers, developmental retardation, kidney damage, and yet death is the occurrence of excessive exposure. Therefore, the step must be taken to reduce the effluent load in river Ganga. They recorded different sources of HMs in sediment and river water that need to be strongly supervised to the enhancement of the environment, and domestic sewage discharge and industrial effluent should be reduced.

In this continuation, few studies on physicochemical variables and heavy metals concentration in Indian RWQs are presented in Tables 13.3 and 13.4, respectively.

Table 13.3 Overall mean/range of numerous physiochemical variables in different rivers of India

Rivers	Location	pH	EC	TDS	DO	BOD	COD	NO ₃ ⁻	Cl ⁻	SO ₂ ⁴⁻	HCO ₃ ⁻	Turb	TA	TH	PO ₄ ³⁻	References
Chambal	Madhya Pradesh	6.95 -8.96	222-854	200-550	5.54-9.02	0.12- 18.08	2.0-68.35	0.35- 7.35	-	-	-	0.11-126.33	-	-	-	Srivastava et al. (2017)
Damodar	West Bengal	7.93	384.44	253.86	-	-	-	0.98	8.18	26.84	109.33	-	-	-	0.29	Banerjee and Gupta (2013)
Hindon	Uttar Pradesh	7.40 - 7.89	83-504	222.2-2426.3	3.10 -4.03	27-51	85.0-337.4	106-245	201-1326	36.4-162.4	-	28.7- 109.3	347.0-596.3	235.1-459.9	-	Suthar et al. (2010)
Ganga	Uttarakhand	7.17	192.04	413.39	10.26	1.84	9.86	0.05	6.72	-	-	3.31	60.12	81.74	-	Bhutiani et al. (2016)
Ganga	Uttarakhand	9.4	85.2	38.6	10.0	4.3	-	-	22.1	-	18.8	-	70.4	101.2	4.2	Haritash et al. (2016)
Kali	Uttar Pradesh	7.13	1281.2	655.6	-	24.3	110.8	31.1	69.2	29.6	277	7.7	301.8	185.9	3.50	Singh et al. (2020)
Ghaghara	Uttar Pradesh	8.083	323.367	226.5	7.76	2.802	11.683	0.4291	7.4816	16.541	-	-	140.3	-	0.0682	Singh et al. (2017)
Gandak	Bihar	8.179	241.1	170.9	7.322	2.277	12.459	0.2387	4.838	22.158	-	-	112.547	-	0.0642	Singh et al. (2017)
Mahanadi	Orissa	7.39	4.665.2	2.461.3	-	-	-	-	1572.2	56.43	-	-	87.9	592.38	-	Sundaray et al. (2009)
Tapi	Gujarat	8.27	290	-	4.95	5.45	79.5	0.53	36.08	-	-	23.8	77.67	137.67	0.67	Gaur. (2018)

All values in mg/L except pH, EC (µs/cm), Turb (NTU)

Table 13.4 Comparison of average heavy metals concentrations (mg/L) in different rivers of India

S. N	Rivers	Regions	Cd	Cu	Cr	Fe	Ni	Pb	Mn	Zn	References
1	Hindon	Uttar Pradesh	–	0.006	0.015	0.226	0.024	0.037	0.129	0.058	Jain and Sharma (2006)
2	Achankovil	Kerala	0.006	0.224	–	11.85	–	0.072	0.699	0.415	Prasad et al. (2006)
3	Koel (Brahmani)	Orissa	–	0.006	0.010	0.481	0.024	0.001	0.030	0.031	Sundaray (2010)
4	Ganga River	West Bengal	0.01	0.01	–	0.8	0.14	0.12	0.26	0.06	Aktar et al. (2010)
5	Damodar		0.30	3.95	11.55	0.480	–	–	–	–	Chatterjee et al. (2010)
6	Kabini	Karnataka	–	27.44	21.79	63.55	–	–	21.70	53.95	Hejabi et al. (2011)
7	Brahmani	Orissa	0.001	0.001	–	0.020	0.015	0.012	0.024	0.015	Reza and Singh (2010)
8	Mahanadi		0.0009	0.0083	0.0036	0.1893	0.0101	0.008	0.0198	0.0292	Sundaray et al. (2012)
9	Subarnarekha	Jharkhand	bdl–0.02	0.01–0.03	0.01–0.023	–	bdl–0.03	bdl–0.38	–	0.07–0.49	Banerjee et al. (2016)
10	Yamuna	Delhi NCR	0.02	0.11	0.05	–	0.05	0.1	–	0.69	Bhattacharya et al. (2015)
11	Yamuna		0.0476	2.1518	0.1471	10.488	0.3755	0.1164	–	1.5007	Bhardwaj et al. (2017)

(continued)

Table 13.4 (continued)

S. N	Rivers	Regions	Cd	Cu	Cr	Fe	Ni	Pb	Mn	Zn	References
12	Kali (East)	Uttar Pradesh	0.06	–	0.06	1.53	–	0.13	–	24.71	Mishra et al. (2018)
13	Kali		0.0774	0.1987	0.1338	0.5316	0.2515	0.3134	0.2524	0.2377	Singh et al. (2020)
14	Ganga	Uttar Pradesh	0.020–0.150	0.020–0.080	0.030–0.090	0.590–0.680	0.220–0.305	0.060–0.190	–	0.200–0.270	Niveshika et al. (2016)
15	Ganga	Uttarakhand-Uttar Pradesh	0.60–13.10	bdl-36.0	–	–	–	2.40–26.90		bdl-106.30	Goswami and Sanjay (2014)

not recorded, bdl below detection limit

13.5 Approaches of River Water Quality Evaluation

13.5.1 Water Quality Index

Water quality indexes (WQIs) are internationally accepted statistical approaches to determine the pollution status by categorizing quality classes (excellent, good, poor, inferior, and unfit for human use). WQI is the most reliable measure of surface and groundwater pollution and can be used effectively to execute water quality updating programmers. The WQI transforms multifaceted water quality information into secure data that is intelligible and useable by people. Water quality lists facilitate the assessment of the water quality profile of a river over its entire stretch and recognize the zones where the difference between the required and current water quality is sufficiently large to necessitate critical pollution control measures (Srivastava et al. 2017; Kumar et al. 2021). This index accounts for a general assessment of water quality on numerous levels that affect the capacity of a stream to sustain life. Numerous studies have been conducted on WQI in India by different researchers (Table 13.5).

Table 13.5 List of different WQIs for monitoring of various rivers in India

Area	Rivers	WQI	References
Tamil Nadu	Cauvery	Tiwari and Mishra	Kalavathy et al. (2011)
Madhya Pradesh	Chambal	NSFWQI	Srivastava et al. (2017)
South Bengal	Damodar	CCMEWQI	Haldar et al. (2016)
Entire river	Godavari	NSFWQI	Chavan et al. (2009)
Uttar Pradesh	Hindon	CPI	Mishra et al. (2016)
Entire river	Hindon	Tiwari and Mishra	Sharma et al. (2014)
Ujjain	Kshipra	NSFWQI	Gupta et al. (2012)
Madhya Pradesh	Narmada	CCMEWQI, NSFWQI, Weighted arithmetic	Gupta et al. (2017)
Gujarat	Sabarmati	Weighted arithmetic mean	Shah and Joshi (2017)
Gujarat	Sabarmati	NSFWQI	Haldar et al. (2014)
Himachal Pradesh	Swan	NSFWQI, OIP	Sharda et al. (2017)
Delhi NCT	Yamuna	OIP	Katyal et al. (2012)
Entire river	Yamuna	Customized NSFWQI	Sharma et al. (2008)
Uttar Pradesh	Kali River	Weighted arithmetic mean	Singh et al. (2020)
Uttarakhand	Ganga	CPI	Kumar et al. (2020)
Uttarakhand	Ganga	CCMEWQI, NSFWQI	Kumar et al. (2021)

NSFWQI: National Sanitation Foundation Water Quality Index; OIP: Overall Index of Pollution; CCMEWQI: Canadian Council of Ministers for Environment Water Quality Index; CPI: Comprehensive pollution index

Jindal and Sharma (2011) studied Sutlej RWQ at Ludhiana (Punjab) in different seasons during 2006–2007. For the calculation of water quality rating and WQI, nine variables were measured. The average values of each variable were compared with ICMR, BIS, and WHO norms. The WQI was found 32.84, 51.01, and 132.66 at sites S1, S2, and S3, respectively. This showed that the river water was unsafe for human use at sites S2 and S3 and might be used only for irrigation, aquaculture, and industrial application. Sharma and Kansal (2011) studied the river Yamuna using WQI to explain the contamination level in the river for 10 years period (2000–2009). They also determine the significant contaminants influencing the RWQ during its course through the city. The range of water quality is found “good to marginal” class at Palla and “poor” class at all other sites. The RWQ at different sites is mainly affected by wastewater release produced from the National Capital Territory (NCR, Delhi), entering the Yamuna River through numerous drains.

Prasad et al. (2013) developed a web-based system to express the surface water quality in the imprecise condition of observed data. Eight variables were examined in surface water, in which four variables i.e. pH, DO, BOD, and FC were applied for the WQI computation following Maharashtra Pollution Control Board (MPCB) water quality norms of category A-II for the best-designated application. The investigation explained that river points in a specific year were in a very bad class with 0–38% certainty level, which is not suitable for drinking uses. Samples in the “bad” and “medium to good” classes had certainty levels between 38–50% and 50–100%, respectively. The remaining sample was a “good to excellent” class, appropriate for drinking uses, with certainty levels between 63–100%. This web system is helpful for the concerned authorities and policymakers that allowing them to obtain the expected output in a shorter time.

Mishra et al. (2015) assessed the heavy metal contamination (Cd, Pb, Fe, Cr, and Zn) in Kali River apply Nemerow pollution index (NPI), in pre- and post-monsoon seasons in 2014. NPI computed for drinking water quality norms and found 5.04 in pre-monsoon and 7.08 in post-monsoon, whereas regarding inland water quality norms established as 4.37 in pre-monsoon and 3.62 in post-monsoon. Heavy metals analysis results revealed that Zn and Pb are the major variables accountable for river water pollution. Comprehensively NPI showed that river water was extremely polluted (i.e. $NPI > 3$) in pre- and post-monsoon seasons, due to surface runoff, dredging, other associated human activities, and the release of urban/industrial effluents into Kali River. Further, Mishra et al. (2018) also evaluated the effect of heavy metal contamination (Zn, Cr, Fe, Cd, and Pb) using the heavy metal pollution index (HPI) in the Kali River at seven locations in pre-monsoon and post-monsoon in 2014. HPI was established to be 6.79 in pre-monsoon and 4.98 in post-monsoon season, which is higher than the crucial value ($HPI \gg 1$). The study explained that the Kali river stretch was extremely polluted concerning heavy metals, and recommended that the wastewater produces from industrial units must be treated before release into the river.

Bhutiani et al. (2016) assessed the river Ganga environs at Uttarakhand and calculated WQI by investigating 16 physicochemical variables based on NSFQI to

evaluate the appropriateness of water for irrigational, drinking, and other applications. Application of NSFQI to evaluate the RWQ over 11 years displays small fluctuations in water quality. Results also showed that solid and liquid waste pollutants, sewerage, or organic nature are the major causes of pollution. Mishra et al. (2016) estimated Hindon RWQ at 28 sampling locations of western Uttar Pradesh (WUP) applying the CPI, considering the eleven environmental variables in 2013–14. The results of CPI showed that the Hindon River was extremely polluted (CPI = 2.68–7.12).

Jaiswal et al. (2019) studies characterized the extensive evaluation of physical and chemical conditions in RWQ of the entire Yamuna stretch (India). Computed WQI was “excellent” to “good” in the upper region, with BOD average values of 2.1 mg/L in rainy and 2.4 mg/L in the non-rainy season. While, WQI was “poor” to “marginal” in the middle region, with BOD mean values of 13.1 and 32.3 mg/L in rainy and non-rainy seasons, respectively. Additionally, WQI values better to “good,” and “excellent” class in lower region and BOD reduced to 1.9 and 1.8 mg/L in rainy and non-rainy seasons, respectively.

The globally accepted coherent approach of WQIs and multivariate statistical models (PCA and CA) were utilized in the dataset to assess the spatial–temporal fluctuation and contamination source recognition and apportionment river Ganga in Uttarakhand (Kumar et al. 2021). Total 22 hydro-chemical variables were analyzed by collecting the samples from 20 different vertically elevated monitoring locations for different seasons. The seasonal variation in RWQ by the CCMEWQI showed the quality class at a marginal level in summer (62.16), monsoon (59.96), and post-monsoon (60.20) season, whereas in winters (71.18), water quality was in fair condition. The present observations contribute to the usefulness of these statistical methodologies to interpret and understand large datasets and also provide reliable information to reduce the tediousness and cost of water quality monitoring and assessment programs.

13.5.2 Multivariate Statistical Approach to Monitoring the River Water Quality

The multivariate statistical analysis involves concurrent evaluation of more than two variables of water quality. All statistical systems concerned with the instantaneous breakdown of numerous measurements on several diverse variables comprise the multivariate analysis (Manoj and Padhy 2014). Some commonly used multivariate statistical models (or environmetrics) for environmental data analysis are factor analysis (FA), cluster analysis (CA), and discriminant analysis (DA). FA, which consists of principal component analysis (PCA), is a statistical method utilized to reduce the dimensionality of a dataset comprising a considerable number of inter-related variables (Singh et al. 2004). This reduction method includes a conversion of the dataset into a new dataset of variables, i.e., termed principal components (PCs).

These PCs are organized in reducing an array of significance and are orthogonal, i.e., non-correlated (Panda et al. 2006). Some of the advantages of PCA are:

1. PCA gives information on the major consequential variables, which explain the entire data set providing data reducing with the least loss of original data.
2. PCA helps the recognition of contamination sources based on shortened variables, like spatial (contamination originate from human activities) and temporal (climatic and seasonal) (Razmkhah et al. 2010; Rizvi et al. 2016).

CA is a technique for establishing a large quantity of data into convenient very important heaps. It is an information-reducing tool that makes sub-clusters which are convenient than a single dataset. Like FA, it examines the inter-association among the variables. This method also aids in assume the data on the contamination sources and inter-relationship among different contamination sources. Hierarchical agglomerative cluster analysis (HACA) is a technique that shows perceptive resemblance associations among any individual sample and the total data set and is usually displayed as a tree diagram, i.e., dendrogram (Panda et al. 2006; Rizvi et al. 2016). The Euclidean metric usually details the uniformity among two samples. A Euclidean metric can be expressed by the variation among investigative data from both samples (Zheng et al. 2015).

Since RWQ evaluation demands working with large datasets, numerous advanced statistical tools were practiced. Environmetrics like PCA and CA have been used to identify possible sources that can influence aquatic bodies to improve the perception of water quality and the actual status of the study region. These techniques have been mainly dependable in providing a new and unique sympathetic of the association between a range of different contaminants (Wang et al. 2013; Barakat et al. 2016). These techniques are crucial for trustworthy monitoring of river water resources and quickly finding solutions to deterioration problems in river water. Numerous studies on the application of multivariate techniques/enviro-metrics to assess the RWQ have been carried out nationwide by various researchers (Table 13.6).

Singh et al. (2004) reported various environmetrics to evaluate spatial-temporal fluctuations and interpret a substantial complex RWQ dataset collected in examining the river Gomti River in UP, India. The multifaceted data matrix (17,790 measured data) was analyzed with various environmetrics like CA, FA/PCA, and DA. CA displayed good outcomes rendition 3 dissimilar clusters of resemblance among the sampling locations indicating the various RWQ variables. PCA recognized six factors, i.e. liable for the data framework describing 71% of the entire variance of a dataset and permitted to cluster the chosen variables as per general characteristics and assess each cluster's frequency on the comprehensive fluctuation in RWQ. DA displayed the best outcomes for reducing data and pattern recognition in a spatial-temporal investigation. DA presented five variables managing over 88% right rendezvous in a temporal investigation, whereas nine variables to manage 91% right rendezvous in a geographical investigation of 3 dissimilar areas in the catchment. Hence, DA permitted a decrease in the spatiality of the huge dataset, defining few indicator variables accountable for huge fluctuations in RWQ. This research shows the need and effectiveness of environmetrics for the monitoring and analyzing

Table 13.6 Application of multivariate techniques for monitoring of RWQs in India

Region	Rivers	Multivariate statistics/environmetrics	References
Uttarakhand	Ganga	PCA, CA	Kumar et al. (2021)
Uttarakhand	Ganga	PCA, HCA	Kumar et al. (2020)
Uttar Pradesh	Hindon	PCA, HCA	Mishra et al. (2016)
Madhya Pradesh	Chambal	PCA, DCA, CCA	Srivastava et al. (2017)
Gujarat	Sabarmati	PCA	Haldar et al. (2014)
Uttar Pradesh	Kali	PCA, HCA	Singh et al. (2020)
Uttar Pradesh	Hindon	PCA, HACA	Rizvi et al. (2016)
Uttar Pradesh	Ramganga	DA, HCA	Gurjar and Tare (2019)
West Bengal	Damodar	PCA	Banerjee and Gupta (2013)
Delhi	Yamuna	PCA	Bhardwaj et al. (2017)

Detrended correspondence analysis (DCA); Canonical correspondence analysis (CCA)

huge datasets to obtain the best information regarding the RWQ and plan of observing networks for efficient water resources supervision.

Kumar et al. (2020) attempted to evaluate the long-term (1989–2016) hydro-chemical parameters of Ganga RWQ at five u/s sites of Uttarakhand i.e. Uttarkashi, Tehri, Rudraprayag, Devprayag, and Rishikesh, applying a CPI and multivariate statistical method (PCA and CA). These techniques were applied to classify, sum up expensive datasets and clustering similar contaminated region along the river stretches. PCA established the input source of nutrients in the river from both human and natural sources. Additionally, the u/s RWQ evaluated was established to be good in comparison to the extremely polluted d/s area.

13.6 Conclusions

This comprehensively reviewed the importance of water and various characteristics of RWQ on a national scale and concluded that the majority of Indian rivers are degrading day by day through different anthropogenic reasons, causes, and sources. Hence, in current scenarios, meticulous monitoring of RWQ concerning physico-chemical, heavy metal, and bacteriological parameters is necessary. Simultaneously, the application of multivariate statistical approach and computing WQI, CPI is also important to find out the actual status of RWQ. Because, rivers have reservoir of ecological diversity and provide important services to communities. River and other surface water qualities is mainly affected by various anthropogenic activities such as fast industrialization, urbanization, improperly managed landfills, landscape change, pollutants (chemical fertilizers and pesticides), runoff from agricultural fields, cities

runoff, municipal drainage mixing, dumping solid or semi-solid wastes in river catchments, which need to be examined and controlled by adopting following remediation techniques:

- Efficient working of ETPs for industrial effluents, STPs for municipal wastewaters. Upgrading or establishment of advanced ETP and STP technologies and ensure complete treatments (primary, secondary and tertiary stage)
- The present ETPs and STPs need to be tested for its efficiency, reliability and technological parameters by self-reliant departments (tech-efficiency-reliability verification).
- Based on effluents/wastewater characteristics, following advanced remediation/treatment techniques could be adopted inside the industrial/municipal regions, which is addressed by numerous reviewers:
 - Bioremediation/phytoremediation technique (by using microbes, algae, exotic and aquatic plants species)
 - Advanced oxidation processes (Fenton's Reagent, Peroxonation, Sonolysis, Ozonation, Ultraviolet Radiation-Based AOP, Photo-Fenton Process, Heterogeneous Photocatalysts, using catalytic nanomaterials)
 - Chitosan-based magnetic adsorbents (for toxic metals)
 - Photoelectro-Fenton process as efficient electrochemical advanced oxidation.
 - Treatment with UV light, sunlight, and coupling with conventional and other photo-assisted advanced technologies
- Identify major drain in urban and peri-urban region; treat their water before release or confluence with surface water body.
- Need to strict implication of numerous rules and regulations followed by national agencies at ground level for improvement of all surface water qualities
- Preventive measure viz stops discarding of solid waste/garbage in its catchment areas as well as creating awareness among community.
- Precise application of chemical fertilizers and pesticide in agricultural field.
- Besides that, monitoring of RWQs at specific intervals is important for find out major causative factors.
- Minimum generation of wastewaters, recycling and reuse is also a significant optional method.

Competing Interests

The authors declare that they do not have any personal or financial conflict of interests.

References

- Aktar MW, Paramasivam M, Ganguly M, Purkait S, Sengupta D (2010) Assessment and occurrence of various heavy metals in surface water of Ganga river around Kolkata: a study for toxicity and ecological impact. *Environ Monit Assess* 160(1):207–213

- Anju A, Ravi SP, Bechan S (2010) Water pollution with special reference to pesticide contamination in India. *J Water Resour Protect*
- Ayyam V, Palanivel S, Chandrakasan S (2019) Coastal ecosystems of the Tropics-adaptive management. Springer, Singapore
- Babbar R (2014) Pollution risk assessment based on QUAL2E-UNCAS simulations of a tropical river in Northern India. *Environ Monit Assess* 186(10):6771–6787
- Banerjee S, Kumar A, Maiti SK, Chowdhury A (2016) Seasonal variation in heavy metal contaminations in water and sediments of Jamshepur stretch of Subarnarekha river, India. *Environ Earth Sci* 75(3):265
- Banerjee US, Gupta S (2013) Impact of industrial waste effluents on river Damodar adjacent to Durgapur industrial complex, West Bengal, India. *Environ Monit Assess* 185(3):2083–2094
- Barakat A, El Baghdadi M, Rais J, Aghezzaf B, Slassi M (2016) Assessment of spatial and seasonal water quality variation of Oum Er Rbia River (Morocco) using multivariate statistical techniques. *Int Soil Water Conser Res* 4(4):284–292
- Bhardwaj R, Gupta A, Garg JK (2017) Evaluation of heavy metal contamination using environmental and indexing approach for River Yamuna, Delhi stretch, India. *Water Sci* 31(1):52–66
- Bhattacharya A, Dey P, Gola D, Mishra A, Malik A, Patel N (2015) Assessment of Yamuna and associated drains used for irrigation in rural and peri-urban settings of Delhi NCR. *Environ Monit Assess* 187(1):1–13
- Bhutiani R, Khanna DR, Kulkarni DB, Ruhela M (2016) Assessment of Ganga river ecosystem at Haridwar, Uttarakhand, India with reference to water quality indices. *Appl Water Sci* 6(2):107–113
- CGWB (Central Ground Water Board) (2017) Dynamic Ground Water Resources of India. CGWB, New Delhi
- Chatterjee SK, Bhattacharjee I, Chandra G (2010) Water quality assessment near an industrial site of Damodar River, India. *Environ Monit Assess* 161(1):177–189
- Chaudhry FN, Malik MF (2017) Factors affecting water pollution: a review. *J Ecosyst Ecography* 7(225):1–3
- Chavan AD, Sharma MP, Bhargava R (2009) Water quality assessment of the Godavari River. *Hydro Nepal J Water Energy Environ* 5:31–34
- CPCB (2016). <https://cpcb.nic.in/openpdf.php?id=TGF0ZXN0RmlsZS9MYXRlc3RfMTE4X0ZpbmFsX0RpcmVjdGlvb3VudG85NTY0LnBkZg>. Accessed 14 June 2021
- CPCB (2021) National inventory of sewage treatment plants. <https://cpcb.nic.in/openpdf.php?id=UmVwb3J0RmlsZXMvMTIyOF8xNjE1MTk2MzIyX2I1ZGlhcGhvdG85NTY0LnBkZg>. Accessed 14 June 2021
- CPCB (2015) Polluted river stretches in India criteria and status. Retrieved from <http://cpcb.nic.in>
- CWC annual report 2013–14. <http://cwc.gov.in/sites/default/files/annual-report-0402-2013-14.pdf>
- CWC (2005) Water data-complete book. Govt. of India, New Delhi. http://cwc.gov.in/sites/default/files/Water_Data_Complete_Book_2005.pdf
- CWC (2015) Annual report 2015–16. Retrieved from http://cwc.gov.in/main/downloads/Annual_ReportCWC_2015-16.pdf
- Dadhwal V, Sharma J, Bera A, Salunkhe S, Bankar N, Singh DV, Paithankar Y, Paul Kalsi A, Gupta P, Agarwal C K, Tembhrney W M, Jain R, Kumar N, Abraham NS, Azhagesan R, Banerjee A, Kumar R, Ranjan P, Sharma P, Bhaskaran R (2014) Watershed atlas of India
- Du Plessis A (2017) Freshwater challenges of South Africa and its upper Vaal River. Springer, Berlin, Germany, pp 129–151
- Garg P (2012) Energy scenario and vision 2020 in India. *J Sustain Energy Environ* 3(1):7–17
- Gaur S (2018) An updated review on quantitative and qualitative analysis of water pollution in west flowing Tapi River of Gujarat, India. *Environ Pollut*, 525–547
- Ghannam HE, El Haddad ESE, Talab AS (2015) Bioaccumulation of heavy metals in tilapia fish organs. *J Biodiversity Environ Sci* 7(2):88–99
- Ghosh S, Mistri B (2015) Geographic concerns on flood climate and flood hydrology in monsoon-dominated Damodar river basin, Eastern India. *Geography J*

- Girija TR, Mahanta C, Chandramouli V (2007) Water quality assessment of an untreated effluent impacted urban stream: the Bharalu tributary of the Brahmaputra River. India. *Environ Monit Assess* 130(1):221–236
- Gómez-Baggethun E, Gren A, Barton DN, Langemeyer J, McPhearson T, O'Farrell P, ... Kremer P (2013) Urban ecosystem services. urbanization, biodiversity and ecosystem services: challenges and opportunities
- Goswami DN, Sanjay SS (2014) Determination of heavy metals, viz. cadmium, copper, lead and zinc in the different matrices of the Ganges River from Rishikesh to Allahabad through differential pulse anodic stripping voltametry. *Int J Adv Res Chem Sci (IJARCS)* 1:7–11
- Gupta N, Pandey P, Hussain J (2017) Effect of physicochemical and biological parameters on the quality of river water of Narmada, Madhya Pradesh. India. *Water Sci* 31(1):11–23
- Gupta RC, Gupta AK, Shrivastava RK (2012) Assessment of water quality status of holy river Kshipra using water quality index. *J Indian Water Resour Soc* 32(1–2):33–39
- Gurjar SK, Tare V (2019) Spatial-temporal assessment of water quality and assimilative capacity of river Ramganga, a tributary of Ganga using multivariate analysis and QUEL2K. *J Clean Prod* 222:550–564
- Halder D, Halder S, Das P, Halder G (2016) Assessment of water quality of Damodar River in South Bengal region of India by Canadian council of ministers of environment (CCME) water quality index: a case study. *Desalin Water Treat* 57(8):3489–3502
- Halder S, Mandal SK, Thorat RB, Goel S, Baxi KD, Parmer NP, ... Mody KH (2014) Water pollution of Sabarmati River—a Harbinger to potential disaster. *Environ Monit Assess* 186(4):2231–2242
- Haritash AK, Gaur S, Garg S (2016) Assessment of water quality and suitability analysis of River Ganga in Rishikesh. India. *Appl Water Sci* 6(4):383–392
- Hawkes SJ (1997) What is a "heavy metal"? *J Chem Educ* 74(11):1374
- Hejazi AT, Basavarajappa HT, Karbassi AR, Monavari SM (2011) Heavy metal pollution in water and sediments in the Kabini River, Karnataka. India. *Environ Monit Assess* 182(1):1–13
- Jain CK, Sharma MK (2006) Heavy metal transport in the Hindon river basin. India. *Environ Monit Assess* 112(1):255–270
- Jain CK, Bhatia KKS, Seth SM (1998) Assessment of point and non-point sources of pollution using a chemical mass balance approach. *Hydrol Sci J* 43(3):379–390
- Jaishankar M, Tseten T, Anbalagan N, Mathew BB, Beeregowda KN (2014) Toxicity, mechanism and health effects of some heavy metals. *Interdiscip Toxicol* 7(2):60
- Jaiswal M, Hussain J, Gupta SK, Nasr M, Nema AK (2019) Comprehensive evaluation of water quality status for entire stretch of Yamuna River. India. *Environ Monit Assess* 191(4):1–17
- Jindal R, Sharma C (2011) Studies on water quality of Sutlej River around Ludhiana with reference to physicochemical parameters. *Environ Monit Assess* 174(1):417–425
- Kalavathy S, Sharma TR, Sureshkumar P (2011) Water quality index of river Cauvery in Tiruchirappalli district, Tamilnadu. *Arch Environ Sci* 5:55–61
- Kashyap R, Verma KS, Bhardwaj SK, Mahajan PK, Sharma JK, Sharma R (2016) Water chemistry of Yamuna river along Ponta Sahib industrial hub of Himachal Pradesh, India. *Res Environ Life Sci* 9:277–281
- Katyal D, Qader A, Ismail AH, Sarma K (2012) Water quality assessment of Yamuna River in Delhi region using index mapping. *Interdiscip Environ Rev* 13(2–3):170–186
- Kumar A, Matta G, Bhatnagar S (2021) A coherent approach of water quality indices and multivariate statistical models to estimate the water quality and pollution source apportionment of river ganga system in Himalayan region, Uttarakhand, India. *Environ Sci Pollut Res*, 1–16
- Kumar A, Mishra S, Taxak AK, Pandey R, Yu ZG (2020) Nature rejuvenation: Long-term (1989–2016) vs short-term memory approach based appraisal of water quality of the upper part of Ganga River. India. *Environ Technol Innov* 20:101164
- Lal K, Kaur R, Rosin KG, Patel N (2016) Low-cost remediation and on-farm management approaches for safe use of wastewater in agriculture. In: *Innovative saline agriculture*. Springer, New Delhi, pp. 265–275

- Letchinger M (2000) Pollution and water quality, neighbourhood water quality assessment. Project oceanography
- Mandal P, Upadhyay R, Hasan A (2010) Seasonal and spatial variation of Yamuna River water quality in Delhi, India. *Environ Monit Assess* 170(1):661–670
- Manju S, Sagar N (2017) Renewable energy integrated desalination: a sustainable solution to overcome future fresh-water scarcity in India. *Renew Sustain Energy Rev* 73:594–609
- Mishra S, Kumar A, Shukla P (2016) Study of water quality in Hindon River using pollution index and environmetrics. India. *Desalination Water Treat* 57(41):19121–19130
- Mishra S, Kumar A, Yadav S, Singhal MK (2015) Assessment of heavy metal contamination in Kali River, Uttar Pradesh, India. *J Appl Nat Sci* 7(2):1016–1020
- Mishra S, Kumar A, Yadav S, Singhal MK (2018) Assessment of heavy metal contamination in water of Kali River using principle component and cluster analysis. India. *Sustain Water Resour Manag* 4(3):573–581
- Misra AK (2010) A river about to die: Yamuna. *J Water Resour Prot* 2(5):489
- MoEFCC (2019) National Status of Wastewater Generation and Treatment
- MoWR, GoI (2008) National water mission under National Action Plan on Climate Change. Government of India ministry of water resources
- Niveshika, Singh S, Verma E, Mishra AK (2016) Isolation, characterization and molecular phylogeny of multiple metal tolerant and antibiotics resistant bacterial isolates from river Ganga, Varanasi, India. *Cogent Environ Sci* 2(1):1273750
- Panda UC, Sundaray SK, Rath P, Nayak BB, Bhatta D (2006) Application of factor and cluster analysis for characterization of river and estuarine water systems—a case study: Mahanadi River (India). *J Hydrol* 331(3–4):434–445
- Pandey G, Madhuri S (2014) Heavy metals causing toxicity in animals and fishes. *Res J Animal Veterinary Fishery Sci* 2(2):17–23
- Pathak SS, Mishra P (2020) A review of the Ganga river water pollution along major urban centres in the state of Uttar Pradesh, India. *Int Res J Eng Technol* 7(3):1202–1210
- Paul D (2017) Research on heavy metal pollution of river Ganga: a review. *Annals of Agrarian Sci* 15(2):278–286
- Paul D, Sinha SN (2015) Isolation and characterization of a phosphate solubilizing heavy metal tolerant bacterium from River Ganga, West Bengal, India. *Songklanakarin J Sci Technol* 37(6):651–657
- Poddar R, Qureshi ME, Shi T (2014) A comparison of water policies for sustainable irrigation management: the case of India and Australia. *Water Resour Manage* 28(4):1079–1094
- Prasad MBK, Ramanathan AL, Shrivastav SK, Saxena R (2006) Metal fractionation studies in surficial and core sediments in the Achankovil river basin in India. *Environ Monit Assess* 121(1):77–102
- Prasad P, Chaurasia M, Sohony RA, Gupta I, Kumar R (2013) Water quality analysis of surface water: a Web approach. *Environ Monit Assess* 185(7):5987–5992
- Razmkhah H, Abrishamchi A, Torkian A (2010) Evaluation of spatial and temporal variation in water quality by pattern recognition techniques: a case study on Jajrood River (Tehran, Iran). *J Environ Manage* 91(4):852–860
- Reza R, Singh G (2010) Heavy metal contamination and its indexing approach for river water. *Int J Environ Sci Technol* 7(4):785–792
- Rizvi N, Katyal D, Joshi V (2016) A multivariate statistical approach for water quality assessment of river Hindon, India. *Int J Environ Ecol Eng* 10(1):6–11
- Schwarzenbach RP, Egli T, Hofstetter TB, Von Gunten U, Wehrli B (2010) Global water pollution and human health. *Annu Rev Environ Resour* 35:109–136
- Shah KA, Joshi GS (2017) Evaluation of water quality index for River Sabarmati, Gujarat, India. *Appl Water Sci* 7(3):1349–1358
- Sharda AK, Sharma HC, Bhushan B (2017) Temporal variation of surface water quality in the Swan River catchment in Himachal Pradesh India. *Hydro Nepal J Water Energy Environ* 20:55–61

- Sharma D, Kansal A (2011) Water quality analysis of River Yamuna using water quality index in the national capital territory, India (2000–2009). *Appl Water Sci* 1(3):147–157
- Sharma MK, Jain CK, Singh O (2014) Characterization of point sources and water quality assessment of river Hindon using water quality index. *J Indian Water Resour Soc* 34(1):53–64
- Sharma MP, Singal SK, Patra S (2008) Water quality profile of Yamuna river, India. *Hydro Nepal J Water Energy Environ* 3:19–24
- Singh G, Patel N, Jindal T, Srivastava P, Bhowmik A (2020) Assessment of spatial and temporal variations in water quality by the application of multivariate statistical methods in the Kali River, Uttar Pradesh, India. *Environ Monit Assess* 192:1–26
- Singh H, Singh D, Singh SK, Shukla DN (2017) Assessment of river water quality and ecological diversity through multivariate statistical techniques, and earth observation dataset of rivers Ghaghara and Gandak, India. *Int J River Basin Manag* 15(3):347–360
- Singh KP, Malik A, Mohan D, Sinha S (2004) Multivariate statistical techniques for the evaluation of spatial and temporal variations in water quality of Gomti River (India)—a case study. *Water Res* 38(18):3980–3992
- Srivastava P, Grover S, Verma J, Khan AS (2017) Applicability and efficacy of diatom indices in water quality evaluation of the Chambal River in Central India. *Environ Sci Pollut Res* 24(33):25955–25976
- Sundaray SK (2010) Application of multivariate statistical techniques in hydrogeochemical studies—a case study: Brahmani-Koel River (India). *Environ Monit Assess* 164(1):297–310
- Sundaray SK, Nayak BB, Bhatta D (2009) Environmental studies on river water quality with reference to suitability for agricultural purposes: Mahanadi river estuarine system, India—a case study. *Environ Monit Assess* 155(1):227–243
- Sundaray SK, Nayak BB, Kanungo TK, Bhatta D (2012) Dynamics and quantification of dissolved heavy metals in the Mahanadi river estuarine system. *India. Environ Monit Assess* 184(2):1157–1179
- Suthar S, Nema AK, Chabukdhara M, Gupta SK (2009) Assessment of metals in water and sediments of Hindon River, India: impact of industrial and urban discharges. *J Hazard Mater* 171(1–3):1088–1095
- Suthar S, Sharma J, Chabukdhara M, Nema AK (2010) Water quality assessment of river Hindon at Ghaziabad, India: impact of industrial and urban wastewater. *Environ Monit Assess* 165(1):103–112
- Vaishaly AG, Mathew BB, Krishnamurthy NB (2015) Health effects caused by metal contaminated ground water. *Int J Adv Sci Res* 1(2):60–64
- Vörösmarty CJ, McIntyre PB, Gessner MO, Dudgeon D, Prusevich A, Green P, Glidden S, Bunn SE, Sullivan CA, Liermann CR, Davies PM (2010) Global threats to human water security and river biodiversity. *Nature* 467(7315):555–561
- Walsh CJ, Roy AH, Feminella JW, Cottingham PD, Groffman PM, Morgan RP (2005) The urban stream syndrome: current knowledge and the search for a cure. *J N Am Benthol Soc* 24(3):706–723
- Wang Y, Wang P, Bai Y, Tian Z, Li J, Shao X, Li BL (2013) Assessment of surface water quality via multivariate statistical techniques: a case study of the Songhua River Harbin region. *China. J Hydro-Environ Res* 7(1):30–40
- Wato T, Amare M, Bonga E, Demand BBO, Coalition BBR (2020) The agricultural water pollution and its minimization strategies—a review. *J Resour Dev Manag.* 10, 64–02
- World Resources Institute (WRI) 2019 Aqueduct Global Maps 3.0 Data. Retrieved from: <https://www.wri.org/resources/data-sets/aqueduct-global-maps-30-data>
- Xiao-jun W, Jian-yun Z, Shahid S, Xing-hui X, Rui-min H, Man-ting S (2014) Catastrophe theory to assess water security and adaptation strategy in the context of environmental change. *Mitig Adapt Strat Glob Change* 19(4):463–477
- Zheng LY, Yu HB, Wang QS (2015) Assessment of temporal and spatial variations in surface water quality using multivariate statistical techniques: A case study of Nenjiang River basin. *China. J Central South Univ* 22(10):3770–3780

Part IV
Techniques for Landscape Management
Under Large Uncertainty

Chapter 14

Adapting to Climate Change: Towards Societal Water Security in Semi-arid Regions



Manas Ranjan Panda and Yeonjoo Kim

Abstract As water plays a vital role in the life support system of the planet, the issue of water scarcity creates an insecurity which need to be overcome for the enhancement of socio-economic balance. Such condition affects more than billion people globally, and most of them live in the semi-arid regions where the available water resources are under threat. As per Food and Agriculture Organization (FAO), 12.2% of total global land is semi-arid zone. Based on the projected climate change, millions more people will be living under such conditions in the coming decades. However, various attention has been given to the eradication of water scarcity problems over this region, only few changes are remarkable in terms of field application. The water governance policies made by the local or national authorities must keep an eye to distinguish properly between various extreme events such as interannual droughts, continuous dry spells and long-term climate aridification. In general, few common contrasting situations are observed to cope with different water-scarcity dilemmas. The most vulnerable countries or region should adapt their water policy in order to sharpen the water shortage condition. The developing countries should take the decisions wisely to pursue the win-win approaches by selecting the most advantageous measures. In this chapter, various adaptive measures taken in the recent past in arid and semi-arid regions of Australia, Brazil, India and other south Asian countries are discussed. The basic fundamental approach for adaptive management for climate change will be providing social learning to the stakeholders to recognize their inter dependence as well as differences. The rethinking will be always required between local governance and stakeholders in order to manage the water for the most common uses such as irrigation, crop processing, domestic, industrial and other environmental uses. However, the large-scale adaption to global change is only possible by integrated river basin management (IRBM) plan by defining the medium- and long-term goals. Various adapting methods for water stress condition are discussed and also domain specific advance technology can play a vital role in such conditions. The aim of this chapter is to discuss various measures taken by the society or stakeholders to adapt

M. R. Panda (✉) · Y. Kim

Department of Civil and Environmental Engineering, Yonsei University, Seoul 03722, South Korea

e-mail: manas@yonsei.ac.kr

the changing trend of water availability due climate extremes in the semi-arid zones of the world.

Keywords Societal water security · Water shortage · Dry spells · Climate aridification · Semi-arid · Integrated river basin management (IRBM)

14.1 Introduction

The importance of water resources for survival and economic development are always intricately connected to the prosperity of individuals and well-being of the communities. Water can execute an important part in the insecurity or deterioration of peace due to its potential for conflict, strife and contention. This is very much related to the surface water and groundwater, where the transboundary distribution occurs between two or more communities, states or nations. As a result, equitable relations between neighboring communities, states or countries are closely linked to the effectiveness of local laws, national laws, international conventions, that allows equal access to the transboundary water resources (Andrade et al. 2021; Azhoni et al. 2016, 2017). Water security consists of diverse technical, monetary, environmental, social and judicial components. The state of public property of water resources, mentioned by various laws, allows public or government officials to achieve public service objectives. As a matter of fact, the establishment of water authorities at various levels seen to be promoting different policies, which place the water in the service of socio-economic development (Azhoni et al. 2016, 2017). Such conditions are more common in water scarce countries because the water management programs are planned accordingly to control the surface and groundwater resources. However, sometimes the excessive withdrawal from the groundwater threatens the water resources sustainability (Nalau et al. 2018).

The arid as well as semi-arid drylands carry an important role in Earth's biophysical environments. The impact of climate variability and change resulting water scarcity and low land productivity in those regions triggered the vulnerability to the local communities. The unanticipated change is characterized by biophysical limitations such as low annual mean precipitation, rising temperatures, erratic rainfall, recurring droughts, and remarkable seasonal and inter-annual variations, triggers the vulnerability of these drylands towards climatic variability and change (Ramarao et al. 2019; Gaur and Squires 2018). The 40% of the global land area is covered by these drylands, and shelter to more than 2.5 billion people (Gaur and Squires 2018). The persistent water scarcity over this region prompting several ecological constraints such as low nutrients and organic content in soil, desertification, soil degradation, disappearance of biodiversity which ultimately impact the livelihoods of surrounding local communities (Gaur and Squires 2018).

The high-level declaration happened at the Second World Water Forum, which took place in Hague in 2000, focused on providing water security in the twenty-first century. The goal was set for ensuring the protection and improvement of different

sources such as freshwater resources, coastal ecosystem as well as other related ecosystems to achieve sustainability are also promoted (GWSP 2011). The basic need of an individual to access sufficient safe water at a reasonable price for a healthy as well as productive life and at the same time vulnerable should be protected from the risks of water-borne hazards were given prime attention (GWSP 2011). There are two basic dimensions of safeguarding the societal water security first, to fulfill the basic water needs for their socio-economic production; second, to reduce water related risk, particularly during the flood and drought situations, to a defensible level (Ramarao et al. 2019).

The impact of the adverse climatic behavior becomes a threat for the low-income and vulnerable people inhabiting in the dry land areas; either in terms of life or wealth and sometimes in both aspect (Allen 2018; Olsson et al. 2014). For such conditions or variability, they are facing unreasonably the most and carrying the unavoidable stress for adaptation. Therefore, the concern for suitable adaptation actions is more important and which can provide ideal resilience towards climate variability and change. The implementation of adaptation measures faces different barriers, which includes lack of prevailing and locally applicable information, institutional constraints, improper management of financial procedure, lack of adequate technology and sometimes neglecting the of inclusion of conventional technique for adaptation strategies (Nalau et al. 2018; Eisenack et al. 2014; Barnett and O'Neill 2010). This shows an adaption deficit existing towards changing climate and extreme events at various levels in terms of social, financial and technological aspects (Asfaw et al. 2018; Milman and Arsano 2012). Such increasing adaptation deficits is not only limited to certain regions but seen are globally (IPCC 2014; Pachauri et al. 2014).

Increasing frequencies and intensities of hydrological extremes like floods and droughts are the main/prime consequences of climate change, and its following impact is going to be realized more severely in developing countries (Heo et al. 2015). Studies have been carried out in different parts of the globe to identify the severe impact of climate change on available water resources (Andrade et al. 2021; Azhoni et al. 2016, 2017; Blakeslee et al. 2020; Bressiani et al. 2015; Gondim et al. 2018; Heo et al. 2015; Lemos et al. 2020; Moors et al. 2011; Mostafa et al. 2021; Ribeiro Neto et al. 2014; Singh et al. 2018; Venkataramanan et al. 2020; Ziervogel et al. 2019) and adaptation strategies (Singh and Chudasama 2021). Among all stakeholders, agriculture is a pragmatic water-intensive sector sensitive to climate change. Climate change is one of the critical drivers of uncertainty in river flow which further widen the gap between irrigation water availability and demand. Studies in Brazil found that if the current practice follows, it is going to be challenging to meet the irrigation water demand in the Jaguaribe River basin, Brazil in the near future (Gondim et al. 2018). This chapter will be focusing on different adaptation strategies for water security at societal levels due to climate change and how to cope with water scarce situation in arid regions at a community level.

14.2 Global Semi-arid Zones and Water Scarcity

The coastal region of Brazil, Northern India, Western coast of India, Iran, Egypt, the USA, Mexico, Spain, Cape Verde, and Australia etc. are the major semi-arid zones of the world and the socioecological dynamics of these dry lands are not well known as well as very much complex. The increasing population density, water scarcity condition pushing the region towards a more vulnerable world (Adame et al. 2021; Poulter et al. 2014). In these regions the water insecurity consequences in reduced crop yields, hydropower production, and hampering the cooling process of thermal power plant, which can subsequently hike the food and energy prices.

The water scarcity indicators

Various methods have been developed by different research groups across the globe to quantify the water scarcity. However, the common method is relied on annual average data and implemented on a large scale (national or regional) on the basis of readily available data. The two most common indicators to define or measure the water stress are: first, evaluating the per capita water availability; the second, determining the withdrawal to availability. Both the indicators include a specific scaling with conventional households that defines water stress and water scarce situations. The most common method of describing water scarcity is the “Water Stress Indicator” (WSI) of Falkenmark et al. (1989). The WSI quantifies the water resource abundance or scarcity on the basis of the available freshwater resource to the population over a region or in a river basin and, taken as the important factor of the water demand. Hence, the Falkenmark indicator, alternatively called as “water crowding index” and which is commonly used in many studies on the basis demographic projections. The “Water Stress Indicator” of Falkenmark categorized into four different stress levels based on per capita water availability as: (i) No stress ($>1700 \text{ m}^3/\text{year}/\text{capita}$), (ii) Stress ($1000\text{--}1700$), (iii) Scarcity ($500\text{--}1000$), and absolute scarcity ($<500 \text{ m}^3/\text{year}/\text{capita}$), where the typical criteria of estimating water resources are procured from mean annual runoff (Raskin et al. 1997). is also proposed a water scarcity indicator to evaluate and interpret the water stress by quantifying the ratio of annual withdrawals to available water resources and equally adopted by many studies due to its easiness. Thus, the Withdrawal to Water Resources (WWR) can be considered one of the widely used water resource vulnerability index that can be used to capture more efficiently the concept of water uses instead of demand. In recent times, various studies using both the WSI and WWR indices in terms of measuring water scarcity due to their relative easiness and also, these indicators applied using annual averaged data at different scales (country or state or basin-wise). The scarcity level is characterized by both of the indicators using various methods which highlight the critical aspects of water scarcity by complementing each other, however, none of them emphasized the conditions for functional access to water by the users. For a certain quantity of resources and population, a country or community may be less vulnerable if it has already executed, beyond its exploitation limits. Hence, a

sufficiently huge quantity of its resources, that guarantee for certain a level of water availability compatible for the living standard of its populations.

14.3 Water Management Approaches; Quality-Quantity Perspective

14.3.1 Water Conservation

Water conservation is one of the cost-effective ways of securing “new” water supply (Arlosoroff 2015). Multiple approaches can be used in this strategy to apply in any sector by focusing on fulfilling the water needs at the demand-side management. The basic principles of water conservation programs include technological, economical, and educational criteria, e.g. promotion of sustainable water use and energy efficient technologies for water, awareness to various economic policies, educating people regarding specific local and national regulations in terms of specific restrictions regarding water use (especially during drought conditions), implementing technologies to overcome water leakages, and street campaigning to enhance public awareness (Cominola et al. 2015; Arlosoroff 2007). There is a confusion between water conservation and water-use efficiency, however, both are related, but have distinct concepts, i.e., water-use efficiency has the potentiality to trigger the increased water use (Scott et al. 2014). The participation of various entities such as governing bodies, households, farmers, commercial businesses, and industrial plants etc. are required for water conservation. Hence, this kind of practice is influenced by complex regulatory bodies and sociotechnical interactions. Sometimes, the media coverage of extreme events (such as drought), engaging the stakeholders by public officials, and local political interferences can make remarkable change to the existing system (Brown 2017; Hess et al. 2016). Many successful programs have been carried out for water conservation at different parts of the globe, for example, in Israel, a national strategy which indulges circulation of both, water-efficient technology and regulatory actions at various sectors (Tal 2006). In Israel, the water regulation is done by a total water metering system which keep on monitoring and determine the rate for water use and also decides the block rate system. The national water carrier system also helps the water users to trade their surplus water to manage for more efficient use (Arlosoroff 2007).

14.3.2 Reuse of Wastewater

The wastewater releasing from various sectors i.e., municipal, industrial and agricultural can be reused upon proper treatment. The reuse can increase the availability of water and reduce reliability on external water sources but at the same time the

quality become more important factor for the users. For instance, reuse of direct potable water needs proper treatment but can reduce the energy requirement needed for the transportation of water from the source to the user and also reduces the stress on the natural ecosystem (Rice and Westerhoff 2015). Many water treatment plants collect the water which originated from wastewater effluent at the upstream sources. However, sometimes the direct potable reuse is avoided by the public due to perception issues and becomes more concerning for the water-supply organizations if any safety failure occurs while wastewater treatment (NRC report 2012). The use of different-colored pipes is adopted in certain areas across the globe for the reclaimed wastewater distribution and commonly known as “dual reticulation”. Generally, it helps in distinguishing the reclaimed wastewater from potable water supply pipes. However, this type of system is not cost effective for the domestic supply but can be more efficient source of supply particularly for the industrial or commercial purpose i.e., industries or power plants because it requires new infrastructure (Tang et al. 2007).

The indirect way of recycling includes agricultural exchanges and different ways of aquifer recharge which can be done at a societal level. The nexus can be possible between urban and rural areas in which urban entity can trade its treated water to a rural community and in exchange they can access the water from the rural sources. The treated urban water is used for agriculture in the rural system but considering the water quality some specific agricultural applications can be done. In the city of Phoenix, USA, such urban–rural-water nexus can be seen where the city transfers its treated wastewater to the Roosevelt Irrigation District especially for the cultivation of non-edible crops and in exchange withdraw an equal volume of water elsewhere in the aquifer (Silber-Coats and Eden 2017). The perception concerns can be changed by enforcing strong policies, public education efforts for wastewater treatment and reuse as happened in Singapore (Luan 2013). This case study focuses the best way of wastewater reuse as a gift for the alternate source of water and simultaneously keeping the priority of societal concerns regarding the safety and cost-effectiveness.

14.3.3 Source Protection

The main goal of source protection measure is to maintain the quality of water from the extraction points. This practice is not new, centuries back, certain type of source protection practice can be found in communities which restricted specific near water sources. This ancient practice can be seen in Babylonian Talmud, where slaughterhouse and tanneries operations were restricted within a radial distance of 25 m from a well and the Yoruba tribes in Africa forbade activities like bathing and washing clothes near wells (Salzman 2017). However, in recent times the regulations are extended beyond the domestic uses in order to create the scope of water uses for recreation (e.g., water sports, aesthetic use etc.). The land use land cover change or intensive agricultural activities can induce the sediment loss and nutrient runoff which eventually causes degradation of watersheds can impact and for which the

downstream users need to pay more in water treatment (McDonald et al. 2016). Hence, it is easy to control the point source contamination but difficult to regulate the non-point source pollution. For example, the receiving bodies in the semi-arid region of Mexico i.e., Chesapeake Bay and the Gulf of Mexico, where the pollutants intruding from the upstream sources have deteriorated the water quality and converted into hypoxic areas and dead zones. Hence, the diffuse nature of contaminants is a major concern for the local authority and dependent community to minimize these non-point sources. Such innovative water governance practices discussed in this section are required both for quantity and quality maintenance under climate change-induced weather variability conditions. (Loecke et al. 2017; Gain et al. 2016; Lankoski and Ollikainen 2013).

14.3.4 Managed Aquifer Recharge

The recharging of aquifers is done by using surface water through various artificial methods and which is very much feasible to enhance water security across the dry land (specifically in semi-arid zones) areas of the globe. The most common ways are reducing the overexploitation of groundwater, storing of water in ponds and lakes during the surplus seasons, and maintaining the water availability conditions in the period of surface water scarcity (Casanova et al. 2016). The planned utilization water for recharging the aquifers is considered as managed aquifer recharge (MAR) (Dillon 2005). In different environments MAR has been rehearsed using various methods for more than a century (Casanova et al. 2016; Weeks 2002). Due to its viability and effectiveness, MAR is commonly used with various sources of water, which mostly includes harvested rainwater (mostly in the ponds or lakes) and river water (Stefan and Ansems 2018).

In certain cases, the treated wastewater is used for MAR purpose and can be withdrawn at a later time from the aquifer for water supply (Asano and Cotruvo 2004). The direct injection of wastewater into the aquifer may arise different issues in terms of water quality such as organic and inorganic chemicals, nutrients, salinity and turbidity, etc. and hence, causes the evaluation of MAR (Page et al. 2018). The risk of urging a variety of contaminants while aquifer recharge is done by runoff water from municipal areas or treated wastewater; however, some of the pollutants can be reduced by natural processes inside aquifer while few still retained and cause risk to human health (Casanova et al. 2016). Therefore, the emphasis on setting up flawless guidelines and regulations are given importance to protect groundwater resources while using the MAR and maintaining the water quality level (Dillon 2005). Several examples of implementing successful MAR can be seen throughout the world, one among which is in the semi-arid regions of southern India, constructing check dams across rivers to retain the surface runoff and increase the groundwater recharge (Renganayaki and Elango 2013). Various studies show that these dams increasing groundwater levels and enhanced the water quality significantly by reducing salinity levels, fluoride and arsenic concentrations in the groundwater. It resulted not only

enhancing the livelihood of local community due to better farm productivity and in certain cases the time spent by the women of various rural community of the region to fetch water have been reduced significantly also documented (Renganayaki and Elango 2013). The public perceptions towards the fairness and faith in decision making by the governing bodies, and implementation of suitable protection measures towards water quality decides the socio-economic approval of MAR (Mankad and Walton 2015). Despite the fact that MAR various benefits, but such complex interactions depict how different local variabilities related to societal stigmas in water quality used for aquifer recharge purpose of the region. The management authority associated with this, should play an influential role for the adoption of such water management practice by the communities around the world.

14.3.5 Desalination of Water

The high-water demand and water scarce situations across the arid as well as semi-arid regions of the world forcing the people as well as concerned authority towards an alternative source of water. In such circumstances, the desalination technique for water is gaining popularity to support the increasing water demands where fresh-water sources are limited. There are 18,500 desalination plants operating globally and supporting the demand for more than 86.8 million m³/day by mid-2015 (Amy et al. 2017). Recent venture in the technology related to desalination have enabled the process more efficient and cost-competitive. The thermal-based and membrane-based are two commonly used desalination processes. Thermal-based technologies works on the principle of converting water into vapor state and then condense this vapor in order to get potable water by supplying thermal energy to seawater (Loecke et al. 2017). Thermal technologies mainly used in the regions of high-water salinity and low energy cost, (Caribbean and the Middle East countries). The widely used thermal-based processes are multi-stage flash (MSF), multi-effect distillation (MED), and vapor compression distillation (McDonald et al. 2016). Furthermore, adoption of gradual phasing in renewable energy sources for supplying power to the desalination plants, can help in long-term sustainability of desalination. However, certain challenges are still existing in reducing energy demands and simultaneously managing waste products which have adverse environmental effects produced during desalination process (Amy et al. 2017; Harandi et al. 2017). The concentration may vary significantly based on the source water quality and volume e.g., ranging from 2.5 g/L to 80 g/L of total dissolved solids (TDS) for brackish water and seawater respectively. With higher salt concentration and other contaminants, such as heavy metals, nitrate, and radioactive materials (naturally present) can exist with high concentration in the brine (Xu et al. 2013). Hence, the management of high concentration is a promising challenge which impelling the implementation of desalination technology. The disposal of brine in an ocean outfall cause settling on the floor which can be toxic to marine ecosystem and can also cause hypoxic conditions. Therefore,

seawater desalination facilities are designed with diffusers at the outfalls to maintain a mixing condition of discharged brine to the oceans (Amy et al. 2017). For instance, the first seawater desalination plant of Australia set up in Perth have an outfall which contains 40 diffusion ports along 600-m pipe (Water Use Association 2011). The projected estimation of desalinated water is $192 \times 106 \text{ m}^3/\text{day}$ by 2050 and currently, Saudi Arabia stands tall in producing desalinated water in the world and has the potential to meet 60% of total water demand using desalination plants (Frank et al. 2017; DeNicola et al. 2015). Other countries in the middle East such as Kuwait and Qatar where 100% of the water used is produced through v desalination (Blanco-Marigota et al. 2017). Despite the widespread use of desalination process, it is still controversial because of the expensiveness of technology used to produce water. Furthermore, it has many environmental effects, for example, huge amount of waste products and high greenhouse gas can affect the marine ecology as discussed in this section (Sepher et al. 2017; Ritcher et al. 2013). Therefore, the continuous improvement in the technology is required, and at the same time prime focus must be given to minimize the adverse health and environmental effects. Better management practice for brine discharges along with highly efficient desalination plants can make the desalination as a cost-effective and sustainable option. This can be a better alternative adaptation source of freshwater around the arid and semi-arid coastal regions of the world in the changing climate.

14.4 Policy and Responses from International Organizations

The basic approach of adaptive management is social learning, through which people can distinguish between their interdependence and differences, help them to execute collective action and resolve the conflicts. That will help to overcome barriers and create new chances for innovative technologies to implement. After the Copenhagen meeting in 2009, many international organizations such as include the Food and Agriculture Organization (FAO) of the United Nations, the International Water Management Institute (IWMI) and the International Network of Basin Organizations (INBO) triggered their participation in analyzing water policies related to climate change adaptation. As per the FAO, more focus should be given on the water-oriented activities such as storages, water use efficiency improvements, water accounting, data gathering, farming activities. They emphasized on altering the crop patterns, and further development of crop breeding. The large-scale fluctuations happen due to droughts however, the water storage at various forms (such as surface water sources, soil moisture and groundwater storages) will be needed protects the stakeholders. The instant solutions for the water scarcity can be managed from surface storages i.e. small reservoirs and natural wetlands. The beneficial practices (soil management, rainwater harvesting and conservation tillage) can be used in farming to improve soil moisture capacity and so as groundwater by recharge. The farmers mostly depend

upon rainfed irrigation are the primary victims during droughts and could be encouraged to use alternative or supplementary irrigation technique to overcome the risk of crop yield reduction and starvation. The efficient water use irrigation systems, should be implemented which reduce the often-large water losses. The concern for increasing water scarcity and unpredictable variability, stated by IWMI should be required to think seriously, for the better management of water in agricultural production and at the same time to integrate the solutions in other sectors (domestic, environmental and industrial) of water use. The emphasis should be given on three things regarding the water use by the users; (i) the source of water, (ii) the benefits (iii) how to manage after its use i.e., wastewater management. The adaptation to the changing hydrological extremes helps to differentiate between prolonged dry spells, severe droughts and long-term aridification of the local climate.

The INBO suggests to give effort on developing a comprehensive, integrated and stable management system for water resources, and that should be based on the assessments of water availability and socio-economic, socio-cultural and geo-political realities. The proper basin management can be done by integrated information systems in accordance with water availability, water use, external polluting forces and dependent ecosystems, and simultaneously paying enough attention to land use changes. The adaptation behaviors to the changing climate would benefit from proper basin management plans satisfying medium- and long-term goals. It is very much necessary for the planning processes included within basin management to rely on integrated information systems on a priority basis and include the dialogues, negotiations, decision making criteria and evaluation guidelines. The coordinated basin approach and two-way understanding of the 'upstream–downstream' users can build a proper protection against the climate extremes (both floods and droughts) at basins and sub-basins scales.

Water security approach in different parts of the globe

Several studies showed the vital importance of water security across the (Gupta and Pahl-Wostl 2013; Bogardi et al. 2012; Pittock and Connell 2010). In recent times, the water strategy at different levels for water security are being promoted by both the International Water Resources Association (IWRA) and the World Water Congress (WWC) which encourages various adaptive measures and Integrated Water Resources Management (IWRM). The issues found at community, catchment and country scales must be present at the global scale otherwise, consideration of water security at global perspective urges new types of issues which needs to be addressed as well. The global perspective also features the desirability of establishing policy and operational interdependence between water security and sustainable development. Global water security is a concept which encourages inclusion of a broad social-ecological system which involves the security for water, food, energy, and other environmental function. Although the understandings of water security for different regions or countries, may differ but the goal for development in regional water security strategies can be decided by global water security framework. This global framework has the potentiality to focus prominent water security issues (such as regional flood control, managing drought disaster, regulating water pollution,

and bio-diversity or eco-system conservation) in specific region, while carrying the objectives of global water security.

Further, studies in Egypt found that the productivity of wheat will decline, and irrigation water demand for the wheat crop is likely to increase by 6.2 and 11.8% in 2050 and 2100, respectively. Andrade et al. (2021) advocated decreasing rainfall and rising temperature as an effect of climate change in Brazil; there will be less precipitation in the wet season and significantly less in the dry season, which will reduce the water yield and surface runoff. However, a significant increase in the potential evapotranspiration. Further, available water resources may fail to support sufficiently for the demand of various sectors like population, economic and environmental. Different adaptation strategies like water-loss reduction, wastewater collection and reuse, rainwater collection have the potential to meet 23% of future water demand (Ribeiro Neto et al. 2014). Further inter-basin water transfer of the São Francisco River has a positive impact on water supply and has the potential to meet the domestic water demand. However, industries and irrigation need demand-side management (Ribeiro Neto et al. 2014). Changes in socio-economic development and projected changes in the timing and quantity of runoff become a challenging task for water resources managers in developing countries (Moors et al. 2011). Some developing countries need decentralization of decision and implementation power in the water sector. Vertical integration of strategic link of scientific know-how to integrate national and sub-national level institutions is the demand of the time to mitigate climate change impact on water sector efficiently (Ziervogel et al. 2019). Further inter-institutional network to be strengthened, and participation and flexibilities of the governing bodies must be empowered to make the water sector resilient to climate change (Azhoni et al. 2016).

The urban- rural-water nexus plays an important role in maintaining the water demand both in urban and rural areas from a shared stock of finite water resources. Against the changing climate, the rising water demands in fast-growing urban areas are leading to many water-related conflicts with its surrounding co-dependent rural areas (Sukhwani et al. 2022). Such rapid growth in urban areas, enhanced the water demands projection to increase by 50 to 80% (Florke et al. 2018; Garrick et al. 2019). While one in four large cities is now facing the water stress condition globally, the simultaneous increasing demands for water-intensive sectors like food and energy are also raising indirect water-stress concerns (Cosgrove and Loucks 2015; Mancosu et al. 2015; Zhang et al. 2019). Addressing the water-energy-food nexus has therefore become very much sensitive to maintain the sustainable urban development due to the increasing demand for all these three inextricably linked resources (Djehdian et al. 2019; Sukhwani et al. 2019). The poor water governance is frequently cited as the key reason for such urban-rural conflicts, it is also recognized as a potential pathway to resolve them (Sukhwani et al. 2022).

Nowadays, in Nagpur Region of Central India, water stress has become a subject of serious concern. Sukhwani et al. (2022) stated that the water demands in Nagpur City are primarily met through the multipurpose Pench Dam, but due to the recent declining water availability in the dam has raised serious concerns for irrigation in the Pench command areas. To support the limited understanding of present water

conflicts in the wider Nagpur Metropolitan Area, this study used a specific set of secondary data related to the Pench Project and its water utilization trends. There was a continuous reduction in irrigated area and more exploitation of groundwater use for irrigation noticed. The cross-sectoral and transboundary implications of increasing water transfer to Nagpur City was revealed. To address these issues, this study then suggested a feasible governance strategy based on mutual benefit sharing and multi-stakeholder engagement for the water resources.

The impact of climate change and the reliability of adaptation towards the change has been observed at the household level. The household-level coping strategies in Africa or South Asia involves (1) Access: storing, purchasing, building infrastructure, and sharing water, (2) Use: changing pattern of food consumption, adopting alternative agricultural practices (3) Quality: maintaining hygiene, water treatment was the most common strategy, (4) Reliability: changing routines or relocating or shifting their homes altogether (Venkataramanan et al. 2020). Developing strategies in the water sector should imbibe the current state of the art technology by considering future impact and should be proactive and flexible enough to incorporate the efficient scientific know-how for better water resources management. Uncertainty in climate change can be coped by focusing on the most vulnerable individuals, engaging the society as a whole, taking into confidence the local leadership, building a sustainable adaptive society, reducing disaster risk and 'Zero Victim' goal to hydrological extremes like floods (Heo et al. 2015).

14.5 Conclusion

This chapter focused the importance of water security and adaptive approaches of society at all scales, and also considered the water security from climate change perspective. While considering the arid and semi-arid countries, the initial steps of the national water security is to raise awareness depending upon the resource's limits. Since, there are not enough resources to meet all demands, the race for water becomes more acute and the dependency for the same watershed or basin become interdependent. The understanding of hydraulic installations to deploy surface water and groundwater resources available in various forms such as dams, boreholes, reservoirs, transfer chains, etc. is very efficient in maintaining water supply and use. It is more prominent in water scarce countries, because it helps to cope with scarcity and encourage the development of various economic activities.

However, within these limits, the water resource needs to be managed in a sustainable way to guarantee for the conservation of pristine environment and the protection of the resource. The water security becomes more consequential at the national scale only when it benefits all the inhabitants and encourages sustainable economic growth, employment and social cohesion. To achieve such goals, policy makers need to understand the direct and indirect relationships between the water sector and the national economy and simultaneously the water managers should execute different sectoral policies in a standard way. While discussing the various policy management

and challenge across the globe, we focused the numerous ways to adopt the science and innovation to overcome the water scarcity conditions in the semi-arid regions. The action demonstrates for the establishment of coalition between willing society and capable researchers, policy makers working in concert with organizations and governing bodies, to address the systemic and mitigating water security challenges. The challenging scale is huge and as per our current understanding regarding inter-linked global water system is inadequate to manage or mitigate thoroughly. However, adaptation approaches as a society can strengthen our ability to face. The goal of blue planet can be achieved by collective respond a common problem in a determined way and lay the foundations for a sustainable 'Blue Planet'.

References

- Adame MF, Reef R, Santini NS, Najera E, Turschwell MP, Hayes MA, ... Lovelock CE (2021) Mangroves in arid regions: ecology, threats, and opportunities. *Estuarine Coastal Shelf Sci* 248:106796
- Allen MR (2018) Framing and context. In: Global warming of 1.5 C: an IPCC special report on the impacts of global warming of 1.5 c above pre-industrial levels and related global greenhouse gas emission pathways, in the context of strengthening the global response to the threat of climate change. Sustainable Development, and Efforts to Eradicate Poverty
- Amy G, Ghaffour N, Li Z, Francis L, Linares RV, Missimer T, Lattemann S (2017) Membrane-based seawater desalination: present and future prospects. *Desalination* 401:16–21
- Andrade CW, Montenegro SM, Montenegro AA, Lima JRDS, Srinivasan R, Jones CA (2021) Climate change impact assessment on water resources under RCP scenarios: a case study in Mundaú River Basin, Northeastern Brazil. *Int J Climatol* 41:E1045–E1061
- Arlosoroff S (2007) Water Demand management—a strategy to deal with water scarcity: Israel as a case study. In: Water resources in the middle east. Springer, Berlin, Heidelberg, pp 325–330
- Asano T, Cotruvo JA (2004) Groundwater recharge with reclaimed municipal wastewater: health and regulatory considerations. *Water Res* 38(8):1941–1951
- Asfaw S, Pallante G, Palma A (2018) Diversification strategies and adaptation deficit: evidence from rural communities in Niger. *World Dev* 101:219–234
- Azhoni A, Holman I, Jude S (2016) Contextual and interdependent causes of climate change adaptation barriers for water management: responses from regional and local institutions in Himachal Pradesh, India. In: EGU general assembly conference abstracts, pp EPSC2016–10022
- Azhoni A, Holman I, Jude S (2017) Adapting water management to climate change: institutional involvement, inter-institutional networks and barriers in India. *Glob Environ Chang* 44:144–157
- Barnett J, O'Neill S (2010) Maladaptation. *Global Environ Change* 20(2):211–213
- Blakeslee D, Fishman R, Srinivasan V (2020) Way down in the hole: adaptation to long-term water loss in rural India. *Amer Econ Rev* 110(1):200–224
- Blanco-Marigorta AM, Lozano-Medina A, Marcos JD (2017) The exergetic efficiency as a performance evaluation tool in reverse osmosis desalination plants in operation. *Desalination* 413:19–28
- Bogardi JJ, Dudgeon D, Lawford R, Flinderbusch E, Meyn A, Pahl-Wostl C, ... Vörösmarty C (2012) Water security for a planet under pressure: interconnected challenges of a changing world call for sustainable solutions. *Current Opin Environ Sustain* 4(1):35–43
- Brown KP (2017) Water, water everywhere (or, seeing is believing): the visibility of water supply and the public will for conservation. *Nature Cult* 12(3):219–245
- Casanova J, Devau N, Pettenati M (2016) Managed aquifer recharge: an overview of issues and options. *Integr Groundwater Manag*, 413–434

- Cominola A, Giuliani M, Piga D, Castelletti A, Rizzoli AE (2015) Benefits and challenges of using smart meters for advancing residential water demand modeling and management: a review. *Environ Model Softw* 72:198–214
- Cosgrove WJ, Loucks DP (2015) Water management: current and future challenges and research directions. *Water Resour Res* 51(6):4823–4839
- de Almeida Bressiani D, Gassman PW, Fernandes JG, Garbossa LHP, Srinivasan R, Bonumá NB, Mendiando EM (2015) Review of soil and water assessment tool (SWAT) applications in Brazil: challenges and prospects. *Int J Agric Biol Eng* 8(3):9–35
- DeNicola E, Aburizaiza OS, Siddique A, Khwaja H, Carpenter DO (2015) Climate change and water scarcity: the case of Saudi Arabia. *Ann Glob Health* 81(3):342–353
- Dillon P (2005) Future management of aquifer recharge. *Hydrogeol J* 13(1):313–316
- Djehdian LA, Chini CM, Marston L, Konar M, Stillwell AS (2019) Exposure of urban food–energy–water (FEW) systems to water scarcity. *Sustain Cities Soc* 50:101621
- Eisenack K, Moser SC, Hoffmann E, Klein RJ, Oberlack C, Pechan A, ... Termeer CJ (2014) Explaining and overcoming barriers to climate change adaptation. *Nat Climate Change* 4(10):867–872
- Falkenmark M, Lundqvist J, Widstrand C (1989) Macro-scale water scarcity requires micro-scale approaches: aspects of vulnerability in semi-arid development. In: *Natural resources forum* (Vol 13, No 4, pp 258–267). Oxford, UK: Blackwell Publishing Ltd
- Flörke M, Schneider C, McDonald RI (2018) Water competition between cities and agriculture driven by climate change and urban growth. *Nature Sustain* 1(1):51–58
- Frank H, Rahav E, Bar-Zeev E (2017) Short-term effects of SWRO desalination brine on benthic heterotrophic microbial communities. *Desalination* 417:52–59
- Gain AK, Giupponi C, Wada Y (2016) Measuring global water security towards sustainable development goals. *Environ Res Lett* 11(12):124015
- Garrick D, De Stefano L, Yu W, Jorgensen I, O'Donnell E, Turley L, ... Wight C (2019) Rural water for thirsty cities: a systematic review of water reallocation from rural to urban regions. *Environ Res Lett* 14(4):043003
- Gaur MK, Squires VR (2018) Drylands under a climate change regime: implications for the land and the pastoral people they support. In: *Climate variability impacts on land use and livelihoods in drylands*. Springer, Cham, pp 319–334
- Gondim R, Silveira C, de Souza Filho F, Vasconcelos F, Cid D (2018) Climate change impacts on water demand and availability using CMIP5 models in the Jaguaribe basin, semi-arid Brazil. *Environ Earth Sci* 77(15):1–14
- Gupta J, Pahl-Wostl C (2013) Global water governance in the context of global and multilevel governance: its need, form, and challenges. *Ecol Soc* 18(4)
- Harandi HB, Rahnema M, Javaran EJ, Asadi A (2017) Performance optimization of a multi stage flash desalination unit with thermal vapor compression using genetic algorithm. *Appl Therm Eng* 123:1106–1119
- Heo J, Yu J, Giardino JR, Cho H (2015) Water resources response to climate and land-cover changes in a semi-arid watershed, New Mexico, USA. *Terrestrial Atmosph Oceanic Sci* 26(4)
- Hess DJ, Wold CA, Hunter E, Nay J, Worland S, Gilligan J, Hornberger GM (2016) Drought, risk, and institutional politics in the American Southwest. In: *Sociological forum* (Vol 31, pp 807–827)
- IPCC (2014) Fifth Assessment Synthesis Report; Cambridge University Press: Cambridge, UK New York, NY, USA
- Lankoski J, Ollikainen M (2013) Innovations in nonpoint source pollution policy—European perspectives. *Choices* 28(3):1–5
- Lemos MC, Puga BP, Formiga-Johnsson RM, Seigerman CK (2020) Building on adaptive capacity to extreme events in Brazil: water reform, participation, and climate information across four river basins. *Reg Environ Change* 20(2):1–13
- Loecke TD, Burgin AJ, Riveros-Iregui DA, Ward AS, Thomas SA, Davis CA, Clair MAS (2017) Weather whiplash in agricultural regions drives deterioration of water quality. *Biogeochemistry* 133(1):7–15

- Luan IOB (2013) Singapore water management policies and practices. In: Asian perspectives on water policy. Routledge, pp 109–124
- Macoscu N, Snyder RL, Kyriakakis G, Spano D (2015) Water scarcity and future challenges for food production. *Water* 7(3):975–992
- Mankad A, Walton A (2015) Accepting managed aquifer recharge of urban storm water reuse: the role of policy-related factors. *Water Resour Res* 51(12):9696–9707
- McDonald RI, Weber KF, Padowski J, Boucher T, Shemie D (2016) Estimating watershed degradation over the last century and its impact on water-treatment costs for the world's large cities. *Proc Natl Acad Sci* 113(32):9117–9122
- Milman A, Arsano Y (2012) Climate adaptation in highly vulnerable regions: the politics of human security in Gambella, Ethiopia. CLICO case study (on file with authors)
- Moors EJ, Groot A, Biemans H, van Scheltinga CT, Siderius C, Stoffel M, ... Collins DN (2011) Adaptation to changing water resources in the Ganges basin, northern India. *Environ Sci Policy* 14(7):758–769
- Mostafa SM, Wahed O, El-Nashar WY, El-Marsafawy SM, Abd-Elhamid HF (2021) Impact of climate change on water resources and crop yield in the Middle Egypt region. *AQUA Water Infrastr Ecosyst Soc* 70(7):1066–1084
- Nalau J, Becken S, Mackey B (2018) Ecosystem-based Adaptation: a review of the constraints. *Environ Sci Policy* 89:357–364
- Olsson L, Opondo M, Tschakert P, Agrawal A, Eriksen S, Ma S, ... Zakeldeen S (2014) Livelihoods and poverty: climate change 2014: impacts, adaptation, and vulnerability. Part A: global and sectoral aspects. Contribution of working group II to the fifth assessment report of the intergovernmental panel on climate change. In: *Climate change 2014: impacts, adaptation, and vulnerability. Part A: Global and Sectoral Aspects*. Cambridge University Press, pp 793–832
- Pachauri RK, Allen MR, Barros VR, Broome J, Cramer W, Christ R, ... van Ypserle JP (2014) Climate change 2014: synthesis report. Contribution of working Groups I, II and III to the fifth assessment report of the Intergovernmental Panel on Climate Change. *Ipcc*, p 151
- Page D, Bekele E, Vanderzalm J, Sidhu J (2018) Managed aquifer recharge (MAR) in sustainable urban water management. *Water* 10(3):239
- Pittock J, Connell D (2010) Australia demonstrates the planet's future: water and climate in the Murray-Darling Basin. *Int J Water Resour Dev* 26(4):561–578
- Poulter B, Frank D, Ciais P, Myeni RB, Andela N, Bi J, ... van der Werf GR (2014) Contribution of semi-arid ecosystems to interannual variability of the global carbon cycle. *Nature* 509(7502):600–603
- Ramarao MVS, Sanjay J, Krishnan R, Mujumdar M, Bazaz A, Revi A (2019) On observed aridity changes over the semi-arid regions of India in a warming climate. *Theoretical Appl Climatol* 136(1-2) 693–702. <https://doi.org/10.1007/s00704-018-2513-6>
- Raskin P, Gleick P, Kirshen P, Pontius G, Strzepek K (1997) Water futures: assessment of long-range patterns and problems. *Comprehensive assessment of the freshwater resources of the world*. SEI
- Renganayaki SP, Elango L (2013) A review on managed aquifer recharge by check dams: a case study near Chennai, India. *Int J Res Eng Technol* 2(4):416–423
- Ribeiro Neto A, Scott CA, Lima EA, Montenegro SMGL, Cirilo JA (2014) Infrastructure sufficiency in meeting water demand under climate-induced socio-hydrological transition in the urbanizing Capibaribe River basin–Brazil. *Hydrol Earth Syst Sci* 18(9):3449–3459
- Rice J, Westerhoff P (2015) Spatial and temporal variation in de facto wastewater reuse in drinking water systems across the USA. *Environ Sci Technol* 49(2):982–989
- Richter BD, Abell D, Bacha E, Brauman K, Calos S, Cohn A, ... Siegfried E (2013) Tapped out: how can cities secure their water future? *Water Policy* 15(3):335–363
- Salzman J (2017) *Drinking water: a history* (Revised Edition). Abrams
- Scott M (2014) Natural disasters, climate change and non-refoulement: What Scope for Resisting Expulsion under Articles 3 and 8 of the European Convention on Human Rights?. *Int J Refugee Law* 26(3):404–432. <https://doi.org/10.1093/ijrl/euu036>

- Sepehr M, Fatemi SMR, Danehkar A, Moradi AM (2017) Application of Delphi method in site selection of desalination plants. *Global J Environ Sci Manag* 3(1):89
- Silber-Coats N, Eden S (2017) Water Banking, Recharge, and Recovery in Arizona. Arroyo. University of Arizona. Water Resources Research Center, Tucson, AZ, pp 2–16
- Singh C, Osbahr H, Dorward P (2018) The implications of rural perceptions of water scarcity on differential adaptation behaviour in Rajasthan, India. *Regional Environ Change* 18(8):2417–2432
- Singh PK, Chudasama H (2021) Pathways for climate change adaptations in arid and semi-arid regions. *J Clean Prod* 284:124744
- Stefan C, Ansems N (2018) Web-based global inventory of managed aquifer recharge applications. *Sustain Water Resour Manag* 4(2):153–162
- Sukhwani V, Shaw R, Mitra BK, Yan W (2019) Optimizing Food-Energy-Water (FEW) nexus to foster collective resilience in urban-rural systems. *Progress Disaster Sci* 1:100005
- Sukhwani V (2022) Stakeholder perception of addressing water stress in nagpur, India
- Sukhwani V, Shaw R (2022) Conjoint assessment of rural water security and system sustainability in Nagpur India. *Int J Disaster Resilie Built Environ* 13(3) 351–367. <https://doi.org/10.1108/IJD-RBE-08-2021-0093>
- Tal A (2006) Seeking sustainability: Israel's evolving water management strategy. *Science* 313(5790):1081–1084
- Tang SL, Yue DP, Ku DC (2007) Engineering and costs of dual water supply systems. IWA Publishing
- Venkataramanan V, Collins SM, Clark KA, Yeam J, Nowakowski VG, Young SL (2020) Coping strategies for individual and household-level water insecurity: a systematic review. *WIREs Water [Internet]* 2020; 7.[Cited 2020 Sep 1]
- WaterReuse Association (2011) Seawater concentrate management. WaterReuse Association White Paper
- Weeks EP (2002) A historical overview of hydrologic studies of artificial recharge in the US Geological Survey. In: US Geological Survey Artificial Recharge Workshop Proceedings, pp 2–4
- Xu P, Cath TY, Robertson AP, Reinhard M, Leckie JO, Drewes JE (2013) Critical review of desalination concentrate management, treatment and beneficial use. *Environ Eng Sci* 30(8):502–514
- Zhang X, Chen N, Sheng H, Ip C, Yang L, Chen Y, ... Niyogi D (2019) Urban drought challenge to 2030 sustainable development goals. *Sci Environ* 693:133536
- Ziervogel G, Satyal P, Basu R, Mensah A, Singh C, Hegga S, Abu TZ (2019) Vertical integration for climate change adaptation in the water sector: lessons from decentralisation in Africa and India. *Reg Environ Change* 19(8):2729–2743

Chapter 15

Challenges and Opportunities of Water Security in Latin America



**Eduardo Saldanha Vogelmann, Juliana Prevedello,
Kelen Rodrigues da Veiga, and Gabriel Oladele Awe**

Abstract Latin America is currently home to approximately 700 million people, a population that is expected to grow even more. In addition, we can see the growth of cities, industries and agriculture, facts that have raised concerns about water security, an agenda that is highlighted in all countries, considering the available quantity and quality. Despite concentrating a significant portion of the world's freshwater reserve, due to the expansion of agriculture and especially the pollution of many rivers and lakes, today practically all countries face some kind of difficulty regarding the supply of drinking water or sanitation to the population. In addition, some countries have become a world reference in the extraction of ores such as gold, copper and iron. Currently, mining and deforestation for illegal logging and possible expansion of agricultural areas have contributed to the degradation of surface water and aquifers. In this worrying scenario, it is also worth mentioning the lack of enforcement of environmental legislation and the existence of few agreements and policies between nations aimed at strengthening integrated river basin management plans. Actually, studies evaluating the issue of water security in Latin America in an integrated way, with basin-scale planning, with the interaction of different nations, in addition to the exchange of experiences and establishment of cooperation agreements are topic that still lacks clarification and intense scientific debate, comparing realities, identifying the biggest challenges and proposing solutions. Thus, the present text seeks to contribute to the analyze of water security in Latin America in a comprehensive way, basing the main current aspects most relevant in relation to the conservation and preservation of this important natural resource that is the water. For this, the main challenges to be faced in this century in Latin America were listed and discussed,

E. S. Vogelmann (✉)

Institute of Biological Sciences, Federal University of Rio Grande, Rio Grande, Brazil

e-mail: eduardovogelmann@furg.br

J. Prevedello · K. R. da Veiga

Institute of Oceanography, Federal University of Rio Grande, Rio Grande, Brazil

G. O. Awe

Department of Soil Resources and Environmental Management Department, State University, Ado Ekiti, Nigeria

which are the impacts of megacities, climate change, lack of policies and implementation of laws, expansion of agriculture and deforestation, increased industrialization, expansion of activities mining, sewage treatment and the lack of transboundary watershed management programs.

Keywords Natural resources · Rivers · Water quality · Water pollution

15.1 Introduction

World demand for water has been increasing at a rate of about 1% per year since the 1980s, due to population growth, socioeconomic development and changes in consumption patterns (WWAP 2019). In addition, climate change and its effects on extreme hydrological events predict large spatial and temporal variations in water cycle dynamics. This can further aggravate discrepancies between water supply and demand in the various regions of the world. In this context, water security has become one of the main challenges today, as more than two thirds of the global population already live in water-scarce areas, a population expected to grow to 9.1 billion by 2050, reflecting an exponential increase in water consumption for various uses (UNESCO 2012).

Considering the definition of water security presented by the United Nations and several other environmental, academic and political bodies, which has been promoted because of its contribution to the maintenance of life and this should be the main focus of those who manage water resources and the society in general (United Nations 2013). However, for this, it is essential to increase investments in water infrastructure and sanitation, improvement of water resources management (planning, control of water use, monitoring, operation and maintenance of water systems, among others), as well as measures for risk management. Thus, the improvement of water management becomes essential towards ensuring the sustainable fulfillment of these demands (Mahlknecht et al. 2020).

Latin America is a region with an immense continental area, variations in geology, relief, water and mineral resources. Each country has its own particularities and often show striking differences even within their own territory. However, what is observed in relation to water resources is that many have similar problems and, therefore, despite these differences pointed out in other aspects, the countries are similar, such as the population's income inequality, low level of education, intensive exploitation of environmental resources, fragility of mechanisms and institutions for environmental protection, among others. Another important aspect is that many of these Latin American countries have always had access to water in quantity and quality, especially in the case of populations located in the Amazon and Central America regions, where large volumes of rainfall are observed during most of the year, fact that contributed to the neglect with the preservation of water resources, which until a few years ago were still abundant, mainly in these regions (Mahlknecht et al. 2020; Tzanakakis et al. 2020). However, this situation has been changing and every year

the population feels more strongly the direct impacts of the lack of management and care on this important resource. This demonstrates the need for studies evaluating the issue of water security in Latin America, also in an integrated way, with basin-scale planning, with the interaction of different nations, in addition to the exchange of experiences and establishment of cooperation agreements, a topic that still lacks clarification and intense scientific debate, comparing realities, identifying the biggest challenges and proposing solutions (Melo and Johnson 2017).

Thus, the present text seeks to contribute to the analyze of water security in Latin America in a comprehensive way, basing the main current aspects most relevant in relation to the conservation and preservation of this important natural resource that is the water. For this, the main challenges to be faced in this century in Latin America were listed and discussed, which are the impacts of megacities, climate change, lack of policies and implementation of laws, expansion of agriculture and deforestation, increased industrialization, expansion of activities mining, sewage treatment and the lack of transboundary watershed management programs.

15.2 Definitions and Concepts About Water Security

The term “water security”, especially in the last two decades, has been discussed by different government agencies and researchers in different ways. The concept presented and used in the Global Water Partnership in 2012 (Rio + 20) is in line with the definitions of (Gray and Sadoff 2007) that conceptualize water security as “acceptable quantity and quality for health, livelihood, ecosystem and production plus the risks related to water for people, the environment and economies”. At this time, water security was mainly related to water availability, with partial mention of other related issues, such as vulnerability to flood events or environmental disasters. A few years later, the United Nations (2013) introduced a new global definition for water security that was now defined as “ensuring sustainable access to quality water, adequate to maintain livelihoods, human well-being and socio-economic development; ensure protection against water pollution and water-related disasters; preserve ecosystems in a climate of peace and political stability”.

Recently, Cook and Bakker (2012) conducted extensive research on the definitions of this term in international literature and found this term was associated with different approaches including industrial use, energy, transportation and natural disasters. In this regard, it can be inferred that mainly over the last decade, the term has been used more widely and associated, around the world, not only with water availability, but also with other aspects that are directly linked to the quality or quantity of available water resources.

Thus, over time, broader and more generic definitions have emerged, broadening the scenarios involving water security, which for many is still closely linked to

water scarcity in quality and/or quantity. In this context, we highlight the definition proposed by Organization for Economic Co-operation and Development (2013) which includes in its conceptual definition of water security and its association with risk management. Thus, Organization for Economic Co-operation and Development (2013) mentions that water security is the management of four types of risks: risk of water scarcity to meet demand; water quality risk from deterioration due to contamination of water systems; risk of flood overflow; and risks to the sustainability of water and environmental systems. Thus, the new concepts seek to cover beyond the risks of physical scarcity and lack of potability, the lack of integrated resource management and resilience to environmental disasters and climate change, problems that currently plague different nations and is currently being disseminated even among the Latin Americans (Tzanakakis et al. 2020).

15.3 Challenges of Water Security in Latin America

15.3.1 *Megacities*

Lack of water security is, in addition to a problem related to nature, a problem linked to the development of the society. At the beginning of this decade, half of the population of Latin American and Caribbean countries still lived in cities with less than 500,000 inhabitants. However, 14% of the world population are already in the so-called megacities and about 80% lived in urban areas. Cities with a population of over 5 million are considered megacities. In 2012, the eight megacities in Latin America—Mexico City, Sao Paulo, Buenos Aires, Rio de Janeiro, Lima, Bogota, Santiago and Belo Horizonte—had a concentration of over 65 million people (França et al. 2012).

In 2019, the United Nations noted in its report “World Population Prospects 2019”: forecast a growth of up to 18% in the population of Latin America by 2050 (United Nations 2019), demonstrating a population growth rate superior to North America, Europe and Asia. This reality has brought new challenges for the sustainable development of cities, given that the environmental impacts caused by urban centers, associated with their dependence on natural resources is exponential (Banhe and Lopes 2016).

According to the data from the UN-Habitat Report: “The State of Latin American and Caribbean Cities”, in which it was found that water supply in Latin America and the Caribbean in 2012 reached 92% of the urban population. In the same period, Brazil had over 90% of the population with access to piped water, just less than that of the urban populations of Chile and Uruguay. Still, it is estimated that 40% of treated water is lost due to infrastructure problems in the supply network (França et al. 2012).

Other problems with water in large cities are: over-exploitation of groundwater, industrial pollution, agricultural pollution, and contamination from the discharge

of fresh sewage into waterways. São Paulo and Mexico City, two of the largest metropolises in Latin America, have experienced quite similar demographic growth and urbanization processes, leading to problems related to water management, where there has been over-exploitation of neighboring aquifers and watersheds. In São Paulo, the problem is related to the high population which is concentrated in the upper part of the water supply basin, making the amount of available water insufficient to meet the demands of the inhabitants. In Mexico City, currently, only 2% of the water used by the population is superficial, while 68% comes from aquifers and 30% from neighboring basins. The main problem is the fact that the volume exploited in this region is much larger than the recharge capacity, an unsustainable practice over time (Izazola and Carmo 2004).

15.3.2 *Climatic Changes*

Climate change can be quite evident in changing water regimes, often resulting from variations in rainfall patterns and, consequently, in river runoff. In many areas of the globe, such processes, accelerated by the phenomenon of global warming, strongly impact the availability of water to the populace (Castro 2012).

Among the main aspects observed in Latin America in relation to climate change is the heavy reliance on Andean thawing for urban and agricultural sectors. According to the Intergovernmental Panel on Climate Change, mountain glaciers are sensitive indicators of climate change, and the threat to their existence reflects direct problems for some countries on the continent, such as Bolivia. La Paz, as well as other major Latin American cities, will have water scarcity problems, as glaciers account for up to 15% of supply throughout the year (Sempris 2009). Similarly, in Peru, there are communities that depend on glacial waters for agricultural use, domestic consumption and hydropower, who will be strongly affected if glaciers disappear (Franco 2016).

Sea-level rise due to melting glaciers could also affect coastal cities, where more than 70% of the Latin American population lives. Countries such as Mexico, Brazil, Cuba, Bahamas and Argentina are considered more likely to be impacted as a result of this phenomenon (Franco 2016).

Another impact emphatically associated with climate change is the change in rainfall. Increasing rainfall could lead to increased flooding (Banhe and Lopes 2016). The southern El Niño oscillation causes extreme drought conditions in the central Pacific region of the Pacific Ocean, while in northern Mexico, the phenomenon could lead to greater rainfall (Sempris 2009). However, periods of low rainfall could cause water scarcity in parts of the continent, such as along the Amazon River or the reduction of water flow in the La Plata basin at some periods of the year (Castro 2012). Lack of rainfall could also trigger drinking water scarcity, as well as cause threats to the security of energy supply due to reduced power generation by hydroelectric plants (Sempris 2009; Franco 2016).

Brazil could suffer from the effects on her water resources depending on the region. Changes include increased arid conditions in the center of the northeast region of the country and southern Amazonia, and precipitation and runoff in the southern Brazilian region (ANA 2016). Climate change tends to affect, in addition to surface water, renewable groundwater recharge rates and the level of aquifers. In northeastern Brazil, it is estimated that there will be a 70% reduction in groundwater recharge by 2050 (ANA 2016).

On the other hand, in an attempt to mitigate these impacts, some countries are signing global agreements to reduce pollution and greenhouse gas emissions, such as the Kyoto Protocol, signed in 1997 with the participation of all Latin American countries. These alignment actions of the Latin American countries for sustainability have contributed significantly to mitigating the possible impacts caused by climate change (Banhe and Lopes 2016).

15.3.3 Politics and Legislations

World discussions on water resources began at the 1977 United Nations Water Conference in Argentina, marking the first intergovernmental meeting to discuss actions to avert water crisis at the end of the century. This meeting produced a set of ten resolutions addressed to United Nations agencies, governments and the international community at large. Subsequently, the International Decade of Drinking Water Supply and Sanitation (1981–1990), the International Conference on Water and Environment (1992) and the Earth Summit (1992) were all events aimed at the conservation of water resources and the right access to portable water for everyone.

All of these meetings were pioneers to guide water policies in countries, especially the International Conference on Water and Environment with its principles of guiding and making recommendations at local, national and international levels. These principles formed the basis of the management model called Integrated Water Resources Management (IWRM), with the general aim of bringing together state and non-state actors such as higher bodies, regulatory and supervisory bodies, river basin bodies, service providers, local authorities and non-governmental organizations (civil society and users), as well as international agreements between countries for shared water resources (Villar 2019). Integrated management would be the main tool for achieving water security, ensuring basic needs of the population, food security, ecosystem protection, good management and equitable sharing of water resources.

In most Latin American countries, water management, with the definition of competencies and responsibilities, has been established by law, where each country establishing her own national water resources policy and created National Water Regulatory Agencies. From these laws and their instruments, the State becomes the central body and has the decision-making power over water resources, besides carrying out the inspection. Major laws specify ways of allocating water rights; environmental management related to water use, water quality parameters, land use planning and the conduct of financial management (Villar 2019).

Water management is generally a shared responsibility between levels of government, but in a bid to improve the management process, some countries have incorporated watersheds as a territorial management unit by forming watershed institutions and organizing their policies, specific and appropriate to the local reality. These institutions work together with the actions of the states or provinces and municipalities, as well as social participation through associations of water users and civil society. For example, Argentina, Brazil, Dominican Republic, Guatemala and Mexico have functioning basin organizations and have sought to organize their water policies based on this territorial unit (Villar 2019).

Brazil has been trying to establish water security indices or degrees through studies and relationships with various areas such as sanitation, agriculture and irrigation, urban and industrial water demand with water availability and future demand scenario. The results of these studies serve as a database for the diagnosis of the water resources situation and have guided government actions in the implementation of plans and projects for critical drought and flood situations. Other environmental policies for the preservation and maintenance of ecosystems directly affect the conservation of water resources. One of such is the Brazilian Forest Code (Law 12.651/2012), which establishes the obligation to maintain a minimum range of vegetation area around water bodies. Most countries in Latin America have tried to develop their water policies in this same trend, as is the case with Argentina, Uruguay, Paraguay, and Peru.

However, it is also worth noting that for all Latin American countries the challenges of water resources management in the next years strongly needs government support, regulating, inspecting, financing and promoting public programs and policies in a more integrated manner for that the agriculture, industry, tourism, energy, transportation and sanitation/health, among others, can have access the water resources in a sustainable way.

15.3.4 Agriculture

Processes such as carbon dioxide fixation and temperature control require plants to transpire huge amounts of water. Several crops use water at rates between 300 and 2000 L per kilogram (kg) of dry matter from the crops produced. It is estimated that in the USA, 1 ha of maize, with crop yield of about 9000 kg/ha, transpires approximately 6 million L of water during the growing cycle, while 1 to 2.5 million L/ha evaporates from the soil to the atmosphere (Pimentel 2004). This means that to complete the cycle, the crop requires about 800 mm of rain (8 million L/ha). These values underscore the dependence and need of the resource to guarantee production. In abundant rainfall, the need for supplemental irrigation is not abundant (Fraiture and Wichelns 2010). However, when analyzing the reality of northeastern Brazil, northern Chile and most of the Mexican territory, there is a great dependence on water resources to guarantee crop production. In these places, there is a strong relationship between water availability and food security for the region or nation.

However, it is noteworthy that in addition to the production of vegetables and grains, a large amount of water is used for animal protein production which requires significantly more water than vegetable production (Fraiture and Wichelns 2010). This high demand does not refer to water consumption by the animal itself, but to the volume involved in the production of pastures and grains.

As South America was notoriously formed by economies based on production and food, such as Brazil, Paraguay, Argentina, Chile and Uruguay, it is estimated that there will be an increase in cultivated area and indirectly increased water to meet crops demand. In addition, many producers have invested in the purchase of irrigation equipment as a way to avoid losses due to lack or erratic distribution of rainfall. In most cases, water for irrigation comes from surface water (rivers and lakes) which is reflected in the reduction of water availability in rivers, conflicting with other uses such as industrial and urban water supply (Fraiture and Wichelns 2010).

However, it is not only the growing demand for the resource that makes agriculture a conflicting point regarding water resource conservation. Especially in the last two decades, the use of pesticides in crops has been intensified, associated with the application of highly soluble mineral fertilizers (Yong and Jiabao 1999). This combination has negatively affected the environment, contributing to the contamination of surface water as well as groundwater (Loannis et al. 2006). Despite the mobilization of Latin American society and Europeans (destination of most food exported) in the face of the rampant use of pesticides, there is currently no policy discouraging this model of agriculture and, therefore, it is estimated that in the future, the problems of water contamination by pesticide residues, veterinary medicines and eutrophication problems from nitrogen and phosphorus loads continue unabated, negatively impacting the environment and especially the population (Yong and Jiabao 1999; Loannis et al. 2006).

15.3.5 Deforestation

Deforestation and anthropogenic transformations in land use have important implications for climate, ecosystems, sustainability and species survival. Forests currently cover only about one third of the planet's surface. Between 2000 and 2012, urban sprawl, farmland conversion, logging and forest fires resulted in the loss of 1.5 to 1.7 million km² of tree cover, or approximately 3.2% of global forest cover (FAO 2016a).

Recent research shows that tropical and subtropical forests play a fundamental role in the global hydrological cycle, being responsible for the transport of atmospheric humidity, cloud formation and rainfall on a regional scale (Ellison et al. 2017). On average, at least 40% of rainfall on earth originates from evapotranspiration, with major contributions in some regions, such as the Prata River basin, where evapotranspiration from the amazon rainforest contributes over 70% of rainfall (Van der Ent et al. 2010). Also, riparian forests protect water resources, thus contributing

to stabilization of slopes and slopes, sediment and nutrient retention, flood protection and regulation of water temperature (MMA 2017).

The Food and Agriculture Organization of the United Nations (FAO) divided the world into 230 major river basins, with historically 67.8% of forest cover. About 40% of river basins lost more than half of their forest cover in 2014, causing negative effects on water conservation and water quality. According to the Global Forest Resources Assessment (FAO 2016b), currently 25% of the world's forested areas are being managed to protect soil and water, especially in North and Central America (71%) and Asia (33%). In other regions, there is a trend of forest reduction, such as in Europe, Africa and South America. According to FAO studies, the annual loss of forests in South America and the Caribbean during 2000–2005 was about 4.7 million ha, accounting for 65% of global losses. However, the deforestation rate fell in South America between 2005 and 2010. Only in Brazil did the reduction of deforestation rate in 70% between 2004 and 2016 after the implementation of the Action Plan for the Prevention and Control of Legal Deforestation (PPCDAM). Recent data from the Deforestation Monitoring Project in the Legal Amazonian Satellite (PROCEDES) recorded an increase in deforestation by 13.7% between August 2017 and July 2018 compared to previous 12 months—the worst result in 10 years (MMA 2018).

There is a need to drastically reduce deforestation worldwide, especially in South America and the Caribbean, which account for about 57% of the world's primary forests, and which are home to the most important biodiversity and conservation standpoint. In Latin America, Costa Rica is one of the countries that has stand out in relation to the maintenance and sustainable exploitation of forests, mainly because it attracts a large number of tourists seeking to enjoy preserved natural environments. This policy adopted by the country aims to adding greater economic value to forests and encouraging the conservation of ecosystems through sustainable forest management.

15.3.6 Industrialization

Historically, Latin America has sustained its growth almost exclusively on the exploitation of natural resources and as a result, many countries in the region have economies that are less diversified and excessively dependent on their raw materials (Pamplona and Caccimali 2017). This has become even more pronounced in recent decades, especially in light of the migration and current expansion of industries in Asian countries, which have become the main consumers of commodities extracted or produced in Latin countries (Etzkowitz and Brisolla 1999). However, efforts are currently being intensified by building a local industry capable of promoting import substitution, driven mainly for job creation, ensure economic growth and improve the balance of trade among countries such as USA, China, and European Union. With

the projected population increase and, consequently, an upward trend in domestic consumption, Latin America presents a favorable scenario for industrialization and should see an increase in the number of new consumers and industries for durable goods in the coming decades (Pamplona and Caccimali 2017).

However, there are some substantial differences in the industrialization process between Latin America and South Asia, which has notoriously attracted investors for labor exploitation and the absence of restrictive environmental legislation, which has ensured a rapid expansion based on consumption of non-renewable energy (coal), factors that have culminated in the intensification of environmental problems such as air and water pollution (Etzkowitz and Brisolla 1999). On the other hand, there is a differentiated possibility of development in Latin America, since most countries have environmental policies that value the conservation of the environment and more restrictive laws, which lead to a process of industrialization with stricter rules which are the case in South Asia, for example. Another important factor is the predominance of hydropower use, which, despite the inherent damage to the river dam, is considered a much less harmful renewable energy source when compared to coal and natural gas, which are non-renewable sources and currently promoted in Asian industry.

Nevertheless, currently in several Latin American countries, there is increasing concentration of the population in the coastal region, associated with increase of populations in megacities, with the formation of industrial complexes which are concentrated mainly in three countries namely Brazil (São Paulo—which has the largest industrial park in Latin America, Manaus Free Zone, and Zona da Mata in the Northeast); Argentina (Buenos Aires, Córdoba, Tucumán, Rosario, Mendoza); and Mexico (Guadalajara, Mexico City, Vera Cruz, Tampico). This conception of the growth of industrial zones linked to large urban centers, despite being engaged with many of the principles of sustainable development, has serious environmental consequences, as these centers become major “drains of environmental resources,” mainly water and energy. In addition, there is large production of liquid, solid and gaseous effluents, with potential effects given the magnitude of concentrated emission in a small spatial area, hindering its dissipation in the environment. In Latin America, one of the most obvious examples is the case of Mendoza, Argentina, located in an arid region with very low annual rainfall, where industrial activity competes with agriculture on the scarcest resource in the region, water (Lavie et al. 2015). Currently, the lack of this resource already impacts on the development of new ventures in the region, making it impossible to expand industrial activity and agriculture (Lavie et al. 2015). Similar cases are also reported in Mexico (Aguilar et al. 2003). Even in Brazil, which owns approximately 12% of the world’s freshwater reserves, the water issue may prove to be a hindrance in the industrialization process, since the rivers that cross the city of São Paulo are among the most polluted in the world and the years of carelessness associated with high consumption have recently caused an unprecedented crisis in the city’s water supply system between 2014 and 2015 (Marengo et al. 2015). In addition, Brazil has most of its industrial complexes near major centers and in the coastal region, while the largest abundance of water and hydroelectric power production potential is in the Amazon region and the Paraná River basin, which is little inhabited and industrialized.

Thus, it is evident the need to rethink the industrialization process in Latin America, which has been following the usual model of urban planning, with the concentration of industries near the major centers, seeking the potentialization of mutual expansion by the association of consumer market, supply of labor and formation of industrial complexes/poles. Because, despite the possible economic benefits, this model implies the increasing supply of natural resources to the regions where urbanization intensifies, resources that, in a contradictory way, are not concentrated, but distributed in the territory, being many times more abundant in regions very away from the industrialized region.

15.3.7 Mining Extraction

The extraction of non-renewable natural resources has been intensified in recent years in Latin America. The World Bank and other international financial institutions have encouraged countries to commit to the growth of the extractive industry as a growth strategy for developing countries (Arellano 2011). According to Walter (2014), the extraction of raw material in Latin American countries jumped from 2,400 million tons in the 1970s to 8,300 million tons in 2009. Since the nineteenth century, mining activity has been of great economic importance. Latin American countries (Bebbington 2011) and Canada are one of the largest investing countries in this continent (Arellano 2011). According to Bebbington (2011), Latin America is mainly responsible for the extraction of copper, bauxite, iron, silver, gold, lead, molybdenum, nickel, tin, zinc, niobium, selenium, antimony, lithium, iodine, coal, tantalite. and manganese. However, gold is the main target of exploitation in these countries, accounting for 42% of the metals extracted, followed by lithium, used as a raw material for the manufacture of batteries (Hilson 2002). In 2015, the continent attracted a significant part of global spending on exploration activities, with Chile, Peru, Mexico, Brazil, Colombia and Argentina with high quotes (Hilson 2002).

According to the liberal economic discourse, revenues from mining activities can increase the Gross domestic product (GDP), boost economic growth, and reduce a country's poverty and unemployment rates (Arellano 2011). Besides the developmental discourse, except for Brazil, the environmental theme in the mining segment was not a priority during the 1980s in developing countries. This phenomenon is added to the economic and political problems faced by several Latin American countries, making it impossible to follow international environmental trends (Bebbington 2011).

Although mining-related regulations exist in many Latin American countries, for the most part, there are no specific laws or regulations setting standards for monitoring and remedying possible damage (Cordy et al. 2011). However, there is a consensus in the sector on the need to develop policies that guarantee the existence of opportunities,

but linked to sustainable development, integrating environmental concerns, human development—considering social goals and economic development (Hilson 2002). According to the Environmental Justice Atlas (EJ Atlas) database, there are potential human threats to water security in virtually every country in Latin America (EJ Atlas 2019). Figure 15.1 presents human threats to water security and conflicts related to mineral extraction in Latin American countries.

According to Hilson (2002), the region is the target of investments in part because the Latin American continent is still subject to this comprehensive exploration in supplying the global market. In Bolivia and Colombia, for example, there is no legal



Fig. 15.1 Map outlining area with restriction of quantity or quality of water for human consumption and points where there are conflicts related to mining in Latin America. (Source adapted from (EJ Atlas 2019)

definition of mining environmental responsibility or compensation for environmental damage. In Chile, there are large-scale deteriorated parts of abandoned mines. In Colombia, the existence of illegal and/or small-scale mines causes mercury to spill into rivers (Cordy et al. 2011).

Among the possible negative impacts, it is possible to highlight the deterioration of the water quality downstream of the mined areas. This is due to the fact that the potential for water contamination increases when it comes into contact with the extracted mineral (Soni 2019; Kunz 2020). Nearby waters suffer from acidification and pollution processes caused by oils, chemicals and heavy metals (Mechi and Sanches 2010). These can also reach groundwater, aggravating the impacts caused. Other possible impacts are the lowering of the water table and the alteration of the hydrological regime of watercourses and aquifers, through the use for mining and beautification processes (Mechi and Sanches 2010; Kunz 2020). An example of this is the expansion of desalinated water infrastructure due to new mining projects in the Atacama region of Chile that has disrupted water supply arrangements for communities and compromised access to groundwater (Kunz 2020). According to Hilson (2002), one of the challenges of the mining industry is to find an appropriate water source for mining projects. The author also states that companies are focused on reducing water consumption in their processes or using other non-potable sources such as seawater.

15.3.8 Sanitation

Access to clean, quality water is fundamental to the existence and survival of society. Risks to water quality increase as the world's population grows and as the demand for water increases. Thus, accessing areas with adequate sanitation helps to prevent the existence of diseases and possible vectors for human health. For example, in Central America, floodwater has been increasing the number of vector-borne diseases, such as dengue and malaria, as well as the transmission of rodent-borne pathogens to humans (Sempris 2009).

Although water supply is close to total for the urban population of Latin America, however this appears not be the case for sanitation services for the same countries. According to França et al. (2012), there are still 74 million people in the Latin American continent without adequate access to sanitation and less than 20% of wastewater is treated before it is disposed off.

In 2015, WHO (2017) data showed that only 23% of the Latin American population had access to safe sanitation. While most of the population had access to sewage collection (63%), 11% of the Latin American and Caribbean population had access to limited services or the service was non-existent (Fig. 15.2).



Fig. 15.2 Proportion of Latin American population using at least the basic sanitation service in 2015 (WHO 2017)

In the same period, 91 to 100% of the population has sewage collection services in Argentina, Chile, Uruguay, Paraguay, Venezuela, French Guiana, Cuba, Puerto Rico, Costa Rica and El Salvador. Brazil, Peru, Ecuador, Colombia, Suriname, Guyana, Panama, Nicaragua, Honduras, Belize, Mexico, Jamaica, and the Dominican Republic had 76 to 90% of its population served with sewage collection services, while Bolivia and Guatemala had between 50 and 75% of its population served with these services. In Haiti, less than 50% of the population has access to sanitation services (WHO 2017). Thus, the urgent need for investments regarding the treatment of sewage in Latin American countries is evident, because despite the great evolution experienced in relation to the supply of treated water to the population experienced in the last decades in the Latin countries confirmed the same evolution in relation to the effluent treatment and it is still common to find cities where it is not the effluent produced.

15.3.9 Integrated Management of National and Transboundary Basins

When a river flows across different countries, government of each country pays less attention to improve the water quality of their river basin portion, as the benefits of their efforts are especially received by countries downstream (Giri 2021). Although it has not yet achieved its due priority in the analysis of international relations, the issue of sharing transboundary surface waters is of great importance to most countries, as most countries have their territories in international watersheds (Wolf et al. 1999). As an aggravation, many of these nations already suffer, or will suffer in the medium term, from water deprivation scenarios. Based on this, it can be concluded that the development of an institutional and legal apparatus to regulate the use of water resources on an international scale is one of the biggest challenges facing water-sharing countries, as it clashes with the sovereignty of countries and the prevalence of national legislation on water use (Giri 2021; Ribeiro et al. 2015).

There are currently 263 international basins and 145 nations that have their territories in these basins, and out of this, 21 nations are fully embedded in shared river basins, while another 12 have more than 95% of their area within one or more basins with geographical particularity (UNESCO 2003). In Latin America, one can cite the example of Brazil, which has about 60% of its territory coinciding with transboundary watersheds, as it is drained by two of the five largest in the globe (Amazon and Platinum) (UNESCO 2003).

In order to minimize these deleterious effects of competition between nations, efforts have been made in Latin America, especially in recent decades, to build cooperation agreements and shared management of transboundary water resources (Giri 2021). Among the main ones listed in Table 15.1 is the Amazon Cooperation Treaty (TCA), signed on July 3, 1978 by Brazil, Colombia, Bolivia, Ecuador, Guyana, Peru, Suriname and Venezuela. This agreement deserves mention among the others already established in Latin America due to two factors, (i) robust legal and administrative instrument established between eight different nations that aims to maintain the balance between economic growth and environmental preservation; and (ii) coverage of the entire territory of the amazon basin which is invaluable to the planet and currently suffers from degradation. However, in relation to the agreements, it is noteworthy that many of them still lack effective implementation, since many of the policies provided for in the agreements are not effectively implemented by both or only the countries participating in the agreement (Wolf et al. 1999).

Table 15.1 List of main transboundary treaties on shared management of water resources in Latin America

Year	Treaty	Participating Countries
1906	Rio Grande o Bravo water distribution treaty	Mexico and USA
1969	Silver basin treaty	Argentina, Brazil, Bolivia, Paraguay and Uruguay
1973	Treaty of hydroelectric use of the waters of the Paraná River of shared sovereignty between Brazil and Paraguay	Brazil and Paraguay
1975	Uruguay River statute	Argentina and Uruguay
1977	Cooperation agreement for the use of natural resources and the development of the Lagoa Mirim basin	Brazil and Uruguay
1978	Amazon cooperation treaty	Brazil, Bolivia, Colombia, Ecuador, Guiana, Peru, Suriname and Venezuela
1979	Tripartite agreement on technical and operational cooperation between Itaipú and corpus	Argentina, Brazil and Paraguay
1980	Treaty to harness the shared water resources of the Uruguayan border	Brazil and Argentina
1986	Trifinio Plan	El Salvador, Guatemala and Honduras
1987	Agreement on the institutionalization of lake Titicaca's water system	Peru and Bolivia
1991	Cooperation agreement for the use of natural resources and development of the Quaraí River basin	Brazil and Uruguay
1992	Cooperation for border development of the sixaola river binational basin	Costa Rica and Panama

References

- Aguilar AG, Ward PM, Smith CB (2003) Globalization, regional development, and mega-city expansion in Latin America: analyzing Mexico City's peri-urban hinterland. *Cities* 20:3–21
- ANA (Agência Nacional das Águas) (2016) *Mudanças Climáticas e Recursos Hídricos: avaliações e diretrizes para adaptação*. Brasília: ANA, GGES, p 93
- Arellano JM (2011) Mining in Latin America: the interplay between natural resources, development, and Freedom. *Inquiries J Stud Pulse*, 3 p
- Banhe A, Lopes J (2016) Gestão de riscos das mudanças climáticas: uma análise sobre oportunidades de colaboração entre governos locais e empresas na América Latina. In: *Mudanças climáticas: o desafio do século*. Rio de Janeiro: Fundação Konrad Adenauer, Cadernos Adenauer xvii, 169 p
- Bebbington A (Ed) (2011) *Social conflict, economic development and the extractive industry: evidence from South America*. Routledge, 256 p
- Castro JE (2012) A gestão da água na América Latina. *Desafios do Desenvolvimento*, Ano 9, nº 7.
- Cook C, Bakker K (2012) Water security: debating an emerging paradigm. *Glob Environ Chang* 22:94–102

- Cordy P, Veiga MM, Salih I et al (2011) Mercury contamination from artisanal gold mining in Antioquia, Colombia: the world's highest per capita mercury pollution. *Sci Total Environ* 410:154–160
- EJ Atlas (2019) Mining conflicts in Latin America. Environmental Justice Atlas. Disponível em: <https://ejatlas.org/featured/mining-latam>. Accessed 8 Aug 2019
- Ellison D, Morris CE, Locatelli B et al (2017) Trees, forests and water: cool insights for a hot world. *Glob Environ Chang* 43:51–61
- Etzkowitz H, Brisolla SN (1999) Failure and success: the fate of industrial policy in Latin America and South East Asia. *Res Policy* 28:337–350
- FAO (Food and Agriculture Organization of the United Nations) (2016a) Global forest resources assessment: how are the world's forests changing? Roma, 137 p
- FAO (Food and Agriculture Organization of the United Nations) (2016b) El Estado de los bosques del mundo 2016b. Los bosques y la agricultura: desafíos y oportunidades en relación con el uso de la tierra. Roma, 137 p
- Fraiture C, Wichelns D (2010) Satisfying future water demands for agriculture. *Agric Water Manag* 97:502–511
- França BC, Cunha JVQ, Custódio MB et al (2012) Síntese dos pontos abordados pelo Relatório “O Estado das Cidades da América Latina e Caribe 2012: rumo a uma nova transição urbana”. Estudo Técnico SAGI, nº 15. Brasília—DF, 14 p
- Franco KM (2016) Enfrentamento das mudanças climáticas na América Latina e Caribe, pp 123–144. In: Mudanças climáticas: o desafio do século. Rio de Janeiro: Fundação Konrad Adenauer, Cadernos Adenauer xvii, 169 p
- Giri S (2021) Water quality prospective in Twenty First Century: Status of water quality in major river basins, contemporary strategies and impediments: a review. *Environ Pollut* 271:116332
- Gray D, Sadoff CW (2007) Sink or Swim: water security for Growth and development. *Water Policy* 9:545–571
- Hilson G (2002) An overview of land use conflicts in mining communities. *Land Use Policy* 19:65–73
- Izazola H, Carmo RL (2004) México e São Paulo: expansão metropolitana, desigualdade social e a questão da água. In: I Congresso da Associação Latino Americana de População, ALAP, Caxambu—MG—Brasil
- Kunz NC (2020) Towards a broadened view of water security in mining regions. *Water Security* 11:100079
- Lavie E, Hévin J, Le Drezen Y (2015) Accès à l'eau potable, problèmes de gouvernance et vulnérabilités: le cas de la municipalité de Las Heras (agglomération de Mendoza, Argentine). *L'Ordinaire des Amériques*, 218 p
- Loannis KK, Dimitra GH, Triantafyllos AA (2006) The status of pesticide pollution in surface waters (rivers and lakes) of Greece. Part I. *Rev Occur Levels Environ Pollut* 141:555–570
- Mahlknecht J, González-Bravo R, Loge FJ (2020) Water-energy-food security: a Nexus perspective of the current situation in Latin America and the Caribbean. *Energy* 194:116824
- Marengo J, Nobre CA, Seluchi M et al (2015) (2015) A seca e a crise hídrica de 2014–2015 em São Paulo. *Revista USP* 10:31–44
- Mechi A, Sanches DL (2010) Impactos ambientais da mineração no Estado de São Paulo. *Estudos Avançados* 24:209–220
- Melo MC, Johnsson RMF (2017) O Conceito emergente de Segurança Hídrica. *Sustentare* 1:72–92
- MMA (Ministério do Meio Ambiente) (2017) Índice de Prioridade de restauração florestal para segurança hídrica: uma aplicação para as regiões metropolitanas da Mata Atlântica. Brasília, DF, 48 p
- MMA (Ministério do Meio Ambiente) (2018) Taxa de desmatamento na Amazônia Legal. Available in: <https://www.mma.gov.br/informma/item/15259-governo-federal-divulga-taxa-de-desmatamento-na-amaz%C3%B4nia.html>. Accessed 15 Aug 2019
- Organisation for Economic Co-operation and Development (OCDE) (2013) Water Security for Better Lives. OECD Publishing, OECD Studies on Water, p 173p

- Pamplona JB, Cacciamali MC (2017) O paradoxo da abundância: recursos naturais e desenvolvimento na América Latina. *Estudos Avançados* 31:251–270
- Pimentel D (2004) Livestock production and energy use. In: (Matsumura R (ed) *Encyclopedia of energy*. San Diego, CA: Elsevier, pp 671–676
- Ribeiro CR, Bermudez OB, Leal AC (2015) A Gestão Compartilhada de Águas Transfronteiriças, Brasil e Colômbia. *Mercator* 14:99–118
- Sempris E (2009) Climate change and freshwater in Latin America and the Caribbean. *UN Chronicle*, 156 p
- Soni AK (2019) Mining of minerals and groundwater in India. Groundwater—resource characterization and management aspects. *IntechOpen: London, UK*, pp 249–283
- Tzanakakis VA, Paranychianakis NV, Angelakis AN (2020) Water supply and water scarcity. *Water* 12:2347
- UNESCO (2003) *Water for People, Water for Life: The First UN World Water Development Report*. Scientific and Cultural Organization (UNESCO) and Berghahn Books, Paris, United Nations Educational, p 36p
- UNESCO (United Nations Education, Scientific and Cultural Organization) (2012) *The united nations world water development report 4: managing water under uncertainty and risk*. UNESCO, 68 p
- United Nations (2013) *Water security & the global water agenda: a un-water analytical brief*. UN University, Hamilton, Canada
- United Nations (Department of Economic and Social Affairs, Population Division) (2019) *World population prospects 2019: highlights*. United Nations, 39 p
- Van der Ent RJ, Savenije HH, Schaefli B et al (2010) Origin and fate of atmospheric moisture over continents. *Water Resour Res* 46:1–12
- Villar PC (2019) *Governança Hídrica Na América Latina*. ANA: Capacitação para a gestão das águas. Available <https://capacitacao.ana.gov.br/conhecerh/handle/ana/78>. Accessed 13 Aug 2019
- Walter M (2014) *Political ecology of mining conflicts in Latin America: an analysis of environmental justice movements and struggles over scales*. PhD Thesis programme in Environmental Sciences. Universitat Autònoma de Barcelona. Institut de Ciència i Tecnologia Ambientals, 194 p
- WHO (World Health Organization), UNICEF (United Nations Children’s Fund) (2017) *Progress on drinking water, sanitation and hygiene: 2017 update and SDG baselines*. WHO Library Catalogue-in-Publication Data, World Health Organization and United Nations Children’s Fund, p 114p
- Wolf AT, Natharius JA, Danielson JJ et al (1999) *International River Basins of the World*. *Int J Water Resour Dev* 15:387–427
- WWAP (World Water Assessment Programme) (2019) *The United Nations world water development report 2019: leaving no one behind*. UNESCO Publishing, 186 p
- Yong L, Jiabao Z (1999) Agricultural diffuse pollution from fertilizers and pesticides in China. *Water Sci Technol* 39:25–32

Chapter 16

Contribution of GIS to the Mapping of the Sensitivity of the Flood's Hybrid Multi-criteria Decision Approach: Example of the Wadi Tamlest Watershed (Agadir, Morocco)



Abderrahmane Wanaim, Mustapha Ikirri, Mohamed Abioui , and Farid Faik

Abstract Since the end of the last century, climate change has generated qualified pluviometric events favoring the triggering of flash floods characterized by very high speeds and fairly short rise times. These floods caused extensive damage and paralyzed all activities in the flooded regions, as was the case during the last event in November 2014 which left behind a significant body of human and material damage in the different regions of Morocco. The Wadi Tamlest watershed located north of the Agadir city is a good example of areas affected by floods. The FHI (Flood Hazard Index) method was applied to study these extreme phenomena and to determine their lateral extensions using six factors influencing the floods (accumulation of flow, distance from the main wadis, drainage density, land use, slope, and permeability). This method made it possible to map with great precision the areas vulnerable to flooding throughout the Wadi Tamlest watershed. Finally, the application of the FHI method is more advantageous in basins not equipped with hydrometric stations but seems less precise in terms of defining the water heights downstream of the basin.

Keywords Climate change · Flooding · Damage · FHI (Flood Hazard Index) · Wadi Tamlest · Morocco

A. Wanaim · M. Ikirri · M. Abioui (✉) · F. Faik
Department of Earth Sciences, Faculty of Sciences, Ibn Zohr University, Agadir, Morocco
e-mail: m.abioui@uiz.ac.ma; abioui.gbs@gmail.com

A. Wanaim
e-mail: a.wanaim@uiz.ac.ma; abdougeologue@gmail.com

M. Ikirri
e-mail: mustapha.ikirri@edu.uiz.ac.ma; ikirimustapha@gmail.com

F. Faik
e-mail: f.faik@uiz.ac.ma; faikfarid@yahoo.fr

16.1 Introduction

The climate changes that the globe is currently experiencing, generate qualified rainfall events favoring the triggering of flash floods characterized by very high current speeds and rises in the water level in a very short time (e.g. Jenkinson 1955; Herschy 2002; Kundzewicz and Menzel 2003; Kundzewicz 2003; Hanson et al. 2007; Campion and Venzke 2013; Kabenge et al. 2017; Wang et al. 2021; Yoo et al. 2021; Ikirri et al. 2021, 2022; Echogdali et al. 2022a, b, c, d, e; Aswathi et al. 2022). These phenomena are considered the most harmful disaster that threatens the Earth in recent years, causing environmental and socio-economic consequences in the affected floodplains. The exceptional floods cause enormous problems with very negative socio-economic and environmental consequences (e.g. Francou and Rodier 1967; Crippen and Bue 1977; Hallegatte et al. 2007; Jonkman et al. 2008; Merz and Thieken 2009; Saidi et al. 2010; Pulvirenti et al. 2011; Jongman et al. 2012; Aich et al. 2015; Cobbinah and Anane 2015; Sun et al. 2016; Mendez and Calvo-Valverde 2016; Lu et al. 2018). Several theories, numerical models, and statistics have been developed to describe the behavior of flood phenomena. Climatically, Morocco is classified as a semi-arid to the arid region. Rainfall is generally low and irregular with strong spatial and temporal variations. Due to the impact of climate change, the country has experienced, in recent years, numerous floods in several regions (e.g. Hulme et al. 2001; Saidi et al. 2010; Feng et al. 2013; Wongsa 2014; El Alaoui El Fels and Saidi 2014; El Alaoui El Fels et al. 2018; El Morjani et al. 2016; Echogdali et al. 2018a, b, 2022a, b, c, d, e; Saad et al. 2019; Bennani et al. 2019; Ikirri et al. 2021, 2022; Aswathi et al. 2022; Benjmel et al. 2022; Ait Haddou et al. 2022). Among the most frequent and deadly disasters that Morocco has experienced:

- The floods of the wadi Ourika in 1995,
- The floods of wadi Maleh in 2002,
- The floods of Tangier, Nador, Fnideq, Boulmane (October 2008),
- Agadir 1956, 1977, 1996, 2010 and 2014,
- The floods of Guelmim and Sidi Ifni (November 2014).

The Agadir region is a perfect example since it has suffered numerous damages following the floods of the wadi Tamlest that occurred in the years 2010 and 2014. These exceptional events are due to heavy rainfall during the winter cycles. The study of lateral extensions seems essential in this region. It will allow decision-makers in the hydraulic field to delimit the areas at risk of flooding and security with these events. This is the reason why a multi-criteria analysis method (AHP) was used for the mapping of flood risk areas in the Tamlest catchment area. This analysis consists of introducing a Flood Risk Index (FHI) to assess these areas at the watershed scale. Six parameters are involved (flow accumulation, distance from the drainage network, density of the drainage network, slope, permeability, and land use) (Kazakis et al. 2015; Elkhrachy 2015; Echogdali et al. 2018a, b, 2022a, b, c, d, e; Talha et al. 2019; Ikirri et al. 2021, 2022; Aswathi et al. 2022). The relative

importance of each parameter and the severity of flooding were related to the weight values. The final risk map is developed after overlaying the selected factors.

16.2 Study Area

The watershed of the Wadi Tamlest, the subject of this study, is located in southern Morocco, between longitude 9°29'50" and 9°36'50" latitude 30°23'20" and 30°30'16", northeast of the city of Agadir. It covers an area of 11.66 Km² with a perimeter of about 18.57 km; the elevation of the surface varies between 84 and 419 m (Fig. 16.1). The length and width of the basin are respectively 7.78 and 1.49 km. The coefficient of Gravius is about 1.53; the basin is, therefore, longer than wide. This basin is located in a semi-arid climatic context; it is characterized by the interference of the cold currents of the Atlantic Ocean and the hot currents coming from the South. The average temperature is 25 °C, with a maximum of 40 °C and a minimum of 10 °C. The average annual rainfall is around 200 mm. The concentration–time is calculated by the formulas of Kirpich (1940) and Spanish that give underestimated values, while the Tc calculated by the formula Giandotti (1934) gives an overestimated value, but the Tc calculated by the formula of Turraza is comparable to those calculated by the formula of Ventura. It is concluded that the average time of concentration that the waters take to arrive at the outlet is 15 h this is related to the shape of the catchment Tamlest, in the case of a circular catchment waters gather quickly towards the outlet (Table 16.1).

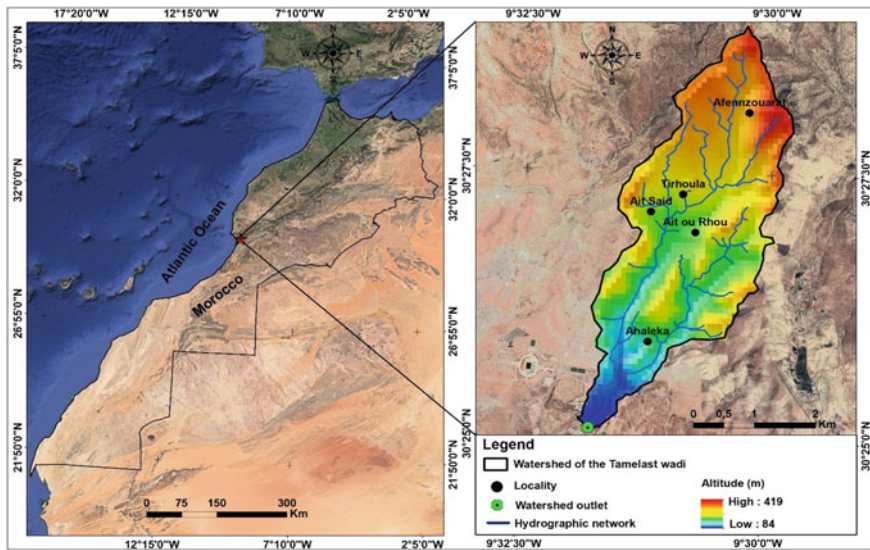


Fig. 16.1 Geographical context of the Wadi Tamlest watershed

Table 16.1 Time of concentration retained for Wadi Tamlest

Methods	Kirpich	Espagnole	Turraza	Ventura	Giandotti	Tc Average
TC (h)	0.031	12.516	22.647	21.484	9.52	15

The geomorphology of this basin is characterized by a dominance of mountains; the southern edge of the Western High Atlas, its plant cover is dominated by plants of Argan and euphorbia. The morphometric parameters of this basin are represented in Table 16.1 and are calculated using SIG software (Roche 1963, 1986). These parameters are of great importance, on the one hand, for understanding the direct influence of the shape of the basin on the generation of floods, and on the other hand, for the calculation of hydrological parameters such as the time of concentration. The slope of the Wadi Tamlest watershed is significant, it varies from 0° and 27° on the beds of the tributaries and downstream of the basin to 64° on the slopes upstream of the basin (Fig. 16.2a). The hydrographic network of the Wadi Tamlest watershed is dense and well-branched. It is characterized by its specific shape in “Y”. The ramification of the network is more pronounced upstream than downstream, given the geological accidents very abundant in the medium and high altitudes. Strahler’s classification (Strahler 1957) has four classes of which the watercourse identified as order 4 is apparent only downstream of the basin, specifically from the confluence of the two wadis Tamlest and Ahalka which will meet downstream, after crossing two-thirds of the basin, to form the Wadi Tamlest (Fig. 16.2b). Floods are more devastating downstream than upstream, both as a result of the gathering of surface water from the entire watershed of Wadi Tamlest. As for the density of drainage, the total length extracted from all the watercourses of the catchment area of Wadi Tamlest is about 8239.34 m; these watercourses are distributed over an area of 11,662 Km², which gives a density of drainage (Dd) of about 0.70 km⁻¹ (Dubreuil 1974).

$$Dd = \frac{\sum Li(Km)}{A(Km^2)} \quad (16.1)$$

16.2.1 Geology of the Wadi Tamlest Watershed

The Wadi Tamlest watershed extends on the southern flank of the anticline of Ait Lamine located on the southern edge of the Western High Atlas. The basin is represented by marine formations which are generally dolomitic limestones and clays of Coniacian age followed by dolomitic sandstones, dolomites, and yellow clays of Santonian and Campanian. The Maestrichtian is constituted by dolomitic limestones and clays. These formations are surmounted by the sandstone and lumachellic limestones of Oligocene and ancient Pliocene followed by the detrital formations of Villafranchian. The Quaternary is represented by conglomeratic shell sandstones,

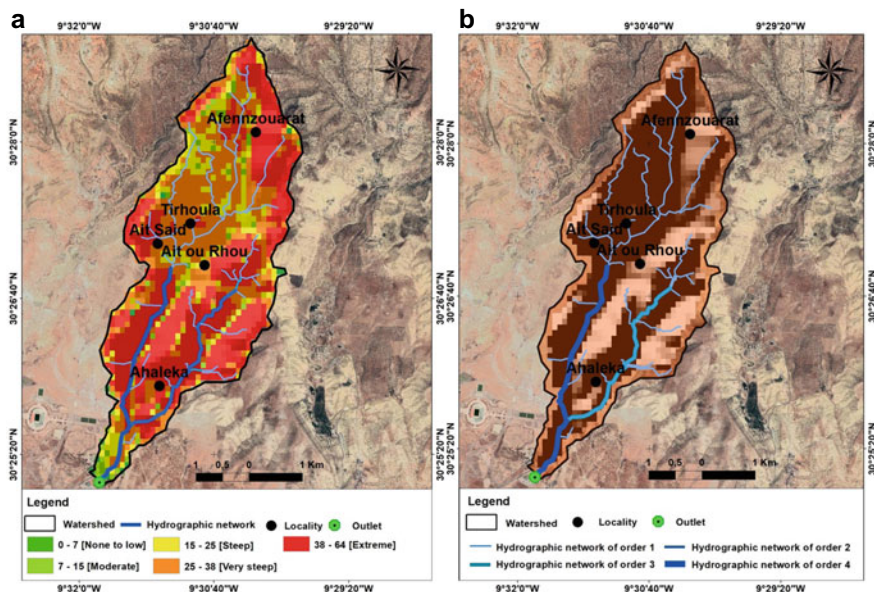


Fig. 16.2 Wadi Tamlest watershed: **a** slopes, and **b** Strahler classification

conglomerate marls, and soft lumachelles and these formations form most of the terraces of the basin (Fig. 16.3a). From a permeability point of view, the Wadi Tamlest watershed is formed by formations generally impermeable (90%), which amplifies the magnitude of flooding in the basin, hence an intense runoff. These formations constitute a major risk by amplifying the destructive power of floods. The permeable formations in the basin come mainly from soil erosion (10%) (Fig. 16.3b).

16.2.2 Hydrological Behavior and Consequences of Flooding

The hydrometric regime of the watershed of Wadi Tamlest is exclusively related to rainfall and is characterized by high water in the fall (first rain) and winter. Maximum rainfall is generally recorded in November and December. The basin does not flow until after the first rains in October or November. The flows of the tributaries of the basin consist of one component, a series of short but fairly strong floods that can occur several times a year depending on the intensity and duration of the rainfall sequences. All the morphological and lithological characteristics analyzed above have an obvious influence on the power of floods. The Wadi Tamlest watershed has no meteorological and hydrometeorological station, which forces us to confine ourselves to the realities on the ground and the damage caused by flooding to understand at what level the basin of Wadi Tamlest has been affected by flooding. In 2010 and 2014, like all regions of Morocco, the Wadi Tamlest watershed was subjected to

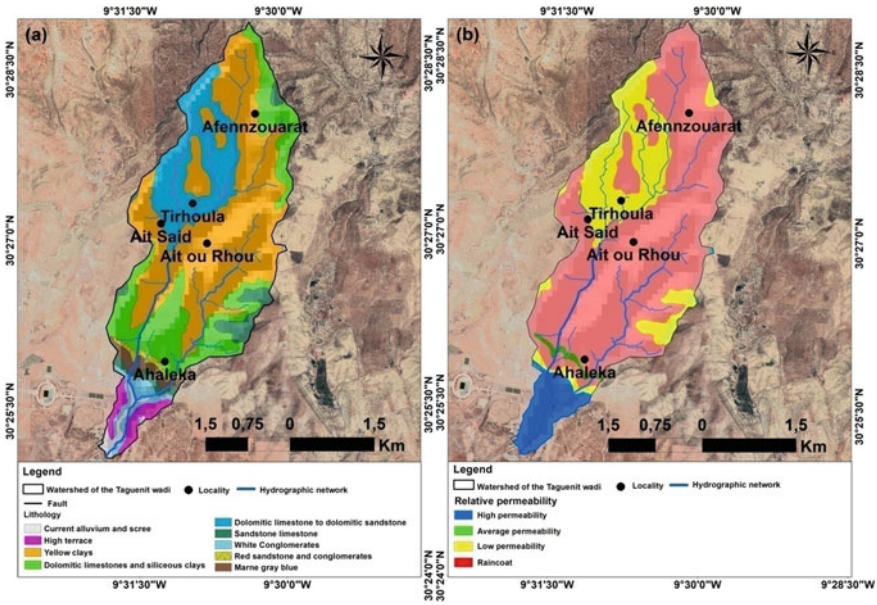


Fig. 16.3 Wadi Tamlest watershed: a geological map, and b permeability map

extreme rainfall that occurred within hours. These torrential rains caused catastrophic floods. The event of November 2014 is characterized by an infamous flood, by its material, and socio-economic damage (Fig. 16.4a, b). The 2010 flood is characterized by the enormous volume of water mobilized (Fig. 16.4c, d), which washed away many materials, vehicles, and infrastructure. Some new houses in the Al-Houda and Tikiouine neighborhoods, the sports complex in Tilila, and the green areas of Tassila were submerged by water and mud. The sectors of energy and trade were also damaged by these floods, indeed, nearly twenty commercial stores and two cafes were affected, at the level of the district Al-Houda and Tilila, so the supply of goods was also affected by the cutting of roads. In addition to this is the leaching of waste at the landfill Tamlest and the flow of leachate. These destructions have induced the stagnation of this liquid, in places, and its infiltration into the soil, causing their eutrophication and environmental pollution.

16.3 Spatialization of Flood Extent

16.3.1 Methodology

The study of flood risks in the watershed of Wadi Tamlest is based on the application of an approach of the flood risk index (FHI). This approach consists in delimiting the



Fig. 16.4 Photos showing infrastructure damage to urban areas during the 2010 and November 2014 floods

most vulnerable areas to flooding phenomena in this small basin by the multi-criteria analysis AHP (Saaty 1977, 1990a, b, 2012; Patrikaki et al. 2018). This analysis was used based on the combination of the selected factors in the basin, taking into account the relative weights according to the methodology shown in Fig. 16.5 (see Saaty 1990a, b; Kazakis et al. 2015; Rahmati et al. 2016; Patrikaki et al. 2018; Echogdali et al. 2018a, b, 2022a, b, c, d, e; Ali et al. 2020; Ikirri et al. 2021, 2022; Aswathi et al. 2022). The AHP multi-criteria analysis is a complex computational approach using matrix algebra. The matrix was used to extract the weight of each factor to take into account its relative importance in the calculation of the FHI (Elkhrachy 2015; Franci et al. 2016).

16.3.2 Factors Used in FHI

The flood risk index method was developed and implemented in a GIS (Geographic Information System) environment, taking into account six flood factors namely: flow accumulation (F), distance to the river system (D), drainage density (Dd), watershed land use (U), slope (S) and watershed geology (G). The selection of these factors in this study was theoretically based on their relevance, their rates of contribution to flood risk as well as the local conditions of the watershed, as indicated in the literature (Saaty 1990a, b; Haan et al. 1994; Patrikaki et al. 2018; Echogdali et al. 2018a, b, 2022a, b, c, d, e; Ikirri et al. 2021, 2022; Aswathi et al. 2022).

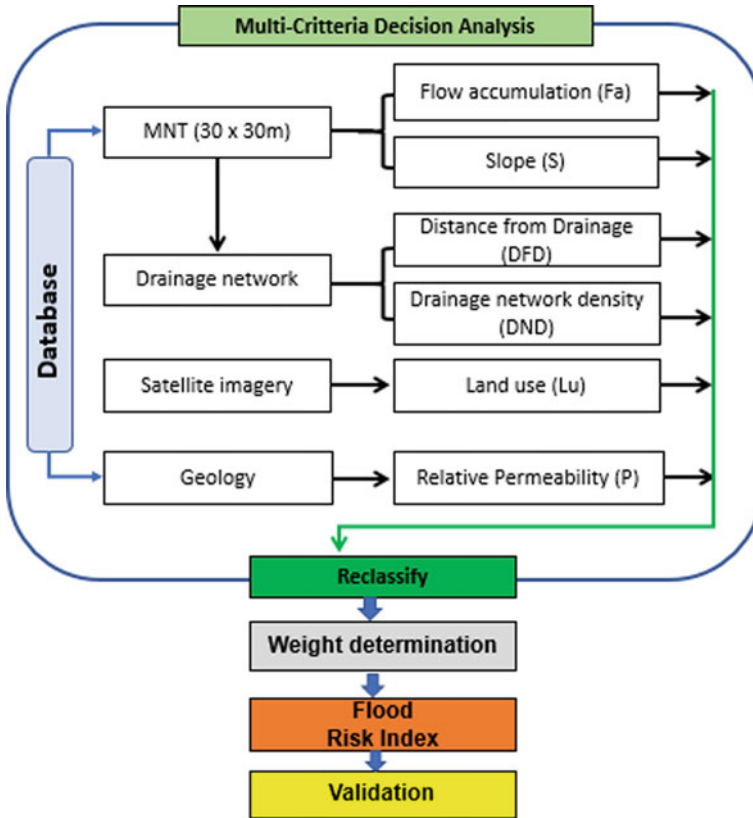


Fig. 16.5 Diagram of the methodology of the model applied to the flooding of the Wadi Tamlest watershed

The data for each factor was reclassified to correlate with flood risk. The values of the different classes used for this basin were between 2 and 10, where 2 indicate a lower risk and 10 is defined for a higher risk. Table 16.2 represents the weights of each factor.

- Flow accumulation: flow accumulation is a more important factor in delineating the area’s most vulnerable to flood risk. However, flow accumulation is the sum of water flowing downslope in the watershed. High values (13,258) of flows indicate areas of concentrated flow and therefore higher flood risk (Avagyan et al. 2018; Patrikaki et al. 2018; Ikirri et al. 2021, 2022) (Fig. 16.6a).
- Distance from the hydrographic network: the distance from the main channels was proposed and defined in Kazakis et al. (2015), Echogdali et al. (2018a, b, 2022a, b, c, d, e), Gao et al. (2020), Ikirri et al. (2021, 2022), and Aswathi et al. (2022). This distance indicates a level of flood risk in each area progressively further from the drainage system. Areas less than 100 m from the wadi are heavily flooded,

Table 16.2 Morphometric parameters of the Wadi Tamlest

Area (Km ²)	11.662
Perimeter (Km)	18.57
Gravelius index	1.5
High elevation (m)	419
Low elevation (m)	84
Wadi length (m)	8239.34
Slope index	0.021
Specific height difference (m)	0,072
Slope (%)	4.07
Equivalent Length (Km)	7.783
Equivalent Width (Km)	1.498

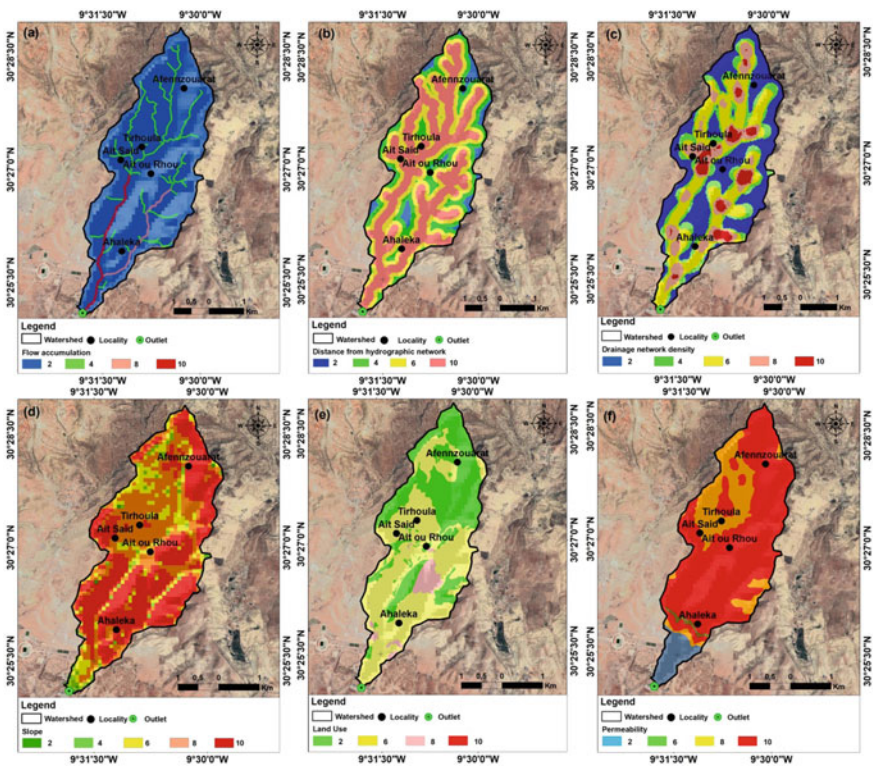


Fig. 16.6 Spatial distribution of factors in the Wadi Tamlest watershed: **a** Flow accumulation, **b** Distance from hydrographic network, **c** Drainage network density, **d** Land use, **e** Slope, **f** Permeability

while the risk effect decreases for distances greater than 100 m. On the other hand, the effect of this criterion is diminished for distances greater than 300 m. This explains why the distance from the drainage network has been given significant weight in the methodology (Fig. 16.6b).

- **Drainage network density:** Drainage density is an indicator that is proportional to the paths of concentration, flow accumulation, and flood probability. This factor influences the time of concentration of the basin. In the Tamlest catchment, the drainage density is varied between 0 and 5.12 m/km², in this case, the risk of flooding is proportional to the density of the drainage network. The classes of the density of the drainage network have been defined according to Jenks (1967) and Ikirri et al. (2021, 2022) (Fig. 16.6c).
- **Land use:** the soil cover determines the infiltration of rainwater into the soil, roads, and urban constructions in general, decreasing the infiltration of water which increases the water flow. While the vegetation favors the infiltration by their root system (Weng 2001; Franci et al. 2016; Ikirri et al. 2021, 2022). The urban area of the Wadi Tamlest is located downstream of the basin which allows more water to flow in the form of floods to this area. A large part of the basin area has bare soil and less dense vegetation, which were assigned rates of 6 and 4 respectively (Franci et al. 2016; Echogdali et al. 2018a, b, 2022a, b, c, d, e; Ikirri et al. 2021, 2022; Aswathi et al. 2022) (Fig. 16.6d).
- **Slope:** is a factor that influences the amount of surface runoff and infiltration. It allows the identification of areas that have shown high susceptibility to flooding (Aaron and Venkatesh 2009; Fernandez and Lutz 2010; Kazakis et al. 2015; Echogdali et al. 2018a, b, 2022a, b, c, d, e; Ikirri et al. 2021; Aswathi et al. 2022). In this study, the slope factor was classified according to the model applied by Demek (1972). For the Wadi Tamlest watershed, the low slope areas are located in the downstream part, while the high slope areas were located in the mountainous parts in the north of the watershed (Fig. 16.6e).
- **Permeability:** the geology of the basin is an important factor in the study of flood phenomena because it can amplify the magnitude of floods (Echogdali et al. 2018a, b, 2022a, b, c, d, e; Ikirri et al. 2021, 2022; Aswathi et al. 2022). It includes soil type, soil texture, and parent rock. The Quaternary of the Wadi Tamlest watershed is characterized by formations that are generally permeable. Whereas the carbonate and clay formations are generally not very permeable to impermeable. The permeable formations favor the infiltration of water, therefore they have been classified by 2, because of their greater capacity of infiltration, on the contrary, the impermeable rocks have been evaluated at 10 (Kazakis et al. 2015) (Fig. 16.6f).

The thematic maps in Fig. 16.6 illustrate the spatial distribution of factor values used for floodplain mapping in the Wadi Tamlest watershed.

16.3.3 Relative Weight of Factors

The weight of each factor A was defined according to the Analytical Hierarchy Process (AHP) (Saaty 1990a, b; Ikirri et al. 2021, 2022). It is calculated after it has been ranked according to the relative importance of each factor determined from the bibliography (Saaty 1990a, b; Kazakis et al. 2015; Ikirri et al. 2021, 2022). Then, once all factors are sorted hierarchically, a pairwise comparison matrix is created. By taking the principal eigenvector of the pairwise comparison matrix between the AHP factors, this matrix is of dimension 6 × 6 and the diagonal elements are equal to 1 (Table 16.3). The pairwise comparison matrix data were taken as input for the determination of the weights of different factors. A good approximation to this result was obtained by summing the values in each column of the comparison matrix, then dividing each element of the matrix by its column total, and finally calculating the average of the elements in each column of the normalized matrix (Drobne and Lisec 2009; Razandi et al. 2015). The degree of coherence of the matrix was calculated by the coherence ratio (CR) which allows the comparison between the coherence index (CI) of the matrix against the coherence index of a random type matrix (RI). The CR defines the probability of comparison between the coherence index and the ratio index.

$$CR = \frac{CI}{RI} \tag{16.2}$$

Table 16.3 Classes of the factors and weights

Factor	Class	Rating	Weight	factor	Class	Rating	Weight
Flow accumulation (pixels)	8637–13,258	10	3.31	Density of the drainage network (m/km ²)	3.53–5.12	10	1.34
	4404–8637	8			2.73–3.53	8	
	2179–4404	6			1.96–2.73	6	
	677–2179	4			1.12–1.96	4	
	0–677	2			0–1.12	2	
Distance from the drainage network (m)	0–100	10	3.08	Slope (%)	0–11.46	10	0.71
	100–200	8			11.46–21.58	8	
	200–300	6			21.58–34.06	6	
	300–400	4			34.06–50.58	4	
	400–475	2			50.58–85.99	2	
Land use	Bare ground	6	1.08	Permeability	High permeability	10	0.49
	Vegetation	4			Medium permeability	8	
	Dwelling/controlled landfill	2			Low permeability	6	

Hence the CI represents the consistency index calculated using Eq. (16.2):

- If the value of $CR \leq 0.10$ the matrix is acceptable.
- If the value of $CR \geq 0.10$ it is necessary to revise the judgments.

$$CI = \frac{\lambda_{max} - n}{n - 1} \tag{16.3}$$

CI represents the consistency index calculated according to Eq. (16.3), which is the random index calculated from the average consistency index of a randomly generated sample of 500 pairwise comparison matrices. Where, λ_{max} represents the maximum eigenvalue of the comparison matrix and (n) the number of criteria. RI is the random index whose value depends on the number (n). The values of RI are given in Table 16.4 (Saaty 1977).

Subsequently, after normalizing the matrix (Table 16.5), the eigenvector λ_{max} of the matrix is calculated and the consistency of the set of judgments is also checked, ensuring that the AHP method suggests that the consistency ratio (CR) is less than or equal to the value of (10%) (Saaty 2012). With CI is calculated for $\lambda_{max} = 6.54$, $n = 6$ and $RI = 1.24$. So the consistency ratio is calculated as $CR = 0.08$. The value of CR is lower than the threshold (0.1), therefore the consistency of the weights is confirmed.

Table 16.4 Pair-wise comparison matrix of different factors

Factor	Flow accumulation (pixels)	Distance from the drainage network (m)	Density of the drainage network (m/km ²)	Land use	Slope (%)	Permeability
Flow accumulation (pixels)	1	2	3	3	5	4
Distance from the drainage network (m)	1/2	1	6	3	4	6
Density of the drainage network (m/km ²)	1/3	1/6	1	2	3	3
Land use	1/3	1/3	1/2	1	3	2
Slope (%)	1/5	1/4	1/3	1/3	1	3
Permeability	1/4	1/6	1/3	1/2	1/3	1

Table 16.5 Random indices were used to calculate the consistency ratio

<i>n</i>	1	2	3	4	5	6	7	8	9	10
RI	0	0	0.58	0.9	1.12	1.24	1.32	1.41	1.45	1.49

16.4 Results and Discussions

Equation 16.4 linearly combines the selected factors, taking into account the relative weights. This indicates the overlay of the thematic maps in Fig. 16.6 in a GIS environment to determine the flood risk index in the Tamlest watershed.

$$FHI = \sum_{i=6}^n (w_i * X_i) \tag{16.4}$$

$$FHI = 3.31 * (\text{Flow accumulation}) + 3.08 * (\text{Distance from hydrographic network}) + 1.34 * (\text{Drainage network density}) + 1.08 * (\text{Land use}) + 0.71 * (\text{Slope}) + 0.49 * (\text{Permeability})$$

With, W_i is the weight of factor i , X is the factor i , and n is the number of factors.

The weights used in the index calculation assess the impact of each flood-causing factor on the FHI; flow accumulation was considered the most influential factor in the FHI, followed by drainage distance, drainage network density, land use, and slope, while permeability was the least influential factor. These factors were ranked in the order of 2 to 10, where 10 indicates higher risk and 2 indicates a low risk based on the class values of the factors. The overlay of factors was performed by linearly combining the thematic maps with different weights in a GIS environment. The flood risk map is created in the end. The result of the FHI model is shown in Fig. 16.7 defining five classes of flood vulnerability. The areas with very high, high, and medium risk represent respectively 14.25%, 25.15%, and 30.44% of the total surface of the basin. While, the low and very low-risk areas constitute 15.06% and 17.10% of the basin area respectively (Tables 16.6 and 16.7).

The majority of the flooding occurred in large flood plains around the main channel of the wadi. The flood areas closest to the Tamlest River were occupied by vegetation, residential buildings, and the new landfill with massive damage to infrastructure including the road. More than 68.84% of the basin area has a very high to medium sensitivity while the 31.16% of the basin area corresponds to low to very low flood risk. The floods recorded in the years 2010 and 2014 confirmed the results of FHI, with a proportional distribution of areas affected by flooding, according to the level of risk indicated on the flood risk map. The areas located in the west of the basin, mainly composed of narrow and more or less deep river beds, proved to be more susceptible to flooding due to the accumulation of high flows, proximity to the drainage system, slope, and geology. The low susceptibility to flooding in the central and northern parts of the basin was generally attributed to the steep slope and presence of permeable

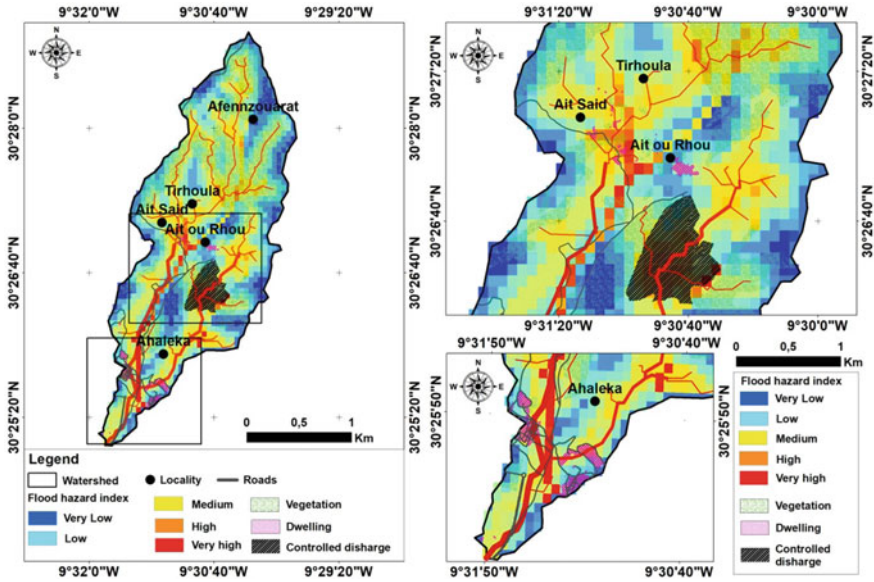


Fig. 16.7 Flood risk map obtained from the FHI

Table 16.6 Standardized flood hazard factors and factor weights

Factor	Flow accumulation (pixels)	Distance from the drainage network (m)	Density of the drainage network (m/km ²)	Land use	Slope (%)	Permeability	Weight
Flow accumulation (pixels)	0.38	0.51	0.27	0.27	0.31	0.31	3.31
Distance from the drainage network (m)	0.19	0.26	0.54	0.54	0.31	0.24	3.08
Density of the drainage network (m/km ²)	0.13	0.04	0.09	0.09	0.20	0.18	1.34
Land use	0.13	0.09	0.04	0.04	0.10	0.18	1.08
Slope (%)	0.08	0.06	0.03	0.03	0.03	0.06	0.71
Permeability	0.10	0.04	0.03	0.05	0.05	0.02	0.49

Table 16.7 Fraction of areas at risk of flooding in the watershed of Wadi Tamlest

Flood risk	Area (Km ²)	Percentage (%)
Very high	1.66	14.25
High	2.93	25.15
Medium	3.54	30.44
Low	1.75	15.06
Very low	1.99	17.10

formations. Flow accumulation and distance to the drainage network are the most influential factors for the IHF, which is consistent with a similar study by Ikirri et al. (2021, 2022). Slope and permeability are the least influential factors in the Wadi Tamlest watershed. Indeed, other factors such as the density of the hydrographic network and land use influence the concentration–time of runoff and infiltration water, which further increases the probability of flooding.

Flood control is following the planning of the fight against cures at the watershed level, including flood maintenance and flood retention, lowering the flood peak upstream of the basin; construction of dams, and reinforcement of banks. In the Wadi Tamlest watershed, gabions are structures applied upstream of the basin (Fig. 16.8a). A gabion or gabion structure is a modular retaining structure consisting of parallel-piped elements made of double-twisted steel mesh with variable galvanization, filled with a material having a specific granulometry and weight. They are permeable, resistant, and flexible structures, recently introduced in several fields. In the hydraulic field, gabions have a great capacity to adapt to ground settlements and to resist unexpected loads. They are mainly used for: the protection of banks against erosion, control of river bed movement, delimitation of the minor bed, and defense against floods. The dam is the artificial structure cut and built across the watercourse of Wadi Tamlest, to protect the urban area of Tilila and El-Houda located downstream of the basin.

The realization of this work allowed regulating the very random flow of the watercourses of the catchment area of the Tamlest wadi. It also allowed mitigating the damage caused by floods by storing the volumes of water of exceptional and sudden floods. The dyke is a raised earthen structure that delimits the two sides of a river to allow the water to rise without overflowing the bed. It is set up to divert the waters of the chaâbas and wadis; Imounsis, Oualhour, and Tamlest towards Wadi Ighzer Laarba located at Drarga. The use of the FHI (Flood Hazard Index) method and the satellite image allowed us to delimit with priority, the agglomerations such as dwellings (e.g. Tamlest and Tighoula villages) and the dump of Tamlest located in the zones with a strong risk of flooding. It is suggested that protective walls be built. Similar to the detour flood protection embankments except that they do not modify the banks and are made of aluminum (Fig. 16.8b). Floodwalls have been used to control floods that protect cities and industrial facilities around the world. And this is without causing major alterations to the landscape, combining optimal protection against the risk of flooding with maximum preservation of the physical and hydraulic characteristics of the watershed.

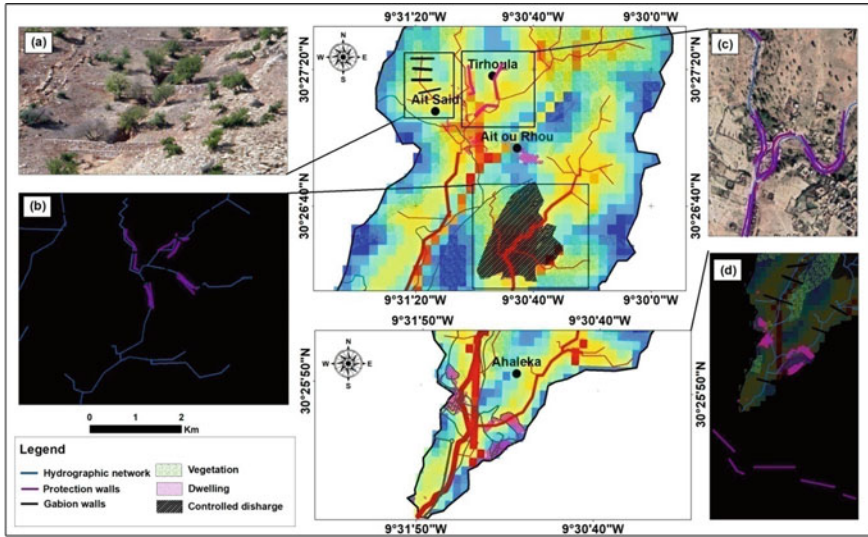


Fig. 16.8 Examples of developments applied in the Wadi Tamlest watershed; **a, b** gabion walls, and **c, d** protective walls

16.5 Conclusion

The relief of the High Atlas, the Atlantic Ocean, and the Sahara are generally the three factors that influence the semi-arid climate of the Agadir city, which is characterized by the scarcity of rainfall and sometimes extreme rainy periods, which causes floods that negatively affect the environment, the economy, and the population. The study of floods in the catchment area of Wadi Tamlest located in the northeast of the city from the mapping of flood risks by the FHI (Flood Hazard Index) method has allowed us to locate the flood-prone areas. This consists in introducing a multi-criteria index taking into account six factors (flow accumulation, distance to the drainage network, density of the drainage network, slope, permeability, and land use). The classification of these factors according to the importance of each one with the others is linked to the weight values that are calculated according to the Analytical Hierarchy Process (AHP). Overlaying, the information from these factors results in a flood risk map showing that the majority of the flooded areas are occupied generally by residential buildings, the Tamlest landfill, and agricultural fields, which pose a threat to human life and vegetation cover. To mitigate the risk of flooding, the Agadir Municipality has built a dam on Wadi Tamlest and flood protection embankments to divert the river, which is currently under construction. Despite these developments, the Wadi Tamlest still leads to flooding in the Agadir city, which is why it is necessary to consider other more effective protection systems.

Acknowledgements Our sincere gratitude is offered to the editor Dr. Vivek Gupta and an anonymous reviewer for the very useful comments and suggestions on the earlier of the manuscript. This

research was partly supported by the Department of Earth Sciences, Faculty of Sciences, Ibn Zohr University, through an ongoing internal project. No seniority of authorship is implied by the order of names; this paper is the product of a true and entirely equal collaboration. All authors have approved the final version of the manuscript. The authors are much obliged to the Springer proofreading team for handling the work, sending reviews, and preparing the proof.

References

- Aaron C, Venkatesh M (2009) Effect of topographic data, geometric configuration and modeling approach on flood inundation mapping. *J Hydrol* 377(1–2):131–142
- Aich V, Liersch S, Vetter T, Andersson J, Muller E, Hatermam F (2015) Climate or Land use? Attribution of changes in river flooding in the Sahel Zone. *Water* 7(6):2796–2820
- Ait Haddou M, Wanaim A, Ikirri M, Aydda A, Bouchriti Y, Abioui M, Kabbachi B (2022) Digital elevation model-derived morphometric indices for physical characterization of the Issen basin (Western High Atlas of Morocco). *Ecol Eng Environ Tech* 23(5):285–298
- Ali SA, Parvin F, Pham QB, Vojtek M, Vojteková J, Costache R, Linh NTT, Nguyen HQ, Ahmad A, Ghorbani MA (2020) GIS-based comparative assessment of flood susceptibility mapping using hybrid multi-criteria decision-making approach, naive Bayes tree, bivariate statistics and logistic regression: a case of Topľa basin, Slovakia. *Ecol Indic* 117:106620
- Aswathi J, Sajinkumar KS, Rajaneesh A, Oommen T, Bouali EH, Binoj Kumar RB, Rani VR, Thomas J, Thrivikramji KP, Ajin RS, Abioui M (2022) Furthering the precision of RUSLE soil erosion with PSInSAR data: an innovative model. *Geocarto Int.* <https://doi.org/10.1080/10106049.2022.2105407>
- Avagyan A, Manandyan H, Arakelyan A, Piloyan A (2018) Toward a disaster risk assessment and mapping in the virtual geographic environment of Armenia. *Nat Hazards* 92(1):283–309
- Benjmel K, Amraoui F, Aydda A, Tahiri A, Yousif M, Pradhan B, Abdelrahman K, Fnais MS, Abioui M (2022) A multidisciplinary approach for groundwater potential mapping in a fractured semi-arid terrain (Kerdous Inlier, Western Anti-Atlas, Morocco). *Water* 14(10):1553
- Bennani O, Trambly Y, Saidi MEM, Gascoïn S, Leone F (2019) Flood hazard mapping using two digital elevation models: Application in a Semi-Arid environment of Morocco. *Eur Sci J* 15(33):338–359
- Campion BB, Venzke JF (2013) Rainfall variability, floods and adaptations of the urban poor to flooding in Kumasi, Ghana. *Nat Hazards* 65(3):1895–1911
- Cobbinah PB, Anane GK (2015) Climate change adaptation in rural Ghana: indigenous perceptions and strategies. *Clim Dev* 8(2):169–178
- Crippen JR, Bue CD (1977) Maximum flood flows in the conterminous United States. US Geol Surv Water Supply Pap 1887, United States Government Printing Office, Washington, DC
- Demek J (1972) Manual of detailed geomorphological mapping. Academia, Prague
- Drobne S, Liseč A (2009) Multi-attribute decision analysis in GIS: weighted linear combination and ordered weighted averaging. *Informatica* 33(4):459–474
- Dubreuil P (1974) Initiation à l'analyse hydrologique. ORSTOM, Paris
- Echogdali FZ, Boutaleb S, Jauregui J, Elmouden A (2018a) Cartography of flooding hazard in semi-arid climate: the case of Tata valley (South-East of Morocco). *J Geograph Nat Disasters* 8(1):1–11
- Echogdali FZ, Boutaleb S, Elmouden A, Ouchchen M (2018b) Assessing flood hazard at river basin scale: comparison between HECRAS-WMS and flood hazard index (FHI) methods applied to El Maleh basin, Morocco. *J Water Resour Prot* 10(9):957–977
- Echogdali FZ, Kpan RB, Ouchchen M, Id-Belqas M, Dadi B, Ikirri M, Abioui M, Boutaleb S (2022a) Spatial Prediction of flood frequency analysis in a semi-arid zone: a case study from the Seyad Basin (Guelmim Region, Morocco). In: Rai PK, Mishra VN, Singh P (eds) *Geospatial*

- technology for landscape and environmental management: sustainable assessment and planning. Springer, Singapore, pp 49–71
- Echogdali FZ, Boutaleb S, Taia S, Ouchchen M, Id-Belqas M, Kpan RB, Abioui M, Aswathi J, Sajinkumar KS (2022b) Assessment of soil erosion risk in a semi-arid climate watershed using SWAT model: case of Tata basin, South-East of Morocco. *Appl Water Sci* 12(6):137
- Echogdali FZ, Boutaleb S, Bendarma A, Saidi ME, Aadraoui M, Abioui M, Ouchchen M, Abdelrahman K, Fnais MS, Sajinkumar KS (2022c) Application of analytical hierarchy process and geophysical method for groundwater potential mapping in the Tata basin, Morocco. *Water* 14(15):2393
- Echogdali FZ, Boutaleb S, Kpan RB, Ouchchen M, Bendarma A, El Ayady H, Abdelrahman K, Fnais MS, Sajinkumar KS, Abioui M (2022d) Application of fuzzy logic and fractal modeling approach for groundwater potential mapping in semi-arid Akka basin, Southeast Morocco. *Sustainability* 14(16):10205
- Echogdali FZ, Boutaleb S, Kpan RB, Ouchchen M, Id-Belqas M, Dadi B, Ikkiri M, Abioui M (2022e) Spatialization of flood hazard using flood hazard index method and hydrodynamic modeling tools in a semi-arid environment: a case study of Seyad basin, south of Morocco. *J Afr Earth Sci* 196:104709
- El Alaoui El Fels A, Saidi MEM (2014) Simulation et spatialisation du risque d'inondation dans une vallée anthropisée. Le cas de la vallée de l'Ourika (Haut Atlas, Maroc). *Eur Sci J* 10(17):210–223
- El Morjani ZEA, Saif Ennasr M, Elmouden A, Idbraim S, Bouaakaz B, Saad A (2016) Flood hazard mapping and modeling using GIS applied to the Souss river watershed. In: Choukr-Allah R, Ragab R, Bouchaou L, Barceló D (eds) *The Souss-Massa River Basin, Morocco*. Springer, Cham, pp 57–93
- Elkhrachy I (2015) Flash flood hazard mapping using satellite images and GIS tools: a case study of Najran City, Kingdom of Saudi Arabia (KSA). *Egypt J Remote Sens Space Sci* 18(2):261–278
- El Alaoui El Fels A, Alaa N, Bachnou A, Rachidi S (2018) Flood frequency analysis and generation of flood hazard indicator maps in a semi-arid environment, case of Ourika Watershed (Western High Atlas Morocco). *J Afr Earth Sci* 141:94–106
- Feng X, Porporato A, Rodriguez- Iturbe I (2013) Changes in rainfall seasonality in the tropics. *Nature Clim Change* 3(9):811–815
- Fernandez DS, Lutz MA (2010) Urban flood hazard zoning in Tucumán Province, Argentina, using GIS and multicriteria decision analysis. *Eng Geol* 111(1–4):90–98
- Franci F, Bitelli G, Mandanici E, Hadjimitsis D, Agapiou A (2016) Satellite remote sensing and GIS-based multi-criteria analysis for flood hazard mapping. *Nat Hazards* 83(1):31–51
- Francou J, Rodier J (1967) *Essai de classification des crues maximales observées dans le monde*. Cah ORSTOM Ser Hydrol 4(3):19–46
- Gao YQ, Liu YP, Lu XH, Luo H, Liu Y (2020) Change of stream network connectivity and its impact on flood control. *Water Sci Eng* 13(4):253–264
- Giandotti M (1934) Previsione delle piene e delle magre dei corsi d'acqua. *Ist Poligr Dello Stato* 8:107–117
- Haan CT, Barfield BJ, Hayes JC (1994) *Design hydrology and sedimentology for small catchments*. Academic Press, San Diego
- Hallegratte S, Hourcade JC, Dumas P (2007) Why economic dynamics matter in assessing climate change damages: illustration on extreme events. *Ecol Econ* 62(2):330–340
- Hanson CE, Palutikof JP, Livermore MTJ, Barring L, Bindi M, Corte-Real J, Ulbrich U (2007) Modelling the impact of climate extremes: an overview of the MICE project. *Clim Change* 81(1):163–177
- Herschey RW (2002) The world's maximum observed floods. *Flow Meas Instrum* 13(5–6):231–235
- Hulme M, Doherty R, Ngara T, New M, Lister D (2001) African climate change: 1900–2100. *Climat Res* 17(2):145–168
- Ikkiri M, Faik F, Boutaleb S, Echogdali FZ, Abioui M, Al-Ansari N (2021) Application of HEC-RAS/WMS and FHI models for extreme hydrological events under climate change in the Ifni

- River arid watershed from Morocco. In: Nistor MM (ed) *Climate and land use impacts on natural and artificial systems: mitigation and adaptation*. Elsevier, Amsterdam, pp 251–270
- Ikirri M, Faik F, Echogdali FZ, Antunes IMHR, Abioui M, Abdelrahman K, Fnais MS, Wanaim A, Id-Belqas M, Boutaleb S, Sajinkumar KS, Quesada-Román A (2022) Flood hazard index application in arid catchments: case of the Taguenit Wadi watershed, Lakhssas, Morocco. *Land* 11(8): 1178
- Jenkinson AF (1955) The frequency distribution of the annual maximum (or minimum) values of meteorological elements. *QJR Meteorol Soc* 81(348):158–171
- Jenks GF (1967) The data model concept in statistical mapping. *Int Yearb Cartograph* 7:186–190
- Jongman B, Kreibich H, Apel H, Barredo JI, Bates PD, Feyen L, Gericke A, Neal J, Aerts JCJH, Ward PJ (2012) Comparative flood damage model assessment: towards a European approach. *Nat Hazards Earth Syst Sci* 12(12):3733–3752
- Jonkman SN, Bočkarjova M, Kok M, Bernardini P (2008) Integrated hydrodynamic and economic modelling of flood damage in the Netherlands. *Ecol Econ* 66(1):77–90
- Kabenge M, Elaru J, Wang H, Li F (2017) Characterizing flood hazard risk in data-scarce areas, using a remote sensing and GIS-based flood hazard index. *Nat Hazards* 89(3):1369–1387
- Kazakis N, Kougiass I, Patsialis T (2015) Assessment of flood hazard areas at a regional scale using an index based approach and analytical hierarchy process: application in Rhodope-Evros Region, Greece. *Sci Total Environ* 538:555–563
- Kirpich ZP (1940) Time of concentration of small agricultural watersheds. *Civ Eng* 10(6):362–365
- Kundzewicz ZW (2003) Extreme precipitation and floods in the changing world. *IAHS Publ* 280:32–39
- Kundzewicz ZW, Menzel L (2003) Flood risk and vulnerability in the changing world. In: *International Conference Towards natural flood reduction strategies*, Warsaw (Abstract Book)
- Lu C, Zhou J, He Z, Yuan S (2018) Evaluating typical flood risks in Yangtze River Economic Belt: application of a flood risk mapping framework. *Nat Hazards* 94(3):1187–1210
- Mendez M, Calvo-Valverde L (2016) Development of the HBV-TEC hydrological model. *Procedia Eng* 154:1116–1123
- Merz B, Thielen AH (2009) Flood risk curves and uncertainty bounds. *Nat Hazards* 51(3):437–458
- Patrikaki O, Kazakis N, Kougiass I, Patsialis T, Theodossiou N, Voudouris K (2018) Assessing flood hazard at river basin scale with an index-based approach: the case of Mouriki, Greece. *Geosciences* 8(2):50
- Pulvirenti L, Chini M, Pierdicca N, Guerriero L, Ferrazzoli P (2011) Flood monitoring using multi-temporal COSMO-SkyMed data: image segmentation and signature interpretation. *Rem Sens Environ* 115(4):990–1002
- Rahmati O, Zeinivand H, Besharat M (2016) Flood hazard zoning in Yasooj region, Iran, using GIS and multi-criteria decision analysis. *Geomat Nat Hazards Risk* 7(3):1000–1017
- Razandi Y, Pourghasemi HR, Neisani NS, Rahmati O (2015) Application of analytical hierarchy process, frequency ratio, and certainty factor models for groundwater potential mapping using GIS. *Earth Sci Inform* 8(4):867–883
- Roche M (1986) *Dictionnaire français d'hydrologie de surface*. Masson, Paris
- Roche C (1963) *Hydrologie de surface*. Gauthier-Villars, Paris
- Saad A, Milewski A, Benaabidate L, El Morjani ZEA, Bouchaou L (2019) Flood frequency analysis and urban Flood modelling of Sidi Ifni basin, Southern Morocco. In: *The International archives of the photogrammetry, remote sensing and spatial information sciences, XLII-4/W19, PhilGEOSS x GeoAdvances 2019*, Manila, Philippines, 14–15 November
- Saaty TL (2012) *Decision making for leaders: the analytics hierarchy process for decisions in a complex world*, 3rd edn. RWS Publications, Pittsburgh
- Saaty TL (1990a) How to make a decision: the analytic hierarchy process. *Eur J Oper Res* 48(1):9–26
- Saaty TL (1990b) An exposition of the AHP in reply to the paper remarks on the analytic hierarchy process. *Manage Sci* 36(3):259–268
- Saaty TL (1977) A scaling method for priorities in hierarchical structures. *J Math Psychol* 15(3):234–281

- Saidi MEM, Daoudi L, Aresmouk MEH, Fniguire F, Boukrim S (2010) Les crues de l'oued Ourika (Haut Atlas, Maroc): Événements extrêmes en contexte montagnard semi-aride. *Comun Geol* 97(1):113–128
- Strahler AN (1957) Quantitative analysis of watershed geomorphology. *Tans Am Geophys Union* 38(6):920–931
- Sun Y, Wendi D, Kim DE, Liang SY (2016) Development and application of an integrated hydrological model for Singapore freshwater swamp forest. *Procedia Eng* 154:1002–1009
- Talha S, Maanan M, Atika H, Rhinane H (2019) Prediction of flash flood susceptibility using fuzzy analytical hierarchy process (FAHP) algorithms and GIS: a study case of Guelmim region in southwestern of Morocco. In: *The international archives of the photogrammetry, remote sensing and spatial information sciences, XLII-4/W19, PhilGEOS x GeoAdvances 2019, Manila, Philippines, 14–15 November*
- Wang K, Wang Z, Liu K, Cheng L, Bai Y, Jin G (2021) Optimizing flood diversion siting and its control strategy of detention basins: a case study of the Yangtze River, China. *J Hydrol* 597:126201
- Weng Q (2001) Modeling urban growth effects on surface runoff with the integration of remote sensing and GIS. *Environ Manage* 28(6):737–748
- Wongsa S (2014) Simulation of Thailand flood (2011). *Int J Eng Technol* 6(6):452–458
- Yoo C, Cho E, Na W, Kang M, Lee M (2021) Change of rainfall-runoff processes in urban areas due to high-rise buildings. *J Hydrol* 597:126–155

Chapter 17

Flood Assessment Along Lower Niger River Using Google Earth Engine



Adeyemi O. Olusola, Oluwatola Adedeji, Lawrence Akpoterai, Samuel T. Ogunjo, Christiana F. Olusegun, and Samuel Adelabu

Abstract The Niger basin plays a critical role in the achievement of Nigeria’s agricultural targets through irrigation, dry season farming, and fish habitats. The seasonality of the river discharge along the lower Niger River creates the possibility of two extremes—drought and flood. The risk of flood has not been adequately monitored on the continent. In this study, the possibility of remotely sensing flood incidences along the lower Niger River was considered. Sentinel-1 imagery was incorporated within the Google Earth Engine infrastructure to map the region before and after the flood event of 20th September 2020 using a change detection approach. This is done by dividing the after-flood mosaic by the before-flood mosaic, resulting in a raster layer showing the degree of change per pixel. The impact of the flood event on the human and socio-economic livelihoods within the region was also evaluated. The flood event was found to affect about 108,587 people, 9,123 ha of cropland, and 2,056 ha of the urban area. The possibility of assessing flood extent, risk, and impact using remotely sensed data will help in humanitarian services, disaster planning and mitigation, and environmental evaluation for policy formulation.

A. O. Olusola (✉)

Faculty of Environmental and Urban Change, York University, 4700 Keele Street, Toronto M3J 1P3, Canada

e-mail: olusolaadeyemi.ao@gmail.com

A. O. Olusola · S. Adelabu

Department of Geography, University of the Free State, Bloemfontein, South Africa

L. Akpoterai

Department of Geography, University of Ibadan, Ibadan, Nigeria

O. Adedeji

Crop Ecophysiology and Precision Agriculture Laboratory, Texas Tech University, Lubbock, TX, USA

S. T. Ogunjo

Department of Physics, Federal University of Technology, Akure, Ondo, Nigeria

C. F. Olusegun

Faculty of Physics, Institute of Geophysics, University of Warsaw ul, 02-093 Pasteura 5, Warszawa, Poland

Keywords Google Earth Engine · SAR · Niger-Benue Confluence · Nigeria · Flood

17.1 Introduction

Natural disasters are catastrophic events, with atmospheric, geological, and hydrological origins, that can cause fatalities, property damage and social environmental disruption (Sivakumar 2005; Israel and Briones 2012; Adedeji et al. 2021; Orimoloye et al. 2021a, b). Examples of these disasters include droughts, floods, earthquakes, hurricanes, landslides. These disasters continue to occur with increasing impacts and oftentimes lead to loss and damages of properties and livelihoods at a local or global scale (Loayza et al. 2009). These disasters often affect agriculture; production cycles are disturbed, plants and livestock are lost, agricultural facilities and infrastructures are damaged, and workers lose their means of livelihood (Sivakumar 2005; Adedeji et al. 2021). This, therefore, affects food security (FAO 2002) and may impede overall economic growth, especially where agriculture accounts for a large share of gross domestic product and employment. There are several types of these disasters that affect agriculture; however, this study examines floods, since agriculture depends largely on water availability.

A flood, an overflow of water that submerges land, can be defined as any relatively high water flow that overtops the natural or artificial banks in any portion of a river or stream (Adedeji et al. 2021). Floods have a serious impact on agriculture and food production. Floods are water-related natural disasters that affect a wide range of environmental factors and activities related to agriculture, vegetation, human and wildlife, local and regional economies (Jeyaseelan 2003). Agriculture is the largest consumer of water and, therefore, the most sensitive to flooding hence the impact of flood most often than not results in extensive loss not only in terms of loss and damages in currency but emotional well-being of the farmer. Boyle et al. (1998) classified flood damages into tangible and intangible. Tangible damages are associated with direct contact with the floodwater, whereas the latter does not involve contact but results as an effect of flood occurrence. For instance, the occurrence of a flood disaster could lead to an epidemic that destroys crops and livestock. In this case, the impact is intangible/indirect, unlike when floodwater erodes soils, damages crops, and displaces or kills livestock. All these however impacts the agricultural economy.

Climate change is closely associated with the increase in magnitude and frequency of floods (IPCC 2014; Adedeji et al. 2021). There is a direct influence of global warming on changes in precipitation and heavy rains (Min et al. 2011). With increased rainfall amount, intensity, and frequency, flooding occurs (Adeola et al. 2021). Since more precipitation occurs as rain there is increased runoff and risk of flooding in early spring, especially over continental areas (Adeola et al. 2021). This is common in all parts of the world, as well as in Africa. Africa which is located in the tropics receives intense temperature and consequently rainfall effects, and this is further intensified by climate change, making the region very prone to flood events. However, one of

the limiting factors to adequate monitoring of precipitation in Africa is the large inequality in the density of weather stations across space. As a result, there are areas where climate information from ground data is still not available. In essence, there is the need to use available sources with better coverage though compromising for in-situ observations. One of such available sources is the use of remote sensing technology.

Remote sensing techniques make it possible to obtain and distribute information rapidly over large areas using sensors operating in several spectral bands, mounted on aircraft or satellites (Jeyaseelan 2003; Adedeji et al. 2021) or flown as aerial vehicles. The digital image acquired by these platforms overcomes several of the challenges related to traditional in-situ observations. Advancements in remote sensing technology helps in real-time monitoring, early warning, and quick damage assessment of flood disasters (Dhakal et al. 2002; Jeyaseelan 2003; Adedeji et al. 2021). With remote sensing techniques, landscape descriptive information proves to be useful before, during and after disasters, for prevention, detection and mapping, and impact assessments, respectively. Development in remote sensing techniques has evolved from optical to radar remote sensing, this transition has provided all-weather capability, a unique breakthrough for tropical countries with cloud constraints on optical sensors (Adedeji et al. 2021).

At the early stages of satellite remote sensing, optical sensors were used as the primary tool for obtaining remotely sensed data. Data available were obtained from Landsat Multispectral Scanner (MSS), Thematic Mapper (TM), Enhanced Thematic Mapper (ETM), SPOT, AVHRR, among others, with improvement in satellite imagery resolution. Flood impact assessment, using remote sensing, dates back to the 1970s, with the use of MSS data. MSS data were used for flood impact assessment and mitigation in the United States–Iowa, Arizona, Mississippi basin, among others (Hallberg et al. 1973; Morrison et al. 1973; Deutsch and Ruggles 1974; Rango et al. 1974).

In flood studies, MSS band 7 (0.8–1.1 μm) has been found particularly suitable for distinguishing water or moist soil from a dry surface due to strong absorption of water in the near-infrared range of the spectrum (Smith 1997). This is the same for Landsat TM band 4, but the Landsat TM NIR band cannot be used optimally in developed land use areas such as downtown commercial or industrial areas. The main reason is that the NIR band reflects very little energy from asphalt areas, appearing black in the imageries. Therefore makes it easy to confuse developed areas with water. Wang et al. (2002) successfully solved this problem by adding Landsat TM band 7 to the NIR (band 4) band to delineate the inundated areas. In TM band 7 (2.08–2.35 μm) images the reflectance from water, paved road surfaces, and rooftops differ significantly and therefore in the Band4 + Band7 image, it becomes easier to choose the density slice for extracting the floodwater. But in some cases, a simple density slice or supervised classification is not enough to identify the inundated area accurately. It involves the use of further indices. In addition, high and medium spatial resolution satellite images like NOAA-AVHRR, and SPOT-HRV are used to produce different kinds of flood-related thematic information, depending on the data acquisition time (Tholey et al. 1997). The application of remote sensing and GIS has proven to be

very efficient and cost-effective in flood impact assessment and management. The use of very high-resolution imageries like IKONOS or SPOT 5 has not been very popular yet in the field of flood management due to its high price, but it is likely that these imageries would be available at a reasonable price and would be widely used for flood mapping (Sanyal and Lu 2004). However, AVHRR, which is available at both low prices and less technical requirements, is effective and good for developing countries (Sheng et al. 2001). The six-hour revisit capability of NOAA satellites has been of utmost advantage for flood assessment, and potential use for monitoring.

The single most important constraint to flood monitoring is the obstruction caused by cloud covers (Melack et al. 1994; Adedeji et al. 2021) and this is observed with the use of optical sensors. This problem was solved with the development of microwave remote sensing which can penetrate cloud covers. One of these microwave remote sensing approaches used in flood assessment is the Synthetic Aperture Radar (SAR) imagery (Chen et al. 1999; Adedeji et al. 2021). SAR imagery can show a sharp distinction between water and land, making it easy to identify flooding activities. Although there is a clear distinction between land and water using SAR imagery, rough water surface appears in a brighter tone in the SAR imageries than the calm water (Yang et al. 1999), hence making it difficult to accurately determine areas of turbulent flooding. Also, forest covers create obstructions to accurately identify inundated areas from a SAR image (Hess et al. 1990). The use of Radar in flood monitoring and forecast has been growing in the literature (Giustarini et al. 2015; Landuyt et al. 2018; Huang and Jin 2020; Amitrano et al. 2020). This stems from the peculiarity of Radar images and the properties of water (see Adedeji et al. 2021). As pointed out by Adedeji et al. (2021), smooth surfaces are specular reflectors, hence they appear dark on a Radar image. With the advent of cloud computing platforms such as Amazon Web Services and Google Earth Engine, accelerated computations over large coverage are becoming a possibility. Google Earth Engine (GEE) combines a multi-petabyte catalog of satellite imagery and geospatial datasets with planetary-scale analysis capabilities. Even though GEE is open source and archives several hundreds of datasets such as but not limited to Landsat, Sentinel and MODIS, very few studies have been able to leverage this platform in the assessment and monitoring of flood events (Fig. 17.1). Hence, this study aims to assess the September 2020 flood events along the Lower Niger in Nigeria using Google Earth Engine and Sentinel-1 imagery.

The choice of use regarding available Radar images (Sentinel-1 especially) on GEE for flood monitoring has been few and far in-between (Fig. 17.2) and collaborations across countries, institutions and academics have been very poor even though microwave remote sensing has widely demonstrated its potential in the continuous monitoring of our rapidly changing planet (Amitrano et al. 2021).

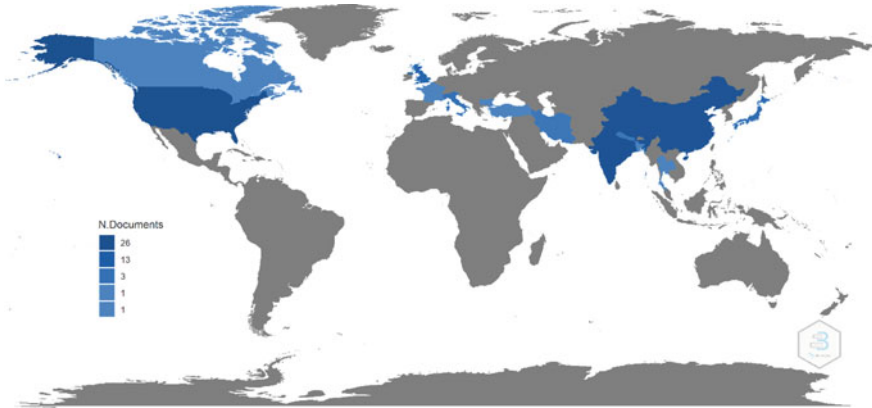


Fig. 17.1 Overview of flood studies indexed in Scopus (www.scopus.com) from 2017–2021 across countries using Google Earth Engine and Radar

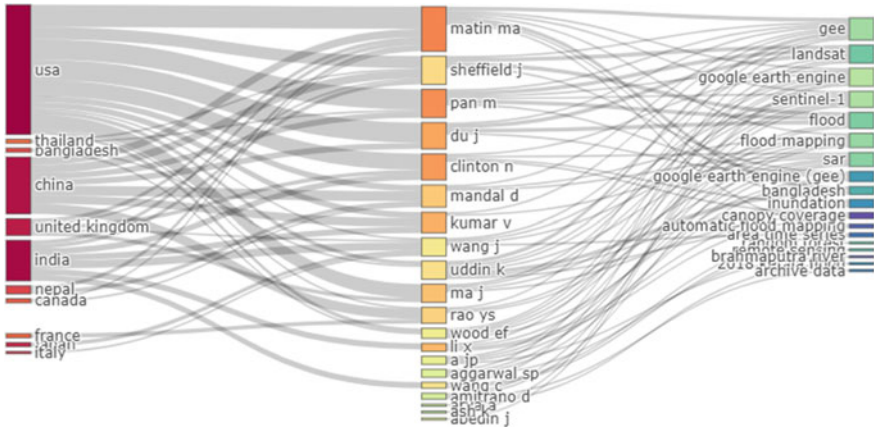


Fig. 17.2 Three-field plot showing available studies on flood using SAR on GEE

17.2 Study Area

The Niger River is the main river draining West Africa. It is the third-longest river in Africa. Along several sections, the river is dammed for various reasons such as but not limited to irrigation, hydroelectricity and water supply. As a result of these, the regime of the river is greatly impaired and its hydrology is very unique. The entire stretch of the river has been divided into several sections for easy identification and political reasons. The Niger River extends about 4,180 km with a drainage area of 2,117,700 km². Its source is in the Guinea Highlands in southeastern Guinea near the Sierra Leone border. It runs in a crescent through Mali, Niger, on the border with Benin and then through Nigeria, discharging through a massive delta, known



Fig. 17.3 Study area map showing the river stretch in blue between Idah and Onitsha. *Source* Google Earth Engine

as the Niger Delta, into the Gulf of Guinea in the Atlantic Ocean. For this study, the lower stretch of the river between Idah and Onitsha, shortly before it forms a delta, forms the study area (Fig. 17.3). This stretch is very dynamic, contains so much flow within its channel and is influenced by the regime of River Benue, Kainji Dam and the release of water from the Lagdo Dam. Lagdo Dam is a reservoir located in the Northern Province of Cameroon and covers an area of 586 km². The influence of water release from Lagdo Dam has been documented as one of the reasons for flood events along this stretch in Nigeria.

17.3 Methodology

The flood extent for the study area (Fig. 17.3) was created using a change detection approach on Sentinel-1 (SAR) data. To assess the number of potentially exposed people, affected cropland and urban areas, additional datasets were employed. Flood extent mapping and its socioeconomic impact was carried out in Google Earth Engine by adapting the process provided by UN Spider (<https://un-spider.org/advisory-support/recommended-practices/recommended-practice-google-earth-engine-flood-mapping/step-by-step>).

17.3.1 Data Sources

For this study, secondary datasets were used. These include Sentinel-1, Level-1, Ground Range Detected (GRD). The imagery is preprocessed and has undergone the apply-orbit-file (updates orbit metadata); Analysis-Ready-Data (ARD) border noise removal; Thermal noise removal; radiometric calibration (computes backscatter intensity using sensor calibration parameters); terrain-correction (orthorectification) and conversion of the backscatter coefficient (σ°) into decibels (dB). In addition, the European Commission's Joint Research Centre (JRC) Global Surface Water Dataset, the JRC Global Human Settlement Population Layer and the MODIS Land Cover Type Product were all combined to estimate the impact of the flood event from the Sentinel-1 on human and socio-economic livelihoods (Fig. 17.4).

17.3.2 Data Analysis

The Sentinel-1 GRD archive, called ImageCollection in Google Earth Engine, is filtered-clipped to the boundaries of Lower Niger (Fig. 17.2). The filtered ImageCollection is then reduced to the selected periods (before and after the flood event). This script in GEE uses a simple, straight-forward change detection approach, where the after-flood mosaic is divided by the before-flood mosaic, resulting in a raster layer showing the degree of change per pixel. High values (bright pixels) indicate high change, low values (dark pixels) point toward little change. To compute the area of the flood extent, a new raster layer is created calculating the area in m^2 for each pixel, taking the projection into account. By summing up all pixels, the area information is derived and converted into hectares. To estimate the number of exposed people, the code uses the JRC Global Human Settlement Population Layer. It contains information on the number of people living in each cell. To intersect the flood layer with the population layer, the flood extent raster first needs to be reprojected to the resolution and projection of the population dataset (Fig. 17.4). To estimate the amount of affected cropland, the MODIS Land Cover Type product was chosen. The dataset has a spatial resolution of 500 m and is updated yearly. It is the only global dataset on Land Cover currently available in Google Earth Engine. The Land Cover Type 1 band consists of 17 classes with two cropland classes (Fig. 17.3). Affected urban areas are calculated the same way as the previous two steps, using the MODIS Land Cover Type dataset (Fig. 17.4). The link to the code is provided here: <https://code.earthengine.google.com/f5c2f984c053c8ea574bfcd4040d084e>.

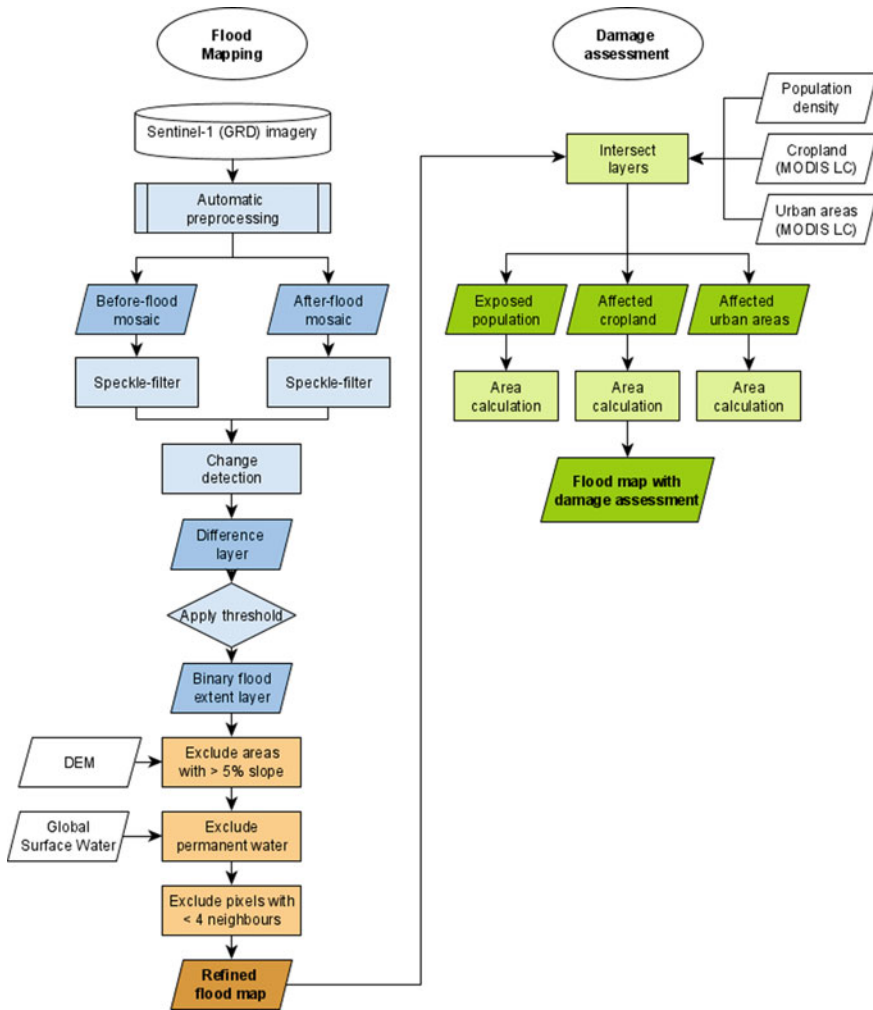


Fig. 17.4 Workflow of GEE performing flood monitoring before and after a flood event

17.4 Results

Flood events, as presented in this study, leverages the use of remote sensing for rapid and efficient means to capture their extent and impact (e.g. Amitano et al. 2020; Orimoloye et al. 2021a, b; Avand et al. 2021; Adedeji et al. 2021; De et al. 2022; Zhang et al. 2022). Sentinel-1, SAR, has the potential for the continuous monitoring of hazards, especially in the light of the changing climate (Amitrano et al. 2020). In addition, the use of synthetic aperture radar (SAR) sensors is a crucial value-added in the mapping of flooding due to their all-weather and all-time imaging characteristics,

ensuring the availability of the acquisition independently of illumination and weather conditions (Amitrano et al. 2018). Figure 17.5 shows before and after the flood event. The backscatter effect is seen as the difference between the two images. A flat water surface acts as a specular reflector which scatters the radar energy away from the sensor. This causes relatively dark pixels in radar data which contrast with non-water areas (Figure 17.5). The flood extent is seen in the image with the yellow circle. The entire flood extent is about 35,987 ha (Fig. 17.6).

Based on the JRC Global Human Settlement Population Layers and the MODIS Land Cover Type, about a hundred and eight thousand five hundred and eighty-seven (108,587) people were exposed, nine thousand one hundred and twenty-three (9123) ha of cropland wasted and two thousand and sixty-five hectares of the urban

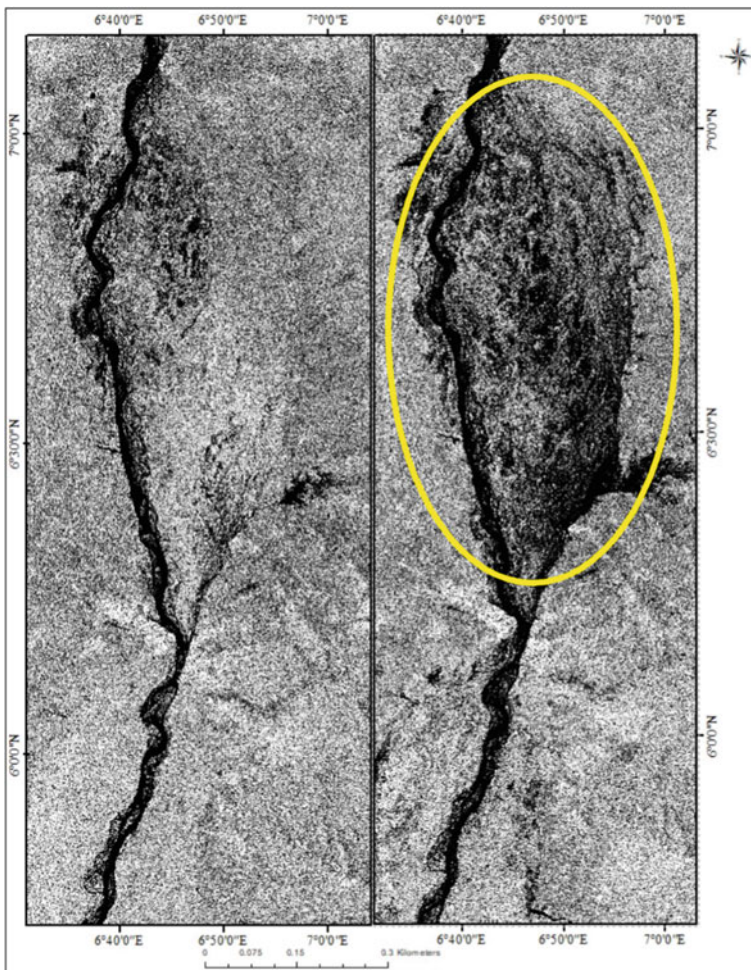


Fig. 17.5 Sentinel-1 showing before and after flood event along Lower Niger in Nigeria

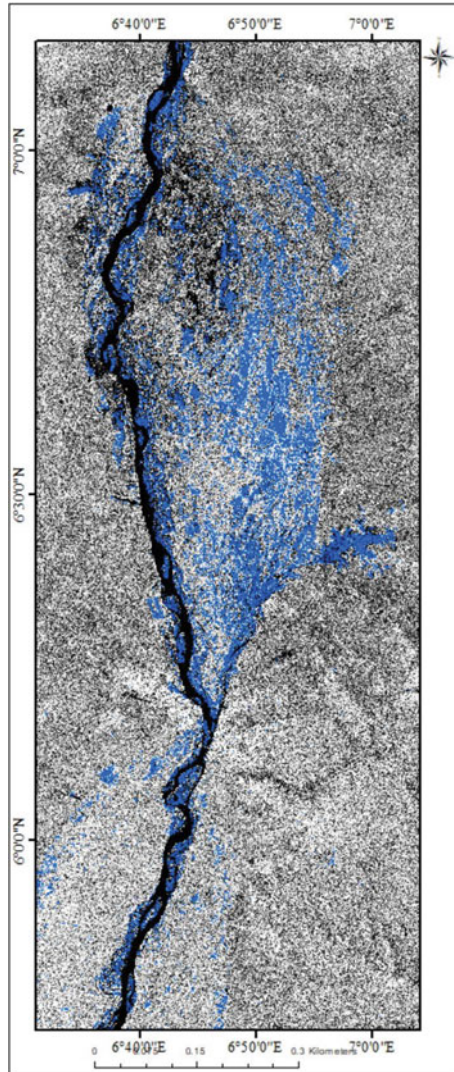


Fig. 17.6 Flood extent showing inundated buildings on Sentinel-1

area inundated as a result of this singular flood event (Fig. 17.6). The impact of this isolated event on the socio-economic livelihood and mental health of the people lasts longer. Hence, the direct and indirect cost of flood disasters becomes priceless. Despite the computing skill required, the availability of Sentinel-1, open-source data, and the unrestricted use of GEE has paved the way for effective and efficient assessment of flood events. Synthetic Aperture Radar (SAR) data are currently the most reliable resource for flood assessments, though still subject to various uncertainties,

which can be objectively represented with probabilistic flood maps. Moreover, the growing number of SAR satellites, especially Sentinel-1 has increased the likelihood of observing a flood event from space through at least a single SAR image. This is set to help middle and low-income countries in establishing flood monitoring networks using open-source data and free-to-use cloud computing platforms such as GEE.

17.5 Discussion

The occurrence of floods across different parts of the world has severe implications on agricultural production and some other sectors of the economy. With the changing climate and occurrence of weather extremes, leading to recurrent flood cases, it is of utmost importance to understand how to effectively monitor and assess these natural disasters. Flood monitoring and assessment would help address food security, implement climate-adaptive agriculture, and avoid agricultural revenue loss (Adedeji et al. 2020, 2021). As shown in this study and some others, the use of Radar has proven to be effective in assessing flood impact (Ekeu-wei et al. 2018; Ganji et al. 2019; Ekeu-wei et al. 2020; Adedeji et al. 2021; Uddin and Matin 2021). Ekeu-wei et al. (2018) in their study on the applications of open-access remotely sensed data for flood modelling and mapping in developing regions highlighted the importance of open access remotely sensed data and the effectiveness of Radar data in flood modelling and mapping to support flood management strategies along Lower Niger section in Nigeria. Furthermore, in another study, Uddin and Matin (2021) using bi-temporal Sentinel-1 Synthetic Aperture Radar (SAR) images acquired before and on the day of the flood event indicated that 95.16% of the actual flooded areas were classified as very high and high flood hazard classes, demonstrating the high potential SAR for flood hazard mapping. The usage of Synthetic Aperture Radar (SAR) satellite imagery for flood extent mapping constitutes a viable solution with fast image processing, providing near real-time flood information to relief agencies for supporting humanitarian action. The high data reliability as well as the absence of geographical constraints, such as site accessibility, emphasize the technology's potential in the field (<https://un-spider.org/advisory-support/recommended-practices/recommended-practice-flood-mapping>). To support this claim by UN-SPIDER, Adedeji et al. (2021) affirmed that Synthetic Aperture Radar (SAR) images had high potentiality for flood analysis. These studies and many more have shown the possibilities in the use of Synthetic Aperture Radar in flood monitoring. This use of SAR has increased in recent years with the availability of Sentinel-1 due to its free-to-use and revisit time. As pointed out by Uddin and Matin (2021) the last few decades have seen an increase in the frequency, intensity, and duration of floods mapping and monitoring. This is partly due to SAR availability and cloud computing platforms such as GEE (Olusola and Adelabu 2021). GEE allows for replicability and easy sharing of codes for manipulation and rapid monitoring.

GRD as used in this study is raising more and more interest among users due to its reduced computational demand for information extraction and availability on cloud

exploitation platforms, like the Google Earth Engine (Amitrano et al. 2019). Tiwari et al (2020) in their study on flood inundation mapping concluded that observations from Sentinel-1 SAR data using the Otsu algorithm in GEE can act as a powerful tool for mapping flood inundation areas at the time of the disaster, and enhance existing efforts towards saving lives and livelihoods of communities and safeguarding infrastructure and businesses. Mudi and Das (2022) in their study on flood hazard mapping in Assam posited that the GEE platform requires lesser data processing capabilities and less time than other traditional approaches. The authors concluded that the choice of using GEE and Sentinel-1 SAR data ensures rapid flood assessment and enables real-time mapping, which is particularly important for the decision-makers to develop flood controlling measures, mitigation, relief, and rescue planning. In essence, rapid mapping of flood and risk assessment especially across scales is a possibility due to the emergence of cloud computing platforms such as GEE accessibility of short-revisit Sentinel-1A radar data (Devrani et al. 2021). A similar position by Ruiz-Ramos et al. (2020) where the authors concluded that using Sentinel-1 time series data and the Google Earth Engine (GEE) platform, we were able to map temporal open water and temporal flooded vegetation areas were mapped in a continuous and near-real-time basis. They posited that the outcomes derived from their study significantly contribute to identifying the hydrological mechanisms of the region of study while providing essential and valuable information for rapid response and environmental impact assessment.

As against optical sensors such as Landsat TM, ETM, AVHRR, MODIS, and their challenges such as but are not limited to their coarse nature, long revisit interval, weather bias, and spatial coverage, the use of SAR especially Sentinel-1 offers greater possibilities and better opportunities. The advantages of optical data include its wide availability, long historical data, ease of access, and low-cost rate. Hence, hybrid studies using a fusion of both optical and microwave sensing could provide better accuracy, especially when combined with deep learning techniques.

17.6 Conclusion

More complex studies on flood impact assessments have employed integrated models which combine optical and radar sensors, with volunteered geographical data, ground data, machine learning functions, and/or artificial intelligence to eliminate the individual challenge posed by each method. The results obtained from such studies have been more accurate and precise. An improved remote sensing flood assessment technique in the generation of flood hazard maps, fusing remote sensing and volunteered geographical data, using machine learning carried out cloud computing platforms are research frontiers, especially in data scarce regions.

With improvement in remotely sensed data and advancements in techniques of analysis, the occurrence of these disasters, through detailed empirical studies, can be planned for, and its effects on the agricultural economy mitigated. This will aid the development of well-informed policy decisions concerning agricultural land use

and production. Developing countries, which often bear the brunt of these impacts, can as well adopt low-cost technology and simple data requirement models to also contribute efforts to the effective management of these disasters.

References

- Adedeji O, Olusola A, Babamaaji R, Adelabu S (2021) An assessment of flood event along lower Niger using Sentinel-1 imagery. *Environ Monit Assess* 193(12):1–17
- Adedeji O, Olusola A, James G, Shaba HA, Orimoloye IR, Singh SK, Adelabu S (2020) Early warning systems development for agricultural drought assessment in Nigeria. *Environ Monit Assess* 192(12):1–21
- Adeola OA, Adeyemi O, Onyemaenu V (2021). Rainfall–runoff in conterminous tropical river basins of Southwestern Nigeria. *African Geogr Rev*, 1–16
- Amitrano D, Di Martino G, Iodice A, Riccio D, Ruello G (2018) Unsupervised rapid flood mapping using Sentinel-1 GRD SAR images. *IEEE Trans Geosci Remote Sens* 56(6):3290–3299
- Amitrano D, Guida R, Ruello G (2019) Multitemporal SAR RGB processing for Sentinel-1 GRD products: Methodology and applications. *IEEE J Sel Topics Appl Earth Observ Remote Sens* 12(5):1497–1507
- Amitrano D, Di Martino G, Guida R, Iervolino P, Iodice A, Papa MN, Riccio D, Ruello G (2021) Earth environmental monitoring using multi-temporal synthetic aperture radar: a critical review of selected applications. *Remote Sens* 13(4):604
- Avand M, Moradi H (2021) Using machine learning models, remote sensing, and GIS to investigate the effects of changing climates and land uses on flood probability. *J Hydrol* 595:125663
- Boyle SJ, Tsanis IK, Kanaroglou PS (1998) Developing geographic information systems for land use impact assessment in flooding conditions. *J water resour Plann Manage* 124(2):89–98
- Chen P, Liew SC, Lim H (1999) Flood detection using multitemporal Radarsat and ERS SAR data, In: *Proceedings 20th Asian conference of remote sensing, Hong Kong, 22–25 November*
- De A, Upadhyaya DB, Thiyaku S, Tomer SK (2022) use of multi-sensor satellite remote sensing data for flood and drought monitoring and mapping in India. In: *Civil engineering for disaster risk reduction*. Springer, Singapore, pp 27–41
- Deutsch M, Ruggles F (1974) Optical data processing and projected applications of the erts-1 imagery covering the 1973 Mississippi river valley floods. *JAWRA J Amer Water Resour Assoc* 10(5):1023–1039
- Devrani R, Srivastava P, Kumar R, Kasana P (2021) Characterization and assessment of flood inundated areas of lower Brahmaputra River Basin using multitemporal synthetic aperture radar data: a case study from NE India. *Geological J*
- Dhokal AS, Amda T, Aniya M, Sharma RR (2002) Detection of areas associated with flood and erosion caused by a heavy rainfall using multi temporal Landsat TM data. *Photogramm Eng Remote Sens* 68(3):233–239
- Ekeu-wei IT, Blackburn GA (2018) Applications of open-access remotely sensed data for flood modelling and mapping in developing regions. *Hydrology* 5(3):39
- Ekeu-wei IT, Blackburn GA (2020) Catchment-scale flood modelling in data-sparse regions using open-access geospatial technology. *ISPRS Int J Geo Inf* 9(9):512
- FAO (2002) *World Agriculture: Towards 2015/2030*. Summary report, food and agricultural organization of the United Nations, Rome
- Ganji K, Gharachelou S, Ahmadi A (2019) Urban's river flood analysing using sentinel-1 data case study:(gorganrood, aq'qala). *Int Arch Photogr Remote Sens Spat Inform Sci* 42:415–419
- Giustarini L, Vernieuwe H, Verwaeren J, Chini M, Hostache R, Matgen P, Verhoest NE, De Baets B (2015) Accounting for image uncertainty in SAR-based flood mapping. *Int J Appl Earth Obs Geoinf* 34:70–77


- Hallberg GR, Hoyer BE, Rango A (1973) Application of ERTS1 imagery to flood inundation mapping. NASA Special Publication No. 327, Symposium on significant results obtained from the earth resources satellite 1, Vol 1, Technical presentations, section A, pp 745–753
- Hess LL, Melack JM, Simonett DS (1990) Radar detection of flooding beneath the forest canopy: a review. *Int J Remote Sens* 11(7):1313–1325
- Huang M, Jin S (2020) Rapid flood mapping and evaluation with a supervised classifier and change detection in Shouguang using Sentinel-1 SAR and Sentinel-2 optical data. *Remote Sensing* 12(13):2073
- IPCC (2014) Climate change 2014: impacts, adaptation and vulnerability. IPCC WGIIAR5 Technical Summary. http://ipccwg2.gov/AR5/images/uploads/WGIIAR5-TS_FGDall.pdf. Accessed 19 August 2014
- Israel DC, Briones RM (2012) Impacts of natural disasters on agriculture, food security, and natural resources and environment in the Philippines. In: Sawada Y, Oum S (eds.), Economic and welfare impacts of disasters in east asia and policy responses. ERIA Research Project Report 2011–8, Jakarta: ERIA, pp 553–599
- Jeyaseelan AT (2003) Droughts & floods assessment and monitoring using remote sensing and GIS. In *Satellite remote sensing and GIS applications in agricultural meteorology* (Vol 291). World Meteorol. Org. Dehra Dun, India Geneva, Switz
- Landuyt L, Van Wesemael A, Schumann GJP, Hostache R, Verhoest NE, Van Coillie FM (2018) Flood mapping based on synthetic aperture radar: an assessment of established approaches. *IEEE Trans Geosci Remote Sens* 57(2):722–739
- Loayza N, Olaberría E, Rigolini J, Christiaensen L (2009) ‘Natural disasters and growth going beyond the averages’, policy research working paper 4980, The World Bank East Asia and Pacific Social Protection Unit & Development Research Group, 40 p. <http://gfdr.org/docs/WPS4980.pdf>. Accessed 20 Feb 2012
- Melack JM, Hess LL, Sippel S (1994) Remote sensing of lakes and floodplains in the Amazon Basin. *Remote Sens Rev* 10:127–142
- Min SK, Zhang X, Zwiers FW, Hegerl GC (2011) Human contribution to more-intense precipitation extremes. *Nature* 470(7334):378–381
- Morrison RB, Cooley ME (1973) Assessment of flood damage in Arizona by means of ERTS-1 imagery. In: NASA. Goddard space flight center Symposium on significant results obtained from the ERTS-1, Vol. 1, Sect. A and B (No. PAPER-W6)
- Mudi S, Das P (2022) Flood hazard mapping in Assam using sentinel-1 SAR data. In: *Geospatial technology for environmental hazards*. Springer, Cham, pp 459–473
- Olusola A, Adelabu SA (2021) Estimating total precipitable water distribution across Free State Province, South Africa using remote sensing data and tools. In: 2021 IEEE international geoscience and remote sensing symposium IGARSS. IEEE, , pp 7164–7167
- Orimoloye IR, Belle JA, Olusola AO, Busayo ET, Ololade OO (2021a) Spatial assessment of drought disasters, vulnerability, severity and water shortages: a potential drought disaster mitigation strategy. *Nat Hazards* 105(3):2735–2754
- Orimoloye IR, Olusola AO, Ololade O, Adelabu S (2021b) A persistent fact: reflections on drought severity evaluation over Nigerian Sahel using MOD13Q1. *Arab J Geosci* 14(19):1–18
- Rango A, Anderson AT (1974) Flood hazard studies in the Mississippi river basin using remote sensing 1. *JAWRA J Amer Water Resour Assoc* 10(5):1060–1081
- Ruiz-Ramos J, Berardi A, Marino A, Bhowmik D, Simpson M (2020) Assessing hydrological dynamics of Guyana’s North Rupununi Wetlands using sentinel-1 Sar imagery change detection analysis on google earth engine. In: 2020 IEEE India geoscience and remote sensing symposium (InGARSS), IEEE, pp 5–8
- Sanyal J, Lu X (2004) Application of remote sensing in flood management with special reference to monsoon Asia: a review. *Nat Hazards* 33:283–301
- Sheng Y, Gong P, Xiao Q (2001) Quantitative dynamic flood monitoring with NOAA AVHRR. *Int J Remote Sens* 22(9):1709–1724

- Sivakumar MVK (2005) Impacts of natural disasters in agriculture, rangeland and forestry: an overview. In: Sivakumar MVK, Motha RP, Das HP (eds) *Natural Disasters and extreme events in agriculture*. Springer Hiderberg Berlin, New York, pp 1–22
- Smith LC (1997) Satellite remote sensing of river inundation area, stage and discharge: a review. *Hydrol Process* 11:1427–1439
- Tholey N, Clandillon S, Fraipont P (1997) Flood surveying using Earth observation data. *Proceedings of the Eurisy Colloquim “earth observation and the environment: benefits for central and eastern European countries”*, Budapest, pp 77–88
- Tiwari V, Kumar V, Matin MA, Thapa A, Ellenburg WL, Gupta N, Thapa S (2020) Flood inundation mapping-Kerala 2018; Harnessing the power of SAR, automatic threshold detection method and Google Earth Engine. *PLoS ONE* 15(8):e0237324
- Uddin K, Matin MA (2021) Potential flood hazard zonation and flood shelter suitability mapping for disaster risk mitigation in Bangladesh using geospatial technology. *Progress Disaster Sci*, 100185
- Wang Y, Colby JD, Mulcahy KA (2002) An efficient method for mapping flood extent in a coastal flood plain using Landsat TM and DEM data. *Int J Remote Sens* 23(18):3681–3696
- Yang C, Zhou C, Wan Q (1999) Deciding the flood extent with Radarsat SAR data and image fusion. In: *Proceedings 20th Asian conference of remote sensing*, Hong Kong, 22–25 November
- Zhang L, Xia J (2022) Flood detection using multiple Chinese satellite datasets during 2020 China summer floods. *Remote Sens* 14(1):51

Chapter 18

Contribution of Geomatics to the Hydrological Study of an Ungauged Basin (Taguenit Wadi Watershed, Lakhssas, Morocco)



**Mustapha Ikirri, Farid Faik, Said Boutaleb, Mohamed Abioui ,
Abderrahmane Wanaim, Amine Touab, Mouna Id-Belqas,
and Fatima Zahra Echogdali**

Abstract Since the end of the last century, climate change has generated extreme pluviometric events favoring the triggering of flash floods, characterized by very high velocity and short rise times. These floods cause a lot of damage and thus, modified the activities in the flooded regions. Watershed of the Taguenit Wadi in the Western Anti-Atlas is a better example to study the effects of these extreme phenomena such as the last event in November 2014. The latter have indeed caused a lot of human and material damage, as well as the destruction of infrastructure and loss of soil. In

M. Ikirri · F. Faik · S. Boutaleb · M. Abioui (✉) · A. Wanaim · A. Touab · M. Id-Belqas ·
F. Z. Echogdali

Department of Earth Sciences, Faculty of Sciences, Ibn Zohr University, Agadir, Morocco
e-mail: m.abioui@uiz.ac.ma; abioui.gbs@gmail.com

M. Ikirri
e-mail: mustapha.ikirri@edu.uiz.ac.ma; ikirimustapha@gmail.com

F. Faik
e-mail: faikfarid@yahoo.fr; f.faik@uiz.ac.ma

S. Boutaleb
e-mail: saidboutaleb1@yahoo.fr; s.boutaleb@uiz.ac.ma

A. Wanaim
e-mail: a.wanaim@uiz.ac.ma; abdougeologue@gmail.com

A. Touab
e-mail: amine.touab@edu.uiz.ac.ma

M. Id-Belqas
e-mail: mouna0959@gmail.com; mouna.id-belqas@edu.uiz.ac.ma

F. Z. Echogdali
e-mail: echogdalifatimazahra@gmail.com; fatimazahra.echogdali@edu.uiz.ac.ma

A. Touab
Souss-Massa Hydraulic Basin Agency, Agadir, Morocco

this paper, a Flood Hazard Index (FHI) method was applied to study these extreme phenomena and determine their lateral extensions. Moreover, this method made it possible to map with great precision the areas vulnerable to flooding throughout the Taguenit Wadi basin. The FHI method is more advantageous in the basins, which are poorly gauged but seem to be less precise in terms of defining the water levels downstream of the basin.

Keywords Climate change · Flooding · Flood Hazard Index (FHI) · Watershed · Anti-Atlas · Morocco

18.1 Introduction

Nowadays, water scarcity is an omnipresent reality, and with soaring demand in the future, it continues to be a precious resource. But, manifestations of water resources as the main cause of contrasting catastrophes such as water-excessive (floods), and water-deficient events like droughts, and desertification, owing to the effects of climate change (Bouramtane et al. 2020); interrogate the mismanagement by the stakeholders. Albeit these, the scenario of arid regions is difficult due to scarcity of flows, absence of morphogenic floods, and difficulty in performing a natural tracing or continuous monitoring of the flow (Bouramtane et al. 2020). However, the occurrence and violence of rain events, floods represent a real risk in arid regions on water resources management.

Floods have the greatest potential for destruction and increasingly affect a large number of people. In recent decades, the world has been affected by severe flooding, causing thousands of deaths, disruption of economic activities, and infrastructures destructions (e.g. Tang et al. 1992; Lekuthai and Vongvisessomjai 2001; Kundzewicz 2003; Campion and Venzke 2013; Cobbinah and Anane 2016; Lu et al. 2018). The flooded phenomena have been studied by several researchers, particularly on the development of theories, numerical models, and statistical methodologies to describe flood behavior and space–time evolution (e.g. Hallegatte et al. 2007; Benkirane et al. 2020; Gao et al. 2020, Ikirri et al. 2021, 2022; Wang et al. 2021).

Morocco, located in North-West Africa, is characterized by some arid and semi-arid river watersheds. It is facing unpredictable rainfall patterns and is subject to various hydrological constraints (Benkirane et al. 2020). In this country, climate variations are highly unpredictable, and the decreasing precipitation amounts resulted in the scarcity of surface water resources (Heiß et al. 2020). However, several Morocco regions have been subject to a considerable history of flooding phenomena (e.g. Saidi et al. 2010; El Morjani et al. 2016; El Alaoui El Fels et al. 2017, 2018; Echogdali et al. 2018a, b, 2022a, b, c, d; Bennani et al. 2019; Saidi et al. 2020). Historical information during 1980–2014 shows different disastrous human and economic consequences of the floods in Morocco (Table 18.1).

The regions of the western Anti-Atlas, particularly on the south-west, have been affected by numerous flooding events; with special relevance to the famous flood

Table 18.1 Disastrous consequences of the main floods in Morocco (1980–2014)

Disaster	Killed people		Economic damages		
	Date	Killed	Disaster	Date	Cost (US\$ X 1000 000)
Flood	1995	730	Flood	1995	15
Earthquake	2004	628	Flood	1996	55
Flood	2002	80	Drought	1999	900
Flood	1997	60	Extreme temperature	2000	809
Flood	1995	43	Flood	2001	2200
Flood	2003	35	Flood	2002	2,00
Flood	2010	32	Earthquake	2004	400
Mass movements dry	1988	31	Storm	2005	50
Flood	2008	30	Flood	2009	200
Flood	1996	25	Flood	2010	100
Flood	2010	100	Flood	2014	5.200
Flood	2014	50	Flood	2018	1.500
Flood	2018	150	Flood	2020	1210

that occurred on the 28th November 2014, which affected the city of Guelmim and the town of Sidi Ifni (Ikirri et al. 2021, 2022).

Flood hazard still looms large over the years due to population growth and socio-economic development, as well as climate change as a result of global warming. The Taguenit Wadi watershed, located in the Lakhssas region (west coast), has recorded numerous bigger floods, with the prominent during 2006, 2010, and 2014, and causing a great deal of damage to infrastructure, loss of soil, and untold suffering to the population (Fig. 18.1). This calls for regular characterization and river monitoring to protect the various infrastructures and human activities of the area.

As a measure, flood risks on a basin-scale were quantified, especially using flood hazard indexes methodologies (e.g. Tehrany et al. 2013, 2014; Elkhrahy 2015;



Fig. 18.1 Damage to the infrastructure of the village of Lakhssas during the floods of November 2014. **a** degradation of the National Road No.1; **b** deterioration in the inter-provincial roads connecting Lakhssas village and Ifni city

Kazakis et al. 2015; Rahmati et al. 2016; Kabenge et al. 2017; Echogdali et al. 2018a, b, 2022a, b, c, d; Ikirri et al. 2021, 2022; Ait Haddou et al. 2022). The study of simulated floods on the Taguenit Wadi watershed and their spatial extension is essential to enable hydraulic operators to delimit the higher risk of flooding areas. Attending to the crucial relevance of this topic, the main aim of the present study is the application of the Flood Hazard Index (FHI) method to delimit the most vulnerable flood areas. This index is based on the modeling of annual rainfall and its comparison with the geomorphological data of the basin deduced from the processing of satellite images and the Digital Terrain Model (DTM).

The identification of more vulnerable flood areas with a higher risk of flooding on the Taguenit Wadi watershed is defined, and adequate management of water resources and urbanized occupation areas is provided.

18.2 Study Area: Geomorphology and Hydro-Climatology of the Taguenit Wadi Watershed

The catchment area of the Taguenit Wadi, between latitudes 29°10'30" to 29°28'30", and longitudes 9°52'30" to 10°43'30", covers an area of 131.52 km². The altitude varies between 577 and 1204 m (Fig. 18.2a), decreasing overall from east to west. The slopes, which are generally steep, vary from a few degrees (0° and 15°) on the terraces of the tributary river beds and downstream of the river basin to 64° on the upstream slopes (Fig. 18.2b).

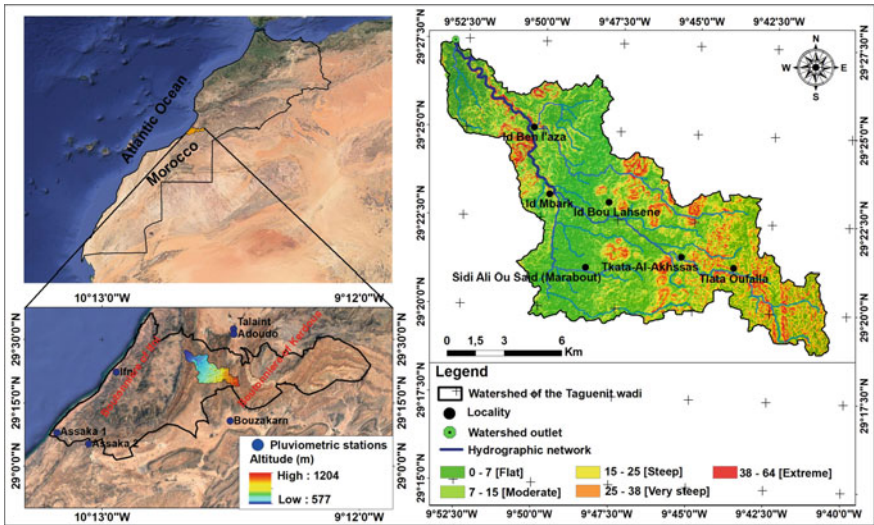


Fig. 18.2 Watershed of Taguenit Wadi River: Geographical setting, hypsometry, and Slopes variation

The average annual rainfall, recorded at the Adoudou station located 15 km north of the basin, is 133 mm. Aridity relatively increases from west to east, due to the increasing distance from oceanic influences. The average temperature is 26 °C, with a maximum of 45 °C and a minimum of 12 °C (Ikirri et al. 2021, 2022).

Morocco has an excellent and diverse coverage due to its geology and structural elements with a consequent highly diverse geomorphology and a variety of landform types (e.g. Dill et al. 2019). The geomorphology of the basin area is characterized by the dominance of the mountains of the western Anti-Atlas range, with cover vegetation dominated by Argan and euphorbia plants. The trunk river and tributaries flow only after the first rains in October or November. The dominant surface water flow is from SE-NW (Fig. 18.2a). The hydrographic network is dense and well-branched, with a specific “Y” shape. The branching of the network is more pronounced upstream than downstream. The time of concentration of the water calculated using the Giandotti equation is 14 h. In this region, flash floods cause much human and material damage, produced by intense rains resulting in short periods of flooding, usually several hours. Some arid and semi-arid basins in Morocco are facing unpredictable rainfall patterns and are subject to various hydrological constraints.

The Taguenit Wadi basin is part of the Lakhssas plateau, located in the Western Anti-Atlas chain, on the west coast of Morocco. The Anti-Atlas forms a vast anticline, extending from the Atlantic Ocean South-Westward to Hamada of Guir North-Eastward (Bouramtane et al. 2020). The study area is located between the two Precambrian massifs of Kerdous and Ifni and is characterized by a continuous transition between the facies of the Upper Neoproterozoic and those of the Lower to Middle Cambrian. These geological formations are composed, from bottom to top, by carbonate facies (Tamjout dolomites and lower limestones), dolomitic limestones, marly limestones with intercalations of dolomitic-sandstone, and finally upper limestones (e.g. Sdzuy and Geyer 1988; Benssaou and Hamoumi 2003; Soulaïmani and Bouabdelli 2005).

From a structural characterization, the area is in a synclinal structural position, affected by Hercynian movements, and characterized by a heterogeneous deformation that is intensified in the center region of the basin. All the area is generally faulted, with the main directions of NNE-SSW, NE-SW, E-W, and ENE-WSE (Fig. 18.3a). The lithology of the Taguenit Wadi basin is dominated by impermeable and low permeability formations that represent 80% of the basin area (Fig. 18.3b). Therefore, these formations constitute a major risk by amplifying the destructive power of floods in the basin. The medium to high permeability formations is mainly concentrated on the north and correspond to the very coarse detrital limestone intercalations (Fig. 18.3).

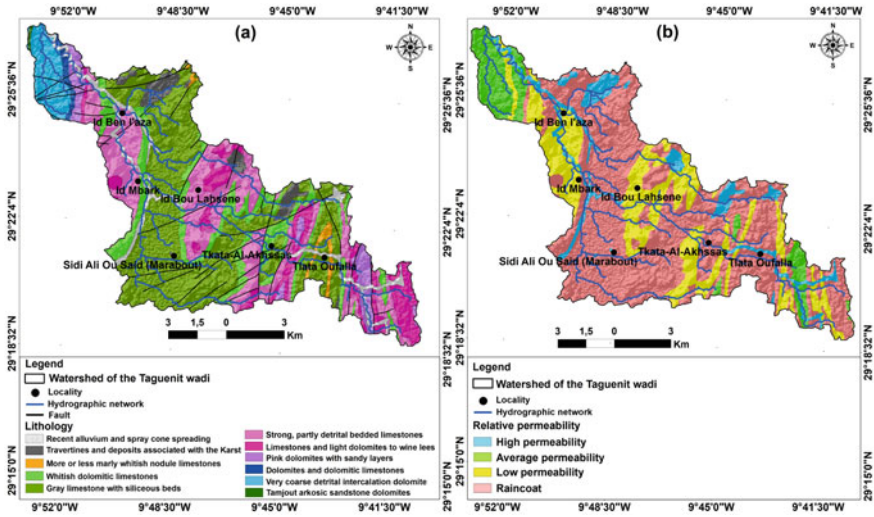


Fig. 18.3 Taguenit Wadi watershed: a Geological map; b Spatial distribution of rocks permeability

18.3 Materials and Methods

18.3.1 Flood Mapping Methodology

The Flood Hazard Index (FHI) model has been developed to define flood risk areas from a regional perspective (e.g. Elkhrachy 2015; Kazakis et al. 2015; Franci et al. 2016; Echogdali et al. 2018a, b, 2022a, b, c, d; Patrikaki et al. 2018; Ali et al. 2020; Benjmel et al. 2020, 2022; Ikirri et al. 2021, 2022). The FHI index is intended to identify vulnerable areas of flooding risk.

The FHI is based on the Analytical Hierarchy Process (AHP) multi-criteria decision analysis, considering the contribution of weights of seven hydro-geo-morpho-climatic factors, namely: Rainfall intensity (I), Slope (S), Flow accumulation (Fa), Drainage Network Density (DND), Distance from Drainage (DFD), relative Permeability of the catchment (P) and catchment Land Use/Cover (LUC). The choice of these factors is theoretically based on their relevance to flood risk (Fig. 18.4).

18.4 FHI Factors

The factors considered in the spatial flood map are extracted from the DEM, with 30mx30m, for slope and flow accumulation, while permeability was extracted from the Lakhssas geological map on a scale of 1:100,000. The drainage network of the area was obtained using DEM data and used to produce the drainage network

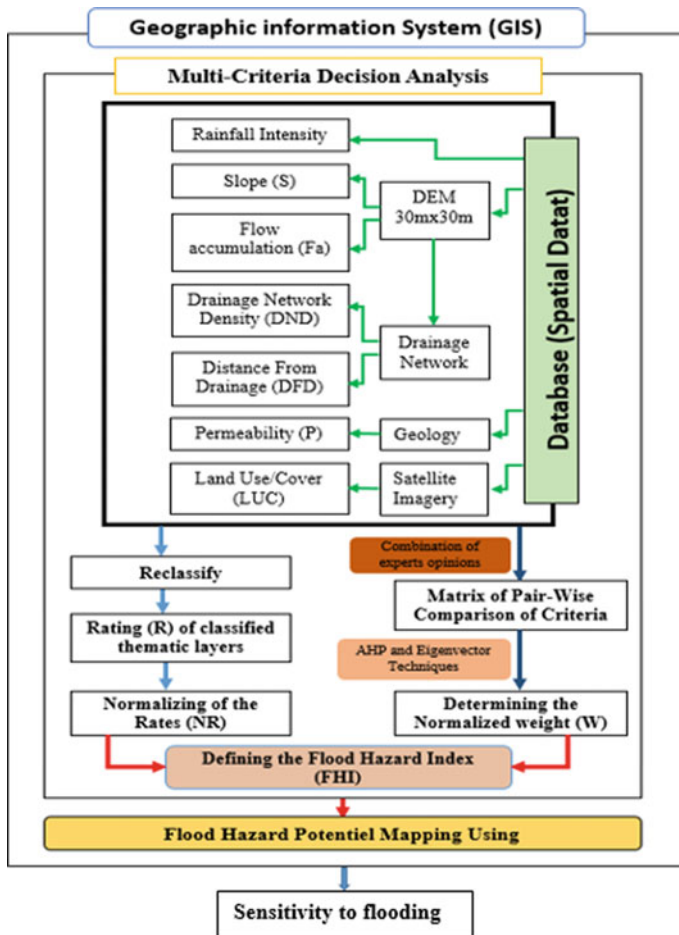


Fig. 18.4 Schematic diagram of integration of hydrological and AHP models in a Geographical Information System (GIS)

density and distance from drainage. As regards rainfall, the spatial distribution map was deduced from a regional extrapolation, including four meteorological stations bordering the basin, namely: Adoudou, Talaint, Sidi Ifni, Assaka 1, Assaka 2, and Bouzakarne. Land Use was obtained using satellite images from the region. All the information was organized in a database using ArcGIS software.

Each of the seven factors was reclassified, with a rating, according to the impact degree on the flood risk. Then, depending on local conditions, each factor was assigned with a value between 2 and 10, with an increase of vulnerability risk (Table 18.2).

- **Flow accumulation (Fa)**: Flow accumulation corresponds to the accumulated water flow to a specific cell drained from the cells located upstream. High values

Table 18.2 Defined factor classes and corresponding ratings adopted for this study (*Source* Collated from various references cited within this chapter)

Factor (Units)	Class	Rating
Fa: Flow accumulation (Pixels)	97,503,24–147,996	10
	45,849,74–97,503,24	8
	23,795,43–45,849,74	6
	6,384,14–23,795,43	4
	0–6,384,14	2
DFD: Distance from drainage (m)	0–200	10
	200–400	8
	400–700	6
	700–1000	4
	1000–2000	2
DND: Drainage Network Density (km/km ²)	4,53–5,67	10
	3,40–4,53	8
	2,26–3,40	6
	1,13–2,26	4
	0–1,13	2
I: Rainfall Intensity (mm)	134,60–137,71	10
	131,50–134,60	8
	128,40,197–131,5,050,049	6
	125,29–128,40	4
	122,19–125,29	2
LU: Land use/Cover (Pixels)	Dwelling	10
	Wadi	8
	Bare ground	6
	Vegetation	2
S: Slope (degree)	0–7	10
	7–15	8
	15–25	6
	25–38	4
	38–64	2
P: Permeability (Pixels)	Impermeable	10
	Low permeability	8
	Average permeability	6
	High permeability	4

of F factor indicate areas of higher concentrated water flow and therefore a higher risk of flooding (Kazakis et al. 2015; Patrikaki et al. 2018; Ikirri et al. 2021, 2022). In the study area, this factor varies in a range between 0 and 147,996, with the highest values coinciding with the water flow of the main tributaries of Taguent Wadi (Table 18.2; Fig. 18.5a).

- **Distance From Drainage (DFD):** The spatial distance of a region to the river system is a crucial factor in the delimitation of flood vulnerability zones. As the distance to the river system decreases, the degree of flood risks will increase (Kazakis et al. 2015; Echogdali et al. 2018a, b; Ikirri et al. 2021, 2022). Distances located below 200 m to the river system will correspond to areas of higher flood vulnerability. Otherwise, the areas located away from 400 m to the river system seem to present a lower or absence of flood risk. Almost the area presents a

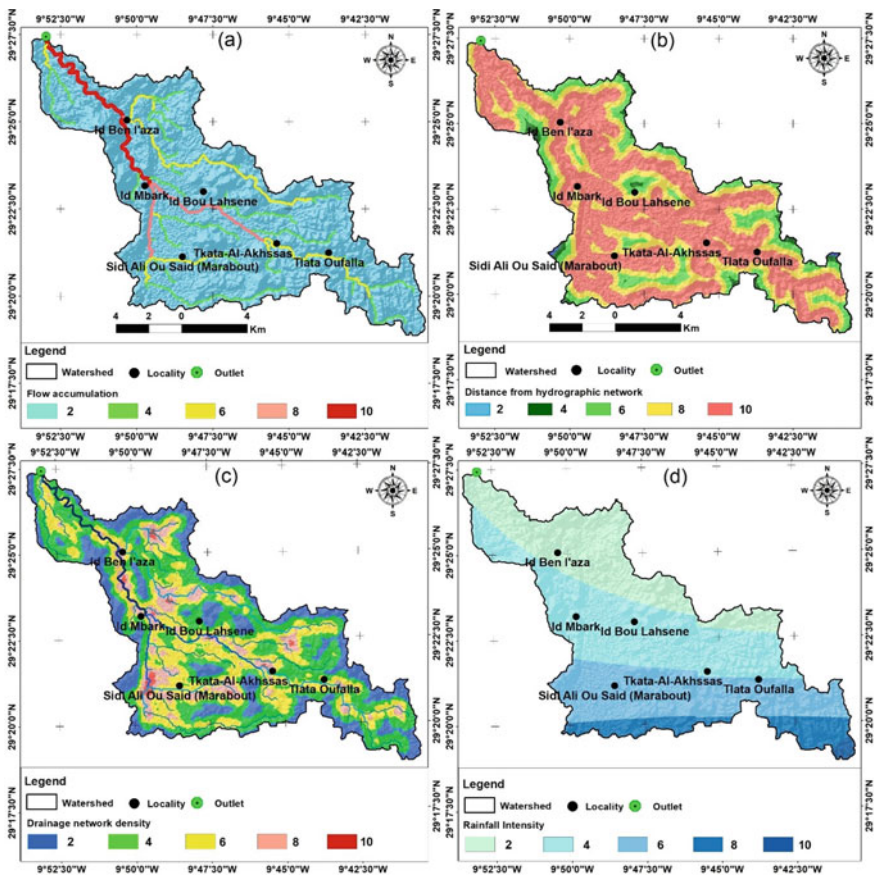


Fig. 18.5 Spatial distribution of flood assessment factors in the Taguent Wadi watershed: **a** Flow accumulation; **b** Distance from drainage; **c** Drainage network density; **d** Rainfall Intensity

high flood vulnerability particularly associated with the drainage network system (Table 18.2; Fig. 18.5b).

- **Drainage Network Density (DND):** Drainage network density is proportional to the cumulative water volume from upstream to downstream the river basin (Echogdali et al. 2018a, b; Ikirri, et al. 2021, 2022). In the Taguenit Wadi watershed region, DND values range from 0 to 5.67 km/km², with the lower class concentrated on the basin region (Table 18.2; Fig. 18.5c).
- **Rainfall Intensity (I):** This factor was interpolated using the inverse weighted method from selected points (Yoo et al. 2005, 2021; Patrikaki et al. 2018). In the Taguenit Wadi watershed region, rainfall intensity varies between 122, 19 to 137,71 mm, with the decrease values from the north to the south, and the highest rainfall values are recorded in the southern part of the basin (Table 18.2; Fig. 18.5d). The spatial distribution of rainfall intensity in the study area is presented in Fig. 18.5d.
- **Slope (S):** The slope of the area influences surface runoff and water infiltration (Aaron and Venkatesh 2009; Patrikaki et al. 2018; Ikirri et al. 2021, 2022). The slope classes vary between 0 and 64° (Table 18.2) and were defined according to the model applied by Demek (1972). The lower slope areas are concentrated downstream, while the higher slope areas are concentrated in the mountainous regions, located in the north of the basin (Fig. 18.6a).
- **Land use (LU):** The type of land use determines the infiltration of rainwater into the soil and the resulting runoff (e.g. Weng 2001; Aich et al. 2015; Kazakis et al. 2015; Franci et al. 2016; Patrikaki et al. 2018; Ikirri et al. 2021, 2022). Forests generally favor infiltration through the root system of trees and plants, whereas roads and buildings reduce infiltration of this water and increase surface runoff. In the Taguenit catchment area, the land use data has been reclassified into four classes displayed in Table 18.2. The village of Lakhssas, located in the center of the basin area and equipped with several infrastructures (e.g. roads, tracks, shops, and dwellings), which amplify the occurrence of floods downstream as it generally contains impermeable materials (Fig. 18.6b).
- **Permeability (P):** In the Taguenit Wadi watershed, the impermeable or poorly permeable rocks, such as crystalline rocks, promote surface runoff. This factor was reclassified in four classes, varying between 4 to 10, according to models established by Ouma and Tateishi (2014), Kazakis et al. (2015), Echogdali et al. (2018a, b), Franci et al. (2016), and Ikirri et al. (2021, 2022). About, 80% of the basin's formations are impermeable or with a low permeability, which offers an environment conducive to the higher probability of strong floods development. Carbonate formations, with lower permeability, strongly favoring runoff, were assigned a weight of 10 (Table 18.2), while the lowest weight (class 2) is attributed to those with high permeability corresponding to the Quaternary formations, which extend over 20% of the Taguenit Wadi watershed (Fig. 18.6c).

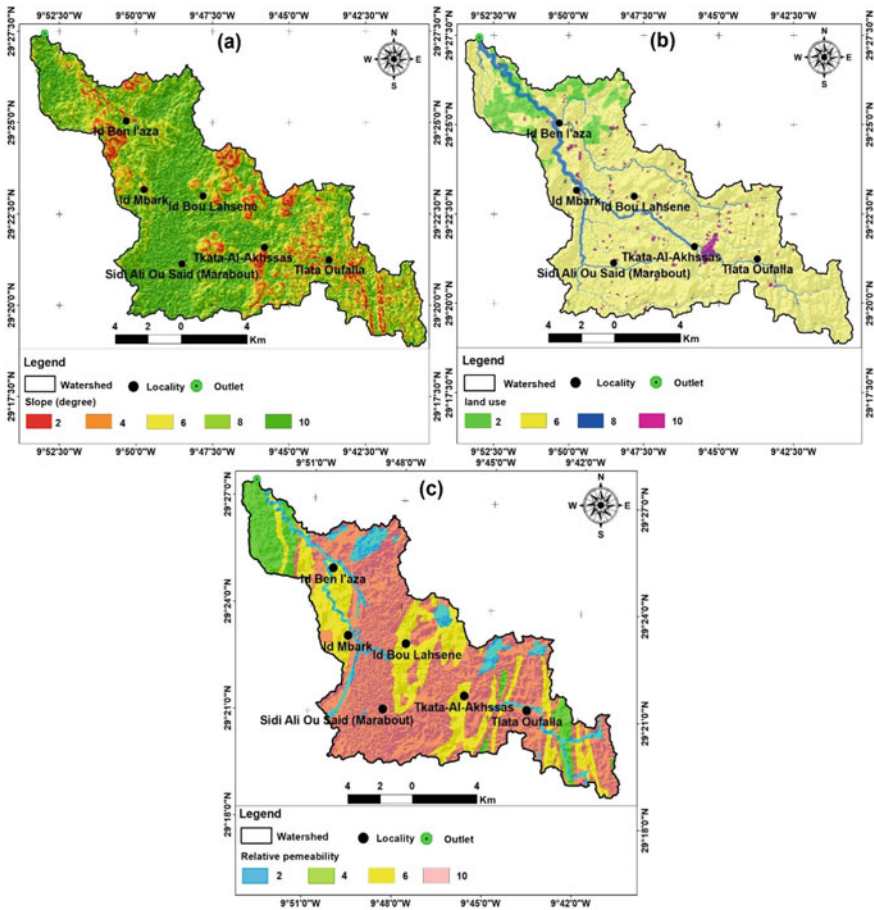


Fig. 18.6 Spatial distribution of flood assessment factors in the watershed of the Taguenit Wadi watershed (continuation): a Slope; b Land use; c Permeability

18.4.1 Relative Weight of Factors

The weights of the factors applied in Taguenit Wadi watershed were determined using AHP (Fig. 18.4) (e.g. Saaty 1990a, b; Kazakis et al. 2015; Echogdali et al. 2018a, b, 2022a, b, c, d; Ikirri et al. 2021, 2022). The AHP methodology is a mathematical approach used to characterize complex problems, with a varying number of factors. Once all the factors are hierarchically sorted, a pairwise comparison matrix is constructed to allow meaningful comparison between the assessments of the factors. The relative importance of each factor was determined by five numerical scales, as shown in Table 18.3.

The applied matrix is of a dimension 7×7 and the diagonal elements are equal to 1. The factors are structured hierarchically in Table 18.4.

Table 18.3 Numerical expression of the relative importance of factors

Importance	Scale
Very important	1
Moderate	1/2
Less important	1/3
Moderately less important	1/4
Much less important	1/5

Table 18.4 Pair-wise comparison matrix of flood influencing factors for AHP

Factors	Flow accumulation	Distance from drainage	Drainage network density	Rainfall intensity	Land use	Slope	Geology (or permeability)
Flow accumulation	1	2	3	5	3	5	4
Distance from drainage	1/2	1	6	4	3	4	6
Drainage network density	1/3	1/6	1	3	2	3	3
Rainfall Intensity	1/5	1/4	1/3	1	2	2	2
Land use	1/3	1/3	1/2	1/2	1	3	2
Slope	1/5	1/4	1/3	1/2	1/3	1	3
Permeability	1/4	1/6	1/3	1/2	1/2	1/3	1
n = 7	$\lambda_{max} = 7,65$		RI = 1,32		CR = 0,08		

The values presented in each row determine the correlation between two considered factors. The addition of each column value to the comparison matrix and dividing each element of the matrix by its column total could be calculated the average of the elements in each column of the matrix (Saaty 1990a, b; Razandi et al. 2015). The normalized weights for individual flood factors are presented in Table 18.5.

The average of the rows of the normalized matrix represents the corresponding weight (w) to each factor. In the Taguenit Wadi watershed area, flow accumulation is considered as the most relevant factor in the FHI index, followed by drainage distance, drainage network density, rainfall intensity, land use, slope, and permeability.

Otherwise, it will be necessary to assess the consistency of the determined AHP eigenvector matrix. The consistency of the matrix could be assessed using the consistency ratio (CR) (Eq. 18.1). This ratio defines the probability of comparison between the consistency index (CI) of the matrix with respect to the index ratio (RI) of a random type of matrix (Saaty 1990a, b; Echogdali et al. 2018a, b; Ikirri al. 2021, 2022).

Table 18.5 Normalized weights determined for each flood factor

Factors	Flow accumulation	Distance from drainage	Drainage network density	Rainfall Intensity	Land use	Slope	Geology	Weight
Flow accumulation	0,36	0,48	0,26	0,34	0,25	0,27	0,19	2,73
Distance from drainage	0,18	0,24	0,52	0,28	0,25	0,22	0,29	2,54
Drainage network density	0,12	0,04	0,09	0,21	0,17	0,16	0,14	1,43
Rainfall Intensity	0,07	0,06	0,03	0,07	0,17	0,11	0,10	0,71
Land use	0,12	0,08	0,04	0,03	0,08	0,16	0,10	0,85
Slope	0,07	0,06	0,03	0,03	0,03	0,05	0,14	0,55
Permeability	0,09	0,04	0,03	0,03	0,04	0,02	0,05	0,40

Table 18.6 Random indices (RI) used to calculate the consistency ratio (CR)

n	1	2	3	4	5	6	7	8	9
RI	0	0	0.58	0.9	1.12	1.24	1.32	1.41	1.45

n: number of factors selected

$$CR = \frac{CI}{RI} \tag{18.1}$$

With CR as the consistency ratio, CI represents the consistency index, calculated using Eq. (18.2), and RI corresponds to the random index dependent on the number of selected factors (n) (Table 18.6).

This index is calculated from the average consistency index of a randomly generated sample of 500 pairwise comparison matrices. If the CR value is ≤ 0.10 , the matrix is acceptable; and if the CR value is ≥ 0.10 , it is necessary to revise the judgments due to the inconsistency.

$$CI = \frac{\lambda_{max} - n}{n - 1} \tag{18.2}$$

The consistency index (CI), will depend on the λ_{max} that corresponds to the maximum value of the comparison matrix, and (n) is the number of factors. The CI is calculated for $\lambda_{max} = 7.54$, $n = 7$ and $RI = 1.32$. The eigenvector λ_{max} of the matrix is calculated and the consistency of all the judgments is also checked, making sure that the AHP method suggests that the obtained CR value is less than or equal to 0.1(Saaty 1977; Saaty and Vargas 2012). Since the value of $CR = 0.08$ is less than the threshold (0.1), the consistency of the weights and weights is confirmed.

The seven selected factors were superimposed linearly with their weights calculated previously. The flood risk index is calculated using Eq. (18.3):

$$FHI = \sum_{i=6}^n (w_i * X_i) \quad (18.3)$$

With X_i : classification of the factor at each point, W_i : weight of each factor, and (n) number of factors.

In Taguenit Wadi watershed area, FHI was applied using the Eq. (18.4):

$$\begin{aligned} FHI = & [2, 73 * (\text{Flow accumulatoin})] + [2, 54 * (\text{Distance From Drainage})] \\ & + [1, 43 * (\text{Drainage Network Density})] + [0, 71 * (\text{Rainfall Intensity})] \\ & + [0, 85 * (\text{Land Use})] + [0, 55 * (\text{Slope})] + [0, 4 * (\text{Permeability})] \end{aligned} \quad (18.4)$$

Flood sensitivity is an analysis to test and evaluate the extent of flooding and to determine the predictive accuracy of the selected model (Koks et al. 2015a, b). Some models use the ratio of affected features to total vulnerable features to determine the flood vulnerability of an area (Hall et al. 2005; Pappenberger et al. 2008; Moel et al. 2012). The variable 'flood depth' could be added to determine flood sensitivity as the degree of affected features is directly related to the flood depth. The flood sensitivity is calculated according to Eq. (18.5).

$$S = \frac{R_{affected}}{R_{total}} * 100\% \quad (18.5)$$

With S is the flood sensitivity score; $R_{affected}$ is the number of affected entities; R_{total} is the amount of total vulnerable entities.

18.5 Results and Discussion

Analysis of the results obtained from the linear combination of the selected factors shows that the three most relevant factors for the determination of flood vulnerability are flow accumulation, distance to the drainage system, and density of the river system. Five flood risk classes, varying from very low to very high, were defined according to the flood risk map of the Taguenit Wadi watershed area (Fig. 18.7). The respective areas corresponding to the different degrees of flood risk vary from 8.29% (very high risk), 20.38% (high risk), 31.47% (moderate risk), 15.36% (low risk), and 24.50% (very low risk)(Table 18.7). Most flood areas are located on the large flood plains extending westwards from the main Taguenit Wadi. Outside the alluvial zones, with general high flood risk, it should be noted that the zones located downstream of the catchment area, on the way to the Id-Mbark village, are the most vulnerable to

high flood occurrences. These areas correspond to the road networks (National Road N°1, provincial roads N°1911, 1918 and tracks), village sites (Lakhssas village, Tlat Oufia, and Idchaoud), and the areas located close to the alluvial banks of the Taguenit Wadi (Fig. 18.7).

In addition to the three factors mentioned above, it seems that the difference in the lateral extension of flood risks in the Taguenit Wadi catchment area is also due to the effect of the topography of the alluvial plains on either side of the main wadi. Several topographic profiles transverse to the main river course reflect a variable morphology from one sector to another. The steepness of the wadi valley varies from 6 m, at the level of profile, 1 to 10 m at the level of profile 2 and could reach 35 m at the level of profile 6 (Fig. 18.8). The areas of low valley incision automatically induce an overflow of water beyond the minor bed. The strong reliefs in the upstream region favor a significant encasement of the valleys that limits the lateral extension of water in these areas. The village of Lakhssas, the largest and most populous commercial center in the region with 5,000 inhabitants, suffers greatly from these extreme and repetitive flood events (Ikirri et al. 2021, 2022). Of the 50 villages in the study area, only 11 villages are located in a low to medium-risk flood zone. The remaining 80%

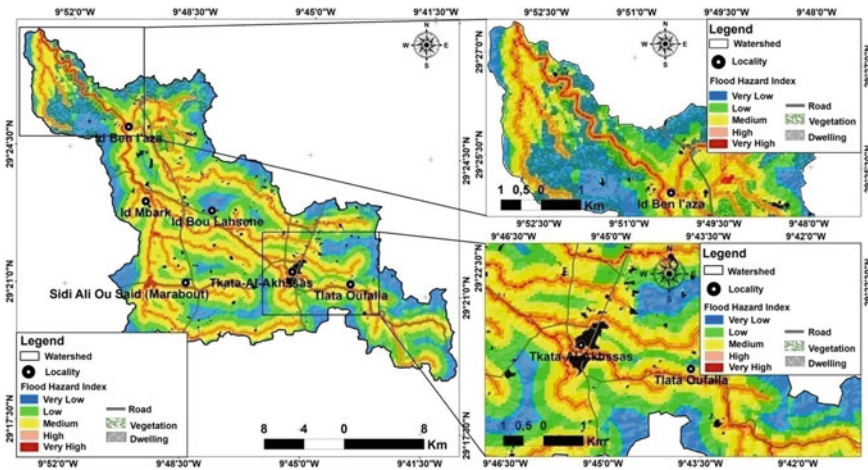


Fig. 18.7 Map of areas vulnerable to flooding in the Taguenit Wadi watershed

Table 18.7 Percentage of degree flood risk areas in the Taguenit Wadi watershed

Degree of flood risk	Area (km ²)	Percentage (%)
Very high	10,89	8,29
High	26,77	20,38
Medium	41,34	31,47
Low	20,36	15,36
Very Low	32,16	24,50

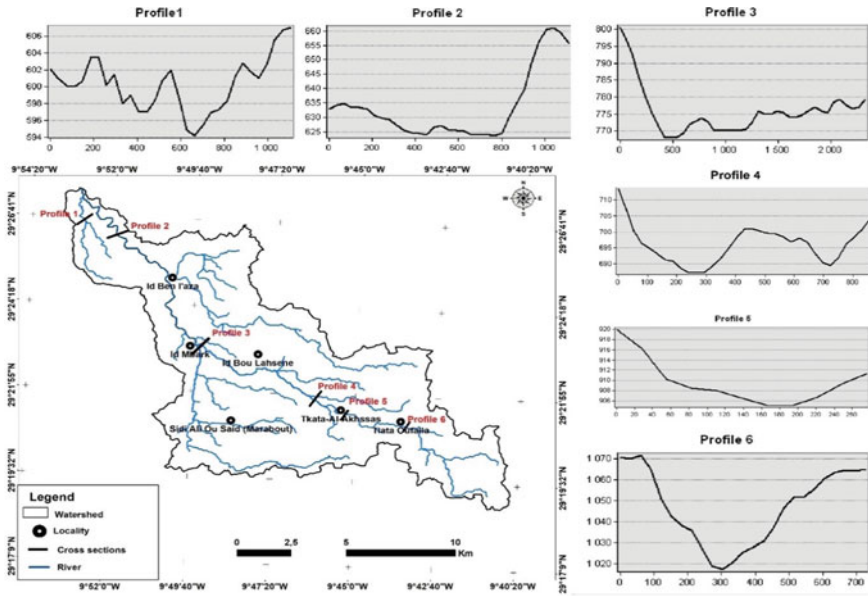


Fig. 18.8 Topographic profiles at six cross-sections in the watershed of Taguenit Wadi area

of agrarian villages face the danger of flooding risk and occupy the alluvial plains of various tributaries.

The flood sensitivity test relates the potential damage to the corresponding flood extent for each land use type. In the study area, the flood sensitivity scores for each land use type tend to increase with increasing proximity to the main wadi (Fig. 18.9). The extent of land use damage is therefore significant. The flood sensitivity of three land use types could be individualized into two different categories: high sensitivity (residential) and medium to low sensitivity (roads and agriculture). Residential areas should be avoided in high flood risk areas, while land use with medium to low flood sensitivity (roads and agriculture) are suitable in these flood risk areas. These results will allow for better planning of stream restoration to reduce losses and damages during floods in the Taguenit Wadi watershed.

The spatial validation of the lateral extension of floods areas at the level of the Taguenit Wadi watershed was also carried out by the fieldwork observations of the water level during a few floods, especially the one of the year 2018, and by a survey of the local population. The obtained results from these surveys corroborate with FHI model results. Considering a few differences, the obtained results could be used in future land use plans on the Taguenit Wadi basin region. In the absence of hydrometric data, the FHI model allowed us, despite the limited number of integrated data, to establish a map of the lateral spread of floods. Nevertheless, it does not provide any indication of the height of the water in these zones, which does not allow us to approach the danger of these flood zones in a more precise manner.

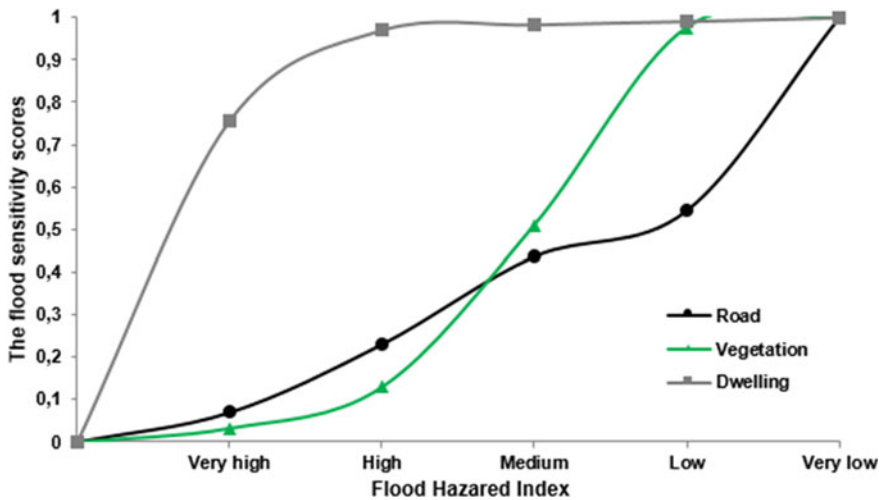


Fig. 18.9 Flood Hazard Index (FHI) versus Flood sensitivity scores

The Taguenit Wadi watershed with a high risk of flooding deserves special attention, especially in the inhabitable, agricultural, and infrastructure areas, to avoid disasters caused by extreme flood events. This basin must be equipped with hydrological and hydraulic infrastructures that allow for regular monitoring of water flows in, at least, three different zones of the main course (e.g. upstream, middle, and downstream). The measured hydrological data should be considered by an intergovernmental regional committee that could announce warnings in case of high floods to evacuate people, livestock, and property, and minimize the associated consequences.

On the developmental plans for the Taguenit Wadi watershed, it would be judicious to limit the effect of floods whose origin is at the level of the upstream basin by the construction of a flood control dam. This infrastructure will allow for the reduction of the velocity of floodwater, which will increase the time of contact between the alluvium and the water, and the consequent gradual water infiltration and a strong supply of the alluvial layers largely used by the local farmers. On the margin of both the tributaries and trunk river, it is recommended to develop the slopes with benches, protective sills, and dikes. The purpose of the benches is two-fold: to control water erosion and to reduce surface runoff by promoting infiltration.

The proposed measures and solutions to the Taguenit Wadi watershed, considering the geomorphological characteristics, are represented in Fig. 18.10. In addition, it is important to set up Flood Risk Management Strategies (FRMSs), established by the local authorities, which define prohibition zones and prescription zones, which are constructible under reserve. The implementation of Flood Risk Management Strategies (FRMSs) will impose to act on the existing to reduce the vulnerability of elements. The challenges to be faced are mainly financial since funding is currently directed towards large basins and agricultural plains of the northern and central regions of Morocco.

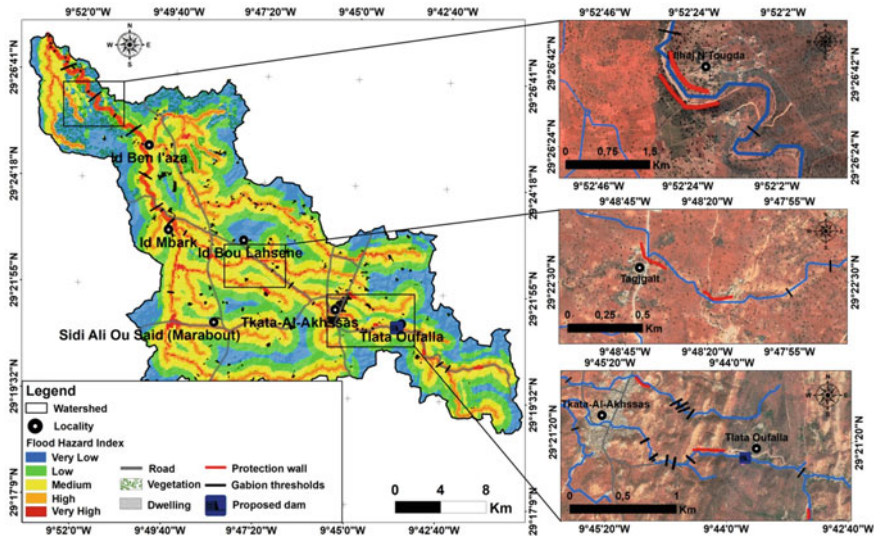


Fig. 18.10 Proposed measures to be applied to the Taguenit Wadi watershed

The study of flood risks in non-equipped basins is of paramount importance, especially in agricultural mountainous regions. Water operators, as well as decision-makers, should encourage the enhancement of infrastructures of these basins (e.g. hydrological stations, dams, dikes) to avoid the dangers related to the impacts of floods, mainly associated with extreme events. In these regions, it is also recommended to ban new construction in flood-prone areas, in addition to the establishment of a flood warning system involving government sectors (e.g. firefighters, River Basin Agencies, municipalities, and Ministry of the Interior). Furthermore, a reforestation program will be crucial on the alluvial plains to improve the water infiltration associated with floodwaters. The construction of bridges on the main roads exposed to flood risks is also mandatory to avoid the disruption of road traffic, which sometimes lasts several days during flood periods.

18.6 Conclusion

The scarcity of water in most drought-affected regions is not only caused by a low or unpredictable rainfall pattern, but also by a lack of capacity to conserve and manage rainwater resources in a sustainable manner (Bathis and Ahmed 2016). The high probability of flooding and climate change, leading to the multiplication of extreme events, highlights the importance of good water resources planning (Bouramtane

et al. 2020). Therefore, the determination of characteristics describing the magnitude, frequency, and response of the watershed to extreme hydrological events is particularly important.

Modeling of the hydrological behavior of watersheds has become unavoidable and hence, it is better to understand issues related to the management of water resources or one of the different facets of hydrological risk. The uncontrollable behavior of floods led to the establishment of preventive models to tackle the consequences. Therefore, it is necessary to define a methodology for predicting flash floods to take preventive measures and reduce damage and losses from the occurrence (Benkirane et al. 2020).

The identification of flood risks in the Taguenit Wadi watershed using the FHI multi-criteria analysis method allowed for a better delineation of exposed areas to flood risks that must be considered in future land use plans and territorial planning. More than half of the Taguenit Wadi watershed area is considered as a very high to medium flood sensitivity region, especially in the downstream section. The main factors impacting most of the floods occurrences are the flow accumulation, distance to the drainage system, and density of the river system. However, the impact of the alluvial topography, which determines the spread of the floods, according to the state of the embankment of the main watercourse valley, should also be considered.

Despite the absence of hydrometric data from the Taguenit Wadi watershed region, the FHI model could be considered as a relevant modeling tool on a first approach to the mapping of flood-prone areas.

The obtained results with the application of the FHI model will allow the proposal of solutions and/or recommendations to avoid larger flood impacts. As an example, Taguenit Wadi watershed could be suggested for the implementation of specific equipment on hydrological stations, for instance in three zones of the basin area, construction of an upstream dam that will promote a decrease of water flow speed and, consequently, a downstream gradual water infiltration, the construction of benches and dikes along with the valley's limits and finally the installation of a vigilance system to allow the previous announcement of strong floods.

Acknowledgements We appreciate the valuable comments and constructive suggestions from the co-editor Dr. Swatantra Kumar Dubey and an anonymous reviewer. Most data presented in this work were collected from 2020 to 2022, as part of the PhD thesis of the first author under the supervisor of Profs. Farid Faik and Said Boutaleb at Ibn Zohr University, Morocco. The authors are much obliged to the Springer proofreading team for handling the work, sending reviews, and preparing the proof.

Author statement All authors have approved the final version of the manuscript.

Data Availability All data generated or analyzed during this study are included in the manuscript.

References

- Aaron C, Venkatesh M (2009) Effect of topographic data, geometric configuration and modeling approach on flood inundation mapping. *J Hydrol* 377(1–2):131–142

- Aich V, Liersch S, Vetter T, Andersson J, Muller E, Hatermam F (2015) Climate or land use? Attribution of changes in river flooding in the Sahel Zone. *Water* 7(6):2796–2820
- Ait Haddou M, Wanaïm A, Ikirri M, Aydda A, Bouchriti Y, Abioui M, Kabbachi B (2022) Digital Elevation Model-Derived Morphometric Indices for Physical Characterization of the Issen Basin (Western High Atlas of Morocco). *Ecol Eng Environ Tech* 23(5): 285–298
- Ali SA, Parvin F, Pham QB, Vojtek M, Vojtekova J, Costache R, Linh NTT, Nguyen HQ, Ahmad A, Ghorbani MA (2020) GIS-based comparative assessment of flood susceptibility mapping using hybrid multi-criteria decision-making approach, naïve Bayes tree, bivariate statistics and logistic regression: a case of Topla basin, Slovakia. *Ecol Ind* 117:106620
- Bathis K, Ahmed SA (2016) Rainfall-runoff modeling of Doddahalla Watershed—an application of HEC-HMS and SCN-CN in ungauged agricultural watershed. *Arab J Geosci* 9(3):170
- Benjmel K, Amraoui F, Boutaleb S, Ouchchen M, Tahiri A, Touab A (2020) Mapping of groundwater potential zones in crystalline terrain using remote sensing, GIS techniques, and multicriteria data analysis (Case of the Ighrem Region, Western Anti-Atlas, Morocco). *Water* 12(2):471
- Benkirane M, Laftouhi N, El Mansouri B, Salik I, Snineh M, El Ghazali FE, Kamal S, Zamrane Z (2020) An approach for flood assessment by numerical modeling of extreme hydrological events in the Zat watershed (High Atlas, Morocco). *Urban Water J* 17(5):381–389
- Bennani O, Druon E, Leone F, Trambly Y, Saidi ME (2019) A spatial and integrated flood risk diagnosis: Relevance for disaster prevention at Ourika valley (High Atlas-Morocco). *Disaster Prev Manag* 28(5):548–564
- Benssaou M, Hamoumi N (2003) Le graben de l'Anti-Atlas occidental (Maroc): contrôle tectonique de la paléogéographie et des séquences au Cambrien inférieur. *CR Geosci* 335(3):297–305
- Benjmel K, Amraoui F, Aydda A, Tahiri A, Yousif M, Pradhan B, Abdelrahman K, Fnais MS, Abioui M (2022) A multidisciplinary approach for groundwater potential mapping in a fractured semi-arid terrain (Kerdous Inlier, Western Anti-Atlas, Morocco). *Water* 14(10):1553
- Bouramtane T, Yameogo S, Touzani M, Tiouiouine A, El Janati M, Ouardi J, Kacimi I, Valles V, Barbiero L (2020) Statistical approach of factors controlling drainage network patterns in arid areas. Application to the Eastern Anti Atlas (Morocco). *J Afri Earth Sci* 162: 103707
- Campion BB, Venzke JF (2013) Rainfall variability, floods and adaptations of the urban poor to flooding in Kumasi, Ghana. *Nat Hazards* 65(3):1895–1911
- Cobbinah PB, Anane GK (2016) Climate change adaptation in rural Ghana: indigenous perceptions and strategies. *Clim Devel* 8(2):169–178
- Demek J (1972) Manual of detailed geomorphological mapping. Czechoslovak Academy of Sciences, Prague
- Dill HG, Kaufhold S, Techmer A, Baritz R, Moussadek R (2019) A joint study in geomorphology, pedology and sedimentology of a Mesoeuropean landscape in the Meseta and Atlas Foreland (NW Morocco). A function of parent lithology, geodynamics and climate. *J Afri Earth Sci* 158:103531
- Echogdali FZ, Boutaleb S, Jauregui J, Elmouden A (2018a) Cartography of flooding hazard in semi-arid climate: the case of Tata valley (South-East of Morocco). *J Geogr Nat Disast* 8(1):214
- Echogdali FZ, Boutaleb S, Elmouden A, Ouchchen M (2018b) Assessing flood hazard at river basin scale: comparison between HECRAS-WMS and flood hazard index (FHI) methods Applied to El Maleh Basin, Morocco. *J Water Resour Prot* 10(9):957–977
- El Alaoui El Fels A, Alaa N, Bachnou A, Rachidi S (2018) Flood frequency analysis and generation of flood hazard indicator maps in a semi-arid environment, case of Ourika watershed (western High Atlas, Morocco). *J Afri Earth Sci* 141:94–106
- El Alaoui El Fels A, Bachnou A, Alaa N (2017) Combination of GIS and mathematical modeling to predict floods in semiarid areas: case of Rheraya watershed (Western High Atlas, Morocco). *Arab J Geosci* 10(24):554
- Elkhrachy I (2015) Flash flood hazard mapping using satellite images and GIS tools: a case study of Najran City, Kingdom of Saudi Arabia (KSA). *Egypt J Remote Sens Space Sci* 18(2):261–278
- El Morjani ZEA, Seif Ennasr M, Elmouden A, Idbraim S, Bouaakaz B, Saad A (2016) Flood hazard mapping and modeling using GIS applied to the Souss river watershed. In: Choukr-Allah

- R, Ragab R, Bouchaou L, Barceló D (eds) *The Souss-Massa River Basin, Morocco*. Springer, Cham, pp 57–93
- Echogdali FZ, Kpan RB, Ouchchen M, Id-Belqas M, Dadi B, Ikirri M, Abioui M, Boutaleb S (2022a) Spatial prediction of flood frequency analysis in a semi-arid zone: a case study from the Seyad Basin (Guelmim Region, Morocco). In: Rai PK, Mishra VN, Singh P (eds) *Geospatial technology for landscape and environmental management: sustainable assessment and planning*. Springer, Singapore, pp 49–71
- Echogdali FZ, Boutaleb S, Taia S, Ouchchen M, Id-Belqas M, Kpan RB, Abioui M, Aswathi J, Sajinkumar KS (2022b) Assessment of soil erosion risk in a semi-arid climate watershed using SWAT model: case of Tata basin, South-East of Morocco. *Appl Water Sci* 12(6):137
- Echogdali FZ, Boutaleb S, Bendarma A, Saidi ME, Aadraoui M, Abioui M, Ouchchen M, Abdelrahman K, Fnais MS, Sajinkumar KS (2022c) Application of Analytical Hierarchy Process and Geophysical Method for Groundwater Potential Mapping in the Tata Basin, Morocco. *Water* 14(15):2393
- Echogdali FZ, Boutaleb S, Kpan RB, Ouchchen M, Bendarma A, El Ayady H, Abdelrahman K, Fnais MS, Sajinkumar KS, Abioui M (2022d) Application of Fuzzy Logic and Fractal Modeling Approach for Groundwater Potential Mapping in Semi-Arid Akka Basin, Southeast Morocco. *Sustain* 14(16):10205
- Franci F, Bitelli G, Mandanici E, Hadjimitsis D, Agapiou A (2016) Satellite remote sensing and GIS-based multi-criteria analysis for flood hazard mapping. *Nat Hazards* 83(1):31–51
- Gao YQ, Liu YP, Lu XH, Luo H, Liu Y (2020) Change of stream network connectivity and its impact on flood control. *Water Sci Eng* 13(4):253–264
- Hall JW, Tarantola S, Bates PD, Horritt MS (2005) Distributed sensitivity analysis of flood inundation model calibration. *J Hydraul Eng* 131(2):117–126
- Hallegatte S, Hourcade JC, Dumas P (2007) Why economic dynamics matter in assessing climate change damages: illustration on extreme events. *Ecol Econ* 62(2):330–340
- Heiß L, Bouchaou L, Tadoumant S, Reichert B (2020) Multi-tracer approach for assessing complex aquifer systems under arid climate: case study of the River Tata catchment in the Moroccan Anti-Atlas Mountains. *Appl Geochem* 120:104671
- Ikirri M, Faik F, Boutaleb S, Echogdali FZ, Abioui M, Al-Ansari N (2021) Application of HEC-RAS/WMS and FHI models for the extreme hydrological events under climate change in the Infi River arid watershed from Morocco. In: Nistor MM (ed) *Climate and Land Use Impacts on Natural and Artificial Systems: Mitigation and Adaptation*. Elsevier, Amsterdam, pp 251–270
- Ikirri M, Faik F, Echogdali FZ, Antunes IMHR, Abioui M, Abdelrahman K, Fnais MS, Wanaim A, Id-Belqas M, Boutaleb S, Sajinkumar KS, Quesada-Román A (2022) Flood hazard index application in arid catchments: Case of the Taguenit Wadi watershed, Lakhssas, Morocco. *Land* 11(8):1178
- Kabenge M, Elaru J, Wang H, Li F (2017) Characterizing flood hazard risk in data-scarce areas, using a remote sensing and GIS-based flood hazard index. *Nat Hazards* 89(3):1369–1387
- Kazakis N, Kougias I, Patsialis T (2015) Assessment of flood hazard areas at a regional scale using an index-based approach and Analytical Hierarchy Process: Application in Rhodope-Evros region, Greece. *Sci Total Environ* 538:555–563
- Koks EE, Jongman B, Husby TG, Botzen WJ (2015a) Combining hazard, exposure and social vulnerability to provide lessons for flood risk management. *Environ Sci Policy* 47:42–52
- Koks EE, Bočkarjova M, de Moel H, Aerts JC (2015b) Integrated direct and indirect flood risk modeling: development and sensitivity analysis. *Risk Anal* 35(5):882–900
- Kundzewicz ZW (2003) Extreme precipitation and floods in the changing world. In: Blöschl G, Franks S, Kumagai M, Musiak K, Rosbjerg D (eds) *Water resources systems-hydrological risk management and development*. IAHS Press, Wallingford, pp 32–39
- Lekuthai A, Vongvisessomjai S (2001) Intangible flood damage quantification. *Water Resour Manage* 15(5):343–362
- Lu C, Zhou J, He Z, Yuan S (2018) Evaluating typical flood risks in Yangtze River Economic Belt: application of a flood risk mapping framework. *Nat Hazards* 94(3):1187–1210

- Moel HD, Asselman NEM, Aerts JCJH (2012) Uncertainty and sensitivity analysis of coastal flood damage estimates in the west of the Netherlands. *Nat Hazards Earth Syst Sci* 12(4):1045–1058
- Ouma YO, Tateishi R (2014) Urban flood vulnerability and risk mapping using integrated multi-parametric AHP and GIS: methodological overview and case study assessment. *Water* 6(6):1515–1545
- Pappenberger F, Beven KJ, Ratto M, Matgen P (2008) Multi-method global sensitivity analysis of flood inundation models. *Adv Water Resour* 31(1):1–14
- Patrikaki O, Kazakis N, Kougias I, Patsialis T, Theodossiou N, Voudouris K (2018) Assessing flood hazard at river basin scale with an index-based approach: The case of Mouriki, Greece. *Geosciences* 8(2):50
- Rahmati O, Zeinivand H, Besharat M (2016) Flood hazard zoning in Yasooj region, Iran, using GIS and multi-criteria decision analysis. *Geomat Nat Hazards Risk* 7(3):1000–1017
- Razandi Y, Pourghasemi HR, Neisani NS, Rahmati O (2015) Application of analytical hierarchy process, frequency ratio, and certainty factor models for groundwater potential mapping using GIS. *Earth Sci Inform* 8(4):867–883
- Saaty TL, Vargas LG (2012) The seven pillars of the analytic hierarchy process. Models, methods, concepts & applications of the analytic hierarchy process, vol 175. Springer, Boston, MA, pp 23–40
- Saaty TL (1990a) How to make a decision: the analytic hierarchy process. *Eur J Oper Res* 48(1):9–26
- Saaty TL (1990b) An exposition of the AHP in reply to the paper “remarks on the analytic hierarchy process. *Manage Sci* 36(3):259–268
- Saaty TL (1977) A scaling method for priorities in hierarchical structures. *J Math Psychol* 15(3):234–281
- Saidi ME, Daoudi L, Aresmouk MEH, Fnguire F, Boukrim S (2010) The Ourika floods (High Atlas, Morocco), extreme events in semi-arid mountain context. *Comun Geol* 97:113–128
- Saidi ME, Saouabe T, El Alaoui El Fels A, El Khalki EM, Hadri A (2020) Hydro-meteorological characteristics and occurrence probability of extreme flood events in Morocco High Atlas. *J Water Clim Change* 11(S1):310–321
- Sdzuy K, Geyer G (1988) The base of the Cambrian in Morocco. In: Jacobshagen VH (ed) *The Atlas System of Morocco*. Springer, Berlin, Heidelberg, pp 91–106
- Soulaimani A, Bouabdelli M (2005) Le Plateau de Lakhssas (Anti-Atlas occidental, Maroc): Un graben fini-précambrien réactivé à l’hercynien. *Ann Soc Géol Nord* 2(2):177–184
- Tang JC, Vongvisessomjai S, Sahasakmontri K (1992) Estimation of flood damage cost for Bangkok. *Water Resour Manag* 6(1):47–56
- Tehrany MS, Pradhan B, Jebur MN (2014) Flood susceptibility mapping using a novel ensemble weights-of-evidence and support vector machine models in GIS. *J Hydrol* 512:332–343
- Tehrany MS, Pradhan B, Jebur MN (2013) Spatial prediction of flood susceptible areas using rule based decision tree (DT) and a novel ensemble bivariate and multivariate statistical models in GIS. *J Hydrol* 504:69–79
- Wang K, Wang Z, Liu K, Cheng L, Bai Y, Jin G (2021) Optimizing flood diversion siting and its control strategy of detention basins: a case study of the Yangtze River, China. *J Hydrol* 597:126201
- Weng Q (2001) Modeling urban growth effects on surface runoff with the integration of remote sensing and GIS. *Environ Manage* 28(6):737–748
- Yoo C, Cho E, Na W, Kang M, Lee M (2021) Change of rainfall-runoff processes in urban areas due to high-rise buildings. *J Hydrol* 597:126155
- Yoo C, Jung KS, Kim TW (2005) Rainfall frequency analysis using a mixed Gamma distribution: evaluation of the global warming effect on daily rainfall. *Hydrol Process* 19(19):3851–3861

Exploring Linkages Among Soil–Water, Agriculture, and Climate Change—A Summary

Swatantra Kumar Dubey, Prakash Kumar Jha, Pankaj Kumar Gupta, Aliva Nanda, Vivek Gupta

Introduction

One of the significant effects of climate change is changing the quality and availability of water resources, which has a direct impact on crop output. Agriculture is today, as it has always been, vulnerable to losses caused by unfavorable weather events and climatic conditions (Rosenberg 1992; Altieri et al 2015). The agricultural sector is the most vulnerable because it directly affects people's lives. An integration of efforts is urgently required to improve research on how climate change affects forests, agriculture, animal husbandry, aquatic life, and other natural organisms. Climate change, the outcome of “global warming,” has now started showing its impacts worldwide (Bhattacharya 2019). Climate is the primary determinant of agricultural productivity which directly impacts on food production across the globe. The agriculture sector is the most sensitive sector to climate change because the climate of a county determines the nature and characteristics of vegetation and crops. Studies on climate impacts and adaptation strategies are increasingly becoming major areas of scientific concern, e.g. impacts on the production of crops such as maize, wheat and rice and other crops (Dhungana et al. 2006; Dubey and Sharma 2018; Mauget et al. 2021; Himanshu et al. 2021; Gunawat et al. 2022) water resources in the river basin catchments (Wilby et al. 2006; Digna et al. 2017) forests (Lexer et al. 2002), industry (Harleet al. 2007) and the landscape (Dockerty et al. 2006).

Climate change, including variations in temperature and precipitation, has a significant impact on food production systems because it can cause pest and disease outbreaks that reduce harvests and eventually jeopardize the nation's food security (Anwar et al. 2013; Bhattacharya 2019). It will be important to manage resources

like soil, water, and biodiversity carefully in order to deal with the effects of climate change on agriculture. The majority of current research has focused on the effects of single climatic factors and paid little attention to how developed agronomic methods affect crop water usage efficiency (Choudhary et al. 2016; Bhattacharya 2019). By utilizing a multi-disciplinary approach, remote sensing and satellite imaging can also aid in future projections for the most vulnerable agro-ecosystems and providing corrective strategies. Additionally, this can aid in developing responses, preparations, and plans for managing agro-ecosystems in the event of extreme occurrences like water scarcity, heat waves, floods, and others. Climate smart agriculture is also an imperative prerequisite for enhancing the yields and quality of production. Agriculture and climate change are closely intertwined. The fast pace of climate change will affect agro-ecosystems and their output in a significant way. Therefore, it is imperative that we get ready for the challenges ahead to battle the effects of climate change and preserve food security for both humans and other living things.

This summary's goals are to present an overall evaluation of how well soil, water, and agriculture are adapting to climate change and to examine the most significant methodological approaches that have recently been established to carry out such an evaluation. In order to provide a baseline against which to compare the effects of climate change, current patterns are utilized to forecast a plausible scenario of future agricultural production, climate change excluded. This overview is broken down into four main sections to help readers understand how agriculture, water, and soil use relate to climate change.

A.1 Soil–Water Hydrological Consideration

Mountains are important for human existence as they are the center of biodiversity and various ecosystem services. Mountains around the world are significant sources of freshwater and provide room for a large amount of water storage. At the same time, mountains are most vulnerable to changing climate, which is also true for the Himalayan Region. Topographically and geographically diverse Himalaya, also known as the water tower of Asia, has the third-largest deposit of ice and snow and is the source of 10 major rivers. However, our understanding of the different components of Himalayan hydrologic cycles is still in the developing phase (Qazi et al. 2017; Nanda et al. 2019). Further, the Himalayas are also very prone to natural hazards like flash floods, landslides, and erosion in the changing climate conditions. But, the unavailability of high-resolution long-term datasets, financial and logistic constraints, and unavailability of detailed field studies, keep our hydrological understanding of the Himalayan region in the nascent phase.

Thus, this book provides a detailed review of Himalayan Hydrology (Chap. 1), which discusses the data scarcity issue and problems related to maintaining long-term hydro-meteorological sites in Himalayan terrain and hydrological differences between 'Himalayan catchments' and 'Alpine catchments due to variation in rain-snow pattern. This chapter discusses different approaches and models to estimate

and predict the discharge of the Himalayan River in gauged and ungauged basins during high and low flow conditions. Further, a brief review of suitable climate models to study the impact of climate change on the Himalayan region is presented in this chapter. The hydrological processes, i.e., runoff generation mechanisms, vary temporally and spatially in the Himalayan region and are also understudied in these topographically diverse regions (Sarkar et al. 2015; Nanda and Sen 2021). Where many large-scale hydrological models ignore hydrological processes caused by macropores, i.e., preferential flow and subsurface flow, at the same time, a new semi-distributed rainfall-runoff model called Hilly Watershed Hydrologic Model (HWHM) for studying water balance in macropores-dominated hilly river basins has been presented in Chap. 2. The case study of the HWHM model has been presented for one of the river basins of the eastern Himalayas, i.e., the Subhansiri river basin, at a spatial resolution of 1 km². Overall, Chap. 2 discusses issues related to rainfall-runoff partitioning, water storage, and variation in subsurface flow in a preferential flow-dominated system.

Chapter 3 describes the coupled ANN-SCS model for simulating rainfall-runoff in one of the sub-catchments of the Brahmaputra River basin, i.e., the Pagladiya watershed. This catchment has severe issues of downstream erosion and flood due to deforestation. Authors used LULC maps for 2000 and 2010 using Landsat satellite-based data of 30 m resolution by supervised classification technique used for runoff simulation for the period 2004–09 and 2010–17. The presented hydrological model will be helpful in planning land use and carefully managing soil, water, and vegetation resources, employing suitable management practices and structural works. Connecting to the first theme of our book, i.e., soil–water hydrological consideration, Chap. 4 discusses soil erosion mapping using the RUSLE model. This study focused on the erosion-prone Mohamed Ben Abdelkrim El Khattabi Dam watershed of Morocco, and it will be helpful for planning soil conservation activities and reducing dam siltation. Overall, we tried to cover the different hydrological perspectives of the mountainous watersheds in the first four chapters.

A.2 Water-Agriculture-Climate Linkage

Drought is a definite after effect of climate change and has a severe impact on agriculture productivity and cascading impact on global food security (Burke and Lobell 2010). As a mitigation measure, greater dependence on irrigation would be required. Over two-thirds of global renewable water resources are annually being used for irrigation, and the demand is projected to increase by 20–30% due to increased drought conditions (Kadiresan and Khanal 2018). This might lead to a reduction in water quantity and quality, increasing competition for freshwater resources from other sectors of the economy, and changes in water policy (Hamdy et al. 2003). Therefore, saving water along with maximizing agriculture productivity in a water-scarce era will have to be carried out by using the available resources very efficiently.

Chapter 5 describes Recent years have seen a significant increase in the investigation of soil moisture retrieval using remote sensing using electromagnetic spectra from the optical/thermal to the microwave regions. This has resulted in the development of several algorithms, models, and products that can be used in practical applications. Due to a lack of resources, low-income economies find it difficult to apply remote sensing technologies to estimate soil moisture. The methods used to estimate soil moisture in Zimbabwe via remote sensing are critically examined in the current study, Chap. 6 discusses Gamma, Beta, Gaussian, Student T, and Uniform were all taken into consideration in this study as the marginal probability distribution functions for rainfall and river discharge that best fit the data. Three copula functions—Gumbel, Clayton, and Frank—were also used to study the relationship between rainfall and river discharge. According to the results, Lokoja’s rainfall and river discharge were most suited to Student T’s dispersion. Additionally, it was discovered that the Frank copula offers the best model for the relationship between rainfall and river discharge using the Akaike Information Criteria.

Thus, Chap. 7 highlights the phenotyping of drought tolerant and resilient cultivars of different crops using drone. An alternative to higher rates of irrigation is to develop newer crop varieties resilient to drought stress. Though there are extensive breeding programs for numerous crops, the traditional breeding process is slow. Phenotyping crops for physiological and morphological traits could be used as proxies for drought tolerance traits. However, extensive in-situ field data collection is constrained by time and resources. Remote data collection and machine learning techniques for analysis offer a high-throughput phenotyping (HTP) alternative to manual measurements that could help faster breeding for stress tolerance. Using HTP methods such as remote sensing, statistics, and machine learning can be faster options to phenotype plants for better water use efficiency and drought tolerance. Along with direct measurements, using aerially derived vegetation indices can be used as predictors for phenotype estimation. Machine learning can also be used to convert the derived indices and crop models into a field map. Machine learning and aerial imagery can, therefore, help in creating high-resolution spatiotemporal field maps for individual phenotypes or vegetation indices which are easier to visualize. This field map can not only be used for breeding but for agronomic purposes to pinpoint requirements of amelioration and corrective measures instead of the blanket application of farm inputs. These techniques could be further extended to aid in variable rate input application, such as irrigation, and be a step towards precision agriculture.

The Chap. 8 highlights sustainable water management practices for intensified agriculture and explained the different aspects of agriculture. The study covered sustainable water use, perspectives for agricultural land and water use towards 2050, water-saving practices for intensified agriculture, enhancing water productivity under intensified agriculture, real-time crop and water management options for intensified agriculture, breeding for enhancing water productivity and role of institutions and policymakers. The Chap. 9 highlights about water management strategies at the field based on crop growth stages, root-zone water requirements and subsurface water requirements. Deficit irrigation (DI) is an optimizing strategy that can reduce the demand for irrigation and improve water productivity. DI is used as

a water-saving irrigation strategy around the world where water supply is limited under erratic climate situations with minimal to minor yield loss. An efficient application of DI requires careful assessment of crop water requirements, knowledge of the water-sensitive growth stages and proper irrigation scheduling based on the DI approach adopted. In addition, an understanding of the role of factors such as crop (and cultivar), soil, climate and different management practices under limited water scenarios is required. DI helps in improving water use efficiency by regulating stomatal guard cell for minimizing transpiration loss, improves photosynthesis to transpiration ratio, and reduces soil evaporation.

A.3 Soil–Water Quality Consideration

Subsurface water resources have dynamic interactions with ground surface and its prevailing environmental conditions (Sophocleous 2002). Climate variability affects subsurface water resources both directly by altering surface water flux and indirectly via changes in groundwater extraction patterns (Gupta et al. 2022). Any such alteration in the (sub)-surface water flux may affect the bio-geochemical makeups of the subsurface environment, which directly results in modification of the fate, and transport of existing pollutants at the site (Earman and Dettinger (2011)). Thus, the knowledge on the role of varying climatic conditions on geochemical characteristics and pollutant transport in the subsurface is required for the management of the subsurface hydrological resources, especially soil–water quality (Gupta and Yadav 2019). To bridge the knowledge gap regarding fate, transport, and remedial of pollutants under climate change conditions, we have included three chapters (Chaps. 10 and 11) in this book. Further, these chapters provide a better understanding of the linkage among subsurface hydrology-pollutants mobility and its implications.

Chapter 10 entitled “Recent Advances in the Occurrence, Transport, Fate, and Distribution Modeling of Emerging Contaminants-A Review”, authored by Ashraf et al., has provided excellent background on the fundamental of fate and transport mechanisms of emerging pollutants in the subsurface. First, the chapter has highlighted the occurrence, sources and types of pollutants and the processes involved in their fate and transport in vadose and saturated zones. Thereafter, the chapter has presented different techniques to estimate pollutant loads in the subsurface under climate change conditions. This study has pointed that the requirement of an appropriate model is of utmost important for risk assessment under changing climate conditions. We are sure that the results of this study can be utilized in policy making and hence controlling emerging contaminants in nature.

Likewise, Chap. 11 entitled “Management and Remediation of Polluted Soils Using Fertilizer, Sawdust and Horse Manure Under Changing Tropical Conditions”, authored by Mustapha and Okeke, has presented a case study of treatment of potential toxic substance using fertilizer, sawdust, and horse manure under changing tropical conditions. They have studied a combination of treatments to cadmium, chromium, lead, and total petroleum hydrocarbon contaminated soils by applying

NPK (nitrogen, phosphorous, and potassium) fertilizer, sawdust, horse manure and exposure to oxygen. Very importantly, this study is an excellent example of nature-based low-cost climatic solutions to polluted sites suffering from multiple contaminations. Thus, we are confident that the results of this study can be useful for many polluted sites around the globe. Based on this study, our especial recommendation to the field manager is to utilize nutrient enhanced bioremediation to achieve the degradation of petroleum hydrocarbon and heavy metals in oil-contaminated soils under the prevailing tropical conditions.

Further Chap. 12 entitled “Impacts of Blend Diesel on Root Zone Microbial Communities: *Vigna radiata* L. growth assessment study”, authored by Gandhi et al., has demonstrated the toxicity of target pollutants i.e., diesels on soil microbial communities and on vegetation (*Vigna radiata* L.) growth. This study has highlighted that the use of Proteobacteria may improve the biodegradation of organic contaminants in soils. In this study, another nature-based low-cost climatic solution i.e., use of neat biofuel as a substrate or plant stimulator has been suggested. We also recommend the use of neat biofuel in soil improves proteobacterial communities to take care of hydrocarbon-polluted soils. Chapter 13 explained the on various processes, causes, and sources of river water pollution in India. To fulfill escalating human demands, there is an urgent need for clean water. River water is abundant in ecological life and is essential to the survival of all living things. Still, because of several human-made activities, it is currently the most endangered ecosystem. In order to determine the true health of river water ecosystems, careful monitoring of river water quality (RWQs), evaluation of multiple variables (physicochemical, bacteriological, pathogenic), and heavy metals content are essential indicators.

Most of the countries are researching in the area of hydrogeology and trying to see the implications under climate change conditions. This is due to linkage of pollution and climate change is one of the major challenges before concern authorities, scientists, policy makers, politicians and other who has interest. This is a timely book to provide very accurate information, data, methods, model, and policy statements on linkage of hydrogeology and climate science to the global audience.

A.4 Techniques for Landscape Management under Large Uncertainty

Climate change is altering hydrological behavior of most of the regions around the world. Studies report that the hydrological extremes such as droughts and floods may increase in frequency and magnitude. Therefore, to adapt to climate change, we would require better tools and techniques for better management, planning and policymaking. In Sect. 4, the recent advancements in the techniques to assess the impacts, identify the risk and to adapt to climate change for water management to increase the water security has been discussed. Two chapter (Chaps. 14 and 15) provides reviews of the current condition, challenges and potential solution reled to the water

security in developing regions of Africa and Latin America. Next three chapters in this section provides great insights in identifying the flood hazard, vulnerability, risk, and sensitivity.

Chapter 14 discusses water scarcity and security in the semi-arid regions of the world, related policies, and approaches for climate adaptation. Water is a critical resource for life support on the planet. This chapter deepens our understanding of the issues in semiarid regions related to water scarcity in different countries of the world. Further, this chapter also helps us in understanding various indicators used for water scarcity quantification. Moreover, the approaches used in water management worldwide, such as water conservation, reuse of wastewater, source protection, managed aquifer recharge, and desalination of water have also been discussed. Furthermore, a detailed discussion on policies and approaches being adopted by different countries for building water security is also discussed.

Chapter 15 discusses different aspects of water security-related challenges in Latin America. The chapter first introduces us to the current water scenario in Latin American countries and dives deeper into how we can define water security in the region. Further, this chapter provides us with the details of the current challenges of water security in the region. The challenges that have been discussed in detail are: megacities, climate change, lack of policies and implementation of laws, expansion of agriculture and deforestation, increased industrialization, expansion of activities in mining, sewage treatment, and the lack of transboundary watershed management programs. Overall, this chapter provides great insights into current issues related to water security in Latin America.

Chapter 16 analyses the flood risk in the Wadi Tamlest watershed of Morocco. In this chapter, an analytical hierarchical processing-based method has been developed to map the flood risk in the flood-prone Wadi Tamlest watershed north of Agadir in Morocco. Authors have utilized the Flood Hazard Index method, which considers six different factors: flow accumulation, distance to the river system, drainage density, watershed land use, slope, and watershed geology. The adopted methodology proves to be an excellent tool for the ungauged watersheds where it is challenging to find the exact flood history.

Chapter 17 presents a Google Earth Engine (GEE) based approach for flood inundation mapping utilizing Sentinel-1 imagery for Niger River basin in Nigeria. The chapter starts with introducing us with the problems of flood management and issues of proper monitoring technique. Further, authors iterate the importance of remote sensing in flood monitoring and explains various remote sensing techniques used for flood monitoring and mapping. Furthermore, authors highlight how Synthetic Aperture Radar (SAR) imagery can be an important tool for flood monitoring. This study utilizes the simple change detection approach in GEE to identify the flooded area. Authors conclude that the Sentinel imagery-based flood assessment technique is reliable and robust and can be utilized in the region with data scarcity.

Chapter 18 discusses the contributions of the geomatics techniques for studying the flood hazard in Taguenit Wadi watershed, Lakhssas, Morocco. The chapter starts with highlighting the importance of management of the hydrological extremes especially in developing countries like Morocco. Further, authors focus on flood hazard

and reviews the major historical flooding events occurred in Morocco. Flood Hazard Index (FHI) has been developed for Taguenit Wadi watershed using analytical hierarchical processing. Distribution of the rainfall, digital elevation model (DEM) of 30 m resolution, geological maps were used to identify the flood hazard by computing slope, flow accumulation, drainage network, drainage density, distance from the stream, permeability etc. Flood sensitivity has also been quantified in this study. After identifying the flood risk authors propose the intervention measures to reduce the flooding risk in the basin.

References

- Altieri MA, Nicholls CI, Henao A, Lana MA (2015) Agroecology and the design of climate change-resilient farming systems. *Agron Sustain Dev* 35(3):869–890
- Anwar MR, Liu DL, Macadam I, Kelly G (2013) Adapting agriculture to climate change: a review. *Theoret Appl Climatol* 113(1):225–245
- Bhattacharya A (2019) Global climate change and its impact on agriculture. *Changing climate and resource use efficiency in plants*, pp 1–50
- Burke M, Lobell D (2010) Food security and adaptation to climate change: what do we know?. *Climate Change Food Secur*, 133–153
- Choudhary M, Ghasal PC, Kumar S, Yadav RP, Singh S, Meena VS, Bisht JK (2016) Conservation agriculture and climate change: an overview. *Conserv Agric*, 1–37
- Dhungana P, Eskridge KM, Weiss A, Baenziger PS (2006) Designing crop technology for a future climate: an example using response surface methodology and the CERES-Wheat model. *Agric Syst* 87(1):63–79
- Digna RF, Mohamed YA, Van Der Zaag P, Uhlenbrook S, Corzo GA (2017) Nile River Basin modelling for water resources management—a literature review. *Int J River Basin Manag* 15(1):39–52
- Dockerty T, Lovett A, Appleton K, Bone A, Sünnerberg G (2006) Developing scenarios and visualisations to illustrate potential policy and climatic influences on future agricultural landscapes. *Agr Ecosyst Environ* 114(1):103–120
- Dubey SK, Sharma D (2018) Assessment of climate change impact on yield of major crops in the Banas River Basin, India. *Sci Total Environ* 635:10–19
- Earman S, Dettinger M (2011) Potential impacts of climate change on groundwater resources—a global review. *J Water Climate Change* 2(4):213–229
- Gunawat A, Sharma D, Sharma A, Dubey SK (2022) Assessment of climate change impact and potential adaptation measures on wheat yield using the DSSAT model in the semi-arid environment. *Nat Hazards* 111(2):2077–2096
- Gupta PK, Yadav BK (2019) Subsurface processes controlling reuse potential of treated wastewater under climate change conditions. In: *Water conservation, recycling and reuse: issues and challenges*. Springer, Singapore, pp 147–170
- Gupta PK, Yadav BK, Sharma D (2022) Impacts of climatic variability on subsurface water resources. In: *Advances in Remediation techniques for polluted soils and groundwater*. Elsevier, pp 171–189. <https://doi.org/10.1016/B978-0-12-823830-1.00003-1>
- Hamdy A, Ragab R, Scarascia-Mugnozza E (2003) Coping with water scarcity: water saving and increasing water productivity. *Irrigation Drainage: J Int Commiss Irrigation Drainage* 52(1):3–20
- Harle KJ, Howden SM, Hunt LP, Dunlop M (2007) The potential impact of climate change on the Australian wool industry by 2030. *Agric Syst* 93(1–3):61–89

- Himanshu SK, Fan Y, Ale S, Bordovsky J (2021) Simulated efficient growth-stage-based deficit irrigation strategies for maximizing cotton yield, crop water productivity and net returns. *Agric Water Manag* 250:106840
- Kadiresan K, Khanal PR (2018) Rethinking irrigation for global food security. *Irrig Drain* 67(1):8–11
- Lexer MJ, Hönninger K, Scheifinger H, Matulla C, Groll N, Kromp-Kolb H, ... Englisch M (2002) The sensitivity of Austrian forests to scenarios of climatic change: a large-scale risk assessment based on a modified gap model and forest inventory data. *Forest Ecol Manag* 162(1):53–72
- Mauget SA, Himanshu SK, Goebel TS, Ale S, Lascano RJ, Gitz DC III (2021) Soil and soil organic carbon effects on simulated Southern High Plains dryland Cotton production. *Soil Tillage Res* 212:105040
- Nanda A, Sen S (2021) A complex network theory based approach to better understand the infiltration-excess runoff generation thresholds. *J Hydrol* 603:127038
- Nanda A, Sen S, McNamara JP (2019) How spatiotemporal variation of soil moisture can explain hydrological connectivity of infiltration-excess dominated hillslope: Observations from lesser Himalayan landscape. *J Hydrol* 579:124146
- Qazi NQ, Bruijnzeel LA, Rai SP, Ghimire CP (2017) Impact of forest degradation on streamflow regime and runoff response to rainfall in the Garhwal Himalaya, northwest India. *Hydrol Sci J* 62(7):1114–1130
- Rosenberg NJ (1992) Adaptation of agriculture to climate change. *Clim Change* 21(4):385–405
- Sarkar R, Dutta S, Dubey AK (2015) An insight into the runoff generation processes in wet subtropics: Field evidences from a vegetated hillslope plot. *CATENA* 128:31–43
- Sophocleous M (2002) Interactions between groundwater and surface water: the state of the science. *Hydrogeol J* 10(1):52–67
- Wilby RL, Whitehead PG, Wade AJ, Butterfield D, Davis RJ, Watts G (2006) Integrated modelling of climate change impacts on water resources and quality in a lowland catchment: River Kennet, UK. *J Hydrol* 330(1–2):204–220